SPECIFICATION OF THE QUALITY OF IONISING RADIATIONS FOR UNIFIED DOSIMETRY IN RADIOBIOLOGY AND RADIOLOGICAL PROTECTION

Ali Salem Alkharam

A Thesis Submitted for the Degree of PhD
at the
University of St Andrews

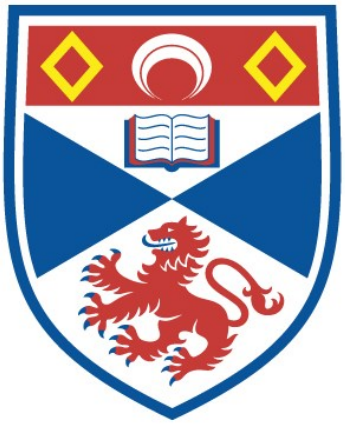

1997

SPECIFICATION OF THE QUALITY OF IONISING RADIATIONS FOR UNIFIED DOSIMETRY IN RADIOBIOLOGY AND RADIOLOGICAL PROTECTION

ALI SALEM ALKHARAM (B.Sc., M.Sc.)
RADIATION BIOPHYSICS
DEPARTMENT OF PHYSICS AND ASTRONOMY
UNIVERSITY OF ST. ANDREWS.

SPECIFICATION OF THE QUALITY OF IONISING RADIATIONS FOR UNIFIED DOSIMETRY IN RADIOBIOLOGY AND RADIOLOGICAL PROTECTION

by

ALI SALEM ALKHARAM
B.Sc. Nuclear Engineering (Oregon State University)
M.Sc. Theoretical Physics (University of Garyounis)

A thesis submitted for the degree of Doctor of Philosophy.
University of St. Andrews
St.Andrews, Fife KY16 9SS,
United Kingdom.

April 1997

Content of the Thesis

Declaration

I, A.S. Alkharam, hereby certify that this thesis, which is approximately 60,000 words in length, has been written by me, that it is the record of work carried out by me and that it has not been submitted in any previous application for a higher degree.

This research has been carried out in the Department of Physics and Astronomy in the University of St. Andrews under the supervision of Dr. D.E. Watt.

Date ..... Signature of candidate

.....

(A.S. Alkharam)

Certification

I hereby certify that the candidate A.S. Alkharam, has fulfilled the conditions of the Resolutions and Regulations appropriate for the Degree of Doctor of Philosophy in the University of St. Andrews and that the candidate is qualified to submit this thesis in application for that degree.

Date .....

Signature of supervisor

.....

Dr. D.E. Watt

(Research Supervisor)

List of Publications

(1) Watt, D.E. and Alkharam, A.S., 1994. Charged-Particle Track Structure Parameters for Application in Radiation Biology and Radiation-Chemistry. Int.J.Quant.Chem. **S2**, 195-207.

(2) Watt, D.E., Alkharam, A.S., Child, M.B., and Salikan, M.S., 1994 Dose as a Specifier in Radiobiology for Radiation Protection, Radiat.Res. **139**, 249-251.

(3) Watt, D.E., and Alkharam, A.S., 1995. A Feasibility Study of Scintillator Microdosimeters for Measurement of the Biological Effectiveness of Ionizing-Radiations. Radiat.Prot.Dosim. **61**, 211-214.

(4) Alkharam, A.S. and Watt, D.E. 1997. Risk Scaling Factors for Chromosome Aberrations, Mutations and Oncogenic Transformations with Respect to Mammalian Cells. Radiat.Prot.Dosim. **70**, 537-540.

(5) Alkharam, A.S. and Watt, D.E. Simulation Modelling of Radiation Induced Double Strand Breaks in the DNA of Mammalian Cells (in preparation).

(6) Alkharam, A.S., McDougall, I.C. and Watt, D.E. Simulation of Double Strand Breaks in the DNA of Mammalian Cells by γ-radiation on NE102 Plastic Scintillator (in preparation).

(7) Alkharam, A.S. and Watt, D.E. Radiobiological Database: Cellular Inactivation, Dicentrics, Mutations, Oncogenic Transformations, and DNA Strand Breaks. (to be published in University of St-Andrews Report, **BIOPHYS/8/ 1997**).

Acknowledgements

I wish to express my appreciation to my supervisor, Dr. D.E. Watt, for the valuable guidance, help, advice, encouragement and simulating discussions throughout the course of this work. His friendliness, and willingness are exemplary manners of a supervisor and a gentleman.

I am indebted to the technical assistance of Physics Department at the University of St-Andrews in particular to L. Kirk, J. Park, J. Clark, and all others in the mechanical and electrical workshops. I would like to extend my thanks to my colleagues in the Radiation Biophysics Unit for their constructive discussions.

Finally I would like to thank the Faculty of Science at the University of Garyounis (Benghazi-Libya) for awarding me this scholarship and other relevant assistance for my study.

Dedications

in the memory of my mother **SASIA F. ALGHANIE**

I also dedicate this to the followings: my father: SALEM A. ALKHARAM; my wife NAGWA A. ELZYANI; my children NARGES, JASER, SALEM, AREGE and AHMED; my brothers JAMAL, SAMI, MOHAMMED and SHARIFF; my sisters: FAIROOZ and FARIAL for your continouse support, encouragement, patience and understanding.

Abstract

It is widely agreed in radiobiological and biophysical research that the DNA is the dominant target which can lead to terminal biological damage in the form of cancer or cell death. A main objective in radiation protection is to set the limits of the possible harmful effects to the general population exposed to ionising radiation at low level (environmental level). The initial slope of the dose-response curve is found to be an appropriate parameter to achieve this objective. Bench mark data sets of the initial effects of ionising radiation on cells *in vitro* were formed which include both physical characterisation of the radiation and the radiobiological parameters. These data-bases include the mammalian cell end-points: cellular inactivation, chromosome dicentrics, HPRT mutations and oncogenic transformations. On the molecular scale, the data-bases include single-strand and double strand breaks induced in the DNA of both mammalian and non-mammalian cells. Analysis of bio-effect mechanisms of damage to mammalian cells in terms of the quality parameter 'mean free path for linear primary ionisation' for ionising radiation, strongly suggest that there is a common mechanism for the biological endpoints of dicentrics, mutations, and oncogenic transformations. A unified response is obtained for all types of heavy ions and all cells which show: a common inflection point at inter-spacing distance equivalent to $\lambda_0 = 1.4 \pm 0.5$ nm, a saturation region at $\lambda < \lambda_0$ and almost constant slope for $\lambda > \lambda_0$. The lethal lesions are identified as dsb's in the intracellular DNA. It follows that radiation risk factors can be determined on the basis of simple ratios to the inactivation cross sections. The size of these genes are found to be in close proximity to the optimised saturation levels. The probabilities of risk with respect to inactivation, for chromosome dicentrics, oncogenic transformations, and mutations of the HPRT gene are respectively 0.18, 1.6×10^{-4} and 2.91×10^{-5}. The same analysis shows that sparsely ionising radiations, which have lower effect cross-sections by an order of magnitude or more, can never reach saturation.

Analysis of the molecular dsb's of DNA produced in mammalian cells by heavy ions shows a lower saturation cross-section of 0.83 μm^2 which may be compared with the geometrical cross-section of 3.5 μm^2. The difference is attributed to a higher packing factor. Calculations using earlier endpoint saturation cross-sections show that 4 dsb's in DNA of a human lymphocyte cell are needed to induce a chromosome dicentric, 100 dsb's in DNA of a C3H10T1/2 cell are needed to inactivate an oncogene, and 3500 dsb's in DNA of a V79 cell are needed on average to delete an HPRT mutant.

The feasibility to design a new dosimetric system which would have a unified response, as described above, is considered. NE102A plastic scintillators of 20 μm thickness are found to be a potentially good prospect for detecting weak ionising radiation. By adjusting the concentration of the activator, the mean of the random distance between centres can be modified to simulate the strand-pair distribution of the DNA in mammalian cells. Thus it is possible to simulate the yield of dsb's in DNA damage as those paired centres spaced by about 1.8 nm and to distinguish them from other unwanted pairs of activated sites with different spacings. Using a ^{60}Co-γ radiation source, and starting from the knowledge of the equilibrium slowing down spectrum of electrons in plastic scintillator, the yields of photons and paired events with an inter-spacing distance of ~ 1.8 nm can be calculated. As may be expected, the results show that the combination from the paired events is very small compared to the total scintillation yield but of the same order as that of double strand breaks in mammalian cells. The resulted simulation showed a yield of 10^{-2} dsb's/keV which is in close proximity with the theoretical result, for a 4 MeV alpha particle, of 7×10^{-3} dsb's/keV. Both the theory and preliminary experimental investigation with a semi-infinite disc of plastic phosphor, 20 μm thick, reveals that the method is potential promising but more detailed study is required on the process for extraction of the desired signal from the practical device.

Table of Contents

Chapter 1

Chapter 2

Chapter 3

Chapter 4

Chapter 5

Chapter 6

Chapter 7

Appendix A

List of Tables

List of Figures

List of abbreviations and Notations

α^{-1}	Radiosensitivity parameter in Gy^{-1}
ABE	Absolute Biological Effectiveness
ALARA	As Low As Reasonably Achievable
β	Relative speed of ion or particle (v/c)
BD	Biological Dosimeter
BEIR	Biological Effects of Ionizing Radiation.
C	Source Concentration (e.g. excitons/cm^3)
c	Speed of light (3 x 10^8 m/s)
D	Absorbed dose (Gy)
dE/dx	Stopping power (keV/μm)
dL/dE	Scintillation efficiency (photons/keV)
dL/dx	Specific luminescence (photons/μm)
DNA	Deoxyribonucleic Acid
DRA	Dual Radiation Action
dsb's	double strand breaks
E_F	Fermi energy level (eV)
E_G	Gab energy (eV)
F	Fano factor
ϕ	fluence (cm^{-2})
GDRA	Generalized Dual Radiation Action
H	Dose Equivalent (H=NQD)
HCP	Heavy Charged Particle
HSET	Hit-Size Effectiveness Theory
ICRP	International Commission on Radiological Protection
k	Boltzman constant (1.380622 x 10^{-23} J/^{o}K)
λ	Mean free path for linear primary ionisation (nm)
L(E)	Light yield

$L_{100,D}$	Dose average restricted linear energy transfer (keV/μm)
$L_{100,T}$	Track average restricted linear energy transfer (keV/μm)
L_D	Dose average linear energy transfer (keV/μm)
LET	Linear Energy Transfer (keV/μm)
LMD	Locally Multiplied Clusters
λ_o	Inter-strand spacing constant = 1.8 nm
L_T	Track average linear energy transfer (keV/μm)
MT	Molecular Theory
NCRP	National Council for Radiation Protection
PCC	Premature Chromosome Condensation
PLIM	Pairwise Lesion Interaction Model
Q or QF	Quality Factor
RBE	Relative Biological Effectiveness ($\alpha_i/\alpha_{X\text{-rays}}$)
rem	roentgen-equivalent-man
σ_{eff}	Effective cross-section (μm^2)
σ_g	Geometrical cross-section (μm^2)
σ_o	Saturation cross-section (μm^2)
SPJ	Superconducting Tunnel Junction
ssb's	single strand breaks
Sv	Sievert
T_δ	Kinetic energy of δ-rays (keV)
TERS	Threshold-Energy Repair-Saturation Model
TSM	Track Structure Theory
UNSCEAR	United Nation Scientific Committee on the Effects of Atomic Radiation.
W	W value which is defined as energy require to produce an ion pair
Z	Absorber atomic number
z	Particle or ion atomic number
z*	Effective charge value (density)

Chapter 1

INTRODUCTION

Background and Scope

Throughout the existing nature since its creation, man has been exposed to ionising radiation. From naturally existing sources in our environment, such as ^{22}Na in drinking water, ^{40}K in living tissues, radioactive elements in rocks and stones, cosmic rays and associated induced activities. In 1895, man-made radiation sources were added to those occurring naturally. In our modern life, the role of technology implies the use of radiation almost everywhere: in industry, medicine, agriculture and research. As a result of the pragmatic use of radiation, assessment of the level of hazards of radiation has to be evaluated to optimise the efficiency in use and to minimise potential health risks of radiation.

1-1 Radiation Protection and Dosimetry

Ionising radiation interacts with biological matter to induce various physical and chemical effects in the molecular scale that can cause biological alterations, figure 1-1. These alterations may lead to harmful damage e.g. cataract, cancer. Radiation protection concerns the protection of workers, members of the public, and patients undergoing diagnosis and therapy against the harmful effects of ionising radiation [NCRP-116, 1993]. The relative proportion of the population requiring protection against radiation sources is summarised in table 1-1.

Table 1-1 Scope of radiation protection.

Sources and Practices	Radiation Protection Concepts and Actions Apply to
Natural Radiation	All Humanity
Medical Applications	Large part of population
Nuclear Power	Large Groups of people
Industrial, Research, Other Uses	Small Group of People
Space Flight	Few Individuals

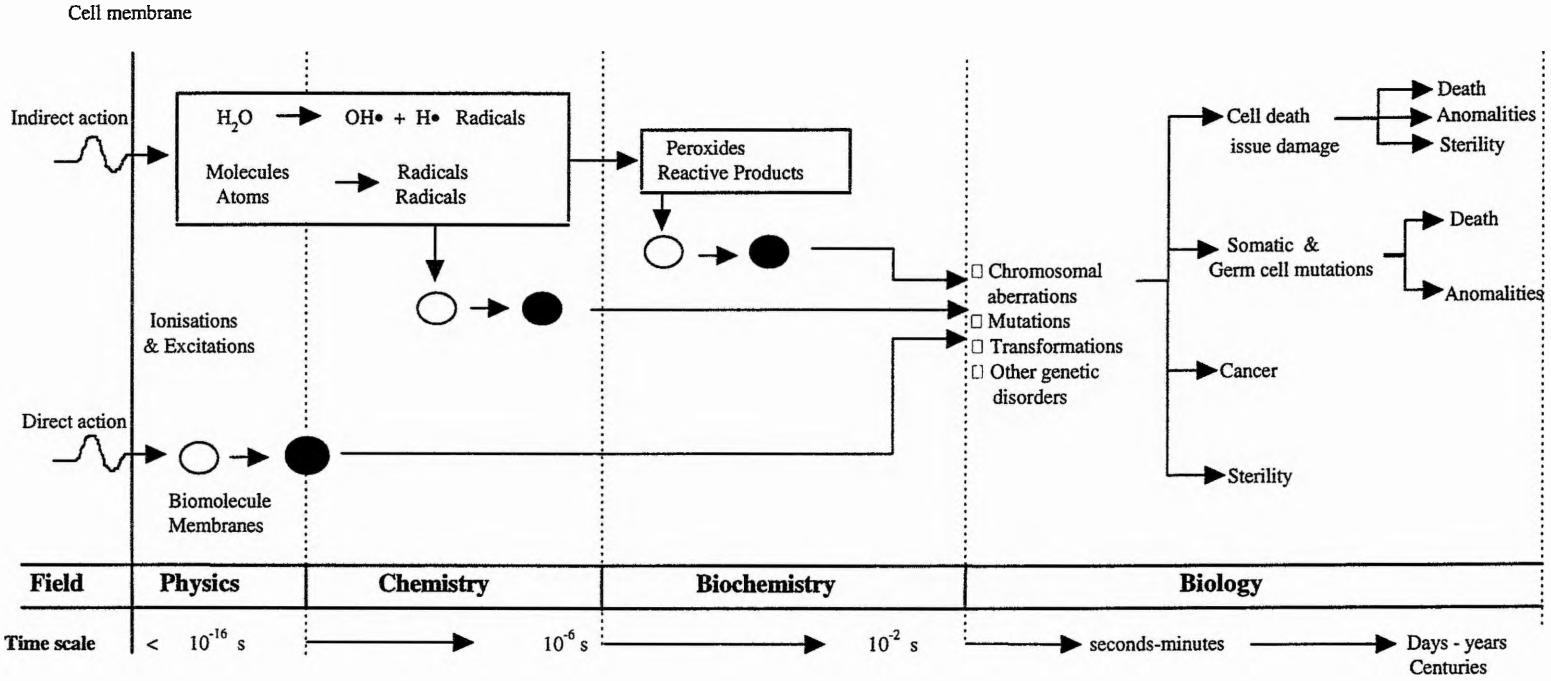

Figure 1-1 Chains of effects from the initial physical action of radiation to the final biological changes.

Ionising radiation is capable of producing harmful effects to the exposed individuals. The effects are known as somatic effects if they become manifest in the exposed individual and as genetic effects if the effect is an off-spring [Cember, 1983].

For radiological protection, radiation effects can be generally categorised as either deterministic effects (non-stochastic) or stochastic effects [Mitchel, 1991]. The severity of deterministic effects varies with dose, above an observed threshold. Stochastic effects on the other hand are probabilistic in nature. Effects may occur long after the exposure. Stochastic effects are expressed in terms of risk and not in terms of severity, as no radiation threshold is observed. Deterministic effects can be avoided by setting limits of exposure to below the threshold. Stochastic effects cannot be avoided entirely because they occur even at low dose and dose rate [Sinclair, 1995].

Both deterministic and stochastic effects are quantified in the present system of dosimetry, in units of dose (D in gray; Gy) or its derivatives such as equivalent dose (H in sievert ; Sv) or effective equivalent dose [Shapiro, 1981]. Cancer risk is quantified in terms of probability per unit equivalent dose (Sv^{-1}).

For radiological protection regulatory commission such as the International Commission for Radiological Protection (ICRP), and National Council on Radiation Protection and Measurements (NCRP) sets their rules (independently) to asses damage to both public and workers in the radiation fields (quantities and units based on ICRU). Both the ICRP and NCRP make recommendations that avoid the occurrence of deterministic effects by setting limits which discourage exposures above the threshold for these effects. The philosophy of both agencies seeks to minimise stochastic effects to reasonable safe levels in relation to other hazards faced by both workers and individuals in the public sector. Thus, along with their limits, they use the principle of keeping exposure as low as reasonably achievable (the ALARA priciple). The protection recommendations of both bodies as, at 1993 are summarised in table 1-2. Their recommendations differ in the path ways toward achieving desired level. However the final commutative levels are the same.

Table 1-2 ICRP (1991) and NCRP (1993) Radiation Protection Recommendations.

	ICRP		NCRP	
EP	**Limit**	**AE**	**Limit**	**AE**
Occupational	20 mSv/y (over 5 years)	20 mSv	50 mSv/y Age x 10 mSv	10 -20 mSv average
Public	1 mSv/y (over 5 years)	1 mSv	1 mSv/y (continous) 5 mSv/y (occasional)	1 mSv (continous) 5 mSv (occasional)
NID			10 μSv/source/year	10 μSv/source

1 rem = 10 mSv NID = Negligible Individual Dose y= year
AE= Annual equivalent EP= Exposed population

Genetic effects have been studied in a variety of species and assessed in detail by the United Nations Scientific Committee on the Effects of Atomic Radiation (UNSCEAR) [UNSCEAR, 1988]. Estimates of genetic risk in the mouse are extrapolated to man. The total genetic risk in an exposed population is estimated to be 1×10^{-2} Sv^{-1}. Based on data from A-bomb survivors, the Biological Effects of Ionising Radiation Committees (BEIR) as well as ICRP and NCRP have studied intensively the developing information on cancer induction since 1972 [Sinclair, 1995]. UNSCEAR and BEIR and ICRP found the risk for high dose exposure to A-bomb survivors, to be 10×10^{-2} Sv^{-1}. ICRP then divides the high dose rate risk by a dose and dose rate effectiveness factor (DDREF) which is assigned the value 2. Both ICRP and NCRP support a nominal value of 5×10^{-2} Sv^{-1} for the general population and 4×10^{-2} Sv^{-1} for workers. Additional components (morbidity of nonfatal cancer and genetic effects) enhance these values to 7.3×10^{-2} Sv^{-1} for a population of all ages and 5.6×10^{-2} Sv^{-1} for workers.

It should be noted here that all the above estimates refer to low LET radiation viz. X- and γ-rays (sparsely ionising radiations). High LET radiations, such as neutrons and alpha particles (densely ionising radiation), were present to a small degree at Hiroshima and Nagasaki. These radiations are more effective than sparsely ionising radiations in producing biological damage. Their relative effectiveness is expressed in terms of the radiation quality factors Q or the radiation weighting factor w_R. Both Q, and w_R are designated to convert absorbed energy to equivalent dose for relation

to biological damage. Table 1-3 shows the radiation weighting factors w_R for the different types of radiations [ICRP-60, 1990].

Table 1-3 Radiation Weighting Factors as recommended by ICRP-60, 1990.

Type and energy range	Radiation Weighting Factor, w_R
Photons, all energies	1
electrons and muons, all energies*	1
Neutrons, energy < 10 keV	5
10 keV to 100 keV	10
> 100 keV to 2 MeV	20
> 2 MeV to 20 MeV	10
> 20 MeV	5
Protons, other than recoil protons, energy > 2 MeV	5
Alpha particles, fission fragments, heavy nuclei	20

* excluding Auger electrons emitted from nuclei bound to DNA.

In the present dosimetry system, and according to the latest relevant ICRP report [ICRP-60, 1990], the equivalent dose $H_{T,R}$ throughout tissue T due to radiation R is given by $H_{T,R} = w_R D_{T,R}$, where $D_{T,R}$ is the average absorbed dose in the tissue or organ. The effective dose E, in which the new radiation protection limits are expressed is defined as $E = \Sigma_{T,R} w_T H_{T,R}$, where w_T is the tissue weighting factor for organ which represents its relative contribution to the total detriment when the whole body is irradiated (w_T is independent of the type of radiation). Thus the risk of induced cancer from a given absorbed dose of heavy ions is 20 x the risk from low-LET (X- of γ-rays).

The radiation quality factor, Q, which is equivalent to w_R is a function of the LET of the ionising radiation. Table 1-4 shows the correlation between Q and the unrestricted LET in water [ICRP-60, 1990]. The same relationship is also represented in figure 1-2. The dose equivalent H, and the quality factor Q are related by H = N Q D where currently N = 1 for non-physical modifying factors, and D is the average absorbed radiation dose.

Table 1-4 Specified Q-L relationship.

L (keV/μm)	Q(L)
< 10	1
10 - 100	0.32 L- 2.2
> 100	$300/L^{1/2}$

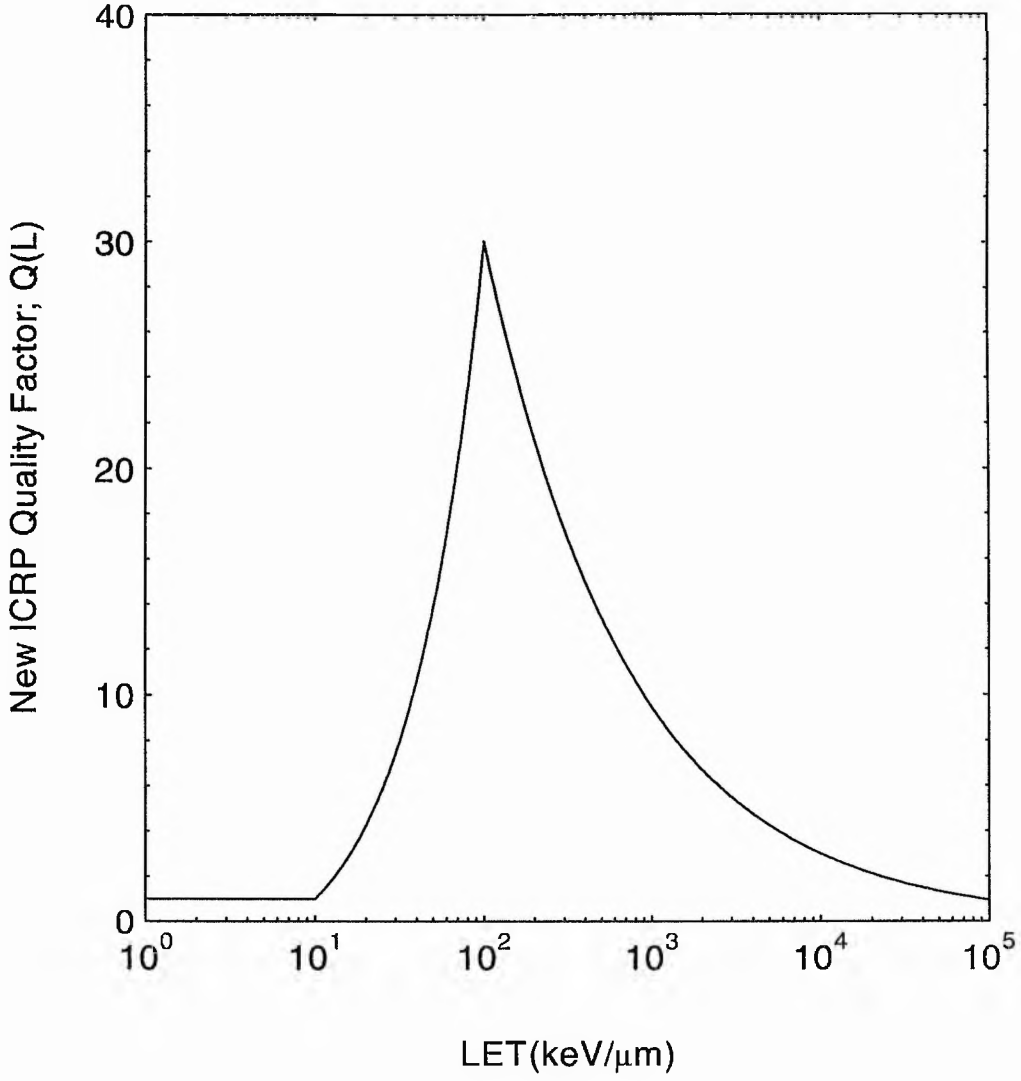

Figure 1-2 NCRP radiation quality factor Q as a function of LET.

Although the quality parameter Q can be expressed as a function of microdosimetric lineal energy y, no unique biological basis exists for fixing the associated volume and size for y (see section 1-2-3 for the definition of y).

In this contest we see that both the weighting factor w_R and the radiation quality factor Q are artificial quantities. Their job is simply to quantify effects other than photons or electrons. Further, the dependency of Q on linear deposition parameters such as LET is subject to controversy because of its fundamental limitations as will be discussed in section 1-3-1.

1-2 Dosimetry and Microdosimetry

1-2-1 Quantities and basic principles

Ionising radiation is classified as either directly ionising radiation or indirectly ionising radiation. The former includes all charged particles e.g. electrons, protons, and alpha particles, heavy ions. The second type includes all neutral radiations e.g. photons (X-rays and γ-rays) and neutrons. Photons primarily interact with biological matter (mainly water) through photo-electric, Compton scattering and pair production. However neutrons interact with matter to produce damage via the product recoils. Proton- and oxygen-recoils are considered the most important in biological matter. Charged particles interact with electrons of biological matter primarily via Coulomb interaction. In all processes involved with both types of radiations, a complex shower of electrons is produced. The spectrum of these charged particles changes with depth through the build up region, reaches equilibrium and then falls under transient equilibrium conditions according to the attenuation of the primary incident radiation. The spectrum charged particle at equilibrium is commonly used in dosimetric calculations.

The basic fundamental unit for absorbed dose is gray, which is defined as the amount of energy absorbed per unit mass of the irradiated media. Other dosimetric quantities commonly used in radiation fields, are the fluence, ϕ (particles/μm^2), flux density (fluence rate), $d\phi/dt$ (particles/μm^2-s), energy fluence F(keV/μm^2) and energy flux density (energy fluence rate) dF/dt(keV/μm^2-s).

1-2-2 The absorbed dose

Absorbed dose D is the quotient dE/dm, where dE is the mean energy imparted by ionising radiation to matter in a volume element and dm is the mass of the matter in that volume element [ICRU-19, 1971]. It is an average quantity and its SI unit is Gy (J/kg). The energy E imparted by ionising radiation to the matter in a volume is $E=R_{in} - R_{out} + \Sigma Q$ where:

R_{in} is the radiant energy incident on the volume i.e. the sum of all energies of ionising radiations enter the volume.

R_{out} is the radiant energy from the volume. i.e. the sum of all ionising radiations energy leaving the volume.

ΣQ is the sum of all changes in the rest mass energy of constituents which occur in the volume i.e. nuclear transformations.

For X- and γ-rays the absorbed dose is given by $D = \Sigma_j \phi_j E_{\gamma j} \Sigma_{i,j} (\mu_{en}/\rho)_{i,j} \times 1.6 \times 10^{-13}$ Gy where ϕ is the photon fluence, E_γ is the photon energy in MeV and μ_{en}/ρ is the mass energy absorption coefficient (m^2/kg).

1-2-3 Microdsimetry and microdosimetric quantities

Microdosimetry is a science that deals with the spatial, temporal, and energy-spectral distribution of energy imparted stochastically in cellular and sub-cellular biological structures, and attempts to relate these distributions to biological effect [Attix, 1986].

A few definitions which are specifically relevant to microdosimetry, have been introduced [ICRU-36, 1983 ; Rossi, 1996]:

i. Energy deposit ε_i : defined as the energy deposited in a single interaction I and given by the expression $\varepsilon_i = T_{in} - T_{out} + Q_{\Delta m}$ where T_{in} is the energy of the incident ionising radiation, T_{out} is the sum of energies of ionising radiation leaving the interaction and $Q_{\Delta m}$ the change of the rest mass energy of the atom and all particles

involved in the interaction ($Q_{\Delta m} > 0$ indicate decrease of rest mass and $Q_{\Delta m} < 0$ indicate increase of rest mass).

ii. Energy imparted ε : is the sum of all energy deposits ε_i and may be due to more than one energy deposition event, that is statistically independent along the particle track.

iii. Specific energy (imparted) z: is the ratio of the energy (ε) imparted in a microscopic mass m i.e. z= ε/m. The specific energy z is a stochastic analogue for the absorbed dose.

iv. Lineal energy y: is the ratio of energy imparted (ε) in a single energy-deposition event to a microscopic volume by the mean chord length ℓ of that volume i.e. $y = \varepsilon/\ell$. The lineal energy is a stochastic analogue for the LET.

v. Five classes of tracks: In microdosimetry it is convenient to define names for 5 classes of tracks that traverse a spherical volume. These are:

Insider: Particles originating in the volume may lose their entire energy in the volume.

Starter: particles originating in the volume may leave the volume before losing all their energy.

Stopper: particles originating outside the volume may enter the volume and stop within the volume.

Crosser: particles originating outside the volume may cross the volume, depositing only part of their energy in the volume.

Glancer: particles 'brush' the wall of the volume so that only δ-rays associated with the track enter it.

1-2-4 The art of dosimetry

The basic objective of radiation dosimetry is to predict the most probable effects of radiation perturbation on an object of interest, presumably biological. This task can be achieved if the biological perturbations can be measured as a function of the

radiation quality. There are two types of dosimeters biological dosimeters and physical dosimeters.

(i) Biological dosimeters: Biological dosimeters (BD) are those based on direct measurement of the biological effects induced by ionising radiations [Wolf, 1991]. They mainly rely on two factors: the production (or frequency) of occurrence of damage which is specific to ionising radiation, and the background rate of these effects. The latter must be very low compared with those induced by the ionising radiation. Examples for BD's associated with different endpoints are those which can measure the frequency of unstable chromosome aberrations (dicentrics, rings) in peripheral lymphocytes [Doloy, 1991], micronuclei (MN) function [Verhaegen, 1994], and measurement of somatic mutations [Martin, 1991 ; Nakamura, 1991]. Although micronuclei are easier to score than aberrations, their quantitative relations to the dose of ionising radiations are well less understood. Moreover their great variability from person to person disqualify them from being use as a biological dosimeter [Wolf, 1991]. On the other hand, mutations assays are found to be far restricted from being use as a biological dosimeter [Nakamura, 1991]. However, some progress has been claimed in the use of chromosome aberrations as a biological dosimeter [Finnon, 1995] but because of their poor durability and reproducibility they still of limited value [Kakati, 1986]. Above all they are impractical.

(ii) Physical dosimeters: On the other hand physical dosimeters are instruments which measure a property of the physical radiation field and which can be related to the probability of occurrence of the biological effects. Usually the quantity can be related to the radiation quantity either directly or by a statistical treatment. Historically dosimeters have been designed to simulate the desired response , as for example in dose equivalent meters where the response correspond to that of the limits set by ICRP.

The current existing dosimetry system is based on energy deposition parameters e.g. the Linear Energy Transfer (LET). Because of the limitations of this parameter (section 1-3-1), and because of the stochastic nature of the energy dependent parameters such as microdosimetric lineal energy y at sub-cellular levels, new

concepts for dosimetric devices must be defined. Now, it is widely accepted that the DNA is a critical target which is at least partially if not totally responsible as an initiating mechanism leading to subsequent biological endpoints including cell death. Thus, the condensed phase dosimeter (nanodosimeter) to be described later (chapter-5) should take into account the essential molecular shape factors correlated to the lethal damage e.g. induction of double strand breaks in the DNA which has an associated DNA with an inter-strand spacing of 0.34 - 1.8 nm i.e. nanometer dimensions.

1-3 Specificity of Radiation Damage

1-3-1 Radiation quality

Lea had based his target theory on a sensitive volume that may contain critical targets [Lea, 1955]. In his theory, the inactivation of one or more of these targets may lead to cell death. His theory, which has influenced many researchers to this date is based on energy deposition parameters e.g. clusters of ionisations. Today the DNA is considered to be the critical target that may lead to different endpoint effects e.g. chromosome aberrations, mutations, transformations, cancer, and cell death.

To explain the variations in biological responses, and to relate these quantitatively to physical measurements, one needs specify an appropriate radiation quality parameter. One candidate is the linear energy transfer (LET), which is defined as the rate of energy lost per track (energy/length). It was Zirkle, 1952 who first introduced this parameter to specify the responses of Aspegillus spores resulting from alpha and X-rays irradiations. Through the work on inactivations of bacteria by high LET radiation, Howard-Flanders, 1958 suggested that δ-rays contributions should be treated separately by the use of a restricted form of LET (L_Δ), where Δ is the minimum energy of electrons included in the LET. Later the restricted energy parameter was redefined in terms of a 100 eV cut off to exclude δ-rays of energy higher than 100 eV [ICRU-16, 1970]. The LET and its restricted form are significantly different in the cellular and sub-cellular volumes (micro-, and nano-meter dimensions). Because of the simplicity of the LET concept, it is very

commonly used, despite its limitations [Kellerer, 1975 ; ICRU-33, 1980; Varma, 1993; Simmons, 1992] which can be summarised in the following:

i- the LET concept failed to provide information on the particle e.g. on the particle range which could determine whether the particle had penetrated that volume or stopped. In practical radiobiology this is signified by the amount of transferred energy lost by the particle which would show an appreciable change in the value of LET at the entrance and exit of the sensitive volume.

ii- LET describes the energy fate along the track and not around the track. In practical radiobiology, the δ-rays produced specifically by heavy ions, tend to deposit their energy radially outside the main track. Different types of radiations with the same LET could have different track diameters (δ-rays with different kinetic energies, different ranges), and produce different levels of damage.

iii- the LET is an average quantity, it does not address the random nature of energy loss along the track. Because of the stochastic nature of energy deposition at small targets of sub-cellular dimensions, energy deposited in small volumes can vary from zero to maximum kinetic energy of the particles. Thus the prediction of this average value can be more or less than the actual energy deposited in small volumes.

The inappropriateness of LET can be seen from the observations of biological damage in cellular and sub-cellular structure of living organisms where different types of radiations of the same LET can have different biological responses. The limitations and misconceptual practice of LET and related averaged energy parameters to specify the damage of the various effects by ionising radiation in mammalian systems, opens a wider scope of research to develop other suitable radiation quality parameters for better specification of the damage [Watt, 1985; Harder, 1992 ; Katz, 1972].

1-3-2 The criteria of low dose

In radiation protection low dose usually means the dose at environmental levels (e.g. few mGy). In radiation biology, low dose means the lowest dose which shows

biological effects (which may or may not be detected). From the practical aspect of radiation biology this dose could be as low as a few cGy to a few Gy.

Based on microdosimetry a criterium for defining low dose at the cellular level can be reached. In this sense low dose is associated with a critical target which corresponds to the deposition of energy by a single event or none at all [Booz, 1988 ; Kellerer, 1987]. The critical target here is assumed to be the reference mammalian cell nucleus which has a diameter of 8 μm and a typical weight of 270 pg [NCRP-63, 1979]. For this type of analysis a 0.3 mGy of ^{60}Co γ-rays is characterised as being low dose. However 30 mGy for the same condition is considered to be a very high dose.

It is argued that cellular transformations and mutations should be considered as secondary effects in the complex cellular response rather than as the consequence of a specific radiation interaction with specific gene segments [Booz, 1988]. Now it is well understood that the DNA is the lethal target leading to these specific damages including cell death. Thus new concepts should be introduced that take into account the complexity of the DNA organisation in the mammalian cell nucleus. On this basis, low dose may be associated with specific damage in the DNA e.g. a double strand break.

1-3-3 Specifying the damage at cellular and sub-cellular levels

The damage or biological response is measured or calculated from dose-effect or fluence-effect data. The damage can be quantified with either the radiobiological effectiveness (RBE) or the effect cross-section. The former is calculated from the ratio of the radiosensitivity of the ionising particle (α^{-1}_{i}) to the radiosensitivity of 250 kV_p X-rays ($\alpha^{-1}_{x\text{-rays}}$) or ^{60}Co γ-rays (i.e. RBE = $\alpha_i / \alpha_{x\text{-rays}}$). In experimental physics, it has often proved useful to express interaction between particles and target in terms of cross sections. This average quantity represents the probability of interaction in unit area i.e. μm^2. The effective cross-section is related to specific

biological damage, and calculated from both the radiation and biological response parameters.

There seems to be universal agreement in using the RBE-LET to estimate and assess biological damage. However, RBE-LET relation demonstrates the failure of the LET concept to explain uniquely the cellular or sub-cellular effects, figure 1-3. For cell inactivation, the maximum RBE is measured to be around LET = 100 - 150 keV/μm. The region above that corresponding maximum is referred to the overkill region. Howard-Flanders (1958) demonstrated that at LET higher than that corresponding to the maximum RBE, the superabundance of ionisation is wasteful since a cell can be only killed once. Thus the observed reduction in RBE is meaningless. The dependency on cell and ion types is also demonstrated by the RBE-LET curves [Barendsen, 1963]. The RBE values for chromosomal damage (dicentrics and centric rings) in human lymphocytes are usually much higher than those for HPRT mutations. The reason for this difference is unknown since it is expected that both endpoints are related [Hall, 1988]. The failure of LET to predict chromosomal aberration damage (RBE), has lead some authors to examine the microdosimetric parameter, the lineal energy y(keV/μm), which also shows the same fate [Edwards, 1985].

On the other hand, at the molecular level the RBE curve has another shape, particularly if we consider the end-point as the double strand breaks (dsb's) of the DNA in mammalian cells. Based on the initial dsb's data, the RBE values calculated by the different authors for the induction of dsb's in mammalian cells are around unity for light ions up to LET value of 60 keV/μm, then the RBE starts to decrease [Heilmann, 1995]. This conclusion was reached despite the results of an older set of data for dsb's which show a maximum RBE for alpha particles with an LET in the range 100 - 200 keV/μm [Kampf, 1983]. This is in contrast with the RBE values for cell inactivation which has a peak at around LET values of 100-200 keV/μm [Barendsen, 1963]. Thus the correlation between DNA double strand breaks and survival for the same cells and radiation with equivalent LET fails to exist. It was argued that cell killing is a result of residual dsb's [Frankenberg, 1981] and

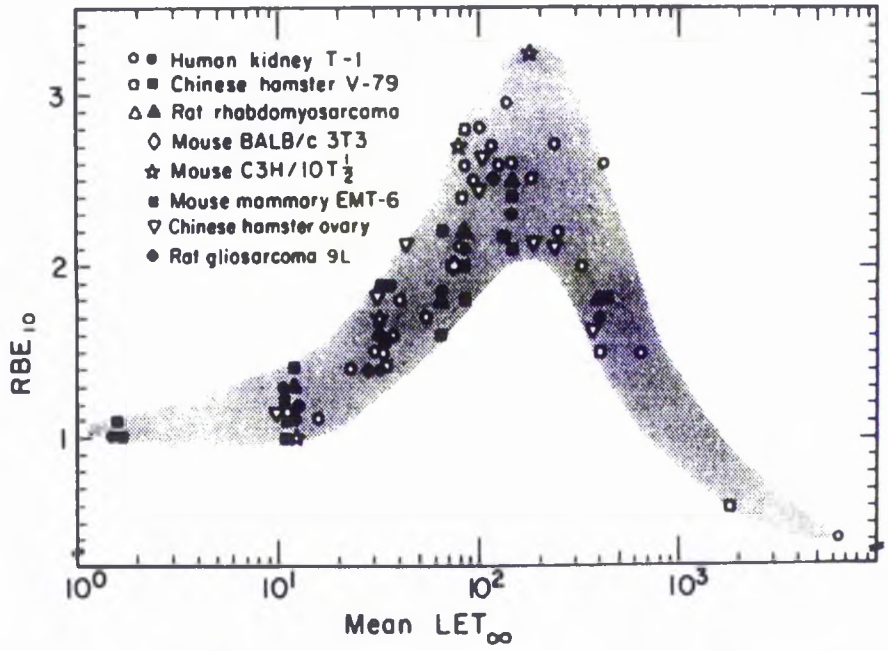

Figure 1-3 The RBE-LET relationship for survival of mammalian cells (*in vitro*) [adopted from Blakely, 1984]. The spread of data and the fall of the RBE demonstrate the failure of the LET to specify biological damage.

models based on the RBE-LET relationship are still the subject of study [Barendsen, 1993; 1994; Taucher-Scholz, 1996].

Thus from studying the RBE-LET relationship, no unique functional behaviour has been found, which suggests the inadequacy of the relationship to clarify our understanding of biological damage mechanisms.

1-3-4 The role of biophysical models in radiation protection

The main objective of radiation protection is the evaluation of the risk at environmental level. Experimentally, at both cellular and sub-cellular levels, the direct measurement of the effects at low dose seems to be impossible. However, exposure experiments with high doses could provide information at the low dose limits if an appropriate method of extrapolating from the higher dose region to the lower dose region, can be devised. A realistic model would help to achieve this priority. Data on biological effects obtained at high doses, used to develop a satisfactory biophysical model, would permit effects at low doses to be deduced [Kellerer, 1972]. Models may also be used to predict the most probable effects at other doses.

Biophysical models are classified as either mechanistic or phenomenological models. While the former seek a conceptual parameterised description based on realistic assumptions related to basic mechanisms, phenomenological models seek a parametrised mathematical description which well fits the range of data of interest. Almost all existing biophysical models contain elements of both mechanistic and phenomenological approaches.

1-3-4-1 Models based on energy depositions in small sites (cluster models)

Theoretical modelling based on energy deposition phenomena was discussed by Lea, 1955. In his hit and target theory he use the notion of specific ionisation which is basically the LET divided by the mean energy to produce an ion pair w_i. Later Howard-Flanders suggested that the cell inactivation resulted from a small number of ionisations in a target of a few nanometer in thickness [Howard-Flanders, 1958]. Most of these models are considered to be mechanistic in nature.

Different approaches have been taken, some of which rely on a theoretical hypothesis e.g. cluster of ionisations in respective critical targets [Goodhead, 1994]. The attempt is mainly to interpret the survival data through the involvement of cellular repair processes. It is suggested that high LET damage can arise from 10 ionisations (> 300 eV) in targets having dimensions of 3-4 nm and low LET radiation damage from 3 ionisations in the same molecular domain (> 100 eV). Various Monte-Carlo codes have been written, to simulate these clusters. Goodhead et al. showed that their predictions agrees quite well with results of HF inactivation by ultra soft C_k X-rays [Goodhead, 1983]. However with high LET, simulations using α–particles and protons in three dimensional codes [Wilson, 1981 ; Charlton, 1985 ; Nikjoo, 1991] the results show agreement for larger critical sizes of 5 -10 nm. These results lead Goodhead et al, 1992 to suggest that the critical size associated with local damage can occur in a nucleosome-sized structure. Further, the prediction of simulating tracks of slow α-particles which produce severs initial damage at sub-cellular and cellular levels, led them to the conclusion of an infinitesimal RBE. Based on their analysis, Goodhead et al., 1990 estimated that 1 Gy of low LET X-rays and γ-rays produce ~ 1000 photons tracks, ~ 100,000 ionising events (energy deposition), 1000 ssb's and 40 dsb's, 0.2 - 0.8 cell deaths, 1 chromosome aberrations and 10-5 mutations.

But since the DNA is identified as the critical target, a number of theoretical models have been developed to study DNA damage in eukaryotic cells under the direct action of ionising radiations or/ and the indirect action of radiation-induced reactive species, such as OH• and H• radicals. These studies depend on the track structure and the ideal linear configuration of the DNA which is often neglects the presence of histones [Charlton, 1988; Nikjoo, 1994; Holley, 1990; Chatterjee, 1990].

Other simulation models are suggested which use a structured DNA configuration and include all the essential parts of the highly organised DNA in 30 nm chromatin matrix (including histones). With simulation of DNA strand breaks induced by monoenergetic electrons, and an energy deposition for event of 25 eV (most probable energy) Pinak et al. concluded that electrons of initial energies from 5 keV to 10 keV have higher probability of energy deposition in a structural part in comparison with

lower or higher energy electrons [Pinak, 1993]. Such conclusion indicates that these electrons which have ranges 800 - 2500 nm may induce double strand breaks only with the aid of water species, particularly OH• radicals. The authors argued that at an energy of the order of 1 keV or lower, energy loss due to straggling becomes important. The same simulation research carried out further by Tomita et al. (1994); two important results were reached, the number of DNA single strand breaks induced per nucleus (diameter of 6 μm) per Gy in pure water is about 10 times that in the cell environment, and that the contribution of the indirect damage decreased as the order of the DNA target model structure increased. The authors concluded that the integrity of the cell nucleus is very important, and parameters related to cell environment should be considered more carefully with the Mont Carlo simulation techniques. On the other hand, Holley and Chatterjee constructed a solenoidal chromatin model of 30 nanometer diameter which was composed of 20 turns of nucleosome and 6 nucleosomes per turn [Holley, 1996]. On the basis of an energy deposition in the primary track core of 100 eV or less for direct collisions and δ-ray knock-on collisions of energies higher than 100 eV, a Monte Carlo simulation code had been developed to incorporate all forms of damage (direct or indirect) on the DNA sites through out the chromatin structure. In their analysis, they argued that the model predicts local clustering damage over 40 bp and, even at larger scale, regional damage of several kilobase pairs. Based on the yields vs. fragment length in bp's, the authors claimed that their model predicts the existence of strong peaks at 85 bp's and 1000 bp's which correspond to the periodicity of DNA about the nucleasome and solenoidal chromatin.

Thus models based on energy depositions in small sites failed to predict interactions at DNA spacing level (within 1.8 nm). In this sense double strand breaks of the DNA are estimated within higher order organisations e.g. nucleosome or chromatin size.

1-3-4-2 Models based on specific types of damage

Models here were developed toward specific needs. The basic input data for mammalian cells include the shape of dose-response curves (shouldered or linear) as specified by fitting parameters.

Kellerer and Rossi had developed the dual radiation action (DRA) model. The model is based on single ionisations in a micron critical target. The model assumes that a pair of lesions of unspecified nature can be induced by a single track (αD component) or via two tracks (βD^2 component). The model was a trial to explain the empirical observation which were related to the relative biological effectiveness of neutrons with respect to X-rays [Kellerer, 1972]. Later a more generalised model suggested by the same authors, included a lower interaction distance in the range 0.1 - 100 nm, and the nature of the lesions which is still unspecified but assumed to be the result of interaction of 2 ssb's [Kellerer, 1978]. The earlier form of the DRA specified damage with the use of a microdosimetric parameter, the mean specific energy z in a μm site, while the generalised DRA was manifested by an artificial distant dependence known as the proximity function t(x). The theory has wide applicability in the science of microdosimetry.

An identical hypothesis by Varma, 1983 led him to formulate a phenomenological model that specified the effects in the cell nucleus with the use of either of the microdosimetric parameters, the specific energy z or the lineal energy y. The model is mainly intended to be used for low dose predictions at cellular level (where spatial energy deposition becomes important).

Katz et al. (1971) formulated a phenomenological model known as the track structure model (TSM). The model is based on two components, the "ion kill" and "γ-kill". The first is associated with the main ion track, while the second one is related to effects dominated by the multiple tracks of δ-rays. Although the nature of damage is unspecified, the events involved in "ion kill" resulted from deposition of 100 keV or more in 2 μm within the track, and that of "γ-kill" the accumulation of 100 keV or more in 2 μm. The model specifies effects using z^{*2}/β^2 and β^2, where z^{*2} is the effective charge of the ion and β^2 is the square of the specific ion velocity. The model seems to

be quite helpful if used in junction with bacteria, virus, enzymes inactivations as well as with the scintillation response of inorganic scintillants based on the "bean bag" and single hit inactivation [Katz, 1982; 1994]. The two components of the model seems to be artificial elements in the sense that those "beans" that escape ion kill have their fate dominated by the γ-kill.

With sub-cellular effects, it was Lea who attributed the two components αD and βD^2 of the aberration yield per cell, y, to the same process, a pairwise interaction between "chromosome breaks", proceeding in competition with their "restitution" [Lea, 1955]. The only difference was that the α component, αD, should be result of intratrack interactions along the tracks of ionising particles, whereas the β component, βD^2, should be due to intertrack interactions between breaks induced by different ionising particles [Harder, 1987]. The theory is further elicited via pairwise lesion, where the nature of lesions related to unrepaired dsb's of the DNA in the chromatin fibre are considered. The damage is specified by the radiation quality parameter the dose average restricted LET, $L_{100,D}$ [Harder, 1992].

Chadwick and Leenhouts (1981) put the first hypothesis for a molecular theory which is also know as the linear-quadratic model (L-Q model). In their model the nature of the damage related to dsb's in the DNA which resulted by two ssb's by OH• radical. The linear component (αD) is assumed to be the result of inducing two ssb's at about 0.5 nm and that the non-linear component (βD^2) is the result of two independent tracks at an associated distance of about 6 nm. The damage is specified with the linear energy transfer (LET) and the ion velocity β. Several dose-response data from a simple relationship to more complicated ones have been tested against the L-Q models [Kellerer, 1972 ; Neary, 1965 ; Elkind, 1984]. For reasons that are not clear, the fundamental assumptions of the model are not widely accepted.

Watt et al. (1989) proposed a unified approach model. This model is based on simple concepts in which damage is specified by the linear primary ionisations $I(nm^{-1})$. The basic hypothesis is related to the induction of two strand breaks as specified by the mean free path for linear primary ionisations of the ionising radiation. Initially the

model had been tested with cell inactivation data, the foundations seems to be promising [Watt, 1989]. A summary of the models referred to in this section along with their main features included in table 1-5.

1-4 Identifying the Important Biological Targets

1-4-1 The organisation of cellular DNA

In both primitive prokaryotic and complex eukaryotic cells the genomic DNA is widely accepted of being the critical target attacked by ionising radiation or the water radicals. Of the various types of damage, the DNA dsb's are considered to be the fatal ones. If these are misrepaired or unrepaired they could lead to mutations or chromosome aberrations.

Unlike all living cells, the DNA in mammalian cells is highly organised. According to the Watson-Crick model, the DNA physical structure is shown schematically in figure 1-4a, where the sugar-phosphate forms the backbone of the strands. Each sugar residue in a repeating backbone of sugar-phosphate units has a heterocyclic base attached as a side chain. Each two bases (complements) of the opposite strands are then combined via weak hydrogen bonding. The strands running in opposite directions twist into a double helix. The cyclic repetition for the molecule on the basis of this model are 0.34 nm per base pair (bp) and 3.4 nm per turn. The strands are separated roughly by 2 nm. The lengths of the DNA varies, e.g. 14 to 73 mm for human cells and 1.6 mm in E.coli, based on 0.34 nm/base pair [McGilvery, 1979]. The actual length of the DNA in human cells if unpacked may reach a length of 2 m .

In living mammalian cells, the genomic DNA is associated with the 5.5 nm histones to form an 11 nm nucleosome array (about 1.75 turns of DNA which is equivalent to 146 bp's) [Stein, 1996]. With the participation of non-histone chromosome (NHC) protein, this primary chromatin fibre is further packaged into higher-order structure to form chromosomes [Benbow, 1992]. The length of chromatin fibre is about 56 mm [Rydberg, 1996]. The physical reconstruction of DNA and the subsequent organisations are shown in figure 1-4b. In mammalian cells each DNA molecule gives

Table 1-5 Biophysical models, their classifications and applications.

	Model	Critical target	lethal event	Radiation quality	Applications	Classification	Authors
1	**GDRA**	Cell Nucleus	not specified	t(x)	Micro- & nano-dosimetry	Mechanistic	Kellerer, Rossi, 1978
2	**HSET**	Cell Nucleus	not specified	z(Gy) ; y(keV/μm)	Microdosimetry	Phenomonological	Bond, Varma, 1983
3	**TSM**	Cell	not specified	β^2 , z^{*2}/β^2	Radial dose distribution	Phenomonological	Katz, 1971
4	**PLM**	Chromatin	dsb's	$L_{100,D}$(keV/μm)		Mechanistic	Harder, 1983, 1987; 1992
5	**MT**	DNA	dsb's	LET(keV.μm) , β	Nanodosimetry	Mechanistic	Chadweick, Leenhout, 1981
6	**TERS**	Nuclosmoes ; DNA	LMD in DNA	threshold energy (15-25eV)		Mechanistic	Goodhead, 1982
7	**ABEM**	DNA	dsb's	λ(nm)	Unified dosimetry	Phenomonological	Watt, 1989

DRA : Dual Radiation Action **GDRA**: Generalized Radiation Action **HSET**: Hit-Size Effectiveness Theory **TSM**: Track Structure Theory
PLI : Pairwise Lesion Model **MT** : Molecular Theory **TERS**: Threshold-Energy, Repair-Saturation Model
ABE : Absolute Biological Effectiveness **LMD** : Locally Multiplied Clusters

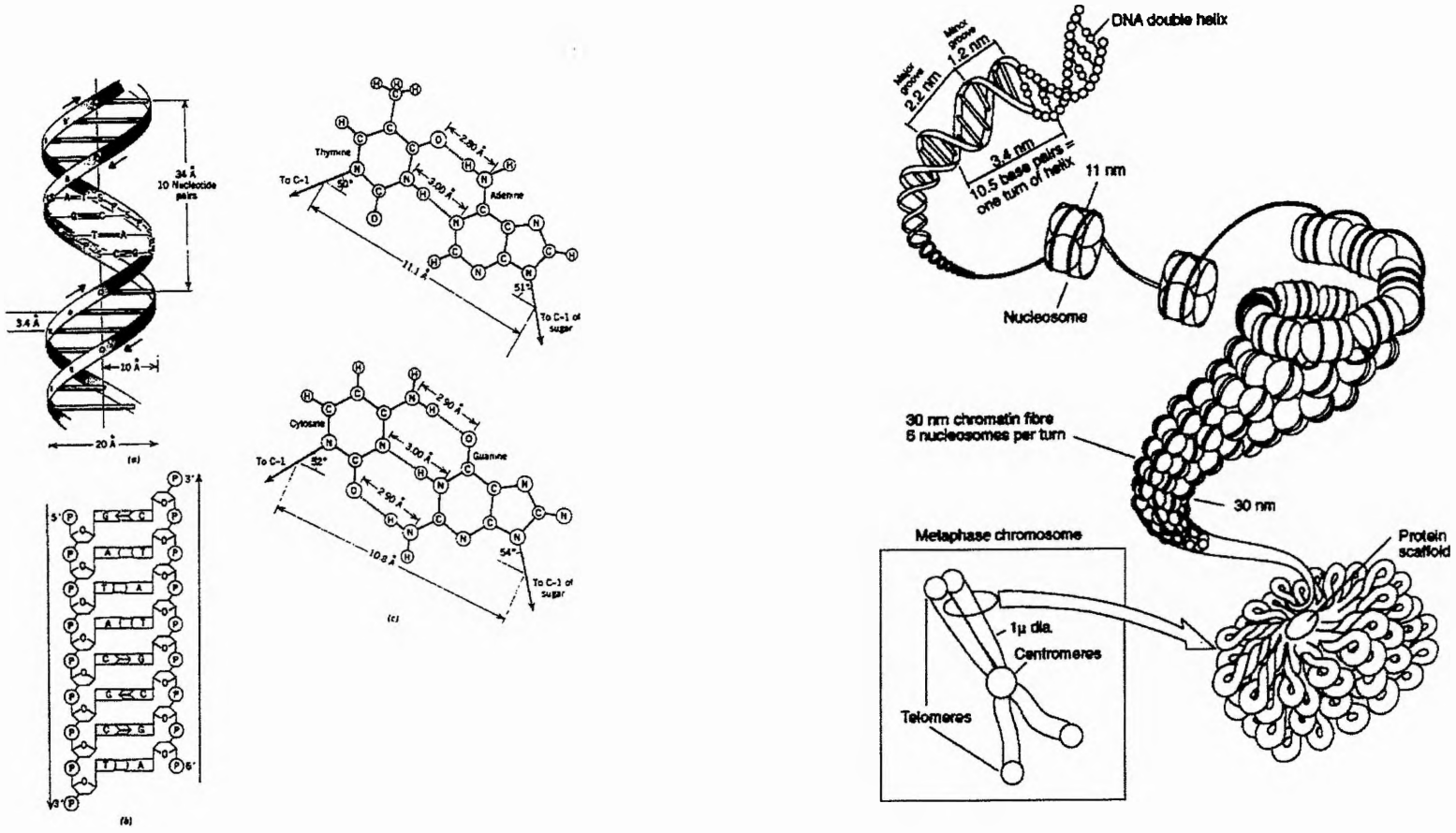

(a) (b)

Figure 1-4 The physical structure of the DNA according to Watson-Crick model shown in a. The physical reconstruction of the subsequent organisations shown as explained in text shown in b.

rise to each of the 46 chromosomes in the cell. The average size of a chromosome in a human cell is estimated to be about 130 Mbp [Sonntag, 1990].

The damaging effects of ionising radiation on the DNA includes ssb's, dsb's, base deletions DNA DNA cross links, DNA protein cross links [von Sonntag, 1987], figure 1-4c outlines the basic damage in the DNA.

1-4-2 The genomes of the chromosomes

As mentioned above, the misrepaired dsb's could lead to mutations or oncogenic transformations. The simplest mutations are known as point mutations, which could be the size of the a base pair. However, only specific genomic alterations (deletions) can be measured in the laboratory with fidelity. Some of the well established specific mutation assays are those associated with HPRT genes. They have the size of 40 kbp's in human cells and 34 kbp's in hamsters. Both genes are located in the lower leg of the X chromosome. On the other hand oncogenic transformations assays which can be detected morphologically at cellular level are associated with genes as small as 1 kbp up to a few Mbp's. Chromosome aberrations, particularly asymmetric ones (dicentrics and centric rings) are considered to be a complex form of mutations, figure 1-5.

1-4-3 The cell nucleus

The cell is considered to be the elementary unit of life. It is associated with the development of complex organisms e.g. egg cell and sperm cell. It contains the genetic material (~ 2 % of nuclear mass). The final effects of ionising radiation is the terminal cell death. For all these reasons, it is justified to define the cell to be the radiation sensitive volume [NCRP-63, 1979]. The diameter of targeted mammalian cell nucleus is taken as 8 μm. This corresponds to a geometrical cross-section σ_g of 50 μm^2. However, flattened cancerous cells have much larger cross-sections e.g. C3H10T1/2 has σ_g of 300 μm^2. In primitive prokaryotic cells, the circular or supercoiled naked DNA is contained within the cellular membrane. The cellular geometrical cross-sections of these cells are much smaller than that of mammalian cells. The DNA content varies among mammalian cells as well as for non-mammalian cells.

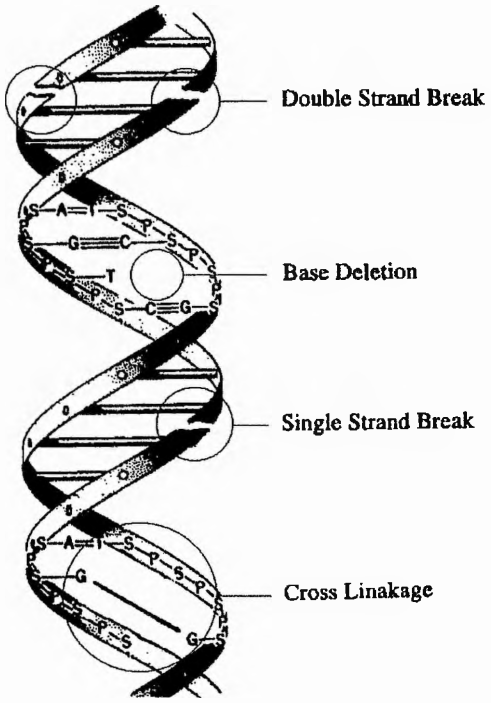

Figure 1-4c The main possible damaging effects by ionising radiation on genomic DNA.

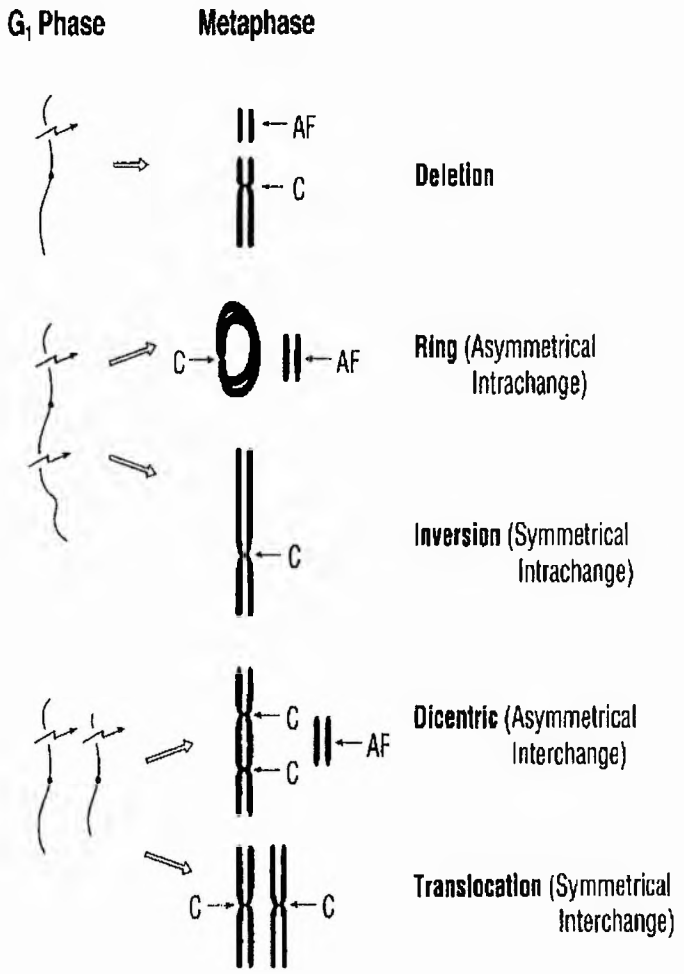

Figure 1-5 Chromosome aberrations types induced by ionising radiation. C= centromere; AF = acentric fragment [adopted from Bender, 1995].

1-5 Statement of Problems

1-5-1 Problems related to mechanisms for biophysical modelling of ionising radiation in biological matter

A fundamental understanding of radiation interactions with biological systems is very important to the interpretation of the radiation effects. There are two sources of data available: the first source is from epidemiological surveys of e.g. uranium mine workers, persons who have suffered accidental over-exposure and from survivors of atomic bomb attacks. The second source is from experimentation in the laboratory using cultured cells, and micro-organisms i.e. bacterial , yeast , and mammalian cells. Confidence in data from the first source is doubtful because of the uncertainties in risk estimates due to the duration of observation and other environmental agents which could add to the fate of these biological targets. Further, the ionising radiation does not cover all ranges of the spectrum (both low LET and high LET) for which the proposed radiation models can be subjected to test.

1-5-2 Problems with the currently accepted dosimetry system

In the currently accepted dosimetry system radiation quantity and quality are characterised in terms of the absorbed dose and linear energy transfer (LET). Radiation effectiveness is expressed in terms of relative biological effectiveness (RBE). At the cellular level for mammalian systems, the RBE shows a maximum value at LET values between 100 - 200 keV/μm. These double valued relationships are shown also for other end points such as HPRT mutations, and chromosome aberrations. However at the molecular level, such as dsb's of the DNA in mammalian cells, the RBE saturates at a value of one for an LET value of about 75 keV/μm, then reduces. This contradicts the earlier conclusion with other end points. It is thus acknowledged that the LET concept is limited in its application and it does not provide a reliable description of damage in the radiation field. Yet, the quality factors and weighting factors which are related empirically to the LET, or to the lineal energy y, are artificial tools. This represents a major drawback for the absolute quantification of damage.

1-5-3 Problems with instrumentation and dosimetric systems

Biological dosimeters, which are based on biological effects induced by ionising radiations with respect to their low background, seem to offer no solution, because of their limited practicability and reproducibility. On the other hand conventional dosimeters which are based on energy deposition parameters e.g. microdosimetry, are handicapped because of their limitations to the absolute measure of ionisations in nanometer dimensions.

1-6 Objectives and Contents

A long-standing objective in radiation protection and radiobiology is to obtain an understanding of the main mechanisms involved in damage to enable prediction of radiation-induced disease from knowledge of the initial exposure. At the fundamental level, the research objective is to find better, more meaningful, methods to predict, quantify and measure the probability of occurrence of the effectiveness of ionising radiations in people, from measurements in the initial radiation field of exposure. In this context radiation quality parameters should be reviewed and tested against the different evaluated biological damage. The main approaches to achieve these objectives are:

1- The data obtained through a technique of cloning in-vitro seems to offer lots of potentials. The desired biological system is activated under certain conditions of exposure toward a biological end-point which specifies the ultimate biological damage due to the interaction of the initial radiation tracks. Thus the main task here is to create a radiobiological data base which contains biological damage parameters along with calculated track structure parameters of ionising radiation. The damage include cellular inactivation, chromosome aberrations, HPRT mutations, oncogenic transformations and DNA breaks. It is intended to contain data on damage, as cited in the literature, that is produced by a wide spectrum of ionising radiation (low and high LET).

2- With the help of this radiobiological data base, it is then possible to compare and evaluate damage as a function of the different track structure parameters, thus testing for a radiation quality parameter which best defines the damage in question.

3- Having identified the radiation quality parameter which specifies all radiation damage uniquely, and possibly absolutely, then it should be reasonable to combine the damage and the quality parameters into a model for predictive purposes and wider testing.

4- Having identified the response function by which ionising radiation induces damage in the biological matter, then it should be possible, with appropriate technology to design a new system of dosimetry which will be independent of the biological target and radiation type. Such an arrangement if successfully developed would be a system of absolute dosimetry. Experimental study of the foundations towards this objective should be carried out.

Details of the work carried out to date are discussed in the following chapters listed. In chapter two, the main targeted track structure parameters are reviewed. Their conceptual foundations and the methods of their evaluations are included. Biological targets are identified. In chapters three and four, the mechanisms of radiation action were studied based on the compiled data base contained in the appendix. In chapter five, possible experimental techniques to investigate the envisaged unified system are reviewed. In chapter six, instrumentations based on thin film plastic scintillators is evaluated, reviewed and tested. In chapter seven, the conclusions, discussion and recommendation for future work is presented.

Chapter 2

PHYSICAL CHARACTERISATION OF IONISING RADIATION FOR SPECIFICATION OF BIOLOGICAL DAMAGE

Ionising radiation interact with biological matter in various ways. Consequently the physical nature of the ionising radiation and the nature and composition of the biological target(s) should be explored in order to understand the mechanisms by which radiation induces radiobiological alterations. It is believed that the genomic DNA in the cell nucleus is the target which if critically damaged leads to cell death. Thus if the visible or microscopic damage by ionising radiation can be identified, then it should be possible to represent the response as a function of an appropriate quality parameter. A good radiation quality parameter should allow prediction of effects for different radiation-quality or type, particularly in the low dose region where the radiation protection limits have their role. Also it can correlate molecular damage with other cellular effects e.g. DNA breaks with chromosomal or cellular damage. The choice of radiation quality parameter can be optimised by modelling these effects. Thus the predictions and scaling of the damage can be estimated properly (chapter 3, and 4). Here in this chapter we will review the basic characterisation of the different types of ionising radiations; introduce the mathematical tools for calculating the radiation quality parameters of interest; and review the interaction of radiations from their early physical interactions up to the manifestation of the biological end-point. The most important parameters related to the chemical phase will be identified. Basic relevant information related to type and content of DNA in living organisms is also introduced.

2-1 Interactions of Ionising Particles

The physical action of ionising radiations, as they interact in a medium, can be classified as directly and indirectly ionising radiation.

(1) *directly ionising radiation*: refer to charged particles which have sufficient kinetic energy, greater than the minimum electron binding energy in the medium, to

produce ionisation by collision. Charged particles of interest in dosimetry are electrons, π-mesons, protons, alpha particles, and accelerated nuclei.

(2) *indirectly ionising radiations*: are uncharged particles that can liberate ionising charged particles through interaction with the medium or that can initiate a nuclear transformation. Indirectly ionising radiations of interest to dosimetry are gamma-rays, X-rays, and neutrons.

The minimum energy of these ionising particles may be as low as 10 eV [Inokuti, 1983]; and the maximum kinetic energies, as in the case of accelerated ions, may reach values of the order of their rest mass.

The dominant interaction of both directly and indirectly fast ionising particles with matter is with the electrons in the target medium. A knowledge of the basic physical processes of radiation interaction and energy transfer is important for the understanding of the action of radiation on living cells.

2-1-1 Heavy charged particles interactions

A heavy charged particle (HCP) traversing matter, loses energy primarily through ionisation and excitations of the atoms to electrons, losing only a small fraction of its momentum in a single collision (i.e. its deflection from the main path is negligible). Thus the HCP through subsequent collisions, travels in almost a straight path in the medium. A non-relativistic expression for the maximum energy transfer T_δ, a single collision (derived from classical mechanics) is given by:

$$T_\delta = \frac{4\, m_e\, M}{(M + m_e)^2}\, E \qquad 2\text{-}1$$

where m_e, M are the masses of electron and HCP respectively, E is the HCP energy. The maximum δ-rays energy can also be calculated from $T_\delta = 1.02\, \beta^2$, where β is the relative velocity of the ion.

The rate at which the HCP loses energy to the atomic electrons along its path in a medium is identified physically as the stopping power of the medium for the particle, S(E). The stopping power can be used to estimate the range of a charged particle. It is also an essential quantity used to evaluate other dosimetric parameters

such as the linear energy transfer; LET. Empirical approximations for stopping power and ranges as well as their tabulations are included in ICRU-37 (1984) and ICRU-49 (1993).

2-1-2 Electrons and Beta particle interactions

Like HCP's , electrons, beta-particles β^+, β^-, interact with matter via excitations and ionisations. However, these particles can lose a considerable fraction of their energy and undergo large deflection in a single collision with atomic electrons. Thus they travel in kinky paths. The maximum energy of δ-rays produced is half the incident particle energy; that is $T_\delta = E_e/2$. The δ-rays are hardly distinguished from the primary electrons. In addition, electrons may interact with the field of the atomic nucleus, in which case they are deflected sharply. The process results in an emission of photons i.e. bremsstrahlung. The rate at which these particles lose energy in matter for the two processes, is given by the collision stopping power $S_c(E) = -(dE/dx)_c$, and by the radiative stopping power (bremsstrahlung) is $S_r(E) = -(dE/dx)_r$.

Radiative process become important at high energy (the threshold for water is about 1 MeV). At very high energy (above 100 MeV), the dominance of radiative over collisional energy loss gives rise to electron-photon cascade showers. Beta particles can also be scattered elastically by atomic electrons, a process which is important for transport of beta rays in matter at low energy. Tabulated data for stopping powers of electrons are found in a number of references [Berger, 1983 ; ICRU-37, 1984 ; Watt, 1989].

2-1-3 Interaction of gamma-radiation with matter

Unlike charged particles, photons can traverse significant thicknesses of matter before they interact with atoms. Energy loss by photons in matter can be one or more of the following; photoelectric absorption, Compton scattering, pair production, and photonuclear reaction. In the first three processes, electrons are produced. Typically, the energy range for which each of these effects is most important (in water) is given in table 2-1.

Table 2-1 Photon interaction thresholds in water.

Process	Energy range
photoelectric absorption	below 15 keV
Compton scattering	100 - 600 keV
pair production	above 1.02 MeV

Cross sections for the different types of interactions for nuclides of importance to radiobiology can be found in a number of references [Hubbell, 1982 ; Evans, 196; Storm, 1970].

2-1-4 Interaction of neutrons with matter

Neutrons are classified according to their energies. Thermal neutrons of energy 0.025 eV, intermediate neutrons of energy between 0.01-0.1 MeV and fast neutrons with energies over 0.1 MeV to 20 MeV. Like photons, neutrons can travel appreciable distances through matter before they interact, via elastic scattering, and non-elastic scattering. The latter includes inelastic scattering, neutron capture and spallation, etc.

The elastic scattering process is important for neutrons with energies up to 14 MeV. The principle scattering nucleus in the absorbing medium for a tissue equivalent system (e.g. water) is the proton. Other important scattering also occurs, resulting in the recoil of oxygen, carbon and nitrogen [ICRU-26, 1977].

2-2 Review of Radiation Quality Parameters

2-2-1 Radiation Quality

All ionising radiations interact with living matter in similar way. At a given absorbed dose different types of radiation induce different degrees of damage. Photon and electron radiations are generally less efficient than fast charged particles and neutrons. For a given system, the inherent damage capability of each type of radiation, for a specified endpoint, is termed the radiation quality. With a good radiation quality parameter, the biological response of an unknown radiation in principle could be predicted from measurements of the distribution of this parameter. In radiation research, the most commonly used parameter for radiation quality are; the linear

energy transfer; LET, adopted by ICRU-36 (1983), the restricted dose average LET, $L_{100,D}$ [Harder, 1992], z^{*2}/β^2 [Butts, 1967], and linear primary ionisation, I_i [Watt, 1985]. The present system of radiation dosimetry for radiobiological protection, is based on the linear energy transfer.

2-2-2 Linear Energy Transfer; LET and its restricted forms

The concept of LET was first introduced by Zirkle et al. (1952). ICRU defines LET as "the linear energy transfer or restricted linear collision stopping power (L_Δ) of charged particles in a medium is the quotient of dE by dl, where dl is the distance traversed by the particle and dE is the mean energy-loss due to collisions with energy transfers less than some specified value Δ" [ICRU-16, 1970]. The energy-loss is sometimes referred to as energy locally imparted. The term locally is associated with the dimension of the site. If this site is considered to be the whole space, then LET, termed as the total L_∞, which is mathematically equal to the collisional stopping power ($LET = dE_l/dl$). If the dimension of the local site is small compared to the range of δ-rays produced by the primary ionising particle, this means that δ-rays will deposit their energy outside the site. The physical quantity restricted LET_Δ is proposed which is mathematically equivalent to the restricted stopping power, that is $LET_\Delta = -(dE/dx)_\Delta$ for energy not exceeding Δ [ICRU-16, 1970]. Thus Δ specifies an energy cut-off and not a range cut-off. Mathematically, the LET is the first moment of energy transfer for the inelastic scattering cross section $\sigma_i(E)$ that is:

$$LET = \int_0^{T_{max,\,\delta}} \sigma_i(E)\, E\, dE \qquad 2\text{-}2$$

The restricted LET is expressed as the second moment of energy transfer which is given by:

$$LET_\Delta = \int_0^{T=\Delta} \sigma_i(E)\, E^2\, dE \qquad 2\text{-}3$$

Physically this quantity is related to straggling. The third moment of energy transfer is related to skeweness.

Secondary electrons generated by primary charged particles not exceeding the cut-off $\Delta = 100$ eV, are included in L_Δ. Those with higher energy are classified as δ-rays which have their own track and are treated separately. Practical radiation fields, with the exception in the case of photon- or neutrons, are usually comprised of charged particles of different types and energies. Thus LET is not single valued. For instance reactor workers are exposed to mixed radiation fields of gamma rays and neutrons, these neutrons ranging from their thermal energy 0.025 eV to energies greater than 10 MeV. The LET would have a spectrum characterised by t(L), the fraction of track length with LET between L and L+dL. Two mean values of LET are defined by ICRU-19 (1971), the track average or the frequency weighted LET; L_T which is represented by the frequency weighted first moment in L i.e. :

$$\bar{L}_T = \frac{\int_0^\infty L\, t(L)\, dL}{\int_0^\infty t(L)\, dL} \qquad 2\text{-}4$$

and the dose averaged LET; L_D, which is represented by the weighted second moment in L, and given by:

$$\bar{L}_D = \frac{\int_0^\infty L^2\, t(L)\, dL}{\int_0^\infty t(L)\, dL} \qquad 2\text{-}5$$

The restricted frequency averaged LET and restricted dose LET are analogously defined [ICRU-16, 1970]. While the total LET distributions are measurable, the restricted LET distribution has to be calculated analytically for a given situation [Howard-Flanders, 1958]. This in turn creates complications in the implementations and limits our use of the present radiation dosimetric system.

2-2-2-1 LET as a radiation quality parameter in the track structure model

In radiobiology damage in biological matter specified with LET. The basis of this model relies on observations depicted from the RBE-LET relations for cells irradiated by ionising radiation. Maximum RBE is found to occur for LET around 100-200 keV/μm, especially with intermediate mass ions (^{10}B, ^{12}C .. etc.) [Barendsen, 1963 ; Todd, 1967]. If the final slopes of the survival curves are used to calculate inactivation cross-sections, Kraft (1991) claims that is possible to specify damage with the use of the $\sigma - L_T$ relationship.

2-2-2-2 Restricted LET as a quality parameter in the pairwise lesion interaction model

Based on the assumption that the damage of two dsb's in the DNA can pairwise interact to cause or form a faulty chromatin cross-link which leads to cytogenetic effects e.g. chromosome aberrations. Harder (1992) had proposed that a model "pairwise lesion interaction" (PLI) based on Lea (1955) and Neary (1965) foundations. Assuming low ionisation/lesion conversion (Poisson processes) the probability of inducing such damage is proportional to:

$$P = 1 - \exp(-\mu) \qquad 2\text{-}6$$

where the number of inactivating molecular products per particle track is Poisson distributed around the mean value μ which is given by:

$$\mu = N \int_0^{\infty} g(t) \left(1 - \exp(-h(t))\right) dt \qquad 2\text{-}7$$

where N is the number of interaction regions traversed by the particle, g(t) and h(t) is the expectation value per time interval Δt of the number of molecular encounters of interactive lesions in a given interaction region of the chromatin, and h(t) is the expectation value of the number of interactions per encounter. Harder argued that μ is a function of LET. However because δ-rays will deposit most of their energy outside of the interaction region, μ can be considered as a function of the restricted dose averaged LET; $L_{D,100}$ [Harder, 1987]. Thus it is possible to predict the cell inactivation cross-sections in terms of the particle fluence ϕ. Assuming that the

number of ionising particles traversing the chromatin is Poisson distributed around a mean value of $\sigma_{g,c}\,\phi$ by :

$$\sigma_i(\mu) = -\frac{d\ln(SF)}{d\phi} = \sigma_{g,c}\left(1 - \exp(-\mu)\right) \qquad 2\text{-}8$$

where $\sigma_{g,c}$ is the geometric cross-section of the chromatin fibre.

2-2-3 Quality parameter in Katz's structure model; z^{*2}/β^2

Butts and Katz (1967) suggested a model formed from calculations of energy densities around an ion track in the medium. They assumed that all electrons are ejected perpendicularly to the ion path and that they have constant energy loss irrespective of their energy. The distribution for energy deposition is given by [Katz, 1982] as:

$$f(\varepsilon)\,d\varepsilon = C\,\frac{z^{*2}}{\beta^2}\,\frac{1}{\varepsilon}\,d\varepsilon \qquad 2\text{-}9$$

where C is a coefficient which depends only on the absorbing medium (C=8.5 eV/μm for water), z* is the effective charge on the ion and is given by the empirical expression [Barkas, 1963];

$$z^* = \frac{z}{\left([1-e^{-125\,\beta z^{-2/3}}\right)} \qquad 2\text{-}10$$

where z is the charge number , and $\beta = v/c$ is the relative particle velocity. According to Katz, the probability of inactivating a cell is then given by [Katz, 1982]:

$$P = \left(1 - e^{-z^*/\kappa\beta^2}\right)^m \qquad 2\text{-}11$$

where the parameters κ, and m determine the radiosensitivity of the specific cells to the ionising radiation The radiation quality parameter z^{*2}/β^2 used by Katz is proportional to the yield of δ-rays per unit distance along a fast ion track. Katz

demonstrated that his model works well with single hit targets such as inactivation of enzymes, viruses and bacteria [Katz, 1995].

2-2-4 The mean free path for linear primary ionisation; λ

Watt et al. (1985) proposed a unified model which relies on the linear primary ionisation, I_i. This radiation quality parameter is used to specify the radiation damage in nanometer regions around the ion core. Physically this quantity represents the primary ionisations per unit path and is equivalent to the yield of δ-rays. The probability to inactivate cells or any other specific damage is given by:

$$P = 1 - \exp(-\lambda_o / \lambda) \qquad 2\text{-}12$$

where $\lambda = 1/I$, and λ_o is about 1.8 nm which corresponds to the inter-strand spacing of the DNA. Just as LET is the first moment of energy transfer, the linear primary ionisation; I_i, is the zeroth moment of the inelastic scattering cross-section, which is given by:

$$I_i = \frac{dP}{dx} = K \int_{E_0}^{E_{max}} \sigma_i(E)\, dE \qquad 2\text{-}13$$

where the lower integrand part E_o is the ionisation potential and can be taken as 10 eV, which is near the minimum threshold energy for inducing ssb's and dsb's of the DNA. The mean free path for linear primary ionisation is calculated from the inverse of I_i , ($\lambda = 1/ I_i$). The mean free path can be a very meaningful radiation quality parameter for specifying radiation damage in nanometer dimensions as will be seen in chapters 3 and 4.

2-2-4-1 The linear primary ionisation of fast ions

The linear primary ionisation (I_i) for accelerated ions was calculated using Bohr's relation [Chen, 1986]

$$I_i = k\left(\frac{z^{*2}}{\beta^2}\right)\left(\frac{1}{I_p} - \frac{1}{T_{\delta,max}}\right) \qquad 2\text{-}14$$

where I_P , is the ionisation potential. $T_{max,\,\delta}$ is the maximum energy of the δ-ray spectrum. The constant k is evaluated from:

$$k = \rho \frac{N_A Z}{M_A} \frac{2\pi e^4}{\varepsilon_o^2 m_e c^2} \qquad 2\text{-}15$$

where ρ, N_A , Z, and M_A in respective order are the density, Avogadro's number, atomic number, and the mass of the absorber. Other symbols have their usual meanings. The linear primary ionisation can also be calculated to a good approximation from the relation:

$$I_i = \frac{\bar{L}}{T_\delta + W} \qquad 2\text{-}16$$

where L , W and T_δ are respectively the track average linear energy transfer, the mean energy to produce a primary ion pair and the average energy transferred to delta rays in a collision. The W values for ions with specific energies greater than 0.5 MeV/amu are deduced from information given in ICRU-reports [ICRU-31, 1979]. For lower energies W is derived from a semi-empirical formulation [Goodman, 1978]. T_δ is the average energy transferred to delta rays in a collision. A compilation of the track structure parameters for heavy ions in water is included in the St-Andrews Report 2-1994. Results are compiled in figures 2-1a, 2-1b, and 2-1c which shows the linear primary ionisation I(nm^{-1}) as a function of different ion types and energies in regions of interest to radiobiology. Also shown in figure 2-2a, b, c, d, and e, are the linear primary ionisation of selected ions (p, ^{4}He, ^{12}C, ^{40}Ar, and ^{238}U) compared to other quality parameters in regions of interest to radiobiology.

2-2-4-2 The linear primary ionisation of photons and electrons

In the case of electron beam exposure, the instantaneous energy values were considered. The collisional stopping power and ranges of electrons with energies higher than 10 keV are based on ICRU-37 (1984). For lower energy electrons, the calculations are based on data obtained from the literature [Iskef, 1983 ; Al-Ahmad, 1984 ; Ashley, 1982 ; Tung, 1983].

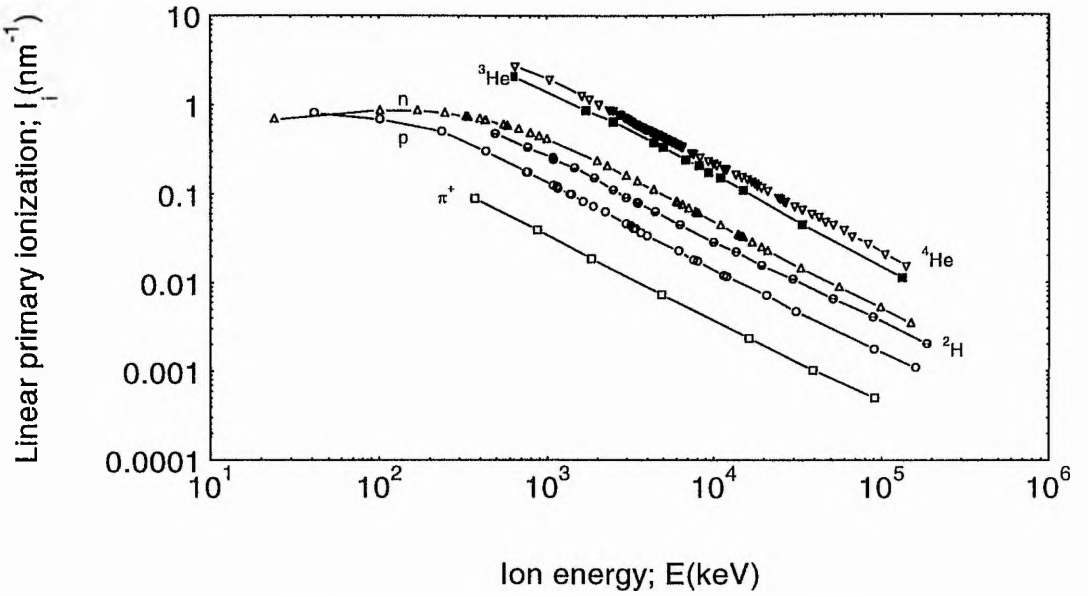

Figure 2-1a Linear primary ionisation vs. light ion energy (up to z=2).

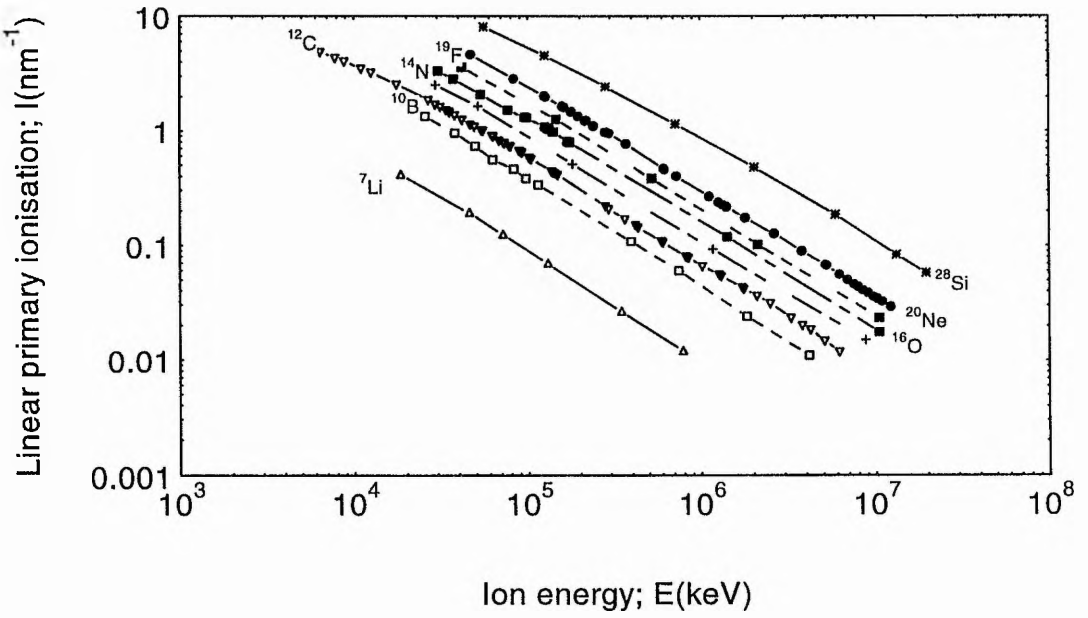

Figure 2-1b Linear primary ionisation vs ion type and energy (z=3 to z=14).

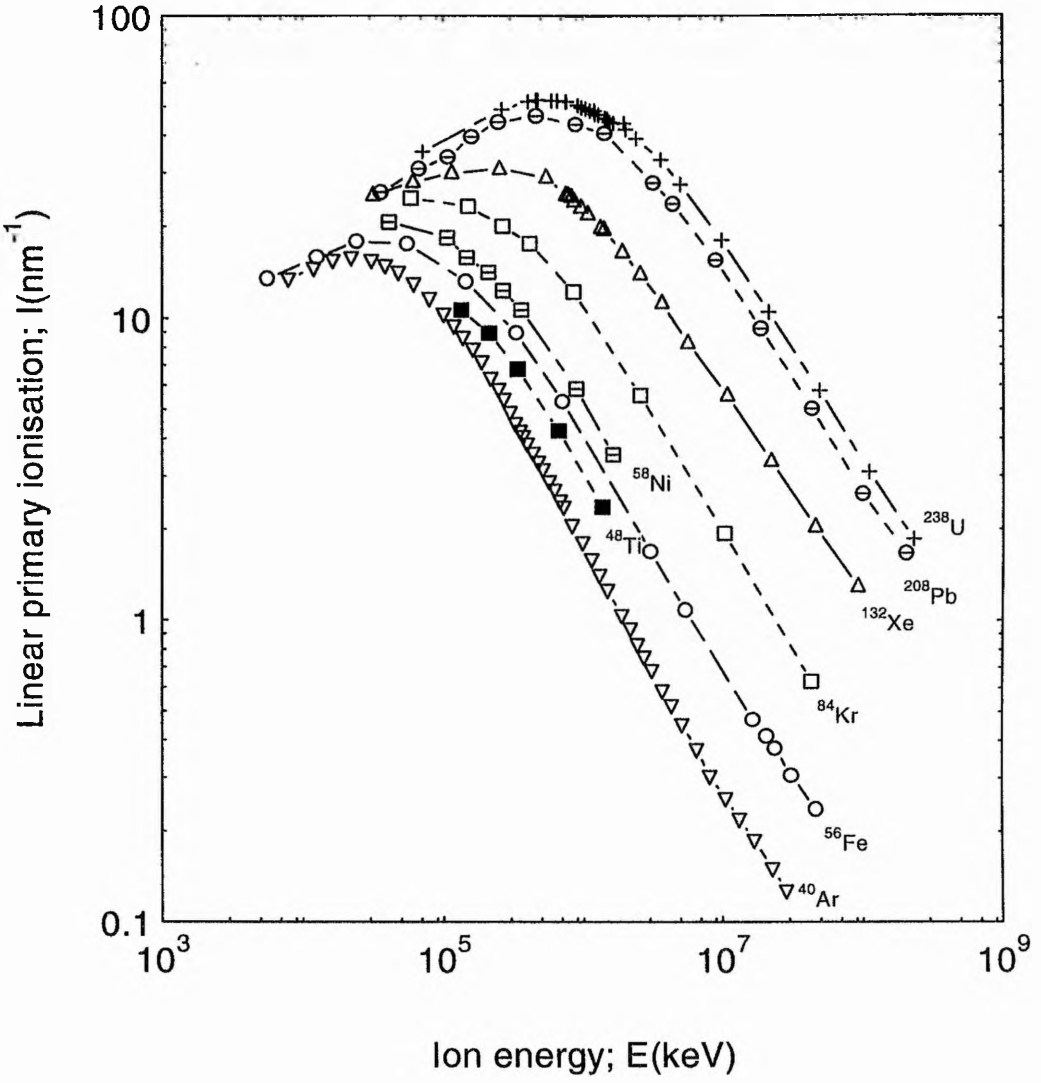

Figure 2-1c Linear primary ionisation vs. ion's type and energy (z=20 to z=92).

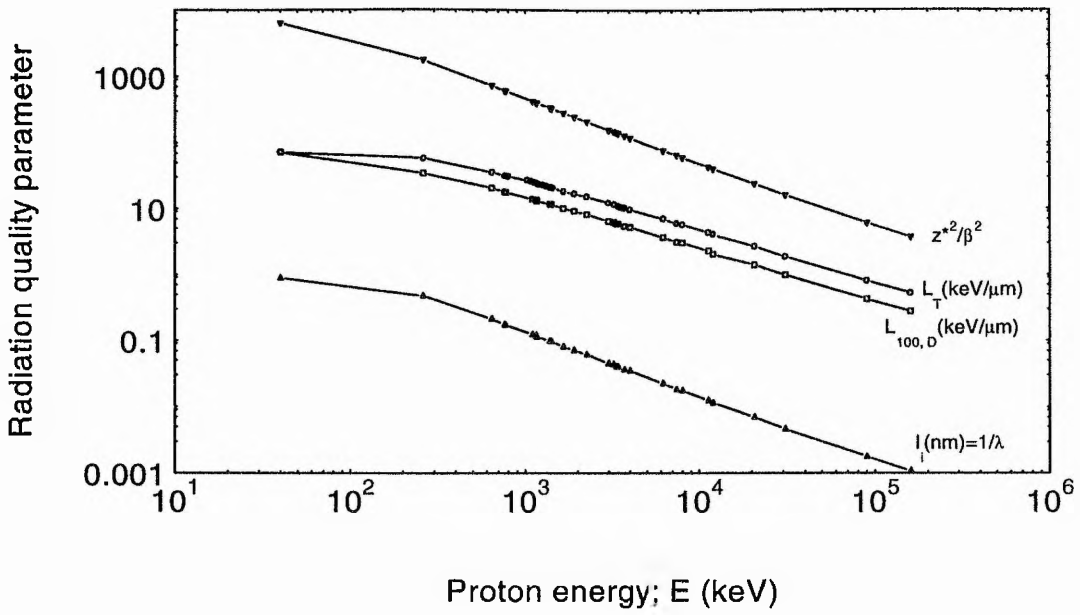

Figure 2-2a Radiation quality parameters for protons.

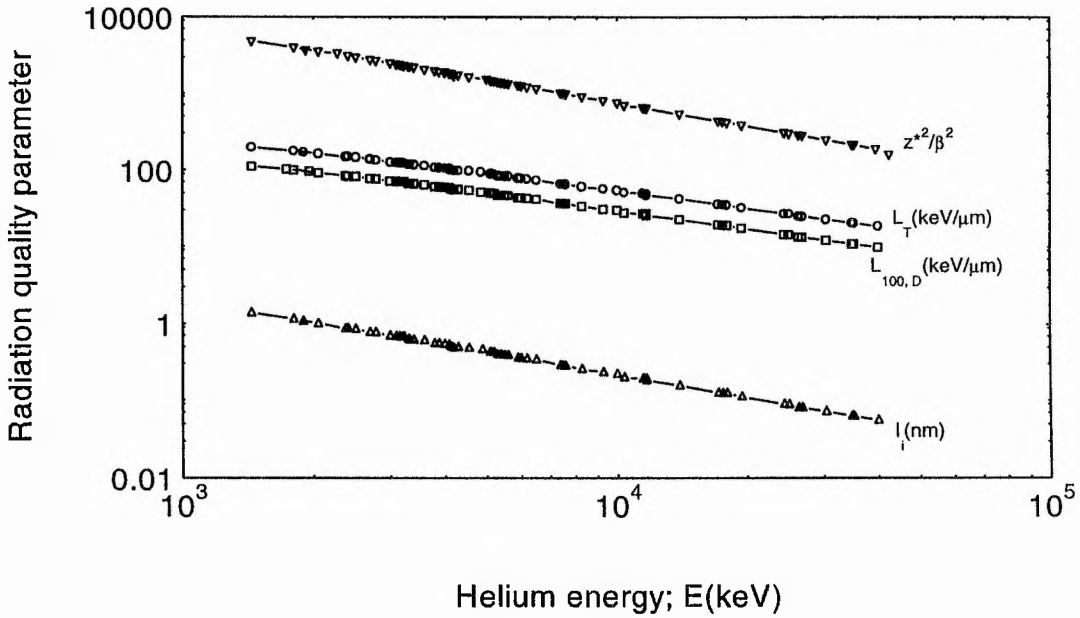

Figure 2-2b Radiation quality parameters for Helium ions.

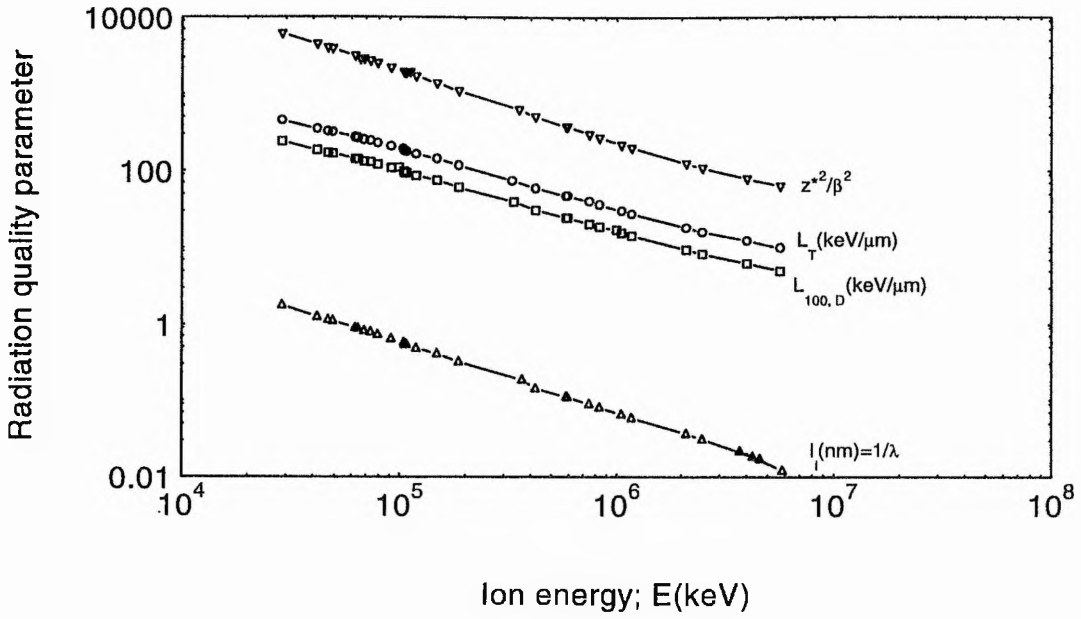

Figure 2-2c Radiation quality parameters for Carbon ions.

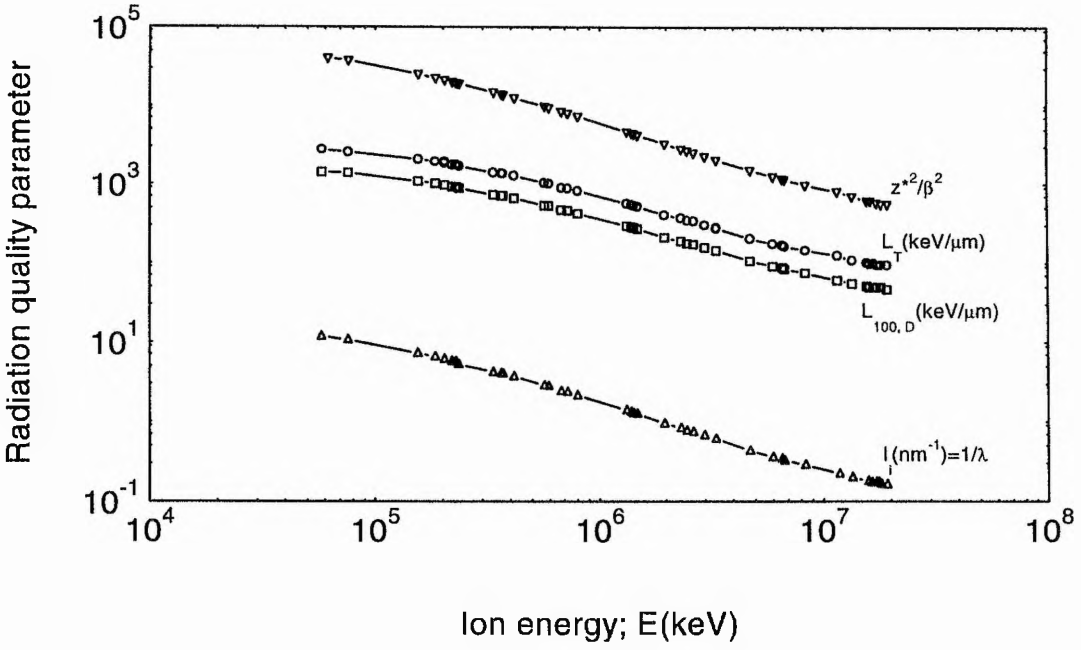

Figure 2-2d Radiation quality parameters for ^{40}Ar ions.

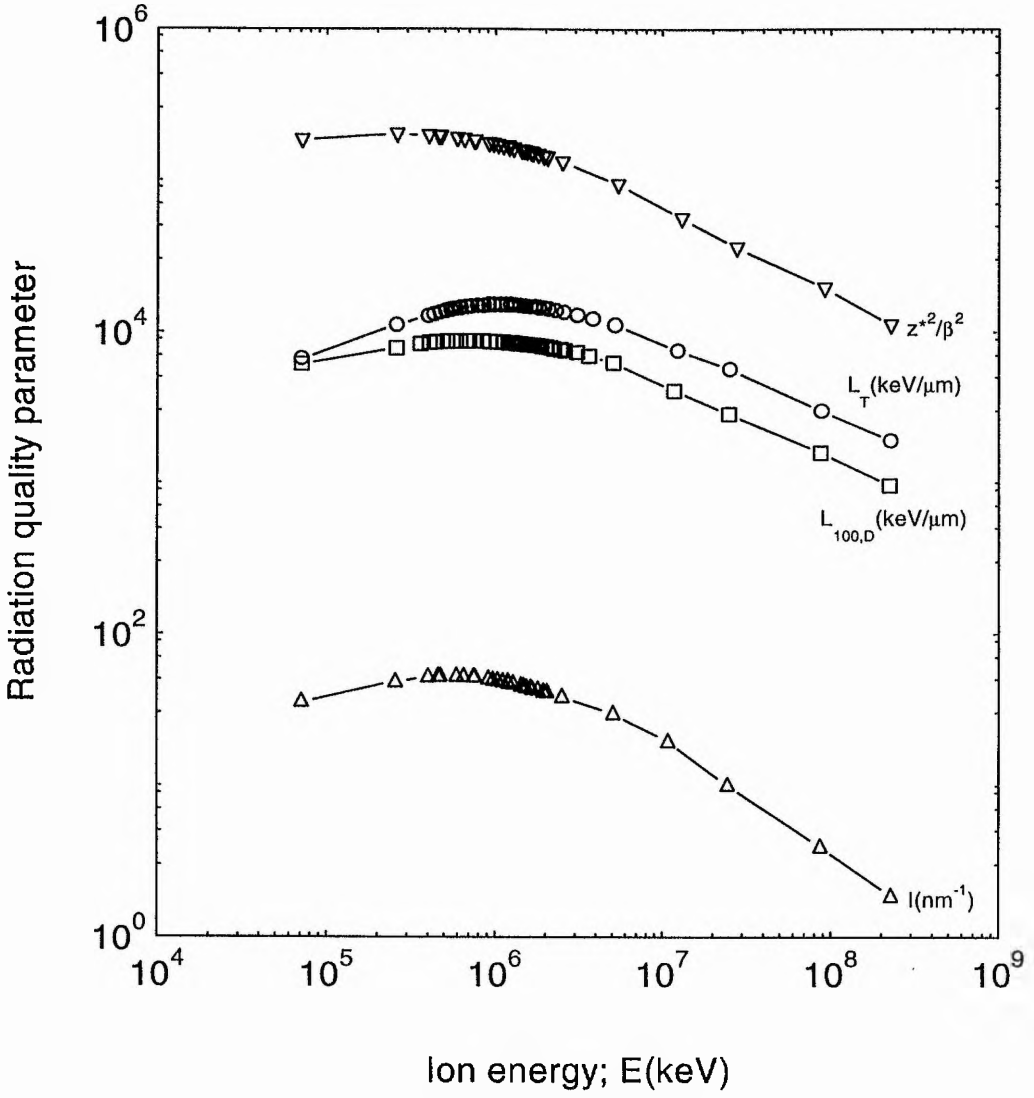

Figure 2-2e Radiation quality parameters for ^{238}U ions.

The situation, however is quite different for photons. The calculation of linear primary ionisation is related to the charged particle equilibrium of electrons produced from the primary Compton and photoelectrons interactions and from subsequent interactions which are produced by the primary electron source [McGinnes, 1959]. For γ-rays from ^{137}Cs and ^{60}Co the effective of the emitted photons were taken to be 0.662 MeV and 1.252 MeV respectively. The X-rays the effective energy E_{eff} of the bremsstrahlung spectra were calculated from data given in literature [Seelentag, 1979 ; Bird, 1979] with consideration of the degree of filtration used by the original authors. The lower cut-off of electron energy was extended to be 30 eV. The effective electron energy, E_{eff}, is determined from the LET distribution. The relevant energy is then used to calculate the linear primary ionisation of electrons either in the equilibrium slowing down or in the primary spectrum, for electrons with energies higher than 10 keV using the empirical relation:

$$I_i = \frac{1.6935 \times 10^{-4}}{\beta^2} \ln(2.325 \times 10^4 \ \beta^2) \quad \text{ionisations / nm} \qquad 2\text{-}17$$

A compilation of the track structure data of electrons in water including a wide energy range is given in the St-Andrews report, (6) 1995 [Watt, 1995], now formally published in Watt (1996). Figure 2-3a shows the calculated linear primary ionisations and the LET for photons (in regions of interest to radiation biology) as a function of maximum photon energy . Figure 2-3b shows the same two radiation quality parameters for electrons as a function of electron energy.

2-2-4-3 The linear primary ionisation of neutrons

Damage to biological material by irradiation with neutrons occurs through the interaction of the recoiled charged particles products, particularly protons. The (n,p) scattering cross-sections were obtained from CINDA, 1992 and the degradation recoil spectrum were calculated directly. The track structure parameters are compiled by Watt, 1996. Figure 2-4 shows the calculated radiation quality parameters, including the linear primary ionisation I, as a function of neutron energies of interest in radiation biology.

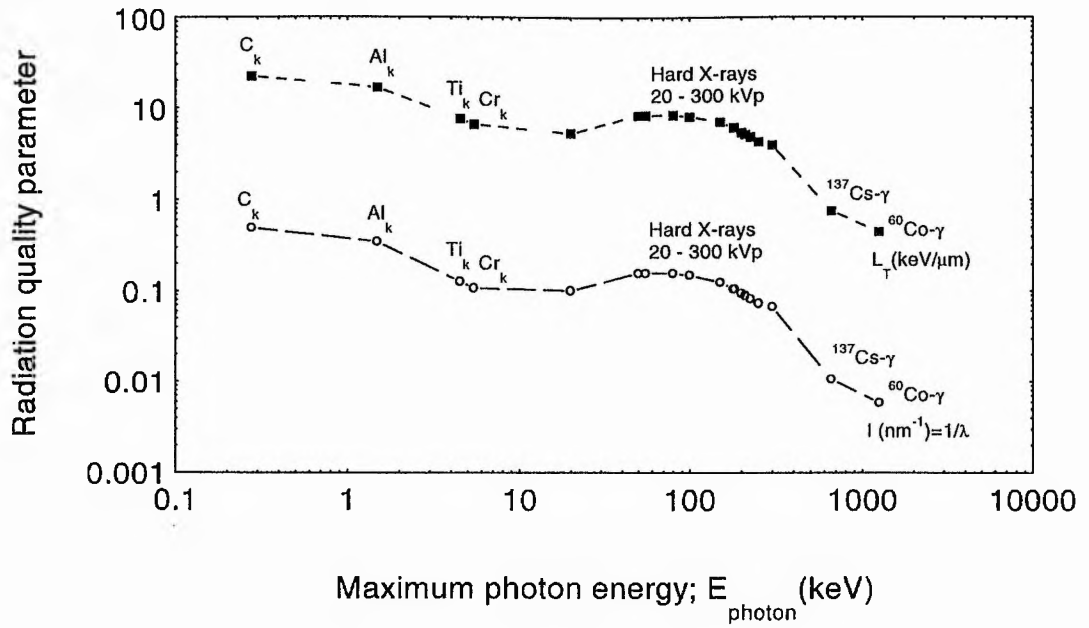

Figure 2-3a Radiation quality parameters for X-rays and γ-rays.

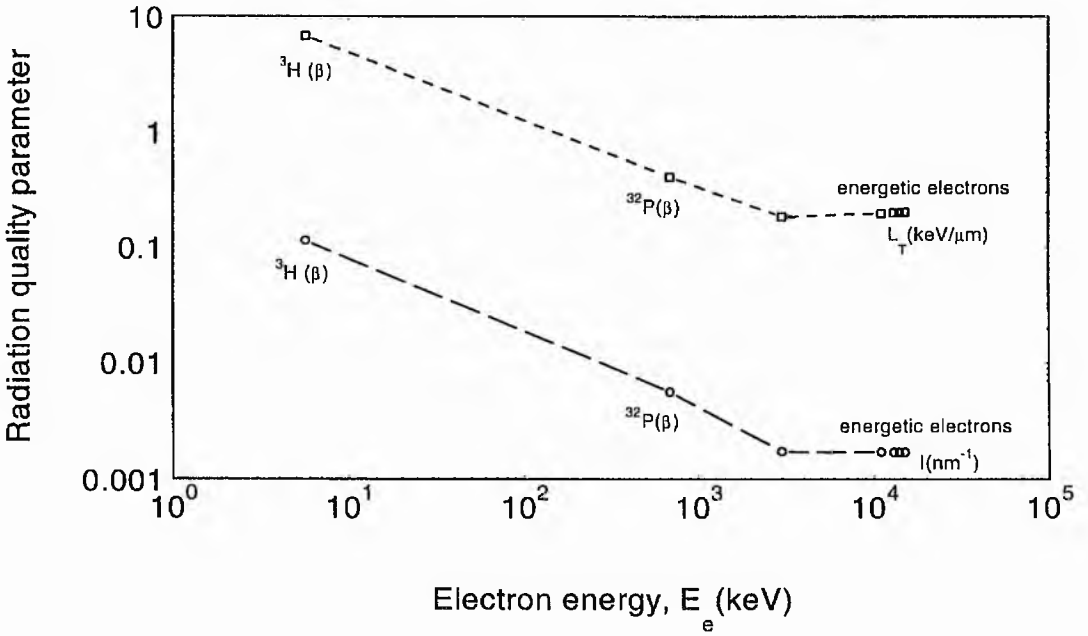

Figure 2-3b Radiation quality pararmeters for electrons.

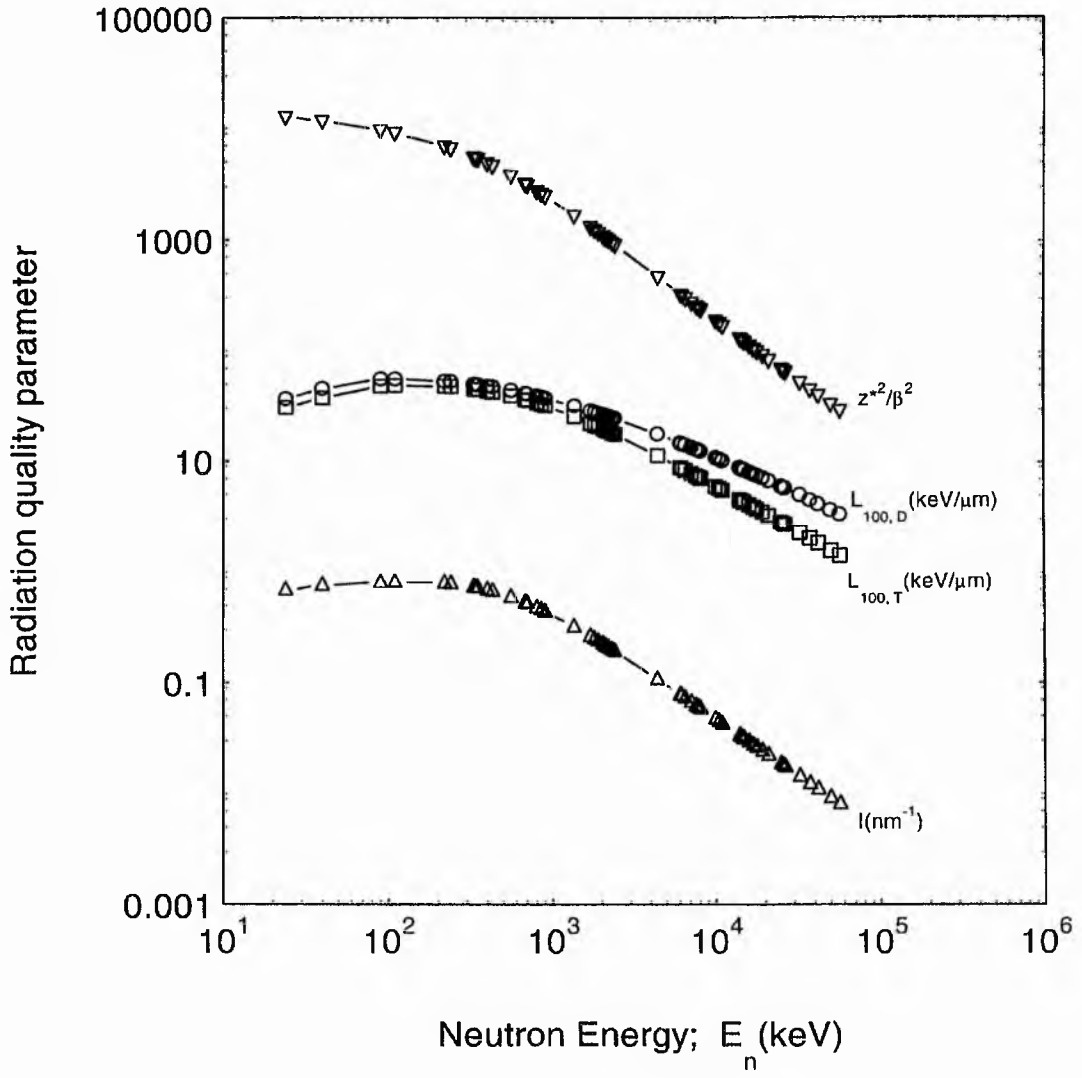

Figure 2-4 Radiation quality parameters fluence-weighted for the proton recoil equilibrium from neutrons in water.

2-3 The Physical, Chemical, and Biological Stages of Radiation Action

2-3-1 Chemical and biological responses to radiation action

Mammalian cells are typically between 70-85% water, 10-20% proteins, and 2-3% lipids. The most common constituent elements which an individual can have are shown in table 2-2 [Raven, 1988 ; ICRP-23, 1978]. They are low atomic weight elements, mostly in the form of water and biochemical compounds, like protein, and Nucleic acids.

Table 2-2 The most common elements in a reference man.

Element	Atomic Number	% of Human Body (W)
Oxygen (O)	8	65
Carbon (C)	6	18.5
Hydrogen (H)	1	9.5
Nitrogen (N)	7	3.3
Calcium (C)	20	1.5
Phosphors (P)	15	1.0
Potassium (K)	19	0.4
Sulphur (S)	16	0.3
Chlorine (Cl)	17	0.2
Sodium (Na)	11	0.2
Magnesium (Mg)	12	0.1

Ionising radiation interacts with the molecules of the biological system. Since water forms the bulk of the biological system by weight, the majority of these interactions will be with water molecules. As the ionising particles traverse through the medium, they lose energy at a rate given by the stopping power S(E), primarily through excitations and ionisations, resulting in ion-electron pairs. These electrons may initiate other reactions in like manner, producing secondary electrons. The absorbed energy in the molecule of the medium, depends on the ionisation potential of water, 12.6 eV, as well as on the average sub-excitation energy of water, 7.4 eV, leading to ionisations, excitations, and super-excitations.

An abundance of secondary electrons is produced in water, as a result of ionisation. Their energy typically ranges from 20 eV to 100 eV [Mozumder, 1966]. They slow

down very quickly, in less than 10-15 μsec. Other various stages of radiation action start. These are summarised in the following sub-sections. If the secondary electrons have enough energy to produce ionsation in the medium, and have distinguishing tracks of their own, then they are called delta electrons, (δ-rays).

2-3-2 Physical Stage

The initial reactions in aqueous solutions, under the radiation action via excitations and ionisations, produce the primary products H_2O^*, (including dissociation products such as the hydroxyl radical, HO•, the hydrogen radical H•, H_2O^+ and the hydrated electron e^-_{aq}. The time scale for this stage is from 10^{-16} to 10^{-12} s.

2-3-3 Pre-chemical stage

The combinations of the preceding reactions with water molecules or hydrogen produce the intermediate products, H^+ ,HO•, H•, OH^-, and the hydrated electron e^-_{aq}. The primary product electrons are slowed down by collision (energy of 100 eV or less) to finally react with water molecules as they are attracted by the permanent dipoles of water molecules, hydrated electrons can be formed. Hydrated electrons have a long lifetime in neutral water, ~ 200 msec, and they are more stable than free electrons.

The ions H^+, OH^- formed in these stages amount to a very small fraction with respect to the distribution of species produced in the dissociation of water. Thus their contribution can be neglected. On the other hand, recombination of radicals and ions can occur immediately, within 10 p-sec. At later times diffusion processes become important.

2-3-4 Chemical stage

The motion of the four chemically active species H_3O^+, OH• , e^-_{aq} , and H•, is controlled by their respective diffusion constants D [Turner, 1986], and their reactive radii, R (table 2-3). They can either interact with one another or become widely separated before interaction. This stage will last for about 1μ-sec.

Table 2-3 Diffusion constants of water products.

Species	Diffusion Constant D X 10^5 (cm^2/s)	R(nm)
OH•	2	0.24
e^-_{aq}	5	0.21
H_3O^+	8	0.03
H•	8	0.042

The fate of the radicals and the molecular decomposition of water can be best quantified by the G-value. The G-value of a reaction is defined as the number of species formed (yield) per 100 eV of energy deposition from the ionising radiation. The initial G-values for primary radiolytic product of water are given in table 2-4.

Table 2-4 The G-values for the water species.

Species	G-values
e^-_{aq}	2.63
H•	0.55
OH•	2.72
H_2	0.45
H_2O_2	0.68
H_2O	4.08
HO_2•	0.008

Adopted from von Sonntag, 1987

The G-value increases with time as the formation of the species of interest increases; or decreases as the reactant species involved are destroyed.

2-3-5 Biological stage

Ionising radiation interacts with biologically important molecules, through two mechanisms. Direct action in the absence of water (dry state), and indirect action in the presence of water.

2-3-5-1 Direct Action

Within the time frame of the initial physical events, the primary ionising charged particle deposits its energy within the biologically important molecule, resulting in excitations and / or ionisation. The unstable excited molecules may undergo

fluorescence process as by emission of photons. The ionised molecule has an excess energy dissipated by the rupture of the covalent bond and scission the molecule into two radicals, whose life span is of the order 10 m-sec.

Breakage of the bond could take place instantly on site, at the site where energy is deposited, or at any other weak bond as the energy absorbed may migrate within the same molecule.

2-3-5-2 Indirect action

Indirect effects are those caused by the interaction of the radiolytic products of water with the biologically important molecules. Since water forms about 80 % of the cell constituents, the importance of the indirect action is suggested.

The direct action of radiation on water molecules may result in excitations, super excitations, or ionisation. Their respective G-values are 0.54, 0.92 and 0.48, [Platzman, 1967].

Experimental evidences has identified the hydroxyl radical $HO_2\bullet$. as the predominant species for reaction with biological molecules. In fact by examining the G-value for radiolytic species of water in table 2-4, the hydroxyl radical is found to have the highest value. Although the hydrated electron has also high G-value, experimental evidence shows that it is of lesser importance in inducing damage to biological molecules. It has been suggested that other radicals such as $^{2}O\bullet$ might play an important role in biological damage [Samuni, 1981].

2-3-5-3 Restoration Processes

Molecules damaged by the action of radiation, can be restored through three mechanisms according to the time scale of their formation, viz. the recombination process, chemical restoration, and enzymatic repair.

Recombination takes place in the very early stages after the irradiation event. It is simply rejoining the ion pairs or radical pairs to reform the original molecule. The time scale for this process 10 psec. If the diffusion process is in control, radicals can migrate, and recombination becomes less likely to occur. Chemical restoration can take place restore the altered molecule to the original state without the intervention of

any biocatylitic steps such as enzymatic action. The time scale for the chemical restoration process is within m-seconds. On a longer time scale, enzymatic repair of damage can occur. Time for this repair takes from minutes to hours [Alpen, 1990].

2-4 Radiation action on Biologically Important Molecules

2-4-1 Macromolecular target in the cell

Ionising radiation induces chemical transformations, that could produce biological alterations of importance to cell survivals. Among those bioactive molecules in the cell, which could be damaged via direct and indirect radiation action, DNA considered to be the critical target. It is the largest molecule in the cell, which carries the genomic information, controlling self-replications, and other biochemical activities, and cell division. The damage under radiation action are equally probable to all molecules of the cell. Enzymes can suffer significant radiolytic damage as a result of direct or indirect action of radiation, and since it is continuously synthesised, damage will soon be replaced. The loss of the vital function of any proportion of the molecule does not cause the loss of the function itself. Whereas in the DNA molecule damage alters the genetic coding, altering cellular function and thus affecting survivals [von Sonntag, 1987].

2-4-2 DNA as the target molecule

The genomic DNA of micro organisms is considered to be the target molecule which may lead subsequently to cell death for the following reasons:

1- On the basis of the physical chemical background, DNA is the largest molecule in the cell, the fatal dose which causes the loss of reproductivity is most likely to damage this molecule.

2- A direct experimental quantitative relationship between the damage induced in DNA and the biological function (reproductive ability) can be established using simple organisms such as bacteriophage and viruses. Depending on the type of virus, the nucleic acid could be single or double stranded DNA.

3- For higher organisms, no direct relation between DNA damage and loss of biological function can be established However loss of function can be correlated with the single and double-strand breaks in DNA.

4- In many organisms, the repair of DNA damage is related to cell survival (ability of the cell to divide).

5- The most sensitive cells to radiation exposure are those which lack the ability to repair DNA, as a result of genetic alteration.

6- Chemical agents which are known to block the repair of DNA damage increase the sensitivity of cells to irradiation.

2-4-3 Reactions of the products of water radiolysis with biological molecules

Following irradiation, free radicals are produced in water. These radicals may interact with biologically important molecules in many different ways [von Sonntag, 1987; Tubiana, 1990]. Although some of these reactions could lead to cellular alterations, the relative importance of each was not completely understood [Coggle, 1983]. The reaction constant for the radicals with DNA is given in table 2-5. The H• radical has a smaller reaction constant compared with the other radicals.

Experimental evidences, obtained through the use of scavengers, shows the relative importance of each of the radicals in their capability to damage the DNA. All experiments show that the OH• radical is the main damaging reactant. Reactions of these species with the DNA, could induce scission of the molecule.

Table 2-5 Reaction constants for water species with DNA.

Reaction	Reaction constant (Mol/s)
OH• + DNA	3.0×10^{8}
H• + DNA	8.0×10^{7}
e-aq + DNA	1.4×10^{8}

Adopted from Alpen, 1990

2-4-4 The variation of the DNA content among living organisms

It is often useful to compare the effective cross-section with the geometric cross-section to test a model, and examine other effects related to the mechanisms of damage, particularly at very high LET where the cross-section reaches saturation damage. To simplify the calculations, the DNA in the cell nucleus is assumed to be compacted into a spherical shape. Then, the geometric cross-section of the DNA; σ_{DNA}, can be calculated from:

$$\sigma_{DNA} = \left(\frac{7.5 \times 10^{11} \sqrt{\pi}\, M}{\rho N_A} \right)^{2/3} \quad \mu m^2 \qquad 2\text{-}18$$

where M is the mass of the nuclear DNA in Dalton, N_A is Avogadro's number, and ρ is the density of the DNA in g/cm^3. The mass of the DNA varies for the different types of cells, e.g. for mammalian cells varies from 3.0 to 3.5 x 10^{12} daltons and for non-mammalian cells varies from 3.4 x 10^5 to 1.0 x 10^{10} daltons [Fasman, 1976]. The density of the dry DNA is about 1.75 gm/cm^3 [Adams, 1992] and the density of the wet DNA is estimated to be about 1.34 gm/cm^3.

The geometrical cross-sections of cell nucleus are estimated from the dimensional data given in Kiefer, 1985 and Sonntag, 1990. Table 2-6 shows the calculated results for the DNA cross-sections and geometrical cross-sections of the cell / nuclei for some prokaryotic and eukaryotic cells. Figure 2-5a shows the variation of the weight of the different DNA in picograms for prokaryotic and eukaryotic cells with their geometric cross sections. Figure 2-5b shows the relation between the DNA cross-sections and the nuclear cross-sections. Figure 2-6c shows the packing ratio of DNA for the different cells against their DNA content (in terms of their nuclear cross-sections). Thus the complexity of mammalian cells is demonstrated by its high molecular weight of the DNA which contains about 6 x 10^9 bp's in a compact form within the cell nucleus (diameter ~ 8 μm) . In condensed form the projected area is about 4 μm^2 which may be compared with about 80 - 100 μm^2 projected cross-sectional area for normal cells nuclei.

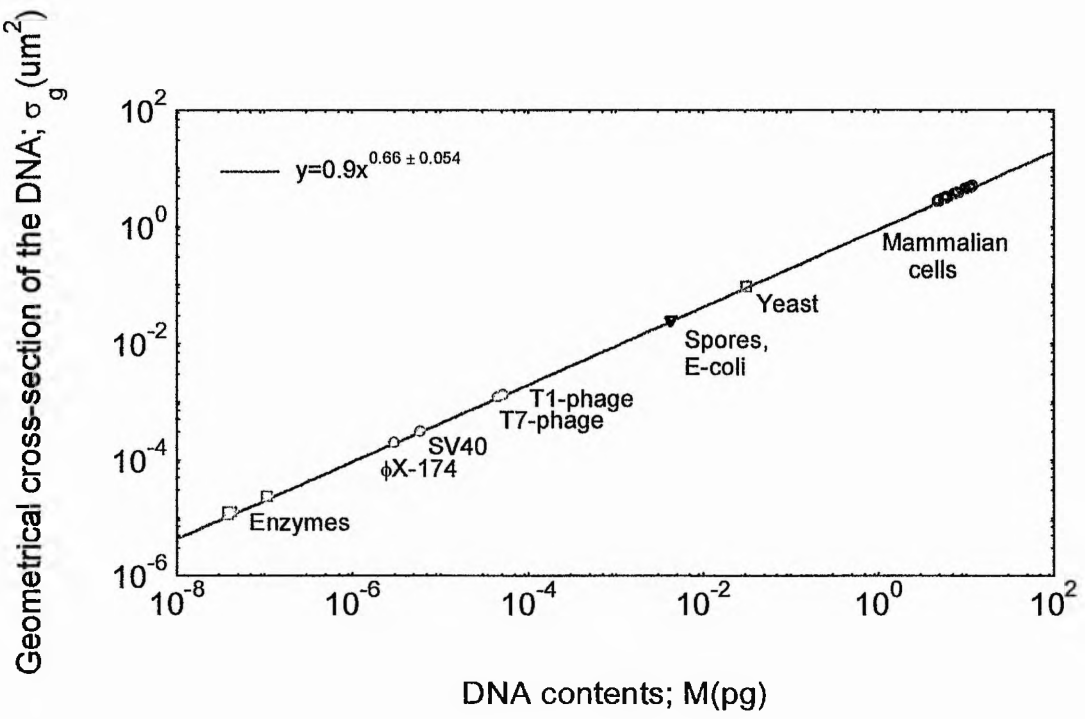

Figure 2-5a Nuclear DNA contents vs. geometrical cross-sections.

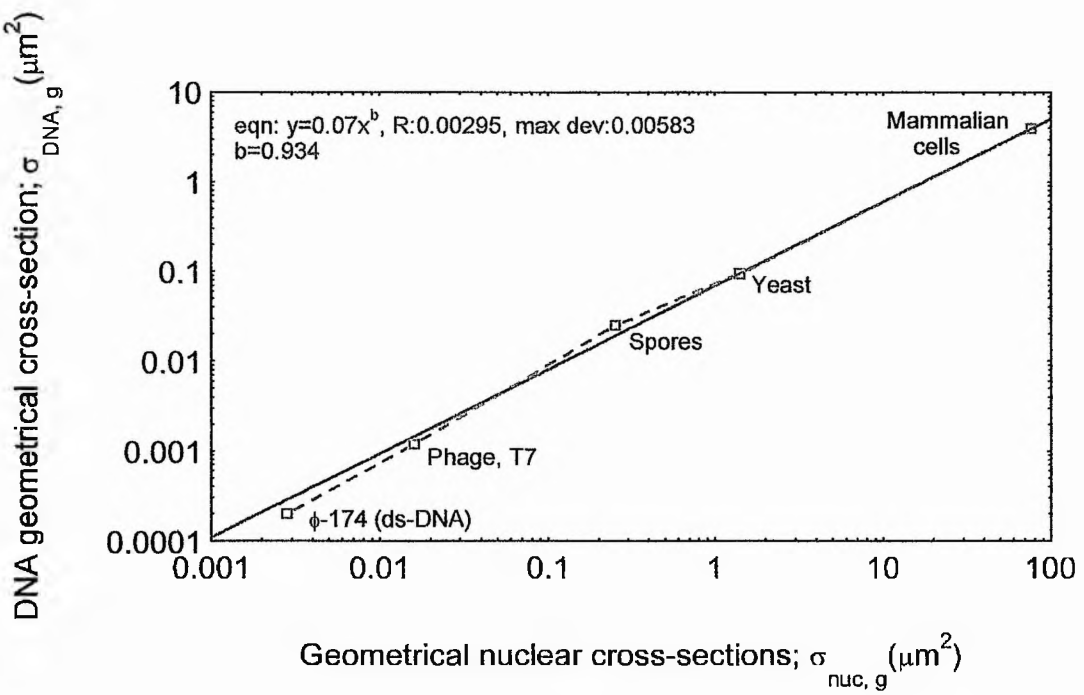

Figure 2-5b Relation between nuclear and DNA geometrical cross-sections.

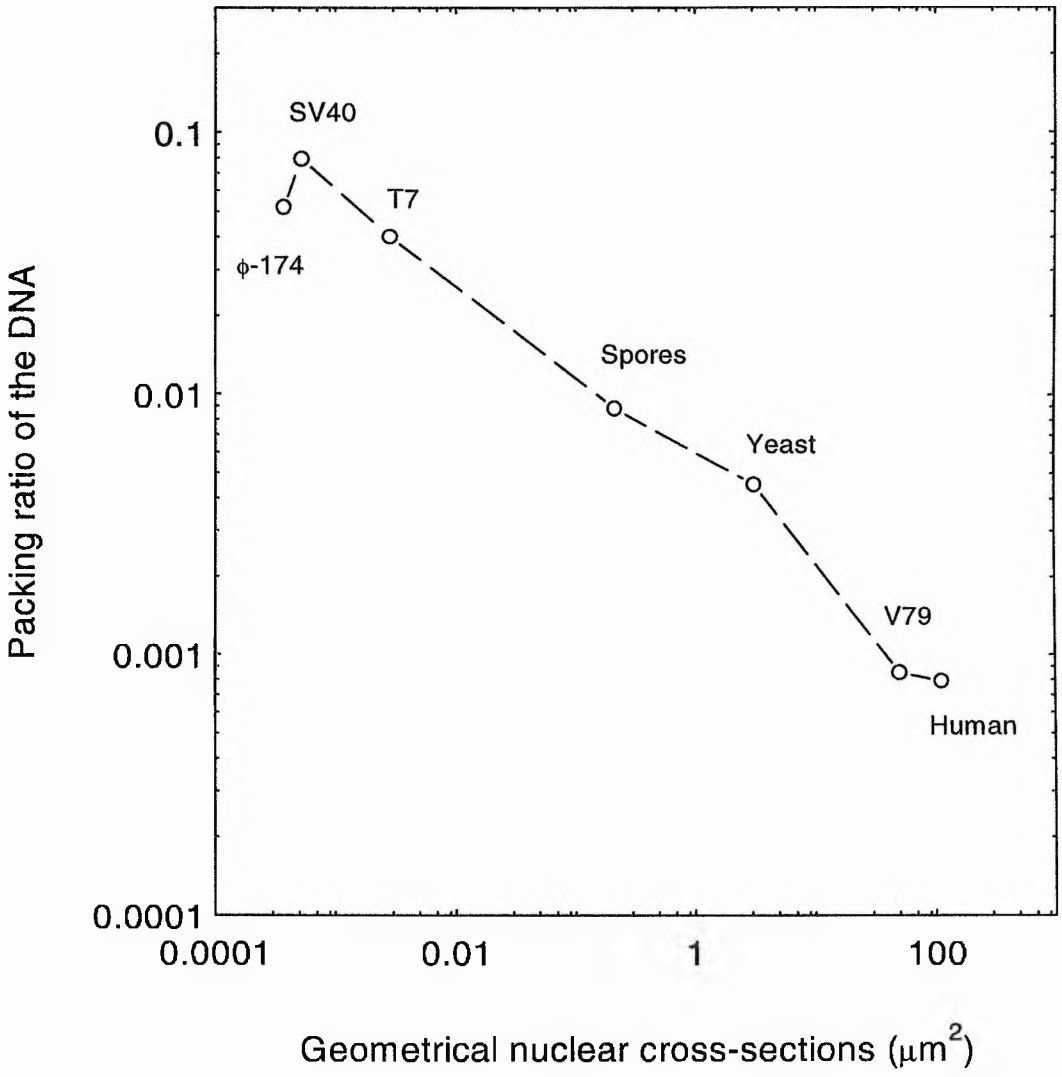

Figure 2-5c Packing ratio of DNA in prokaryotic and eukaryotic cells.

Table 2-6 The DNA variation among simple and complex organisms.

Cell Type/ organism	σ_{ng} (μm^2)*	σ_{DNA} (μm^2)	MW (daltons)
ϕ-174 (ds-DNA)	2.80×10^{-3}	2.0×10^{-4}	3.4×10^{5}
Bacteriophage, T7	1.6×10^{-2}	1.2×10^{-3}	3.7×10^{7}
Bacillus Subtilis	0.2	2.5×10^{-2}	2.5×10^{9}
Yeast	1.4	9.5×10^{-2}	9.6×10^{9}
Mammalian cells	76	4	3.6×10^{12}

* for prokaryotic cells, σ_{ng} is mainly the cellular cross section.

The molecular structure of the DNA plays an important role in determining the micro- and nano-distributions of DNA damage following the exposure of cells to ionising radiation [Oleinick, 1994; Rydberg, 1996; Holley, 1996].

Chapter 3

BIOLOGICAL DAMAGE BY IONISING RADIATION

The action of ionising radiation on cultured mammalian cells was pioneered by the classic experiments of Puck and Marcus [Puck, 1956]. Since then there have been extensive studies on clonogenic survivals and on other well defined biological endpoints. The prominent experimental endpoints investigated include cellular survival and recovery [Deering, 1962 ; Barendsen, 1963 ; Todd, 1967 ; Blakely, 1979 ; Wulf, 1985], chromosome damage [Awa, 1974 ; Edwards, 1980 ; Edwards, 1986 ; Edwards, 1994; Geard, 1985 ; Lloyd, 1976 ; Lloyd, 1978 ; Ritter, 1992 ; Skarsgard, 1967], gene specific mutations [Thacker, 1986 ; Belli, 1991 ; Belli, 1994 ; Cox, 1977 ; Hei, 1988 ; Kranert, 1992 ; Kronenberg, 1994 ; Stoll, 1995], oncogenic transformations [Elkind, 1979; Hei, 1988 ; Miller, 1989 ; Miller, 1995 ; Yang, 1985 ; Bettega, 1992 ; Bettega, 1995] and DNA strand breaks and repair [Ritter, 1977 ; Aufderheide, 1987 ; Heilmann, 1995 ; Jenner, 1992 ; Kampf, 1983 ; Lobrich, 1994 ; Rydberg, 1985 ; Rydberg, 1996]. In the early days, Lea thought that the lethal effects leading to cell killing could be the chromosome aberrations [Lea, 1955]. Now it is believed that with the improved understanding of molecular biology that the nucleur DNA is the lethal target in the cell [Hagen, 1994]. In fact it is believed that the initial damage of DNA (dsb's) by heavy ions could induce cell death, and that the misrepair of the DNA dsb's could induce stochastic damage (mutations and at later stage cancer). Measuring and scaling these damage in relation to each other is still subject of debate. There is no direct experimental evidence from the RBE-LET relations that relates the inactivation of mammalian cells by ionising radiations to the induction of dsb's in the DNA. This could be attributed on one hand to the failure of the energy deposition parameter, such as the LET, to specify the damage and, on the other hand to the inadequacy of the measurements of damage at the molecular level.

3-1 Benchmark Data-base

It is intended here first to survey the literature for the available radiobiological data under the action of both densely and sparsely ionising radiations in mammalian cells. The various biological endpoints, cell survival, chromosome aberrations (dicentrics and rings), specific genomic mutations, oncogenic transformations and DNA ssb's and dsb's are considered. Then a database is constructed which contains the bulk information on both the radiobiological and physical details. The track structure parameters, which include the different quality radiation parameters for the primary radiation, the reduced relativistic ion speed β^2 , z^{*2}/β^2, L_T(keV/μm) , $L_{100,T}$(keV/μm), λ(nm), and the ion range R(μm) are calculated using the energy (or LET) at the centre of the target as available from the original work [Watt, 1994 ; 1996] for light and heavy ions in liquid water. As for neutrons, only the proton recoil track structure are considered (the effect of oxygen recoils are ignored as they are small in liquid water for the neutron energies of interest). The same relevant data structure parameters are calculated for the given energy in the biological target, and include L_D (keV/μm) , $L_{100,D}$ (keV/μm). For electrons and photons, track structure parameters are obtained for the equilibrium spectrum of electrons generated by the initial field [Watt, 1995 ; 1996]. The track structure calculations for heavy ions and neutrons include also the physical parameters for the δ-rays component, the maximum energy of δ-rays T_{max} (keV) and maximum range R_{max} (μm) which is a measure of the penumbra i.e. the extent of the radial distribution of δ-rays from the primary ion core. The radiobiological data include the initial and the final slopes; $\alpha(Gy^{-1})$, $\beta(Gy^{-2})$, of the dose-effect curves for survival and for other endpoints. The slopes quoted are these determined by the original authors whenever available. For other older data, linear quadratic fitting is used to determined the initial slope, $\alpha(Gy^{-1})$. The data base has been continually updated to include literature available up 1996. The physical and radiobiological data so obtained are then used to calculate the effect cross sections.

There are various ultimate objectives for building up this huge radiobiological database:

(1) to identify the main mechanisms responsible for radiation induced biological damage. This information is required for application in radiobiology and radiation protection.

(2) to examine the parameters which best express the radiation quality, and here to test the radiobiological models and their validity.

(3) to justify the basis of the St-Andrews "unified dosimetry model" by application of the biological bench-mark data for dsb's in the DNA.

3-1-2 Mathematical formulations of the effective cross-section

3-1-2-1 Cell Survival

Survivals curves for eukaryotic type, in particular mammalian cells, are generally expressed as the fraction of survival versus dose in gray. A dose of a bout 5 Gy is capable of killing any mammalian cell. The surviving fraction of non-mammalian cells are expressed as a function of the charged particle fluence ϕ in μm^{-2}. It is always a matter of practice to calculate the dose from fluence or vice versa using the charge particle fluence dose conversion relation:

$$\phi = \frac{6.25 \times 10^8 \, D(Gy)}{L_T(keV/\mu m)} \quad (cm^{-2}) \qquad 3\text{-}1$$

It is found that the prokaryotic cells are highly resistant to low dose. Possibly a few hundreds of grays are needed to inactivate them. Thus extrapolating from higher dose to lower dose is difficult to achieve particularly with shoulder type of survival [Schafer, 1980 ; Krasavin,1989]. The situation with mammalian cells is quite different. For one thing the genomic DNA is highly organised, unlike simple prokaryotic or non -mammalian cells, and the lower dose required to inactivate the cells exposed to radiation *in vitro* which is of the order of a few grays (up to 12 Gy) enable us to extrapolate to lower dose regions for the shoulder type. The role of the DNA and its complex order within the mammalian cells and the function of nuclear enzymes contribute to these differences with non mammalian cells. Although the inactivation prokaryotic cells will not contribute much to radiation protection, their

simple structure may provide basic principles related to the mechanism of cell killing. However only radiobiological data for mammalian cells could provide the objectives in the preceding section.

To extract the radiobiological data available in the literature, we need to customise a standard method of calculation. Figure 3-1 shows two types of survival curves, for sparsely ionising radiation (low LET) which is of sigmoid type, and for densely ionising radiation (high LET) which is a purely exponential relation. The nature of the shoulder in the sigmoid type could be attributed to the enzymatic repair of DNA damage [Ward, 1990]. It is assumed from observations that the associated shoulders, as shown in figure 3-1 are due to single tracks in the charged particle equilibrium spectrum [Watt, 1989].

The fraction of survival in terms of the effective cross section; σ_{eff} , as a function of the particle fluence; ϕ and time t is given by:

$$F = \exp[-\sigma_{eff}(\phi, t)\phi] \qquad 3\text{-}2$$

by taking the logarithm of both sides and differentiating, we get

$$\sigma_{eff} = -\frac{\delta(\ln F)}{\delta\phi} \qquad 3\text{-}3$$

for low fluence (low dose) at the initial slope of the survival curve, as shown in figures 3-1a and 3-1b. The total cross section, σ_{tot} is given by

$$\sigma_{tot} = -\frac{\delta(\ln F)}{\delta\phi} = \sigma_{eff} + \phi\frac{\delta\sigma_{eff}}{\delta\phi} \qquad 3\text{-}4$$

For densely ionising radiation (high LET) the last term of equation 3-4 vanishes, and the effective cross section , σ_{eff}, is equal to the initial slope ($\sigma_o = 1/\phi_{37}$). This type of curve is a simple exponential.

However, for sparsely ionising radiation, the dependence of fluence and fluence rate (the dose and dose rate) is very important. To get information on the dependence of

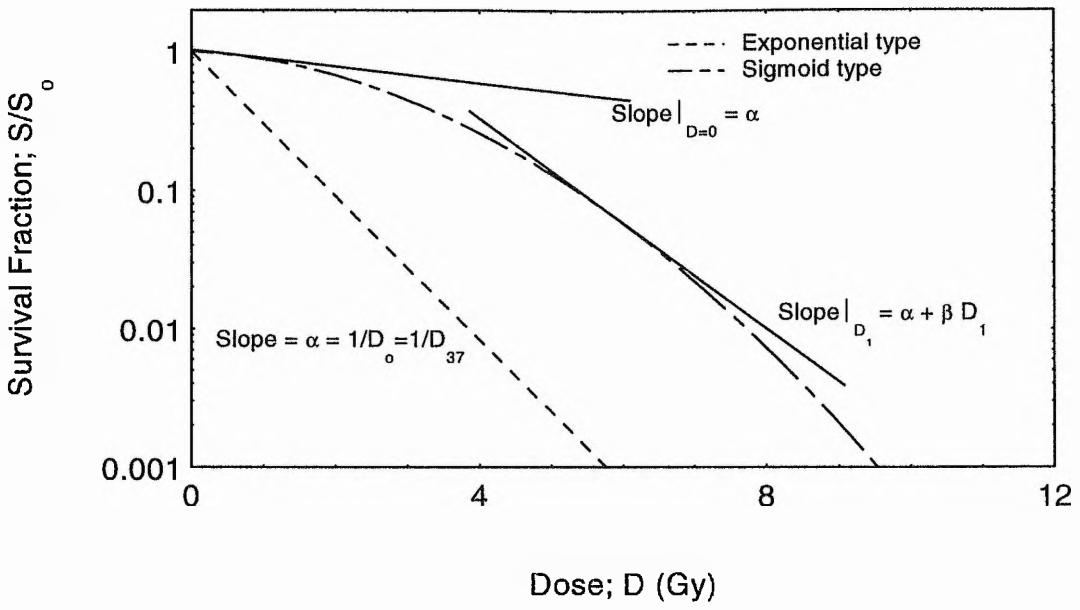

Figure 3-1a The survival fraction of sigmoid and the purely exponential types.

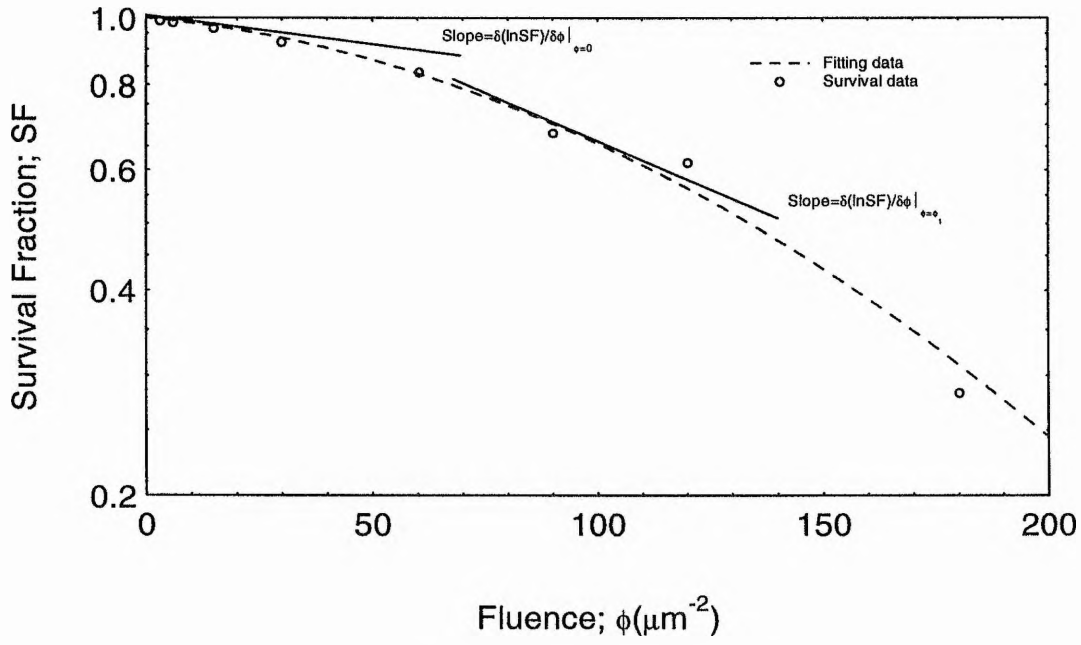

Figure 3-1b Survival fraction derived from dicentrics data expressed as a function of particle fluence. The D-T neutrons data taken from Lloyd, D.C.1984.

the effect cross-section on fluence and fluence rate, the last term in equation 3 viz. $\phi\ (\delta\sigma/\delta\phi)$, must be explored further. To do this, one must plot $\delta(\ln F)/\delta\phi$ versus ϕ for sigmoid survival curves (X-rays, γ-rays, energetic e^- and fast protons and neutrons). An illustration to that is shown in figure 3-2.

Extrapolation of the curve to zero fluence gives the effect cross-section at the initial slope. By exploring the trend with fluence we can get information on the dependence of the cross-section on fluence rate, irradiation time and deduce facts about repair rates as given in the model.

For linear quadratic fittings the survival fraction as a function of dose D, is given by:

$$F = \exp(-\alpha D + \beta D^2) \qquad 3\text{-}5$$

where α and β is the initial slope of the survival curve, β is related to the final slope. The survival fraction as a function of fluence is given by:

$$F = \exp(-\alpha'\phi + \beta'\phi^2) \qquad 3\text{-}6$$

for pure linear survival as in the case of heavy ions with high LET, the second term of both equations 3-5 and 3-6 vanish. By taking the log of equation 3-5, and differentiating with respect to both D, and ϕ we get:

$$\frac{\delta(\ln F)}{\delta D} = -(\alpha + 2\,\beta D) \qquad 3\text{-}7$$

$$\frac{\delta(\ln F)}{\delta\phi} = -(\alpha\frac{\delta D}{\delta\phi} + 2\beta D\frac{\delta D}{\delta\phi}) \qquad 3\text{-}8$$

comparing equations 3-4 and 3-8, we obtain:

$$\alpha\frac{\delta D}{\delta\phi} = \sigma_{eff} \qquad \text{and} \qquad 2\beta D\frac{\delta D}{\delta\phi} = \phi\frac{\delta\sigma_{eff}}{\delta\phi} \qquad 3\text{-}9$$

for heavy ions (high LET) $\beta = 0$, mammalian cell survival varies linearly with both dose and fluence. Using the conversion $\phi = 6.25 \times 10^8\ D/L_T$ (particles-cm^{-2}) or

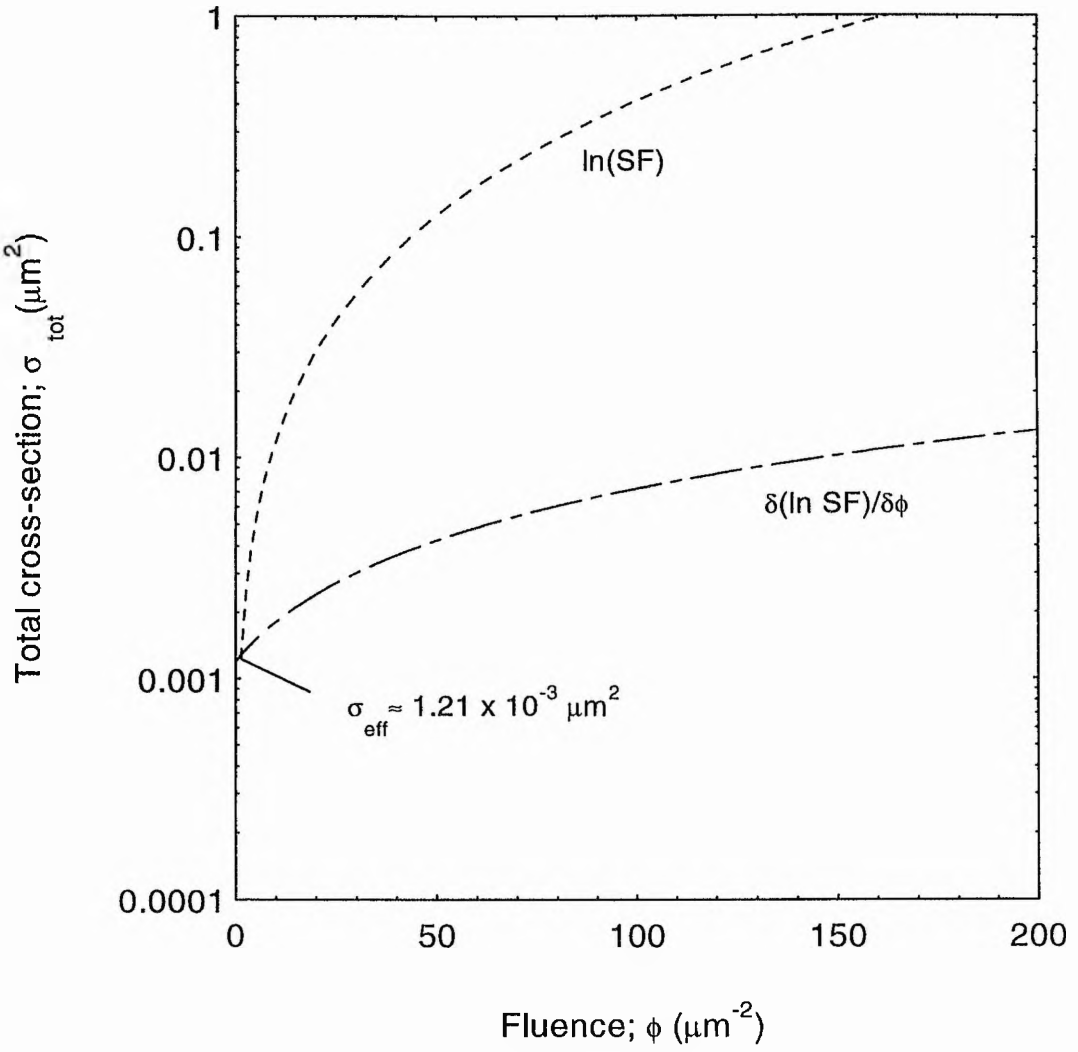

Figure 3-2 Ln(SF) for dicentric production expressed as a function of neutron fluence. The lower curve is the a derivaive of the upper curve. Data analysed using the data depicted from figure3-1b.

$\delta\phi/\delta D=6.25\ /L_T$ (particles/μm^2-Gy), and substituting this for the right hand side of the first expression of equations 3-9, we get:

$$\sigma_{eff} = \frac{\alpha \bar{L}_T}{6.25} \quad \mu m^2 \qquad 3\text{-}10$$

Equation 3-10 is valid for the initial slope for the sigmoid curve, σ_0. The initial slope α_{eff}, can be obtained directly from the dose-survival curve, as in equation 3-5, by differentiating and taking the limits as D = 0. Thus α is given by:

$$\alpha = \left.\frac{\delta(\ln F)}{\delta D}\right|_{D=0} \quad Gy^{-1} \qquad 3\text{-}11$$

3-1-2-2 Specific end-points damage per cell

As for other endpoints e.g. chromosome aberrations, transformations, and specific genomic mutations, the induced damage for a given dose of radiation are expressed as damage/cell-Gy. These specific effective cross sections can be calculated directly from the damage distributions. In literature the frequency of specific damage (e.g. mutations/cell-Gy), usually follow a linear quadratic relation with dose. Mathematically, the specific damage (SD) takes the form :

$$SD = \alpha D + \beta D^2 \quad \text{damage/cell-Gy} \qquad 3\text{-}12$$

for densely ionising radiation with high LET, equation 3-12 reduces to the linear form $SD = \alpha D$. Examples of these types of dose-effect curve are shown in figures 3-3a, and 3-3 b. The selected curves were chosen from the chromosome aberration data base, or elsewhere. The references are quoted in the figure.

3-1-2-2.1 Specific damage cross-section

The survival fraction of irradiated cells can be represented by:

$$SF = \exp(-\sigma_{eff}\ \phi) \qquad 3\text{-}13$$

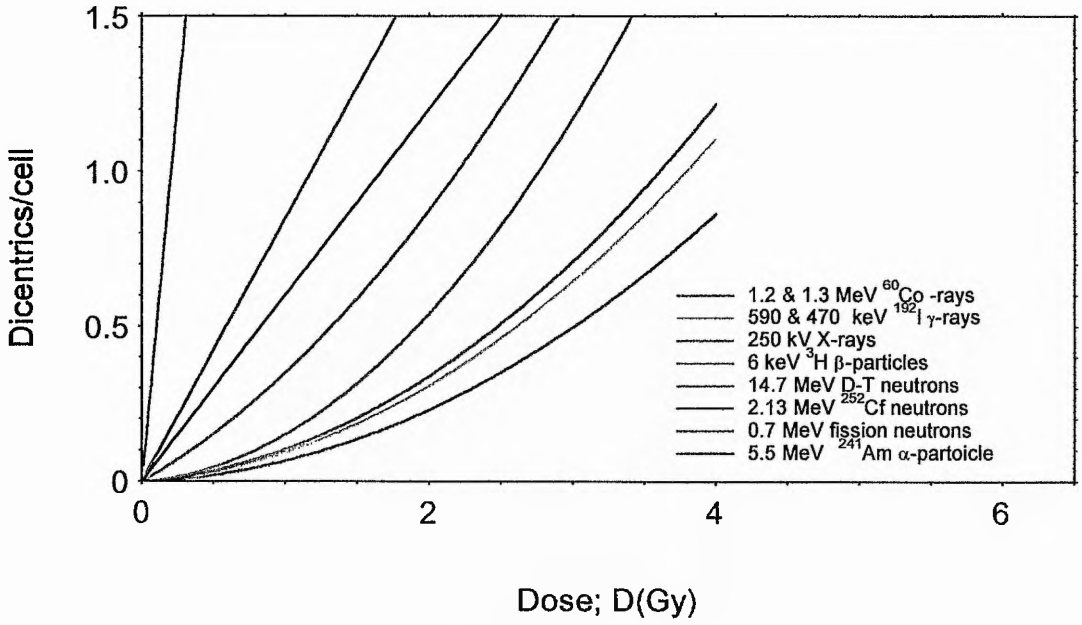

Figure 3-3a Dose-response curves for dicentric chromosome aberrations induced in human lymphocytes.

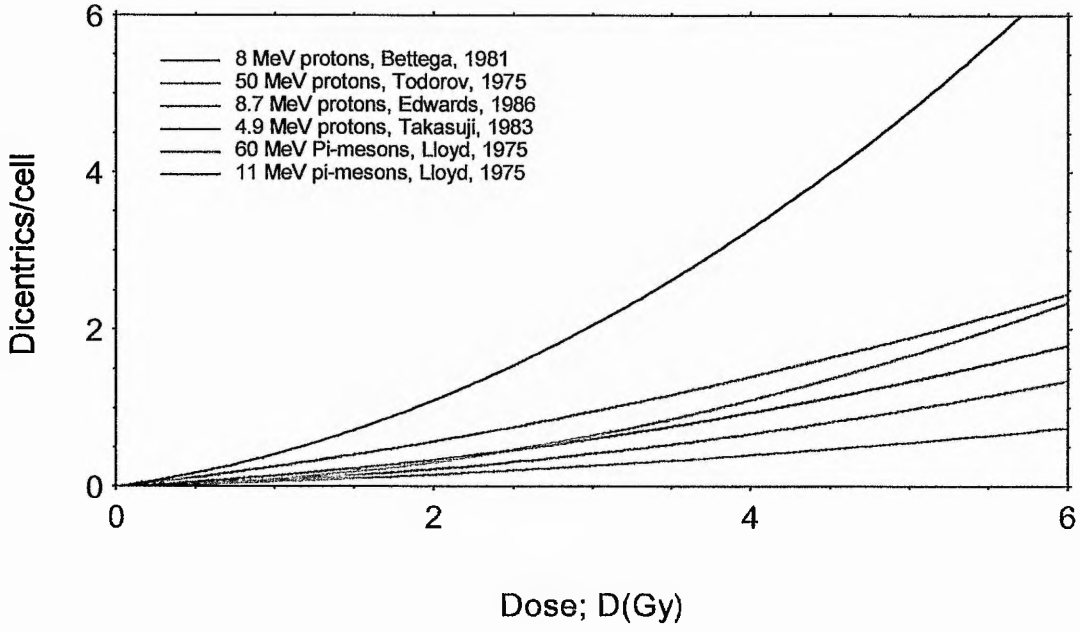

Figure 3-3b Dose-response curves for dicentric chromosme aberrations induced in human lymphocytes.

The inactivation cross-section σ_{eff} for heavy particles is constant depending on radiation and cell types, and independent of fluence (dose), whereas σ_{eff} for sparsely ionising radiation and fast particles is a function of fluence (dose) and possibly fluence rate, (dose rate), and thereby gives a sigmoid curve with shoulder. Thus for heavy ions the survival relations are given by:

$$SF = \exp(-\sigma_o \phi) \qquad 3\text{-}14$$

where $\sigma_{eff} = \sigma_o$, which is given by the relation 3-10 in the preceding section.

For low LET radiation, the fraction of cells not intercepted by tracks is given by $\exp(-\sigma_{eff} \phi)$, where σ_{eff} is the relevant damage cross-section. If we assume the initial number of cells scored by N_o, and the number of cells damaged at any time is given by N_{dam} . Then the ratio of the damaged cells will be given by:

$$\frac{N_{dam}}{N_o} = 1 - \exp(-\sigma_{eff} \phi) \qquad 3\text{-}15$$

and the inactivation cross section can be written as:

$$\sigma_{eff} = - \frac{\ln\left(1 - \frac{N_{dam}}{N_o}\right)}{\phi} \qquad 3\text{-}16$$

The fluence can be calculated from the relation:

$$\phi = 6.25 \times 10^8 \frac{D}{\bar{L}_T} \text{ particles / cm}^2 \qquad 3\text{-}17$$

Thus if we plot the specific inactivation cross-section σ_{eff} vs. the fluence; ϕ, the initial cross-section σ_o can be calculated from the intercept at zero dose (or zero fluence). The initial slope of the σ_{eff} - ϕ curve can give an indication about the dependence of other factors such as repair time, fluence rate, ..etc.

An example of the analysis of specific damage with respect to cells is shown in figure 3-1b where the dicentric frequency induced by D-T neutrons (with an average energy of 14.9 MeV, and track average $L_T \sim 7.9$ keV/μm) is used to calculate the survival fraction, which is then expressed as a function of fluence. The effective cross section at zero fluence is then determined by extrapolation, as shown in figure 3-2.

3-2 Bench-mark Data for Survival

Although DNA is considered to be the most likely lethal target in the cell nucleus, no direct experimental evidence seems to support that. However, it is believed that other biological effects such as chromosome aberrations are the cause of cell killings [Lea, 1955 ; Neary, 1965]. More direct experiments for the role of dsb's in cell killing were provided by experiments with restriction enzymes, in which ionising radiation was found to induce chromosomal abnormalities and cell death [Bryant, 1984; 1988]. Thus cell killing phenomena still, although indirectly related with DNA dsb's, forms the common background to both cytological and molecular biology.

Cells are the basic unit used to define clonogenic survivals in laboratory experiments. Clonogenic survival is defined as the ability of a single cell to give rise to a colony of cells on a petri plate. Modern radiobiological theory is based on cell survival curves, which describes the relationship between the fraction of survival of a population of radiated cells and the dose to which the cells have been exposed. There are a variety of well established lines of both normal and cancer cells, **appendix AI**. The techniques and methods of irradiating the cells and dose measurements in the cells are well developed in many radiobiological centres around the world. Cells are cultured, fed and cultivated under standard protocols. To avoid complexity related to cell cycle phases, only cells irradiated asynchronically in aerated conditions are considered here, with no chemical protectors or sensitisers present.

3-2-1 Calculation of the effective cross-section for survival

It is well accepted that the survival fraction of irradiated living cells generally follows the linear-quadratic dependence on dose (i.e. $SF = \alpha D + \beta D^2$) and a pronounced

shoulder is expected. Although these shoulders are expected with the inactivation of non-mammalian cells, even for high LET radiation, mammalian cells dominated by the linear term (SF= α D). Ordinarily, the initial slope $\alpha(Gy^{-1})$ is used to determine the effective cross section for inactivation, $\sigma(\mu m^2)$, whenever the fitting is carried out by the original authors. In older data, where fitting performed with models, the original data is used to recalculate the initial slope of the linear quadratic model. It is emphasised here that whenever the linear-quadratic model is used, it is mainly for evaluation of fitting purpose to evaluate α (Gy^{-1}) and β (Gy^{-2}).

The inactivation cross section can be evaluated using the concept in the preceding section. Thus assuming the density of water ($1gm/cm^3$) the effective cross section σ_i in μm^2 for cell inactivation is thus given by:

$$\sigma_i = \frac{L_T \alpha_i}{6.25} \quad \mu m^2 \qquad 3\text{-}18$$

The calculations of the inactivation cross sections are carried out for the different cell types (or lines), for mammalian cells in **Appendix AII**. Calculated track structure parameters are also included in the table.

3-2-2 Results and discussion

Mammalian cells unlike other lower eukaryotics or prokaryotics are of special interest in radiation protection. For one thing, although cells are irradiated *in vitro*, they seem to be the only source available in which studies at low dose exposure to radiation can be evaluated consistently. To make use of the data extracted or calculated, the inactivation cross sections, $\sigma_i(\mu m^2)$ which quantify the damage is plotted against the different quality parameters. It is thus important to specify the radiation quality parameter with which the damage is best quantified.

Figure 3-4, shown the inverse of the radiosensitivity parameter, $\alpha(Gy^{-1})$ for Chinese Hamster cells as a function of the LET. The data points are scattered and show no obvious correlation among the ions, or even the cell types. There is a general trend

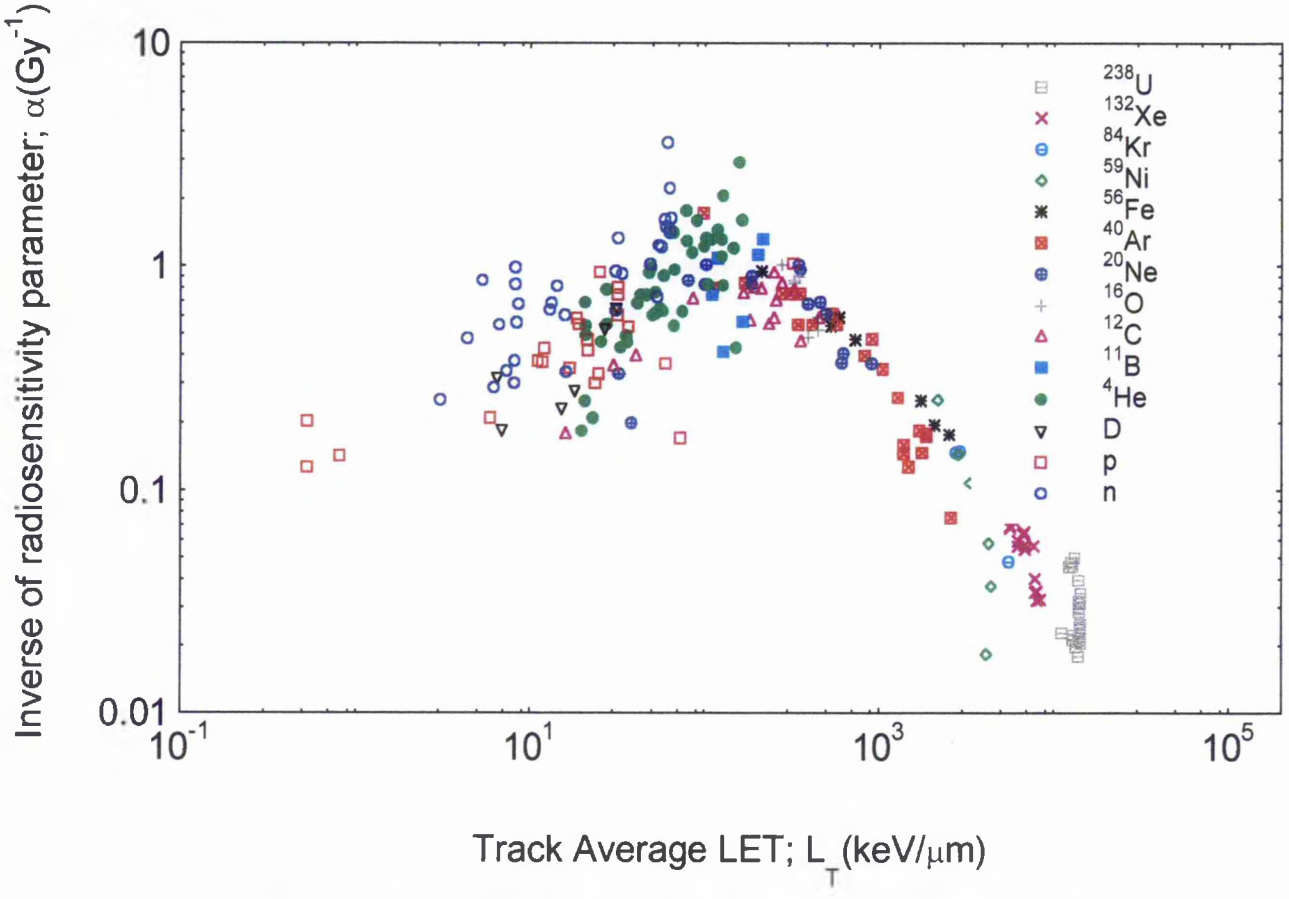

Figure 3-4 Radiosensitivity α^{-1} of hamster cells vs. track average linear energy transfer.

for the ion's inverse radiosensitivity, α_i to reach to maximum damage at about 4 Gy^{-1} between the values LET = 70 - 160 keV/μm, then there is a clear decrease which is interpreted as "overkill region". The lower part of the curve is dominated by the fluctuation of light ions The maximum region shows a concentration of ^4He, while the overkill region is dominated by heavy ions. Since RBE= $\alpha_i / \alpha_{x\text{-ray}}$, where $\alpha_{x\text{-ray}}$ is a reference for 250 kV_p X-rays, α_i is proportional to the RBE values. The poor correlation demonstrates an image of RBE-LET relationship. The same conclusion is reached for other mammalian and non-mammalian cells.

Figures 3-5, 3-6, and 3-7, demonstrate the effective cross sections for inactivation, $\sigma_i(\mu m^2)$ are related to the dose average LET, L_D(keV/μm), restricted dose average LET, $L_{D,\,100}$(keV/μm), and the ion core track structure parameter, z^{*2}/β^2. The single ion character is still shown in the σ_i-L_D relation, especially in the high LET regions and with high atomic numbers (overkill regions). For light ions, the single ion curves show an increasing linear relation (figure 3-5) up to a LET values of 100 -200 keV/mm. At higher LET values, the effective cross section seems with the distinguished-ion-pattern curves to saturate about a fixed value of 40 μm^2 for V79 cells.

At the end of the tracks, the single heavy ion curves, are characterised with the shape of hooks. This phenomena, known by Katz as "thin down", is well studied by a number of researchers [Katz, 1985 ; Kraft, 1987]. This breakdown could be attributed to the effect of the different δ-ray distributions. However with the $L_{D,\,100}$, second moment of energy parameter, the σ_i-$L_{100,D}$ seems to show a better response, and that is owing to the fact that δ-rays contribution is cut down to 100 eV. On the other hand, the ion core structure parameter z^{*2}/β^2 specify damage in the V79 cells in similar manner like the restricted LET. The inactivation cross section increases linearly with z^{*2}/β^2 up to a point at which $z^{*2}/\beta^2 \sim 3000$. The σ_i - z^{*2}/β^2 curve is shown to have a tendency to saturate at higher value z^{*2}/β^2 , however the "thin down" hooks feature this region.

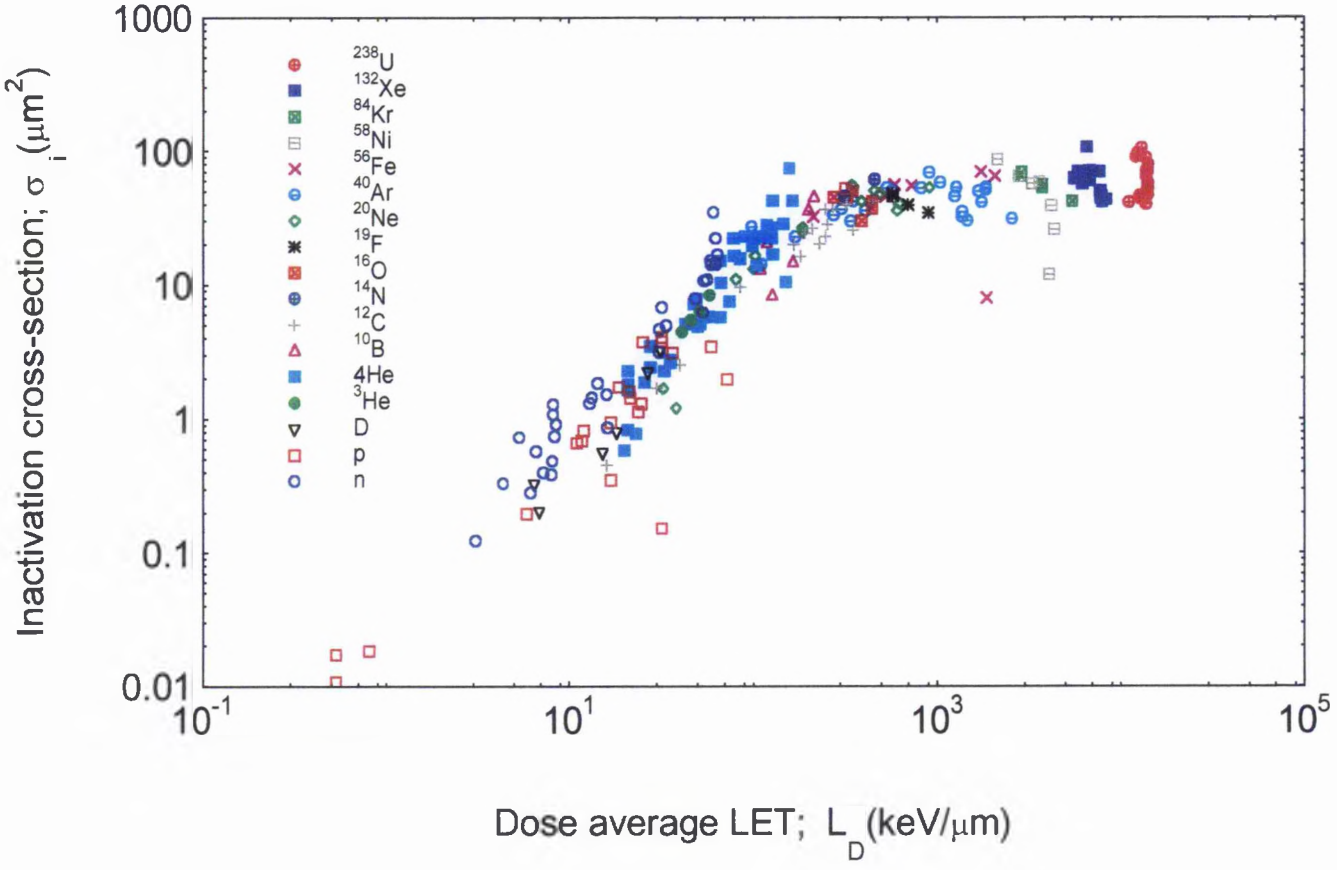

Figure 3-5 Inactivation cross-section of Chinese hamster cells vs. the dose average LET.

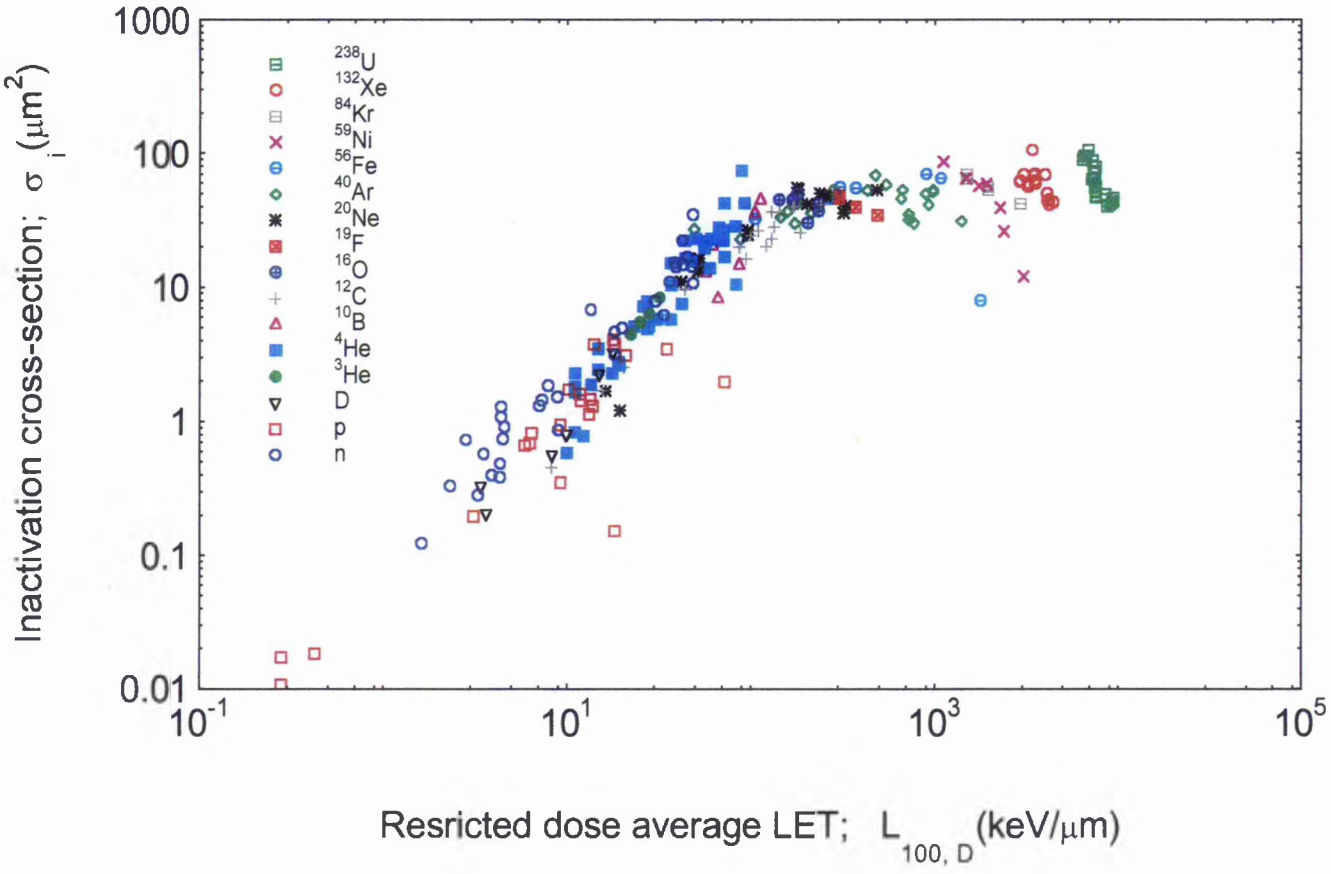

Figure 3-6 Inactivation cross section of Chinese hamster cells vs. the restricted dose average LET.

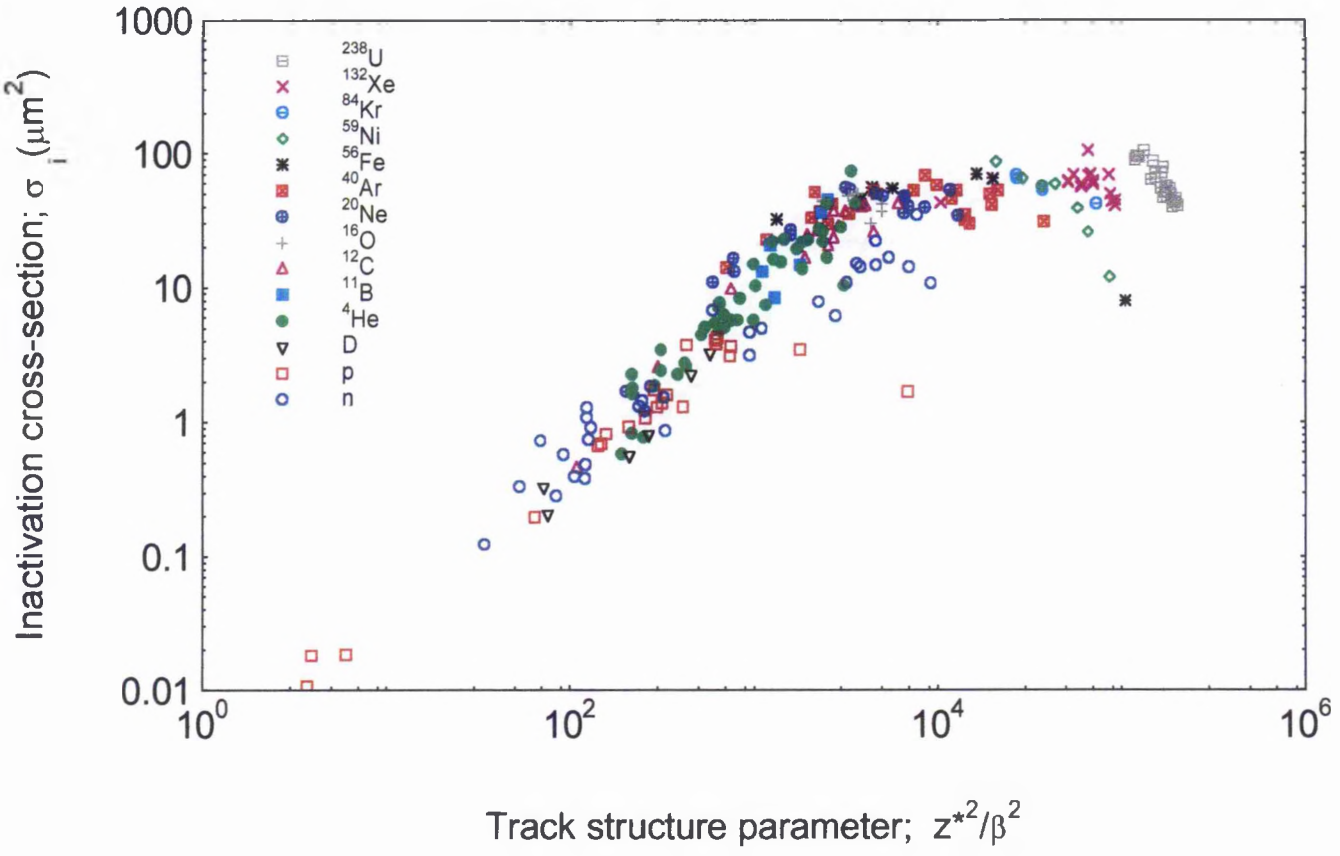

Figure 3-7 Inactivation cross-section of hamster cells vs. the track structure radiation quality parameter z^{*2}/β^2.

Figure 3-8 shows the σ_i-λ response curve of ionising radiation on V79 cells. Here the inactivation cross section is specified in term of the zeroth moment of energy (chapter 2), the mean free path for linear primary ionisation, λ(nm). The general trend of the curve σ_i-λ seems to unify the response of all radiation types (as will be seen later, a distinctive feature of this relation shows independent responses for each of sparsely ionising radiation and densely ionising radiation). The shape of the σ_i-λ curve may be divided into two parts, a pronounced saturated region and a linearly dependent region separated by an inflection point distinguished at λ_o= 1.4 nm. For λ_o< 1.4 nm, the heavy ions with high LET overkill cells, thus forming the saturation region. For V79 cells the saturation cross section is about 40 μm^2. At higher λ values (λ_o> 1.4 nm) the effective cross section increases linearly with decreasing λ until reaching the inflection point. This region is attributed to the effect of densely ionising radiation with low LET, which include light charged particles such as protons or alpha particles or neutral particles such as neutrons. Other mammalian systems show the same response, with higher saturation cross section, such as normal HF cells (67 μm^2) or cancerous C3H10T1/2 cells (240 μm^2). The reason for this variation can be related to their DNA content. However, the variation of responses of the same cell species can be related to other factors Possibly the most important is the shape of the cell during irradiation e.g. whether cells are irradiated in suspension or monolayered (The suspended cells have higher DNA number at risk than flattened cells) and the strain type e.g. V79 or T1 cells once they are subcultured they may lose their orginal identity (i.e. shape or size).

This inter-relation of σ_i and λ is found to hold for all other non-mammalian systems. This is demonstrated in figures 3-9, and 3-10 for yeast and bacteria spores. Watt and collaborators demonstrated that by employing data for single-stranded viruses and enzymes, that the effective cross section continually increases with decreasing λ. [Watt, 1989]. However with double stranded ϕ-174 (replicate form) or bacteriophage (T7) the inflection point is clearly seen at λ_o. Thus the general response of the σ_i-λ

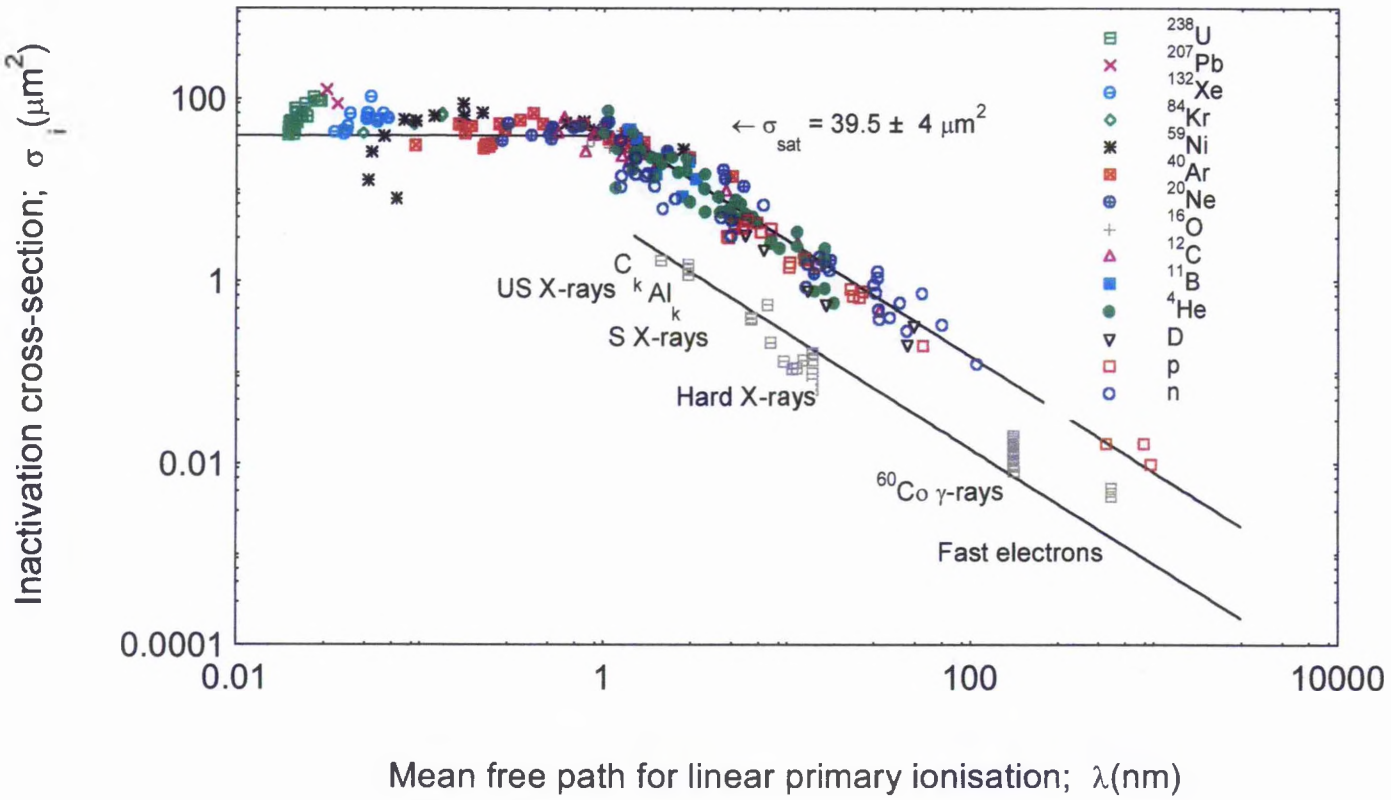

Figure 3-8 Inactivation cross-section of hamster cells vs. mean free path for linear primary ionisation. The ratio of curves at same λ is about 14.

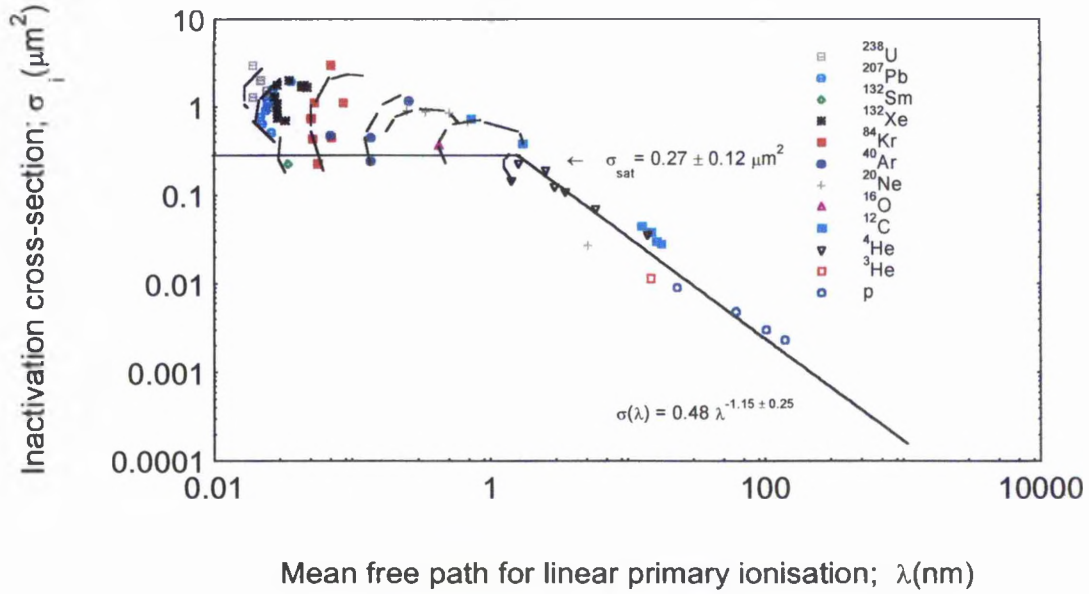

Figure 3-9 Inactivation cross-sections of Yeast (d-211 wild type) vs. mean free path for linear primary ionisation.

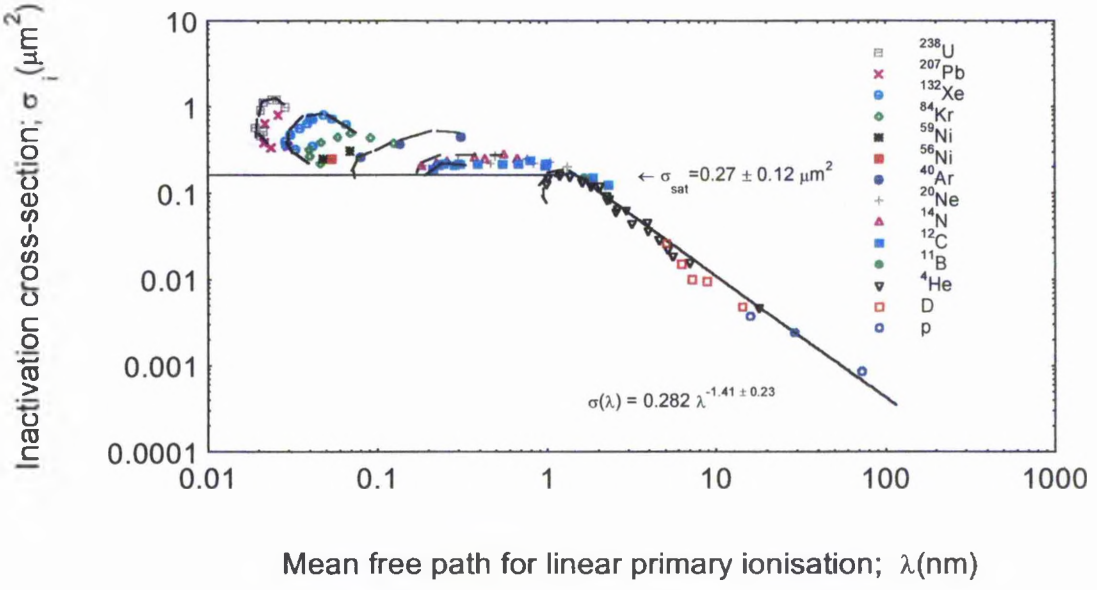

Figure 3-10 Inactivation cross-section of Bacillus subtilis vs. the mean free path for linear primary ionisation.

curve which includes the saturation region, shows a direct dependence on the double stranded DNA content in the cell.

At the saturation region (for $\lambda < \lambda_o$) in mammalian cells, heavy ions with high LET overkill cells. Based on energy deposition principles, these heavy ions in association with high specific ionisations, can create clusters all over the genomic DNA. These clusters can break both sugar phosphate strands in all the chromosomes in the cell. Thus the association of the mean free path of linear primary ionisation with the double strand inter-spacing distance of the DNA is quite clear. It is at this molecular distance that the breaks are involved. At the lower part of the σ_t-λ , or to be specific at $\lambda > \lambda_o$, less dsb's in the DNA are induced by the ionising radiation and thus there is higher probability of survival enzymatic repair processes.

In mammalian cells the geometric cross section is always significantly greater than the saturation cross sections. For example V79 has a saturation cross section of about 40 μm^2 while its geometrical cross section of about 100 μm^2. However for non-mammalian cells (including both prokaryotic or lower eukaryotic cells) the geometrical cross section could of the same order (or less). The ratio of the geometrical cross section to effective cross section, σ_g / σ_i gives an estimate to the number of track(s) that inactivate the cell. Thus, an average of 2-3 tracks is needed to inactivate a mammalian cell, and an average of 1 track is needed to inactivate non-mammalian cells. In this sense, the saturation region is characterised by fewer tracks and a larger number of DNA dsb's, while the linear part of the σ_t-λ is associated with larger number of tracks but fewer DNA dsb's.

For sparsely ionising radiation, the σ_t-λ shape is preserved, however the response is less than that of the densely ionising radiation. The lower sensitivity of this radiation is demonstrated in figure 3-8. It can be seen clearly that the saturation region can never be established with hard X-rays, γ-rays or energetic electrons, but the ultra soft C_k X-rays is very close to the expected inflection point at $\lambda_o = 1.4$ nm. Thus only the linear part of the σ_t-λ response can be is characterised by sparsely ionising radiation.

Hard X-rays, γ-rays and fast electrons are more penetrating than soft X-rays, thus they induce less ionisations. This is seen clearly as the inactivation cross section decreases in that order. The variation of the inactivation cross section for the same ionising particle gives an indication of the dose rate effect e.g. γ-rays in figure 3-8. With this it is easy to realise the misconceptual practise to compare hard X-rays with γ-rays for the calculation of RBE e.g. 250 kV_p and ^{60}Co γ-rays since both quantities have different effect levels (and different LET spectrum), unless using different level of dose rate (very high dose rate for X-rays, and very low dose rate for γ-rays).

The densely ionising radiation is found to be effective by about 15 times the effect of sparsely ionising radiation. This multiplicity effect can be related to the number of DNA segment at risk for the densely ionising radiation compared with that for the sparsely ionising radiation. The damage specification of the mean free path for linear primary ionisation, λ, in the inter-molecular domain reveals this fact. This will be further elicited in the next chapter.

To illustrate some of the features of the σ_i-λ response in mammalian cells, light particles such as protons, will never achieve saturation. The protons, of energy of 80 keV and LET_{max}= 83 keV/μm (Bragg peak), will reach to the highest effective cross section at λ = 1.3 nm. With energy lower than 80 keV (lower LET), the inactivation cross section will decrease because of the proton's shorter range (R<1.4 μm) , in fact some will not be able penetrate the cell nucleus. Thus protons will never reach saturation. However, heavier charged particles, such as alpha particles with energy of 800 keV, and LET_{max}= 230 keV/μm (Bragg peak) will reach saturation at a higher energy of about E = 4 MeV. Thus biological damage at the cellular level are much clearer when they are specified by the mean free path of linear primary ionisation, λ . On the light of the forgoing discussion, it is easy to verify whether a charged particle would inactivate the cell or overkill it. Whereas the use of LET to specify the damage (e.g. RBE-LET) could lead to misinterpretation. This illustrates how some results of clonogenic survival at some of the radiobiological laboratories, because of some experimental errors, in their analyses the RBE decreases at much lower energies than

80 keV [Belli, 1989 ; 1993]. The experimental resolution of this confusion clarified later at another laboratory using the logic of track structure [Folkard, 1996]. With the sense of the σ_t-λ interpretation this confusion could have been cleared up immediately. Figure 3-8 illustrates this arguments.

On the other hand, neutrons will interact with the biological cell nucleus mainly via proton recoil, thus they act just like other light charged particles. As with protons, neutrons can produce saturation damage in the mammalian cells (the reach maximum LET at around $\lambda \sim 2$ nm).

On the light of σ_t-λ relation, a model known as "the St-Andrews unified model" is suggested [Watt, 1989]. The response of all ions seems to follow a universal path characterised by a linear relation between the effect cross section $\sigma_{eff}(\mu m)$, and the mean free path of linear primary ionisation, λ(nm). The basis of this model relies on the molecular scale and the geometry of the DNA (e.g. the DNA interstrand spacing; 1.8 nm, or the space between two conjugate bases; 0.34 nm). Thus the mechanism requires only that the spacing of interactions along the particle track matches that of the mean chord distance through a DNA segment, and at least two interactions coincide with each opposite strand. For sparsely ionising radiation the attack of the oxygen radical species provide the mean interactions at one strand, while the secondary electrons would provide the other [Siddiqi, 1987]. The number of DNA segment at risk in both cases is different, and thus different scales of damage are observed, this is revealed and depicted by the σ_t-λ relation. The elements of this model will be discussed later (Chapter 4).

3-3 Chromosome Aberrations Benchmark Data

Ionising radiation can induce lethal damage to chromosomes. This damage is classified into two types. The first is asymmetrical chromosome-type exchange such as interstitial deletions (dicentrics and centric rings) and usually leads to cell death. The second is symmetrical type (inversions or reciprocal translocations) which are fairly stable and could participate in the late effects of radiation.

Lea, 1955 suggested a theory for chromosome breaks by ionising radiation. The theory outline that chromosome breaks resulted from a cluster of ionisation caused by a single particle track. Later, Neary, 1967 proposed that the primary lesion in a chromosome is activated by an ionising event in a structure of nanometer dimensions. On the basis of the molecular DNA, it has been suggested that there is a link between a DNA dsb's misrepair and chromosomal aberrations of mammalian cells [Helbig, 1995]. This is further elaborated on the basis of the rejoining two dsb's occurred in different chromosomes to form dicentric and an eccentric fragments [Hall, 1994]. The rejoining could also be as a symmetric type which is not lethal but it may activate an oncogene which is related to late effects.

The techniques of cytogenetic experiments, involving the induction of chromosome aberrations in human lymphocytes by ionising radiation, were well established in the 1960s [Bender, 1962]. Cell preparation and irradiation (at G_o) techniques are carried out so that the damaged chromosomes can only be observed in the condensed form in their early metaphase. Although recent technology offers new methods for detecting chromosome aberrations e.g. chromosome painting technique via fluorescence *in situ* hybridization (FISH) [Weir, 1991], but the data in the literature are very limited.

Lymphocytes chromosome aberrations may be classified as stable or unstable. The unstable aberrations include pericentric inversions and translocations, their instability prevent them from being particularly useful for dosimetric purposes. The stable aberrations include dicentrics, centric rings, and acentrics. The reported maximum background frequencies (Y_o) or dicentrics and acentrics aberrations for healthy individuals are $(1.25 \pm 0.25) \times 10^{-3}$ aberrations/cell and $(3.3 \pm 0.4) \times 10^{-3}$ dicentrics/cell respectively [Bauchinger, 1995 ; Mettler, 1985]. Generally dicentric abnormalities are considered to be the harmful type leading to cell death [Lea, 1955; Puck, 1960]. Figures 3-3a and 3-3b show the dose-response curves for the induction of chromosome dicentrics in human lymphocytes [Dufrain, 1980]. With high LET the responses of ionising radiation on lymphocytes are expected to be linearly correlated with dose, whereas with low-LET the relationship is non-linear.

This can be seen quite clearly even for 8 and 50 MeV protons in figure 3-3b [Todorov, 1975 ; Bettega, 1981].

3-3-1 Calculation of the effective cross -section for chromosome aberrations

The frequencies of dicentrics/cell Y is generally related to dose D by the linear quadratic relation:

$$Y = Y_o + \alpha_Y D + \beta_Y D^2 \qquad 3\text{-}19$$

where Y_o is the frequency of spontaneous dicentrics, α_Y is the initial slope (dicentrics/cell-Gy) and β_Y is the coefficient of the quadratic term (dicentrics/cell-Gy^2). The initial slope α_Y is used to calculate the dicentric effective cross section for the induction of dicentrics in chromosomes, σ_Y which is given by:

$$\sigma_Y = \frac{L_T \alpha_Y}{6.25} \quad \mu m^2 \qquad 3\text{-}20$$

The radiobiological data for induction of chromosome aberrations along with calculated effective cross-sections σ_Y are given in **Appendix AIII**. The relevant calculated track structure parameters are also included.

3-3-2 Results and discussion

The effect cross-section, σ_Y for the induction of chromosome dicentrics by ionising radiations is plotted against the various quality parameters. Figures 3-11, 3-12, and 3-13 show the σ_Y-L_D, σ_Y-$L_{100,D}$, and σ_Y-(z^{*2}/β^2) relations. It can be seen that the situation here is quite different from that for inactivation. As the target is getting smaller, the effect of δ-rays will be enhanced. Naturally, these δ-rays would not contribute to local damage, hence their contribution will be outside of the critical target (the chromosomes). Thus the dose average LET, L_D will not be the appropriate parameter to specify the quality of chromosome damage (dicentrics). However the other quality parameters, the restricted dose average LET, $L_{100,D}$, and

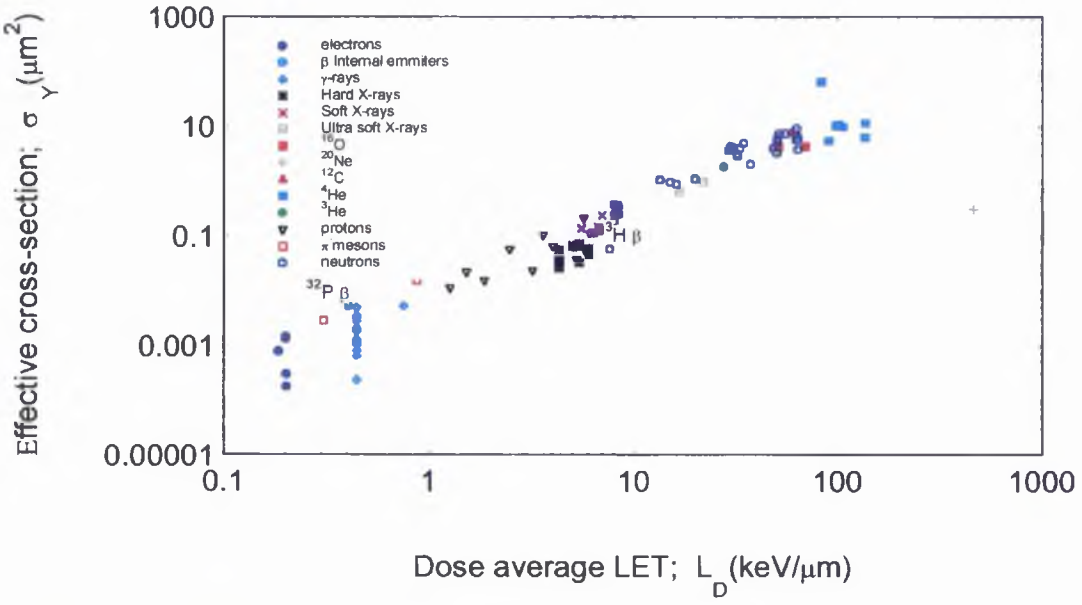

Figure 3-11 Effective cross-section for dicentric induction in human lymphocytes vs. dose average LET.

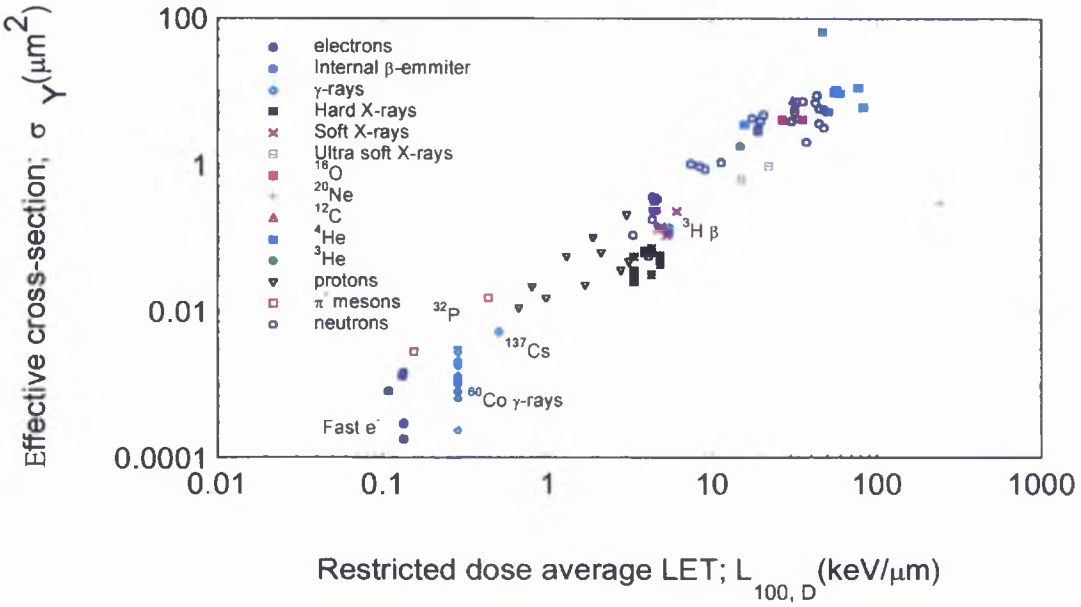

Figure 3-12 Effective cross-section for dicentric induction in human lymphocytes vs. restricted dose average LET.

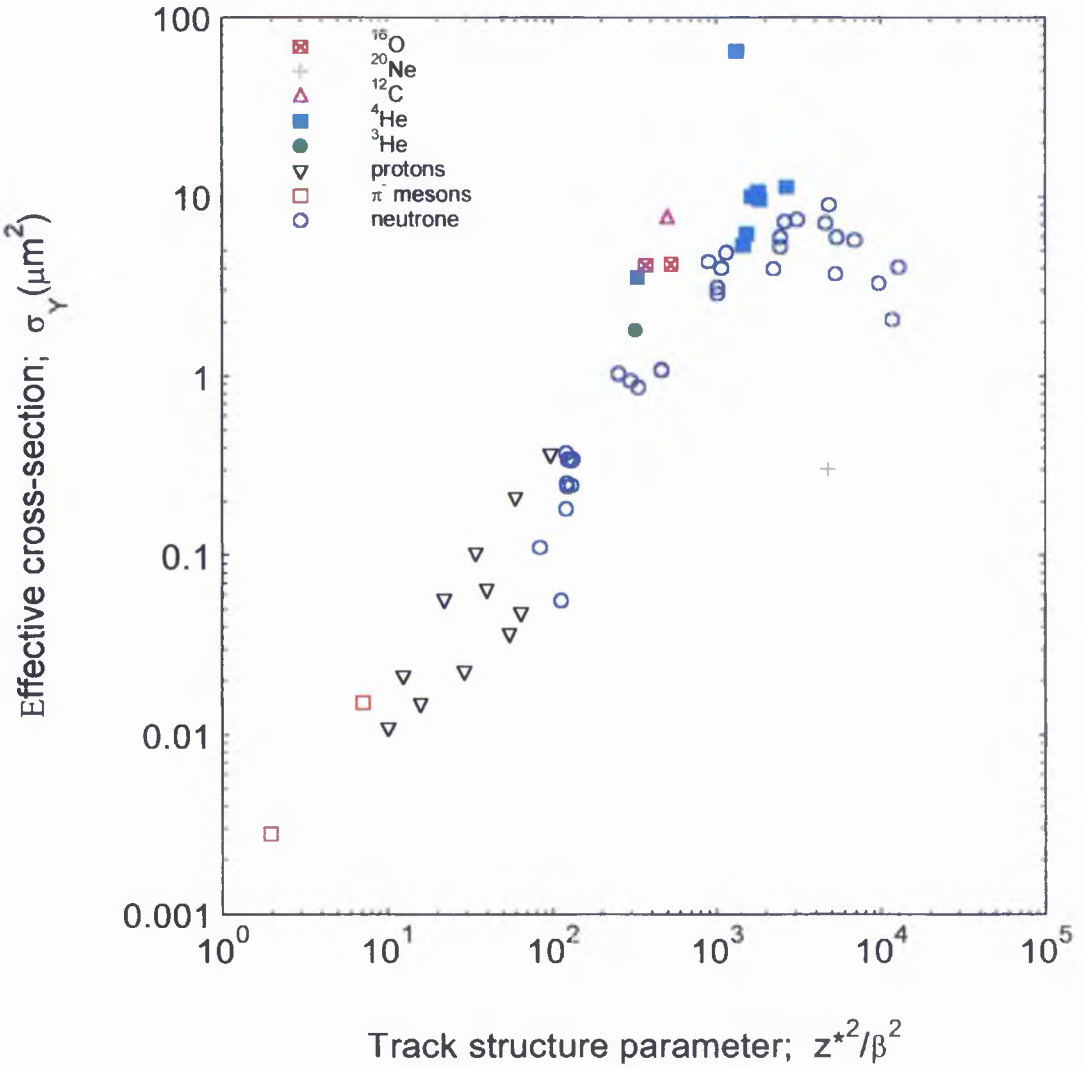

Figure 3-13 Effective cross section for dicentric induction in human lymphocytes vs. track structure parameter z^{*2}/β^2.

z^{*2}/β^2 as explain earlier in the previous section, show a reduction in contribution to the effect of these secondary electron, consequently better representation are obtained.

Figure 3-14 shows σ_Y vs. the mean free path for linear primary ionisation, λ . Unlike the other parameters, λ is still showing its capability to specify the damage better than other parameters. The light ions, including protons and alpha particles, fit quite well except for a few data points. This includes 7.4 , 8.7, and 16.5 MeV protons [Bocian, 1973 ; Edwards, 1986 ; Rimpl, 1990] with underestimated $\alpha(Gy^{-1})$ values, thus leading to lower effective cross sections. With the only set of heavy ion data available in the literature [Edwards, 1994], overestimation of $\alpha(Gy^{-1})$ values have been observed. This includes the two ^{16}O , and ^{12}C ions and the 23.3 MeV α-particle [Takatsuji, 1984] and ^{251}Am α-particle (5.6 MeV) which have $\alpha_Y = 4.9\ Gy^{-1}$ [Duffrain, 1979]. These observed results would lead to higher values of effective cross sections than expected particularly the last data of Dufrain which results in a cross section of about 65 μm^2 (about the size of cell nucleus). An exceptional observation for heavy ion interactions is the ^{20}Ne ion [Edwards, 1994] which can not penetrate the nucleus because of its short range (0.7 μm) thus it falls far below the saturation cross section. On the other hand neutrons were found to respond like other charged particles in the σ_Y–λ plot. This last result is expected, since neutrons would interact with biological material mainly via its recoiled protons. An underestimated $\alpha(Gy^{-1})$ value is found for the of the 16 MeV neutron, thus a lower effective cross section is also observed [Barjaktarovic, 1980].

Like the cell survival σ_1–λ relation, the effective cross-section, σ_Y for dicentrics seems to show a similar trend but with lower response. For $\lambda > 1.5$ nm, the effect cross section σ_Y decreases with increasing λ. This includes almost all the proton data (lower than Bragg peak), π–mesons, neutrons and alpha particles. Neutrons will decrease in response at λ at about 2 nm, however alpha particles do achieve saturation at $\lambda \leq 1.5$ nm. Although with the very few data available at $\lambda < 1.5$ nm, a

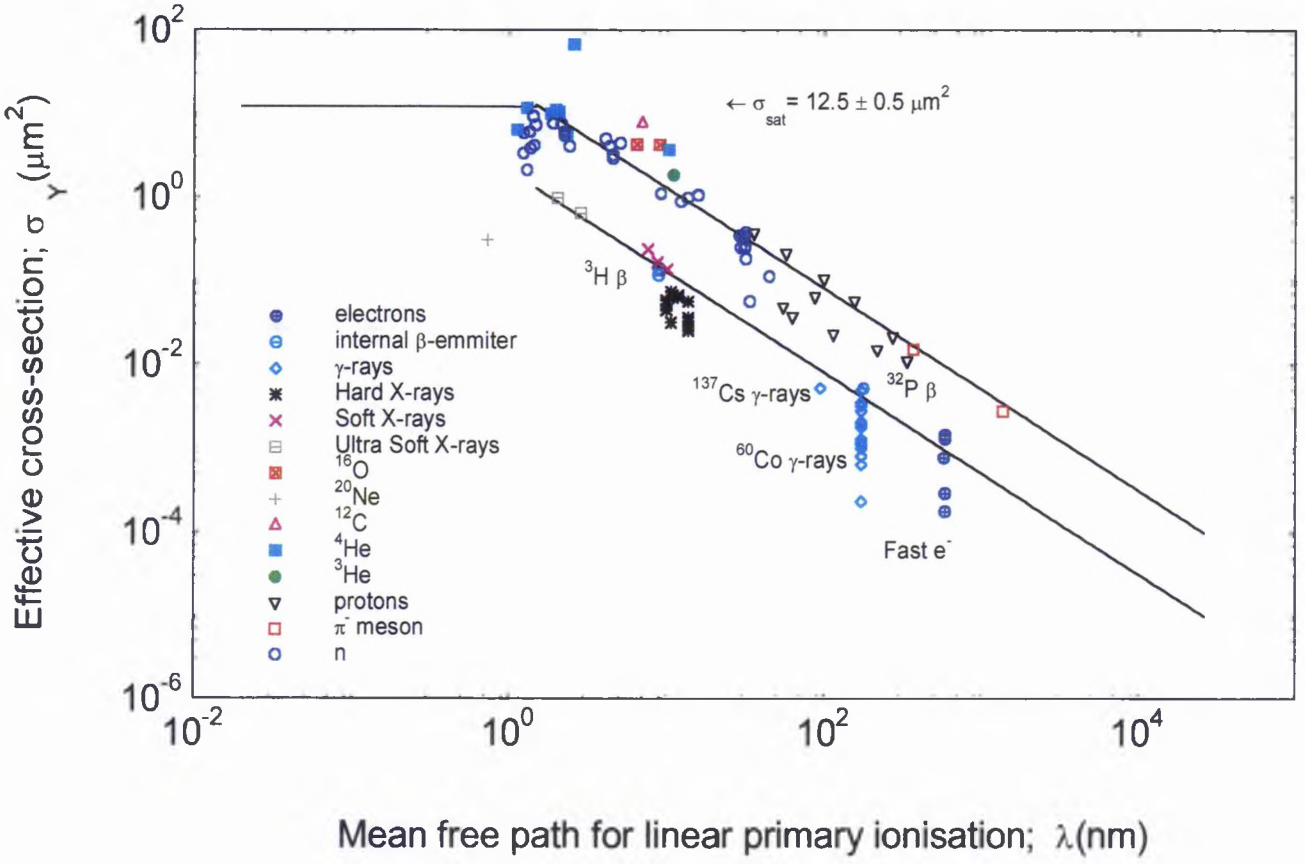

Figure 3-14 Effective cross-section for induction of dicentrics in human lymphocytes vs. mean free path for linear primary ionisation. The ratio of the curves at the same λ is about 11.

saturation region is expected. The saturation cross-section for dicentrics is estimated to be about σ_{sat} =12.5 μm^2. Since the human chromosome has an average size of 130 Mbp, the geometrical cross-section of this chromosome is expected to be about 0.25 μm^2 (estimated from equation 2-18). Thus the total geometrical cross-section (of 46 chromosomes observed at metaphase) will be roughly about 11.5 μm^2. This crude calculation agrees with the resulting saturation cross-section for dicentric induction.

Figure 3-14, shows that σ_Y-λ curve by densely ionising radiation, is higher by 10 folds than that of sparsely ionising radiation ($\sigma_{Y,\ ions}/\sigma_{Y,\ photons}$ = 10 ± 2.5). Like survival, US X-rays are seen to be more effective than any other energetic photons or electrons. Here with σ_Y-λ response for sparsely ionising radiation, incorporated radioactive nuclides seems to fit within the domain of other radiations. Incorporated ^3H β– emitter shows a much higher probability to induce dicentrics than incorporated ^{32}P β-emitter but not as closely effective as with US C_k X-rays. Thus the σ_Y-λ provides means to unify all sparsely ionising radiations just as it does for densely ionising radiations, which include energetic electrons (E > 1 MeV), energetic photons (γ-rays from ^{60}Co, and ^{137}Cs), X-rays (Characteristic and hard X-rays) and incorporated radioactive β-emitters.

One final conclusion should be made in relation to the ratio of the saturation cross-section for dicentric induction to the saturation cross-section for cell inactivation in human lymphocytes. Using saturation cross-sections of responses to heavy ions, σ_Y/σ_i is estimated to be about 1/4. This may be related to the suspected requirement that two double strand breaks (pairwise lesions) are required to produce relevant chromosome damage such as dicentrics [Harder, 1987]. Then the probability for inducing this damage will be equivalent to 2^2.

3-4 Mutations Benchmark Data

Ionising radiation produces a range of damage in DNA, including base modification, ssb's and dsb's breaks of the DNA, and apyrimidinic (AP) sites [Ward, 1988]. These types of damage may result in mutations if they are not repaired with fidelity. Mutation types could be as simple as point mutations, which results of in a mismatch of single base pairs, and as complex as alterations or deletion of larger expressions in specific genes or loci in chromosomes. Despite much work, the molecular mechanisms by which ionising radiation mutates DNA are not well understood. Several studies and techniques have been employed to examine mutations induced by ionising radiation, in specific genes of mammalian cells. One of the well established techniques is associated with cellular deficiency in the purine salvage pathway enzyme hypoxanthine-guanine phosphoribosyl transferase (HGPRT), located on the long arm of X chromosome (q26). The lack of HGPRT is measured by means of the cell resistance to cytotoxic purine analogue 6-thioguanine, (TG) [Cox, 1978]. Based on analysis in the molecular domain, HGPRT mutations classified as partial gene deletion which mainly involve low LET radiation, or full gene deletion which mainly involve high LET radiation [Stoll, 1995].

The HGPRT assay system has been in use by a variety of groups [Cox, 1979 ; Munson, 1979 ; Thacker, 1979 ; Kronenberg, 1989 ; Kranert, 1990 ; Belli, 1992]. Other assays for mutation induction is related to Thymidine Kinase (TK) deficiency in human B-lymphoblastoid cell lines [Kronenberg, 1989 ; 1991], Adenine phosoribosyl-transfears (APRT), and dihydrofolate reductase (DFFR). Different standard protocols for measuring these deficiencies are adopted. The molecular size and locations of these enzymes are included in table 3-1 [Sankaranarayanan, 1991].

Table 3-1 Common mutation assay systems in mammalian cells, their location, size (regions that they span in the genomic DNA).

Mutation loci	cells or line	Location (No-Portion)	Size (kbp)
HGPRT	Mouse Human	 X -q26	34 44
APRT	Hamster Human	16 -q24 3 -p	2.5
TK	Mouse Human	5 17 -q23	 12.9
DHFR	Hamster	5	30

3-4-1 Calculation of effective cross-section for mutations

The mutation frequency M (mutations/cell) is generally a varying as linear-quadratic function of dose and is given by:

$$M = M_0 + \alpha D + \beta D^2 \qquad 3\text{-}21$$

where M_0 , the spontaneous mutation frequency, which is in the range of 2.5 - 4.2 x 10^{-6} mutations/cell [Ward, 1995], α_M is the initial slope (mutations/cell-Gy) and β_M is the coefficient of the quadratic term (mutations/cell-Gy^2). This relation generally holds for sparsely ionising radiation for most mammalian cells. The linear dependency of mutation frequency is revealed for heavy ions. For human lymphocytes the mutation frequency is always linear i.e. $M = \alpha_M D$, with all kinds of ionising radiations [Cox, 1977]. The initial slope α_M of equation 3-21 is used to calculate the effective cross section for mutation induction which is given by:

$$\sigma_M = \frac{L_T \alpha_M}{6.25} \ \mu m^2 \qquad 3\text{-}22$$

Appendix AIV includes most of the published initial slope data, along with the calculated track structure parameters and the effective cross-section σ_M.

3-4-2 Results and discussion

The effective cross-section for HGPRT mutations in mammalian cells (V79 and HF) is tested against the various quality parameters, this is shown in figures 3-15, 3-16, 3-17. Although, it is difficult to draw any definite conclusion due to the few data available with HF, the general trends when compared with the V79 mutation data seems to a show similar response.

The σ_M-L_T relation, as depicted from figure 3-15, is characterised by a single curve, which is well-defined for heavy ions and high LET. At high LET, prediction of the mutation cross section becomes highly uncertain. This is because of the inclusion of δ-rays in the contribution to damage in the saturation region. As for the σ_M-$L_{100\,D}$ relation, as shown in figure 3-16, nothing changes about the shape as compared to full specification of the dose average LET, except for the shift of $L_{100,D}$, and the little reduction in the δ-ray contribution. Figure 3-17 shows the effect cross section for HGPRT induction defined by the ion core parameter z^{*2}/β^2 for V79 cells. The relation seems to show the same single-ion characterisation. In fact the appropriateness of single parameters such as ion specific energies, LET or even z^{*2}/β^2 to represent radiation quality parameters is less for mutations than inactivation [Kranert, 1992 ; Stoll, 1996; Cucinotta, 1995 ; Katz, 1996].

On the other hand, the mean free path for linear primary ionisation, λ(nm) seems to unify the general trends in behaviour for mutation as they do with inactivation data. This is illustrated in figures 3-18a, 3-18b. Like inactivation cross sections, with heavy charged particles on V79, an inflection point is revealed in the σ_M-λ graph at λ_o = 1.4 nm. For higher λ > 1.4 nm, the effective cross section decreases as λ increases with a gradient of about -1.33. In this region neutrons preserve the same identity as other charged particles. It must be emphasised again that light particles such as protons and neutrons can never achieve to saturation. As λ becomes shorter (< 1.4 nm) there is still some fluctuation in the effective cross section. This could be related to the degree of uncertainties in measurements of mutation frequencies, bearing in mind that the effect of δ-rays is more pronounced in this region than in cell inactivation.

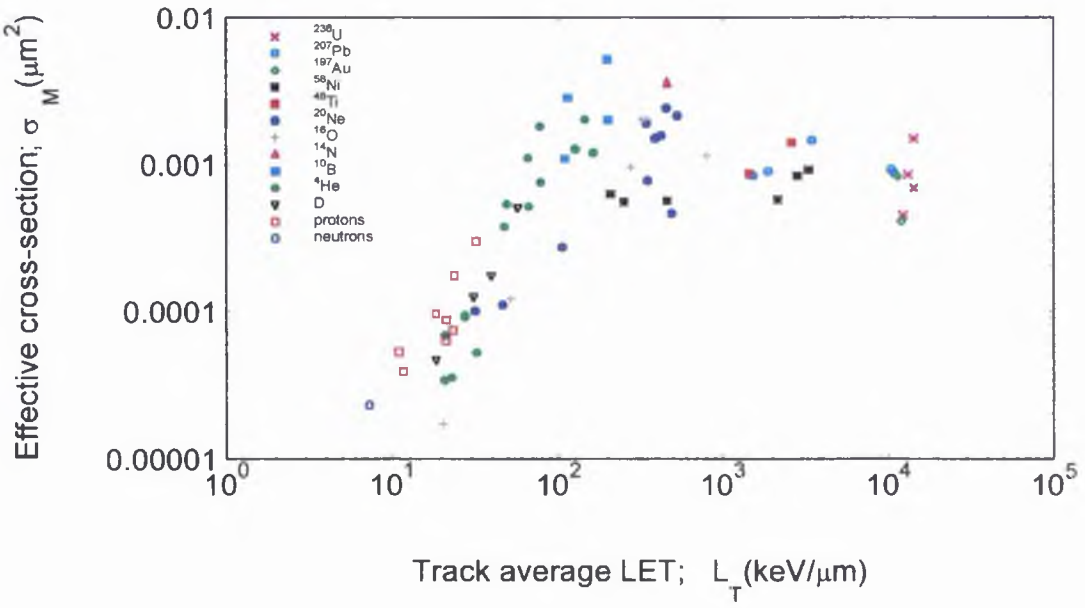

Figure 3-15 Effective cross-section for induction of HPRT mutations in V79 cells vs. the track average LET.

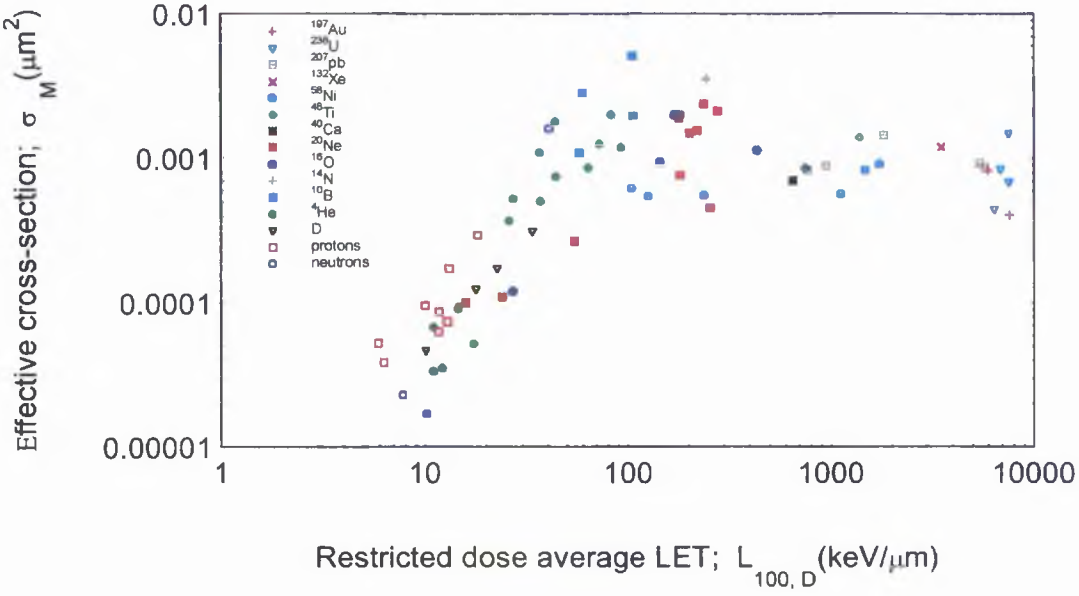

Figure 3-16 Effective cross-section for induction of HPRT mutations in V79 cells vs. the restricted dose average LET.

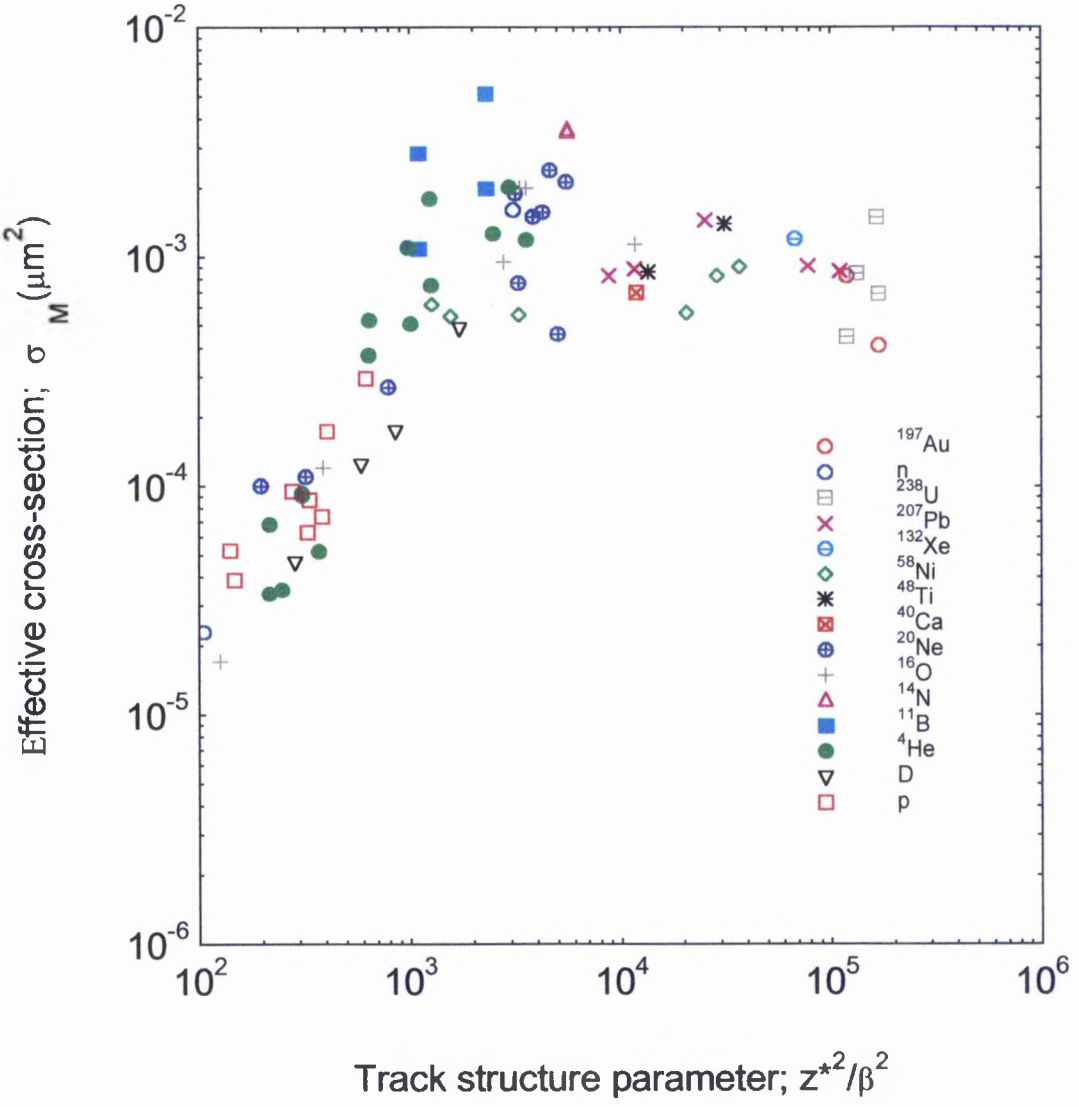

Figure 3-17 The effective cross section for induction of HPRT mutations by ionising radiation in V79 cells vs. the ion core track structure parameter z^{*2}/β^2.

Total deletion of the HGPRT genes is expected in this region. In support of these results, based on table 3-1, the geometric cross section of the 44 kb HGPRT gene is estimated (assuming condensed phase sphere) to be about 1.20 x 10^{-3} μm^2 which is slightly above the saturation cross section obtained for heavy ions in the V79 cells. This is a rather crude estimate and is intended to be used only for comparison of trends.

The restricted dose average LET is also preserved as a good parameter compared to the LET. This is because the effect of δ-rays has been restricted to the action of those less than 100 eV.

Also shown in figure 3-18 are the effect cross sections of sparsely ionising radiation which have their particular curve. It is expected that these radiations characterised by their low LET, would have a lower effective cross section than heavy ions. From figure 3-18 heavy ions are seen to be about 20 times more effective than photons (or electrons) at the same λ (in non saturation region). Unlike the situation with RBE-LET curves (or the σ-LET relation) in which sparsely ionising radiation used as a reference (RBE=1) e.g. 250 KVp X-rays or ^{60}Co γ-rays, this relation ceased to exist with the σ–λ relation. The ultra soft C_k X-rays again is get closer to the saturation region than any other sparsely ionising radiation. This is due to the short range of the induced charged particles in equilibrium (electrons) which have ranges of ~ 7 nm which is within the order of the chromatin fibre diameter (30 nm). Hard X-rays or γ-rays which lie at the middle and end of the linear part of the σ_M-λ curve (λ > 1.4 nm) induce longer range charged electrons, which may escape the chromatin fibre matrix and induce partial deletions of the HGPRT gene only when indirect action of radiation is substantial. Thus C_k X-rays are expected to at least induce partial deletion of the HGPRT gene and consequently more tracks are needed to do that than is the case with heavy ions. Al_k X-rays produce electrons having a range of about 70 nm. Thus they are relatively less efficient than C_k X-rays in inducing DNA dsb's, thus less deletion of the HGPRT gene would be expected. Thus generally the frequency of full deletions is higher with high LET as compared with lower LET.

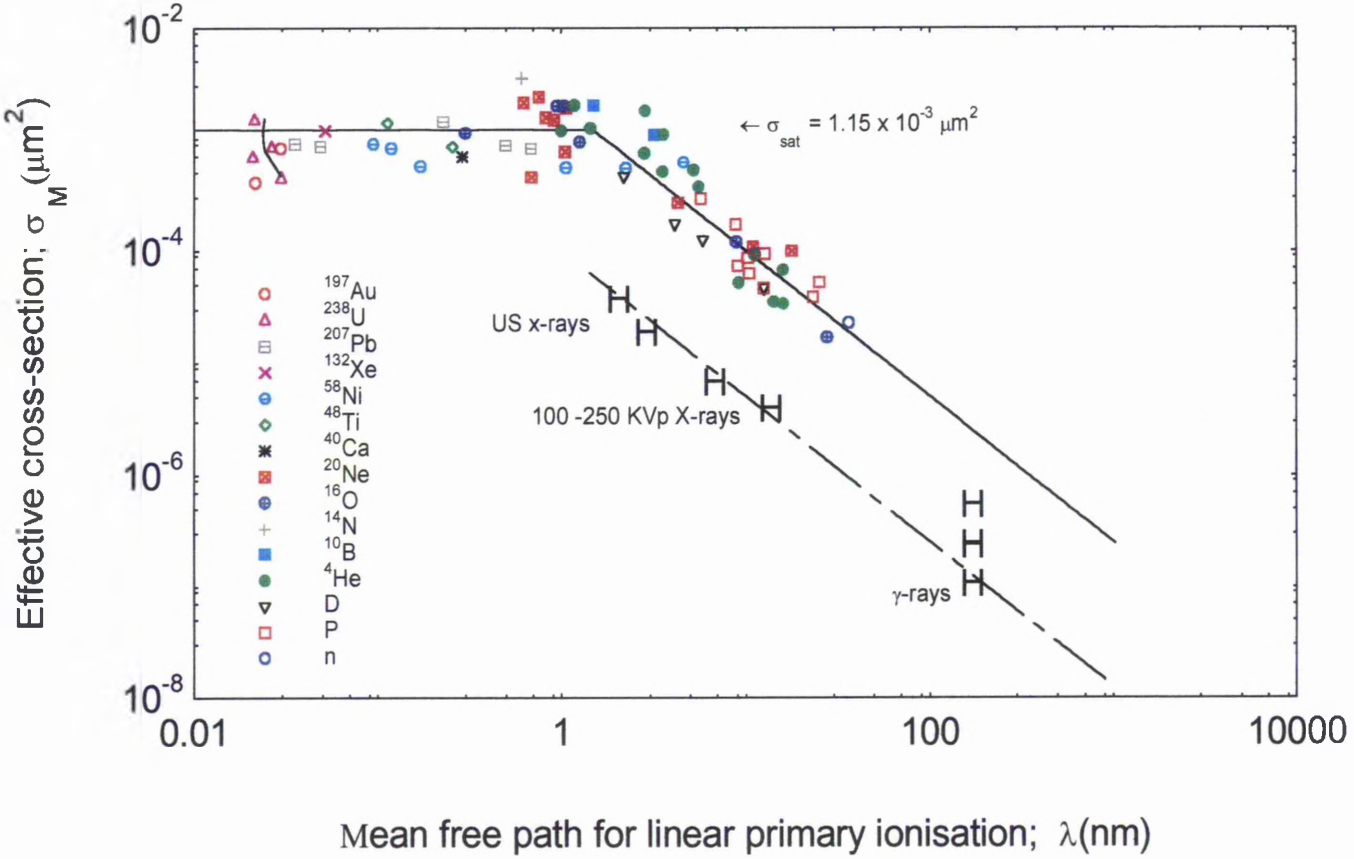

Figure 3-18a Effective cross-section for induction of HPRT mutations in V79 cells vs. the mean free path for linear primary ionisation. The ratio of the upper to the lower curve at the same λ is about 15–20.

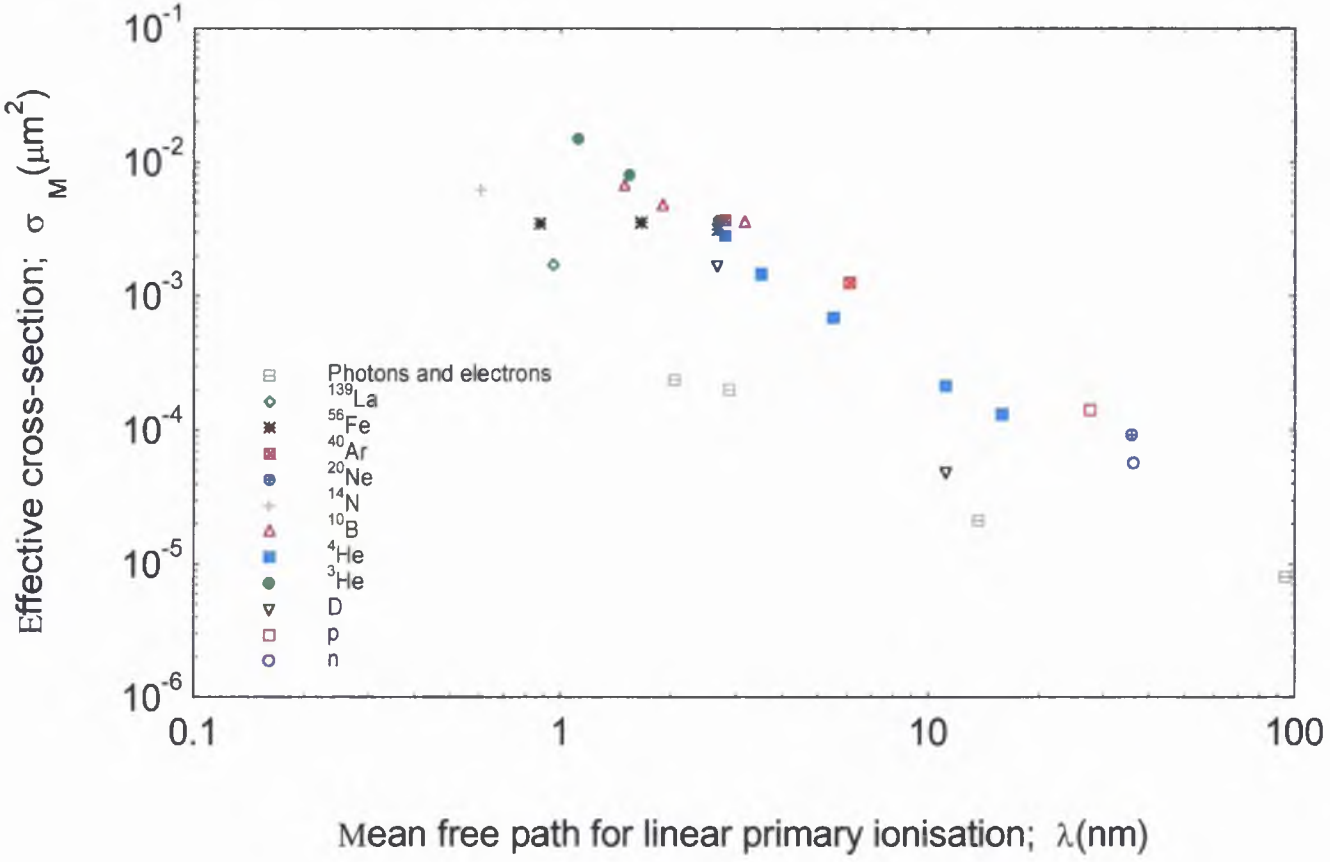

Figure 3-18b Effective cross-section for induction of HPRT mutations in HF cells vs. mean free path for linear primary ionisation.

The foundations of partial and full deletions of specific gene mutations by ionising radiations needed to be verified experimentally at the molecular scale.

Although less data of HGPRT mutation induced by ionising radiation in human fibroblasts (HF) are available than that of V79 (especially in the saturation region), the effective cross section for mutation induction, σ_M of HF is seen to be slightly higher than in V79 cells. The saturation cross section of HF is expected to be about $4 \times 10^{-3}\ \mu m^2$, and the shape of σ_M-λ curve is preserved.

3-5 In vitro Oncogenic Transformation Benchmark

Low doses 0.001 to 0.01Gy are of great concern in radiation protection for public exposure to ionising radiations in vicinity of power plants or within the routine use of medical diagnostics or therapy. It is quite hard to asses the effects of ionising radiation in the region of a lower limit of 0.001Gy, however, it is generally assumed that the linear extrapolation from higher doses to lower doses in single acute exposure can accurately estimate the risk of low dose ionising radiation. Although the exposure of the public to ionising radiation in practical situations can not be considered as a single acute dose, nevertheless the single acute extrapolated low dose can be considered as an upper limit for risk estimate at low doses. The epidemiological data of carcinogenesis from atomic bomb survivals can not be used to estimate the risk because of the complexity involved in analysis of the mixed radiation field. Furthermore, the stochastic nature of these effects may have originated from other chemical and environmental agents. For these various reasons it is thought that assessment of oncogenic transformation provide a good means of estimating the risk of ionising radiation in low dose regions.

Most published work involving *in vitro* transformations has been either performed with primary cultures or with two established lines of Syrian hamster embryos which are directly descendent from the cells *in situ*. The primary cells consist of diploid cells, and have a finite life span. Once the plated cell suspension is treated with radiation or chemical agents, incubated for two weeks to allow colony formation, then

fixed and stained, the transformed clones can be distinguished from the normal clones by their morphology. The spontaneous transformation rate is below 10^{-6} transformations/cell-Gy [Hall, 1981]. For the established cell lines, the same technique of culturing is used except for a longer incubation time to allow sufficient growth after irradiation (usually 6 weeks). The observed spontaneous transformation increases with the frequency of subculturing. Survival measurements are usually carried out for two weeks incubation after irradiation. The most widely used established cell lines for transformation studies are the C3H3T3 and C3H10T1/2. The last is considered to be the most suitable for low-dose studies because of its low spontaneous transformation frequency. By using this assay, it is found that linear extrapolation from higher doses to lower doses for sparsely ionising radiation (or dose rate dependent ionising radiation) does not accurately predict the transformation incidence for smaller single doses.

3-5-1 Calculation of oncogenic-transformation effective cross-section

The oncogenic frequencies per cell, G is generally a linear quadratic dose dependence. The relation is given by:

$$G = G_o + \alpha_G D + \beta_G D^2 \quad \text{oncogenes / cell} \qquad 3\text{-}23$$

where G_o is the spontaneous frequency (below 10^{-6} oncogenes/cell). The oncogenic cross section is related to the initial slope α_G (oncogenes/Gy) and the track average LET by the relation:

$$\sigma_G = \frac{\alpha_G L_T}{6.25} \quad \mu m^2 \qquad 3\text{-}24$$

Radiobiological data which include the initial slope and effective cross section for the induction of oncogenic transformations in C3H10T1/2 cells are tabulated in **Appendix AV**. Also the calculated track structure parameters for the relevant interacting ionising radiations are included in the table.

3-5-2 Results and discussion:

The inactivation cross section of C3H10T1/2 for ionising radiation, plotted as a function of the mean free path for linear primary ionisation, λ is shown in figure 3-19. The hypersensitivity of this cancerous cells are shown to be more persistent than other mammalian cells. The effective cross sections for induction of oncogenic transformations by heavy ions in C3H10T1/2 cells, σ_G, is plotted against various quality parameters (L_D, $L_{100,D}$, and z^{*2}/β^2). These are shown in figures 3-20, 3-21, 3-22. Despite the large uncertainties of the experimental data, no unique correlation were found with these quality parameters.

Figure 3-23 shows σ_G as a function of λ. The heavy ions show the same general trends as they do with the other end-points discussed in the preceding sections. This conclusion is withdrawn, despite that some data points are found to have smaller cross-sections which is caused by underestimation of the oncogenes per viable cells [Hei, 1988 ; Bettega, 1990 ; 1992]. As concluded earlier, a similar relation is found between the oncogenic effective cross-sections, σ_G, and the mean free path for linear primary ionisation, λ . A saturated damage of $\sigma_{sat,G} = 3.93 \times 10^{-2}$ μm^2 is seen as $\lambda \leq 1.4$ nm. For $\lambda > 1.4$ nm, the curve has a gradient of about -1.33. This relation demonstrates the role of damage in the molecular scale, and may imply the influential role of DNA breaks, presumably DNA dsb's, to induce the oncogenes.

On the other hand photons have their own unique σ_G–λ curve (figure 3-23). Again, this shows that sparsely ionising radiation is less effective in inducing oncogenic transformations than densely ionising particles. The C_k ultra-soft X-rays are seen to approach the inflection point at $\lambda = 1.4$ nm, and the corresponding saturation, if seen, would be about 1.13×10^{-4} μm^2. Thus, the σ–λ curve decreases with the same gradient as observed for heavy ions and includes both hard X-rays and γ-rays.

Heavy ions are seen to be about 52 times more effective than photons in inactivating C3H10T1/2 cells, and by about 450 times that of photons for the induction of oncogenic transformations. The genomic damage (oncogenes) involved in the oncogenic

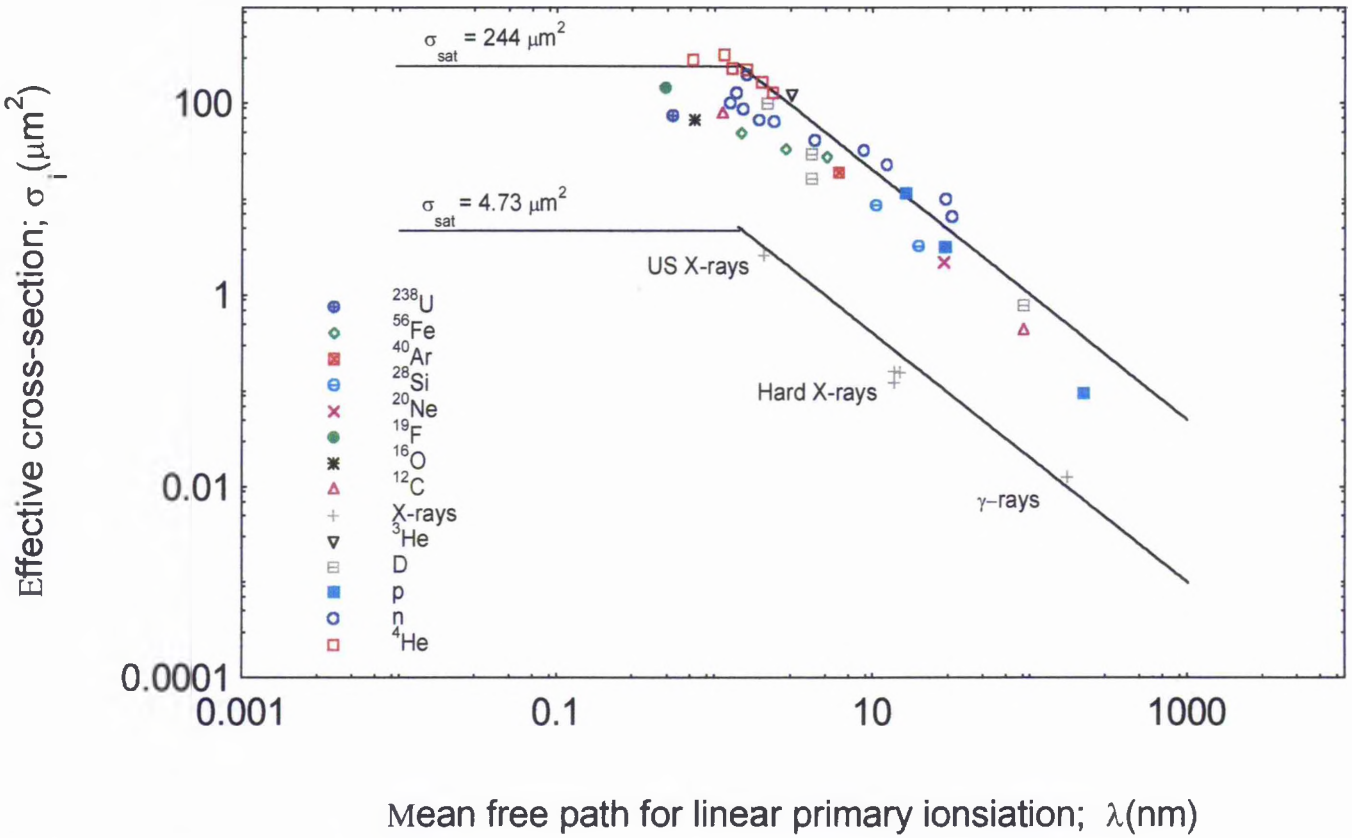

Figure 3-19 Inactivation cross section of C3H10T1/2 vs. mean free path for linear primary ionisation. The ratio of the upper curve to the lower curve at the same λ is about 52.

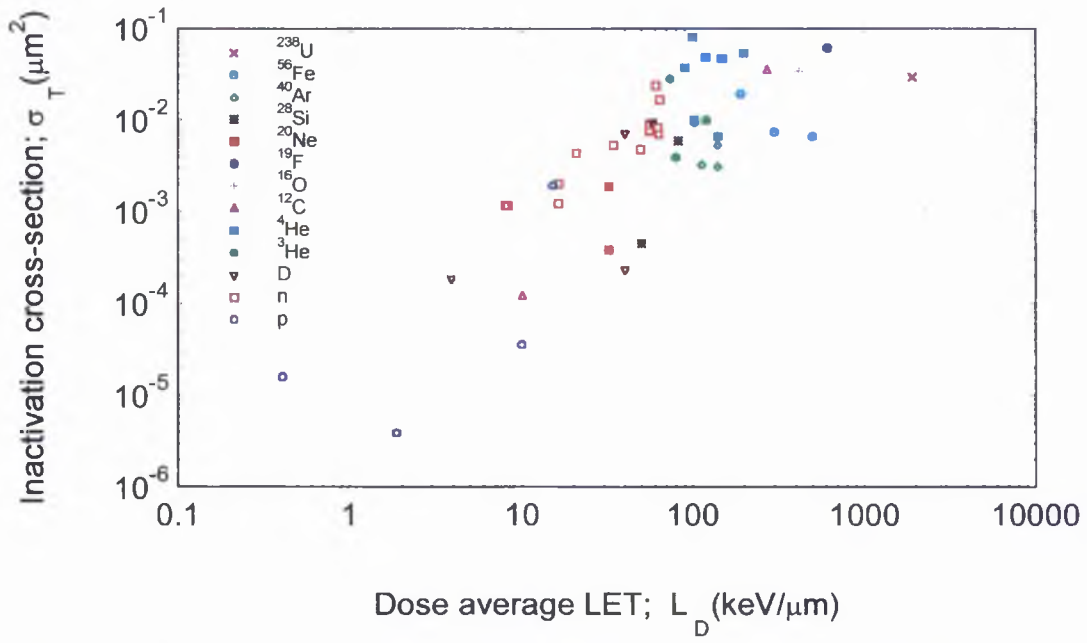

Figure 3-20 Effective cross-section for induction of oncogenic transformations in C3H10T1/2 cells vs. the dose average LET.

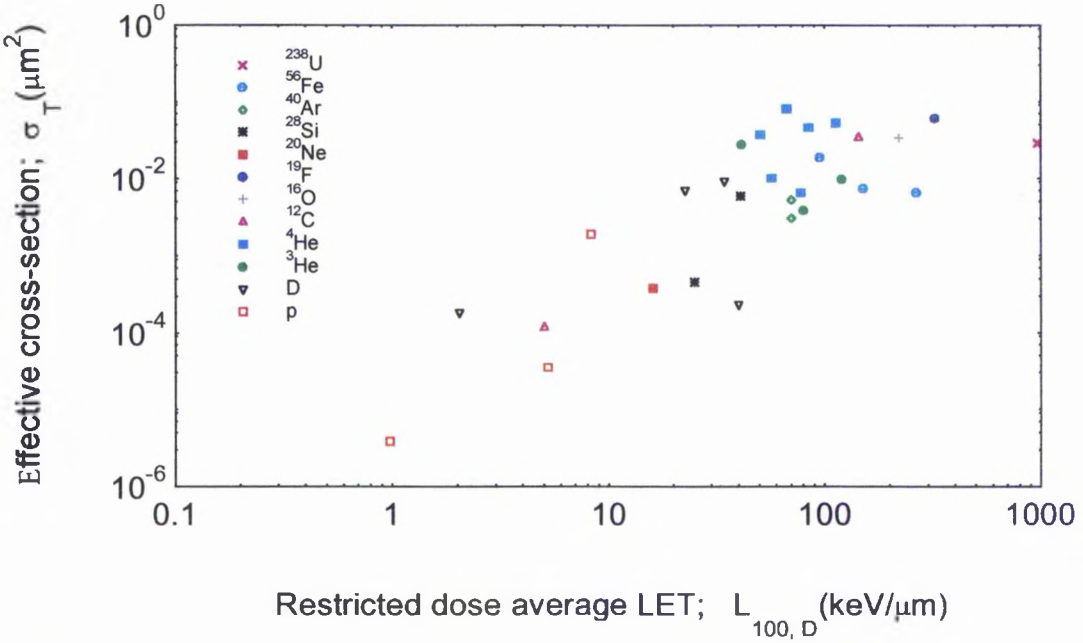

Figure 3-21 Effective cross-section for induction of oncogenic transformations in C3H10T1/2 cells vs. restricted dose average LET.

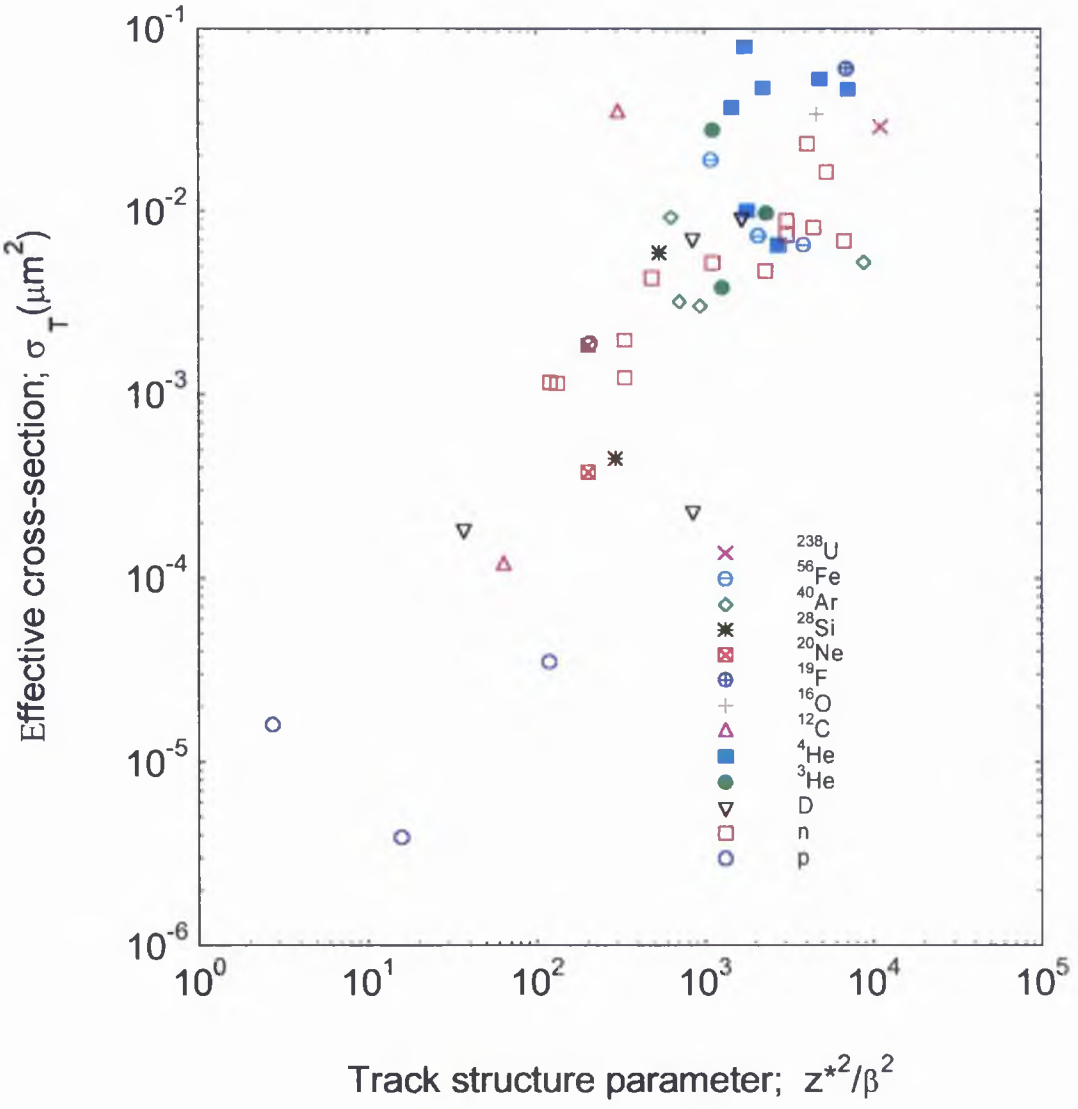

Figure 3-22 Effective cross-section for induction of oncogenic transformations in C3H10T1/2 cells vs. the track structure parameter z^{*2}/β^2.

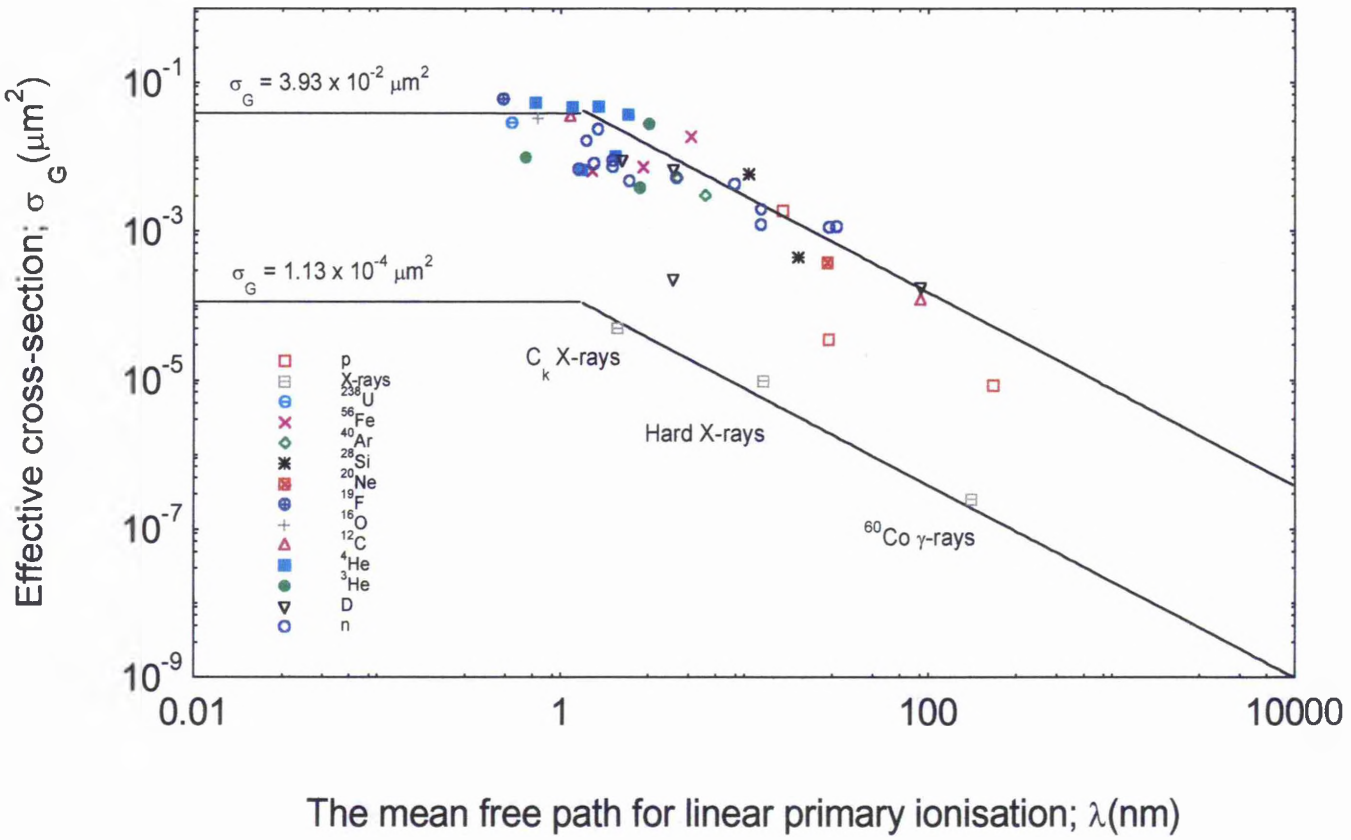

Figure 3-23 Effective cross section for the induction of oncogenic transformations in C3H10T1/2 cells vs. the mean free path for linear primary ionisation, λ. The ratio of the cross-sections at same λ is 450.

transformations, which may lead to cancer or cell death, can be estimated in terms of base pairs (bps). With the assumption that the genome has a condensed spherical shape, and using the formula 2-18 in chapter 2, the size of the genes are estimated to be as much as 8 Mbp's for saturation damage by heavy ions, but only much smaller genes of about 1.2 kbp's for the ultra soft photons. Of course the types and exact sizes of these genes can be found experimentally in the molecular scale. However the size calculated here, within the experimental errors gives only a crude estimate to be used only for comparison.

3-6 Risk Scaling Factors of Biological Damage with respect to Cell Death

One way to obtain a better insight into the mechanism of radiation action inducing cell death is the investigation of the biological effectiveness of different radiation qualities in producing various types of endpoint effects in mammalian cells. Several attempts, based on the RBE-LET relationship, compare various specific types of biological damage with cell survival. Those include studies with chromosome aberrations produced by a wide range of energetic ions with various LET's [Skarsgard, 1967], HGPRT mutations [Cox, 1979], oncogenic transformations [Miller, 1995 ; 1995], and even DNA dsb's [Kampf, 1983]. No simple relation, to correlate the specific damage to cell inactivation, has yet been found.

Here, based on the analysis of results from the foregoing sections, it has been found that the mean free path for linear primary ionisation can specify the damage significantly much better than any of the other quality parameters applied. Radiation damage is found to have the same interdependence on λ if damage is expressed in the form of cross-sections, e.g. common features are the same inflection point, and saturation characteristics of the densely ionising radiation (DIR). The saturation cross-sections, $\sigma_{sat}(\mu m^2)$ for the different endpoints on mammalian cells (V79, human lymphocytes, C3H10T1/2), and the gradient for the linear portion of the $\sigma-\lambda$ relationship are summarised in table 3-2. If we assume that sparsely ionising radiation (SIR) can induce damage in the saturation region, via very low energy

electrons e.g. auger electrons, then the same inflection point is expected as for the heavy ions. The anticipated cross-sections at the point of inflection of SIR are included in table 3-2.

Table 3-2 The fitting parameters of $\sigma-\lambda$ response curves for the different endpoints studied in the preceding sections. This includes their inflection points gradients and saturation cross sections.

End point	RT	λ_o(nm)	$\sigma_{sat}(\mu m^2)$	Gradient
Inactivation (V79)	DIR SIR	1.40 ± 0.5	39.5 ± 4 3.20	-1.27 ± 0.12
Inactivation (C3H10T1/2)	DIR SIR	1.30 ± 0.6	244 ± 20 4.73	-1.31 ± 0.15
Inactivation (Human cells)	DIR SIR	1.46 ± 0.4	70 ± 6.5 11.6	-1.37 ± 0.2
Dicentrics (H.Lymphocytes)	DIR SIR	1.46 ± 0.4	12.5 ± 1.5 1.30	-1.23 ± 0.1
Oncog. Transf. (C3H10T1/2)	DIR SIR	1.37 ± 0.6	$(3.93 \pm 0.5) \times 10^{-2}$ 1.13×10^{-4}	-1.30 ± 0.14
HGPRT Mut. (V79)	DIR SIR	1.40 ± 0.7	$(1.15 \pm 0.3) \times 10^{-3}$ 6.20×10^{-5}	-1.30 ± 0.15

RT:Radiation Type DIR: Densely Ionising Radiation SIR: Sparsely Ionising Radiation

Examination of the details at the molecular and sub-molecular level reveals that the radiation -induced biological endpoints of inactivation, chromosome aberrations, gene mutations and oncogenic transformation are all initiated by the same basic damage mechanism, i.e. attributed to the production of double-strand breaks in the intracellular DNA due to the correlation between the primary ionisation and the spacing of the strands in the DNA. As the shape and properties of the $\sigma-\lambda$ curves is closely similar for all end points studied, the ratio of saturation effect cross sections to those for inactivation can be used as a scaling factor for estimation of risk of occurrence. The significance here is that if a good model can be derived for predicting the inactivation of mammalian cells, the scaling factors can be incorporated to yield the probability of cancer induction, a factor which is of a major importance in radiation protection.

As the slopes of the curves of various biological end points are practically about the same within the experimental errors, it seems justifiable to take the ratio with respect to inactivation to determine the scaling factors for risk estimation. These scaling factors are found to be 0.18, 1.6 x 10^{-4} and 2.91 x 10^{-5} for the induction of chromosome dicentrics, oncogenic transformations and HPRT mutations in respective order. The same scaling coefficients can be predicted by the ratio of predicted saturation cross-sections of sparsely ionising radiations.

3-7 Delta Ray Effects

Charged particles including the heavy ions interact with biological matter in various ways. The mechanisms involved in cellular and subcellular scales which lead either to recoverable or permanent damage can be best understood if specified with the linear primary ionisation e.g. λ. However, high energy heavy ions produce energetic secondary electrons termed as δ-rays. The yield of these δ-rays is proportional to Katz's ion core track parameter, z^{*2}/β^2 (chapter 2). The maximum kinetic energy of the δ-rays, $T_{max,\,\delta}$ is proportional to both its maximum range $R_{max,\,\delta}$ and the speed of the ion, β^2. Figures 3-24 and 3-25 show these relationships [Watt, 1996].

Thus the picture is best considered as in the track structure model: a main ion core characterised by the primary ionising radiation and the cylindrical region around the track which characterises the δ-ray tracks. Thus the parameter z^{*2}/β^2 specifies the yield of δ-rays while β^2 determines the maximum spatial extent δ-rays around the ion track. Whether these δ-rays have any significant role in damaging or multiplying the unsaturated damage within the biologically important sites (critical targets) remains one of the fundamental questions in radiation protection , as well as in radiobiology e.g. in estimating scaling factors for risk coefficients. In other words, it is desired here to clarify the picture through the use of the σ–λ relation.

As has already been seen in the last few sections, the unified σ–λ curve has two regions separated by the inter-molecular inflection point, λ_o. Here, the analysis will be performed in each region independently. In this analysis, only the benchmark

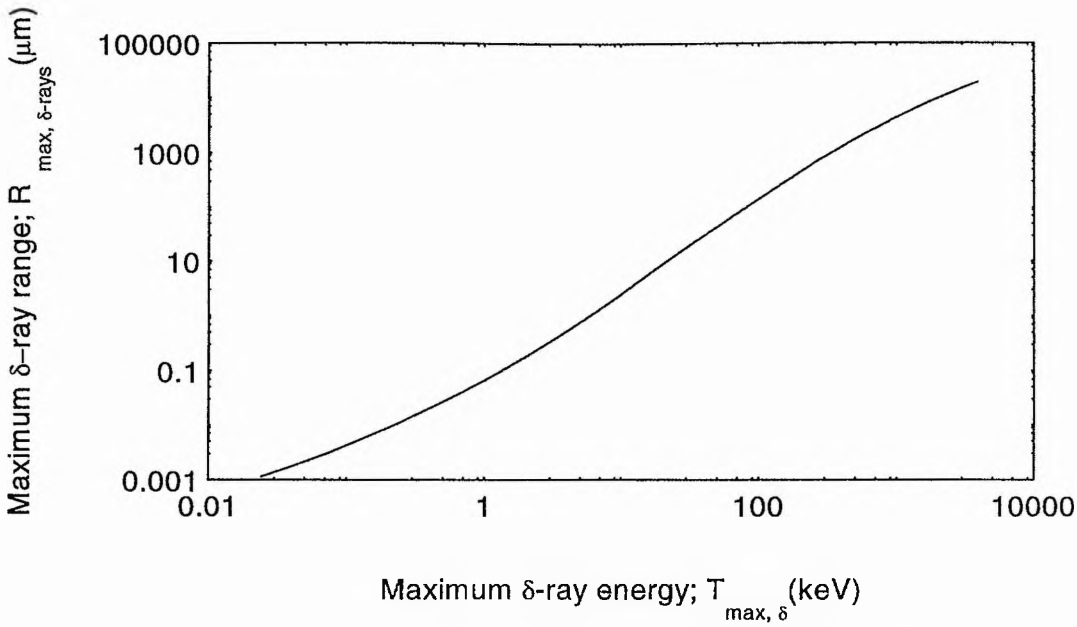

Figure 3-24a Maximum range of delta rays vs. its maximum kinetic energy.

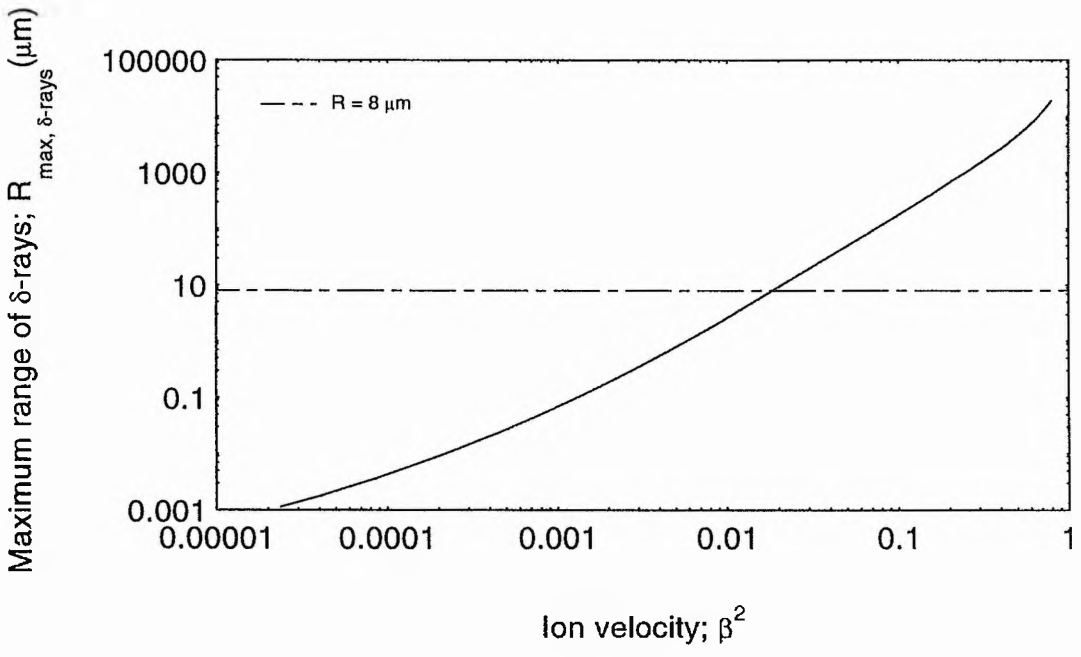

Figure 3-24b Maximum range of delta rays vs. ions velocity.

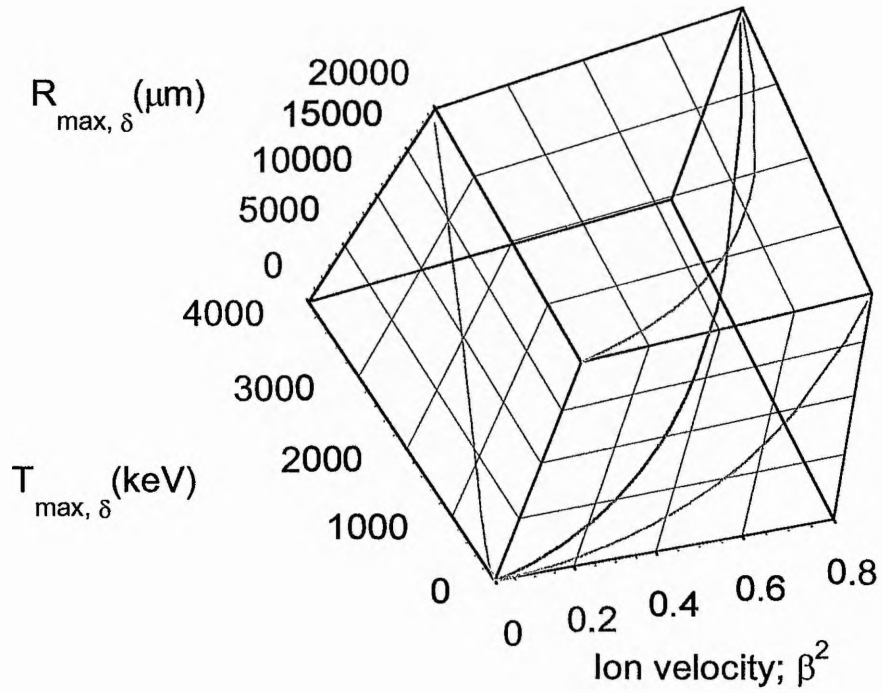

Figure 3-25 Maximum δ-rays range vs. ions velocity and δ-energy

survival data will be used because of the extensive amount of data available. As for other endpoints and because of the correlation between their effective cross-sections and that of survival, the same conclusion is to be expected.

3-7-1 Delta ray effect in the non-saturation region

Since λ is the mean free path for δ-ray production, and proportional to z^{*2}/β^2 for fast ions, the inactivation cross section per δ-rays yield can be calculated from $\lambda\,\sigma_i$ (μm^3). To test the δ-ray effect in this region ($\lambda > \lambda_0$) , $\lambda\,\sigma_i$ is plotted against the factor β^2 or $T_{max,\,\delta}$ within a narrow region ($\Delta\lambda \sim 0$) . In figure 3–26a, a selection of two sets of radiobiological data of human cells (from Appendix AII) are chosen, for which the upper curve $\lambda = 2.8 \pm 0.3$ (nm), and the lower curve $\lambda = 11 \pm 1$ (nm). A clear conclusion can be drawn immediately from figure 3-26a, viz. that the δ-rays do not make any appreciable contribution to the damage since changing their ranges (by increasing β^2 or $T_{max,\,\delta}$) for the different particles or ions does not make any additional contribution. In figure 3-26b. The same conclusion is reached for V79 cells in the narrow selected region of $\lambda = 16 \pm 1$ nm.

Alternately, if we fix the shape (determined by β^2 or $T_{max,\,\delta}$) and plot the damage cross section per δ-ray yield, using the radiobiological data of Todd which seems to be the only data set obtained in the same laboratory with human cells with ^{2}H, ^{4}He, ^{7}Li, ^{11}B and ^{12}C having constant speed ($\beta^2 \sim 1.4 \times 10^{-2}$) [Todd, 1965 ; 1968 ; 1975] again, the δ-rays are found to have negligible effects within errors of about 12 %. Since β^2 determines the shape (in this case δ–ray range ~ 5 μm), and because of the low yield of δ-rays, thus only the linear primary ionisations effectively inactivate the cells. This is demonstrated in figure 3-27.

From the forgoing discussion, we conclude that δ-rays do not play any appreciable role in the lower part of the σ–λ curve ($\lambda > \lambda_o$).

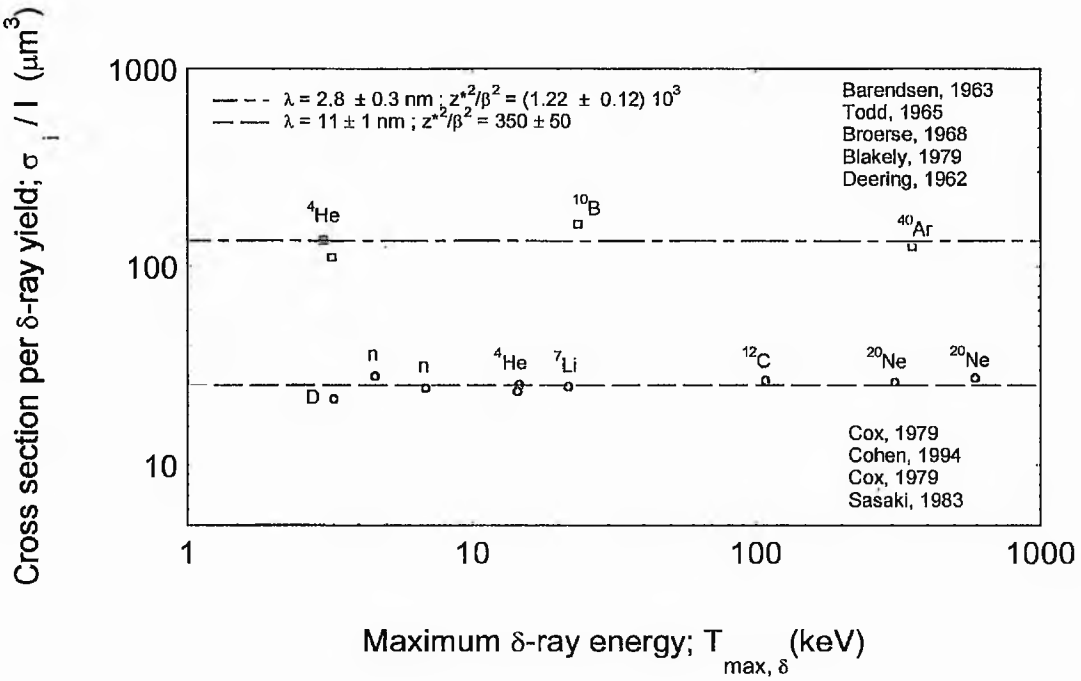

Figure 3-26a Role of delta rays for light charged particles ($\lambda > \lambda_o$) in human cells at constant z^{*2}/β^2.

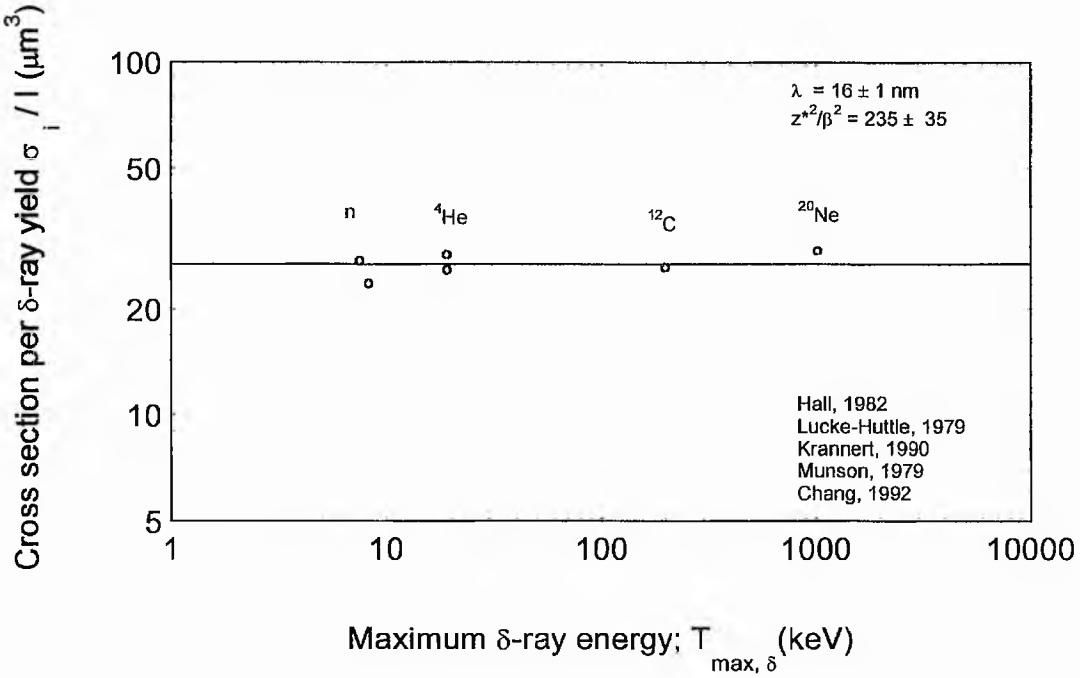

Figure 3-26b Role of delta rays for light charged particles ($\lambda > \lambda_o$) in V79 cells at constant z^{*2}/β^2.

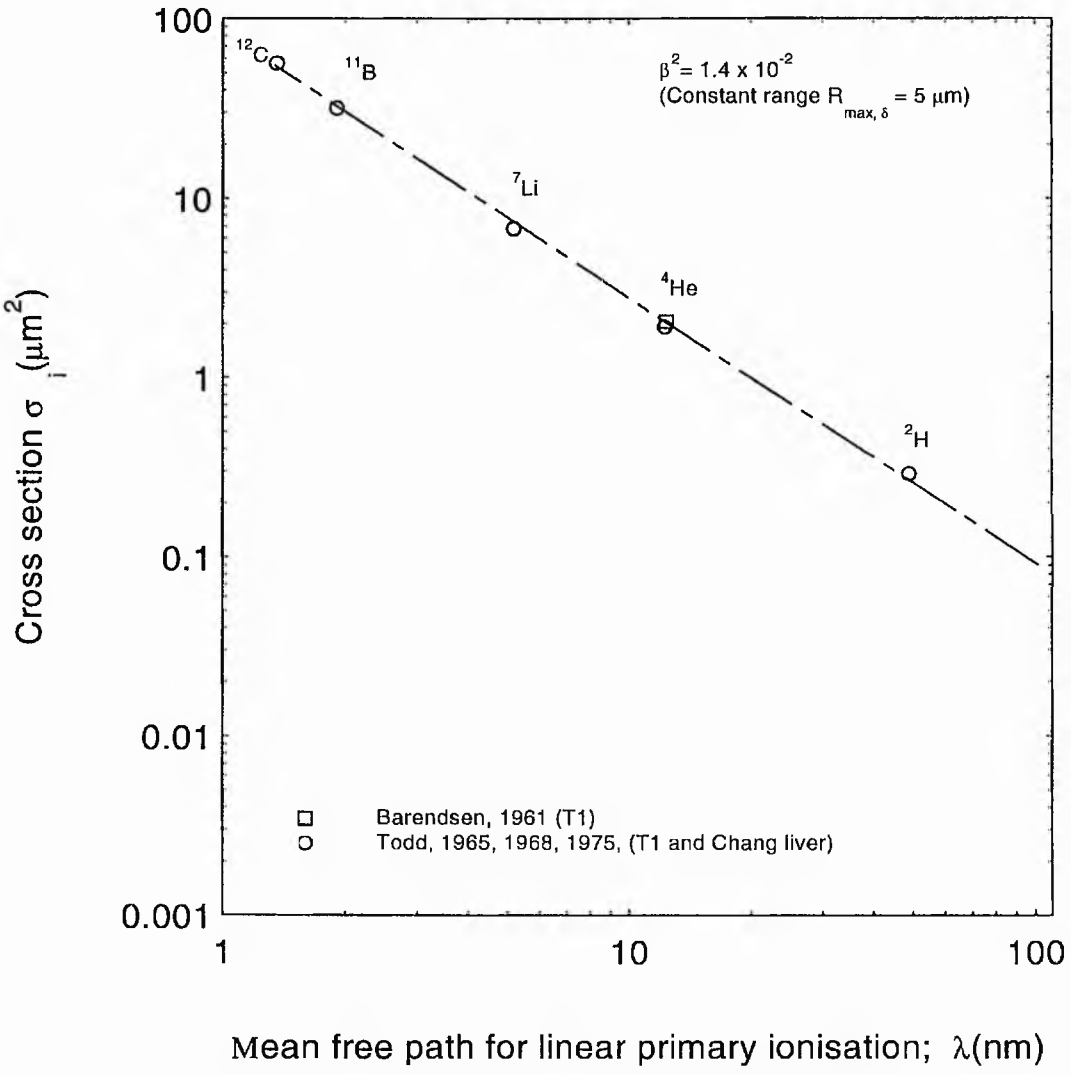

Figure 3-27 Role of delta rays for light charged particels ($\lambda > \lambda_o$) in human cells at constant β^2.

3-7-2 Delta ray effect in the saturation region

In this region ($\lambda > \lambda_o$), as has been seen previously, the yield of δ-rays is enormous. This can be seen very clearly in the $\sigma-\lambda$ curve shown in figure 3-28. It is noticed that for each type of heavy ion action on mammalian cells (^{238}U, ^{132}Xe, ^{58}Ni, ^{56}Fe and ^{40}Ar) the inactivation cross section reaches a maximum value, at different values of λ. The reason for this is lies in the definition of the saturation region. In this region, the primary ionising radiation (high LET heavy ions) kills all cells traversed. Thus the cells suffer saturation damage determined by the effect cross-section for all $\lambda < \lambda_o$. Experimentally, this is evident for the lighter ions such as ^{12}C as shown in figure 3-28 in which saturation damage to cells starts at about the inflection point, then followed by small region of saturation before they start to decrease because of their shorter ion range. However, for heavier ions (high z) featuring a much higher yield of δ-rays having large ranges, the δ-rays may reach and induce damage in neighbouring cells. Therefore the action cross-section for δ-rays, $\sigma_{\delta-rays}$ which depends on the ion type increases with decreasing λ, then a maximum action cross-section; $\sigma_{max,\ \delta-rays}$ (2-3 times that of the saturation cross-section for ^{238}U, and drops to lower values for lower atomic number) is achieved at $\lambda_{max,\ \delta-rays}$ before it starts to decrease. In other words the total cross-section $\sigma_t(\lambda)$ at the saturation region can be expressed as:

$$\sigma_t(\lambda) = \sigma_i(\lambda)\left(1 + \int \sigma_\delta(\lambda)\, d\lambda\right) \qquad 3\text{-}25$$

where $\sigma_i(\lambda)$ is the cross-section of primary ionisations, $\sigma_\delta(\lambda)$ is the action cross-section of δ-rays, and the integral takes care of all δ-rays produced by the primary radiation. Thus in the saturation region, the δ-rays produced would act independently to inactivate neighbouring cells.

The criterion known as the "Thin down" phenomenon is observed in the track of heavy ions approaching the end of their ranges. As the ion slows down, the track first increases in width to a maximum value and the thins down like a sharpened pencil. Generally both the yield (z^{*2}/β^2) and shape (β^2) of δ-rays specify its property. The

dependent role of these parameters is shown in figure 3-29. The three dimensional figure reveal that heavier ions (^{238}U) have higher δ-ray yields with longer ranges compared to that of lighter heavy ions like ^{132}Xe, or ^{40}Ar .

In non-mammalian cells the yield of δ-rays and their spectral shape have greater influence than in mammalian cells. This is expected because of the smaller dimensions of the cells. In fact this might be like a rule of thumb for other smaller biological entities (for all organisms); the smaller the target the larger the number irradiated by the δ-rays.

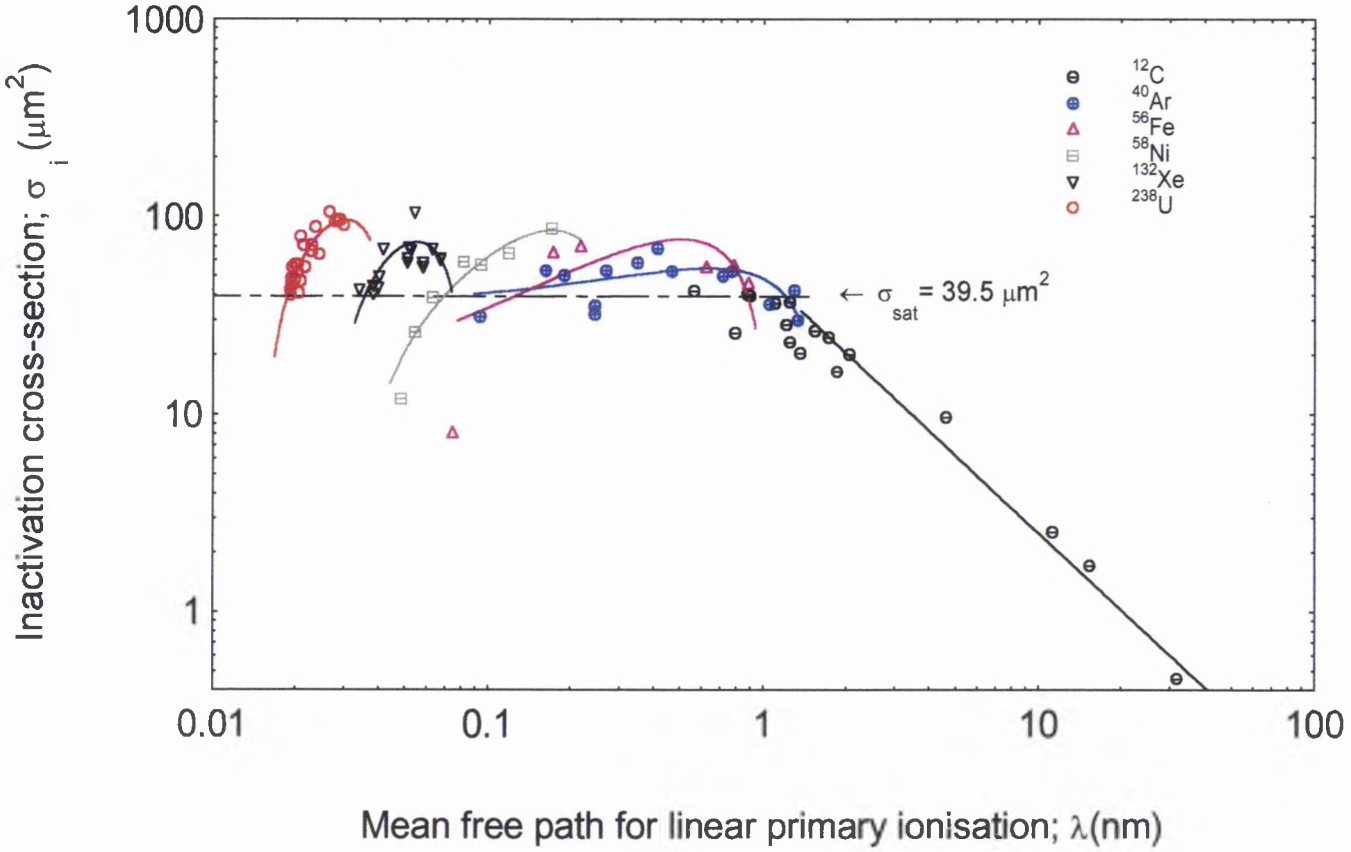

Figure 3-28 Damage due to delta ray production in the saturation region of V79 cells.

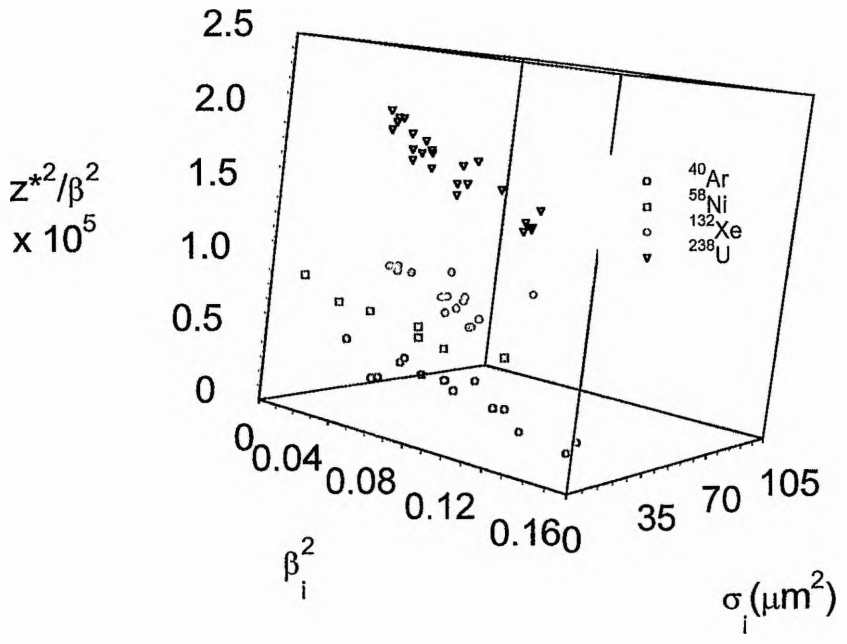

Figure 3-29 Action cross-section of delta rays vs. their shape and yield factors.

Chapter 4

DNA DAMAGE BY IONISING RADIATION

4-1 Introduction

It is generally believed that the DNA is the principal target which initiates damage to mammalian cells by radiation [Painter, 1980]. The damage could be in the form of DNA ssb's, dsb's, sugar damage, DNA-protein crosslinks (dpc) and both intra- and inter-strand DNA-DNA cross links [Hutchinson, 1987]. Although all damage are harmful, only the DNA dsb's considered to be the lethal ones.

On the other hand if repair is allowed, most of the ssb's can be faithfully repaired [Wallace, 1994] but not the dsb's. Radiation-induced dsb's are most likely to remain unrepaired or be misrepaired and lead to cell killing in eukaryotic cells [Frankenberg, 1981 ; Ward, 1988]. It is commonly believed that the majority of the non-repairable lesions are dsb's caused by complex clustered damage [Ward, 1985; Frankenberg-Schwager, 1989].

Low LET radiations (sparsely ionising radiations) produce mainly ssb's in dry DNA. These radiations interact with water in wet DNA and produce hydroxyl radicals e.g. OH• radical which may produce ssb's by direct interaction with the strands of the DNA. The distance travelled by the radical is controlled by its diffusion properties. The dsb's of DNA caused by low LET radiation is mainly produced via the combinational interaction of the radiation and induced radicals with the DNA strands. Thus the damaging effects of low LET radiation are mostly attributed to indirect effects [Roots, 1985 ; Chatterjee, 1996]. High LET (densely ionising) radiation on the other hand is characterised by its small inter-spacing distance (of the order of nanometers or less) between their successive ionisations within the biological material. Thus, high LET radiations produce mostly DNA dsb's and other effects which are mostly irreversible in nature. In considering both the direct and indirect action of radiation with mammalian cells, DNA dsb's are one of their products. These dsb's may go through repair mechanisms, resulting in non-rejoined and

misrejoined (misrepaired) DNA. The non-rejoined DNA dsb's (presumably proportional to the initial dsb's) are thought to lead to cell death, while the misrejoined may lead to other stochastic effects including mutations, transformations, chromosome aberrations, cancer and finally the terminal cell death. It should be emphasised here that although the main mechanisms of ionising radiation leading to many biological effects including cell killing, measurements of both initial and residual dsb's still form one of the problems in quantifying biological damage at the molecular scale. These problems, as mentioned earlier, are related to the diversity of data measured by the different techniques as will be seen in the next sections.

4-2 Measuring Techniques for dsb's in DNA

Several methods are available to detect breaks at the molecular level. The measurements of ssb's pose no problems as it is possible to denature the double stranded DNA to separate the strands, thus the exact molecular weight could be determined by the usual alkaline sucrose density gradient methods or alkaline elution techniques. However methods to determine dsb's are not so sufficient. Here we briefly review the most commonly used three methods to measure the dsb's of the DNA.

4-2-1 Ultra-speed sedimentation in Neutral Sucrose Gradient (USNSG)

USNSG is a standard method of sizing the DNA molecules. This method is used to measure the level of DNA dsb's in irradiated cells [Blocher, 1982]. The basis of USNSG relies on the fact that molecules of similar density and form will sediment when subjected to centrifugal force. Since ionising radiations cause dsb's, the molecular weight of the resulted broken molecules is reduced and thus can be quantitated by the alteration induced in their sedimentation behaviour. The well established physical theory of the sedimentation technique along with its mathematical formulations used to estimate the molecular weight of the broken DNA. The method has been very successful at high speed centrifugation (ultra-speed) with the DNA of prokaryotics, e.g. viruses, bacteria [Neary, 1972; Christensen, 1972] and the lower eukaryotics; e.g. yeast [Frankenberg, 1981 ; 1990]. For mammalian cells lower speed is needed [Kampf, 1983 ; Ritter, 1977 ; Jenner, 1993 ; Belli, 1994], and seemingly

this introduces many technical problems. The method requires high doses to establish the breaks [Blocher, 1982], and has proven to be very laborious.

4-2-2 Non-Denaturing Filter Elution method (NDFE)

NDFE is one of the earliest known techniques for the measurements of DNA dsb's in mammalian cells [Bradley, 1979]. The method is based on the DNA remaining (deposited) on a membrane filter (polycarbonate). The stranded DNA retains its form in the non-denaturing conditions. Elution rates depend on the applied radiation. The assay is found to be sensitive to pH, lysis conditions, elution buffer, chromatin structure and phase of the cell cycle. The system must be calibrated for absolute measurements of DNA dsb's. This is done by inducing a known amount of DNA dsb's incorporated with ^{125}I in the form of ^{125}IdU. Unlike other techniques, the response of measuring the breaks have a linear-quadratic relation with dose and experimentation can be carried within the same scale of dose with the cell survival [Prise, 1989]. The sensitivity of the method is claimed to be an advantage, in which low LET radiation would show a low-dose shoulder similar to that of the cell survival curve. However the method has some shortcomings. For one thing it is not quantitative and reproducibility is poor which questions the reliability of the sensitivity of the method at low doses.

4-2-3 Pulse Field Gel Electrophoresis (PFGE)

In recent years, the induction of dsb's of DNA by radiation can be determined in mammalian cells using PFGE [Blocher, 1989 ; Iliakis, 1991]. Electrophoresis of DNA dsb's through agarose gels allows separation of macromolecules by sizes. If an electric field is applied across the agarose, the molecules are dragged into the gel. The irradiated cells are then placed into plugs which are first referred to an unirradiated control, usually of known smaller molecular weight e.g. yeast. The latest development of electrophoresis allows the use of a pulsed field across the gel to reorient bigger fragment migration (up to 10 Mbp) along the field lines. Several types of PFGE are introduced for the radiation dsb's measurements, among them Clamped Homogeneous Electric Field (CHEF) [Blocher, 1989 ; Rydberg, 1994], Asymmetric Field

Inversion (AFI) [Lobrich, 1993] and Transverse Alternating (TA) field electrophoresis [Iliakis, 1991]. The mechanisms of the various types of PFGE were reviewed by several authors [Chebotarev, 1990 ; Viovy,1992]. In all electrophoresis methods, after the DNA fragments are dragged, the gel is normally stained with ethidium bromide, destained in distilled water and then photographed on negative films using 313 nm UV transilluminator. The images are then used to quantitate the irradiated DNA extracted in the wells by image analysers usually with computer codes and compared with that control (unirradiated sample). The number of dsb's in each lane can be related to the absolute number of DNA dsb's after empirical calibration of the assay through the decay of ^{125}I incorporated into the DNA in the form of ^{125}IdU. The lanes in the gel are cut, assuming an average of about 1 DNA dsb is produced per decay, thus the total number of dsb's in the fragment can be estimated [Iliakis, 1991].

While the mechanism of migration of fragments is fairly well understood using diffusion theory, there are still major limitations to the technique. Most of these limitations related to exploring why the fragments fail to migrate as well as to how they get trapped [Viovy, 1992].

4-2-4 General remarks on detection assays of dsb's

The principle features of most important DNA damage assays, including other techniques not discussed above, are summarised in table 4-1 Generally, USNSG results in an increase in the RBE for dsb with LET [Kampf, 1983 ; Blocher, 1988] in contrast to the use of NDFE technique which shows the same frequency for induction of dsb's by γ- and α-irradiation [Prise, 1987 ; Peak, 1983 ; Blocher, 1988]. Several previous studies using USNSG did not deprotenise the DNA, so that DNA-protein crosslinks may have an influence upon determination of dsb yields [Kampf, 1983]. Above all the high dose required to induce the breaks in both methods, is capable of killing any mammalian cells in any clonogenic experiments.

The several protocols suggested for the PFGE DNA dsb detection assays leads to different dsb spectra even if the same ion types and energies are used. The method which requires high doses to establish dsb's in the DNA is still causing some difficulties. Thus the

Table 4-1 Principal features of the most important DNA assays. Table modefied from Whitaker et al, 1991.

Assay	lessions	Dose Range (Gy)	Principle	Advantages	Disadvantages
SVSC	ssb's dsb's	D ≥ 5 D ≥ 15	Larger DNA fragments sediment further in linear gradient.	Absolute quntity of dsb's	Insensitive at low doses. Anomolous effects in cells with large genomes (mammalian).
FET	ssb's dsb's dpc's base	1 ≥ D ≥2 D ≥ 5 D ≥ 30 D ≥ 1	Larger fragments elute more slowly.	More sensitive than sedimentation. Show quadratic dose dependent. Allows measurements relevant to survival.	Uncertain effects of DNA conformation, cell cylce, cell number, lysis, pH.
PFGE	dsb's	D ≥ 5	Mobility in gel determinedby gel factors and DNA relaxation reorientation rates	Sensitive at doses relevant to cell survival. Heterogeneity of damage/repair can be resumed	Uncertain effects of DNA conformation. Cluster damages are considered as dsb's.
PT	ssb's dsb's	1 ≥ D ≥ 5 D ≥ 40	Fragments have differential solubility.	Rapid, simple. Low cell numbers.	Mysterious nature of lesions. PH critical. Results varies with type of treatment.
AU	ssb's	0.1≥ D ≥ 5	ssb's indicated by ratio of ss ds DNA after partial denaturing with ess.	Assesses topology of DNA conformation. Base damage revealed with ess.	Difficult to asses repair as kinetics of unwinding and rewinding vary.

AU : Alkaline Unwinding ; **FET**: Filter Elution Technique ; **PFGE**: Pulse Field Gel Elecrophoresis ; **PT**: Precipitation Technique ; **SVSC**: Sucrose Velocity Sedimentation Cenrifugation
dpc's: DNA Protein Crosslinks ; **ssb's**: Single Strand Breaks ; **dsb's**: Double Strand Breaks ; **ess**: Endonuclease Sensitive Sites

low dose measurement technique of PFGE is still not applicable [Lobrich, 1994 ; 1996 ; Rydberg, 1996 ; Heilmann, 1995].

Ward et al. have suggested that there are two types of DNA lesions induced by ionising radiation [Ward, 1990]. The first kind resulted from isolated lesions, referred dsb's which have their constituent ssb's close together on opposite strands, the second kind resulted from clustered lesions which are formed of two ssb's which are separated by several base pairs. It is suggested that NDFE and the PFGE techniques could score the second type as dsb's if the hydrogen bonds between the strands are disrupted by sheering forces. This hypothesis suggested that the experimental techniques could enhance the production of extra DNA dsb's in what is called locally multiply damaged sites (LMDS).

It is now accepted that the induction of dsb's is linear with dose, however the result does not mean that the response obtained also has a linear relation with dose. This can be seen clearly from the responses for both NDFE (fraction eluted) and PFGE (fraction released) which are described by sigmoid curves. The situation using the velocity sedimentation technique is quite different as in that case the signal is linearly related to dose [Iliakis, 1991].

Despite the availability of these techniques, several difficulties arise in making an inter-comparison of results using the different assay methods. They are not applicable within the same dose range and they have different sensitivities. Other complicating factors in the interpretation of measurements are associated with the dynamics and complexity of the DNA packing in mammalian cell nuclei as they progress through the cell cycle as well as the dynamics of the organisation of the DNA. These factors make it quite hard both experimentally and theoretically to determine the absolute number of breaks (dsb's and ssb's). The different experimental methods and the various protocols in use add more difficulties in relation to the outcome of the experiments. However, it is argued that the results of all measurements of dsb's in the DNA for the different detection methods in current use can be related [Iliakis, 1991]. Within the last two decades a large amount of data on

DNA dsb's have been produced by a number of authors and at various laboratories and for different ion types and energies.

In simple prokaryotic and lower eukaryotic cells, one may not expect complications correlating DNA dsb's with the cell death since the PGFE method is sensitive enough to measure a single dsb per genome. Thus it possible to carry out dsb measurements within the same dose range as for the survival curves [Micke, 1994 ; Schafer, 1994]. The method also seems to be sensitive enough to assay non-mammalian eukaryotic cells [Lobrich, 1993]. However the situation with mammalian cells, considering the complexity of the DNA organisations, is quite different and the sensitivity issue is still a challenging one .

Our aim here is to analyse the available data of the initial ssb's and dsb's of the DNA in terms of the various radiation quality parameters, and possibly study the mechanism of these effects in relations to other end points including cell inactivation.

4-3 Calculations of the Effective Cross-sections of DNA Breaks

The response to ssb's in the DNA is always expected to be linearly related to dose since it can be considered as a single hit process. The response for velocity sedimentation techniques is assumed also to be linear with dose. However the filter elution- , and pulsed field gel electrophoresis techniques have a response which is non linearly related to dose [Radford, 1988]. This hypothesis is still the subject of research [Ward, 1990]. In other word the linear response (the double strand break yield) G_{dsb} (dsb's/Gy) could have the form:

$$G_{dsb} = \alpha_{dsb} D \qquad 4\text{-}1$$

where α_{dsb} is the linear slope (dsb's/cell-Gy), and is the dose in Gy. The same expression is valid for single strand breaks, with the initial slope α_{ssb}. For the non-linear dose response, as expected from the filter elution method, the yield of dsb's contains an additional quadratic term. Thus the yield G_{dsb} is given by:

$$G_{dsb} = \alpha_{dsb} D + \beta_{dsb} D^2 \qquad 4\text{-}2$$

where α_{ssb} is again the initial slope (dsb's/cell-Gy) and β_{dsb} is the coefficient of the quadratic term (dsb's/cell-Gy^2).

To estimate the yield G (breaks/Gy-Cell) for both types of breaks it is necessary to convert from the different quantities expressed by the original authors to this form. Data on DNA breaks reported in the literature are expressed as breaks/Mb-fragments or breaks/kbp [Rydberg, 1994 ; Lobrich, 1994] or breaks/molecule [Roots, 1990], or breaks /dalton-cell [Belli, 1994]. It should also be noted that these values obtained by different authors using different molecular weight (MW), related to the measurements of the techniques at zero dose, are some times underestimated. The same MW were retained and used to estimate the damage. In general the molecular weight or the number of base pairs of DNA per cell are roughly estimated from their DNA weight in grams per cell (mammalian cells contain around 6 p-gm of DNA). In the surveyed data, DNA irradiated in mammalian cells, whereas in two set of data i.e. for ϕ-174 and T7 bacteriophage, the DNA is extracted from the cells and irradiated in the dry state [Neary, 1972] or in nutrient broth [Christensen, 1972] or in TE buffer [Stanton, 1992]. Details of the type of breaks and the different measuring techniques are shown in table 4-2.

Based on these assumptions the effective cross-sections for inducing dsb's (or ssb's) is given by the relation:

$$\sigma_{dsb} = \frac{L_T(keV/\mu m).\alpha_{dsb}(Gy^{-1})}{6.25\,\rho(g/cm^3)} \quad (\mu m^2) \qquad 4\text{-}3$$

where the L_T is the track average LET; α_{dsb} is the initial number of breaks (ssb's or dsb's) per Gy, and ρ is the density of the medium. The same expression can be used to calculate the effective cross-section for ssb's, σ_{ssb},using the initial slope (linear), α_{ssb}. The effective cross-section for inducing damage to the DNA is a measure of the probability to induce that damage in that area.

Table 4-2 **Details of the various measuring techniques used to determine induced DNA breaks in cells by heavy ions, are shown along with the molecular weights used by the different authors.**

	Cell Line	DNA MW* Dalton	Break's Measuring Techniques				REFERENCE
			SSB's	DSB's	TB's	NRB's	
1	V79-379A		AFE	NFE			Prise, 1989
2	V79-4	2.0000E+09	ASGC	NSGC			Kampf, 1983
3	V79-S171	2.0000E+08			ASGC	ASGC	Ritter, 1977
4	V79				AUT	AUT	Rydberg, 1985
5	V79			NFE	AFE and AUT	AUT	Heilmann, 1993
6	V79	5.4340E+09		NSGC			Jenner, 1992
7	V79	2.1300E+12		NSGC			Belli, 1994 *
8	V79-4	3.0000E+10		NSGC and NFE		NSGC	Jenner, 1993
9	V79	5.0400E+12		PFGE and NFE			Weber, 1993
10	CHO-9			NFE			Baumstark-Khan, 1993
11	EATC	3.5000E+12		NSGC		NSGC	Blocher, 1988
12	T1				AUT	AUT	Roots, 1979
13	GM38A		PFGE	PAGE			Lobrich, 1994 ; Rydberg, 1996
14	Caski	1.0600E+13		PFGE and NFE			Weber, 1993
15	Yeast-d	9.6000E+09		NSGC			Frankenberg, 1981, 1986
16	Yeast-d			PFGE			Lobrich, 1993
17	T7**	2.7000E+07	ASGC	ASGC			Neary, 1970, 1972
18	ϕx-174**	3.4000E+06	NSGC	NSGC			Christensen, 1972
19	SV40**	3.5000E+06		PFGE			Stanton, 1990, 1992, 1993
20	CHO-K1			CFGE			Heilmann, 1995
21	epithelial lens			NFE	AUT	AUT	Aufderheide, 1987

SSB's : **S**ingle **S**trand **B**reaks **DSB's** : **D**ouble **S**trand **B**reaks **TB's** : **T**otal **B**reaks **NRB's** : **N**one **R**ejoined **B**reaks
AFE : **A**lkaline **F**ilter **E**lution **NFE** : **N**eutral **F**ilter **E**lution **ASGC** : **A**lkaline **S**ucrose **G**radient **C**entrifugation
NSGC : **N**eutral **S**ucrose **G**radient **C**entrifugation **AUT** : **A**lkaline **U**nwinding **T**echnique
PFGE : **P**ulse **F**ield **G**el **E**lectrophoresis **CFGE** : **C**onstant **F**ield **G**el **E**lectrophoresis

* DNA Molecular weights used in the cited reference.

** All DNA's are irradiated in cells except T7 (Dry DNA); ϕx-174 (Difco Nutrient Broth) and SV40 (DNA in TEB).

4-4 Data-base for ssb's and dsb's in the DNA

The DNA dsb's and ssb's data for both prokaryotic- and eukaryotic-cells are compiled. Track structure parameters including the mean free path for linear primary ionisation, the restricted dose average LET and ion core track structure parameter, z^{*2}/β^2 were calculated for the ionising radiation inducing these scissions [Watt, 1994 ; 1995]. The effective cross-section of inducing ssb's and dsb's of the DNA are also calculated using the relation given by equation 4-3. Only the initial strand breaks were considered with the exception of one set of data [Ritter, 1977] which is related to the residual breaks (allowing repair) used for comparison. Both radiobiological data and the track structure parameters for ssb's and dsb's of DNA are tabulated in **Appendix AVI** and **AVII.**

4-4-1 Results and discussions

The calculated effective cross-sections of the ssb's of the DNA; $\sigma_{ssb's}$, resulting from the interaction of densely ionising radiations on non-mammalian cells is shown as a function of the mean free path of linear primary ionisation, λ , in figures 4-1a. On a log-scale the effective cross-section for induction of DNA ssb's increases monotonically with decreasing λ. The cross-section $\sigma_{ssb's}$ is expected to be linearly correlated with λ since DNA ssb's production follows the single hit target theory. As based on Katz's theory, the track structure radiation quality parameter z^{*2}/β^2 can specify these types of damage quite well, as shown in figure 4-1b.

The effective cross sections for dsb's in the DNA of mammalian and non-mammalian cells is plotted against the various radiation quality parameters; L_D, $L_{100,D}$, and z^{*2}/β^2 , λ in figures 4-2, 4-3, 4-4, and 4-5.

The effective cross-section, $\sigma_{DNA,\ dsb's}$ for dsb's seems to correlate better with λ than with the other quality parameters. This is consistent with the results obtained in the preceding chapter. Here the discussion will be based on the results demonstrated by the $\sigma_{DNA,\ dsb}-\lambda$ curves.

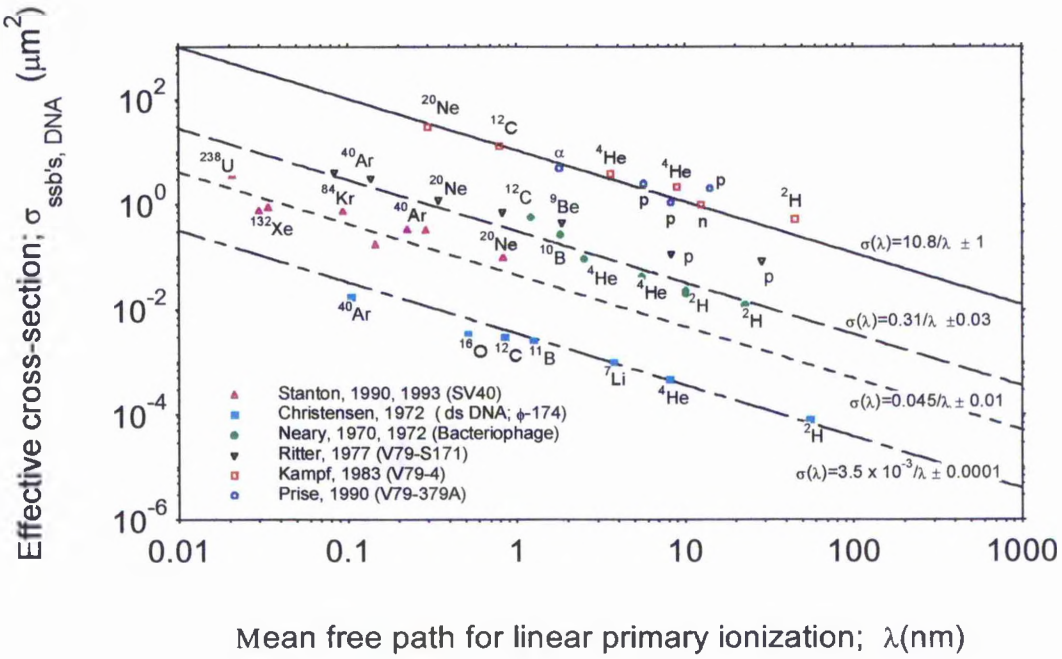

Figure 4-1a Effective cross-section for induction of ssb's in DNA vs. mean free path for linear primary ionisation, λ.

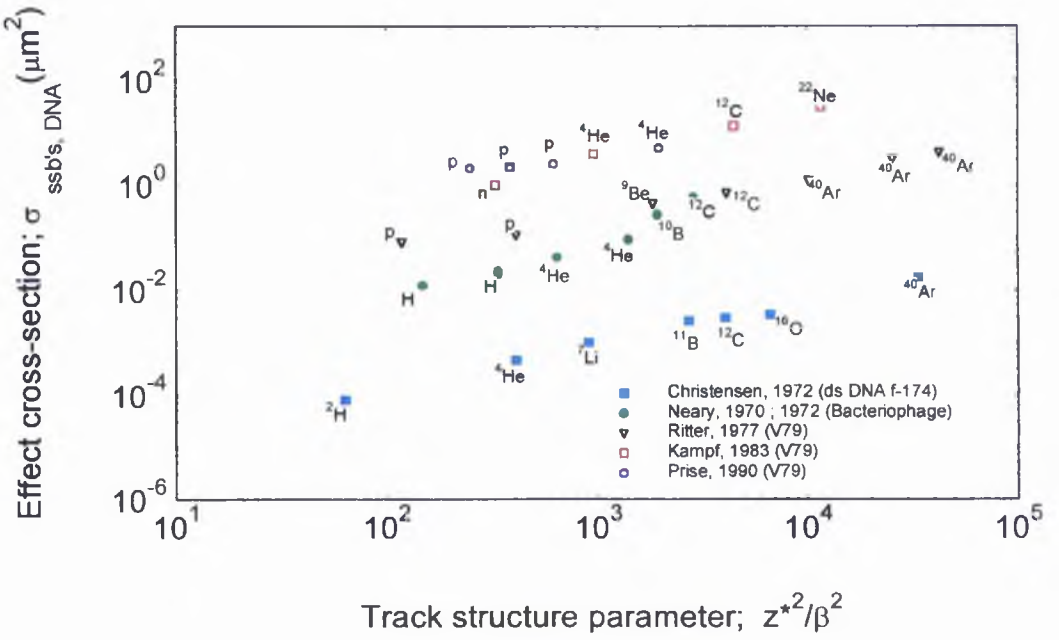

Figure 4-1b Effective-cross-section for ssb's in DNA vs. track structure parameter, z^{*2}/β^2.

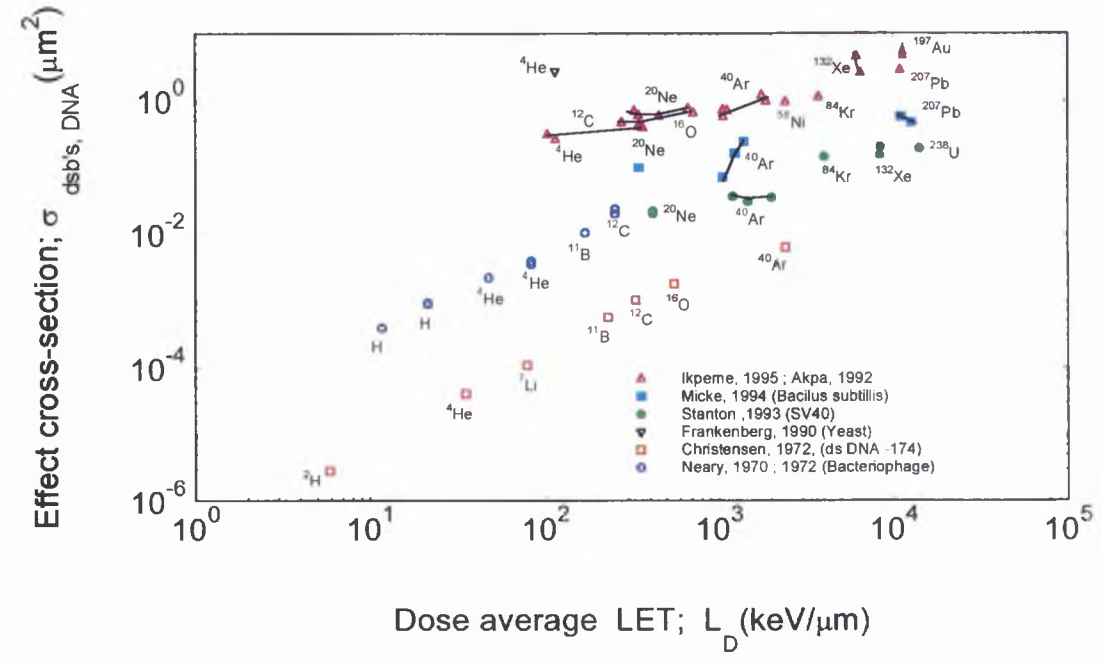

Figure 4-2a Effect cross-section for induction of dsb's in DNA of non-mammalian DNA dsb's vs. LET.

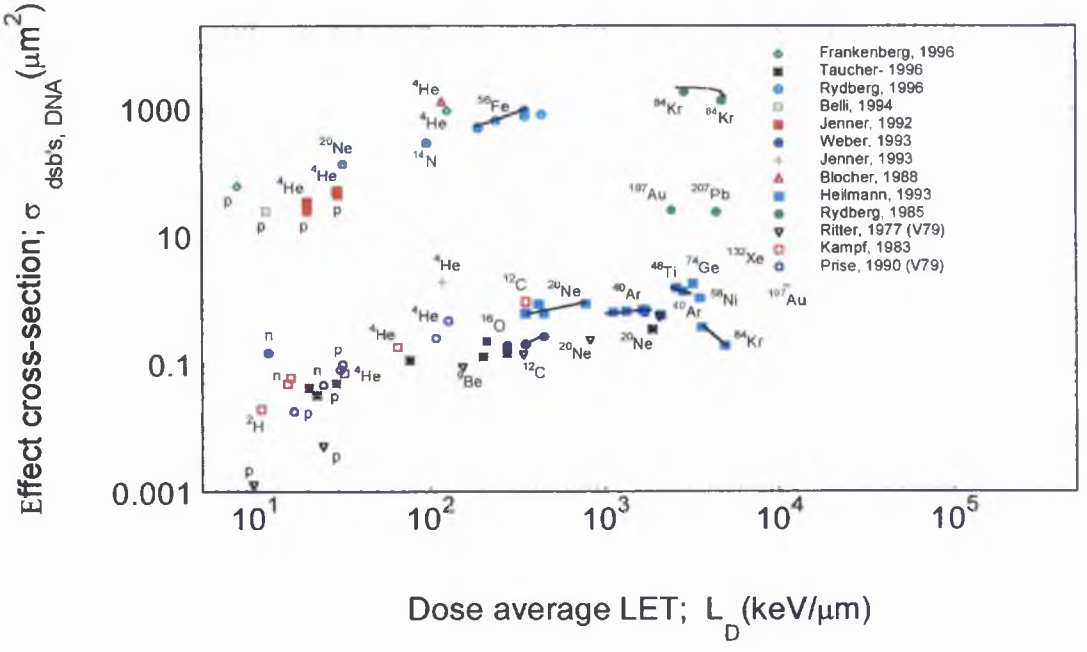

Figure 4-2b Effect cross-section for induction of dsb's in DNA of mammalian cells vs. LET.

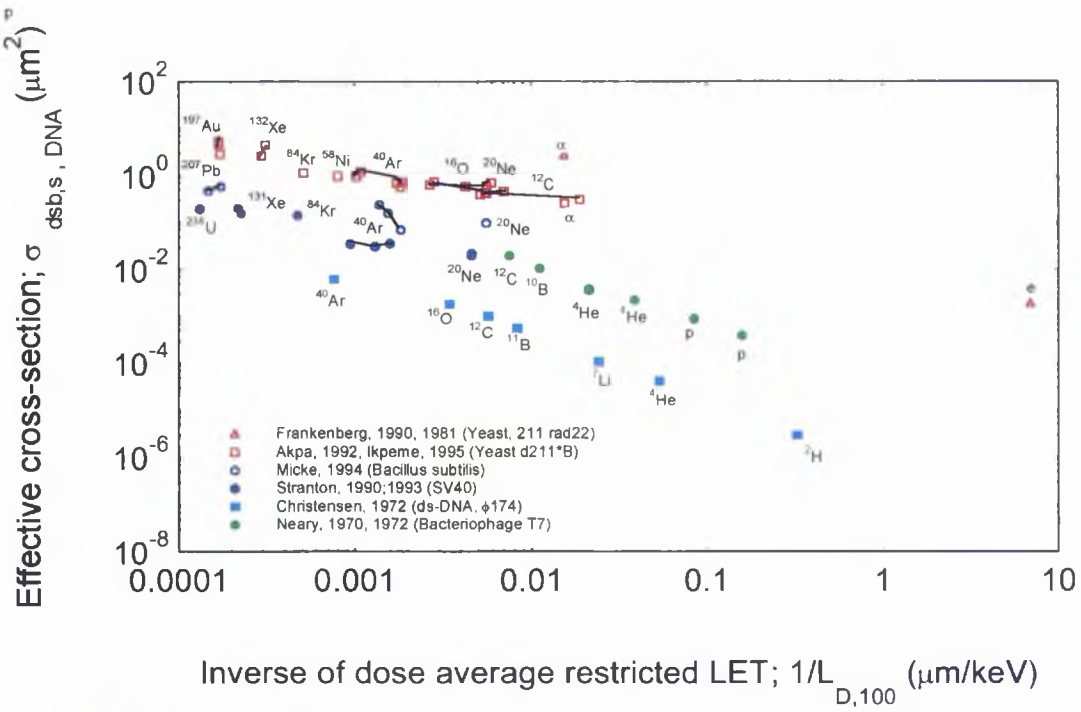

Figure 4-3a Effect cross-section for induction of dsb's in DNA of non-mammalian cells vs. restricted LET.

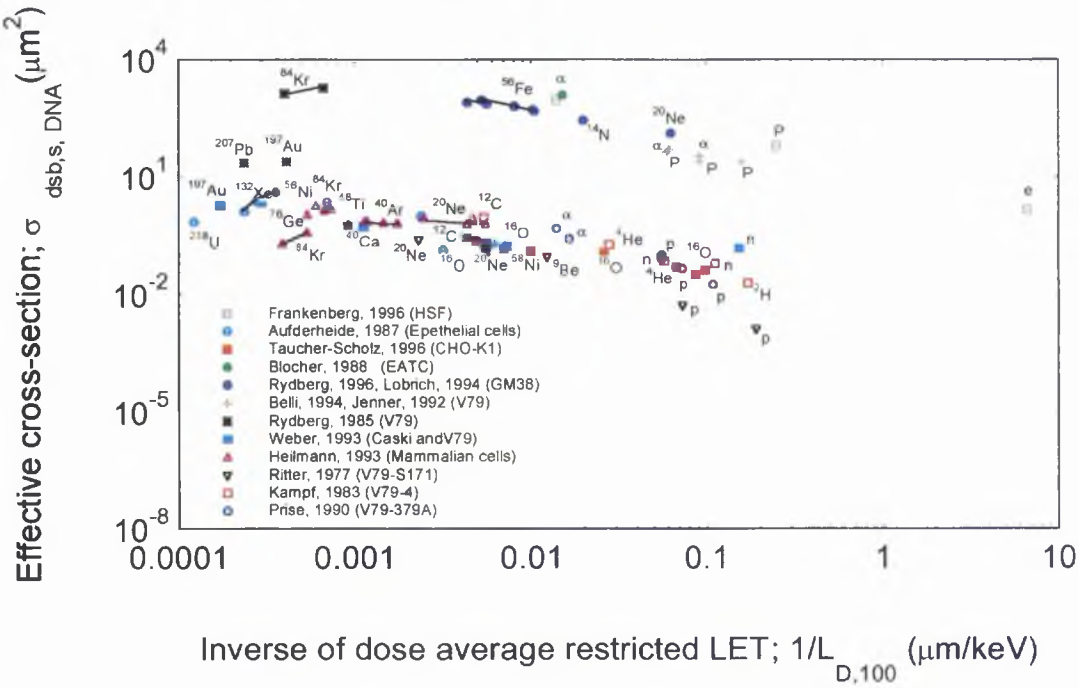

Figure 4-3b Effective cross-section for iduction of dsb's in DNA of mammalian cells vs. restricted LET.

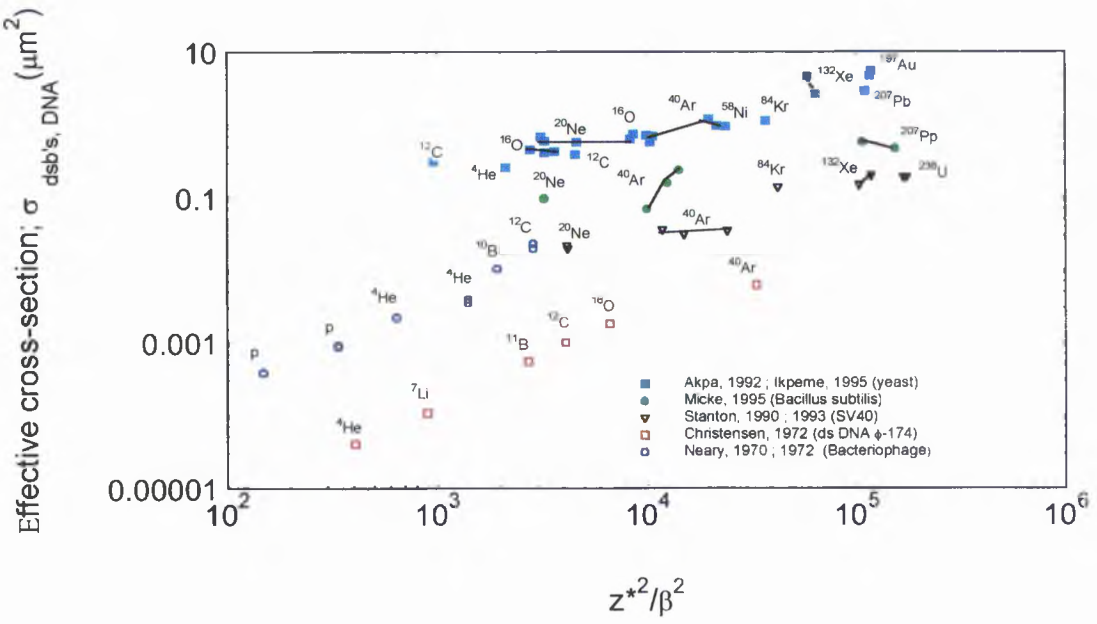

Figure 4-4a Effect cross-section for induction of dsb's in non-mammalian cells vs. track structure parameter z^{*2}/β^2.

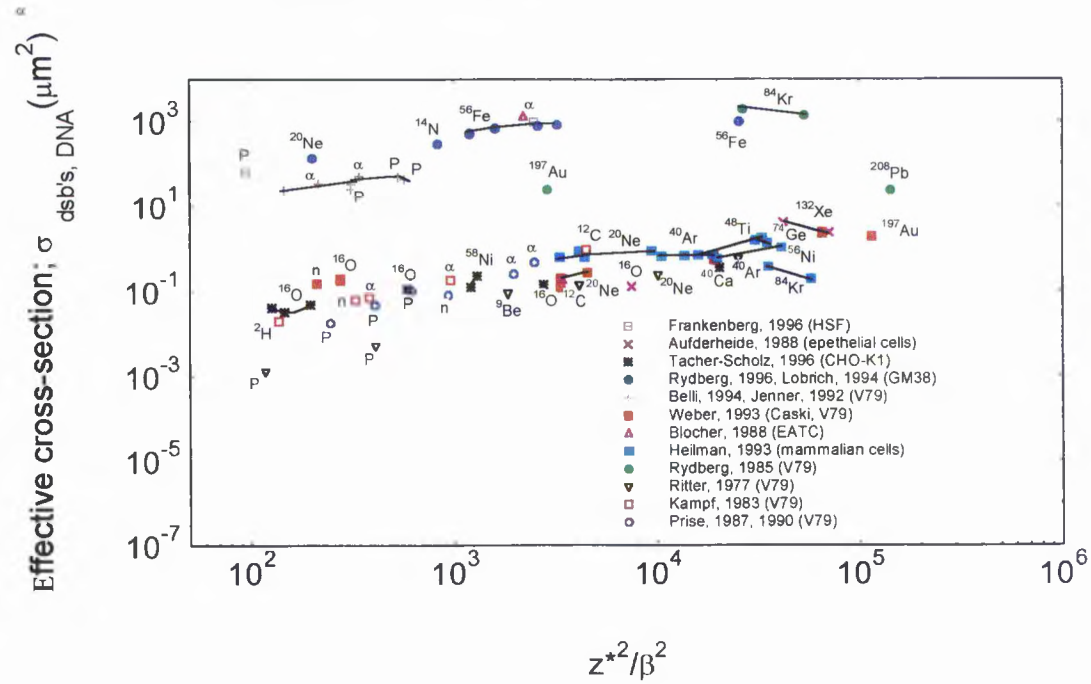

Figure 4-4b Effect cross-section for induction of dsb's in DNA of mammalian cells vs. track structure parameter z^{*2}/β^2.

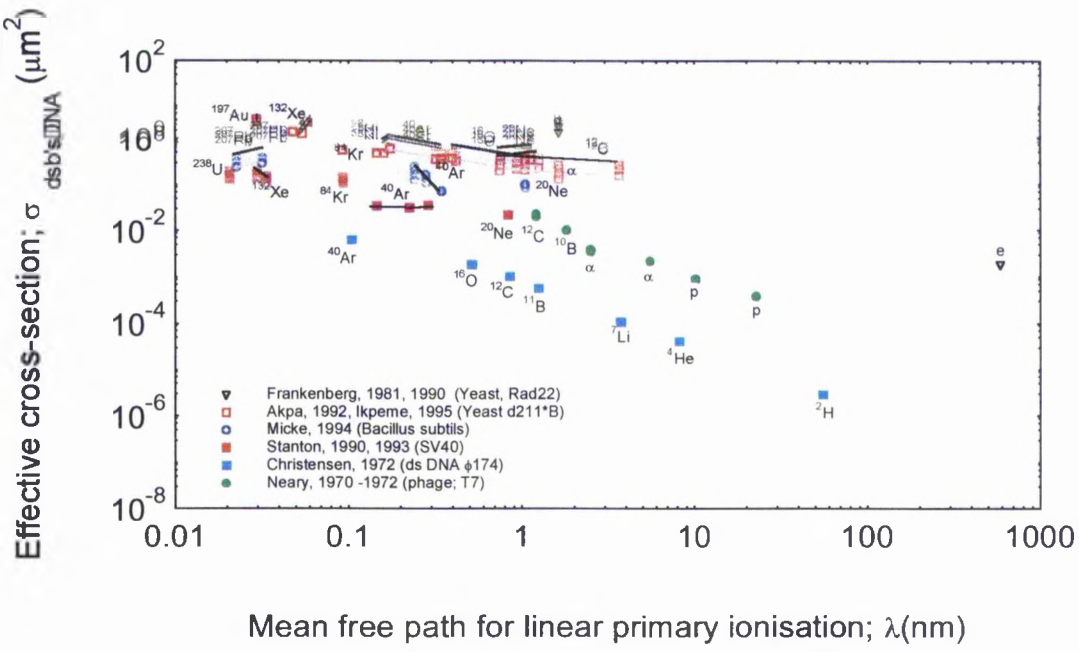

Figure 4-5a Effect cross-secction for induction of dsb's in DNA dsb's in non-mammalian cells vs. mean free path for linear primary ionisation, λ.

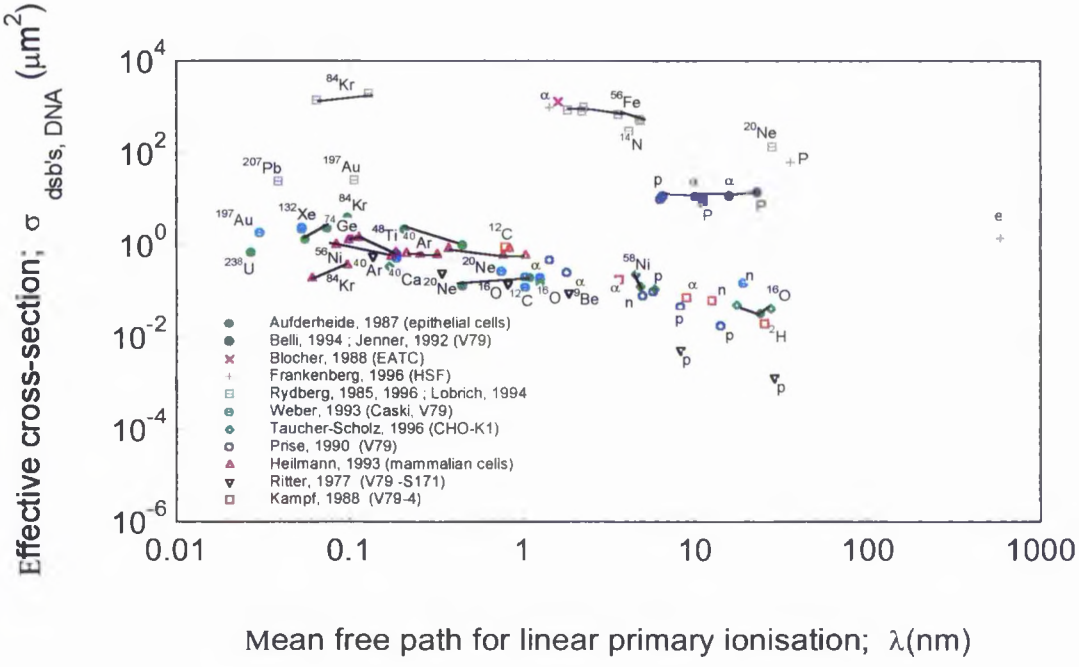

Figure 4-5b Effect cross-section for induction of dsb's in DNA in mammalian cells vs. mean free path for linear primary ionisation, λ.

For non-mammalian cells, there seems to be an agreement among some of the data carried out by the different methods. As it is clear from figure 4-5a, the double stranded DNA break data of ϕ-174 [Christensen, 1972] for low and medium LET ions are less by an order of magnitude than the T7 Bacteriophage [Neary, 1970, ; 1972] in the same region which is expected because of the higher DNA content of the phage. The SV40 data for high LET radiations [Stanton, 1993] have a higher saturation value than expected for the ϕ-174 virus. This may be due to the improvement gained by using pulse field electrophoresis in measuring the SV40 breaks on one hand and due to the depressed results of the ϕ-174 breaks on the other (the lower production of water radicals). However the data for non-mammalian eukaryotic cells (yeast; d211) obtained mostly for heavy ions, show saturation at about 1 μm^2. Higher effective cross-sections up to 5 μm^2 are achieved by using very heavy ions such ^{132}Xe, ^{197}Au, ^{207}pb [Akpa, 1992 ; Ikpeme, 1995]. This may be due to the effect of δ-rays in the saturation region. It is also noted that the saturation cross-section of cell inactivation is about the same order of magnitude as saturation of the DNA dsb's yield and of the geometrical cross section of the yeast nucleus. Fewer data exist in the literature for lighter LET charged particles.

However the situation with mammalian cells is quite a different one, as shown in figure 4-5b. The diversity of data for DNA dsb's (represented by their effective cross sections) shows two distinctive $\sigma-\lambda$ curves. The higher curve has a saturation cross section, σ_{sat} of about 1000 μm^2 which is much higher than the geometrical cross -section, σ_{DNA} of the DNA for the mammalian cells [Rydberg, 1985 ; 1996 ; Blocher, 1988; Lobrich, 1994 ; Frankenberg, 1997]. The scarcity of the data available from the literature at $\lambda > 1.5$ nm, makes it quite difficult to reach a conclusion about the general shape of the curve despite the availability of Belli's and Jenner's data for protons and alpha particles which have lower calculated effective cross sections [Belli, 1994 ; Jenner, 1992]. On the other hand the lower curve reveals a pronounced saturation region of about 0.8 μm^2 which is about 1/5 th of the total geometrical cross-section of the DNA in the cell nucleus. The saturation region of the curve is

characterised by the dsb's produced by heavy ions with high LET on epithelial and V79 cells [Heilmann, 1993]. As with the other endpoints, an inflection point is revealed at about λ=1.5 nm. At higher λ, the effective cross section decreases as λ increases. The available data for mammalian cells in this region are characterised by the low LET radiations [Kampf, 1983 ; Prise, 1990 ; Taucher-Scholz, 1996]. For simple prokaryotic cells, such as SV40, and the bacteriophage T7, the DNA saturation cross-sections are several times larger than the geometrical cross- sections, which may be due to the effect of the δ-rays from the high LET radiation.

Most of the data for dsb's are obtained with substantially large doses to induce sufficiently observable breaks. This contradicts the observed effects in cell inactivation at low doses and for other endpoint. This either suggest that the methods of PFGE are not reliable or the methods of quantifying damage (breaks) are insufficient. Nevertheless the yield of ssb's and dsb's based on effect cross section determine from the initial slopes seems to follow the same trend for most laboratories.

4-5 Modelling Radiation Induced dsb's in DNA

Some models of cell inactivation have a basic criterium that the dsb's in the DNA are the most important fundamental lesion leading to cell death and other related endpoints discussed in the preceing chapter. For radiological purposes, it was also demonstrated that the probability of occurrence of these endpoints can be deduced by scaling from the results for cell inactivations. With the increase of experimental information, particularly for the yields of radiation induced dsb's in the DNA, it was possible to verify that the calculated effective cross section of the breaks are better correlated with the mean free path for linear primary ionisation.

The reliability of the data for DNA breaks (represented in terms of its cross section; σ and specified by the radiation quality parameter; λ) will be subjected to a realistic test by comparing with prediction of the St-Andrews unified model. The model has been derived directly from other end-points. However, the basic studies based on the compilations of these data and the calculated cross sections reveal that there are two distinct σ–λ curves, one of which is an order of magnitude greater than the other.

Although the saturation response of the lower curve is about one fifth of the geometrical cross section of the mammalian DNA (4 μm^2), the curve is found to be more realistic than the other one (stated in section 4-4-1).

4-5-1 The St-Andrews unified model for yields of dsb's in intracellular DNA

The number of dsb's produced in mammalian cells by an incident radiation fluence Φ_i, is $\sigma_B \Phi_i$ where the cross section for the bio-effect is given by:

$$\sigma_B = \sigma_S \left(\varepsilon_2(\lambda) + 2\,\varepsilon_1(\lambda) \left(\frac{\sigma_{ssb}}{\sigma_S} \right) + \left(\frac{\sigma_{ssb}}{\sigma_S} \right)^2 \right) \qquad 4\text{-}4$$

and

$$\sigma_S = \left(\sigma_{g,\,DNA}\; n_0 \; \frac{\bar{R}}{\bar{d}} \right) \qquad 4\text{-}5$$

And hence the probability of inducing a dsb per cell and unit charged particle fluence is given by:

$$\sigma_{dsb} = \frac{\sigma_B}{n_0} = \sigma_{g,\,DNA} \left(\varepsilon_2(\lambda) + 2\,\varepsilon_1(\lambda) \left(\frac{\sigma_{ssb}}{\sigma_S} \right) + \left(\frac{\sigma_{ssb}}{\sigma_S} \right)^2 \right) \qquad 4\text{-}6$$

where the symbols have the following meanings:

d = mean chord length through the cell nucleus.

R = the mean projected range of the relevant tracks. If R>d, R/d=1 which allows for the reduced multiplicity of the targets at risk for 'stopper and insider' tracks.

n_0 = number of targets at risk per track traversal (~ 15 on average), dependent on the compactness of the configuration of the DNA.

$\sigma_{g,DNA}$ = the projected area of the intranuclear DNA - dependent on cell type, but typically 3 to 4 μm^2 for mammalian cells.

σ_S = the saturation cross-section = $\sigma_{g,\,DNA}\, n_0\, R/d$. If R> d, R/d = 1.

$\varepsilon_2(\lambda)$ = the efficiency of dsb production by direct action. $\varepsilon_2(\lambda)$ is taken as the probability that each single-strand of the DNA will receive one or more 'hits' and that there will be zero 'hits' between the strands in a DNA segment i.e. = $\exp(-\lambda_o/\lambda)\,(1-\exp(-1.0/\lambda))^2$ with λ_o =1.8 nm and λ = mean free path for linear primary ionisation for the relevant charged particles.

$\varepsilon_1(\lambda)$ = 1-exp(-1.0/λ) = efficiency for single strand break (ssb) production by direct action in a single DNA strand.

$\sigma_{ssb,\,j}$ is the interaction cross-section for ssb's produced by a line source of OH• radicals, determined by the track restricted LET and the diffusion length [Simmons, 1997 ; Watt, 1994].

4-5-2 Results and discussions

The predicted saturation cross-section for DNA dsb's for asynchronous mammalian cells, using equation 4-4, is about 3.5 μm^2. This is equivalent to the geometrical cross-section of the DNA within the cell nucleus (assumed to be compacted in the form of a sphere). Thus the product of $\sigma_{g,DNA}$ times the average number, n_0 of DNA segments at risk should represent the saturation cross section of cell inactivation calculated in the previous chapter. Ideally, this is about 50 μm^2 for Chinese hamster cells, and is about 65 μm^2 for human cells. With simple calculations, the target multiplicity, n_0 is estimated to be within 12 - 16 for mammalian cells. This number constitutes a factor to account for overlap of the DNA segments along a penetrating charged particle track. In other word this quantity should be a constant for an even amount of intra-nuclear DNA averaged for the exposed cell population.

However, the experimental determination of dsb's in DNA of mammalian cells resulted in saturation cross section of 0.83 μm^2 which is lower than expected. This could be due to several factors. The most convincing one is attributed to the geometrical packing of the DNA within the chromatin fibre matrix. Consequently, for comparison with theory equation 4-4 must be modified to justify and predict the saturation cross

section. Thus the saturation cross-section for cell inactivation (50 μm^2) should be divided by the number of DNA segments at risk (i.e. the target multiplicity $n_0 \sim 15$) which gives the geometrical cross section and then by a factor of 4 to get the measured saturated cross-section ($\sigma_{sat,\ DNA} \sim 0.83\ \mu m^2$). This factor was previously depicted in the last chapter as the ratio of the saturation cross-section for cell inactivation to the saturation cross section for dicentric induction.

A physical explanation for the observed factor of 4 is that two dsb's (pairwise lesions) are required to produce relevant chromosome damage the probability of which is 2^2. Another possible explanation is that the total projected area of the chromatin fibre, considered to be the critical target for the DNA, is about 1100 μm^2 [Rydberg, 1996 ; Holley, 1996] whereas the total projected area of the DNA if freed from its packed configuration is 4000 μm^2 i.e. a ratio of 1 to 4 is revealed. Consequently to compare the model with the measured values of dsb yields, the projected cross section of the DNA in the form of chromatin fibres was take as 0.83 μm^2 rather than 3.5 μm^2.

Upon comparison of the experimental V79 cell data with the prediction of the model, it was found that equation 4-4 is unnecessarily complex, especially in the forms of $\varepsilon_2(\lambda)$ and the presence of components of indirect action. A better fit to the data is given by the simple empirical form:

$$\sigma_{dsb} = \sigma_{g,\ DNA}\left(1 - \exp\left(-\frac{2}{\lambda}\right)^2\right) \qquad 4\text{-}7$$

Equation 4-4 is consistent with the usual expectation that one ionisation in two separate strands of the DNA segment can lead to a double strand break but the implication of equation 4-7 is that the sensitive dimension of the strand is about 2 nm rather than 1 nm. The results are shown in figure 4-6.

Another problem has arisen with the interpretation of damage mechanisms. One would expect that the scaling of the cross sections for the induction of dsb's, on going from complex mammalian cells to smaller prokaryotic cells such as phages, should be

in the ratio of saturation cross sections i.e. the projected areas of the DNA content multiplied by the multiplicity of sites at risk, (σ_s in equation 4-4) . However, if this is tried, the dsb's yields are found to be an order of magnitude below the observed values. In fact the yields of the dsb's scale much more satisfactorily by the ratio of the mean chord lengths through the DNA as shown by the dashed lines in figure 4-6. This linear dependence of the scaling was unexpected and not readily interpreted. Possibly the experimentally measured dsb's are an order of magnitude too large for the phages.

In the forgoing calculations, the contribution of the cross-section in the saturation region, due to the interaction of δ-rays with adjoining biological species has been deliberately omitted [Watt, 1989] in this instance. The excess contribution is expected to increase with decreasing biological target size, as seen in the figures where the excess is above the saturation level indicated by the lines, for $\lambda < 2$ nm. Although it is possible that the probability terms in equation 4-4 may need to be revised, the experimental data appear to be consistent with the generalised interpretation of the basic damage mechanisms vis. that the damage is caused predominantly by single tracks with a quality determined by the mean free path for primary ionisation. If energy transfer to δ-rays is an important damage mechanism for fast particles, one would not expect the observed change of slope at the onset of saturation near 2 nm, forming a sloping plateau for dsb's. The yield of dsb's would be expected to increase almost monotonically with decreasing λ.

It also possible to scale the risk of producing oncogenic transformation and HPRT mutations, bearing in mind the 1/4 geometrical packing factor. The calculations showed that 100 DNA dsb's needed to inactivate an oncogene in C3H10T1/2 and 3500 dsb's needed to delete an HPRT mutant in V79 cells. In fact the ratio of the geometrical cross sections (viz. $\sigma_{g,\ DNA} / \sigma_{g,\ HPRT}$) predict about the same results e.g. geometrical cross-section of HPRT in compact form was already calculated to be about 1.2×10^{-3} μm^2 and the geometrical cross-section of V79 DNA is about 3.5 μm^2 which gives about the same result (3000 dsb's). Again the foundation of this rough estimation needs to be verified experimentally in the molecular scale.

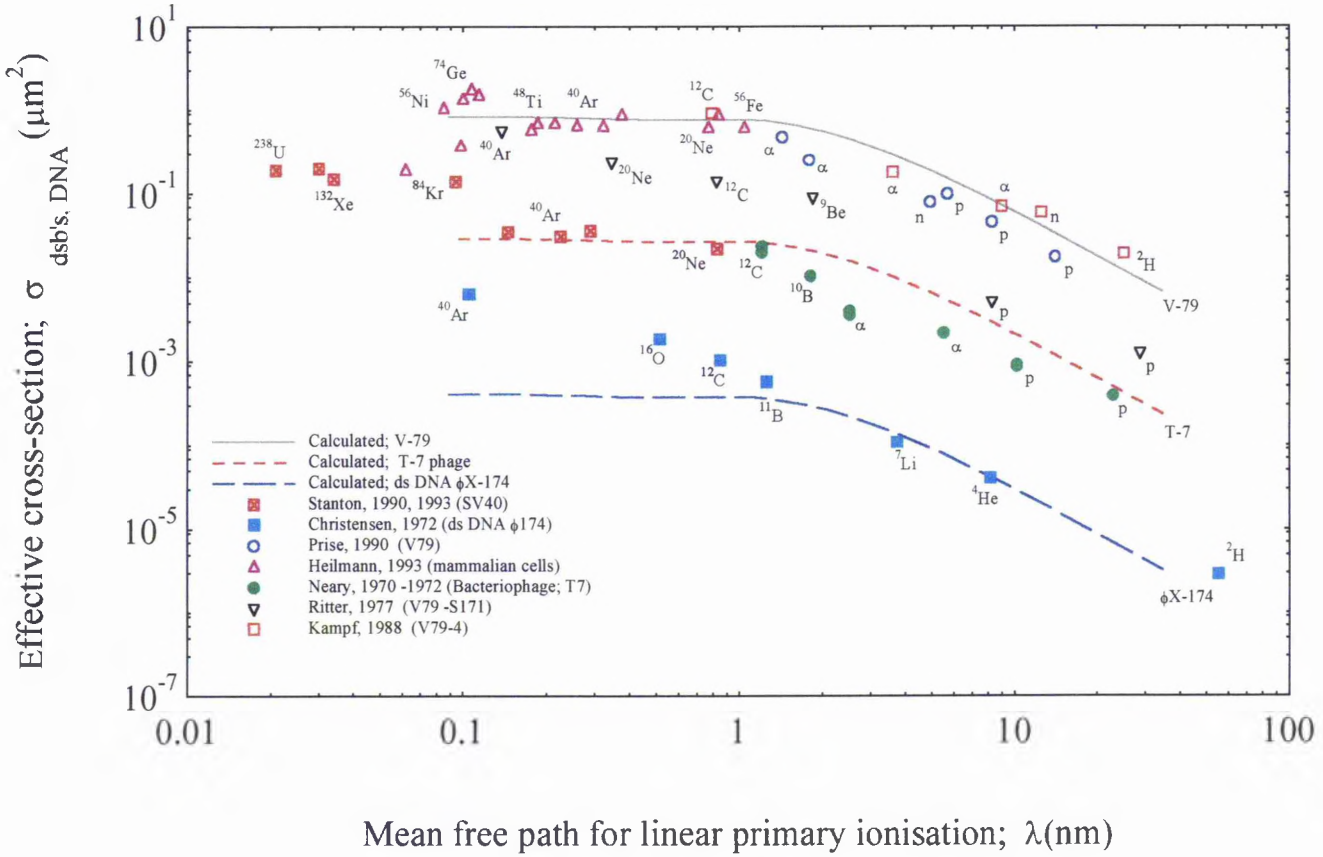

Figure 4-6 Modelling the dsb's induction in DNA.

4-6 Summary and Conclusions

In the last two chapters a number of conclusions related to radiobiological and radiation protection have been reached. They can be summarised is the following:

(1) sparsely ionising radiations are seen always to have lower effective cross-sections than densely ionising-radiations, the reason is simply related to the number of dsb's at risk weighted for the efficiency factor $\varepsilon(\lambda)$. In this sense σ_{eff} for sparsely ionising radiation for the induction of dsb's should be lower than that of densely ionising radiation. This would put a question mark on the data obtained for dsb's in DNA, where X-rays is chosen as the reference i.e. 22 dsb's/Gy [Blocher, 1988], or for the energetic electrons [Frankenberg, 1997]. These data points lie on the same σ-L_T curve(s) but this is seen hypothetically to be wrong as revealed in models based on the σ–λ relation (the St-Andrews unified model).

(2) The shape of σ_{eff}-λ curves is closely similar for all endpoints studied, and all types of radiations whether sparsely or densely ionising. That is to say on a log scale the main features are: a saturation region at λ less than λ_o (1.2 - 1.8) nm, and a linear region (for λ higher than λ_o) of the curve with almost the same gradient for all curves (see section 3-6 and 4-5). Such relations make it quite easy to predict and verify the experimental data. These relations also provide the essential tools to compare damage for sparsely ionising radiation or densely ionising radiation, thus allowing for inter-comparison between them. Moreover the multiplicity of one of them in terms of the other, e.g. the comparison between ultra soft C_k X-rays and ^{60}Co γ-rays for which it was concluded that US X-rays are more effective by a factor of 4 at inducing oncogenic transformation [Frankenberg, 1995]. This indeed provides solid evidence on how the RBE-LET relationship can mislead the interpretation of the specific damage. However such a conclusion is avoided by the σ–λ relation since both radiations have different molecular inter-spacing properties (λ). For this our model, which is based on σ–λ, predicts a much higher value of effectiveness as specified by the different λ's. It is also seen that σ_{eff} in the saturation region is less than the

geometrical cross-sections σ_g, for any specific damage with mammalian cells, except where the δ-rays play a part as in the case for slow heavy ions.

(3) Among all cells, mammalian or non-mammalian, it is seen that sensitivity measures of the σ–λ relation is dependent on volume of the DNA present in the cells. Thus the response, $\sigma(\lambda)$ of cancerous human cells such as T1 or HeLa cells are seen to be higher than normal human cells HF cells at the same λ. However in the molecular level, in scaling from higher order mammalian DNA, the damage in prokaryotic as measured by the dsb's assays are seen to be overestimated (figure 4-7). This is revealed by both the observations of dsb's in the DNA as specified in terms of mean free path for linear primary ionisation, λ and the predictions of St-Andrews unified model.

(4) The model depicted by the σ–λ relation should provide essential information for applications in radiation protection. This is demonstrated by the calculations of the risk scaling factors for the individual endpoints compared with survival. It is also verified that all damage is related to the inter-spacing distances along the mean chords through the DNA. This is expressed intrinsically by mean free path for linear primary ionisation.

(5) The response of the σ–λ relation leads to the concept of a unified dosimetry system, which is based on the induction of the dsb's of the DNA. The unification of all radiobiological data based on the σ–λ for all types of radiations shows the same inflection point, which is related to the inter-molecular spacing within the DNA. With this, and the standards of radiation protection set by the regulation agencies, it is possible to design a unified dosimeter having the same response function to simulate the equivalent DNA breaks (presumably dsb's).

(6) The low dose criteria is found to be inherited in the σ–λ relation. Based on the criteria which is briefly discussed in section 1-3-2, the geometrical cross-section, σ_g of the reference mammalian cells is evaluated to be around 50 μm^2, the low dose condition would imply that $\phi\ \sigma_g < 1$, where ϕ is the particle fluence (particles/μm^2).

With such criteria, it is easy to see that 0.3 mGy of ^{60}Co γ-rays correspond to a single track through the cell nucleus or less, whereas 30 mGy of the same source correspond to about 30 tracks through the cell nucleus (very high dose).

(7) Delta rays dominate the effect in the saturation region. The action cross-section of δ-rays becomes larger with smaller targets. These δ-rays effects do not show any contribution in the non-saturation region ($\lambda > \lambda_o$). The phenomena becomes very important in dealing with instrumentation for example in designing a nano-dosimeter to serve as a unified dosimeter.

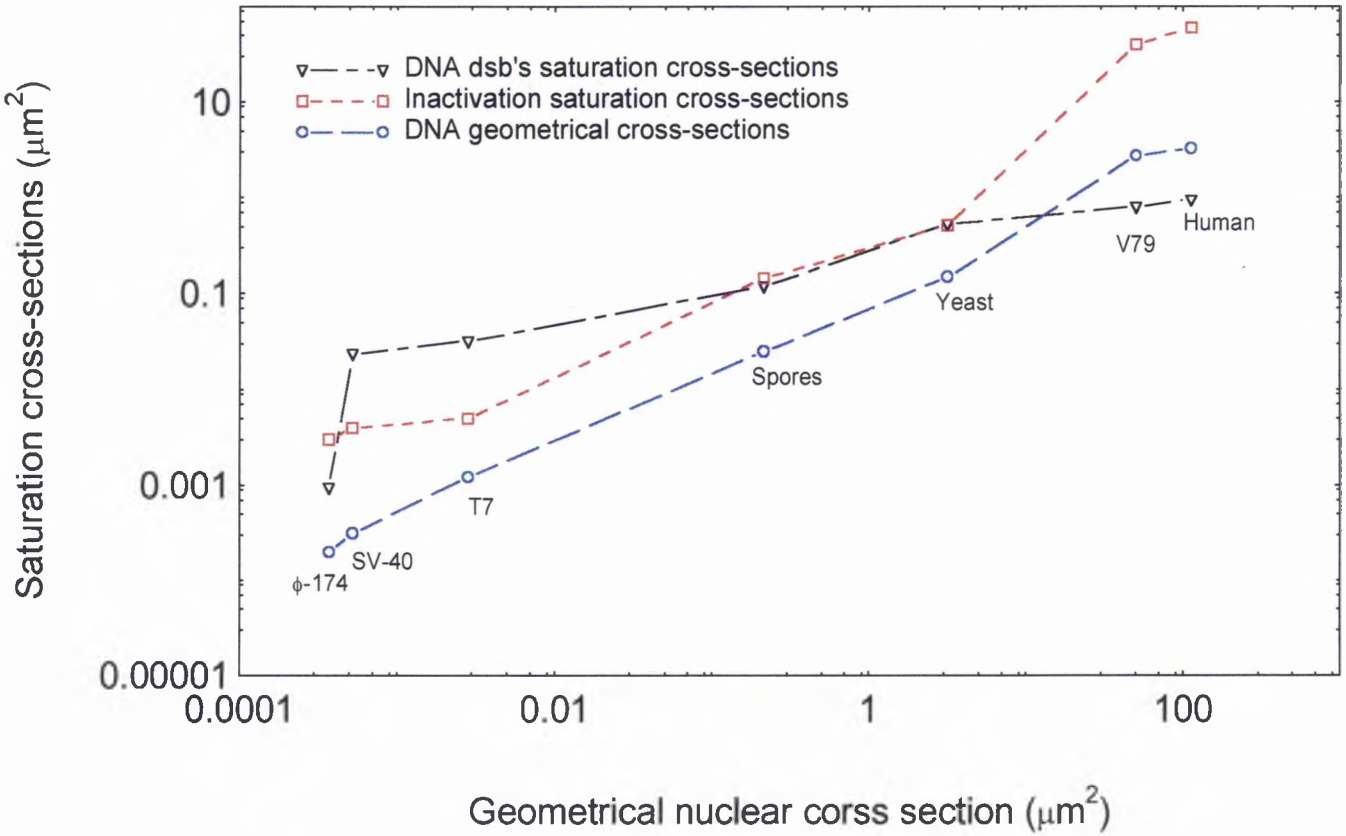

Figure 4-7 Comparison between DNA dsb's cross sections with cell inactivations .

Chapter 5

POSSIBLE EXPERIMENTAL APPROACHES LEADING TO UNIFIED DOSIMETRY

No physical device has yet been constructed which can give a direct measure of the initial biological effectiveness of ionising radiation fields. To achieve this capability, instruments should be conceived which have a response function to radiation which is equivalent to that of mammalian cells. In this chapter we will first define the conceptual and physical parameters for a unified system of radiation dosimetry. Various possible detection devices are then reviewed in terms of their potential for practical implementation of such a system and as a prelude to exploratory experimental work with organic scintillators.

5-1 The Basic Requirements of a Detector for Unified Dosimetry

It was shown in the preceding chapters, that the mean lethal damage in biological targets are primarily due to the interaction of ionising radiation with nuclear DNA, which in turn causes dsb's. Consequently the physical detector should match the effective size of this critical target, further its detection principle should reflect this finding.

It is assumed that the induction of damage by the inter-acting ionising radiation is determined by the stochastically fluctuating inter-ionisation distance. The relative yield, P , of the lesions for unit incident fluence is given by:

$$P = \sigma_g \phi_s \left(1 - e^{-\frac{\lambda_0}{\lambda}} \right) \qquad 5\text{-}1$$

where λ is the mean free path for linear primary ionisation along the charged particle track, λ_o=1.8 nm, is the mean chord length between the DNA strands, σ_g is the saturation cross-section which is the effect cross section of the specified damage at

$\lambda_o \leq 1.8$ nm, and ϕ_s is the pertinent charged particle fluence at charged particle equilibrium (chapter 3, chapter 4). The term $(1-e^{-\lambda o/\lambda})$ is the probability that the significant spacing, λ_o, will occur for a particle with mean free path λ. Watt, 1986 has proposed that the ideal dosimeter should have a response which in effect means the number of coincident ionising events in the DNA spaced at λ_o. Leenhout, 1990 has suggested that the hypothetically ideal detector should measure two energy deposition events along the same track, occurring in two small spheres spaced at a distance of 1.2 nm. This in turn would simulate the two strands of the DNA helix. On the present basis, the response should be based on the linear primary ionisation [Watt, 1986]. Since a single hit detector will only resemble ssb's, our hypothetical detector is capable of measuring dsb's, which are caused by two events spaced at 1.8 nm. Each event could, for example, be a single ion pair depending on the detecting medium. Ideally, if the two detectors are operated in coincidence, the resolution of this detecting system should be capable of distinguishing between two single ionisations within DNA inter-space.

5-1-1 The physical requirements for unified dosimetry

In order to simulate the action of ionising radiation in nanometer regions, i.e. within the DNA, several important requirements must be considered. These requirements either related to the physical and geometrical properties of the DNA or are related to the detector material properties for optimising the signal/noise ratio. These requirements are general in nature and can be summarised as the follows:

1- In order to mirror the DNA segments physically, the desired detection system should consist of thin detectors of 1 nm sensitive dimension (at least two) separated by an insensitive region(s) of dimension about 1.8 nm (mean chord length through the DNA). The detectors should have the same physical, and chemical properties, i.e. be constructed from the same material. If more than n detectors are used, then a probability distribution function f(x) should be employed to interpret the response in terms of those tracks passing through two sites spaced by 1.8 nanometers.

2- The interaction of radiation with the detector media should generate charged particles or corresponding entities (i.e. electrons or photons) which can be both conveniently and efficiently collected. These entities should ideally be linearly related to the number of interaction events at preferable sites (1.8 nm).

3- The unified dosimeter should have a response, similar to that of the bio-effect curves related to the different endpoints, as described in chapter 3 and 4. The mean energy required to induce dsb's in the DNA is of the order 30 eV [Folkard, 1993]. This could be considered as the threshold energy for the signal from a unified dosimeter

4- The signal-to-noise ratio of the detector output should be optimised. This implies that every interaction equal to ,or above, threshold level should be detectable. To achieve this level of optimisation other requirements such as internal and external amplification may be invoked [Knoll, 1989].

5- The detection medium should have a fast response to radiation to match up with the time scale of interaction on the DNA strands (Chapter 2). If coincidence techniques are used then the resolving time should be of the order of nanoseconds.

6- Although DNA shows structural inhomogeneity, the detection system will have a high degree of uniformity in both composition and physical thickness of the material to be used. This requirement will reduce the fluctuations of the measured signals.

7- The molecular DNA within the cell is essentially compacted in a condensed liquid form (chromatin fibre). The physical properties of these liquids are closer to solids than to gasses. Thus the required detector should preferably be in the condensed phase, and preferably tissue equivalent.

8- Availability, practicability, good tensile strength and durability and resistance to radiation damage are desired detection material properties.

9- The interaction cross-sections and mass stopping power of charged particles in the detection material should be the same as for DNA. It is favourable if the electron

densities of both are of the same order of magnitude. Tissue (DNA) equivalence is required.

5-1-2 Mode of operation and interpretation of response

In simulating the radiation action on DNA at the molecular target, several problems may arise. These problems should be handled with care.

The results presented in chapter 4 showed that both the absorbed dose and the RBE are not suitable parameters to quantify the biological damage at the cellular or molecular scale. The measurement of energy deposition at the DNA level might not be realistic. This is due to the stochastic nature of energy deposition at the nanometer level [Kellerer, 1985]. The present dosimetric system including microdosimetry cannot satisfactorily quantify the effect of δ-rays.

More realistic measurements can be made if a threshold can be identified and used. However it is important that analysis will be based on frequency of events i.e. the induction of ssb's in the DNA duplex, and not on energy deposition (chapter 4). The energy involved in the induction of ssb's can therefore be taken as the threshold sensitivity required of each adjacent sites in the unified dosimetric system. Then, interpretation of the detector response will amount simply to counting the interaction frequency corresponding to the sites spaced at 1.8 nm. On the other hand conventional dosimetry relies on energy deposition spectra which are based on the mean energy for production of an ion-pair and may not be suitable for estimating the frequency of events since the mean energy for producing an ion pair is not a constant for slow particles [Goodman, 1978 ; ICRU-37, 1984].

Ideal detectors for unified dosimetry do not necessarily measure the total energy deposited. Rather it is more appropriate and convenient to count ionisation events corresponding to those spaced at 1.8 nm. The peculiarity of using the term nanodosimeters for such devices has evolved historically and it does not have the usual sense of energy deposition [ICRU-36, 1983]. In fact the term is used here only to indicate the nanometer dimensions of the DNA inter-spacing.

In this sense the integral of the response spectrum (IRS) of the unified dosimeter to radiation is given by equations 5-2a and 5-2b:

$$IRS = \sum \frac{\sigma_g}{\sigma_e}\left(1 - \exp\left(-\frac{\lambda_o}{\lambda}\right)\right)\phi_s \qquad ; \lambda > \lambda_o \qquad 5\text{-}2a$$

and

$$IRS = \text{Constant} \qquad ; \lambda = \lambda_o \qquad 5\text{-}2b$$

where σ_g and σ_e are the geometric and effective cross-sections (chapter 3 and 4).

For $\lambda = \lambda_o = 1.8$ nm, the ratio σ_g/σ_e can be made equal to unity. Thus the integral of the response spectrum of an ideal instrument is a direct measure of the absolute biological effectiveness (ABE) of the give radiation. This relation implies that the integral of the area under the peak of a single radiation depends on its mean free path and the charged particle fluence ϕ_s. For mixed radiation fields, the net absolute biological effectiveness will be given by the integral of their response spectra.

5-2 Detectors Based on Secondary Electron Emission

5-2.1 Background and principles

Irradiation of a solid material with the provision of energy more than the gap energy E_G, generally generates an internal electron spectrum. Out of the slowing down electron spectrum, only those electrons with energy less than 50 eV are termed as secondary electron emission; "SEE" [Burlin, 1974]. For an incident beam of electrons with incident energy E_o, the distribution of SEE shows two other groups of electrons with energy higher than 50 eV: the elastically reflected primary electrons (causing a peak at the end of the spectra at E_o) and the re-diffused primary electrons which are related to the slowing down of the primary radiation in the media (their energies are in the range of E_o down to about 50 eV). The yield of these electrons outside the surface is very low. Secondary electrons up to the energy E_G (for Alkali-halides 6.3 eV)

lose their energy primarily through electron -phonon interaction, and involve extremely small energy transfers ~ 0.01 eV. Thus they move through the solid without any multiplication. The other part of the spectrum with energy interval, E_G - 50 eV, lose their energy through a very limited range in the solid due to their interactions with multiple scattering with electrons and phonons. However at the peripheral layer of the material "escape zone", some electrons may escape through the barrier potential. The depth of the zone is a property of the material, independent of the type or energy of the ionising radiation. For metals it is of the order of 10 nm, for semiconductors, and insulators, it may extend up to 50 nm. The lower the work function, the higher the yield of the secondary electrons. The yield also varies with energy of the primary particle. The secondary particle escape probability is a function of depth and it is given by:

$$P(x) = P(0) \exp\left(-\frac{x}{L_s}\right) \qquad 5\text{-}3$$

where x is the depth of the layer, L_s is the average escape length which is related to the escape zone, and P(0) is the escape probability at the exit surface.

Because of stochastic nature of producing SEE, it is not possible to correlate the energy deposited by the primary ionising particle in the surface layer with the number of secondary electrons emitted from the surface. However, the average value of energy expended in the escape zone to produce a secondary electron, analogous to the W-value to create an ion pair in a gas, is used to estimate the average yield per energy deposited. For CsI, W_{see} ~ 7 eV [Akkerman, 1992].

The SEE spectrum has a pronounced peak at 1-3 eV. The maximum yield for metals and semiconductors is in the range 0.6 - 1.7, for insulators it may be up to 20. The time for secondary electron build-up is of the order of 10 psec. Burlin et al. quoted [Baroody, 1950] that the relative secondary electron yield (δ/δ_m) against the relative energy of secondary electrons with respect to the corresponding maximum yield energy (E_o/E_{om}), can be used to deduce a universal yield curve, which is analogous to

the RBE-LET relation [Burlin , 1974]. Despite the observation that the general shape of the yield curves is the same for metals, semiconductors, and insulators, it was not possible to fit them all with a single universal yield curve.

For heavy ions the energy distribution of SEE was found to be the same. Ions with the same velocity, have a yield proportional to the effective charge number z* and it is much higher than that of electrons.

5-2-2 The possibility of using SEE as a unified dosimeter

The main theme is to simulate action of primary ionising particles on biological targets having dimensions around 10 nm or less (e.g. 2 nm for DNA and 10 nm for the nucleosomes). The potential for using secondary electron emission phenomena in microdosimetry was first noted by Burlin, 1974. The idea is explored later in the context of two-target theory [Forsberg,1978 ; 1982]. The authors proposed thin films of C, LiF (properties included in table 5-1) where the two escape zones (surfaces) act as the two detectors, figure 5-1.

Table 5-1 Properties of SEE materials.

Foil	E_G	ρ (gm/cc)	L_s (nm)	L_F (nm)	TE (μm)
C	5.7	2.265	4	10	0.2
CsI	6.3	4.51	30		
LiF	8.0	2.625	24	200	0.5

TE; Tissue Equivalent, L_F ; Film thickness

To simulate target sizes in the nanometer region, at least one secondary electron should be emitted from each side to satisfy the coincident requirements. The secondary electrons could be multiplied and detected by connecting a multistep avalanche counter on both sides. Then with Monte Carlo simulation via electron bombardment, the probability distribution of lineal energy of the SEE's at the entry and exit sides are calculated.

Despite the fact that alkali halides are very good secondary electron emitters when irradiated by ionising radiations, they are not suitable for instrumentation in the unified radiation dosimetric system for a number of reasons:

(1) Although the rediffused electrons from the media can be discriminated by proper instrumentation, some may escape and ionise the gaseous detection media, and thus complicate the analysis of the resulting spectra. Further, there is a chance that the secondary electrons are produced from the inter spacing between the escape zone surfaces and thus contradict the idea of two isolated detectors spaced by non-interactive media.

(2) The alkali halide closest to tissue equivalence is LiF with a density of 2.65 gm/cm^3 (table 5-1). The optimum thin film dimensions for the production of SEE's for the two escape zone surfaces are far from the dimension of the DNA spacing. Also, E_G for LiF is about 8 eV, and the average energy of the maximum yield is about 2 eV, consequently the yield could be very low. This would indicate that the SEE is likely to have very low sensitivity, moreover a single interaction event will be hardly detectable.

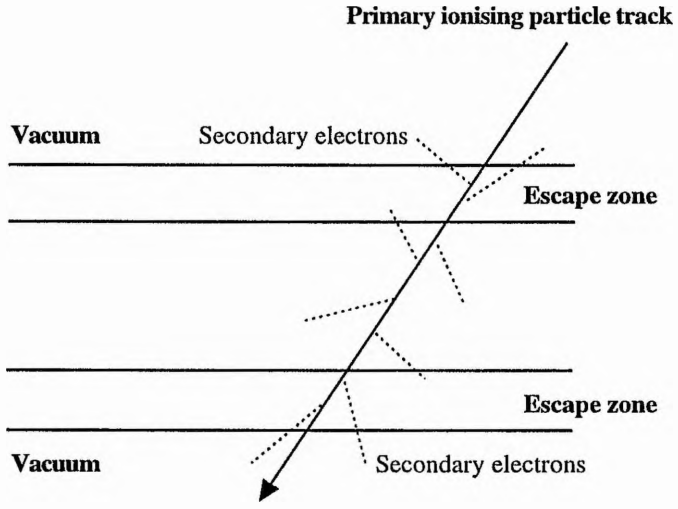

Figure 5-1 A detector based on thin film secondary electron emission.

5-3 Detectors Based on Semiconductivity

5-3-1 Background and principles

The main attraction of semiconductors for nanodosimetry is their high resolution compared to that of scintillators and other conventional detecting systems. The energy required to produce an electron-hole pair is of the order of 4 eV. The main characteristic features of semiconductors are shown in table 5-2.

Table 5-2 Intrinsic properties of semi-condcucting material*.

	Si	Ge
Atomic number, Z	14	32
Density, ρ (gm/cm^3)	2.33	5.32
Number density, N (atoms/cm^3)	4.96 x 10^{22}	4.41 x 10^{22}
Forbidden energy gap, E_G(eV)	1.115	0.665
Intrinsic carrier density, n_i or p_i (cm^{-3})	1.5 x 10^{10}	2.4 x 10^{13}
Intrinsic resistivity, ρ_i (Ω-cm)	2.3 x 10^5	47
Electron mobility, μ_e (cm^2/V.s)	1350	3900
Hole mobility, μ_h (cm^2/V.s)	480	1900
Average energy per electron-hole pair W_p(eV)	3.62	2.96
Dielectric constant	12	16
Fano factor, F (at 77 K)	0.14	0.13

* Adopted from Knoll, 1988

All properties are given at 300 K unless otherwise stated.

The basic properties of pure semiconductors are influenced by one or more of the following [Sze, 1981]:

(1) the addition of impurities of group III (donor impurities) or group IV (acceptor impurities) give rise to a majority carrier of one type or the other (e.g. holes and electrons). Thus these impurities give rise to other classes of semiconductors known as n-type, which arise from semiconductors doped with donor impurities and p-type, which arise from acceptor impurities. If the two types p- and n-types are brought together in good thermodynamic contact, a p-n junction semiconductor will be formed. The majority carrier of n-type is termed as N_D and the majority carrier of p-type is termed as N_A.

(2) changing temperature can alter the physical properties of semiconductors such as the carrier mobilities and resistivities. The probability per unit time that an electron-hole pair is thermally generated is given by the simple classical Boltzman distribution, $P(T)=f(T)\exp(-E_G/kT)$, where $f(T)=CT^{3/2}$, C is constant, k is Boltzman constant, T is the temperature in Kelvin, and E_G is the energy gap between the valence and conduction bands which is of the order of 1 eV in semiconductors (see table 5-2). In the absence of an electric field the thermally created hole-electron pairs would ultimately recombine.

(3) applying an electric field will influence carrier transport. At low electric field E, the carrier drift velocities will be $v_h = \mu_h E$ and $v_e = \mu_e E$, where μ_h and μ_e are the hole and electron mobilities which are of the same order of magnitude. At higher electric field the carrier drift velocities will reach a limiting value which is of the order of 10^7 cm/s in Si. It is preferable to operate semicoductor detectors at the limiting velocity since this will minimise the time of collecting the charge at small dimensions which is typically of few nanoseconds.

It is important to note that no matter what influence there is on the semiconductors, the balance of charges of carries (created or recombined) is always maintained at equilibrium such that the product of carriers of the new class is equal to the product of the carriers of the intrinsic class (e.g. $np = n_i p_i$).

Thus when a charged particle passes through an intrinsic semiconductor, it produces electrons-hole (e-h) pairs along its tracks. For high LET ions, δ-rays will be an essential part of their products, which subsequently lose their energy in producing more e-h pairs. To simplify the process, regardless of the nature and energy of the ionising radiation, the average energy needed to create an e-h pair is defined as ε(eV). The smaller average energy needed to create an e-h pair makes it possible to produce more charge carriers. Thus the detection medium is affected by the radiation energy, the higher energy would narrow the statistical fluctuations in the number of carriers per pulse which leads to a better signal/noise ratio. However, for low energy

radiation, the resolution could be limited by the electronic noise in the preamplifier [Knoll, 1988].

The dependence on particle energy of the average energy per e-h pair, $W_{e\text{-}h}$(eV), has been examined by a number of authors. Not much difference has been found between fast electrons and fast light ions. However, a small difference up to about 2.2% has been noticed between protons and alpha particles and much higher diversities are seen for heavy ions or fission fragments. The ionisation energy ε is seen also to be temperature dependent e.g. ε have lower values for higher temperatures.

Another important parameter is the Fano factor (F) which is defined as the ratio of the observed statistical variance to the fluctuations of carrier number. For the detection of N e-h pair excitations, the intrinsic root mean square energy resolution R(E) is given by $R(E)/E = (F/N)^{1/2}$ and the FWHM = 2.35 R(E) = $2.35(W_{e\text{-}h}\, F\, E)^{1/2}$. Thus to optimise the resolution, the Fano factor must be kept as small as possible. The diversion of the Fano factor from unity is not completely understood. Favourable Fano factors are included in table 5-2.

5-3-2 The possibility of using semiconducting devices as a unified dosimeter

Favourable radiation detector properties can be based on the junction between n- and p-type. Charged carriers are able to migrate from regions of high concentration to low in accordance with Ficks diffusion law. An equilibrium is established, and a potential difference (contact potential) V_o exists between the two regions (typically 0.5 V) and the net current density is zero. Under the influence of an electric field both electrons and holes will move in opposite directions. Thus if a reversed bias V_r is applied, the total potential across the junction becomes $V_o + V_r$. Such potential makes the motions of both electrons and holes hard, thus limiting conduction to very small current. The electric potential ϕ across the junction is governed by Poisson's equation $\nabla^2\phi = -\rho/\varepsilon$ where ρ is the net charge density and ε is the dielectric constant of the medium. The associated electric field E will be related to the electric potential

ϕ by the relation $E= -\nabla\phi$. The charge flow set up by an electric field E across the junction can be measured by an external circuit.

Reverse bias junctions are of practical importance for radiation detection. The region where recombination of electrons and holes form a free charge region at zero bias is known as the depleted region. With a reverse bias V_r the width d of this region is found to be:

$$d = \left(\frac{2\,\varepsilon_d\,V_r}{eN}\right) = \left(2\,\varepsilon_d\,V_r\,\mu\,\rho_d\right)^{1/2} \qquad 5\text{-}4$$

where N is the dopant concentration, whichever has lower dopant level (N_d or N_c), ρ_d is the resistivity of the doped semiconductor ($1/e\mu N$), e is the electric charge, μ is the mobility of the majority carrier and ε_d is the dielectric constant. This part of the junction represents the effective sensitive region for the detector. It has significantly reduced concentrations of carriers (holes and electrons) and therefore higher resistivity. In conventional detectors it is usually required to have a depletion depth but small detector capacitance ($C = \varepsilon_d/d$). Thus this will result in a high internal electric field.

Experience exists on the use of semiconductors as transmission detectors for charged particle identification [Goulding, 1975]. Their high atomic number is an advantage for detecting electrons, however the minimum thickness obtainable is in the order of mg/cm^2 which exceeds the range of these minimum ionising particles.

For detectors in unified dosimetry both the application of reverse bias (to minimise the noise), and shallower depletion regions are targeted. This would imply that doped semiconducting material should be of low dielectric constant or low resistivity.

The use of conventional rectifying diodes, operated at low voltage, will be limited by low-level noise discrimination and tissue equivalence. Although a bias lower than 0.5 V may not be sufficient to draw currents through the junction (thus higher noise could distort the output signal), careful selection of the semiconductor and manipulation of its fabrication and operation conditions may reduce the noise.

However the high atomic numbers of conventional semiconductors make them far from tissue equivalent. On the other hand organic semiconductors which are in the form of polymers seem to offer solutions to these problems. The low atomic weights of their constituents qualify them to be nearly tissue equivalent. The high content of hydrogen in organic semiconductors indicates good prospects for neutron detection. The two detector system which simulates the double strands of the DNA can be constructed by employing the Langmiur-Boldgett technique for making ultra thin films of organic semiconducting material on both sides of a solid substrate [Roberts, 1981]. The semiconducting layers can then be doped with a suitable ionic material. The techniques require ultra vacuum conditions. Despite these, consideration of technical problems related to molecular wiring is still a problem.

Other ideas can be used by implementing multiple junction devices such as transistors e.g. pnp or npn junction devices. Again, the depletion regions represent the target detectors. Their depth can be controlled by the low reverse bias. Thus these sort of devices can be tailored with specifications related to the unified dosimetry system.

Metallic semiconducting compounds have properties which may provide another means of approach to unified dosimetry. Field-effect transistors (FETs) e.g. metal-oxide semiconductor field-effect transistors (MOSFETs), and metal semiconductor field-effect transistor (MESFETs) show their compatibility as radiation sensing devices. They are simple to fabricate and occupy little space on a chip. Nowadays technology is at the stage where, a chip with a density exceeding millions of MOSFETs per chip can be made. Studies related to single event upset (error) by solar radiation to these type of devices in space may provide the necessary tools for implementing them toward a unified dosimetry system [Bradford, 1978 ; Mcnulty, 1980 ; Mnich, 1983 ; Luke, 1988].

5-4. Detectors Based on Superconductivity

5-4.1. Background and principles

The phenomena of superconductivity is based on the superconducting state that is characterised by the condensation of conduction electrons into the ground state, in which they form Cooper pairs with equal and opposite spins. The electron pairs interact via an attractive potential set up by the positive core, and is accomplished by phonon exchange which indeed dominates over the coulomb repulsive potential at temperature lower than the critical temperature T_c. The interactive pair results in the electron state denoted as $2\Delta(T)$ near the Fermi energy level E_F. Cooper pairs are occasionally broken by phonons, resulting in quasiparticles. The number density of quasiparticles N(T) is proportional to the classical Boltzman factor $\exp(-\Delta(T)/kT)$ and so is strongly temperature dependent. By 1986 superconductivity was established at a higher critical temperature T_c for complex oxides, compare to that of low temperature superconductivity for pure metals, i.e. $T_c \sim 1.75\ ^{o}K$. Recently superconductivity was observed at $125\ ^{o}K$. This would reduce the heat load in cryogenic experiments. While the Bardeen-Cooper-Schriefer theory satisfactorily explains the mechanisms involved in low temperature superconductivity, no complete theory is available for high temperature superconductivity.

When an ionising particle such as an electron resulting from an interaction deposits its energy in a superconductor, quasiparticles of the order of 10^9 /MeV above the energy E_F are formed as a result of Cooper pairs. Phonons are radiated with energy $\Omega \geq 2\Delta(T)$. At a later time, recombinations of quasiparticles via interaction with phonons take place. The complexity of the system arises because we are dealing with three fluid systems, quasiparticles, Cooper pairs, and phonons which are also interrelated in different ways. The mechanisms and energy scales of the process quasiparticles, phonons, and their fates (figure 5-2) is discussed in details in a number of references [Booth, 1987].

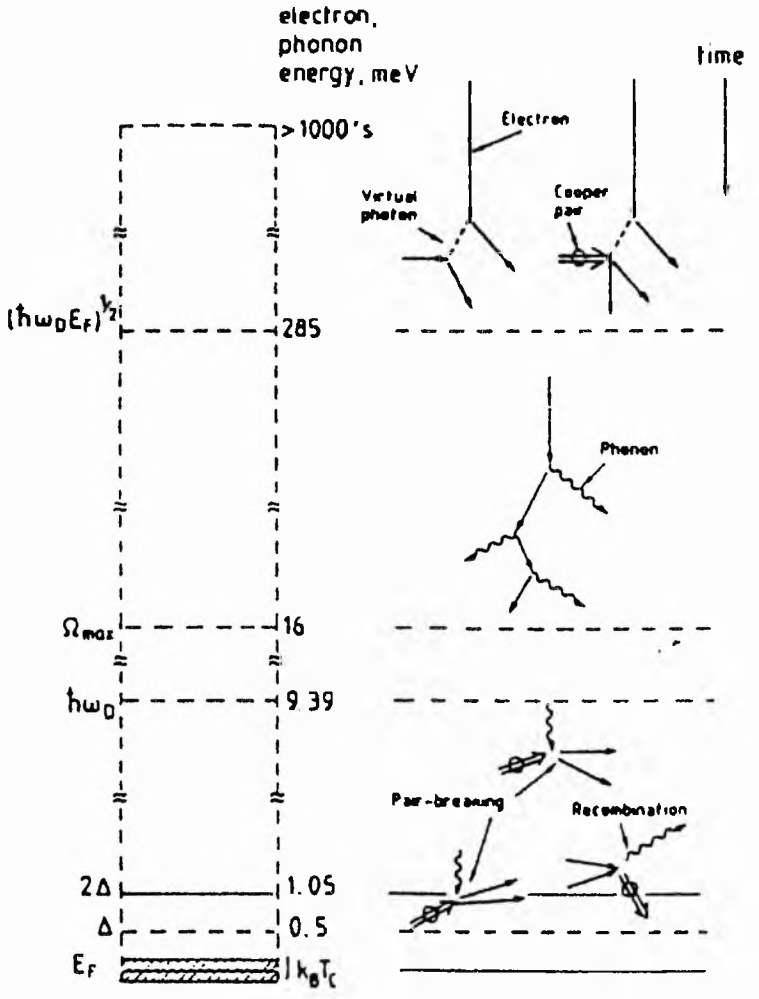

Figure 5-2 The mechanisms and energy scales of the process quasiparticles, phonons, and their fates [adopted from Booth, 1987].

5-4-2 The possibility of using superconducting devices as a unified dosimeter

The motivation for using radiation detectors based on superconducting junction is largely due to the growing interest of measuring the energy of single nuclear particles or quanta which are present randomly in time [Booth, 1996]. In principle superconducting material offers the prospect of high resolution as compared to other detection material such as metals, semiconductors, scintillators...etc. Table 5-3 contains a comparison of the vital important physical parameters for those material [Barone, 1995]. The energy required to create a hole-electron pair in semiconductors is of the order of 4 eV, this energy could produce more than 1000 quasiparticles in superconductors. This number accounts for the predicted statistical improvement in energy resolution.

If two superconductors are separated by a thin layer of insulating material e.g. metal oxide, and a biased voltage is applied between them, a current will flow between the superconductors via quantum tunneling [Baron, 1982]. Superconducting tunnel junctions, (SPJ's), are classified into two types. The first is Giaever type junctions. They are simple contacts with junction thickness ~5-10 nm. Single particle tunnelling can take place which results in depairing the Cooper pairs via thermal activation. The second type is the Josephson type junctions, the thickness of junction is of the order of 1 - 2 nm. Tunnelling results mainly in Copper pairs. The I-V characteristics of the two types are shown in figure 5-3.

Experimentally, for Nb/Al/AlO_x/Al/Nb STJ detectors the best energy resolution width is ΔE = 29 eV for 6 keV X-rays [Joose, 1996] which is still much higher than the theoretical estimates of $\Delta E \sim 4$ eV for 6 keV X-rays [Rando, 1995]. Nevertheless this is a significantly improvement over the $\Delta E \sim 135$ eV for the best Si detectors [Takahashi, 1994]. The energy resolution is proportional to $\varepsilon^{1/2}$ and is more than an order of magnitude better in a superconductor than any other conventional device.

Table 5-3 Comparison of basic properties of the different material properties for radiation detection.

Detector Media	Excitations	ε	ΔE	Examples
Organic Scintillators	photons	60 eV	~ keV's	NE102A
Inorganic Scintillators	electron-holes	20 eV	~ keV's	NaI 300 eV
Semiconductors	electron-holes	1 eV	135 eV	Si 3.6 eV
Superconductors	quasiparticles	1 meV	29 eV	Nb 2.6 meV
Crystals	phonons	0.1 meV	~ 1 eV	lattice vibrations

ε: energy required to create an exciton ; ΔE: resolution

The best way to detect quasiparticles, which are related to the energy deposited by the ionising particles, is by means of STJ's. In principle either a Giaver or Josephson STJ's can be used for unified dosimetry. However, due to the tunnelling probability, Josephson STJ's are employed whenever the zero voltage current, I_c occurs (Josephson supercurrent), as shown in figure 5-3c.

The biased voltage value V_B is usually less than 1 mV. The equivalent circuit diagram is shown in figure 5-4 [Cristiano, 1993]. It is important to suppress the Josephson super current, I_c which exceeds the quasiparticle subgap current by an external applied magnetic field [Barone, 1995]. The junction is represented by a parallel capacitance C_D, the dynamic resistance R_D, the excess quasiparticles current due to interactions by the ionising radiation D_I and the feed back capacitor C_F. The symbols I_N,V_S are the intrinsic junction noise and amplifier noise respectively. The tunnelling barrier and the "detector volume" should be small to maximise the tunnelling rate over the recombination rate, and the energy losses.

Table 5-4 Physical properties of superconducting material [Baron, 1995].

Material	Z	A	ρ g/cm^3	T_C K	T_D K	Δ meV	τ_o ns	τ_o^{ph} ps	$\tau_{\phi\phi}$ ms
Al	13	27	2.69	1.175	420	0.180	110	242	3300
V	23	51	6.11	5.40	383	1.600			
Nb	41	93	8.57	9.25	276	1.515	0.149	417	0.030
In	49	115	7.31	3.408	109	0.540	0.799	169	0.20
Sn	50	119	5.75	3.722	195	0.590	2.30	110	1.60
Ta	73	181	16.65	4.47	258	1.400	1.80	22.7	
Pb	82	207	11.35	7.196	96	1.350	0.196	34	0.006

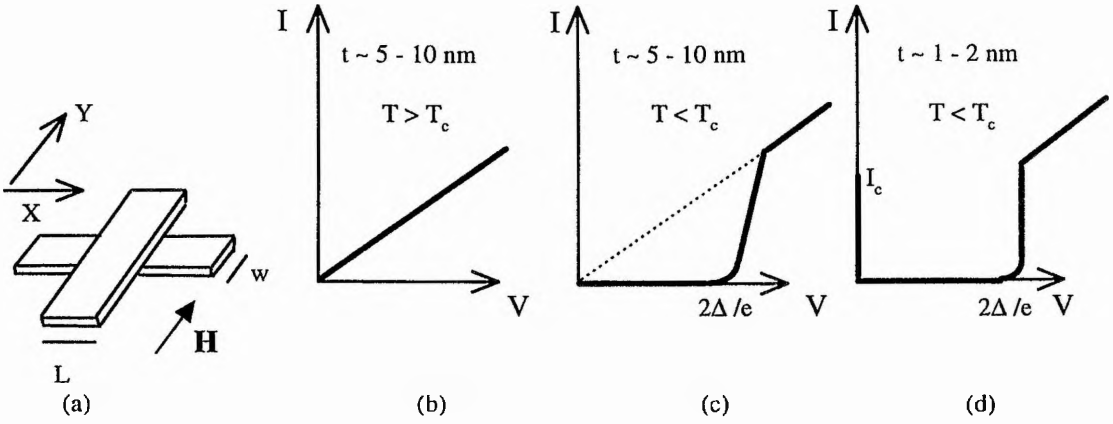

Figure 5-3 Superconductor junction I-V characteristics. (a) Junction structure; (b) I-V curve for junction electrodes in normal state ($T>T_c$) ; (c) I-V curve of superconductive structure ($T<T_c$) ; (d) I-V curve of a Josephson junction (t ~ 1 nm).

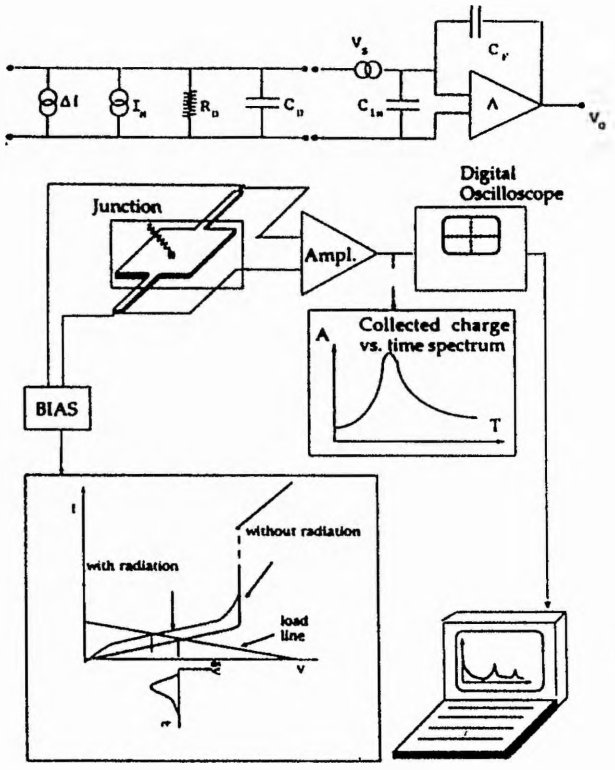

Figure 5-4 A superconductor tunnel junction (STJ) detector equivalent circuit diagram [adopted from Cristiano, 1993].

Several technical requirements reviewed by Baron, 1995 are needed to minimise the losses of quasiparticles. The main problem arises with STJ detector is related to the weak current signal even in the presence of a large number of carriers produced (due to the long time necessary for of collections of the excess quasiparticles by the tunnel junction). This problem can be reduced by the introducing an absorber layer of larger gap material in contact with lower gap material which acts as a trap, as shown in figure 5-5. The idea is that once the quasiparticles are created in the absorber, they diffuse into the lower gap layer, lose their energy by phonon emission, and the quasiparticles are then forced to tunnel through the junction with higher frequency, speeding the tunnelling, and therefore leading to a larger current signal [Booth, 1987 ; 1988].

The structure of Josephson-type Junction, their properties and dimensions, represent a unique advantage for radiation measurements in nanometer dimensions. Such devices could be tailored to fabricate either two single junctions separated by an insulator, or a multiple junction system to serve the purpose of building a unified dosimeter. The unified dosimeteric system would be based on the critical thickness of sensitive volume of the junction(s). e.g. two STJ's separated by an ultra thin inactive substrate with proper external electronic circuits. Then it should be possible to simulate the two strands of the DNA.

Athough STJ's offer much greater potentiality over other detecting media, in terms of energy resolution and the very low bias voltage (~ 0.5 mV) and the consequent better signal to noise ratio, superconductivity may not be the best approach to suit needs at the present time. For example their high density makes them far from tissue equivalent. The availability of superconducting materials and the practicabilities of operation add other disadvantages e.g. they are cryogenic dependent, highly delicate with weak support, and must be operated under high vacuum.

Higher temperature ceramic superconductors, now operable at ~ 70 ^{o}K may offer prospects of alleviating the very low temperature requirements.

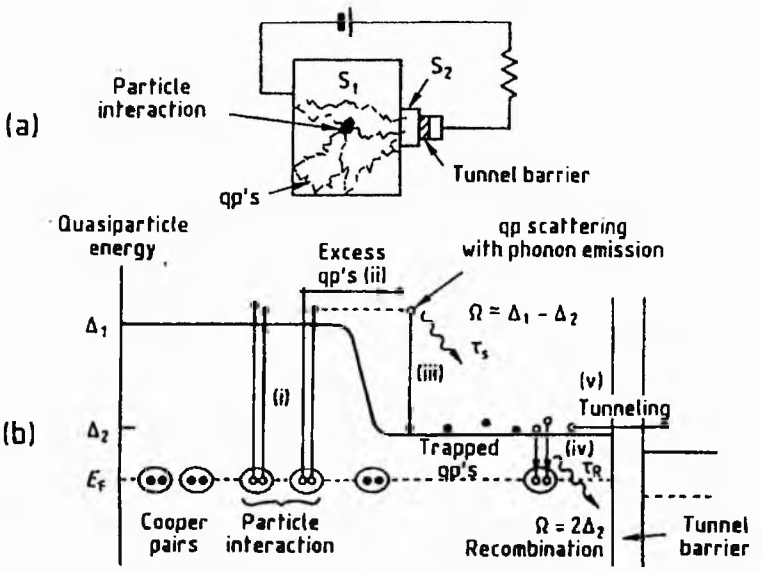

Figure 5-5 Principles of quasiparticles (qp's) trapping showing a trap S2 between the absorber S1 and the tunnel junction (a) and an energy diagram (b) showing the processes (i) creation of excess qp's by a particle interaction, (ii) diffusion of qp's into the trap, (iii) scattering of qps to the new gap edge by phonon emission, (iv) recombination of the qp's in the trap, (v) tunneling of trapped qp's.

5-5 Detectors Based on Scintillating Materials

Many compounds scintillate when exposed to ionising radiations. Light is emitted in response to the ionisation produced by a charged particle. There are two types of scintillating material, organic- and inorganic scintillators. The mechanism of luminescence in organic scintillators is based on the molecular excitations whereas, for the inorganic scintillators it is based on the generation of excitons (e-h pairs) in the impurity energy gap, e.g. NaI(Tl). Both mechanisms have been extensively reviewed in the literature [Birks, 1964 ; Heath,1979 ; Brook,1979].

The need to detect and identify heavy ions is leading to extensive use of scintillators [Menchaca-Rocha, 1993]. The move from traditional solid state methods is mostly related to size and price of semiconductor detectors [Goulding, 1975; 1985].

Despite their limitations, e.g. poor resolution, and the high energy needed (1keV) to create a measurable photons at the face of photodetecting devices (table 5-3), organic scintillators are seen to offer more advantages over the other devices reviewed in the preceding sections. Far from their tissue equivalent properties, the experience of our laboratory from previous years has shown their practicability e.g. they are available in different sizes and shapes (spheres, rods, and thin films), their availability e.g. they can be manufactured at the laboratory with the desirable ratio of their constituents (solvents and solutes). The basic properties of organic scintillators and their feasibility to be used as a unified dosimeter will be reviewed in details in the next chapter.

Chapter 6

ORGANIC SCINTILLATORS & UNIFIED DOSIMETRY

In this chapter the basic physical and chemical properties of organic scintillators are discussed with the ultimate objective of their application to unified dosimetry. The basic physical requirements discussed in chapter 5 are to be met. From data available in the literature, the response of ionising radiation (charged particles) on plastic scintillators will be examined against the various quality parameters. The response and the radiation qualities will be subjected to test of the various models available in the literature including the St-Andrews unified model. A feasibility study for measurements of the biological effectiveness of ionising radiation at nanometer dimensions will be carried out.

6-1 Theory and Mechanism of Scintillations in Organic Material

Organic scintillators are a class of aromatic compounds. Basically they consist of planer benzene rings. They are classified as unitary, binary, ternary, and higher order. A binary scintillator consists of a solvent, sv and a solute ps. Ternary scintillators are made of a solvent and primary solute, ps, and secondary solutes, ss. Secondary solvents sv' may also be used. The most commonly used solvents and solutes are tabulated in table 6-1 [Berlman, 1971 ; Turro, 1978].

Table 6-1 Common solvents and solutes for organic scintillators.

Compounds	Formula	Application
Benzene	C_6H_6	sv
Toluene	$C_6H_5CH_3$	sv
P-Xylene	$C_6H_3(CH_3)_3$	sv
Naphthalene	$C_{10}H_8$	sv'
Biphenyl	$C_{12}H_{10}$	sv'
p-Terphenyl	$C_{18}H_{14}$	ps
PPO	$C_{15}H_{11}NO$	ps
PBD	$C_{20}H_{14}N_2O$	ps
POPOP	$C_{24}H_{16}N_2O_2$	ss
TPB	$C_{28}H_{22}$	ss

sv:solvent sv': secondary solvent ps:primary solute ss:secondary solute
PPO = 2,5-diphenyloxazole ; PBD=2-Phenyl,5-(4-biphenylyl)-1,3,4-oxadiazole
POPOP = 1,4-Bis{2-(5-phenyloxazoly)}-benzene
TPB = 1,1',4,4'-Tetraphenyl-1,3-butadiene

Physical and chemical properties of common solvents and solutes for scintometry can be found in a number of references e.g. Wiel, 1989 and Gusten, 1989.

6-1-1 The mechanism of organic scintillation process

Although not fully understood, the basic mechanisms for light production in organic scintillators is covered in detail in a number of references (e.g. Birks, 1964 ; Brooks, 1979 ; Bransome, 1970). The main components of organic scintillators are an aromatic solvent, X, e.g. xylene or toluene; an aromatic fluorescent primary solute Y, e.g. PPO, PBD and an aromatic fluorescent secondary solute, Z, e.g. POPOP, which acts as a wave shifter to longer wavelength. The molar concentrations of primary solute, $\{Y\} \approx 10^{-2}\ M$, and of the secondary solute $\{Z\} \approx 10^{-3}\ M$.

The process of fluorescence in organic scintillators arises from transitions between energy levels of the molecular structure. This is related to the symmetric properties associated with the π-electronic structure of the organic molecules. The two main electronic sets that form the basic scintillation processes are the singlet state with spin = 0; energy levels S1, S2, S3... and the triplet state (spin=1); energy levels T1, T2, T3... . The spacing of these energy levels are of the order of a few electron volts. The electronic energy levels are subdivided into vibrational levels which have the order of a fraction of eV. Figure 6-1[Birks, 1964] shows energy level representations for the corresponding two electronic states.

Initially, at room temperature (E = 0.025 eV), all molecules are in their ground state S_{00}. Two processes are involved once an ionising particle interacts with the organic scintillator. (i) absorption , which raises the molecule to a higher excited singlet state, and (ii) emission which de-excites those molecules, by the emission of photons to lower vibrational levels in their electronic ground state. The absorption process can occur in the order of pico-seconds. The higher singlet excited states and vibrational states in the first excited electronic states de-excite to S1 through radiationless internal conversion and thermalization to equilibrium states respectively. Organic molecules at S1 then make the transition either to the ground state S0, via the fluorescence process, or to a higher electronic triplet state, T1. The transition from

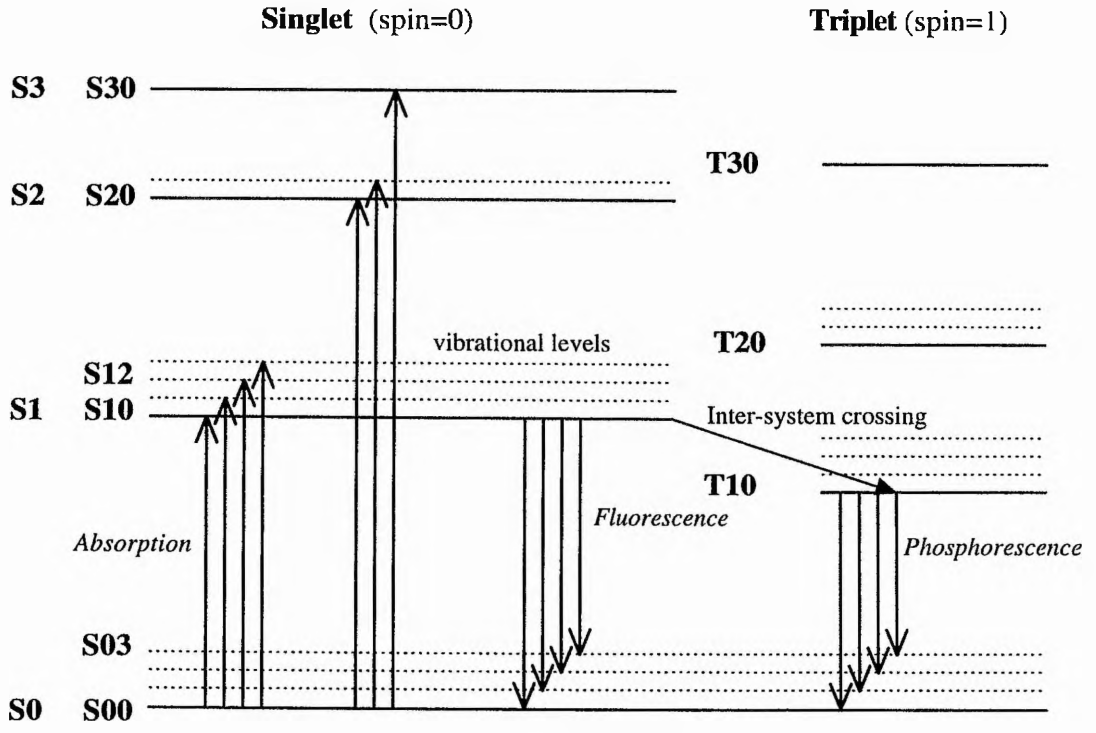

Figure 6-1 Energy levels of an organic molecule with π-electron structure (Adopted from J.B. Birks, 1964).

T1 to S0 is responsible for delayed phosphorescence. These transition processes can be summarised as:

I -	$R_n \rightarrow R_{n-1}$	Internal conversion.
II -	$R_1 \rightarrow {}^*R_1$	Inter-system crossing.
III -	$R_1 \rightarrow R_0$	Fluorescence or internal conversion.
IV -	${}^*R_1 \rightarrow R_0$	Phosphorescence or inter-system crossing.

It is noted that transitions I ($S_n \rightarrow S_{n-1}$ and $T_n \rightarrow T_{n-1}$) are sufficiently rapid (~ 1 ps) that radiative transitions from S_n and T_n are not normally observed and the last transition IV ($T_1 \rightarrow S_0$) phosphorescence occurs as a delayed process (life time ~ up to 1 ms). However not every transition of the third ($S_1 \rightarrow S_0$) or the fourth ($T_1 \rightarrow S_0$) types will result in fluorescence or phosphorescence.

If only the solvent was exposed to ionising radiation, the fluorescent yield would be very low. In some cases it is not even transparent to its own emission wavelengths. The addition of a primary solute could make an efficient scintillator, but non-radiative energy transfer from the main matrix (solute) to the primary solvent could occur. Addition of a secondary solute serves to shift the wavelength from the UV region to the visible blue or green region, via radiative transfer. It should be noted that both the primary and the secondary absorbing and emission spectra interfere, which means that they absorb their own emitted spectra.

6-2 Physical Properties of Organic Scintillators

The basic properties of the most common scintillators in use are listed in table-6-2. It is quite apparent that there are several advantages in using organic scintillators over inorganic scintillators. Organic scintillators have the faster response time of the order of nano-seconds, lower densities and are easy to handle. This is in contrast to the inorganic scintillators which despite their high efficiency, e.g. NaI(Tl), they may be hygroscopic and have higher refractive indexes. Solid organic scintillators are usually more practical than liquid organics due to the containment and geometry problems of the latter. However not all solid organic scintillators are convenient in

practice. For instance, crystalline organics such as anthracene and stilbene are brittle and possess an isotropic response to radiation. Plastic scintillator, available commercially as NE102 offers distinct advantages for the present purpose.

Table 6-2 Classification of commercially available scintillators.

Scintillator	Density, gm/cc	Refractive index, n	Boiling or Melting point, °C	Decay Constant, ns	Wavelength of max. emiss.; nm	H/C ratio	Light output % Anthracene
OP	1.032 - 1.140	1.580 - 1.594	75 - 99	1.6 - 3.3	370 - 495	0.957 - 1.109	46 - 68
OL	0.796 - 1.610	1.380 - 1.508	81 - 350	2.6 - 4.0	420 - 430	0.984 - 2.000	20 - 80
OC	1.160 - 1.250	1.620 - 1.626	125 - 217	4.5 - 30	410 - 447	0.715 - 0.858	50 - 100
IC	3.170 - 7.130	1.775 - 2.357	650 - 1850	70 - 1100	413 - 580	0	20 - 300

OP= Organic Plastics ; **OL**=Organic Liquids ; **OC**=Organic Crystals : **IC** = Inorganic Cystals
Source: Table of Physical constant of Scintillators, Nuclear Enterprises, Inc. 1995.

6-2-1 Plastic scintillators

Plastic scintillators are the solid forms of organic liquid scintillators. They are composed of an aromatic plastic base, which has a benzene ring as an appendant along the polymer backbone, an aromatic primary and secondary fluors. The concentration of the primary fluors ranges from 0.3 - 4 % by weight. The concentration of the secondary fluors ranges from 0.001 - 0.100 % by weight of the plastic base.

Plastic scintillators have been in use in the detection of heavy charged particles for some decades [Muga, 1971; Ajitanand, 1976; Batra, 1984]. They have several advantages over liquids. For example, being solid they can be positioned very easily. They are easy to handle, cheap, and suffer negligible radiation damage at very high doses [Bross, 1992; Ilie, 1993; Wick, 1991; Zorn, 1990]. They are inert to water and air, and to some other chemicals. Their low atomic weight and low density which is about the same as that of water, makes them more closely tissue equivalent. They can be machined into any desired shape or form such as spheres (with diameters ranging from a few microns to several meters) rods or thin films. The most frequently used solvents are polystyrene (PS), polyvinylxylene (PVX), and polyvinyltoluene (PVT). Practical common solutes are p-terphenyl and POPOP. The exact composition of some plastic scintillators are included in various references e.g. Swank, 1954. It is noted here that all concentrations for primary or secondary solutes are optimised for both maximum emission of light and to avoid polymerisation problems [Wolfgang, 1956 ;

Birks, 1964 ; Murray, 1962; Rebourgeard, 1989]. Table 6-3 contains a summary of compositions. Number 3 in the list is commercially code-named as NE102A provided by NE Technology, Edinburgh.

Table 6-3 Composition of common plastic scintillators.

	Solvent	Primary Solute (gm/l)*	Secondary Solute (gm/l)*	Decay time (ns)	$\lambda_{max;}$ nm	Light output % Anthracene
1	PVT	p-Terphenyl (36)	p,p'-diphenstilbene (0.9)	3	380	48
2	PVT	p-Terphenyl (36)	TPB (0.2)	4	445	45
3	PVT	p-Terphenyl (30)	POPOP (0.5)	2.4	423	65

* Gram of solute per 1000 gm of solvent.

The spectral response in the visible region, peaks at 423 nm in the blue part of the spectrum. The decay time is 2.4 ns [Hansen, 1995; Walker, 1969]. The light output of NE102 relative to anthracene is about 65%. The light yield of NE102A is 10 - 15 photons per 1 keV of absorbed energy and the absolute light output for fast electrons is 3% of the energy deposited in the scintillator [Miyajima, 1993 ; Holl, 1988].

6-3 Experimental Response of NE102 to Ionising Radiation

6-3-1 Response to light charged particles

The response of the plastic scintillator NE102 to electrons is found to be linear for particle energies above 125 keV [Birks, 1964; Brannen, 1962]. Experimental data used to reach this conclusion is obtained either directly using electron beams or indirectly via Compton recoil electrons from γ-sources e.g. ^{60}Co and ^{57}Co [Gettner, 1960 ; Prescott, 1961]. The response of NE102 to electrons has been measured over the energy range from as low as of few keV's to the relativistic domain of 20 MeV [Evans, 1959 ; Prescott, 1961; Feist, 1968]. The linear response is valid up to a dose rate of $5x10^{10}$ Gy/sec [Harrah, 1971]. However, the response for protons with the same energies as electrons, at about 1 MeV or less, is lower by a factor of 10, as shown in figure 6-2. The discrepancy is reduced for higher energies [Smith, 1968; Craun, 1970].

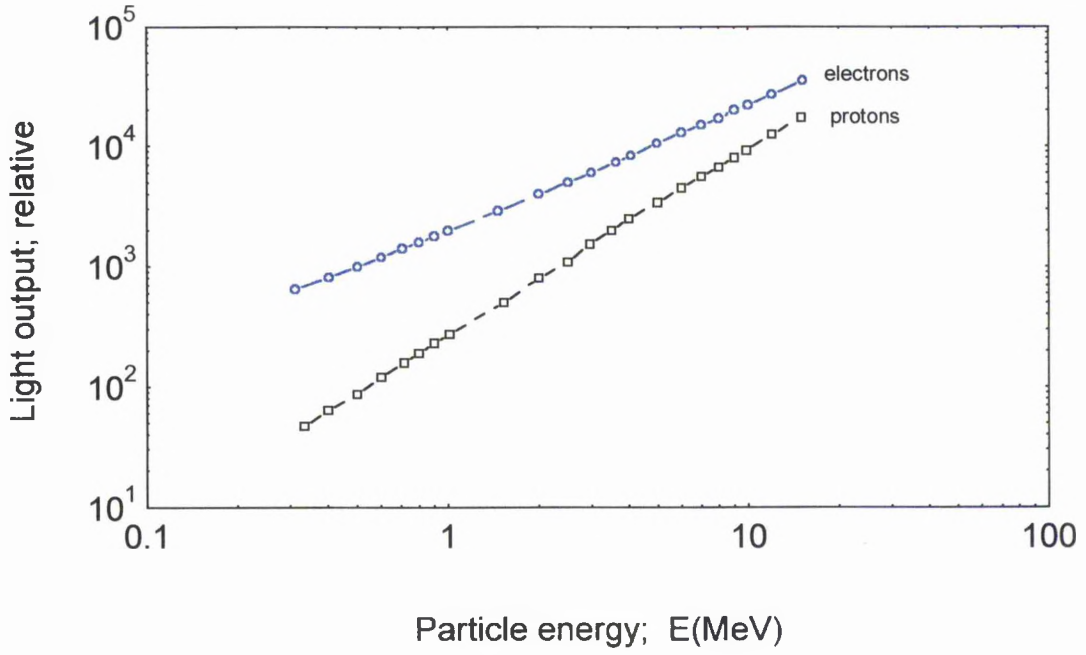

Figure 6-2 Response of NE102A to electrons and protons, Craun, 1970.

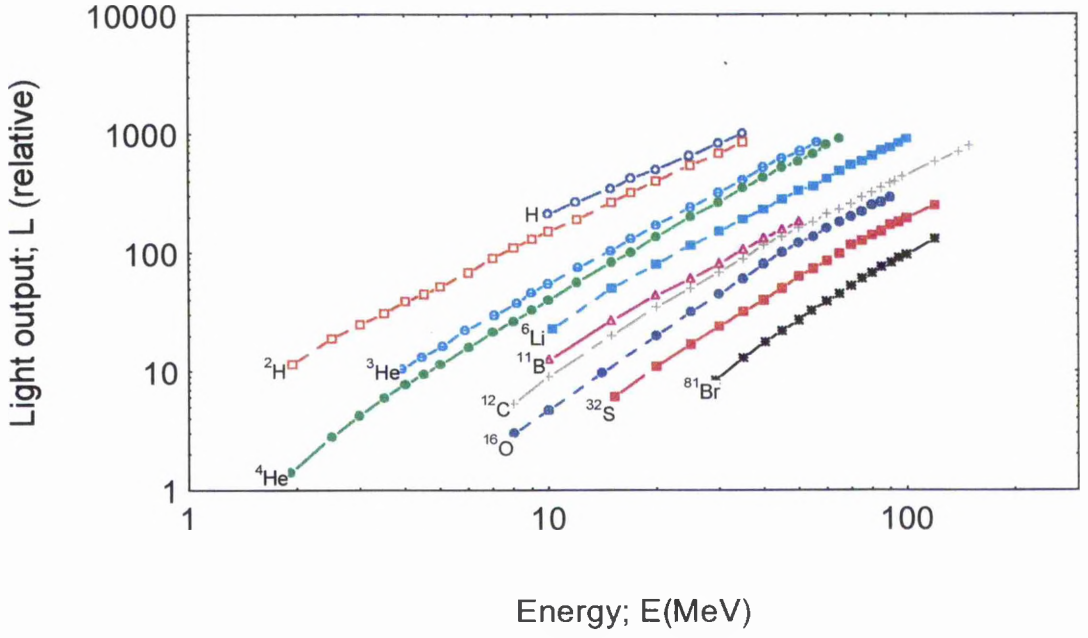

Figure 6.3 The response of NE102A to heavy ions, Becchetti, 1976.

6-3.2 Response to heavy charged particles

The response to protons, and other heavy ions has been studied with particle energies up to a few hundred MeV's [McParland, 1986; Madey, 1978; Flynn, 1964; Muga,1974; Becchetti, 1976; Degtyarenko, 1985]. Figure 6-3 shows the response of plastic scintillators to heavy ions (z=1-35) as with energies up to 170 MeV, fully stopped in the phosphors [Becchetti, 1976]. The non-linearity of response to heavy ions other than protons is clearly evident. Heavier ions are seen to have less response. Lighter ions have a linear response at lower energies.

6-3-3 The response of phosphors to uncharged ionising radiation

X-rays and γ-rays penetrate thin plastic scintillators (NE102A) with minimum interactions, as their photoelectric cross sections are very small, no photo-peaks are observed [Miyajima, 1993]. Nevertheless despite the low efficiency of NE102A plastic scintillators, they still can be used to detect X-rays and γ-rays in terms of their Compton secondary electrons [Evans, 1959; Gettner, 1960; Steinbauer, 1988].

On the other hand, since plastic scintillators have a high hydrogen content, neutrons can be detected quite easily through the proton-recoil process. Response measurement data for neutron energies from l00 keV up to 130 MeV shows a non-linearity response in the energy range below 2.3 MeV [Wishart, 1967; Gettner, 1960; Crabb, 1967; Thornton, 1971]. A linear response is observed at much higher neutron energies, as expected from the response of protons.

6-4 Modelling the Response of Plastic Scintillators

The response of scintillators to charged particles exhibits a decreasing scintillation efficiency, dL/dE, with increasing specific energy loss, dE/dx, of the primary particle. Early experiments using organic and inorganic scintillators [Muga, 1974 ; Voltz, 1966 ; Becchetti, 1976 ; Newman, 1960] suggested that their light response is a function of ion type and not solely determined by their stopping power owing to the fact that different ions of exactly the same dE/dx have been observed to have different light response. A number of theoretical models have been suggested [Birks, 1964; Meyer,

1962; Katz, 1968; Luntz, 1971; Salamon, 1981; Muga, 1974 ; Michaelian, 1994] to identify energy deposition mechanisms and their relation to the luminescence phenomena. The aim of many authors is to find a generalised model that will fit experimental data obtained with both inorganic and organic scintillators. In this section we will survey the main models and thus seek a possible model which fits the response of an ideal unified dosimeter (Section 6-4-7). For every model there is an association between response e.g. effect cross sections, specific luminescence; dL/dx (the mean number of photons emitted per unit path length of the primary particle), and a radiation quality parameter which allows an explanation to the specified mechanisms. Two major observations must be seen in each model, a complete saturation, where the effect cross section is constant, and non-saturation where the effect cross section is proportional to the radiation quality.

6-4-1 Birks and Chou and Wright: Empirical model

On the basis of a theoretical model proposed by Birks, 1951 and 1964, which assumed that the local concentration of damaged molecules along the particle track is proportional to dE/dx, Chou ,1952 has derived a more an extensive formula (known as the modified Birks formula), which has been tested using experimental data [Smith, 1968; Craun, 1970] viz:

$$\frac{dL}{dx} = \frac{A\frac{dE}{dx}}{1 + kB\frac{dE}{dx} + C\left(\frac{dE}{dx}\right)^2} \qquad 6\text{-}1$$

where A (dE/dx) is the light yield in the absence of quenching, kB (dE/dX) is the quenching factor, $C(dE/dx)^2$ is higher order quenching. Hence A is the normal scintillation efficiency, B and C are proportionality constants which can be determined empirically from experimental data. The pulse light yield L(E), can be then found from the integration of equation 6-1. To make use of this relation, it is assumed that when using high energy electrons, the modified Birk's formula predicts that $A = \left.\frac{dL}{dE}\right|_e$, which would lead to the linear response with intensity of light as

predicted experimentally [Craun, 1970]. If a beam of α-particles with high stopping power is used, saturation is likely to take part along the track, then Birk's formula predicts $\frac{A}{kB} = \left.\frac{dL}{dx}\right|_{\alpha}$ which shows the non linear response due to quenching factors within the scintillators [Bluenerd, 1976]. The quenching factor then can be calculated as $kB = \left.\frac{dL}{dE}\right|_{e} \Big/ \left.\frac{dL}{dE}\right|_{\alpha}$. The light response dL/dx for electrons is always larger than that of other charged particles of the same energy. kB is treated as a single adjustable parameter, since there is no means available for measuring k or B separately. kB is calculated for various charged particles over wide energy intervals [Birks, 1964; Badhwar, 1967].

Wright, 1953 proposed that the specific luminescence for NE102 is given by the expression:

$$\frac{dL}{dx} = \alpha \ln\left[1 + \beta \frac{dE}{dx}\right] \qquad 6\text{-}2$$

where α and β are constants to be determined by fitting. The normalisation factor α is determined using the same logic used for Birks' model. The formulation was applied to several charged particles π^{+}, p, ^{2}H, ^{3}H, and ^{3}He on plastic scintillators in the energy range from 1 MeV to 300 MeV [Degtyarenko, 1985; O'Rielly, 1996]. It was argued that the specific luminescence for NE102 essentially depends on both the velocity and the charge of the ion in transit, but not on its mass.

Although the Birks-, Chou-, and Wright-models fit the experimental results quite well within specific energy ranges, it contain no explanation for the physical processes [Mouatassim, 1995]. Their formalisms do not accurately reproduce the measured low energy response of protons and deuterons [Saraf, 1988].

It was shown earlier (chapter 2) that the collision stopping power, LET, is not a satisfactory quality parameter for modelling the effect of ionising radiation on biological volumes. Similarly; in the case of scintillating material, the stopping power fails (as a radiation quality parameter) to fit any of the scintillation models.

This can be seen from the discrepancy between the model and experimental light yields for high energy ions (section 6-5-2-1). This indeed is a definite result which emphasises the parallelism of this quantity for specifying biological damage and the response of physical devices.

6-4-2 The Meyer and Murray δ-ray model

Meyer and Murray, 1963 (MM) treated the scintillation yield in a more fundamental approach. They proposed that dL/dx and dL/dE arise mainly from two sources; the primary column of ionisation centred along the path of the ionising particle and the energetic secondary electrons (δ-rays), which escape beyond the primary column.

MM suggested that dL/dE along the primary column depends on the composition of the scintillators. The radius of the primary column is of the order of a few tens nanometers. The energetic δ-rays, (1-22 keV) produce light with efficiency near unity. In contrast the primary column efficiency is often much lower than unity. The density of δ-rays depends on the charge z, the specific energy E/A, and dE/dx of the incident ion(s). The total specific luminescence dL/dx is then given by:

$$\frac{dL}{dx} = \left(\frac{dL}{dE}\right)_p \left(\frac{dE}{dx}\right)_p + \left(\frac{dL}{dE}\right)_\delta \left(\frac{dE}{dx}\right)_\delta \qquad 6\text{-}3$$

where the subscripts p and δ refer to the primary column and δ-rays, respectively. The fraction of energy deposited outside of the primary column is a given by:

$$F = \frac{\left(dE/dx\right)_\delta}{dE/dx} \qquad 6\text{-}4$$

where the total stopping power $dE/dx=(dE/dx)_p+(dE/dx)_\delta$. Substituting equation 6-4 into equation 6-3 we get an expression for the scintillation efficiency viz.:

$$\frac{dL}{dE} = (1-F)\left(\frac{dL}{dE}\right)_p + F\left(\frac{dL}{dE}\right)_\delta \qquad 6\text{-}5$$

For light ions, the effects of δ-rays vanishes, thus both the scintillation efficiency and specific luminescence are determined mainly by $(dL/dE)_p$, that is:

$$\frac{dL}{dE} = (1-F)\left(\frac{dL}{dE}\right)_p \qquad \text{and,} \qquad \frac{dL}{dx} = \left((1-F)\left(\frac{dL}{dE}\right)_p\right)\left(\frac{dE}{dx}\right) \qquad 6\text{-}6$$

For heavy ions, the scintillation efficiency and the specific luminescence are predominately controlled by the δ-rays, i.e. $(dL/dE)_p << 1$ (due to saturation) and $(dL/dE)_\delta \approx 1$. For such condition we get the following expressions:

$$\frac{dL}{dE} = (1-F)\left(\frac{dL}{dE}\right)_p + F \qquad \text{and,} \qquad \frac{dL}{dx} = \left((1-F)\left(\frac{dL}{dE}\right)_p + F\right)\frac{dE}{dx} \qquad 6\text{-}7$$

From these equations we note that both dL/dx, and dL/dE are determined by the δ-ray production and the saturation of the primary column. The model failed to explain the decline in the scintillation efficiency of CsI for ions with high specific energy [Gwin, 1963].

5-4.3 Katz and Kobetich's δ-ray model

Katz and Kobetich, 1968 (KK), had looked at the δ-ray model of MM from another viewpoint. Since dE/dx contains no information on the spatial distribution of ionisation energy, they suggested that dE/dx is not a suitable parameter for describing both dL/dx and dL/dE. They proposed their hypothesis on the basis that saturated luminescence centres occur due to the deposition of energy in the medium by δ-rays ejected from the primary passing ion. Energy transfer carries the deposited energy from the passive matrix to the luminescence centre. Part of the energy is wasted in the matrix through radiationless decay. Each luminescence centre is associated with a sensitive volume. On the basis of the longer lifetime of excitations compared to the interaction time, Katz, suggested that the scintillation resembles the single target inactivation model in analogy with a model proposed by Lea for the inactivation of viruses and enzymes [Lea, 1955 ; Katz, 1968]. Thus the model demonstrates the

importance of a depletion mechanism for saturation. In their analysis they considered the following:

i- the number of δ-rays generated with a given initial energy: The number of δ-rays per unit length of the ion's track liberated from the stopping material was obtained from the Mott formula [Katz, 1968] for elastic scattering of electrons by the Coulomb field of a nucleus.

ii- the residual energy of these δ-rays after passing a specified radius: Calculated from the empirical relation $R=A\omega_0\{1-B/(1+C\omega_0)\}$ where R is the range of an electron at initial energy ω_0. A, B, and C are constants for a given range of electrons [Kobetich, 1968].

iii- the probability of these δ-rays arriving at this radius when back scattering is considered: Since the low energy electrons follow a complicated route, the fraction of incident electrons that are transmitted by an absorber was taken from an empirical relation given in Katz, 1968.

These ingredients were combined to obtain an expression for the energy flux φ carried by the δ-rays through the cylindrical surface of radius r and with axis as the ion's path. The probability per luminescence centre for the emission of a photon from a region which has absorbed a uniform energy dose of $\rho(r)=-d\varphi/dA$ (where A is the traversed area to ion track) is given by:

$$P = 1 - \exp(-\rho/\rho_0) \qquad 6\text{-}8$$

where ρ_0 is the mean energy density required to excite 63 % luminescence centres of the region. The model seems to show good agreement with the NaI(Tl) data, however it shows poor correlation with other types of scintillant.

6-4-4 Luntz Track-effect model

This model is essentially the same as the MM model in which an imaginary cylinder surrounds the ion track to partition the scintillator into high- and low- energy-deposition regions [Luntz, 1971]. The contribution of the high-density region in

dL/dE is assumed to be negligible because of the non-radiative events that occur in this region (i.e. the e-h recombinations, radiation damage, and lattice heating effects). The luminescence response to energy deposited in the low-density region is assumed to be linearly proportional to the deposited energy. Luntz deduced an empirical form from the numerical results of Katz [Kobetich, 1968], for an energy deposition function which is given by:

$$\rho = k\frac{z^{*2}}{r^2V^2} \qquad 6\text{-}9$$

where r is the radial distance from the ion track. V and z^{*2} are the velocity and the effective charge of the incident ion. For every incident ion in the track-effect model there are two adjustable parameters, one of which determines the radius of the high-density cylinder, and the other which normalises the final L against E_0 curve. The model did not show compatibility with the data for heavy ions on CsI [Newman, 1960].

Luntz and Heymsfield then suggested a modified form of the same model [Luntz, 1972], in which they included the contribution from the high-density region to cope with the non-linearity of the response in the earlier model especially in the low and intermediate ion velocity regions. The model is referred to as "the linear-falloff approach". The regional luminescence response assumed to be proportional to the deposited energy at a radius higher than falloff radius and reduces to zero in the restricted region in the immediate vicinity of the ion track. The core region was determined by V/f_0 where f_0 is the electron natural frequency. The beginning of the falloff is an adjustable parameter of the modified model of Luntz.

6-4-5 Salamon and Ahlen model

Salamon and Ahlen, 1981 (SA) allowed the migration of electron-hole (e-h) pairs away from the region of high pair density and low scintillation efficiency during the lifetime of e-h pairs at room temperature. They assumed the non-radiative quenching of the e-h pairs to be proportional to the square of the pair density n. The transport

equation which allows both simultaneous diffusion and self-annihilation of the e-h pairs is given by:

$$\frac{\partial n}{\partial t} = D \nabla^2 n - Kn^2 \qquad 6\text{-}10$$

where D is the diffusion constant, and K an annihilation constant. The number of NaI molecules required to accommodate one e-h pair is given by η. Thus the main parameters in the model are D, K and η. They argued that the scintillator crystal can accommodate only a limited number of excitons (e-h pairs) and thus the excess number would contribute to prompt quenching in some unknown manner. The authors claimed that their model provides a good fit to data for ions having stopping power from 10 to 5000 MeV-cm^2/gm and with atomic number from 1 to 26 in NaI(Tl) and provides an explanation for the absence of activator depletion as a mechanism contributing to saturation. However, the model fails to fit the low energy ions when compared to the static energy deposition model.

6-4-6 Muga, Grifith and Diksic model

Muga and co-workers, 1974 (MD) assumed that the primary ion makes negligible interactions. Thus the luminescence response in scintillators is mainly due to the scattered electrons. The specific luminescence for thin film is found to be:

$$\frac{dL}{dx} = I n \sigma \qquad 6\text{-}11$$

where I is the number of electrons penetrating the disk, n is the number of scintillator sites per volume, and $\sigma(E)$ is the cross section for luminescence production. σ is taken to be constant independent of electron energy (above 1 keV). The distribution of electrons is determined using the Rutherford scattering formula. The range of electrons in the scintillator is assumed to be linearly proportional to their initial energy. In the saturation region the specific luminescence is determined by the :

$$\frac{dL}{dx} = C\left(\pi r_{sat}^2 \rho_{sat} + \int_{r_{sat}}^{r_{max}} \rho(r)\, 2\pi r\, dr\right) \qquad 6\text{-}12$$

where C is a normalisation constant and $\rho(r)$ is the number density of scattered electrons. Muga and co-workers tested the model [Muga, 1974], concluded that the constant C must be taken as a linearly increasing function of the ion charge z. The model was derived in an attempt to fit the response data for NE102 for heavy ions obtained by the author earlier [Muga, 1974].

6-4-7 Luminescence and linear primary ionisation model

In previous chapters, it was demonstrated that the mean free path for primary ionisation is a better physical quality parameter for describing the action of radiation in living cells. Here we will utilise our knowledge on the response of scintillators and of the forgoing models to apply a new model based on the linear primary ionisation. The model will include both the effects of the incident ion track and the associated δ–rays as a function of their linear primary ionisations. Assuming that there is an optimum spacing for generation of scintillations, and that the conversion efficiency of electrons and ions is about the same, then the specific luminescence will be given by:

$$\frac{dL}{dx} = k_i\, I_i \left[\left(1 - e^{-\frac{I_i(E)}{I_{i,o}}}\right) + \sum_{T=T_{min}}^{T=T_{max}} f(T)\, R_\delta(T)\, I_\delta(T)\, \Delta T\right] \qquad 6\text{-}13$$

where k_i the efficiency for conversion of an ionisation to a scintillation at the fluor centre. $I_i(E)$, $I_{i,o}$ are the linear primary ionisation at energies E, and E_o; $I_\delta(T)$ is the linear primary ionisation for δ-rays at energies T; f(T) is the yield of δ-rays having energy between T and T+ΔT. The first term inside the square bracket is the probability that the optimum mean spacing of primary ionisation is reached. The maximum saturation is expected when all the available excitation levels are stimulated by excitons. The second term inside the square bracket $I_i(E)$, the yield of δ-rays, for every primary ionisation in the core, is averaged over the delta ray energy

of range $R_\delta(T)$. The summation is over all delta ray energies extended from a threshold energy T_{min} to the maximum energy of T_{max}. Below the threshold energy T_{min}, the primary ion track dominates the mechanism. Rewriting equation 6-13 and set the following $a_o=k_i$, and $a_1=1/I_{i,o}$, we get:

$$\frac{dL}{dx} = a_o I_i \left[\left(1 - e^{-a_1 I_i}\right) + \sum_{T=T_{min}}^{T=T_{max}} f(T)\, R_\delta(T)\, I_\delta(T)\, \Delta T \right] \qquad 6\text{-}14$$

Thus for slow light ions, i.e. negligible δ-ray effects, the expression reduces to:

$$\frac{dL}{dx} = a_o I_i \left(1 - e^{-a_1 I_i}\right) \qquad 6\text{-}15$$

for fast very heavy ions the equation 6-13 approximates to:

$$\frac{dL}{dx} = a_o I_i \sum_{T=T_{min}}^{T=T_{max}} f(T)\, R_\delta(T)\, I_\delta(T)\, dT \qquad 6\text{-}16$$

The constants a_o and a_1 are to be evaluated for the phosphor from fitting.

The description here is for inorganic scintillators using the band theory of solids. For organic scintillators the same equations hold, except for the nomenclature. Thus the term exciton(s) will be used interchangeably for both organic and inorganic scintillators. Table 6-4 shows the main models, as discussed in section 6-4, with their principle radiation quality parameters.

Table 6-4 Scintillation models and their specification quality parameter.

Model	Radiation quality	Application
Birks Model, 1964	dE/dx (keV/μm)	Organic Scintillators
MM Model, 1963	$(dE/dx)_p$ and $(dE/dx)_\delta$	Inorganic (CsI)
Harder Model, 1988	$L_{100,D}$	Biological targets
KK Model, 1968	z^{*2}/β^2	Inorganic (NaI(Tl))
Luntz Model, 1972	E_o	Inorganic (CsI)
SA Model, 1981	dE/dx	Inorganic (high energy ions)
MGD Model, 1974	Initial energy E_o	Organic Thin Films NE102
Unified Model, 1989	$I(nm^{-1})$ or $\lambda(nm)$	Unified Dosimetry

6-5 Specifying Luminescence of Plastic Scintillators by Heavy Ions

The non-linearity of the light response means that current scintillator calibration techniques require the measurements of an extensive number of data points (L, dE) for each incident ion. Unknown points are determined by extrapolation or interpolation of an arbitrary n-parameter equation obtained from an overall fit to the existing data. It should be noted that the light response of the plastic scintillators to the various ionising particles obtained by the different authors are relative. The reasons for that is due to the different experimental set-ups, with different photomultipliers, light guides, contact lubricant thickness, electronic gain, ...etc. In other words there is no common mean of results for such a system. However for one specific experiment, to be carried out for all ions, the advantage of using a calibrated source is clear. Out of the many experimental results published by the different authors, we find the data obtained by Becchetti (1974) are the only comprehensive set which were obtained in the same lab with the same apparatus in wide energy ranges. Despite the fact that other experimental data for heavy ions using thin films of plastic scintillators were obtained by different authors [Voltz, 1966; Muga, 1971 ; Muga, 1974], the data either are irrelevant to the circumstances required for modelling or out of physical reality.

6-5-1 Input data and calculations

The physical parameters of the charged particles in the plastic scintillator are calculated using the physical data available for the absorber given in table 6-5 [NE, 1995 ; Voltz, 1966; Paul, 1971]. The values for the ionisation potential of the phosphors were obtained from ICRU-37, 1984.

The aim is to develop a model for the scintillation photon yield and to assess the feasibility of utilising scintillators with a response designed to simulate that of mammalian cells for measurement of bio-effectiveness in a system of unified dosimetry. The calculated parameters and their relation to the specific luminescence are discussed in light of the foregoing sections.

Table 6-5 Physical parameters for NE102A.

Physical Parameter	Value
Constituent atomic numbers, Z_i	H: 1 ; C: 6
Constituent atomic weight, A_i	H: 1.0079 ; C: 12
Constituent fractional weights, w_i/w_t	H: 0.0853 ; C: 0.9147
Constituent mean excitation potential (eV)	H: 19.20 ; C: 81.00
Constituent number of atoms/molecule	H: 10 ; C: 9
Molecular Weight ; dalton	118.178
Nominal Density ; gm/cm^3	1.032
Molecular Density ; mol/gm	5.096×10^{21}
Mean Z/A	3.65
Mean Excitation Potential ; eV	64.68
Electronic Density, NZ ; electrons/cm^3	3.39×10^{22}
Mean energy expected per ion pair; W(eV)	30.00
No of H atoms atoms/cm^3	5.26×10^{22}
No of C atoms atoms/cm^3	4.78×10^{22}

6-5-2 Results and discussions

From the foregoing reviews of modelling the scintillating response, it is quite clear that each model relies on specific radiation quality parameters. Thus, the models will be tested on the basis of their own radiation quality parameters. It is important to bear in mind that all of these models except for the last one are related to a single hit theorem. The differential light output with respect to the ion's energy, dL/dE, calculated using the light response data of the ion's energies on NE102, was shown earlier in figure 6-3 (data of Becchetti et al., 1976). The specific luminescence is the calculated using; dL/dx=(dL/dE)(dE/dx). The track structure parameters for the ions, dE/dx(keV/μm), $L_{100,D}$ (keV/μm), z^{*2}/β^2, and λ(nm), are estimated from Watt's tables (Watt, 1996). Results of the light response of the heavy ions on NE102 as specified with each radiation quality are discussed within the subsequent sections.

6-5-2-1 The LET and its restricted form

Figures 6-4 and 6-5 show the calculated scintillation efficiency dL/dE as a function of ions energies E(MeV), and their stopping power dE/dx (keV/μm) in NE102A. As expected higher scintillation efficiencies are obtained for lower z ions at the same

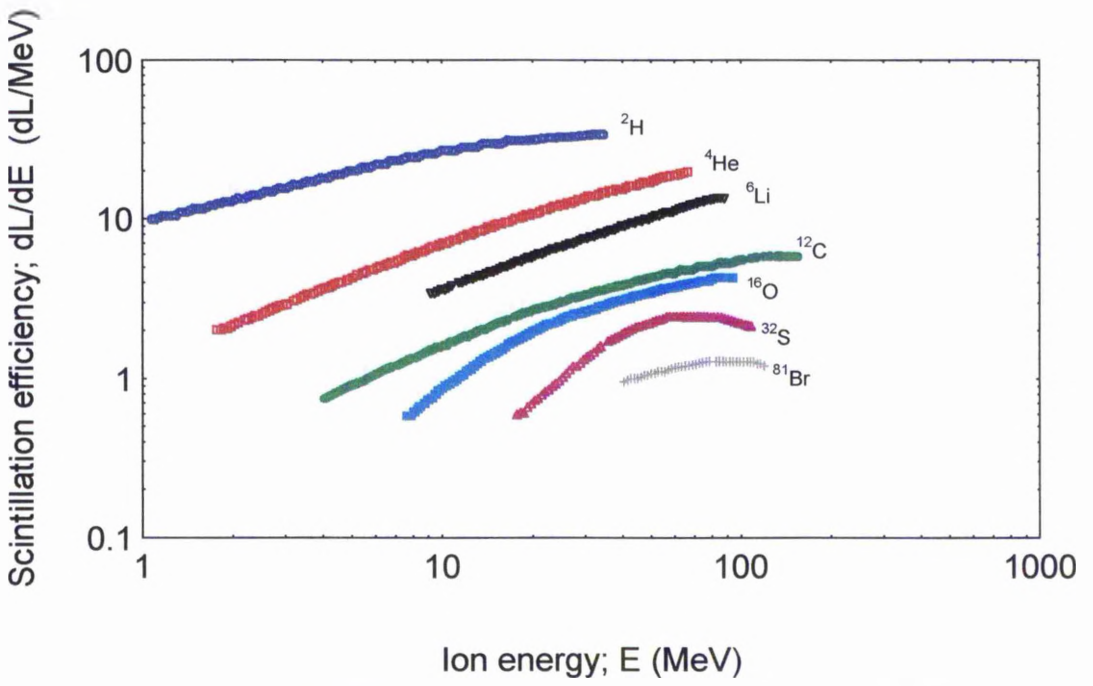

Figure 6-4 Calculated scintillation efficiency dL/dE vs. ion energy in NE102A.

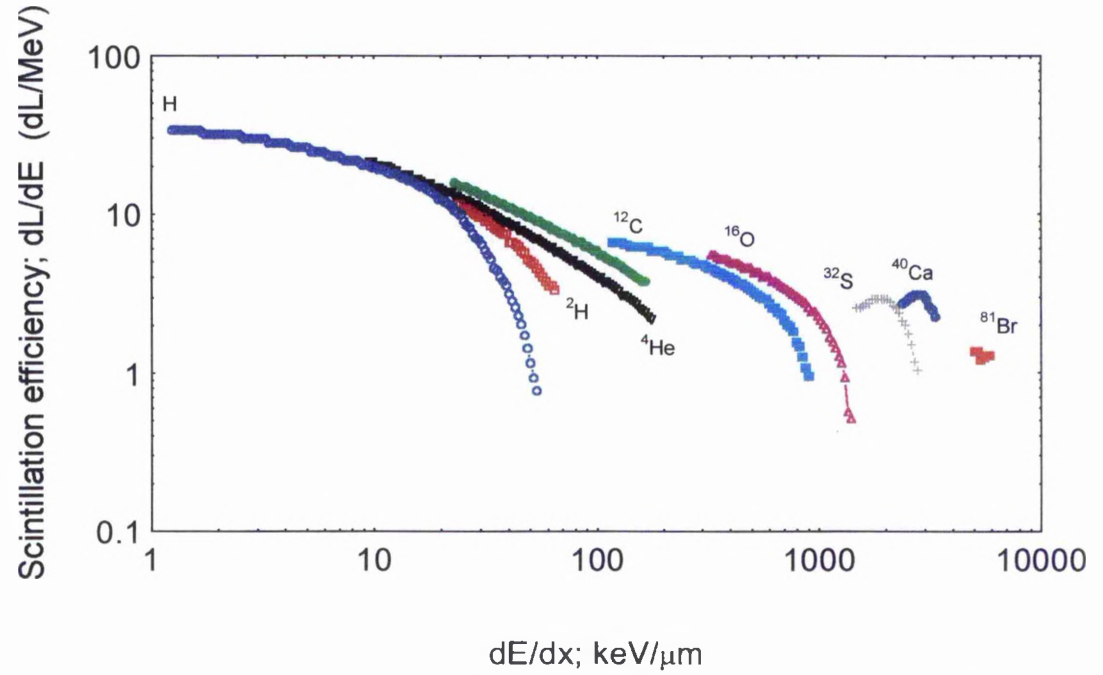

Figure 6-5 Calculated scintillation efficiency dL/dE vs. the stopping power dE/dx in NE102A.

energies. Also observed, in figure 6-5; for same ion type, higher scintillation efficiencies for lower stopping power, with an exception for very heavy ions where they show a maximum value before they start decreasing at lower stopping power (^{32}S, ^{40}Ca, and ^{81}Br).

The specific luminescence dL/dx is also plotted in figures 6-6 and 6-7 against the dose average LET; L_D, and its restricted form $L_{100,D}$. The relationship is initially linear up to LET=20 keV/μm. The specific luminescence on log scale shows a linear, almost unified, relationship at low values of LET for lighter ions (H, ^{2}H, ^{3}He, ^{4}He, ^{6}Li), whereas for the heavier ions (^{11}B, ^{12}C, ^{16}O, ^{32}S, ^{81}Br) a characterised response for each ion is clear, reaching a maximum value before decreasing. For ions of the same L_D, $L_{100,D}$, dL/dx increases with z but is relatively independent of mass.

Harder (1992) proposed the restricted form of LET (or mainly the $L_{100,D}$ parameter) as a radiation quality parameter to quantify biological damages. As seen in chapters 3 and 4, the application of the quality $L_{100,D}$ with micro-biological volumes will eliminate, to some extent, the role of δ-ray damage. On the contrary dL/dx shows almost the same relation as that obtained with L_T. This suggests the importance of δ-rays in activating the scintillation processes.

6-5-2-2 The radiation quality parameter z^{*2}/β^2

Katz and collaborators investigated their version of track structure theory for the prediction of specific luminescence of inorganic scintillators [Katz, 1968]. Their model relies on the dominant effect of δ-rays. Although it shows success in the inactivations of viruses, single-stranded DNA bacteria and thick inorganic scintillators e.g. NaI(Tl), the production of damage is coherently and conceptually correlated with δ-rays and not the primary ions. Butts and Katz (1967) proposed the parameter z^{*2}/β^2 for the specification of radiation quality. The parameter z^{*2}/β^2 is directly related to the δ-ray yield along the track, whereas β, the relative ion velocity, determines the maximum spatial distribution of δ-rays around the track. The effect is considered to be a function of this quality parameter. In fact it was demonstrated

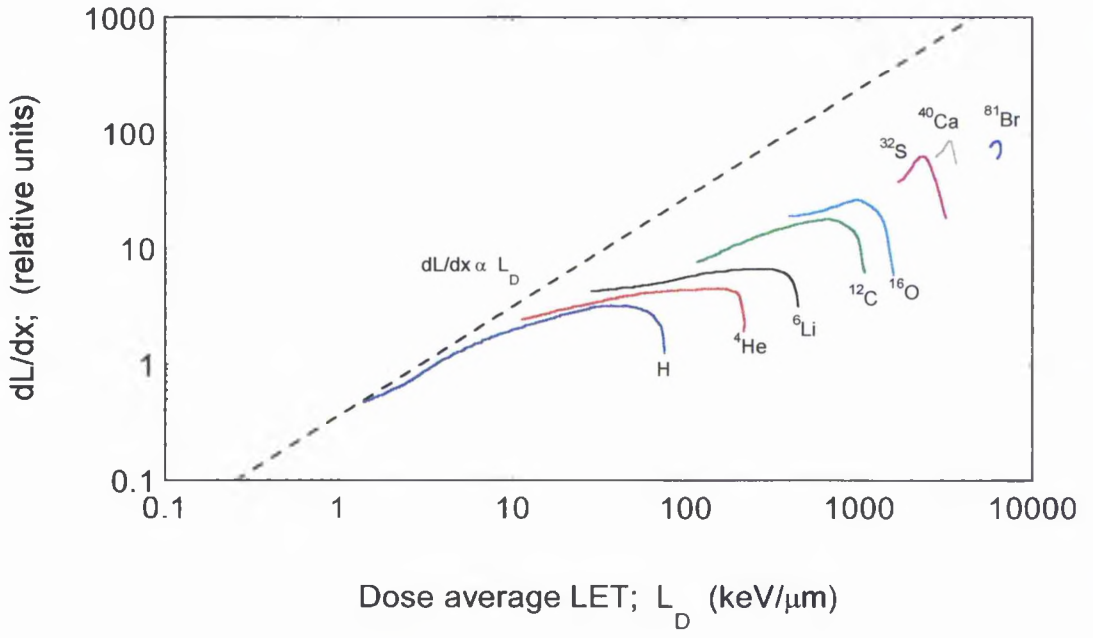

Figure 6-6 Specific fluorescence vs. linear energy transfer in NE102A.

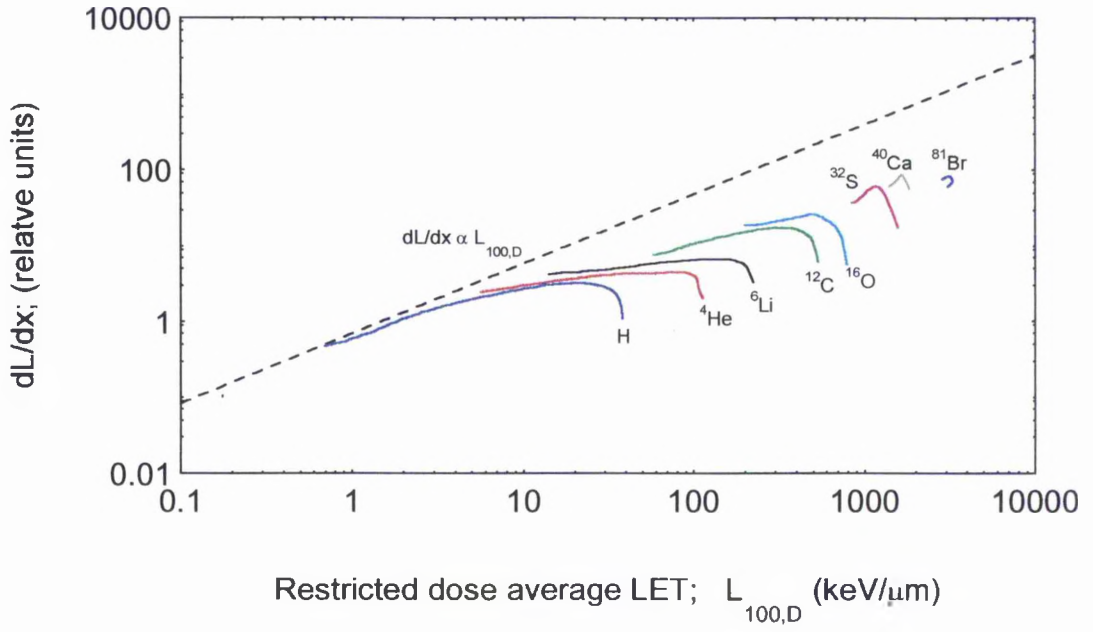

Figure 6-7 Specific fluorescence vs. restricted linear energy transfer in NE102A.

by Katz, 1993; that the effect is described as a single hit detector, and best described by the quality z^{*2}/β^2. The specific luminescence vs. β^2 , and z^{*2}/β^2 are shown in figures 6-8, and 6-9 respectively. It is noted that dL/dx is a decreasing function of β^2 for lighter ions ($z \leq 6$), whereas for the heavier ions ($z>6$), dL/dx increases first and then saturates. For the same β^2, the linear response dL/dx increases with higher z. These figures show by implication the role of δ-rays in stimulating the scintillating material into producing photons. The effect, however, is enormous for the heavier ions.

6-5-2-3 The mean free path for linear primary ionisation λ

Here we will consider the linear primary ionisation for specification of radiation quality as proposed by Watt, et al. 1985. With this parameter, or its inverse, the mean free path λ, a good correlation for the unified model proposed by the same author can be obtained [Watt, 1989]. Figure 6-10 shows the relationship between the specific luminescence and λ. The physical implications are quite clear as expected for the unified approach for nano-biological targets, notably the DNA, an inflection point is revealed clearly at λ=1.8 nm. From the dL/dx-λ plot, the same response is shown for the light ions (H, ^{2}H, ^{3}He, ^{4}He, ^{6}Li) up to the expected point of inflection. The turnover of ^{4}He, and ^{3}He ions is around 2 nm due to the short range of the ions within the sensitive target. The saturation was expected to start with the heavier ions (^{11}B, ^{12}C, ^{16}O, ^{32}S, ^{81}Br) but because of the importance of the effect of δ-rays in that region, the magnification of the effect was enormous. This is due to the total absorption of the ions within the scintillators. However, incativation of biological material shows a different response, particularly with very heavy ions (saturation region) where the critical volumes (DNA) absorb part of the energy (which is enough to 'overkill' the cells) while the δ-rays deposit their energy outside the critical targets.

6-5-2-4 The role of δ-rays

Here the role of δ-rays in scintillation will be explored further with the aid of the mean free path for linear primary ionisation (or z^{*2}/β^2) and the parameter β^2. The plots in figures 6-11a, b and 6-12 show the light response L, the luminescence

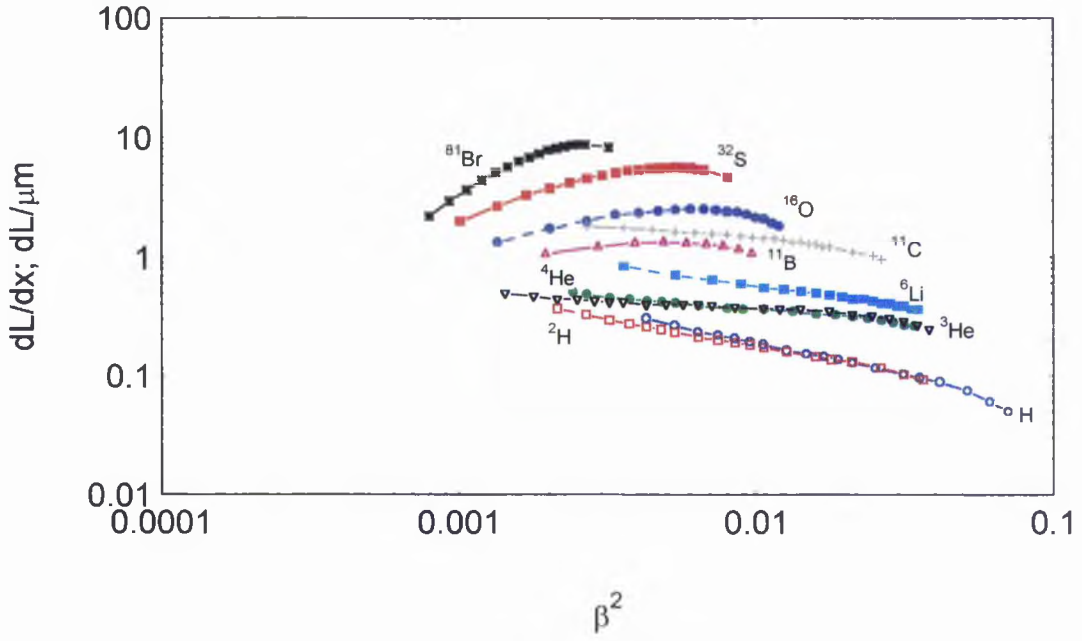

Figure 6-8 Specific fluorescence vs. ion relative velocity.

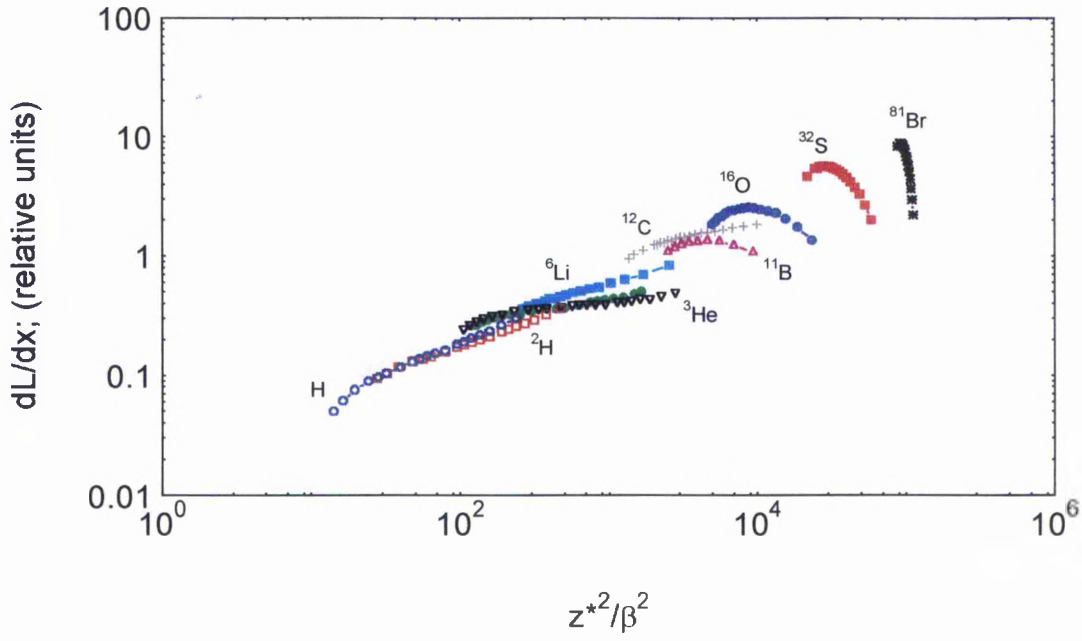

Figure 6-9 Specific fluorescence vs. Katz's quality parameter z^{*2}/β^2.

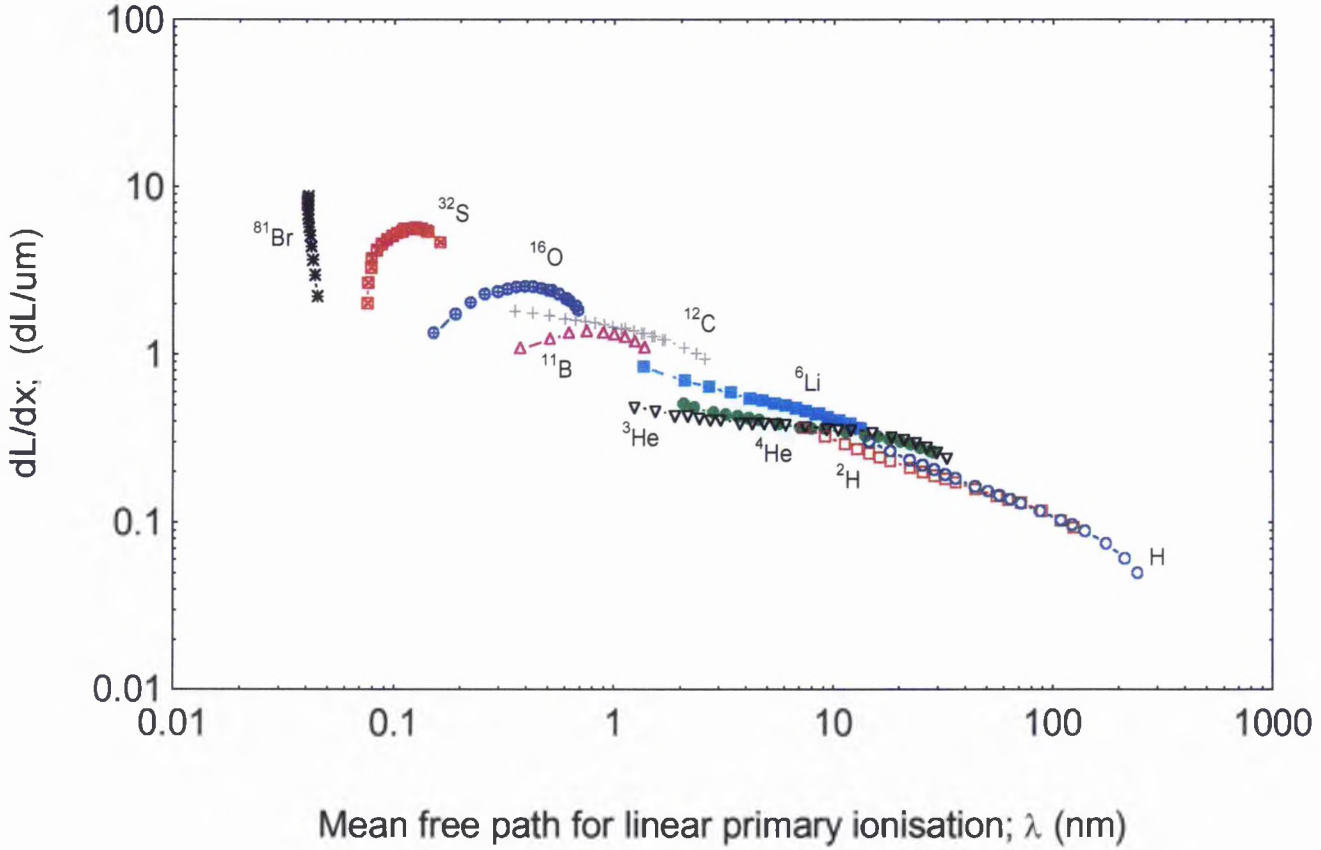

Figure 6-10 Specific fluorescence vs the linear primary ionisation in NE102A.

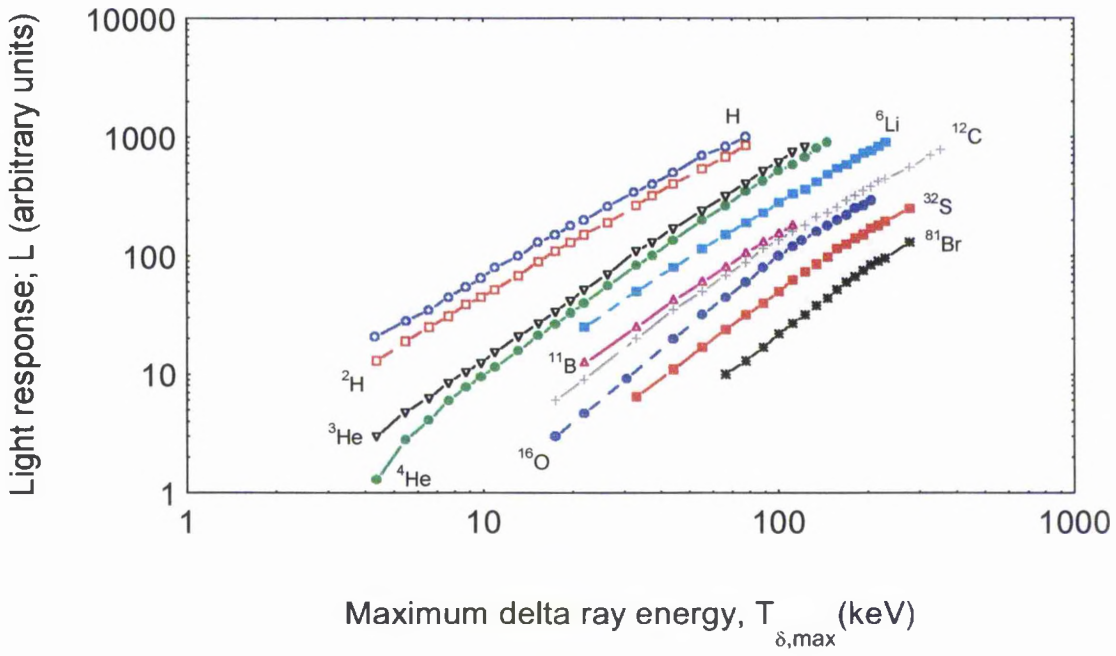

Figure 6-11a Light response of NE102A as a function of maximum delta ray energy.

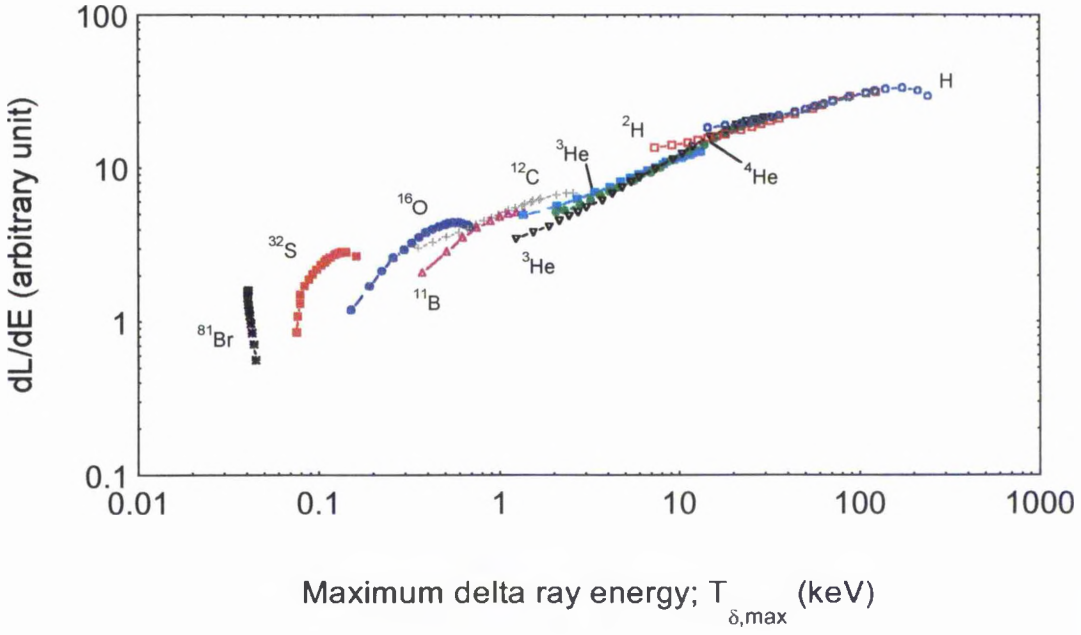

Figure 6-11b Fluorescence efficiency of NE102A vs maximum delta ray energy.

efficiency dL/dE, and the specific luminescence dL/dx as a function of the maximum δ-rays energy produced by the primary ions stopped in the NE102A. The light output generally increases with the kinetic energy of δ-rays and is closer to linearity for lighter ions. The same trend for the luminescence efficiency is observed, except for the heaviest ions (^{81}Br, ^{32}S, and ^{16}O). The observed dependence of the light response on an ion's charge and velocity (section 6-5-2-2) is due to the fact that the δ-ray extension and yield per unit length are, respectively, proportional to the ion's velocity, β, and z^{*2}/β^2. Thus the effect cross sections of the scintillators is determined predominantly by the δ-ray response.

Figure 6-12 on the other hand shows a decreasing specific luminescence for lighter ions ($z<6$) with increasing kinetic energy of the δ-rays produced by the ions, whereas for the heavier ions ($z>6$) dL/dx increases to a maximum and then starts to decrease. The reason for this is that with ionising radiation of lower dE/dx and small δ-ray yields, the contribution of the ion's track core and the penumbra formed by the δ-rays play a role in photon production (e.g. Birks, 1964). However with the higher dE/dx of the ions the role of the track core decreases, and δ-rays play a major part in the production of photons. Thus, unlike the response of a biological detector (chapter 3), the specific luminescence is largely related to the range or energy of the δ-rays.

6-5-2-5 The shape and the yield of the δ-ray spectra

From the past sections, it is apparent that the β^2 of the ion controls the shape of δ-ray spectrum, since it is proportional to the kinetic energy of the δ-rays (and thus approximately to the range), and that z^{*2}/β^2 controls the yield (number) of the δ-rays. Since the mean free bath for the linear primary ionisation, λ, is indeed linearly proportional to β^2/z^{*2} (inversely proportional to the δ-ray yield), a quantitative correlation can be reached using the fixation of one of the parameters β^2 and λ whilst varying the other. Figure 6-13a shows the specific luminescence as a function of β^2. The yield of δ-rays is fixed by the parameter λ. The number of photons per unit length is closer to a constant value for higher fixation of $\lambda>2$nm (lower δ-rays yield),

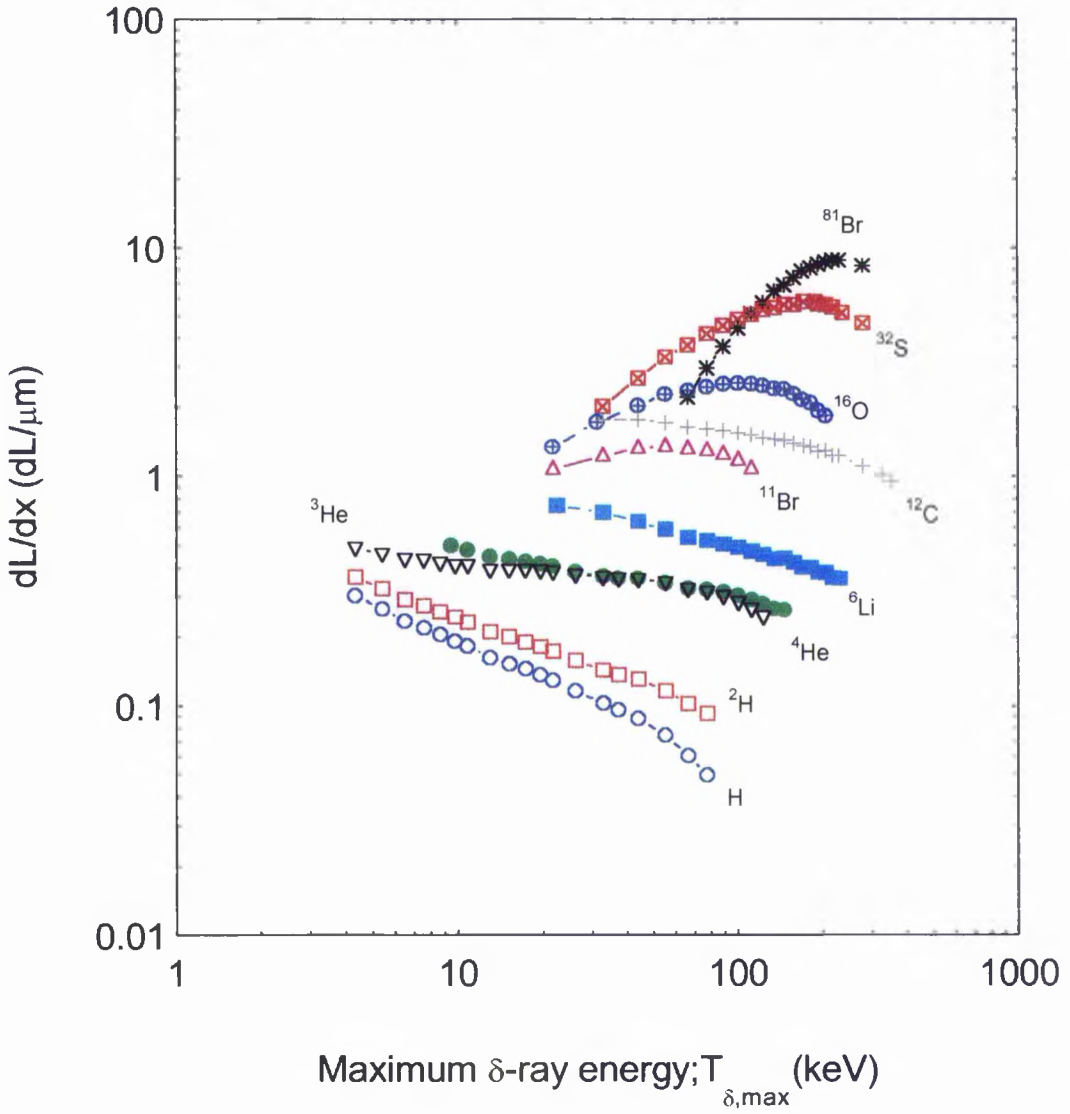

Figure 6-12 Specific luminescence dL/dx vs. maximum δ-ray energy.

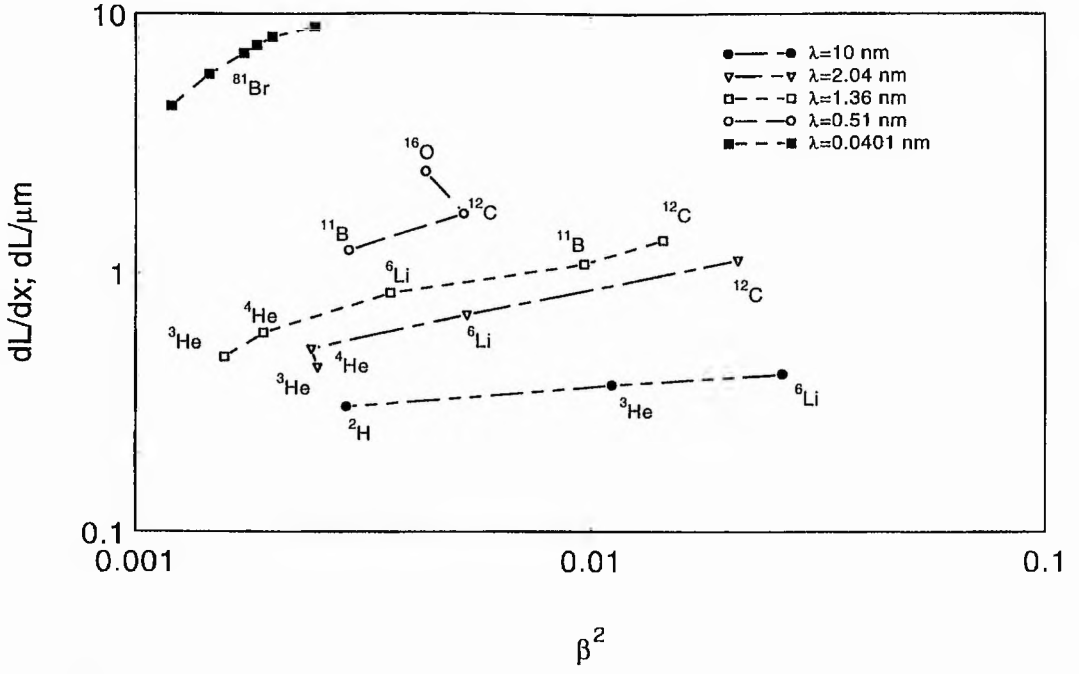

Figure 6-13a The specific luminescence vs ion energies for fixed values of λ.

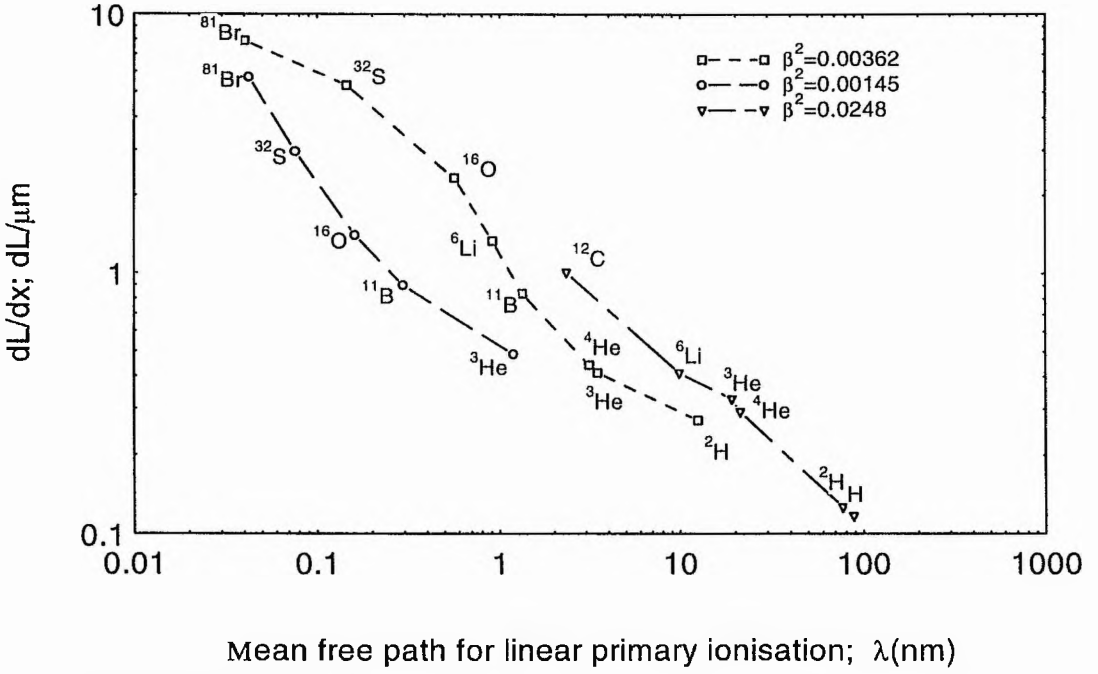

Figure 6-13b Specific luminescence vs. the linear primary ionisation for a fixed ion velocities.

while for lower fixations of $\lambda < 2$ nm, the number of photons per unit length clearly increases with increasing β^2. In Figure 6-13b the specific luminescence is plotted against λ with the parameter β^2 fixed. Although no unique feature is observed, the number of photons per unit length increases as λ decreases for a given fixed ion velocity.

From the past two sections, a very clear conclusion can be drawn. The δ-rays are found to play an important role in both depleting the scintillating centres and producing light quanta. This could be mainly due to two reasons. The thickness of the plastic scintillator, used by Becchetti and co-workers [Becchetti, 1976] in their experimentation, is of the order of a few millimetres. This is sufficient to allow total absorption of the ions and their δ-rays and technically measures the stopping power in the scintillator. Thus it is preferable to measure the response of thin films (of the order of a few microns) to ionising radiation and cover a wide spectrum of LET (monoenergetic heavy ions). This will allow precision in measuring the LET and allow the escape of δ-rays from the thin detector region.

6-6 Scintillators for Measurement of Biological Effectiveness

The basic idea for a nano-device is to simulate the effects of ionising radiation on mammalian cells by using scintillating spheres, or ultra thin films, spaced at 1.8 nm (the approximate interstrand distance of the DNA). Another idea (Harder, 1992) is to use ultra thin scintillating rods implanted in a non-active matrix (e.g. clear perspex).

Provided the appropriate nanometric dimensions are used, δ-rays would have a high probability of escape from the detector elements (spheres or rods) and deposit their energy mainly in the non-active matrix, thus producing no photons. Hence the collected photons will be related to those events produced initially by the primary ionisations in the active volumes. These ideas are presented in figure 6-14.

Preliminary studies, conducted by the present author, using micro-spheres of plastic scintillating material (supplied by Nuclear Enterprise Ltd., Edinburgh), showed the

impracticability of such a device. For one reason the spheres are of inhomogenous mixed sizes. Their diameters ranged from 1 to 50 μm which are much larger than the desired nanometer dimensions needed for a unified dosimeter. However, at the micron level, and with spheres selected to have diameters of about 50 microns dispersed in clear adhesive (UHU, GmbH Germany), lower photon yield was observed because of the poor contact of the spheres with the photomultiplier tube. However, despite their incompatibility for current work, they still have some prospect for application in microdosimetry, as they are of the correct dimensions to simulate damage to e.g. chromosome aberrations.

The impracticability of the micron scintillating volumes to simulate dsb's of the DNA left no other option but to explore the molecular domain of the scintillating material. Thus the ideas explored at the micron levels were extended to utilise the activation cross sections of the scintillating centres, which are of the order of a few nanometer squared (~10 nm^2) depending on the concentration of the fluors.

In this section a new experimental approach is considered for study of the feasibility of employing a modified microdosimetric approach to the measurement of the biological effectiveness of ionising radiations. The idea is based on the assumption that the active centres of the plastic scintillator "fluor solute" can be thought of as an interaction cross-section for the emission of light. By adjusting the concentration of the activator, the mean of the random distance between centres can be modified to simulate the strand-pair distribution of the DNA in mammalian cells. Thus it is possible to simulate the yield of dsb's in DNA damage as those paired centres spaced by about 1.8 nm and to distinguish them from other unwanted pairs of activated sites with spacings different from 1.8 nm. Starting from the knowledge of the equilibrium slowing down spectrum of electrons in the material it is possible to determine the yields of photons and paired events and their relationship to the biological effectiveness.

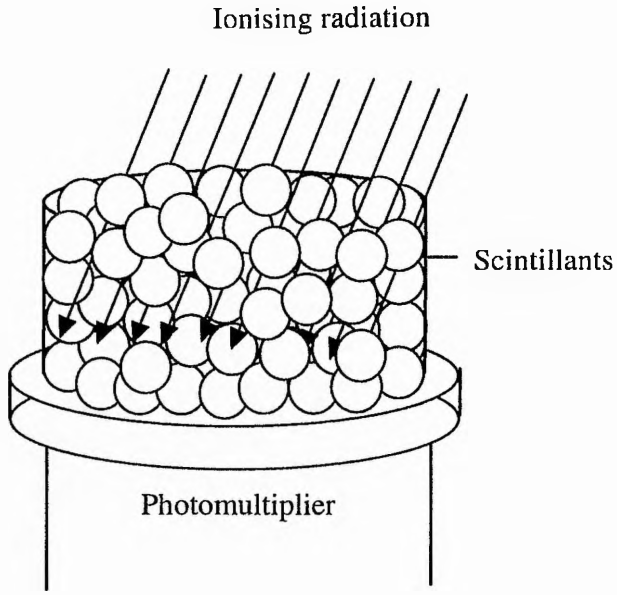

(a) NE102A scintillating micospheres of 10 μm diameter dispersed in clear adhesive.

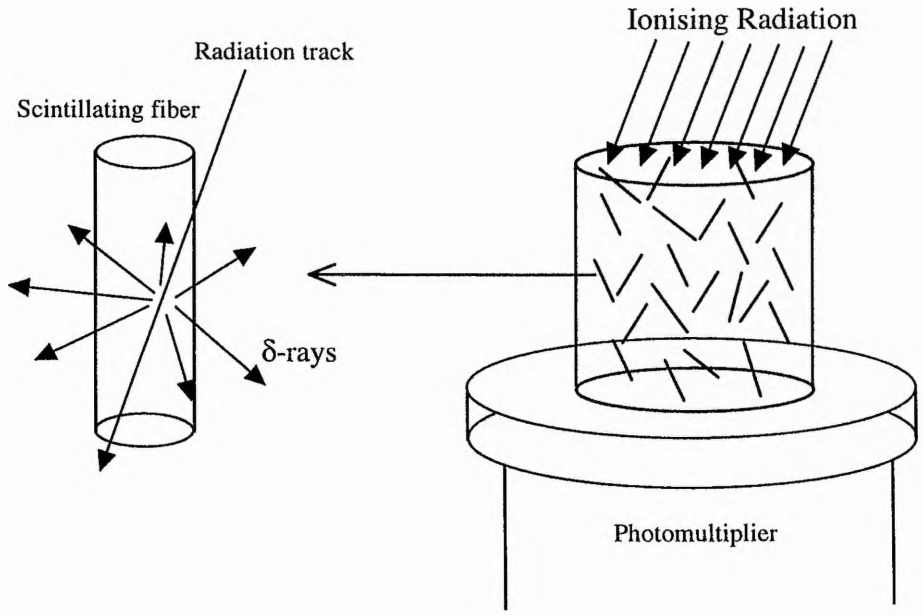

(b) NE102A scintillating fibres in a clear perspex matrix.

Figure 6-14 Simulating the action of ionising radiation on scintillating spheres or rods of micro-dimensions.

6-6-1 Calculation of the photon yield and distribution of activated pairs

By irradiating a thin film of plastic scintillator, NE102, with electrons, X- or γ-rays, the light photon yield can be determined from the resulting spectra. This can be established by first calculating the primary electron and equilibrium electron spectrum generated in the material [Watt, 1989].

The concentration of excitons $C_x(E)$, as a function of electron energy E, and per unit source concentration of electrons is given by:

$$C_X(E) = \phi_{eq}(E)\, I(E) \qquad 6\text{-}17$$

where ϕ_{eq} is the differential fluence spectrum of equilibrium electrons per unit source concentration of electrons generated in the medium. I(E) is the linear primary ionisation for the electron tracks. Assuming that each ionisation give rise to an exciton, then the fluence of excitons per unit source concentration of electrons, ϕ_x, is written as:

$$\phi_x(E) = C_x(E)\, \lambda_x \qquad 6\text{-}18$$

where λ_x is the mean diffusion length for an exciton. In non-scavenging conditions, the diffusion length of an exciton is several microns, but in a phosphor the length is controlled by the fluor concentration.

The probability of activating an active centre in the scintillator is given by:

$$P_a(E) = 1 - \exp\left[-\phi_x(E)\, \sigma_a(E)\, C_a\right] \qquad 6\text{-}19$$

where C_a is the concentration of the active sites in the scintillator (fluor molecules) and σ_a is the cross section for exciton production. The average number of active centres at risk , $N_r(E)$, due to electrons having energy E to E+ΔE in the equilibrium spectrum is given by the expression:

$$N_r(E)\,\Delta E = \frac{\phi_{eq}(E)\,\Delta E}{x_a} \qquad 6\text{-}20$$

where X_a is the mean distance between the active centres, determined from the known concentration of fluor molecules in the phosphor. Numerical integration over the whole spectrum gives the mean total number of active centres at risk:

$$N_{T,a} = \sum_{r,j} N_r(E_j)\,\Delta E = \frac{\sum_j \phi_{eq}(E_j)}{x_a}\,\Delta(E) \qquad 6\text{-}21$$

Based on the assumption that the pairs at risk follow Poisson statistics: assigning P(2) as the probability that paired activator sites spaced at exactly 2 nm will occur in the random distribution with a known mean spacing of x_a per nanometer, which is given by

$$P(2) = \frac{e^{-x_a} x_a^2}{2!} \qquad 6\text{-}22$$

Likewise, assigning H(2,E) as the probability that two or more "hits" will occur, one in each partner of the pair to produce the simulated equivalent of double-strand breaks, is expressed as:

$$H(2,E) = \left[1 - \left(1 + \frac{I}{I_o}\right) e^{-\frac{I}{I_o}}\right] \qquad 6\text{-}23$$

where I is the linear primary ionisation in nm, and I_o is the linear primary ionisation corresponding to a mean free path of 2 nm ($I_o = 1/\lambda_o = 500\ \mu m^{-1}$). Thus the product of equations 6-22 and 6-23 will result in the probability of having two events and spaced by 2 nm.

The mean number of pairs of active centres at risk N_{pr} is obtained by combining equations 6-21 and 6-22, which is expressed as:

$$N_{pr} = P(2)\sum_{r,j} N_r(E_j)\,\Delta E \qquad 6\text{-}24$$

Thus the total yield of photons from the scintillator, Y_{hv} is deduced from the expressions 6-19 and 6-21to be:

$$Y_{hv} = \frac{\sum_j P_a(E_j)\,\phi_{eq}(E_j)\,\Delta E}{X_a} \qquad 6\text{-}25$$

and the total yield of photon pairs is obtained by combining equations 6-22, 6-23 and 6-25, which will be in the form:

$$Y_{pr} = P(2)\,\frac{\sum_j P_a(E_j)\,H(2,E_j)\,\phi_{eq}(E_j)\,\Delta E_j}{X_a} \qquad 6\text{-}26$$

The steps by which these procedures were carried out, as indicated by equations 6-17 to equations 6-26, are presented schematically in figure 6-15.

The ratio of equation 6- 26 to 6-25 gives the efficiency for dsb production, ε_{dsb}, as:

$$\varepsilon_{dsb} = \frac{Y_{pr}}{Y_{hv}} \qquad 6\text{-}27$$

The cross-section for induction of the simulated biological effect, σ_B, is simply the ratio of the average yield of double-strand breaks in the DNA to the total equilibrium particle fluence. Thus σ_B can be expressed as:

$$\sigma_B = \frac{Y_{pr}}{\phi_{i\gamma}\sum_k \omega_k \mu_{tr,k}\,\phi_{T,eq,k}} \qquad 6\text{-}28$$

In equation 6-28, the denominator is summed over the constituent elements type k of the phosphor material. It is the product of the concentration of electrons, $\phi_i\omega_k\mu_{tr,k}$, generated by an initial incident photon fluence ϕ_i, and the total equilibrium fluence per unit source concentration of primary electrons, $\phi_{T,eq,k}$. The product $\omega_k\mu_{tr,k}$ is the

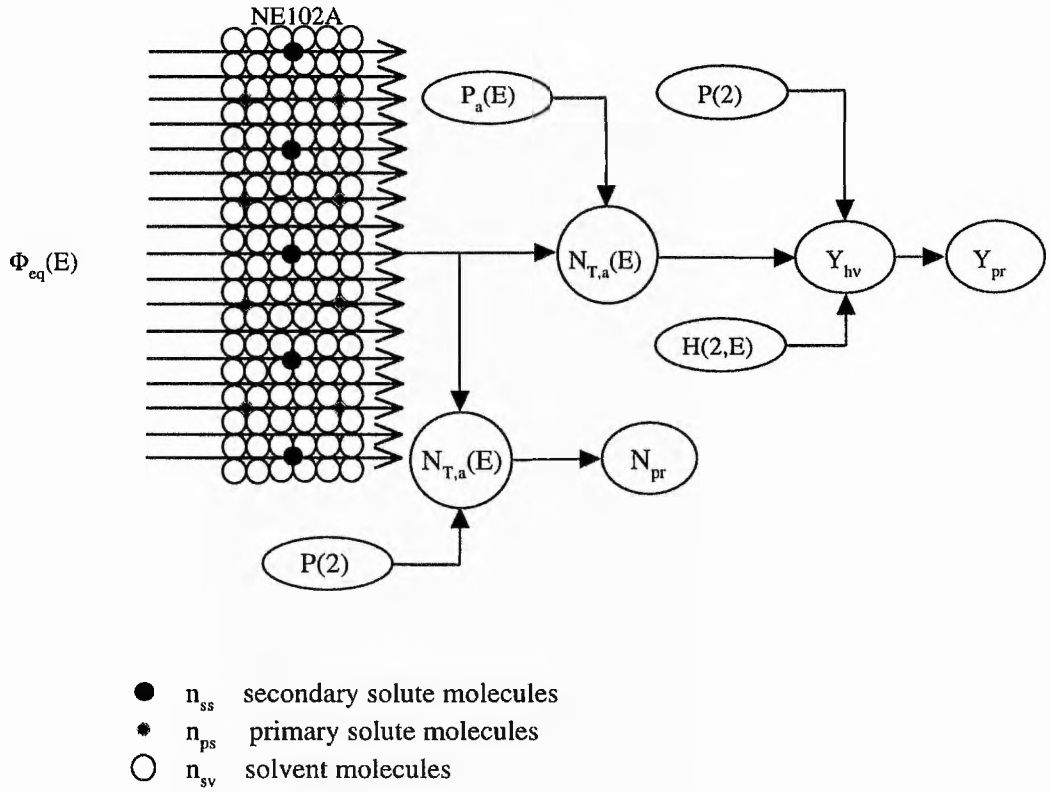

Figure 6-15 Schematic diagram showing the computer simulation steps as carried-out from knowledge of the equilibrium fluence $\Phi_{eq}(E)$. Then the total number of active centres at risk, $N_{T,a}(E)$ and the total yield of photons Y_{hv} can be estimated. Among those, the yield of photons that are simulated and spaced by two nanometers are selected by applying the probability distributions P(2) and H(2,I(E)).

fraction by weight, ω_k, of the mass energy transfer coefficient for the constituent element type k. $\phi_{T,eq}$ is the total equilibrium fluence generated by primary electrons produced by the initial X- or γ-ray interactions in component element, k, of the phosphor material.

6-6-2 Instrument descriptions

6-6-2-1 The photomultiplier

The photmultiplier used in this experiment is a Thorn EMI tube type 9125B. The window is made up of low background borosilicate glass which has a good optical transmission to light in the visible region (wavelength > 300 nm). The photocathode is made up of Bialkali (Sb-Rb-Cs) with an active diameter of 2.3 cm and quantum efficiency of 25 %. The photocathode offers response in the visible blue region and is characterised with its low thermionic emission to maximise the signal to noise ratio, S/N. Thus the low dark current characteristic would enable the tube to detect the very weak light expected from thin films with thicknesses of a few microns. The basic characteristics of the tube are shown in table 6-6. The tube had been selected very carefully for its high performance specifically in conjunction with NE102A. Its spectral response matches the emission spectra of NE102 as shown in figure 6-16.

A maximum voltage of 1500 volts (with negative feedback for stability) was applied to the voltage devider. The dynode resistances (13) are each of 100 kΩ. Stabilising capacitors are incorporated across the last three dynodes, each of 2 μF to maintain current linearity.

The output pulse height rapidly attains equilibrium with a stability coefficient of better than 1 % per day after 10 hours of operation. A magnetic shield is used on top of the tube surface to screen it from any possible surrounding magnetic fields. The PM produces pulses with time constants of ~ 1 μs and the preamplifier time constant is of the order 50 μs, should allow this shape to pass without any change.

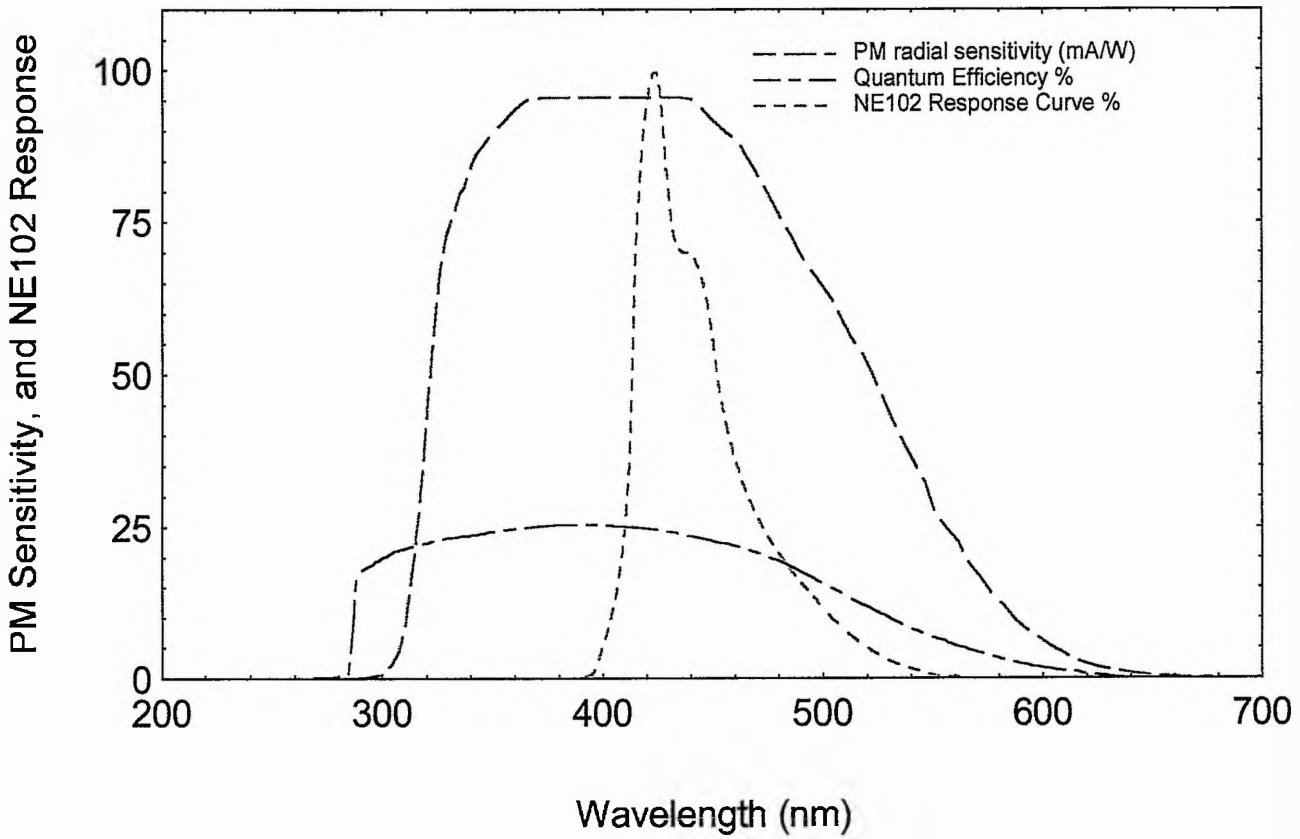

Figure 6-16 Spectral response of the photomultiplier tube vs. the emission spectra of NE102.

Table 6-6 Characteristics of photomultiplier 9125B.

Windows	
material	Borosillicate glass
diameter	29 mm
Index of Refraction	1.48
Photocathode	
Type	Bialkali
active diameter	23 mm
spectral range	310-650 nm
corning blue (typ)	11.0
(min)	7.0
QE at maximum λ (typ)	25%
Dynodes	
number	11
type	linear focused
secondary emitting surface	SbCs
capacitance anode to all dynodes	5 pF
Gain and Dark Current	
voltage for 200 A/lm (typ)	950 V
(max)	1250 V
dark current at 200 A/lm (typ)	0.2 nA
(max)	5 nA
dark current at 20 °C (typ)	100 s^{-1}
Linearity	
The pulse current at which there is 5% deviation from linear amplification.	
Voltage divider A	25 mA
Voltage divider B	100 mA
Rate Effect	
$I_a = 0 \rightarrow 50\ \mu A$	< 2%
Timing Performance	
rise time	4.5 ns
pulse width	7.5 ns
transit time	33 ns
Temperature Coefficient at 20 °C	± 0.1% $°C^{-1}$
Rating (not to exceed 2000 A/lm)	
overall sensitivity	2000 A/lm
V(k-d_1)	300 V
V(d-d)	300 V
V(k-a)	2000 V
Ik(mean)	50 nA
Ia(mean)	100 μA
temperature (operating)	-30 to +60 °C

6-6-2-2 The detection assembly

The plastic scintillator films NE102A of thickness 20 μm were specially made by Nuclear Enterprises. Their thickness uniformity has been tested using both a mechanical micrometer (Digimatic model IDf-122E) with resolution of 1μm and magnetic induction (Minitest 2000 by Electro-Physik, Köln).

A current sensitive preamplifier should generally have low input impedance to convert fast current pulses coming from the photomultiplier to a voltage pulse. Here the preamplifier used was selected to match the impedances of the PMT and the amplifier. The output to input ratio is of the order 500 mV/mA.

Typical pulses with a fast rise time of 20 ns and a long decay time from an ORTEC-448 research pulser were introduced to the preamplifier. Pulses of the order of 5 mV from the preamplifier are fed into the amplifier for shaping and further amplification. The semi-Gaussian shaping was made with differentiating and integrating time constants of 2 μs. Clear pulses of 160 mV height, were measured at the amplifier output.

Signal output pulse shapes from the amplifier have been tested using radiation sources and the research pulser: two γ-sources (^{60}Co, ^{137}Cs) and a beta source (^{90}Sr/^{90}Y). The 20 micron thin film plastic scintillator target (NE102A) introduced on the EMI photomultiplier 9125B which is operated with an optimum applied 820 volts. A 5 mm plastic was sandwiched between the source and the scintillator, which is positioned on the PM, to ensure charge particle equilibrium. The bipolar mode of the amplifier was selected. The amplifier gain was set at 100 and a shaping time constant of 2.0 μs. The pulses were introduced at the rate of 20 pulses/s with a fixed fast rise time of 50 ns and a long decay time of 50 μs and negative polarity. Stable pulses of the order 400 mV, 300 mV, and 170 mV in respective order for ^{60}Co, ^{137}Cs, and ^{90}Sr has been measured for both matched signals. The performance of the other components have been tested and fully responded within the expected scales.

The basic components of the integrated detection system and types are shown in figures 6-17a, b.

6-6-2-3 Experimental arrangement

In experimentation with the γ-ray sources, a slab of perspex of 5 mm thickness was introduced, to establish electron charged particles equilibrium at the entrance to the NE102 thin film. The perspex is covered with a TiO_2 water based emulsion paint (NE560) which has (90-95%) reflectivity for the emission spectra of NE102A in the range 400-600 nm. A thin layer of silicone oil was applied to the surface of the thin film and the photomultiplier to maintain good optical coupling.

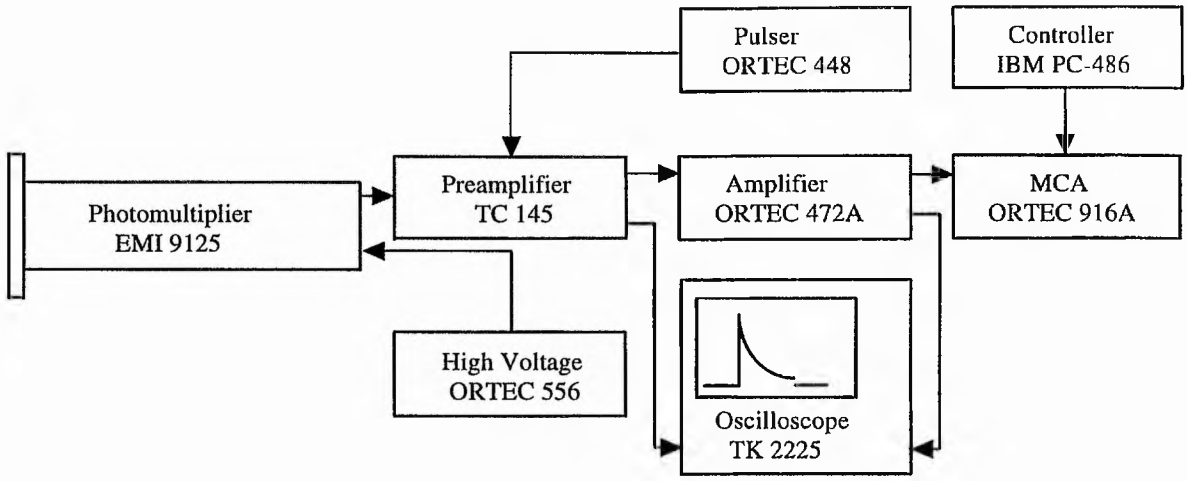

Figure 6-17a Scintillation detection assembly.

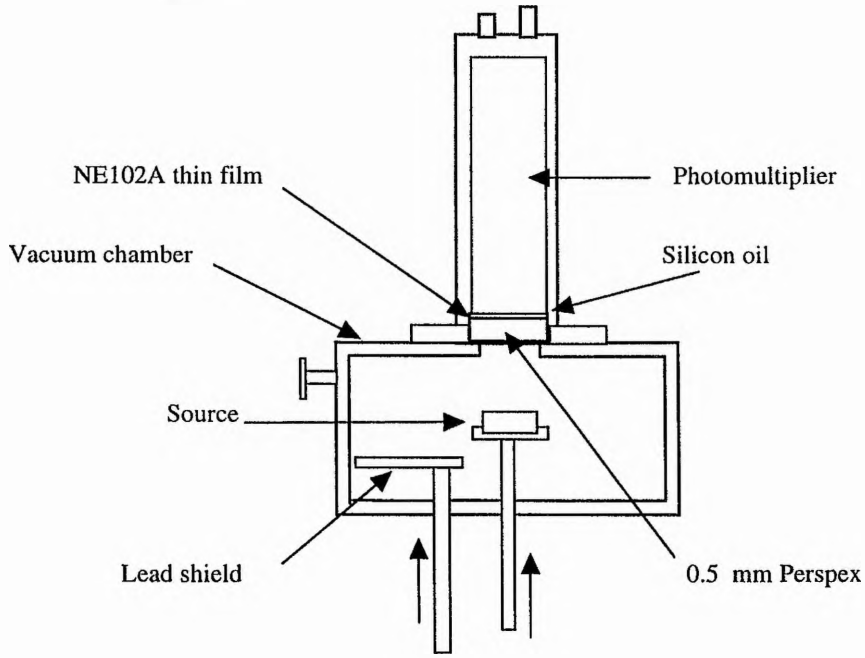

Figure 6-17b Detector-photomultiplier arrangement.

For the purpose of testing the NE102A thin film and examining its feasibility toward unified dosimetry, γ-radiation is considered to be more convenient than other radiation. For one thing, γ-rays deposit only a small portion of their total energy in the medium and, as they are sparsely ionising, they do not cause saturation. Thus knowing the equilibrium charged particle spectrum within the scintillator, it is possible to evaluate the main components required for examining the system.

6-6-3 Results and calculations

Slowing down electron spectra at equilibrium for ^{60}Co and ^{137}Cs; figures 6-18, calculated from an analytical formula [Watt, 1996], were obtained as a preliminary to evaluation of the data given by equations 6-17 to 6-28. The semi-infinite layer of NE102A phosphor of 20 micron thick served as the test device.

The pulse height spectra of γ-rays from ^{60}Co, ^{137}Cs, and β-rays from $^{90}Sr/^{90}Y$ are shown in figures 6-19 a, b. From knowledge of the microdose spectra, the energy of equilibrium electrons that stopped in the 20 μm thickness is estimated to be about 32 keV (LET ~ 15 keV/μm) [Watt, 1996]. The threshold for these electrons to produce measurable light quanta is about 1 keV. The photon yield of the testing sources are calculated as a function of charged particles at equilibrium (electrons). The results are shown figures 6-20 a, b, c. Electrons with low energies up to 5 keV (LET = 4 to about 12 keV/μm) produce a high, well resolved light output. This is in contrast with those electrons at the end of track (LET > 15 keV/μm) which show a large spread of the light output.

6-6-3-1 Modelling experimental output

The formulation of the unified model for thin films of organic scintillators (section 6-4-7) is based on track segment experiments with fast heavy ions. However, in our analysis here, the spectra obtained from γ-sources are based on the charged particle equilibrium produced by the primary radiation. Thus here knowledge of the equilibrium slowing down fluence per unit concentration and the properties of the scintillator material will be utilised to model the results.

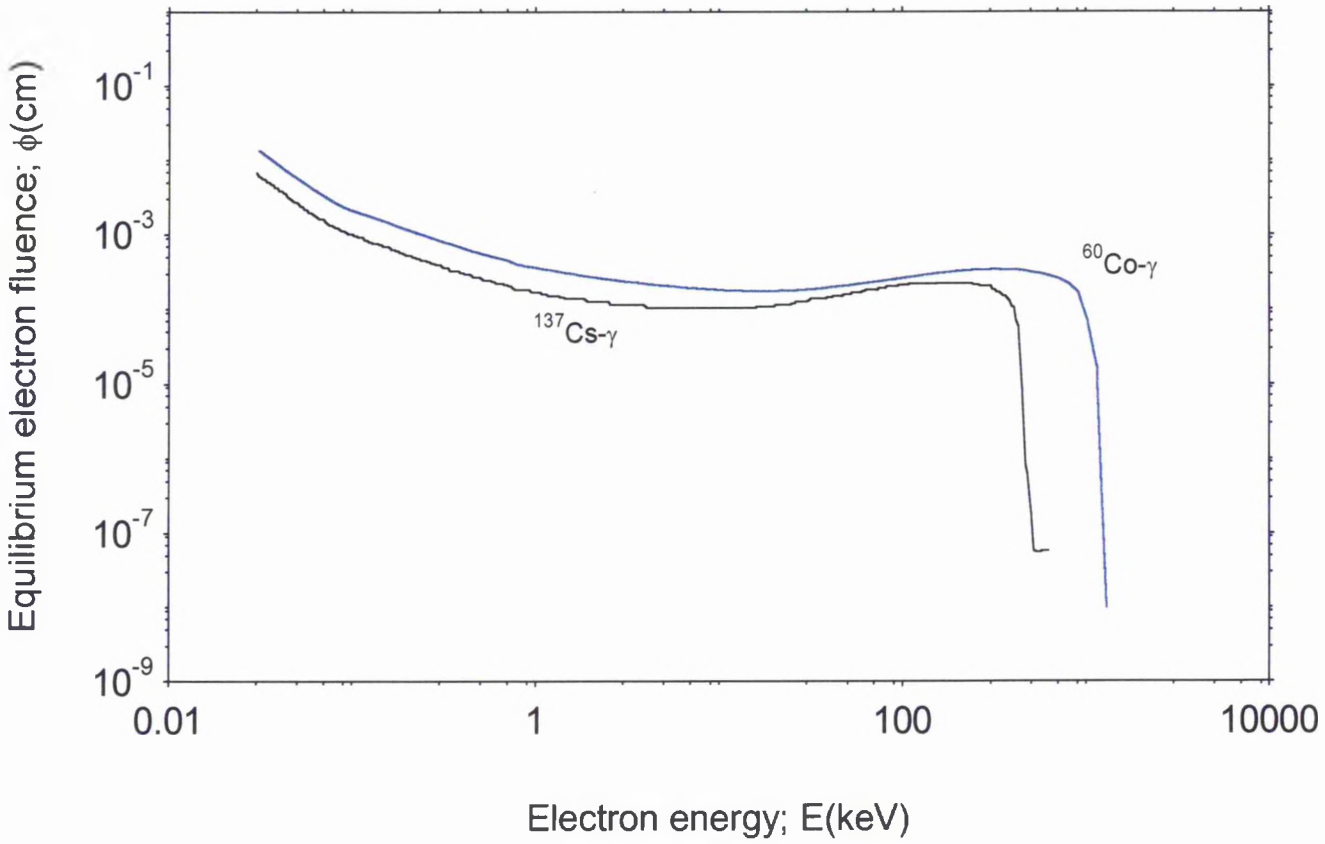

Figure 6-18 Equilibrium Electron Spectrum in Water: γ-sources. The Source concentrations per γ-rays of ^{60}Co and ^{137}Cs are $N\sigma_{tr} = 2.98 \times 10^{-2}$ and 3.26×10^{-2} respectively.

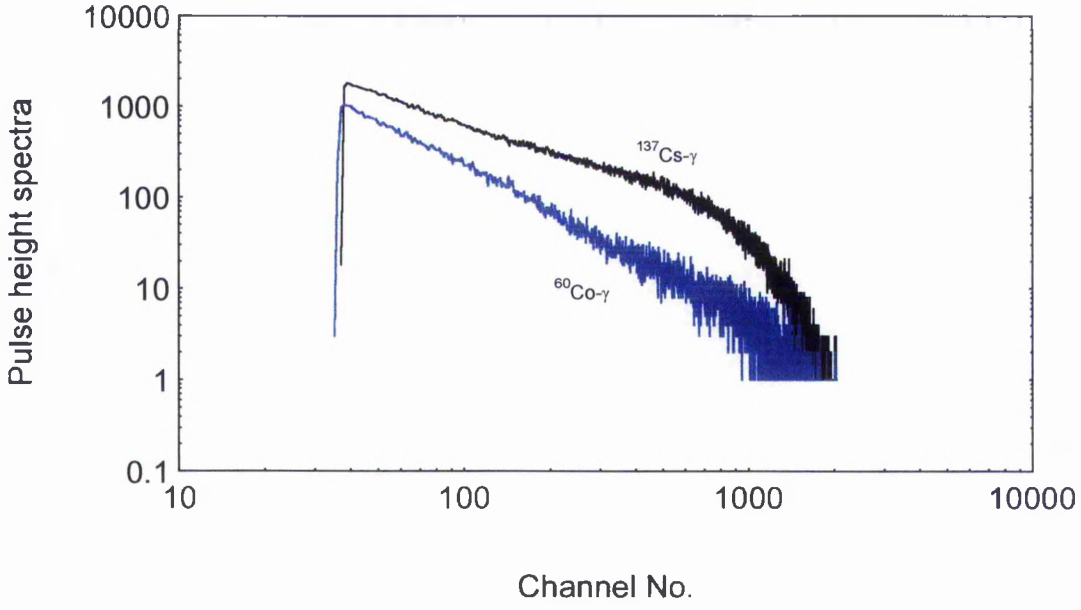

Figure 6-19a γ-ray pulse spectra recorded by an ORTEC MCA.

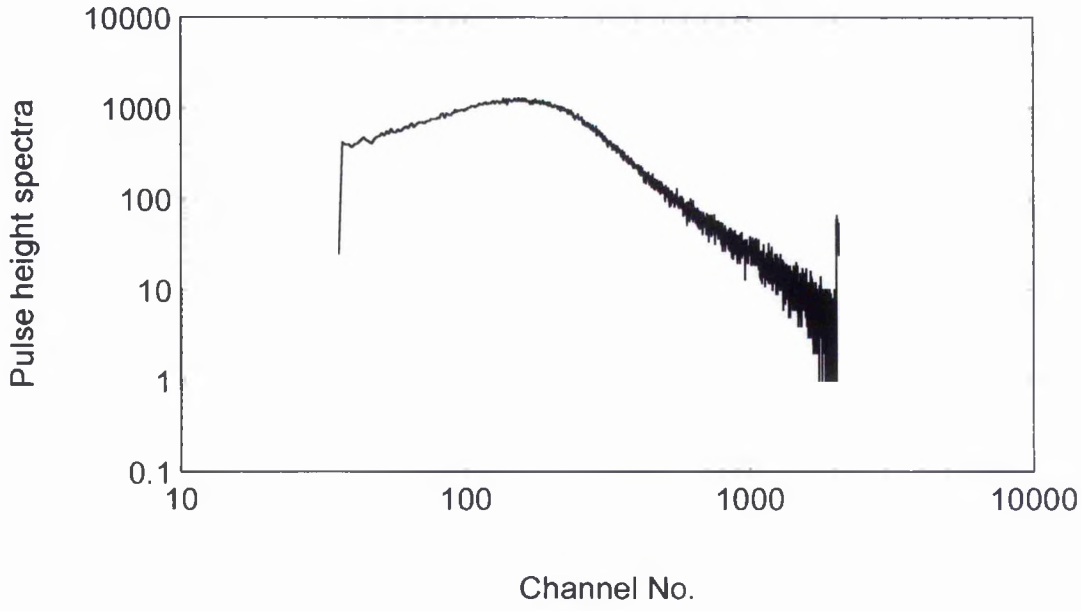

Figure 6-19b $^{90}Sr/^{90}Y$ β-ray pulse spectra recorded by an ORTEC MCA.

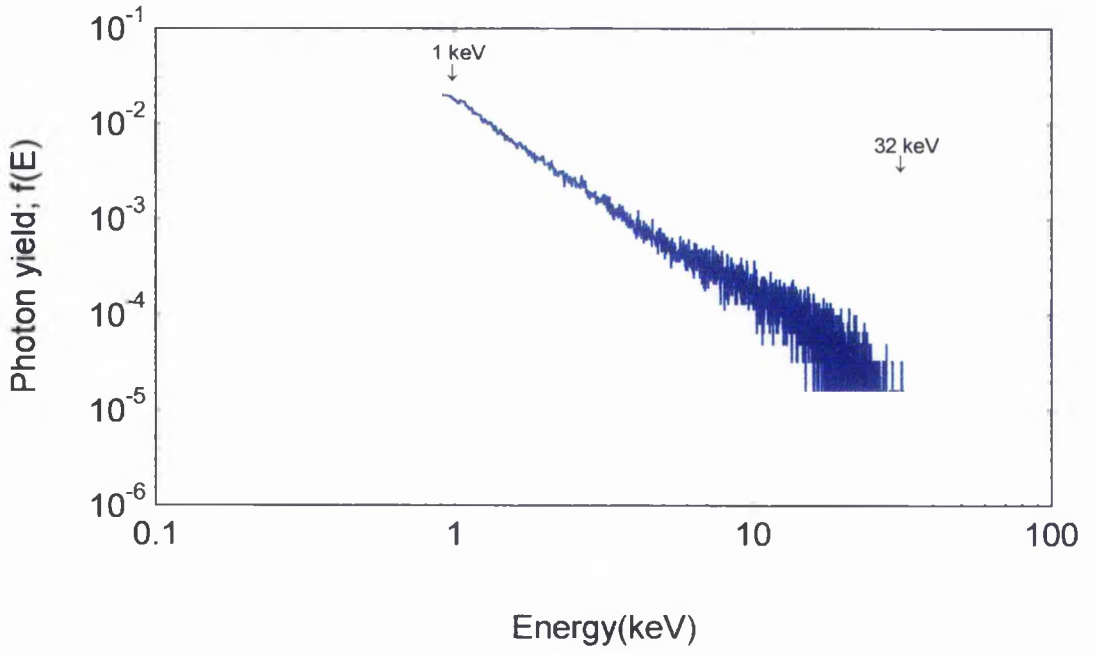

Figure 6-20a Experimental light yield spectra of equilibrium electrons for ^{60}Co-γ rays.

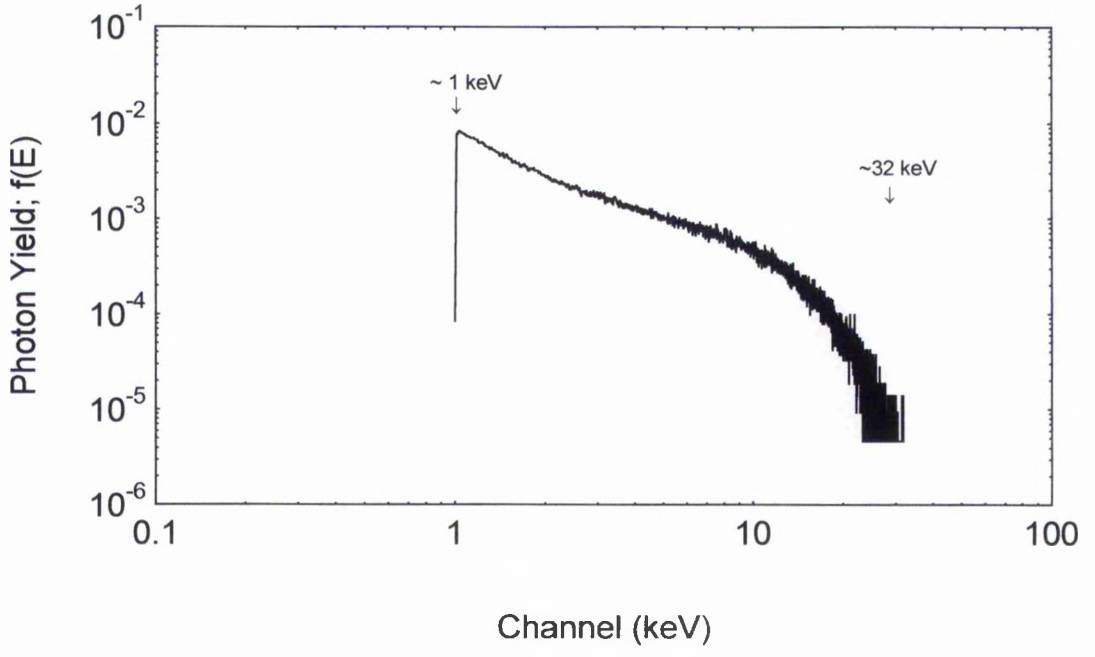

Figure 6-20b Experimental light yield spectra of equilibrium electrons for ^{137}Cs-γ rays.

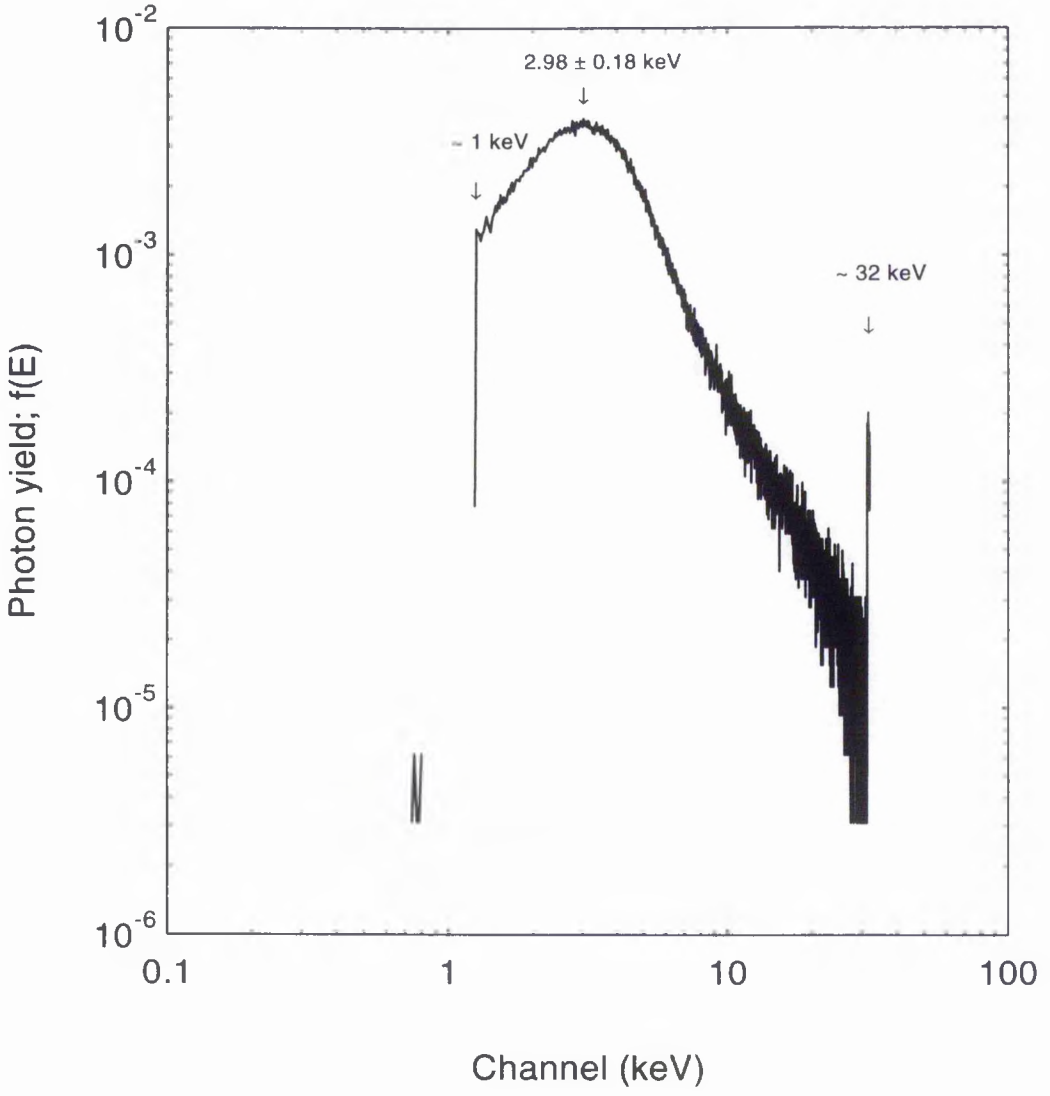

Figure 6-20c Experimental light yield for equilibrium electrons for $^{90}Sr/^{90}Y$-β source.

Because of the higher efficiency of scintillation induced by electrons, the relation dL/dx=S dE/dx derived from Birks' formula (section 6-4-1) still holds. Thus the total experimental light yield, L(E), is given by:

$$L(E) = \int_0^E f(E)\, dE \qquad 6\text{-}29$$

where f(E) is the relative light output as shown in figure 6-20a.

However for charged particles (electrons) at equilibrium, produced in the thin film, within the energy range of 1 - 30 keV, the energy absorption spectra will be given by:

$$G(E) = \Phi_{eq}(E) \overline{\frac{dE}{dx}} \qquad 6\text{-}30$$

where $\Phi_i(E)$ is the fraction of the total fluence for electrons which is given by:

$$\Phi_i(E) = \frac{\phi_i(E)}{\int_0^E \phi(E)\, dE} \qquad 6\text{-}31$$

and dE/dx is the average stopping power of the charged particles equilibrium (electrons).

The total light output produced by the charged particles at equilibrium will be proportional to the energy absorption function G(E). Thus a constant of proportionality, A, from the experimental and theoretical calculations can be found; such that A = G(E)/f(E). Figure 6-21b shows the calculated energy absorption function G(E) based on equation 6-30, the radiation quality parameters in figure 6-21 a, and the experimental light output L induced by the ^{60}Co-γ ray source. Thus the experimental results are found to be in good agreement with the theoretical result using the equilibrium fluence of the electrons which produce light in the phosphor.

The lower gain of the experimental spectrum is due to several factors where energy is dissipated outside the thin film. These include loss of energy in the light pipe, loss of energy due to light transmission from the film to the PM surface through the silicone layers, loss due to conversion of photons to photoelectrons in the photocathode material

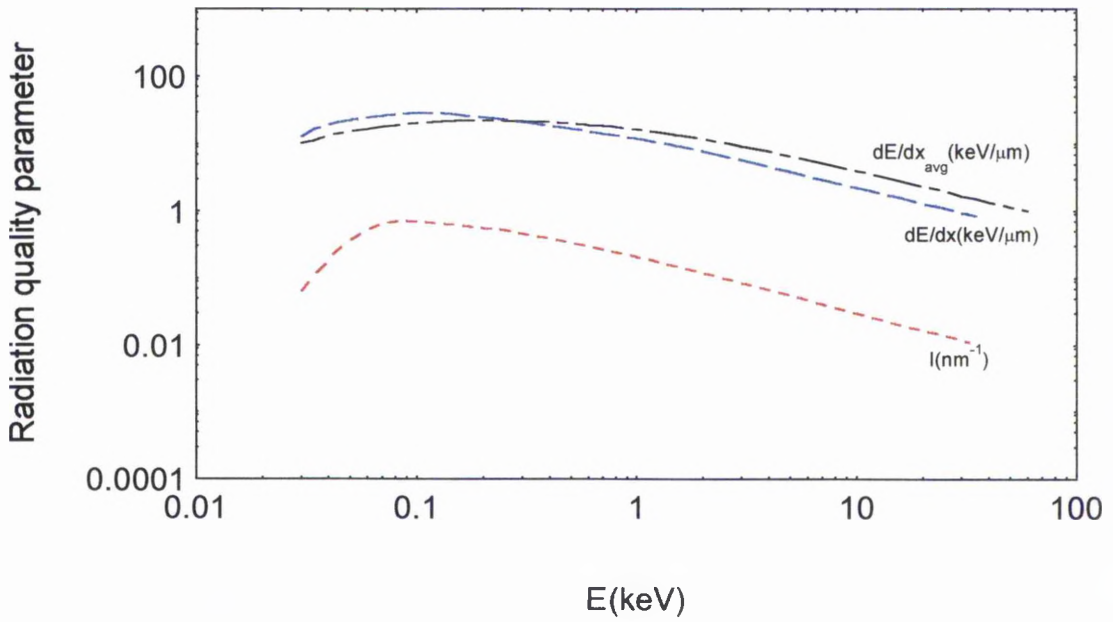

Figure 6-21a Quality parameters for equilibrium electrons in NE102A plastic scintillator.

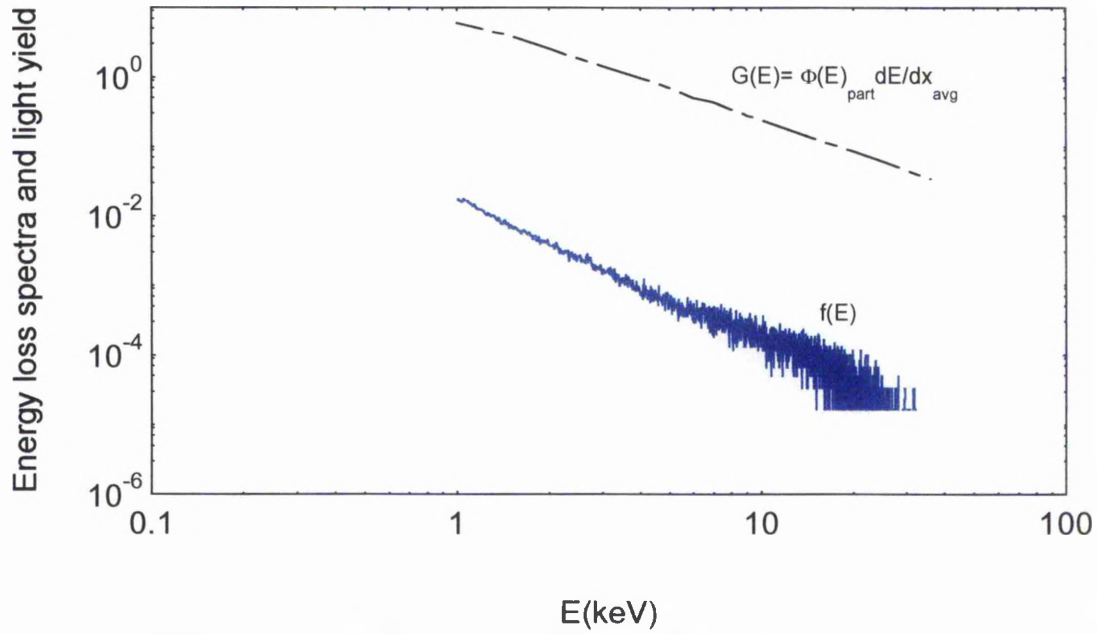

Figure 6-21b Relation between energy loss per equilibrium charged particles and light yield of ^{60}Co-γ source in 20 μm NE102A plastic scintillator.

of the PM. The value of the proportionality constant, A, which includes these factors, is found to be about 1.2 x 10^3 $keV^2/\mu m$. This factor is related to the scintillator properties as well as to the radiation type. However, accounting for these discrepancies, the 20 micron NE102A thin films are found to be a potentially good prospect for detecting weak ionising radiation.

6-6-3-2 Total photon and dsb's simulation

Assuming that the phosphor is uniformly distributed in a solvent e.g. PVT or Xylene, the fraction of the fluor (p-terphenyl) by weight is about 3.0 % (table 6-3). The density of the scintillant is about 1.03 g/cm^3 and the molecular weight of fluor is about 230 g/mole (table 6-2), thus the volume occupied by the fluor molecule is about 1.2 x 10^{-20} cm^3 , and the mean distance between two fluor molecules in the main matrix is estimated to be about 3 nm. This represents twice the approximate distance over which the activator competes for excitons.

Hence, for the rest of the calculations, only ^{60}Co-γ spectra will be considered. Starting from the equilibrium slowing down spectra of ^{60}Co-γ radiation, the total yield of scintillation photons, $Y_{h\nu}$, and the yield of paired scintillations, Y_{pr}, which represent the dsb's are calculated by the computer code NANOSPECTRA, appendix BI. The resulted yield as a function of energy deposited in the 20 μm NE102A plastic scintillator is shown in figure 6-22.

The very small yield, Y_{pr}, of simulated dsb's for ^{60}Co-γ radiation is consistent with expectations and with the known low efficiency of biological damage due to electron irradiations relative to heavy particles [Watt,1989]. We know from our past experience that 4 MeV α-particles are capable of saturating the biological damage. At the molecular level this saturated damage is of the order of the geometrical cross-section area of the DNA, $\sigma_g \sim 4\ \mu m^2$. Thus the frequency of damage is estimated to be about 2.52 x 10^{-1} dsb's/Gy-cell. For a dose of 1 Gy, the energy absorbed in the nuclear DNA is about 36 keV, results in an estimated figure of 7 x 10^{-3} dsb's/keV. In fact this is not too bad when compared to the figure of $Y_{pr} \sim 10^{-2}$ dsb's/keV for

the ^{60}Co-γ radiation. On the other hand the initial ssb's of the DNA can only be considered as 0.1 % of the total light yield (0.089 ssb's/keV) of which about 10 % estimated as dsb's of the DNA. Using microdosimetry nomenclature [Caswell, 1966] for particle tracks in micron spheres 'insider' and 'stopper' electrons are found to be most damaging on an individual track basis. On the other hand, the individual tracks of 'crosser' and 'starter' electrons are found to be much less effective biologically, even though they contribute most to the total events.

Significant enhancement of the wanted signal at the expense of the unwanted signal could be achieved by utilising coincidence techniques to resolve the respective contributions thereby making a considerable enhancement of the 'signal to background' ratio of events. As a very large portion of the energy deposited is seen to be wasted in relatively unimportant events, these results clearly demonstrate the limitation of absorbed dose as a quantity for interpretation of radiation damage in mammalian systems [Watt, 1994]. Another observation is that very low energy electrons (less than 300 eV) can contribute significantly to the overall electron damage. Instrumentation should therefore be designed to analyse electron events above about 40 eV. Organic scintillators with photomultiplier tubes typically have a threshold of about 1 keV. However it is possible that this is not too serious a disadvantage as often the frequency of events having sizes greater than 1 keV, when weighted by the statistical probability of damage per track, dominates the total effect. Enhancement of sensitivity at low energies may be possible by appropriate adjustment to the fluor concentration to ensure a mean spacing of less than 3 nm. A fluor concentration of 20 % by weight is found to be appropriate for this task.

In conclusion NE102A is found to have some advantageous features which have a parallel with the physico-chemical processes known to be fundamental to the initiation of radiation damage in mammalian cells. The proposed method has the potential to record radiation effects at the nanometer level in the condensed phase, a dimension which is known to be of fundamental importance for biological effects [Colauti, 1994].

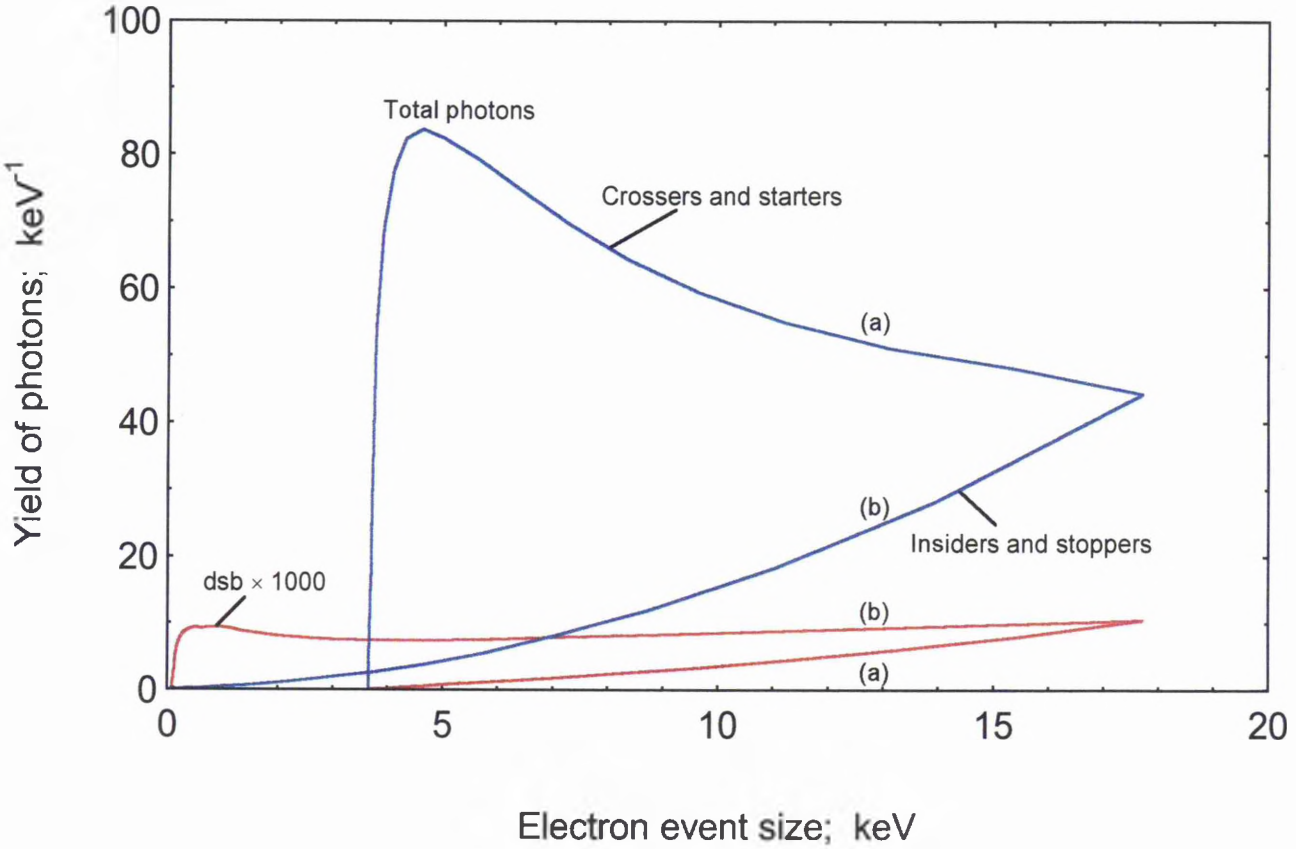

Figure 6-22 Simulation of photon yield within 20 μm plastic scintillator by ^{60}Co-γ rays.

Chapter 7

CONCLUSION AND FUTURE PROPOSALS

From the forgoing studies in chapter 3 and 4, we concluded that all the biological effects for the different end points; chromosome aberrations, HPRT specific mutations, oncogenic transformations and cell inactivation are all closely related if their damage, quantified by the effective cross-sections, σ, is represented as a function of the mean free path for linear primary ionisation, λ(nm). For these end points it is seen that they all preserve the same shape characteristics in a σ–λ plot e.g. they have same gradient for $\lambda > \lambda_o$; the damage saturation region ($\lambda < \lambda_o$) is closely related to the geometrical cross-sections, σ_g, of the biological targets; and all curves have the same inflection point at $\lambda = \lambda_o \sim 1.4$ nm. The biological damage is seen to be related to the dsb's of the DNA, as the point of inflection is in close proximity to the inter-strand distance (mean chord length ~ 1.4 nm). The simple correlation allowed estimation of risk scaling factors of the various end points as related to cell killing [Alkharam, 1997]. The probabilities of risk with respect to inactivation, for chromosome dicentrics, oncogenic transformation, and of mutations of the HPRT gene are respectively 0.18, 1.6×10^{-4} and 2.91×10^{-5}. More experiments on all endpoints using the same species and charged particles with low and high LET at the same laboratory are encouraged. With the provision of both inactivation data and their experimental errors, a better estimation for more profound interpretation of the (λ–σ) response can be reached.

The situation with specific molecular damage (e.g. ssb's and dsb's of the DNA in cells) is quite different. Although, the data on DNA strand breaks of viruses [Christensen, 1972 ; Stanton, 1990], bacteriophage [Neary, 1972] and mammalian cells [Prise, 1990 ; Kampf, 1983; Weber, 1993 ; Belli, 1994 ; Heilmann, 1995 ; Taucher-Scholz, 1996] are made available, the same conclusions related to the shapes of the σ–λ curve were reached [Alkharam, 1997]. However, the damage associated

with the different organisms (prokaryotics and eukaryotics) do not scale by their geometrical proportions. These controversial differences may be related to the different experimental techniques used and to the different experimental protocols (chapter 4).

For mammalian cells, the saturation cross-sections were found to be about 1 μm^2, which is about one fourth of the geometrical cross-section of DNA packed into a solid form. If this result is confirmed by more experimental measurements with the same species and same strain (e.g. V79), then this will provide another meaning of the geometrical packing factor of the chromatin in the nucleus. Another interpretation is reached if one considers the chromosomes as the lethal target [Harder, 1992], then the probability to induce pairwise lesions is proportional to $1/2^2$. Calculations using earlier endpoint saturation cross-sections show that four dsb's in the DNA of a human lymphocyte cell are needed to induce a chromosome dicentric ; 100 dsb's in DNA of a C3H10T1/2 cell are needed to inactivate an oncogene and 3500 dsb's in DNA of a V79 cell are needed to delete an HPRT mutant. Experiments on measurements of dsb's in DNA in the same laboratory and using the same experimental protocols with different charged particles (LET spectrum ~ 1 keV/μm to ~ 1000 keV/μm) on different species (viruses, bacteria, and mammalian cells) are also encouraged for better evaluation.

An overall conclusion may be drawn from these studies: that there is a universal response function, which has an inflection point at $\lambda_0 \sim 1.8$ nm. Indeed this can only be related to the DNA double strand breaks, where spatial dimensions are of the order of the inter-strand distance of the DNA. For radiation protection it is sufficient to express the yield of dsb's of the DNA as a function of the mean free path for linear primary ionisation. The measuring device has many criteria for radiation protection application; most important are, credibility, reproducibility, practicability and availability. Thin film plastic scintillators are found to be potentially viable for this purpose. Preliminary experimentation to model the effects of ionising radiation on these detection media show their credibility of measuring low level radiation e.g. at

environmental background. In these experimentations simple probability functions were applied to find those primary solutes at risk and whose active cross-section area is similar to that of the DNA (10 nm^2). The interaction of ionising radiation with these active centres results in the emission of fluorescent photons (scintons). Among those scintons, only those which have originated from two hits on phosphor centres spaced at a mean chord length of 2 nm are considered to simulate the action of ionising radiation on DNA (dsb's). The 20 μm NE102A plastic scintillators are found to be suitable detecting media for this purpose. The resulting simulation showed a yield of 10^{-2} dsb's/keV which is in close proximity with the theoretical result for a 4 MeV alpha particle of 7 x 10^{-3} dsb's/keV.

In practice, interpretation of the instrumental reading will sometimes be required for an unknown radiation source (e.g. γ-ray source), in which case knowledge of the mean linear primary ionisation for each event is required (because of the role of the probability, H(2,E) in equations 6-23). Therefore, for successful interpretation of the required signals from a practical device, it will be necessary to distinguish between signals arising from:

(i) 'Wanted' pairs of emitted scintons originating at the desired spacing of ~ 1.8 nm from those 'unwanted' pairs separated by other distances.

(ii) Signals for equal energy event sizes, and therefore equal number of scintons, due to tracks which have different ionisation rates e.g. a fast 'crosser' compared with a 'stopper' of the same event size, etc.

To overcome these problems, it is proposed first to investigate representations of the trends of the fraction of 'crosser' plus 'starter' and 'insider' plus 'stopper' components with respect to the total events, for different radiation fields, and secondly to observe the event frequency spectra in the phosphor layer as a function of the integral number of scintons emitted per event plotted as abscissa. The latter number spectrum implicitly contains information on the event size spectral components. Hybrid photomultiplier tubes (HPMT's) with single-photon sensitivity are found to be

capable of resolving single and plural photon emissions [van Geest, 1991]. Unlike the conventional PM's, photoelectrons produced on the photocathode are accelerated through a focused electrostatic negative potential of 10 kV - 15 kV. The electrons then impinge on a reversed biased silicon diode, thus generating electron-hole pairs. The detecting system exhibits a number of features; higher gain and lower electronic (dark current) and thermal noise. The most important feature is that the system can differentiate between single a plural events specifically for weak sources [D'Ambrosio, 1994a]. The well resolved Gaussian shaped peaks can be simulated via Poisson statistics [D'Ambrosio, 1994b]. Leutz, 1995 reviewed the basic principles of scintillating fibres along with HPMT's.

Currently, at our research laboratory, we are utilising our knowledge along with these new generation tubes to explore their feasibility for absolute dosimetric measurements. Figure 7-1, shows a typical response of ^{137}Cs-γ rays as measured by HPMT using NE102 thin film plastic scintillator. The second peak shows double events which have arrived at and are sensed by the system. More detailed statistical probabilities are needed to separate those events correlated with scintons emitted from two phosphor centres spaced at 1.8 nm. The compilation of experimental biological data obtained earlier (chapter 3 and chapter 4) are now available to enable testing and comparison of the response of the proposed device.

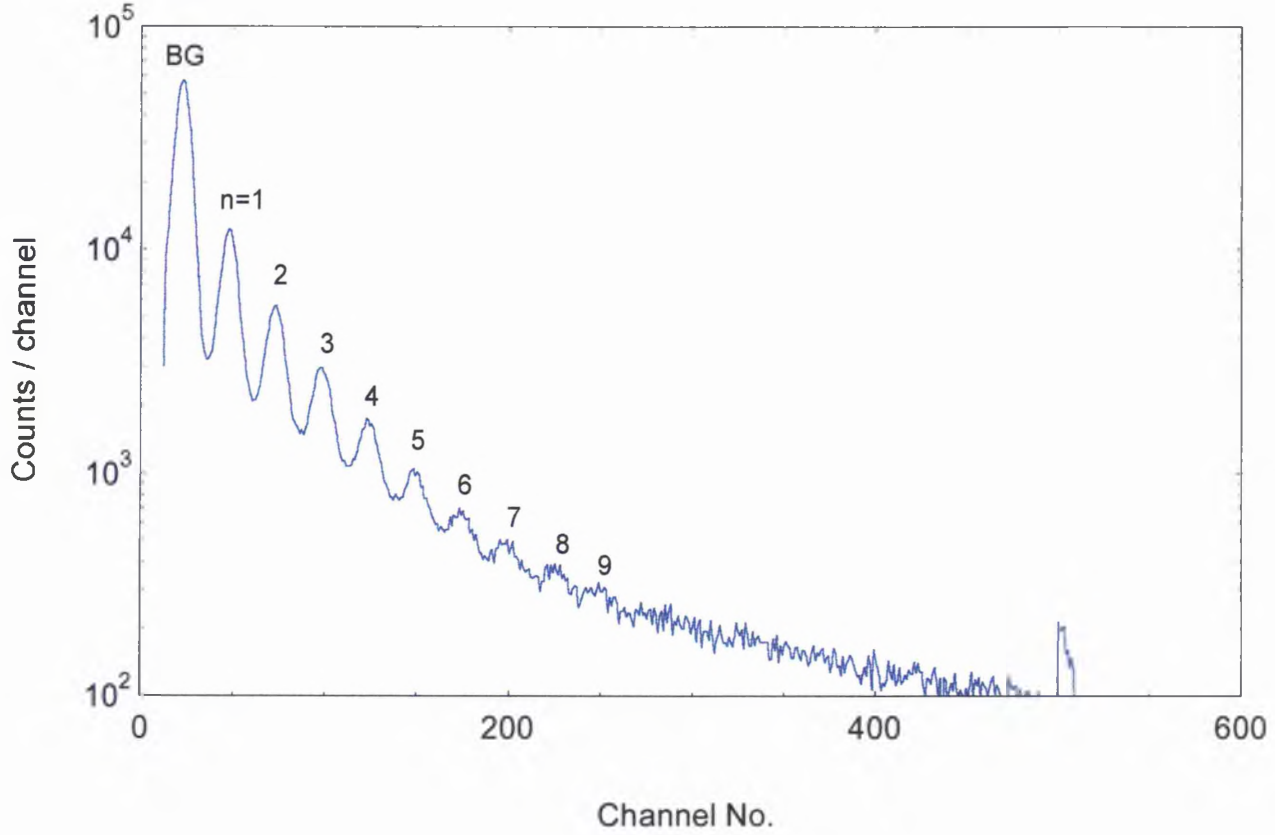

Figure 7-1 Hybrid photomultiplier tube spectral response from ^{137}Cs-γ rays on 20 μm NE102A plastic scintillator.

REFERENCES

Adams, R. L. P., J. T. Knowler, et al. (1992). **The Biochemistry of The Nucleic Acids.** London, Chapman and Hall.

Ajitanand, N. N., and Iyengar, K. N. (1976). "On The Technique of Preparation of High Quality Thin Film Scintillators." Nucl. Instrum. Meth. **133**: 71-74.

Akkerman, A., A. Gibrekhterman, et al. (1992). "Monte Carlo Simulations of Secondary Electron Emission from CsI Induced by 1-10 keV X-rays and Electrons." J.Appl.Phys. **72** : 5429-5436.

Akpa, T. C., K. J. Weber, et al. (1992). "Heavy Ion-induced DNA Double Strand Breaks in Yeast." Int.J.Radiat.Biol. **62:** 279-287

Al-Ahmad, K. O. and D. E. Watt (1984). "Stopping Power of Low Energy Electrons (<10 keV) in Solid Polyethylene." J. Phys. D: Appl. Phys. **17**: 1899-1904.

Alkharam, A. S. and D. E. Watt (1997). "Risk Scaling Factors from Inactivation to Chromosome Aberrations, Mutations and Oncogenic Transformations in Mammalian Cells." Radiat. Prot. Dosim. **70, No.1-4**: 537-540.

Alpen, A. L. (1990). **Radiation Biophysics.** London, Prentice-Hall International.

Ashley, J. C. (1982). "Stopping Power of Liquid Water for Low Energy Electrons." Radiat. Res. **89**: 25-31.

Attix, F. H. (1986). **Introduction Radiological Physics and Radiation Dosimetry.** New York, John Wiley & Sons, Inc.

Aufderheide, E., H. Rink, et al. (1987). "Heavy Ions Effects on Cellular DNA: Strand Break Induction and Repair in Cultured Diploid Lens Epithelial Cells." Int.J.Radiat.Biol. **51**: 779-790.

Awa, D., W. Dewey, et al. (1974). "Measurement of Radiation-induced DNA Double Strand Breaks by Pulsed Field Electrophoresis." Radiat.Res. **122**: 181-187.

Badhwar, G., C. Deney, et al. (1967). "The Non-linear Response of the Plastic Scintillator NE102." Nucl. Instr. Meth. **57**: 116-120.

Barendsen, G. W. (1993). "Sublethal Damage and DNA Double Strand Breaks have Similar RBE-LET Relationships: evidence and implications." Int.J.Radiat.Bilol. **63**: 325-330.

Barendsen, G. W. (1994). "RBE-LET Relationships for Different Types Of Lethal Radiation-Damage In Mammalian-Cells - Comparison with DNA dsb and an Interpretation of Differences in Radiosensitivity." Int.J.Radiat.Bilol. **66**: 433-436.

Barendsen, G. W. and H. M. D. Walter (1963). "Effects of Different Ionizing Radiations on Human Cells in Tissue Culture." Radiat. Res. **18**: 106-119.

Barjaktarovic, N. and R. K. Savage (1980). "RBE for d(42 MeV)-Be Neutrons based on Chromosome-type Aberrations Induced in Human Lymphocytes and Scored in Cells at First Division." Int.J.Radiat.Biol. **37**: 667-675.

Barkas, W. H. (1963). **Nuclear Research Emulsions.** New York, Academic Press Inc.

Barone, A. (1995). "Why Superconductive Detectors?" Nucl.Phys.B **44**: 645-666.

Barone, A. and G. Paterno (1982). **Physics and Applications of the Josephson Effect.**. London, Wiley.

Batra, R. K. and A. C. Shotter (1984). "Passage of Fission Fragments Through Thin Film Plastic Scintillators." Nucl.Instrum. Meth.Phys.Res.B **5**: 14-19.

Bauchinger, M. (1995). "Cytogentetic Research after Accident Radiation Exposure." Stem Cell, **13, Suppl.1**: 182-190.

Becchetti, F. D. (1976). "Response of Plastic Scintillator Detectors to Heavy Ions, Z≥35, E≤170 MeV." Nucl.Instr.Meth. **138**: 93-104.

Belli, M., F. Cera, et al. (1994). "Inactivation Induced by Deutrons of Various LET in V79 Cells." Radiat.Prot.Dosim. **52**: 305-310.

Belli, M., F. Cera, et al. (1991). "Mutation induction and RBE-LET relationship of low-energy proton in V79 cells." Int.J.Radiat.Biol. **59**: 459-465.

Belli, M., F. Cera, et al. (1992). "RBE-LET Relationship for Survival and Mutation Induction of V79 Cells Irradiated with Low-Energy Protons: Re-evaluation of the LET Values at the LNL Facility." Int.J.Radiat.Biol. **61** : 145-146.

Belli, M., F. Cera, et al. (1993). "Inactivation and Mutation Induction in V79 Cells by Low Energy Protons: Re-evaluation of the Results at the LNL Facility." Int.J.Radiat.Biol. **63** : 331-337.

Belli, M., F. Cera, et al. (1994). "DNA Double-Strand Breaks Induced by Low Energy Protons in V79 Cells." Int.J.Radiat.Biol. **65**: 529-536.

Belli, M., R. Cherubini, et al. (1989). "RBE-LET Relationship for the Survival of V79 Cells Irradiated with Low Energy Protons." Int. J. Radiat.Biol. **55** : 93-104.

Belli, M., D. T. Goodhead, et al. (1992). "Direct Comparison of Biological Effectiveness of Proton and Alpha-Particles of the Same LET. II. Mutation Induction at the HPRT Locus in V79 Cells." Int.J.Radiat.Biol. **61**: 625-629.

Benbow, R. M. (1992). "Chromosome Structures." Sci.Progress **76**: 425-450.

Bender, M. A. (1995). "Cytogenetic Research in Radiation Biology." Stem Cells **13, Suppl.1**: 172-181.

Bender, M. A. and P. C. Goochi (1962). "Types and Rates of X-ray Induced Chromosome Aberrations in Human Blood Irradiated *in vitro*." Proc.Natl.Acad.Sci. U.S. **48**: 522-532.

Berger, M. J. and S. M. Seltzer (1983). "Stopping Powers and Ranges of Electrons and Positrons." NBS-IR 2550-A, National Bureau of Standards, US Department of Commerce, Washington, D.C.

Berlman, I. B. (1971). **Handbook of Fluorescence Spectra of Aromatic Molecules**. 2nd Ed. New York, Academic Press.

Bettega, D., C. Birattari, et al. (1981). "Energy Deposition by Proton Beams of up to 31 MeV in microscopic volumes." Radiat.Environ.Biophys. **19**: 79-89.

Bettega, D., P. Calzolari, et al. (1992). "Transformation of C3H10T1/2 Cells with 4.3 MeV α Particles at Low Doses: Effects of Single and Fractionated Doses." Radiat. Res. **131**: 66-71.

Bettega, D., P. Calzolari, et al. (1995). "Oncogenic Transformation of C3H10T/12 Cells Exposed to Alpha Particles: Sensitivity Through the Cell Cycle." Radiat.Res. **142**: 276-280.

Bettega, D., P. Calzolari, et al. (1990). "Oncogenic Transformation Induced by High and Low LET Radiations." Radiat.Prot.Dosim **31**: 279-283.

Bettega, D., S. Dubini, et al. (1981). "Chromosome Aberrations Induced by Protons up to 31 MeV in Cultured Human Cells." Radiat. Environ. Biophys. **19**: 91-100.

Birks, J. B. (1951). "Scintillations for Organic Crystals: Specific Fluorescence and Relative Response to Different Radiations." Proc. Phys. Soc. **A64**: 874-880.

Birks, J. B. (1964). **Theory and Practice of Scintillation Counting.** New York, Pergamon Press.

Blakely, E. A., F. Q. Ngo, et al. (1984). Heavy-Ion Radiobiology: Cellular Studies. **In: Advances in Radiation Biology:** edited by J. T. Lett, U. K. Ehmann and A. B. Cox. Orlando, Florida., Academic Press, Inc. **11**: pp 330.

Blakely, E. A., C. A. Tobias, et al. (1979). "Inactivation of Human Kidney Cells by High-Energy Monoenergetic Heavy-Ion Beams." Radiat. Res. **80**: 122-160.

Blocher, D. (1982). "DNA Double Strand Breaks in Ehrlich Ascites Tumor Cells at Low Doses of X-Rays. I. Determination of Induced Breaks by Centrifugation at Reduced Speed." Int.J.Radiat.Biol. **42**: 317-328.

Blocher, D. (1988). "DNA Double-Strand Break Repair Determines the RBE of α-Particles." Int.J.Radiat. Biol. **54**: 761-771.

Blocher, D., M. Einspenner, et al. (1989). "CHEF Electrophoresis, a Sensitive Technique for the Determination of DNA Double-Strand Breaks." Int.J.Radiat.Biol. **56**: 437-448.

Bluenerd, M., D. L. Hendrie, et al. (1976). "Response of Pilot U Scintillator to Heavy Ions." Nucl. Instrum. Meth. **136**: 137-177

Bocian, E., S. Pszona, et al. (1973). "Dose-Response Curve for Chromosome Aberrations in Human Lymphocytes Irradiated with 7.4 Mev Protons *in vitro*." studia biophysica **39**: 167-176.

Booth, N. E. (1987). "Quasiparticles Trapping and the Quasiparticle Multiplier." Appl.Phys.Lett. **50**: 293-295.

Booth, N. E. (1988). "Superconducting Detectors for Nuclear Physics, Particle Physics and Astrophysics, **In: Superconductive Particle Detectors**; edited by A. Barone, Singapore. World Scientific Publications: pp 18-37.

Booth, N. E. and D. Goldie (1996). "Superconductor Particle Detectors." Supercond.Sci.Technol. **9**: 493-516.

Booz, J. and Feinendegen, L. (1988). "A Microdosimetric Understanding of Low Dose Radiation Effects." Int.J.Radiat.Biol. **53**: 13-21.

Bradford, J. N. (1978). "Heavy Ion Radiation Effects in VLSI." Report; Deputy for Electronic technology (RADC/ESR), Hanscom AFB, Massachusetts **01731**.

Bradley, M. O. and K. W. Kohn (1979). "X-ray Induced DNA Double-Strand Break Production and Repair in Mammalian Cells as Measured by Neutral Filter Elution." Nucleic Acid Res., **7**: 793-804.

Brannen, E., and Olde, G. (1962). "The Response of Organic Scintillators to Electron Energy Deposited in them." Radiat.Res. **16**: 1-6.

Bransome, E. D. (1970). **The Current Status of Liquid Scintillation Counting.** New York, Grune and Stratton.

Brooks, F. D. (1979). "Development of Organic Scintillators." Nucl.Instrum.Meth. **162**: 477--505.

Bross, A. D., and Pla-Dalmau, A. (1992). "Radiation Damage of Plastic Scintillators." IEEE Trans. Nucl. Sci. **39**: 1199-1204.

Bryant, P. (1988). "Use of Restriction Endonucleases to Study Relationships Between DNA Double-Strand-Breaks, Chromosomal Aberrations and Other End-Points in Mammalian Cells." Int.J.Radiat.Biol. **54**: 869-890.

Bryant, P. E. (1984). "Enzymatic Restriction of Mammalian Cell DNA Using Pvu II and Bam HI: Evidence for the Double-Strand Break Origin of Chromosome Aberrations." Int.J.J.Radiat.Biol. **46**: 57-65.

Burlin, T. E. (1974). "The Characteristics of Secondary Electron Emission and Some Potential Applications to Microdosimetry, **In: Proceedins of the Fourth Symposium on Microdosimetry**. Luxembourg; edited by J.Booz, R.Eickel and A.Walker. Published by CEC-DGSTIM; EUR 5122 d-e-f: pp 35-55.

Butts, J. J. and R. Katz (1967). "Theory of RBE Heavy Ion Bombardment of Dry Enzymes and Viruses." Radiat.Res. **30**: 855-871.

Caswell, R. S. (1966). "Deposition of Energy by Neutrons in Spherical Cavities." Radiat.Res. **27**: 92-107.

Cember, H. (1983). **Introduction to Health Physics** (2nd. Edition). Oxford, Pergamon Press.

Chadwick, K. H. and H. P. Leenhouts (1981). **The Molecular Theory of Radiation Biology.**. Heidelberg: Spriger-Verlag.

Charlton, D. E., Goodhead, D. T., Wilson, W. E., and Paretzke, H. G. (1985). "The Deposition of Energy in Small Cylindrical Targets by High LET Radiations." Radiat.Prot. Dosim. **13**: 123-125.

Charlton, D. E. and J. L. Humm (1988). "A Method of Calculating Initial DNA Strand Breakage Following the Decay of Incorporated ^{125}I." Int.J.Radiat.Biol. **53**: 353-356.

Chatterjee, A. and W. R. Holley (1990). "A General-Theory of DNA Strand Break Production By Direct and Indirect Effects." Radiat.Prot.Dosim. **31**: 241-247.

Chebotarev, V. Y. and A. N. Rekesh (1990). "Pulsed-Field Electrophoresis in the Investigation of Biological Macromolecules." Mol. Biol. **24**: 488-500.

Chen, C. Z. and D. E. Watt (1986). "Biophysical Mechanism of Radiation-Damage to Mammalian-Cells by X-rays and Gamma-Rays." Int.J.Radiat.Bilol. **49**: 131-142.

Chou, C. N. (1952). "Internal Absorption of Fluorescent Light in Large Plastic Scintillators." Phys.Rev. **87**: 376-377.

Christensen, R. C. and C. A. Tobias (1972). "Heavy-ion-induced Single- and Double-Strand Breaks in ϕX-174 Replicative for DNA." Int. J. Radiat. Biol. **22**: 457-477.

CINDA (1992). **The Index to Literature and Computer Files on Microscopic Neutrons Data.** Vienna, IAEA.

Coggle, J. E. (1983). **Biological Effects of Radiation.** London, Taylor and Francis.

Colautti, P., G. Talpo, et al. (1994). "Measurements of Ionization Distribution around a Particle Track at the Nanometer Level." Radiat.Prot.Dosim **52**: 329-334.

Cox, R. and W. K. Masson (1978). "Do Radiation-Induced Thioguanine-Resistant Mutants of Cultured Mammalian Cells Arise by HGPRT Gene Mutation or X-Chromosome Rearrangement?" Nature **276**: 629-630.

Cox, R. and W. K. Masson (1979). "Mutation and Inactivation of Cultured Mammalian Cells Exposed to Beams of Accelerated Ions. III. Human fibroblasts." Int.J.Radiat.Biol. **36**: 149-160.

Cox, R., J. Thacker, et al. (1977). "Inactivation and Mutation of Cultured Mammalian Cells by Aluminium Characteristic Ultrasoft X-rays. II.Dose-responses of Chinese Hamster and Human Diploid Cells to Aluminium X-rays and Radiations of Different LET." Int.Radiat.J.Biol. **31**: 561-576.

Cox, R., J. Thacker, et al. (1977). "Mutation and Inactivation of Mammalian Cells by various Ionising Radiation." Nature **267**: 425-427.

Crabb, D. G., J. G. McEwen, et al. (1967). "Detection Efficiency of Plastic Scintillation Counters for Neutrons in the Energy Range 20-130 MeV." Nucl. Instr. Meth. **48**: 87-92.

Craun, R. L., and Smith, D. L. (1970). "Analysis of Response Data for Several Organic Scintillators." Nucl.Instr.Meth. **80**: 239-244.

Cristiano, R., L. Esposito, et al. (1993). "Interaction of α-particles with Superconductive Nb/AlO_x/Nb Structure in Single Junction and Array Configurations." Fizika Nizkikh Temperatur **19**: 1065-1070.

Cucinotta, F. A., J. W. Wilson, et al. (1994). "Radiosensitivity Parameters for Lethal Mutagenesis in Caenorhabditis- Elegans." Radiat.Prot.Dosim. **52**: 25-27.

Cucinotta, F. A., J. W. Wislon, et al. (1995). "Effects of Track Structure and Cell Inactivation on the Calculation of Heavy Ion Mutation Rates in Mammalian Cells." Int.J.Radiat.Biol. **69**: 593-600.

D'Ambrosio, C., T. Gys, et al. (1994). "Photon Counting with Hybrid Photomultiplier Tube (HPMT)." Nucl.Instr.Meth. Phys.Res.A **338**: 389-397.

D'Ambrosio, C., T. Gys, et al. (1994). "Further Results on Photoelectron Counting with Small Diameter Scintillating Fibers." Nucl.Instr.Meth.Phys.Res.A **345**: 279-283.

Deering, R. A. and R. Rice (1962). "Heavy Ion Irradiation of HeLa Cells." Radiat.Res. **17**: 774-786.

Degtyarenko, P. V., E. A. Doroshkevitch, et al. (1985). "Response of a Plastic Scintillator Detector to Light Ions with Energies up to Hundreds of MeV." Nucl.Instrum.Meth.Phys.Res.A **239**: 527-528.

Doloy, M. T. (1991). "Dosimetry from Chromosome Aberration Counts in Blood Lymphocytes." Radiprotection **26, No.S1**: 171-184.

Duffrain, R. J., L. G. Littlefield, et al. (1979). "Human Cytogenetic Dosimetry: A Dose-Response Relationship for Alpha Radiation from ^{241}Am." Health Phys. **37**: 279.

Dufrain, R. J., G. L. Littlefield, et al. (1980). "*In vitro* Human Cytogenetic Dose Response system." Oak Ridge Assoc. Univ. Report 1-79-75-2: pp 357-374.

Edwards, A. A. (1994). "The Induction of Chromosomal Changes in Human And Rodent Cells by Accelerated Changed Particles: Early and Late Effects." CEC Progress Report, F13P-CT920064i.

Edwards, A. A., P. Finnon, et al. (1994). "The Effectiveness of High-Energy Neon Ions in Producing Chromosomal- Aberrations in Human-Lymphocytes." Radit.Prot.Dosim. **52**: 299-303.

Edwards, A. A., D. C. Lloyd, et al. (1985). "The Induction of Chromosome-Aberrations in Human-Lymphocytes by Accelerated Charged-Particles." Radit.Prot. Dosim. **13**: 205-209.

Edwards, A. A., D. C. Lloyd, et al. (1986). "Chromosome Aberrations Induced in Human Lymphocytes by 8.7 MeV Protons and 23.5 MeV Helium-3 Ions." Int.J.Radiat.Biol. **50**: 137-145.

Edwards, A. A., V. V. Moiseenko, et al. (1994). "Modeling of DNA Breaks and the Formation of Chromosome-Aberrations." Int. J.Radiat.Biol. **66**: 633-637.

Edwards, A. A., R. J. Purrott, et al. (1980). "The Induction of Chromosome Aberrations in Human Lymphocytes by Alpha-Radiation." Int. J. Radiat. Biol. **38**: 83-91.

Elkind, M. M. (1984). "Repair Processes in Radiation Biology." Radiat.Res. **100**: 425-449.

Elkind, M. M. and A. Han (1979). "Neoplastic Transformation and Dose Fractionation: Does Repair of Damage Play a Role?" Radiat. Res. **79**: 233-240.

Evans, H. C. and E. H. Bellamy (1959). "The Response of Plastic Scintillators to Protons." Proc. Phys. Soc. **74**: 483-385.

Fasman, G. D., Ed. (1976). **Handbook of Biochemistry and Molecular Biology. Vol.II**. New York, CRC.

Finnon, P., D. C. Lloyd, et al. (1995). "Fluorescence *in situ* Hybridization Detection of Chromosomal Aberrations in Human Lymphocytes: Applicability To Biological Dosimetry." Int.J.Radiat.Biol. **68**: 429-435.

Folkard, M., K. M. Prise, et al. (1996). "Inactivation of V79 by Low-Energy Protons, Deutrons and Helium-3 Ions." Int.J.Radiat.Biol. **69**: 729-738.

Folkard, M., K. M. Prise, et al. (1993). "Measurement of DNA Damage by Electrons with Energies Between 25 and 4000 eV." Int.J.Radiat.Biol. **64**: 651-658.

Forsberg, B. (1982). "Derivation of a Dose Mean Value of Lineal Energy from Variance Measurements of a Secondary Electron Emission Current." Nucl.Sci.Engin. **81**: 283-290.

Forsberg, B. J. and T. E. Burlin (1978). "Relations of Secondary Electrons Emission to Microdosimetry and Applications to Two-Target Theory." **In: Proceedings of the Sixth Symposium on Microdosimetry,** Brussels, Belgium; edited by J.Booz and H.G.Ebert. Harwood Academic Publisher, CEC EUR 6064 DE-EN-FR; pp 207-226.

Frankenberg, D., Frankenberg-Schwager, M., et al. (1981). "Evidence for DNA Double Strand Breaks as Critical Lesions in Yeast Cells Irradiated with Aparsely or Densely Ionizing Radiation Under Oxic or Anoxic Conditions." Radiat. Res. **88**: 524-532.

Frankenberg, D., M. Frankenberg-Schwager, et al. (1990). "The Contribution of OH* In Densely Ionizing Electron Track Ends or Particle Tracks to the Induction of DNA Double Strand Breaks." Radiat.Prot.Dosim. **31**(1-4): 249-252.

Frankenberg, D., H. Kuhn, et al. (1995). "0.3 keV Carbon-K Ultrasoft X-rays are Four Times More Effective than γ-rays When Inducing Oncogenic Cell Transformation at Low Doses." Int.J.Radiat.Biol. **68**: 593-601.

Frankenberg, D., C. Steinmetz, et al. (1997). "Yields of DNA Double -Strand Breaks in Human Skin Fibroblasts After Exposure to 18 MeV Electrons, 5 MeV Protons And 3 MeV α-Particles Using Calibrated PFGE." **In: Proceedings of the twelfth Symposium on Microdosimetry**, Oxford. (In Press).

Frankenberg-Schwager, M. (1989). "Review of Repair Kinetics for DNA Damage Induced in Eukaryotic Cells in Vitro by Ionizing Radiation." Radioth.Oncol. **14**: 307-320.

Geard, C. R. (1985). "Chromosomal Aberration Production by Track Segment Charged-Particles as a Function of Linear Energy-Transfer." Radiat.Prot.Dosim. **13**: 199-204.

Gettner, M. and W. Selove (1960). "Pulse Size from Neutrons of 0.14 to 2.3 MeV in Plastic Scintillators." Rev.Sci.Instrum. **31**: 450-451.

Goodhead, D. T. (1994). "Initial Events in Cellular Effects of Ionizing Radiations: Clustered Damage in DNA." Int.J.Radiat.Biol. **65**: 7-17.

Goodhead, D. T., M. Belli, et al. (1992). "Direct Comparison Between Protons and Alpha-Particles of the Same LET: I. Irradiation Methods and Inactivation of Asynchronous V79, HeLa and C3H10T1/2 Cells." Int. J. Radiat. Biol. **61**: 611-624.

Goodhead, D. T. and D. J. Brenner (1983). "Estimation of a Single Property of Low LET Radiations which Correlates with Biological Effectiveness." Phys. Med. Biol. **28**: 485-492.

Goodhead, D. T. and H. Nikjoo (1990). "Current Status of Ultrasoft X-rays and Track Structure-Analysis as Tools for Testing and Developing Biophysical Models of Radiation Action." Radiat.Prot. Dosim. **31**: 343-350.

Goodman, L.J. (1978). "W_N Computed from Recent Measurements of W for Charged Particles." **In: third Synposium on Neutron Dosimetry in Biology and Medicine;** edited by G.Burger and G.Ebert. CEC, EUR-5848.

Goulding, F. S. and B. G. Harvey (1975). "Identification of Nuclear Particles." Ann. Rev. Nucl. Sci. **25**: 167-240.

Gusten, H. and J. Mirsky (1989). "PMP, a Novel Scintillation Solute with a Large Shift." **In: Liquid Scintillation Counting and Organic Scintillators;** edited by H. Ross, J. E. Noakes, and J.D. Spaulding. Chelsea, Michigan., Lewis Publishers, Inc.: 1-7.

Gwin, R. and R. B. Murray (1963). "Scintillation Process in CsI(Tl). I. Comparison with Activator Saturation Model." Phys.Rev. **131**: 501-508.

Gwin, R. and R. B. Murray (1963). "Scintillation Process in CsI(Tl). II. Emission Spectra and Possible Role of Self-Trapped Holes." Phys.Rev. **131**: 508-512.

Hagen, U. (1994). "Mechanisms of Induction and Repair of DNA Double-Strand Breaks by Ionizing-Radiation - Some Contradictions." Radiat.Environ.Biophys. **33**(1): 45-61.

Hall, E. J. (1994). "Molecular Biology in Radiation Therapy: The Potential Impact of Recombinant Technology on Clinical Practice." Int.J.Radiat.Oncol.Biol.Phys. **30**: 1019-1028.

Hall, E. J. and R. C. Miller (1981). "The How and Why of *in vitro* Oncogenic Transformation." Radiat. Res. **87**: 208-223.

Hansen, T. and H. Hugh (1995). "NE102 Cocktail, and Specifications." private communications.

Harder, D. (1987). "Pairwise Lesion Interaction - Extension and Confirmation of The Lea's Model." **Proc. 8th International Congress Radiation Research,** Edinburgh; edited by Fielden, E.M. et al., Taylor and Francis. Vol.2: pp 318-324.

Harder, D. and E. Bartels (1992). "Restricted LET determine the yield of intratrack pairwise lesion interaction." **In: Radiation Research, Atwnticth-Century Perspective;** edited by W.C.Dewey, M. Edington, R.J.M. Fry, E.J. Hall and G.F. Whitmore..London Academic Press, Inc., pp 427-432.

Harder, D., P. Virsik-Peuckert, et al. (1992). "Theory of Pairwise Lesion Interaction." **In: Biophysical Modelling of Radiation Effects;** edited by K.H. Chadwick, G.Moschini, and M.N. Varma. Adam Hilger, Bristol: pp 179-184.

Harrah, L. A. and R. C. Powell (1971). "Dose Rate Saturation in Plastic Scintillators." **In: Organic Scintillator and Liquid Scintillation Counting;** edited by D. L. Horrocks and C.-T. Peng. London, Academic Press.

Heath, R. L., R. Hofstadler, et al. (1979). "Inorganic Scintillators. a Review of Techniques and Applications." Nucl.Instr.Meth. **162**: 431-476.

Hei, T. K., D. J. Chen, et al. (1988). "Mutation Induction by Charged Particles of Defined Linear Energy Transfer" Carcinogenesis **9**: 1233-1236.

Hei, T. K., E. J. Hall, et al. (1988). "Mutation Induction and Relative Biological Effectiveness of Neutrons in Mammalian Cells." Radiat.Res. **115**: 281-291.

Hei, T. K., K. Komatsu, et al. (1988). "Oncogenic Transformation by Charged Particles of Defined LET." Carcinogenesis **9**: 747-750.

Heilmann, J., H. Rink, et al. (1993). "DNA Strand Break Induction, Rejoining and Cellular Recovery in Mammalian Cells after Heavy Ion Irradiation." Radiat. Res. **135**: 46-55.

Heilmann, J., G. Taucher-Scholz, et al. (1995). "Induction of DNA Double-Strand Breaks in CHO-K1 Cells by Carbon Ions." Int.J.Radiat.Biol. **68**: 153-162.

Helbig, R., Z. Zdsienicka, et al. (1995). "The Effect of Deffective DNA Double-Strand-Break Repair on Mutations and Chromosome Aberrations in the Chinese Hamster Cell Mutant XR-V15B." Radiat.Res. **143**: 151-157.

Holl, I., E. Lorenz, et al. (1988). "A Measurement of the Light Yield of Common Inorganic Scintillators." IEEE Trans.Nucl.Sci. **35**: 105-109.

Holley, W. and A. Chatterjee (1996). "Clusters of DNA Damage Induced by Ionizing Radiation: Formation of Short Fragments. I. Theoretical Modeling." Radiat.Res. **145**: 188-199.

Holley, W. R., A. Chatterjee, et al. (1990). "Production of DNA Strand Breaks by Direct Effects of Heavy Charged Particles." Radiat.Res. **121**: 161-168.

Howard-Flanders, P. (1958). "Physical and Chemical Mechanisms in the Injury Of Cells by Ionizing Radiations." Adv.Biol. Med.Phys.: 553-603.

Hubbell, J. H. (1982). "Photon Mass Attenuation and Energy-Absorption Coefficients from 1 keV to 20 MeV." Int.J.Appl. Radiat.Isot. **33**: 1269-1290.

Hutchinson, F. (1987). "Chemical Changes Induced in DNA by Ionizing Radiation." Prog. Nucleic Acid Res. Mol. Biol. **32**: 115-154.

ICRP-23 (1978). Recommendations of the International Commission on Radiological Protection. Reference Man. Pergamon Press, Oxford. New York.

ICRP-60 (1990). Recommendations of the International Commission on Radiological Protection. Pergamon Press, New York.

ICRU-16 (1970). "Linear Energy Transfer." International Commission on Radiation Units and Measurements. Bathesda, Maryland.

ICRU-19 (1971). "Radiation Quantities and Units." International Commission on Radiation Units and Measurements, Bathesda, Maryland.

ICRU-26 (1977). "Neutron Dosimetry for Biology and Medicine." International Commission on Radiation Units and Measurements, Bathesda, Maryland.

ICRU-31 (1979). "Average Energy Required to Produce an Ion Pair." International Commission on Radiation Units and Measurements, Bathesda, Maryland.

ICRU-33 (1980). "Radiation Quantities and Units." International Commission on Radiation Units and Measurements, Bathesda, Maryland.

ICRU-36 (1983). "Microdosimetry." International Commission on Radiation Units and Measurements, Bathesda, Maryland.

ICRU-37 (1984). "Stopping Powers for Electrons and Positrons." International Commission on Radiation Units and Measurements, Bathesda, Maryland.

ICRU-49 (1993). "Stopping Powers and Ranges for Protons and Alpha Particles." International Commission on Radiation Units and Measurements, Bathesda, Maryland.

Ikpeme, S., M. Lobrich, et al. (1995). "Heavy-Ion-Induced DNA Double-Strand Breaks with Yeast as a Model System." Radiat.Environ.Biophys. **34**: 95-99.

Iliakis, G. (1991). "The Role of DNA Double Strand Breaks in Ionizing Radiation-Induced Killing of Eukaryotic Cells." Bioessays **13**: 641-648.

Iliakis, G., D. Blocher, et al. (1991). "Comparison of DNA Double-Strand Break Rejoining as Measured by Pulsed Field Gel-Electrophoresis, Neutral Sucrose Gradient Centrifugation and Non-Unwinding Filter Elution in Irradiated Plateau-Phase CHO Cells." Int. J.Radiat.Biol. **59**: 927-939.

Ilie, S., H. Schonbacher, et al. (1993). "Radiation-Damage Measurements on PVT-Based Plastic Scintillators." Nucl. Phys.B (Proc. Suppl.) **32**: 384-391.

Inokuti, M. (1983). "Radiation Physics as a Basis of Radiation Chemistry and Biology." **In: Applied Atomic Collision Physics** Vol-4; edited by S. Datz, London, Academic Press; pp 179-236.

Iskef, H., J. W. Cunningham, et al. (1983). "Projected Ranges and Effective Stopping Powers of Electrons with Energy Between 20 eV and 10 keV." Phys.Med.Biol. **28**: 535-545.

Jenner, T. J., M. Belli, et al. (1992). "Direct Comparison of Biological Effectiveness Of Protons and Alpha-Particles of the Same LET. III. Initial Yield of DNA Double-Strand Breaks in V79." Int.J.Radiat.Biol. **61**: 631-637.

Jenner, T. J., C. M. de Lara, et al. (1994). "The Induction of DNA Double Strand Breaks in V79-4 Cells by γ- and α-Radiations: Complexity of Damage." Radiat.Prot.Dosim. **52**: 289-293.

Jenner, T. J., C. M. deLara, et al. (1993). "Induction and Rejoining of DNA-Strand Breaks in V79-4 Mammalian Cells Following γ- and α-irradiation." Int.J.Radiat.Biol. **64**: 265-273.

Joosse, K., H. Nakagawa, et al. (1996). "High Quality Nb/Al-Alo_x/Nb Superconducting Tunnel Junctions for Radiation Detection." Appl.Phys.Lett. **68**: 702-704.

Kakati, S., J. R. Kowalczyk, et al. (1986). "Use of Radiation-Induced Chromosomal Damage in Human Lymphocytes as a Biological Dosimeter is Questionable." Cancer Genetics and Cytogenetics. **22**: 137-141.

Kampf, G. and K. Eichhorn (1983). "DNA Strand Breaks by Different Radiation Qualities and Relations to Cell Killing: Further Results after the Influence of α-particles And Carbon Ions." studia biophysica **93**: 17-26.

Katz, R., Sharma, S. C., and Homayoonfar, M. (1972). "Detection of Energetic Heavy Ions." Nucl. Instrum. Meth. **100**: 13-32.

Katz, R. (1993). "A Track Physics Retrospective." Radiat.Prot.Dosim. **47**: 65-68.

Katz, R. (1994). "Dose as a Damage Specifier in Radiobiology for Radiation Protection." Radiat.Res. **139**: 251-253.

Katz, R., B. Ackerson, et al. (1971). "Inactivation of Cells by Heavy Ion Bombardment." Radiat.Res. **47**: 402-425.

Katz, R., A. Cucinotta, et al. (1996). "The Calculation of Radial Dose from Heavy Ions: Predictions of Biological Action Cross-Sections." Nucl.Instrum.Meth.Phys.Res.B **107**: 287-291.

Katz, R., D. E. Dunn, et al. (1985). "Thindown in Radiobiology." Radiat.Prot.Dosim. **13**: 281-284.

Katz, R. and W. Hofmann (1982). "Biological Effects of Low Doses of Ionizing Radiations: Particle Tracks in Radiobiology." Nucl.Instrum.Meth. **203**: 433-442.

Katz, R. and E. J. Kobetich (1968). "Response of NaI(Tl) to Energetic Heavy Ions." Phys. Rev. **170**: 397-400.

Kellerer, A. M. (1975). "Criteria for the Applicability of LET." Radiat.Res. **63**: 226-234.

Kellerer, A. M., Rossi, H. H. (1978). "A Generalized Formulation of Dual Radiation Action." Radiat. Res. **75**: 471-488.

Kellerer, A. M. (1985). Fundamentals of Microdosimetry. **In: The Dosimetry of Ionizing Radiation**; edited by K.R. Kase, B. E. Bjarngard and F.H. Attix, New York, Academic Press. Vol.I: pp 77-162.

Kellerer, A. M. (1987). "Microdosimetry-recent Trends and Applications to Radiobiology and Radiation Chemistry." **In: Proceedings of the Eighth International Congress of Radiation Research; Edinburgh**; edited by E.M.Fielden , J.W.Fowler, J.H.Hendry and D.Scott. London: Taylor and Francis: pp 338-344.

Kellerer, A. M. and H. H. Rossi (1972). "The Theory of Dual Radiation Action." Current Top. Radiat.Res. Quarterly, **8**,: 85-158.

Kiefer, J. (1985). "Cellular and Subcellular Effects of Very Heavy Ions." Int.J.Radiat.Biol. **48**: 873-892.

Knoll, G. E. (1989). **Radiation Detection and Measurements.**, New York, John Wiley & Sons.
Kobetich, E. J. and R. Katz (1968). "Energy Deposition by Electron Beams and δ-rays." Phys.Rev. **170**: 391-396.

Kobetich, E. J. and R. KAtz (1968). "Width of Heavy-Ion Tracks in Emulsion." Phys.Rev. **170**: 405-411.

Kraft, G. (1987). "Radiobiological Effects of Very Heavy Ions: Inactivation, Induction of Chromosome Aberrations and Strand Breaks." Nucl. Sci. Applic. **3**: 1-28.

Kramer, M. and G. Karft (1991). "Heavy ion track structure calculations." **In: Biophysical Modelling of Radiation Effects**; edited by K.H. Chadwick, G.Moschini, and M.N. Varma, 61-68.

Kranert, T., E. Schneider, et al. (1990). "Mutation Induction in V79 Chinese Hamster Cells by very Heavy Ions." Int.J.Radiat. Biol. **58**: 975-987.

Kranert, T., U. Stoll, et al. (1992). "Mutation Induction in Mammalian Cells by Very Heavy Ions." Adv.Space Res. **12 (2-3)**: (2)111-(2)118.

Krasavin, E. A., K. G. Amirtayev, et al. (1989). "Role of DNA Repair Processes in the Biological Efficiency of Heavy Ions." studia biophyscia **133**: 25-31.

Kronenberg, A. (1991). "Perspective on Fast-Neutron Mutagenesis of Human Lymphobastoid Cells." Radiat.Res. **128**: S87-S93

Kronenberg, A. (1994). "Mutation-Induction in Human Lymphoid-Cells by Energetic Heavy-Ions." Adv.Space Res. **14 (10)**: 339-346.

Kronenberg, A. and J. B. Little (1989). "Locus Specificity for Mutation Induction in Human Cells Exposed to Accelerated Heavy Ions." Int.J.Radiat.Biol. **55**: 913-924.

Lea, D. E. (1955). **Actions of Radiations on Living Cells.**, London, Cambridge University Press.

Leutz, H. (1995). "Scintillating Fibers." Nucl.Instr.Meth.Phys.Res.A **364**: 422-448.

Lloyd, D. C., R. J. Purrott, et al. (1976). "Chromosome Aberrations Induced in Human by Neutron Irradiation." Int.J.Radiat.Biol. **29**: 169-182.

Lloyd, D. C., R. J. Purrott, et al. (1978). "Chromosome Aberrations Induced in Human Lymphocytes from ^{252}Cf." Int.J.Radiat.Biol. **34**: 177-186.

Lloyd, D. C., D. H. Reading, et al. (1978). "Expansion of a Negative pi-meson Peak to Cover a Range of Depths Useful for Radiotherapy." Brit. J. Radiol. **51**: 41-45.

Lobrich, M., S. Ikpeme, et al. (1993). "DNA Double-Strand Break Induction in Yeast by X-rays and α-Particles Measured By Pulsed-Field Gel Electrophoresis." Int.J.Radiat.Biol. **64**: 539-546.

Lobrich, M., S. Ikpeme, et al. (1993). "Analysis of the Inversion Effect in Pulsed Field Gel-Electrophoresis by a 2-Dimensional Contour-Clamped Homogeneous Electric-Field System." Analytical Biochemistry **208**: 65-73.

Lobrich, M., S. Ikpeme, et al. (1994). "DNA Double-Strand Break Measurement in Mammalian Cells by Pulsed-Field Gel Electrophoresis: An Approach Using Restriction Enzymes and Gene Probing." Int.J.Radiat.Biol. **65**: 623-630.

Lobrich, M., B. Rydeberg, et al. (1994). "DNA Double-Strand Breaks Induced by High-Energy Neon and Iron in Human Fibrobalsts. II. Probing Individual Noti Fragment By Hybridization." Radiat. Res. **139**: 142-151.

Luke, K. L. and M. G. Buehler (1988). "An Exact, Closed-Form Expression Of The Integral Chord-Length Distribution for the Calculation of Single-Event Upsets Induced by Cosmic Ray." J.Appl.Phys. **64**: 5132-5137.

Luntz, M. (1971). "Track-Effect theory of Scintillation Efficiency." Phys.Rev.B **4**: 2857-2868.

Luntz, M. and R. H. Bartram (1968). "Stopping Power and Luminescent-Response Calculations for Channeling in NaI(Tl) and CsI(Tl)." Phys.Rev. **175**: 468-476.

Luntz, M. and G. M. Heymsfield (1972). "Track-Effect account of Scintillation Efficiency for Random and Channeled Heavy Ions of Intermediate Velocities." Phys.Rev.B **6**: 2530-2536.

Madey, R., F. M. Waterman, et al. (1978). "The Response of NE-228A, NE-228, NE-224, and NE-102 Scintillators to Protons from 2.43 to 19.55 MeV." Nucl. Instr. Meth. **151**: 445-450.

Martin, C., E. Muton, et al. (1991). "Biological Dosimetry- Biochemical- and Cellular-Parameters." Radiprotection **26, No.S1**: 205-221.

McGilvery, R. W. and G. Goldstein (1979). **Biochemistry, A Functional Approach.** Philadelphia, Holt-Saunders Company.

McGinnes, R. T. (1959). "Energy Spectrum resulting from Electron Slowing Down" Circular 597, NBS Wahington DC,.

McNulty, P. J., Farrell, G. E., Wyatt, R. C., Rothwell, P. L., Filz, R. C., and Bradford, J. N. (1980). "Upset Phenomena Induced by Energetic Protons and Electrons." IEEE Trans. Nucl. Sci. **NS-27**: 1516-1522.

McParland, B. J. (1986). "The response of NE-102 plastic Scintillator to Stop He-3 Nuclei." Nucl.Instrum.Meth.Phys.Res.A **251**: 412-413.

Menchaca-Rocha, A., K. Michaelian, et al. (1993). "A New Look at Luminescence and Scintillation Detection." Revista Mexicana de Fisica **39,** Suppl.2: 182-189.

Mettler, F. A. and R. D. Mosleley (1985). **Medical Effects of Ionizing Radiation.** Orlando, Florida 32887, Grune & Stratton, Inc.

Meyer, A. and R. Murray (1962). "Effect of Energetic Secondary Electrons on the Scintillation Process." Phys.Rev. **128**: 98-105.

Michaelian, K. and A. Menchac-Rocha (1994). "Model of Ion-Induced Luminescence Based on Energy Deposition by Secondary Electrons." Phys. Rev. B **49**: 15550-15562.

Micke, U., G. Horneck, et al. (1994). "Double-Strand Breaks in the DNA of Bacillus-Subtilis Cells Irradiated by Heavy-Ions." Adv. Space Res. **14(10)**: 207-211.

Miller, R. C., C. R. Geard, et al. (1989). "Neutron-Energy-Dependent Oncogenic Transformation of C3H10T1/2 Mouse Cells." Radiat. Res. **117**: 114-127.

Miller, R. C., C. R. Geard, et al. (1995). "Neutron-Induced Cell-Dependent Oncogenic Transformation of C3H10T1/2 Cells." Radiat.Res. **142**: 270-275.

Miller, R. C., S. A. Marino, et al. (1995). "The Biological effectiveness of Radon-Progeny Alpha Particles. II. Oncogenic Transformation as a Function of Linear Energy Transfer." Radiat. Res. **142**: 54-60.

Mitchel, C. (1991). "Radiobiological Fundamental in Radioepodemiology and Radiation Protection." Sozil und Praventivmedizen. **36, No.4/5**: 225-229.

Miyajima, M., S. Sasaki, et al. (1993). "Numbers of Scintillation Photons Produced in NaI(Tl) and Plastic Scintillator by Gamma-rays." IEEE Trans.Nucl.Sci. **40**: 417-423.

Mnich, T. M., Diehl, S. E., Shafer, B. D., Koga, R., Kolasinski, W. A., and Ochara Jr., A. (1983). "Comparison of Analytical Models and Experimental Results for Single Event Upset in CMOS SRAMs." IEEE Trans. Nucl. Sci. **NS-30**: 4620-4623.

Mouatassim, S., G. J. Costa, et al. (1995). "The Light Yield Response of NE213 Organic Scintillators to Charged Particles Resulting from Neutron Interactions." Nucl.Instrum.Meth.Phys.Res.A **359**: 530-536.

Mozumder, A., and Magge, J. L. (1966). "Model of Tracks of Ionizing Radiations for Radical Reaction Mechanisms." Radiat. Res. **28**: 203-214.

Muga, L., A. Clem, et al. (1974). "Luminescence Response of Thin Plastic Scintillator Detectors to Fission Fragments from Proton-Induced Fission of ^{232}Th, ^{235}U, and ^{238}U." Nucl.Instr. Meth. **119**: 255-260.

Muga, L. and M. Diksic (1974). "Refined Model of Luminescence Production in Plastic Scintillators." Nucl.Instr.Meth. **122**: 553-558.

Muga, L. and G. Grifith (1974). "Specific Luminescence Studies in Plastic Scintillators." Phys. Rev. B **9**: 3639-3649.

Muga, M. L. (1971). "A Versatile dE/dx Detector for Heavy Mass Nuclear Particles." Nucl. Instr. and Meth. **95**: 349-359.

Munson, R. J., D. A. Bance, et al. (1979). "Mutation and Inactivation of Cultured Mammalian Cells Exposed to Beams of Accelerated Ions. I. Irradiation facilities and methods." Int.J.Radiat.Biol. **36**: 127-136.

Murray, R. B. (1962). "Scintillation Counters." **Nuclear Instruments and Their Uses.** A. H. Snell. London, John Wiley: 82-165

Nakamura, N., S. Umeki, et al. (1991). "Evaluation of Four Somatic Mutation Assays for Biological Dosimetry of Radiation-Exposed People Including Atomic Bomb Survivor." **In: New Horizon in Biological Dosimetry**; edited by B.L. Gledhill and F. Mauro. John Wiley, New York: pp 341-350.

NCRP-63 (1979). "Tritium and Other Labeled Organic Compounds Incorporated in Genetic Material." National Council on Radiation Protection and Measurements, Bethesda, MD.

NCRP-116 (1993). "Limitation of exposure to ionizing radiation." National Council on Radiation Protection and Measurements Bethesda, Maryland.

Neary, G. J. (1965). "Chromosome Aberrations and the Theory of RBE. 1.General Considerations." Int.J.Radiat.Biol. **9**: 477-502.

Neary, G. J. (1970). "The Influence of Radiation Quality and Oxygen on Strand Breaks in Dry DNA." Int.J.Radiat.Biol. **18**: 25-40.

Neary, G. J., V. J. Horgan, et al. (1972). "Further Data on DNA Strand Breakage by Various Radiation Qualities." Int.J.Radiat. Biol. **22**: 525-537.

NE Technology (1995). **Plastic Liquid and Crystal Scintillators, Technical Data.** Edinburgh.

Newman, E. and F. E. Steigert (1960). "Response of NaI(Tl) to Energetic Heavy Ions." Phys. Rev. **118**: 1575-1578.

Nikjoo, H., D. T. Goodhead, et al. (1991). "Energy Deposition in Small Cylindrical Targets by Monoenergetic Electrons." Int.J.Radiat.Biol. **60**: 739-756.

Nikjoo, H., M. Terrissol, et al. (1994). "Comparison of Energy Deposition in Small Cylindrical Volumes by Electrons Generated by Monte-Carlo Track Structure Codes for Gaseous and Liquid Water." Radiat.Prot.Dosim. **52**: 165-169.

Oleinick, N. L., U. Balasubramaniam, et al. (1994). "Nuclear-Structure and the Microdistribution of Radiation-Damage in DNA." Int.J.Radiat.Biol. **66**: 523-529.

Oleinick, N. L. and S. M. Chiu (1994). "Nuclear and Chromatin Structures and Their Influence on the Radiosensitivity of DNA." Radiat.Prot.Dosim. **52**: 353-358.

O'Rielly, G. V., N. R. Kolb, et al. (1996). "The Response of plastic scintillator to Protons and Deutrons." Nucl.Instrum.meth. Phys.Res.A **368**: 745-749.

Painter, T. B. and B. R. Young (1980). "Radiosensitivity in Ataxia Telangiectasia: A New Explanation." Proc.Natl.Acad.Sci.USA **77**: 7315-7317.

Paul, J. M. (1971). "The Density Effect and Rate of Energy Loss in Common Plastic Scintillators." Nucl. Instr. Meth. **96**: 51-59

Pinak, M. and A. Ito (1993). "Energy Deposition in Structural Parts of DNA by Monoenergetic Electrons." J.Radiat.Res. **34**: 221-234.

Platzman, R. (1967). "Energy Spectrum of Primary Activation in the Action of Ionizing Radiation." In: Radiation Research, Proc. 3rd. Int. Congress. Contina d'Ampezzo, Italy, 20-42.

Prescott, J. R. and A. S. Rupaal (1961). "The Specific Fluorescence of Plastic Scintillator NE 102." Can. J. Phys. **39**: 221-227.

Prise, K. M., Davies, S., and Micheal B. D. (1989). "Cell Killing and DNA Damage in Chinese Hamster V79 Cells Treated with Hydrogen Peroxide." Int.J.Radiat.Biol. **55**: 583-592.

Prise, K. M., Davies, S., and Micheal, B. D. (1989). "An Improved Method for the Treatment of Data from DNA Strand Break Measurements Using Filter Elution Techniques with an Internal Standard." Int.J.Radiat.Biol. **55**: 323-330.

Prise, K. M., S. Davies, et al. (1987). "The Relationship Between Radiation-Induced DNA Double-Strand Breaks and Cell Kill in Hamster V79 Fibroblasts Irradiated with 250 kVp X-rays, 2.3 MeV Neutrons or ^{238}Pu α-particles." Int.J.Radait.Biol. **52**: 893-902.

Prise, K. M., M. Folkard, et al. (1990). "The irradiation of V79 Mammalian cells by Protons with Energies Below 2 MeV. Part II. Measurement of Oxygen Enhancement Ratios and DNA Damage." Int.J.Radiat.Biol. **58**: 261-277.

Prise, K. M., M. Folkard, et al. (1989). "Measurement of DNA Damage and Cell killing in Chinese Hamster V79 cells Irradiated with Aluminum Characteristic Ultrasoft X-rays." Radiat. Res. **117**: 489-499.

Puck, T. (1960). "The Action of Radiation on Mammalian Cells." Am. Naturalist **94**: 95-109.

Puck, T. and P. Marcus (1956). "Action of X-rays on Mammalian Cells." J.Experim. Med. **103**: 653-666.

Radford, I. R. (1988). "The Dose-Response for Low-LET Radiation-Induced DNA Double-Strand Breakage: Methods of Measurement and Implications for Radiation Action Models." Int.J.Radiat.Biol. **54**: 1-11.

Rando, N., P. Videler, et al. (1995). "Transmission Electron Microscopy and Atomic Force Microscopy Analysis of Nb-Al-AlO_x-Nb superconducting tunnel junctions detectors." J.Appl.Phys. **77**: 4099-4106.

Raven, P. H. and G. B. Johnson (1988). **Understanding Biology.** St.Louis, Time Mirror/Mosby College Publishing.

Rebourgeard, P., Blumenfeld, H., H., and Bourdinaud, M. (1989). "A simple Method for Measuring the Performance of Plastic Scintillating Material." IEEE Trans. Nucl. Sci. **36**: 150-157.

Rimpl, G. R., E. Schmid, et al. (1990). "Chromosome Aberrations Induced in Human Lymphocytes by 16.5 MeV Protons." Int.J.Radiat.Biol. **58**: 999-1007.

Ritter, M. A., J. E. Cleaver, et al. (1977). "High-LET Radiations Induce a Large Proportion of Non-rejoining DNA Breaks." Nature **266**: 653-655.

Ritter, S., W. Kraft-Weyrather, et al. (1992). "Induction of Chromosome Aberrations in Mammalian Cells After Heavy Ions Exposure." Adv. Space Res. **12(2-3)**: (2)119-(2)125.

Roberts, G. G., P. S. Vincett, et al. (1981). "Technological Applications of Langmuir-Blodgett films." Physics Technology **12**: 69-87.

Roots, R., A. Chatterjee, et al. (1985). "Characterization of Hydroxyl Radical-Induced Damage after Sparsely and Densely Ionizing Irradiation." Int.J.RAdiat.Biol. **47**: 157-166.

Roots, R., W. Holley, et al. (1990). "The Formation of Strand Breaks in DNA after High-LET Irradiation: A Comparison of Data from *in vitro* and Cellular Systems." Int.J.Radiat.Biol. **58**: 55-69.

Rydberg, B. (1985). "DNA Strand Breaks Induced by Low-Energy Heavy Ions." Int.J. Radiat.Biol. **47, No.1**: 57-61.

Rydberg, B. (1994). "Regionally Multiply Damaged Sites: Experimental Evidence. **In: International Workshop on Radiation Damage in DNA: Relationship at Early Times**; edited by J.D.Zimrick, A.F. Fuciarellai, J.H. Miller." .

Rydberg, B. (1996). "Clusters of DNA Damage Induced by Ionizing Radiation: Formation of Short Fragments. II. Experimental detection." Radiat.Res. **145**: 200-209.

Rydberg, B., M. Lobrich, et al. (1994). "DNA Double-Strand Breaks Induced by High-energy Neon and Iron Ions in Human Fibrobasts. I. Pulsed-field Gel Electrophoresis." Radiat.Res. **139**: 133-144.

Salamon, M. H. and S. P. Ahlen (1981). "NaI(Tl) Response to Relativistic Ne, Ar, and Fe Ions." Phys.Rev.B **24**: 5026-5036.

Samuni, A. and G. Czapski (1981). "Radiation Induced Damage in Escheirchia Coli B: The Effect of Superoxide Radicals and Molecular Oxygen." Radiat.Res. **76**: 624-632.

Sankaranarayanan, K. (1991). "Ionizing radiation and genetic risks. II. Nature of Radiation-induced Mutations in Experimental Mammalian *in vivo* Systems." Mutation Res. **258**: 51-73.

Sankaranarayanan, K. (1991). "Ionizing radiation and genetic risks. III. Nature of Spontaneous and Radiation-Induced Mutation In Mammalian *in vitro* System and Mechanism of Induction of Mutation by Radiation." Mutation Res. **258**: 75-97.

Saraf, S. K., N. Al-Niemi, et al. (1988). "Determination of the Light Response of BC-404 Plastic Scintillator for ^{3}He and ^{4}He With Energies Between 3 to 13 MeV." Nucl.Instrum. Meth.Phys.Res.A **288**: 451-454.

Saraf, S. K., C. E. Brient, et al. (1988). "Determination of the Light Response of BC-404 Plastic Scintillator for Protons and Deutrons With Energies Between 1 to 11 MeV." Nucl. Instrum.Meth.Phys.Res.A **268**: 200-203.

Schafer, M., K. Facius, et al. (1980). "Contribution of ion-kill and δ-electrons to Inactivation Cross-sections of Bacillus Subtilis Spores Irradiated with Very Heavy Ions." **In: Proceedings of the Seventh Symposium on Microdosimetry,** Oxford; edited by J. Booz, H.D. Hartfield and H.G. Ebert . Harwood Academic Publisher; CEC EUR 7147 DE-EN-FR: pp 1331-1340.

Schafer, M., R. Facius, et al. (1994). "Inactivation of Individual Bacillus-Subtilis Spores In Dependence on Their Distance to Single Accelerated Heavy-Ions." Adv. Space Res. **14(10)**: 1039-1046.

Schafer, M., C. Schmitz, et al. (1994). "DNA Double-Strand Breaks Induced in Escherichia-Coli-Cells By Radiations of Different Quality." Radiat.Prot. Dosim. **52**: 233-236.

Schafer, M., C. Schmitz, et al. (1994). "Heavy-Ion-Induced DNA Double-Strand Breaks in Cells of Escherichia-Coli." Adv. Space Res. **14(10)**: 203-206.

Seelentag, W. W., W. Panzer, et al. (1979). "A Catalogue of Spectra for the Calibration of Dosimeters." GSF Bericht **560**: 409-422 (GSF, Munich).

Shapiro, J. (1981). **Radiation Protection: A Guide for Scientific and Physicians** (2nd Edition)., Harvard Uni. Press, London.

Siddiqi, M. A. and F. Bothe (1987). "Single- and Double-Strand Break Formation in DNA Irradiated in Aqueous Solution: Dependence on the Dose and OH Radical Scavenger Concentration." Radiat.Res. **112**: 449-463.

Simmons, J. A. (1992). "Absorbed Dose- an Irrelevant Concept for Irradiation with Heavy Charged Particles." J. Radiol. Prot. **12**: 173-179.

Simmons, J. A., P. Cohn, et al. (1983). "Sensitivity of Lung Cells to Alpha Particle Irradiation." In: Proceedings of the Seventh International Congress of Radiation Research. Biology.: B7-27.

Simmons, J. A., P. Cohn, et al. (1996). "Survival and Yields of Chromosomes Aberrations in Hamster and Human Lung Cells Irradiated by Alpha Particles." Radiat.Res. **145**: 174-180.

Simmons, J. A. and D.E.Watt (1997). **Radiation Protection- a Radical Reappraisal.**, Medical Physics Publishers.

Sinclair, W. K. (1995). "Radiation Protection Recommendations on Dose Limits:The Role of the NCRP and the ICRP and Future Developments." Int.J.Radiat.Oncol.Biol.Phys. **31**: 387-392.

Skarsgard, L. D., B. A. Kihlman, et al. (1967). "Survival, Chromosome Abnormalities, and Recovery in Heavy Ion- and X--Irradiated Mammalian cells." Radiat.Res. **Suppl. 7**: 208-221.

Smith, D. L., Polk, R. G., and Miller, T. G. (1968). "Measurement of the Response of Several Organic Scintillators to Electrons, Protons and Deutrons." Nucl. Instr. Meth. **64**: 157-166.

Sonntag, W., G. Knedlitschek, et al. (1990). "The DNA content of some mammalian cells measured by flow cytometry and its infuence on radiation sensitivity." Int. J. Radiat. Biol. **57**: 1183-1193.

Stanton, J., G. Taucher-Scholz, et al. (1993). "Protection of DNA from High LET Radiation by Two OH Radical Scavengers, Tris (Hydroxymethyl) Amino-methane and 2-Mercaptoethanol." Radiat. Environ. Biophys. **32**: 21-32.

Stanton, J., G. Taucherscholz, et al. (1990). "Comparison Between Indirect and Direct Effects for High and Low Let Radiations in SV40 DNA Strand Break Induction." Radiat.Prot.Dosim. **31**: 253-256.

Stein, G. S., J. L. Stein, et al. (1996). "The Maturation of a Cell." Amer.ican Scientific **84**: 28-37.

Steinbauer, E. and O. Benka (1988). "Detection of Low Energy X-rays in Coincidence Measurements Using the Organic Scintillator NE102A." Nucl. Instr. Meth. Phys. Res.A **272**: 834-839.

Stoll, U., B. Barth, et al. (1996). "HPRT Mutations in V79 Chinese Hamster Cells Induced by Accelarated Ni, Au and Pb Ions." Int.J.Radiat.Biol. **70**: 15-22.

Stoll, U., A. Schmidt, et al. (1995). "Killing and Mutation of Chinese Hamster V79 Cells exposed to Accelerated Oxygen and Neon Ions." Radiat. Res. **142**: 288-294.

Stoll, U., E. Schneider, et al. (1995). "Induction of HPRT(-) Mutants in Chinese-Hamster V79 Cells After Heavy-Ion Exposure." Radiat.Environ.Biophys. **34**(2): 91-94.

Storm, E. and H. Isreal (1970). "Photon Cross Sections from 1 keV to 100 MeV for Elements from z=1 to z=100." Nucl.Data Tables **A7**: 565.

Swank, R. K. (1954). "Characteristics of Scintillators." Ann.Rev.Nucl.Sci. **4**: 111-140.

Sze, S. M. (1981). **Physics of Semiconductor Devices**. 2nd ed., John Wiely.

Takatsuji, T. (1984). "Dose-Effect Relationship of Chromosome Aberrations Induced by 23 MeV Alpha Particles in Human Lymphocytes." Int.J.Radiat.Biol. **45**: 237-243.

Taucher-Scholz, G., J. Heilmann, et al. (1996). "Induction and Rejoining of DNA Double-Strand Breaks In CHO Cells After Heavy-Ion Irradiation." Adv. Space Res. **18(1-2)**: 83-92.

Taucher-Scholz, G., J. Heilmann, et al. (1996). "Induction of DNA Strand Breaks by Heavy Ions." Nucl.Instrum.Meth.Phys.,Res.B **107**: 318-322.

Taucher-Scholz, G., J. Heilmann, et al. (1995). "Detection of Heavy-Ion-Induced DNA Double-Strand Breaks Using Static- Field Gel-Electrophoresis." Radiat.Environ.Biophysi. **34**: 101-106.

Thacker, J., A. Stretch, et al. (1979). "Mutation and Inactivation of Cultured Mammalian Cells Exposed to Beams of Accelerated Ions. II. Chinese Hamster V79 Cells." Int.J.Radiat.Biol. **36**: 137-148.

Thacker, J., R. E. Wilkinson, et al. (1986). "The Induction of Chromosome Exchange Aberrations by Carbon Ultrasoft X-rays in V79 Hamster Cells." Int.J.Radiat.Biol. **49**: 645-656.

Thornton, S. T. and J. R. Smith (1971). "Measurements and Calculations of Neutron Detector Efficiencies." Nucl.Instrum.Meth. **96**: 551-555.

Todd, P. (1965). "Reversible and Irreversible Effects of Densely Ionizing Radiations upon the Reproductive Capacity of Cultured Human Cells." Medical College of Virginia Quarterly. **1**: 2-14.

Todd, P. (1967). "Heavy-ion Irradiation of Cultured Human Cells." Radiat. Res. **Suppl. 7**: 196-207.

Todd, P. (1968). "Fractionated Heavy Ion Irrdaiation of Cultured Human Cells." Radiat. Res. **34**: 378-389.

Todd, P. W. (1975). "Heavy-ion Irradiation of Human and Chinese Cells in *vitro*." Radiat. Res. **61**: 288-297.

Todd, P. W., J. T. Lyman, et al. (1968). "Dosimetry and Apparatus for Heavy Ion Irradiation of Mammalian Cells *in vitro*." Radiat. Res. **34**: 1-23.

Todorov, S. L. (1975). "Radiation-induced Chromosome Aberrations in Human Peripheral Lymphocytes. Exposure to X-rays or Protons." Strahlentherapie **149**: 197-204.

Tubiana, M., J. Dutreix, et al. (1990). **Introduction to Radiobiology.**. London, Taylor and Francis.

Tung, C. J. and P. J. Chen (1983). "Energy Loss and Range Straggling for Electrons in Water." **In: Proceedings of the Eighth Symposium on Microdosimetry,** GmbH Jülich, Germany; edited by J. Booz and H.G. Ebert. Harwood Academic Publishers; ECE EUR 8395 EN: pp 243-254.

Turner, J. E. (1986). **Atoms, Radiation, and Radiation Protection.** New York, Pergamon Press.

Turro, N. J. (1978). **Modern Molecular Photochemistry**. Menlo Park, California, Benjamin/Cummings Pub. Co.

UNSCEAR (1988). "Sources, Effects and Risks of Ionizing Radiation,." United Nations Scientific Committee on the Effects of Atomic Radiation (UNSCEAR), #E.88.IX.7. New York: United Nations.

van Geest, L. K. and K. W. J. Stoop (1991). "Hybrid Phototube with Si Target." Nucl.Instr.Meth.Phys.Res.A **310**: 261-266.

Varma, M. N., V. P. Bond, et al. (1993). "Hit-size Effectiveness Approach in Radiation Protection." J.Radiol.Prot. **13,No.4**: 243-258.

Verhaegen, F. and A. Vral (1994). "Micronucleus Induction in Human-Lymphocytes to Low-LET Radiation Qualities, RBE and Correlation of RBE and LET." Radiat.Res. **139**: 208-213.

Viovy, J. L., T. Duke, et al. (1992). "The Physics of DNA Electrophoresis." Contemporary Phys. **33**: 25-40.

Voltz, R., J. Lopes Da Silva, et al. (1966). "Influence of the Nature of Ionizing Particles on the Specific Luminescence of Organic Scintillators." J.Chem.Phys. **45**: 3306-3311.

von Sonntag, C. (1987). **The Chemical Basis of Radiation Biology.** London, Taylor & Francis.

Walker, J. (1969). "Characteristics of Plastic Scintillators in their use as Large Area Particle Detectors." Nucl. Instrum. Meth. **68**: 131-134.

Wallace, S. (1994). "DNA Damages Processed by Base Excision-Repair - Biological Consequences." Int. J.Radiat. Biol. **66**: 579-589.

Ward, J. E. (1988). "DNA Damage Produced by Ionizing Radiation in Mammalian Cells: Identities, Mechanisms of Formation and Repairability." Prog.Nucleic Acids Mol.Biol. **35**: 95-125.

Ward, J. E. (1990). "The Yield of DNA Double-Strand Breaks Produced Itracellularly by Ionizing Radiation" Int.J.Radiat.Biol. **57**: 1141-1150.

Ward, J. F. (1985). "Biochemistryof DNA Lesions." Radiat.Res. **104**: S103-S111.

Ward, J. F. (1986). "Mechanisms of DNA Repair and their Potential Modification for Radiotherapy." Int.J.Radiat.Biol.Phys. **12**: 1027-1032.

Ward, J. F. (1994). "The Complexity Of DNA-Damage - Relevance to Biological Consequences." Int.J.Radiat.Biol. **66**: 427-432

Ward, J. F. (1995). "Radiation Mutagenesis: The Initial DNA Lesions Responsible." Radiat.Res. **142**: 362-368.

Ward, J. F., G. D. D. Jones, et al. (1994). "Biological Consequences of Nonhomogeneous Energy Deposition by Ionizing-Radiation." Radiation Protection Dosimetry **52**: 271-276.

Watt, D. E. (1989). "An Approach Towards a Unified Theory of Damage to Mammalian- Cells by Ionizing-Radiation for Absolute Dosimetry." Radiat.Prot. Dosim. **27**: 73-84.

Watt, D. E. (1989). "On Absolute Biological Effectiveness and Unified Dosimetry." J. Radiol. Prot. **9**: 33-49.

Watt, D. E. (1994). "Heavy-Particle Track Structure Parameters for Biophysical Modeling." Nucl.Instrum. Meth. Phys. Res.B **93**: 215-221.

Watt, D. E. (1994). Track Structure Data for Ionizing Radiations in Liquid Water. Part 2: Heavy Charged Particles; 100 eV/A to 1GeV/A. St-Andrews., Univ. of St-Andrews.

Watt, D. E. (1995). Track Structure Data for Ionizing Radiations in Liquid Water. Part 1: Electrons and Photons. St-Andrews., Univ. of St-Andrews.

Watt, D. E. (1995). Track Structure Data for Ionizing Radiations in Liquid Water. Part 3: Neutrons; 0.5 keV - 100 MeV. St-Andrews., Univ. of St-Andrews.

Watt, D. E. (1996). **Quantities for Dosimetry of Ionizing Radiation in Liquid Water**. London, Taylor and Francis.

Watt, D. E., I. A. M. Alaffan, et al. (1985). "Identification of Biophysical Mechanisms of Damage By Ionizing- Radiation." Radiat. Prot.Dosim. **13**: 1-4.

Watt, D. E. and A. S. Alkharam (1994). "Charged-Particle Track Structure Parameters For Application in Radiation Biology and Radiation-Chemistry." Int.J. Quantum Chem. **(S21)**: 195-207.

Watt, D. E. and A. S. Alkharam (1995). "A Feasibility Study Of Scintillator Microdosimeters for Measurement of the Biological Effectiveness of Ionizing- Radiations." Radiat.Prot.Dosim. **61**: 1-3.

Watt, D. E., A. S. Alkharam, et al. (1994). "Dose as a Damage Specifier in Radiobiology for Radiation Protection." Radiat.Res. **139**: 249-251.

Watt, D. E. and S. J. A. Hill (1994). "An Empirical-Model for the Induction of Double-Strand Breaks in DNA By the Indirect Action of Ionizing-Radiation." Radiat. Prot.Dosim. **52**: 1-4.

Weir, H. G., J. N. Lucas, et al. (1991). "Two-Color Hybridization With High Complexity Chromosome-Specific Probes And a Degenerate Alpha Satellite Probe DNA Allows Unambiguous Discrimination Between Symmetrical and Asymetrical Translocations." Chromosoma **100**: 371-376.

Wick, K., Paul, D., Schroder, P., Stieber, V., and Bicken, B. (1991). "Recovery and Dose Rate Dependence of Radiation Damage in Scintillators, Wavelength Shifters and Light Guids." Nucl. Instr. and Meth. Phys. Res.B **61**: 472-486.

Wiel, J. T. and T. Hegge (1989). Advances in Scintillation Cocktails. In: Liquid Scintillation Counting and Organic Scintillators, editted by Harley Ross, John E. Noakes, and Jim D. Spaulding, LEWIS PUBLISHING, Inc. 51-67.

Wilson, W. E., and Paretzke, H. G. (1981). "Calculation of Distributions for Energy Imparted and Ionization by Fast Protons in Nanometer Sites." Radiat. Res. **87**: 521-537.

Wishart, L.P., R. Plattner, et al. (1967). "Detector For Neutron Time-of-Flight Spectrometry with Improved Response to Low Energy Neutrons." Nucl.Instrum.Meth. **57**: 237-244.

Wolf, S. (1991). "Biological Dosimetry with Cytogenetic Endpoints." **In: New Horizon in Biological Dosimetry;** edited by B.L. Gledhill and F. Mauro. John Wiley, New York.: pp 351-362.

Wolfgang, J. R. (1956). "Scintillation Detectors." **In: Radiation Dosimetry;** edited by G. L. Hine and G. L. Brownell; pp246-297.

Wright, G. T. (1953). "Scintillation Response of Organic Phosphors." Phys.Rev. **91**: 1282-1283.

Wulf, H., W. Kraft-Weyrather, et al. (1985). "Heavy-ion Effects on Mammalian Cells: Inactivation Measurements with Different Cell Lines." Radiat. Res. **134**: S122-S134.

Yang, T. C. and C. A. Tobias (1985). "Mechanism of Radiation-Induced Neoplastic Cell Transformation." In: Proc. of the Berkeley Conf. in honor of Jersy Neyman and J.Kiefer. Vol.1, editors L.M.Lecam, and R.A.Olshen, Wadworth Inc.: pp 343-371

Yang, T. C, L. Craise, et al. (1985). "Neoplastic Cell Transformation by Heavy Charged Particles." Radiat.Res. **104**: S177-S187.

Zirkle, R. E., D. F. Marchbank, et al. (1952). "Exponential and Sigmoid Survival Curves Resulting from Alpha and X-irradiation of Aspergillus Spores." J.Cell.Comp.Physiol. **Suppl.1**: 75-85.

Zorn, C., S. Majewski, et al. (1990). "Preliminary study of Radiation Damage in Liquid Scintillators." IEEE Trans.Nucl.Sci. **37**: 487-491.

Zorn, C. (1990). "Studies in the Radiation Resistance of Plastic Scintillators; Review and Prospects." IEEE Trans.Nucl.Sci. **37**: 504-512.

AI-Established Cell Lines Abbreviations

Common Mammalian Cell Lines

	Cell Line	Derived From
1	Caski	Human Squamous Carcinoma
2	HCLC	Human Chang Liver Cells
3	HF19	Human Lung Fibroblasts
4	HSF	Human Skin Fibroblasts
5	HeLa	Human cervix carcinoma (Helen Lane)
6	IMR-90	Normal Human Lung Fibrobalsts
7	AG1522	Normal Human Skin Fibroblasts
8	A_l	Human-Hamster Hybrid Cells
9	T1	Human Kidney Cells
10	TK6	Human Lymphoblasts
11	GM38A	Primary Human Skin Fibrobalsts
12	EATC	Ehrlich Ascites Tumor Cells
13	L5178Y	Mouse Lymphocytes Leukemia
14	C3H10T1/2	Mouse Embryo
15	MEF	Normal Mouse Embryo Fibroblasts
16	P388F	Mouse Lymphoma Cells
17	3T3	Mouse Fibroblast Cells
18	R-1	Rat Rhadomyosarcoma Tumor
19	9L-21	Rat Brain Gliosarcoma
20	V79	Chinese Hamster Lung Fibroblasts
21	M3-1	Chinese Hamster Femoral Bone Marrow
22	HS23	Hamster Skin Fibroblasts
23	BA14FAF28	Peritoneul Hamster Cells
24	CHO	Chinese Hamster Ovary
25	SHE	Syrian Hamster Embryo
26	GHE	Primary Golden Hamster Embryo
27	BLEC	Bovine Lens Epithelial Cells

Common Fungus, Bacteria cells

1	BSS	Bacillus Subtilis Spores
2	E-Coli	Escherichia coli
3	Yeast d-211	Saccharomyces cerevisiae

Common Viruses

1	SV40	Simian Virus (Papova virus)
2	T1	Bacteriophage
3	ϕx-174	Virus

Common Enzymes

1		Lysozyme
2		Trypsin
3		DNAs

AII Inactivation of Mammalian Cells

All-1 Charged Particles on Hamster Cells

Cells (Types/Lines)	$\alpha(Gy^{-1})$	$\beta(Gy^{-2})$	Ions	E/m (keV/amu)	E(MeV)	$E_{m,a}$(keV)	$R_{m,a}$(μm)	R_β(μm)	L_T(keV/μm)	$L_{100,T}$(keV/μm)	β^2	z^{*2}/β^2	λ(nm)	σ(μm²)	Reference
V79-753B	1.71E-01		p	4.00E+01	4.00E-02	8.71E-02	3.61E-03	8.84E-01	7.23E+01	7.23E+01	8.52E-05	6.38E+03	1.13E+00	1.98E+00	Belli, 1993
V79-753B	3.67E-01		p	2.60E+02	2.60E-01	5.66E-01	3.12E-02	3.95E+00	5.89E+01	3.48E+01	5.54E-04	1.77E+03	2.10E+00	3.46E+00	Belli, 1993
V79-753B	5.36E-01		p	6.40E+02	6.40E-01	1.39E+00	1.07E-01	1.26E+01	3.62E+01	2.08E+01	1.36E-03	7.34E+02	4.67E+00	3.11E+00	Belli, 1993
V79-379A	1.03E+00		p	7.60E+02	7.60E-01	1.66E+00	1.37E-01	1.63E+01	3.19E+01	1.81E+01	1.62E-03	6.18E+02	5.68E+00	5.25E+01	Prise, 1990
V79-753B	7.44E-01		p	7.60E+02	7.60E-01	1.66E+00	1.37E-01	1.63E+01	3.19E+01	1.81E+01	1.62E-03	6.18E+02	5.68E+00	3.79E+00	Belli, 1993
V79	3.00E-02		p	7.60E+02	7.60E-01	1.66E+00	1.37E-01	1.63E+01	3.19E+01	1.81E+01	1.62E-03	6.18E+02	5.68E+00	1.53E-01	Folkard, 1989
V79-753B	8.03E-01		p	7.70E+02	7.70E-01	1.68E+00	1.40E-01	1.66E+01	3.17E+01	1.78E+01	1.64E-03	6.10E+02	5.72E+00	4.07E+00	Belli, 1989
V79-379A	7.40E-01	1.10E-02	p	1.07E+03	1.07E+00	2.29E+00	2.44E-01	2.74E+01	2.53E+01	1.41E+01	2.28E-03	4.39E+02	7.97E+00	2.99E+00	Folkard, 1996
V79-753B	9.38E-01		p	1.10E+03	1.10E+00	2.40E+00	2.38E-01	2.86E+01	2.51E+01	1.40E+01	2.34E-03	4.28E+02	8.08E+00	3.76E+00	Belli, 1989
V79	3.30E-01	6.60E-02	p	1.15E+03	1.15E+00	2.51E+00	2.55E-01	3.07E+01	2.47E+01	1.38E+01	2.45E-03	4.09E+02	8.26E+00	1.30E+00	Folkard, 1989
V79-379A	3.30E-01	6.60E-02	p	1.15E+03	1.15E+00	2.51E+00	2.55E-01	3.07E+01	2.47E+01	1.38E+01	2.45E-03	4.09E+02	8.26E+00	1.30E+00	Prise, 1990
V79	3.00E-01	5.20E-02	p	1.16E+03	1.16E+00	2.53E+00	2.58E-01	3.11E+01	2.36E+01	1.32E+01	2.47E-03	4.05E+02	8.70E+00	1.13E+00	Goodhead, 1992
V79	4.20E-01	1.90E-02	p	1.38E+03	1.38E+00	3.01E+00	3.37E-01	4.10E+01	2.14E+01	1.18E+01	2.93E-03	3.41E+02	1.01E+01	1.43E+00	Goodhead, 1992
V79-753B	4.71E-01	4.40E-02	p	1.41E+03	1.41E+00	3.07E+00	3.49E-01	4.25E+01	2.12E+01	1.17E+01	3.00E-03	3.34E+02	1.02E+01	1.60E+00	Belli,1993
V79-753B	5.86E-01	3.70E-02	p	1.65E+03	1.65E+00	3.60E+00	4.47E-01	5.48E+01	1.85E+01	1.01E+01	3.51E-03	2.85E+02	1.24E+01	1.73E+00	Belli, 1989
V79-379A	4.50E-01	2.80E-02	p	1.83E+03	1.83E+00	4.13E+00	5.38E-01	6.50E+01	1.78E+01	9.74E+00	3.89E-03	2.57E+02	1.31E+01	1.28E+00	Folkard, 1996
V79	1.30E-01	7.80E-02	p	1.90E+03	1.90E+00	4.14E+00	5.59E-01	6.92E+01	1.68E+01	9.19E+00	4.04E-03	2.48E+02	1.41E+01	3.50E-01	Folkard, 1989
V79-379A	3.50E-01	4.50E-02	p	1.90E+03	1.90E+00	4.14E+00	5.59E-01	6.92E+01	1.68E+01	9.19E+00	4.04E-03	2.48E+02	1.41E+01	9.41E-01	Prise, 1990
V79	4.30E-01		p	3.00E+03	3.00E+00	6.54E+00	1.19E+00	1.49E+02	1.19E+01	6.44E+00	6.36E-03	1.57E+02	2.22E+01	8.21E-01	Perris, 1986
V79-753B	3.72E-01	3.60E-02	p	3.20E+03	3.20E+00	6.98E+00	1.32E+00	1.66E+02	1.17E+01	6.27E+00	6.78E-03	1.47E+02	2.29E+01	6.94E-01	Belli,1993
V79-379A	3.20E-01	3.90E-02	p	3.66E+03	3.66E+00	7.79E+00	1.63E+00	2.09E+02	1.06E+01	5.69E+00	7.75E-03	1.29E+02	2.59E+01	5.43E-01	Folkard, 1996
V79	2.10E-01	2.30E-02	p	7.40E+03	7.40E+00	1.62E+01	5.91E+00	7.16E+02	5.87E+00	3.10E+00	1.56E-02	6.42E+01	5.48E+01	1.97E-01	Perris, 1986
V79-WNRE	1.36E-01	3.40E-02	p	7.00E+04	7.00E+01	1.62E+02	3.22E+02	3.98E+04	9.63E-01	5.11E-01	1.35E-01	7.79E+00	4.46E+02	2.10E-02	Wouters, 1996
V79 (B-11-dii FAF28)	1.43E-01		p	9.00E+04	9.00E+01	2.05E+02	4.67E+02	6.37E+04	8.05E-01	4.22E-01	1.67E-01	5.98E+00	5.69E+02	1.84E-02	Wainson, 1972
V79 (Attached)	1.27E-01		p	1.60E+05	1.60E+02	3.78E+02	1.19E+03	1.78E+05	5.29E-01	2.77E-01	2.70E-01	3.70E+00	9.22E+02	1.07E-02	Hall, 1978
V79 (Suspended)	2.03E-01		p	1.60E+05	1.60E+02	3.78E+02	1.19E+03	1.78E+05	5.29E-01	2.77E-01	2.70E-01	3.70E+00	9.22E+02	1.72E-02	Hall, 1978
V79-379A	1.23E+00		D	4.65E+02	9.30E-01	1.01E+00	6.86E-02	1.62E+01	4.29E+01	2.50E+01	9.91E-04	1.01E+03	3.58E+00	8.44E+00	Folkard, 1996
V79-379A	1.10E+00		D	7.00E+02	1.40E+00	1.60E+00	1.23E-01	2.88E+01	3.40E+01	1.94E+01	1.49E-03	6.71E+02	5.16E+00	5.98E+00	Folkard, 1996
V79-753B	6.55E-01		D	8.19E+02	1.64E+00	1.78E+00	1.53E-01	3.63E+01	3.11E+01	1.76E+01	1.74E-03	5.73E+02	5.90E+00	3.26E+00	Belli, 1994
V79-753B	5.29E-01		D	1.03E+03	2.06E+00	2.25E+00	2.16E-01	5.18E+01	2.66E+01	1.49E+01	2.19E-03	4.55E+02	7.40E+00	2.25E+00	Belli, 1994
V79-379A	7.60E-01	1.30E-02	D	1.07E+03	2.14E+00	2.29E+00	2.31E-01	5.48E+01	2.53E+01	1.41E+01	2.28E-03	4.39E+02	7.98E+00	3.08E+00	Folkard, 1996
V79-379A	4.30E-01	5.50E-02	D	1.70E+03	3.40E+00	3.76E+00	4.60E-01	1.15E+02	1.83E+01	1.00E+01	3.62E-03	2.77E+02	1.26E+01	1.26E+00	Folkard, 1996
V79-753B	2.80E-01	3.30E-02	D	1.77E+03	3.53E+00	3.85E+00	4.98E-01	1.23E+02	1.80E+01	9.87E+00	3.76E-03	2.66E+02	1.28E+01	8.06E-01	Belli, 1994

Cells (Types/Lines)	$\alpha(Gy^{-1})$	$\beta(Gy^{-2})$	Ions	E/m (keV/amu)	E(MeV)	$E_{m,d}$(keV)	$R_{m,d}$(μm)	R_i(μm)	L_T(keV/μm)	$L_{100,T}$(keV/μm)	β^2	z^{*2}/β^2	λ(nm)	σ(μm²)	Reference
V79/4	2.33E-01		D	2.25E+03	4.50E+00	4.91E+00	7.36E-01	1.83E+02	1.51E+01	8.23E+00	4.78E-03	2.09E+02	1.62E+01	5.64E-01	Tolkendorf, 1983
M3-1	3.20E-01		D	6.60E+03	1.32E+01	1.44E+01	4.80E+00	1.17E+03	6.43E+00	3.40E+00	1.39E-02	7.16E+01	4.89E+01	3.29E-01	Todd, 1975
V79/4	1.87E-01		D	1.00E+05	1.25E+01	2.29E+02	5.59E+02	1.07E+03	6.86E+00	3.63E+00	1.33E-02	7.54E+01	4.51E+01	2.06E-01	Tolkendorf, 1983
V79-379A	1.33E+00		He-3	1.13E+03	3.39E+00	2.51E+00	2.71E-01	2.47E+01	9.60E+01	5.42E+01	2.41E-03	1.66E+03	2.11E+00	2.04E+01	Folkard, 1996
V79-379A	1.44E+00		He-3	1.39E+03	4.18E+00	3.15E+00	3.53E-01	3.37E+01	8.16E+01	4.60E+01	2.97E-03	1.35E+03	2.62E+00	1.88E+01	Folkard, 1996
V79	9.01E-01		He-3	2.27E+03	6.80E+00	4.94E+00	7.45E-01	7.27E+01	5.80E+01	3.20E+01	4.82E-03	8.29E+02	4.19E+00	8.36E+00	Cherubini, 1994
V79-379A	1.24E+00		He-3	2.30E+03	6.90E+00	5.19E+00	8.22E-01	7.44E+01	5.79E+01	3.19E+01	4.89E-03	8.17E+02	4.22E+00	1.15E+01	Folkard, 1996
V79	7.64E-01		He-3	2.73E+03	8.20E+00	5.96E+00	1.01E+00	9.89E+01	5.15E+01	2.80E+01	5.81E-03	6.80E+02	4.87E+00	6.30E+00	Cherubini, 1994
V79	7.40E-01		He-3	3.10E+03	9.30E+00	6.76E+00	1.25E+00	1.22E+02	4.60E+01	2.48E+01	6.59E-03	6.07E+02	5.81E+00	5.45E+00	Cherubini, 1994
V79	6.82E-01		He-3	3.67E+03	1.10E+01	8.00E+00	1.67E+00	1.62E+02	4.10E+01	2.22E+01	7.79E-03	5.14E+02	6.69E+00	4.47E+00	Cherubini, 1994
V79/4	2.91E+00		He-4	4.50E+02	1.80E+00	9.80E-01	6.50E-02	1.22E+01	1.58E+02	8.93E+01	1.17E-03	3.37E+03	1.04E+00	7.34E+01	Tolkendorf, 1983
V79	1.61E+00		α	5.13E+02	2.05E+00	1.12E+00	7.79E-02	1.14E+01	1.63E+02	9.25E+01	1.10E-03	3.57E+03	9.91E-01	4.20E+01	Kranert, 1992
V79	4.32E-01		He-4	6.00E+02	2.40E+00	1.31E+00	9.73E-02	1.37E+01	1.50E+02	8.30E+01	1.29E-03	3.08E+03	1.15E+00	1.04E+01	Cherubini, 1994
V79-4	1.20E+00		α	6.25E+02	2.50E+00	1.36E+00	1.03E-01	1.43E+01	1.46E+02	8.26E+01	1.34E-03	2.96E+03	1.17E+00	2.80E+01	Thacker, 1982
V79-379A	8.18E-01	6.51E-02	α	7.50E+02	3.00E+00	1.63E+00	1.34E-01	1.81E+01	1.27E+02	7.21E+01	1.61E-03	2.48E+03	1.43E+00	1.67E+01	Prise, 1987
V79	2.06E+00		α	7.50E+02	3.00E+00	1.63E+00	1.34E-01	1.81E+01	1.27E+02	7.21E+01	1.60E-03	2.48E+03	1.43E+00	4.20E+01	Kranert, 1988
CHO-10B	1.32E+00		α	7.90E+02	3.16E+00	1.72E+00	1.45E-01	1.94E+01	1.25E+02	7.08E+01	1.69E-03	2.36E+03	1.46E+00	2.63E+01	Raju, 1991
V79	1.10E+00		α	7.90E+02	3.16E+00	1.72E+00	1.45E-01	1.94E+01	1.25E+02	7.08E+01	1.69E-03	2.36E+03	1.46E+00	2.20E+01	Raju, 1991
V79-4	1.45E+00		α	8.28E+02	3.31E+00	1.80E+00	1.55E-01	2.06E+01	1.18E+02	6.69E+01	1.77E-03	2.25E+03	1.58E+00	2.74E+01	Jenner, 1993
V79-379A	1.31E+00		α	9.50E+02	3.80E+00	2.07E+00	1.91E-01	2.50E+01	1.08E+02	6.12E+01	2.04E-03	1.96E+03	1.79E+00	2.27E+01	Prise, 1990
V79	1.31E+00		α	9.73E+02	3.89E+00	2.12E+00	1.97E-01	2.58E+01	1.07E+02	6.07E+01	2.08E-03	1.92E+03	1.81E+00	2.25E+01	Folkard, 1989
V79	8.27E-01		He-4	1.03E+03	4.10E+00	2.23E+00	2.14E-01	2.79E+01	1.04E+02	5.95E+01	2.20E-03	1.82E+03	1.86E+00	1.38E+01	Cherubini, 1994
V79	1.33E+00		α	1.04E+03	4.14E+00	2.26E+00	2.17E-01	2.83E+01	1.02E+02	5.72E+01	2.22E-03	1.80E+03	1.95E+00	2.17E+01	Min, 1986 / Simmons, 1996
V79/4	1.23E+00		He-4	1.05E+03	4.20E+00	2.29E+00	2.22E-01	3.10E+01	9.87E+01	5.56E+01	2.36E-03	1.69E+03	2.04E+00	1.94E+01	Tolkendorf, 1983
V79	1.59E+00		α	1.30E+03	5.20E+00	2.83E+00	3.07E-01	3.97E+01	8.95E+01	5.02E+01	2.78E-03	1.44E+03	2.34E+00	2.28E+01	Hall, 1972
V79	1.15E+00		α	1.34E+03	5.37E+00	2.93E+00	3.23E-01	4.17E+01	8.43E+01	4.75E+01	2.87E-03	1.39E+03	2.52E+00	1.55E+01	Schlag, 1981
V79	1.29E+00	7.00E-02	He-4	1.48E+03	5.90E+00	3.21E+00	3.74E-01	4.83E+01	7.84E+01	4.39E+01	3.16E-03	1.27E+03	2.79E+00	1.62E+01	Munson, 1979
V79	1.76E+00		He-4	1.50E+03	6.00E+00	3.27E+00	3.84E-01	4.96E+01	7.80E+01	4.36E+01	3.21E-03	1.25E+03	2.81E+00	2.20E+01	Kranert, 1990
V79	6.25E-01		He-4	1.63E+03	6.50E+00	3.54E+00	4.36E-01	5.63E+01	7.40E+01	4.20E+01	3.48E-03	1.15E+03	2.93E+00	7.40E+00	Cherubini, 1994
V79	9.61E-01	9.70E-02	He-4	1.85E+03	7.40E+00	4.03E+00	5.36E-01	6.92E+01	6.67E+01	3.69E+01	3.96E-03	1.01E+03	3.50E+00	1.03E+01	Munson, 1979
V79	5.39E-01		α	1.90E+03	7.60E+00	4.14E+00	5.59E-01	7.22E+01	6.61E+01	3.66E+01	4.06E-03	9.84E+02	3.54E+00	5.70E+00	Wulf, 1985
V79	1.41E+00		He-4	1.90E+03	7.60E+00	4.14E+00	5.59E-01	7.22E+01	6.61E+01	3.66E+01	4.06E-03	9.84E+02	3.54E+00	1.49E+01	Kranert, 1990
V79	6.29E-01		He-4	2.33E+03	9.30E+00	5.07E+00	7.76E-01	1.00E+02	5.70E+01	3.10E+01	4.97E-03	8.05E+02	4.30E+00	5.73E+00	Cherubini, 1994

Cells (Types/Lines)	$\alpha(Gy^{-1})$	$\beta(Gy^{-2})$	Ions	E/m (keV/amu)	E(MeV)	$E_{m,s}$(keV)	$R_{m,s}$(μm)	R_i(μm)	L_T(keV/μm)	$L_{100,T}$(keV/μm)	β^2	z^{*2}/β^2	λ(nm)	$\sigma(\mu m^2)$	Reference
V79-379A	6.49E-01	4.10E-03	He-4	2.50E+03	1.00E+01	5.45E+00	8.75E-01	1.13E+02	5.50E+01	3.01E+01	5.34E-03	7.49E+02	4.55E+00	5.71E+00	Stehenlow, 1994
V79	6.15E-01		He-4	2.60E+03	1.04E+01	5.67E+00	9.33E-01	1.31E+02	5.15E+01	2.78E+01	5.82E-03	6.87E+02	5.03E+00	5.07E+00	Cherubini, 1994
V79	9.82E-01		He-4	2.90E+03	1.16E+01	6.32E+00	1.12E+00	1.45E+02	4.90E+01	2.71E+01	6.19E-03	6.46E+02	5.19E+00	7.70E+00	Kranert, 1990
V79	9.33E-01	2.45E-02	He-4	2.93E+03	1.17E+01	6.38E+00	1.14E+00	1.47E+02	4.76E+01	2.59E+01	6.25E-03	6.40E+02	5.52E+00	7.10E+00	Munson, 1979
V79/4	6.04E-01		He-4	2.93E+03	1.17E+01	6.38E+00	1.14E+00	1.45E+02	4.98E+01	2.71E+01	6.20E-03	6.45E+02	5.19E+00	4.81E+00	Tolkendorf, 1983
V79	7.43E-01		α	3.50E+03	1.40E+01	7.64E+00	1.54E+00	1.99E+02	4.25E+01	2.30E+01	7.47E-03	5.36E+02	6.38E+00	5.06E+00	Wulf, 1985
V79	4.56E-01		α	4.40E+03	1.76E+01	9.60E+00	2.28E+00	2.94E+02	3.57E+01	1.92E+01	9.38E-03	4.27E+02	8.02E+00	2.60E+00	Wulf, 1985
V79	4.86E-01		He-4	4.50E+03	1.80E+01	9.82E+00	2.37E+00	3.06E+02	3.53E+01	1.90E+01	9.59E-03	4.17E+02	8.11E+00	2.75E+00	Kraft, 1982
V79/4	4.33E-01		He-4	4.88E+03	1.95E+01	1.06E+01	2.76E+00	3.54E+02	3.27E+01	1.75E+01	1.04E-02	3.83E+02	8.96E+00	2.27E+00	Tolkendorf
V79	7.87E-01		He-4	6.10E+03	2.44E+01	1.33E+01	4.16E+00	5.18E+02	2.74E+01	1.46E+01	1.30E-02	3.09E+02	1.12E+01	3.45E+00	Kranert, 1990
V79	5.49E-01	4.20E-02	He-4	6.10E+03	2.44E+01	1.33E+01	4.16E+00	5.18E+02	2.74E+01	1.46E+01	1.30E-02	3.09E+02	1.12E+01	2.41E+00	Munson, 1979
M3-1	4.58E-01		He-4	6.58E+03	2.63E+01	1.44E+01	4.77E+00	5.91E+02	2.54E+01	1.35E+01	1.40E-02	2.87E+02	1.23E+01	1.86E+00	Todd, 1975
V79	2.10E-01	4.70E-02	α	7.60E+03	3.04E+01	1.66E+01	6.20E+00	7.62E+02	2.29E+01	1.22E+01	1.61E-02	2.48E+02	1.40E+01	7.70E-01	Goodhead, 1992
V79	5.43E-01		He-4	8.70E+03	3.48E+01	1.90E+01	7.91E+00	9.68E+02	2.07E+01	1.10E+01	1.84E-02	2.17E+02	1.58E+01	1.80E+00	Kranert, 1990
V79	4.91E-01	1.80E-02	He-4	8.73E+03	3.49E+01	1.91E+01	7.95E+00	9.73E+02	2.07E+01	1.10E+01	1.85E-02	2.17E+02	1.58E+01	1.63E+00	Munson, 1979
V79	6.88E-01		α	8.80E+03	3.52E+01	1.93E+01	8.08E+00	9.89E+02	2.06E+01	1.10E+01	1.86E-02	2.15E+02	1.59E+01	2.27E+00	Wulf, 1985
V79	2.50E-01	4.30E-02	α	8.80E+03	3.52E+01	1.93E+01	8.08E+00	9.89E+02	2.06E+01	1.10E+01	1.86E-02	2.15E+02	1.59E+01	8.25E-01	Goodhead, 1992
V79-SH1	1.83E-01		He-4	9.93E+03	3.97E+01	2.17E+01	1.00E+01	1.22E+03	1.98E+01	9.94E+00	2.10E-02	1.91E+02	1.79E+01	5.80E-01	Bird,1975
M3-1	6.71E-01		Li-7	6.59E+03	4.61E+01	1.44E+01	4.78E+00	4.59E+02	6.02E+01	3.17E+01	1.40E-02	6.44E+02	5.20E+00	6.47E+00	Todd, 1975
V79-SH1	2.41E-01		Li-7	9.85E+03	6.90E+01	2.16E+01	9.89E+00	9.30E+02	4.27E+01	2.23E+01	2.08E-02	4.33E+02	7.96E+00	1.64E+00	Bird,1975
V79	1.32E+00		B-10	4.98E+03	4.98E+01	1.09E+01	2.67E+00	1.80E+02	2.14E+02	1.13E+02	9.64E-03	2.51E+03	1.36E+00	4.50E+01	Kranert, 1990
V79	1.12E+00	1.90E-01	B-10	4.98E+03	4.98E+01	1.09E+01	2.67E+00	1.62E+02	2.00E+02	1.06E+02	1.06E-02	2.30E+03	1.49E+00	3.58E+01	Munson, 1979
M3-1	5.61E-01		B-11	6.58E+03	7.24E+01	1.44E+01	4.78E+00	2.79E+02	1.64E+02	8.64E+01	1.40E-02	1.77E+03	1.91E+00	1.47E+01	Todd, 1975
V79-SH1	4.11E-01		B-11	9.17E+03	1.01E+02	2.01E+01	8.70E+00	4.85E+02	1.27E+02	6.61E+01	1.94E-02	1.28E+03	2.65E+00	8.32E+00	Bird,1975
V79	7.40E-01	1.40E-01	B-10	1.07E+04	1.07E+02	2.34E+01	1.15E+01	5.74E+02	1.10E+02	5.71E+01	2.26E-02	1.10E+03	3.16E+00	1.30E+01	R.Munson, 1979
V79	1.08E+00		B-10	1.07E+04	1.07E+02	2.34E+01	1.15E+01	6.31E+02	1.18E+02	6.17E+01	2.06E-02	1.21E+03	2.88E+00	2.04E+01	Kranert, 1990
V79	5.81E-01		C-12	2.40E+03	2.88E+01	5.23E+00	8.18E-01	4.98E+01	4.48E+02	2.42E+02	5.13E-02	6.08E+03	5.61E-01	4.17E+01	Wulf, 1985
V79/4	4.58E-01		C-12	3.47E+03	4.17E+01	7.58E+00	1.52E+00	8.29E+01	3.51E+02	1.87E+02	7.42E-03	4.47E+03	7.90E-01	2.57E+01	Tolkendorf, 1983
V79	7.73E-01		C-12	3.90E+03	4.68E+01	8.51E+00	1.85E+00	9.81E+01	3.26E+02	1.73E+02	8.32E-03	4.02E+03	8.73E-01	4.03E+01	Wulf, 1985
V79	7.70E-01		C-12	4.10E+03	4.92E+01	8.95E+00	2.02E+00	1.06E+02	3.21E+02	1.70E+02	8.75E-03	3.87E+03	8.92E-01	3.95E+01	Wulf, 1985
V79	8.32E-01		C-12	5.20E+03	6.24E+01	1.14E+01	3.11E+00	1.51E+02	2.74E+02	1.44E+02	1.11E-02	3.13E+03	1.10E+00	3.64E+01	Wulf, 1985
V79	6.96E-01		C-12	5.70E+03	6.84E+01	1.25E+01	3.68E+00	1.74E+02	2.54E+02	1.34E+02	1.21E-02	2.87E+03	1.21E+00	2.83E+01	Wulf, 1985
V79	9.27E-01		C-12	6.10E+03	7.32E+01	1.33E+01	4.16E+00	1.94E+02	2.48E+02	1.31E+02	1.30E-02	2.70E+03	1.25E+00	3.68E+01	Wulf, 1985

Cells (Types/Lines)	$\alpha(Gy^{-1})$	$\beta(Gy^{-2})$	Ions	E/m (keV/amu)	E(MeV)	$E_{m,s}$(keV)	$R_{m,s}$(μm)	R_i(μm)	L_T(keV/μm)	$L_{100,T}$(keV/μm)	β^2	z^{*2}/β^2	λ(nm)	σ(μm^2)	Reference
V79	5.81E-01		C-12	6.10E+03	7.32E+01	1.33E+01	4.16E+00	1.94E+02	2.48E+02	1.31E+02	1.30E-02	2.70E+03	1.25E+00	2.31E+01	Kraft, 1982
M3-1	5.48E-01		C-12	6.58E+03	7.90E+01	1.44E+01	4.77E+00	2.19E+02	2.31E+02	1.22E+02	1.40E-02	2.52E+03	1.36E+00	2.03E+01	Todd, 1975
V79	7.85E-01		C-12	7.60E+03	9.12E+01	1.66E+01	6.20E+00	2.76E+02	2.10E+02	1.10E+02	1.61E-02	2.20E+03	1.54E+00	2.64E+01	Wulf, 1985
V79	7.95E-01		C-12	8.70E+03	1.04E+02	1.90E+01	7.91E+00	3.45E+02	1.91E+02	9.97E+01	1.84E-02	1.93E+03	1.73E+00	2.43E+01	Wulf, 1985
V79-SH1	5.67E-01		C-12	8.93E+03	1.07E+02	1.95E+01	8.29E+00	3.60E+02	1.81E+02	9.46E+01	1.89E-02	1.88E+03	1.85E+00	1.64E+01	Bird,1975
V79	7.52E-01		C-12	9.90E+03	1.19E+02	2.17E+01	9.98E+00	4.27E+02	1.66E+02	8.67E+01	2.09E-02	1.71E+03	2.06E+00	2.00E+01	Wulf, 1985
V79	7.09E-01		C-12	3.19E+04	3.83E+02	7.07E+01	7.86E+01	1.91E+03	8.49E+01	4.40E+01	4.84E-02	7.43E+02	4.60E+00	9.63E+00	Lucke-Huttle, 1979
V79	3.96E-01		C-12	6.21E+04	7.45E+02	1.40E+02	2.47E+02	1.09E+04	4.01E+01	2.04E+01	1.21E-01	2.97E+02	1.13E+01	2.54E+00	Lucke-Huttle, 1979
V79	3.56E-01		C-12	8.75E+04	1.05E+03	1.99E+02	4.45E+02	2.03E+04	3.00E+01	1.56E+01	1.65E-01	2.19E+02	1.53E+01	1.71E+00	Lucke-Huttle, 1979
V79	1.78E-01		C-12	2.08E+05	2.50E+03	5.04E+02	1.78E+03	9.34E+04	1.60E+01	8.25E+00	3.32E-01	1.08E+02	3.19E+01	4.56E-01	Lucke-Huttle, 1979
V79	8.30E-01		N-14	3.70E+03	5.18E+01	8.07E+00	1.69E+00	8.26E+01	4.59E+02	2.45E+02	7.90E-03	5.59E+03	6.05E-01	6.10E+01	Kranert, 1990
V79	8.21E-01	-1.90E-02	N-14	3.70E+03	5.18E+01	8.07E+00	1.69E+00	8.26E+01	4.59E+02	2.45E+02	7.90E-03	5.59E+03	6.05E-01	6.03E+01	Munson, 1979
M3-1	9.01E-01		N-14	6.58E+03	9.21E+01	1.44E+01	4.77E+00	1.95E+02	3.16E+02	1.66E+02	1.40E-02	3.38E+03	9.97E-01	4.56E+01	Todd, 1975
V79	5.19E-01		O-16	5.60E+03	8.96E+01	1.22E+01	3.56E+00	1.39E+02	4.46E+02	2.35E+02	1.19E-02	5.00E+03	9.68E+00	3.70E+01	Wulf, 1985
V79	5.89E-01		O-16	5.60E+03	8.96E+01	1.22E+01	3.56E+00	1.39E+02	4.46E+02	2.35E+02	1.19E-02	5.00E+03	9.68E+00	4.20E+01	Wulf, 1985
M3-1	4.81E-01		O-16	6.58E+03	1.05E+02	1.44E+01	4.78E+00	1.77E+02	3.91E+02	2.05E+02	1.40E-02	4.34E+03	8.12E-01	3.01E+01	Todd, 1975
V79	9.00E-01		O-16	8.20E+03	1.31E+02	1.79E+01	7.11E+00	2.49E+02	3.47E+02	1.82E+02	1.74E-02	3.56E+03	9.43E-01	5.00E+01	Kranert, 1990
V79	8.63E-01		O-16	8.70E+03	1.39E+02	1.90E+01	7.91E+00	2.73E+02	3.26E+02	1.70E+02	1.84E-02	2.37E+03	1.02E+00	4.50E+01	Wulf, 1985
V79	8.44E-01		O-16	8.70E+03	1.39E+02	1.90E+01	7.91E+00	2.73E+02	3.26E+02	1.70E+02	1.84E-02	2.37E+03	1.02E+00	4.40E+01	Wulf, 1985
V79	1.02E+00		O-16	1.08E+04	1.73E+02	2.36E+01	1.16E+01	3.87E+02	2.76E+02	1.44E+02	2.28E-02	2.76E+02	1.26E+00	4.50E+01	Weber, 1993
V79	1.02E+00		O-16	1.08E+04	1.73E+02	2.37E+01	1.17E+01	3.87E+02	2.76E+02	1.44E+02	2.28E-02	2.76E+02	1.26E+00	4.50E+01	Weber, 1993
V79	2.39E-01		F-19	2.20E+03	4.18E+01	4.80E+00	7.09E-01	3.96E+01	8.99E+02	4.85E+02	4.71E-03	1.28E+04	2.77E-01	3.43E+01	Wulf, 1985
V79	3.53E-01		F-19	3.80E+03	7.22E+01	8.29E+00	1.77E+00	7.89E+01	6.97E+02	3.71E+02	8.11E-03	8.49E+03	4.02E-01	3.94E+01	Wulf, 1985
V79	4.99E-01		F-19	5.20E+03	9.88E+01	1.14E+01	3.11E+00	1.22E+02	5.74E+02	3.03E+02	1.11E-02	6.58E+03	5.24E-01	4.58E+01	Wulf, 1985
V79	5.24E-01		F-19	5.20E+03	9.88E+01	1.14E+01	3.11E+00	1.22E+02	5.74E+02	3.03E+02	1.11E-02	6.58E+03	5.24E-01	4.81E+01	Wulf, 1985
V79/4	3.67E-01		Ne-22	3.51E+03	7.01E+01	7.65E+00	1.54E+00	6.23E+01	9.05E+02	4.84E+02	6.81E-03	1.16E+04	2.98E-01	5.31E+01	Tolkendorf, 1983
V79-SH1	4.06E-01		Ne-20	6.18E+03	1.24E+02	1.35E+01	4.26E+00	1.38E+02	6.21E+02	3.27E+02	1.31E-02	6.90E+03	5.02E-01	4.04E+01	Bird, 1975
M3-1	3.70E-01		Ne-20	6.58E+03	1.32E+02	1.44E+01	4.77E+00	1.53E+02	6.08E+02	3.20E+02	1.39E-02	6.52E+03	5.16E-01	3.60E+01	Todd, 1975
V79	6.12E-01		Ne-20	8.90E+03	1.78E+02	1.95E+01	8.24E+00	2.41E+02	4.90E+02	2.56E+02	1.89E-02	5.03E+03	6.81E-01	4.80E+01	Kranert, 1990
V79	6.89E-01		Ne-20	9.80E+03	1.96E+02	2.15E+01	9.80E+00	2.80E+02	4.55E+02	2.38E+02	2.07E-02	4.62E+03	7.48E-01	5.02E+01	Kranert, 1992
V79	6.76E-01		Ne-20	1.20E+04	2.40E+02	2.63E+01	1.41E+01	3.86E+02	3.89E+02	2.02E+02	2.53E-02	3.84E+03	9.09E-01	4.20E+01	Kranert, 1990
V79	9.61E-01		Ne-20	1.40E+04	2.80E+02	3.07E+01	1.85E+01	4.96E+02	3.51E+02	1.83E+02	2.94E-02	3.33E+03	1.03E+00	5.40E+01	Weber, 1993
V79	9.61E-01		Ne-20	1.40E+04	2.80E+02	3.07E+01	1.85E+01	4.96E+02	3.51E+02	1.83E+02	2.94E-02	3.33E+03	1.03E+00	5.40E+01	Weber, 1993

Cells (Types/Lines)	$\alpha(Gy^{-1})$	$\beta(Gy^{-2})$	Ions	E/m (keV/amu)	E(MeV)	$E_{m,s}$(keV)	$R_{m,s}$(μm)	R_i(μm)	L_T(keV/μm)	$L_{100,T}$(keV/μm)	β^2	z^{*2}/β^2	λ(nm)	$\sigma(\mu m^2)$	Reference
V79	1.01E+00		Ne-20	1.48E+04	2.96E+02	3.25E+01	2.04E+01	5.44E+02	3.44E+02	1.79E+02	3.11E-02	3.16E+03	1.06E+00	5.54E+01	Kranert, 1992
V79	8.30E-01		Ne-20	3.10E+04	6.20E+02	6.86E+01	7.47E+01	1.93E+03	1.86E+02	9.63E+01	6.34E-02	1.57E+03	2.19E+00	2.46E+01	Ngo, 1981
CHO-SC1 & -tsH1	9.00E-01		Ne-20	3.10E+04	6.20E+02	6.86E+01	7.47E+01	1.93E+03	1.86E+02	9.63E+01	6.34E-02	1.57E+03	2.19E+00	2.67E+01	Chang, 1992
V79	8.26E-01		Ne-20	6.66E+04	1.33E+03	1.50E+02	2.79E+02	7.49E+03	9.98E+01	5.13E+01	1.29E-01	7.75E+02	4.54E+00	1.32E+01	Lucke-Huttle,1979
CHO-SC1 & -tsH1	1.01E+00	1.00E-02	Ne-20	6.75E+04	1.35E+03	1.52E+02	2.85E+02	7.67E+03	1.02E+02	5.23E+01	1.31E-01	7.66E+02	4.45E+00	1.65E+01	Chang, 1992
CHO-SC1 & -tsH1	8.60E-01	2.00E-02	Ne-20	9.03E+04	1.81E+03	2.06E+02	4.69E+02	1.29E+04	8.02E+01	4.17E+01	1.69E-01	5.92E+02	5.76E+00	1.10E+01	Chang, 1992
V79	1.99E-01		Ne-20	2.80E+05	5.60E+03	7.01E+02	2.78E+03	8.50E+04	3.80E+01	1.94E+01	3.96E-01	2.52E+02	1.39E+01	1.21E+00	Lucke-Huttle,1979
CHO-SC1 & -tsH1	3.30E-01	6.00E-02	Ne-20	3.88E+05	7.75E+03	1.02E+03	4.47E+03	1.55E+03	3.21E+01	1.62E+01	5.01E-01	2.00E+02	1.72E+01	1.70E+00	Chang, 1992
V79	1.27E-01		Ca-40	1.06E+04	4.24E+02	2.32E+01	1.13E+01	2.08E+02	1.47E+03	7.67E+02	2.24E-02	1.49E+04	2.35E-01	3.00E+01	Wulf, 1985
V79	2.29E-01		Ca-40	1.41E+04	5.64E+02	3.09E+01	1.88E+01	3.12E+02	1.26E+03	6.54E+02	2.96E-02	1.19E+04	2.88E-01	4.60E+01	Kranert, 1990
V79	7.55E-02		Ar-40	1.90E+03	7.60E+01	4.14E+00	5.59E-01	3.20E+01	2.57E+03	1.39E+03	4.07E-03	3.78E+04	9.32E-02	3.10E+01	Wulf, 1985
V79-SH1	1.74E-01		Ar-40	5.09E+03	2.04E+02	1.11E+01	2.99E+00	9.17E+01	1.85E+03	9.79E+02	1.08E-02	2.13E+04	1.61E-01	5.17E+01	Bird,1975
V79	1.79E-01		Ar-40	5.10E+03	2.04E+02	1.11E+01	3.00E+00	9.23E+01	1.85E+03	9.78E+02	1.09E-02	2.12E+04	1.61E-01	5.30E+01	Wulf, 1985
M3-1	1.47E-01		Ar-40	5.70E+03	2.28E+02	1.25E+01	3.68E+00	1.06E+02	1.76E+03	9.25E+02	1.21E-02	1.97E+04	1.74E-01	4.13E+01	Todd, 1975
V79	1.84E-01		Ar-40	5.90E+03	2.36E+02	1.29E+01	3.91E+00	1.11E+02	1.69E+03	8.91E+02	1.26E-02	1.92E+04	1.88E-01	5.00E+01	Weber, 1993
V79	1.84E-01		Ar-40	5.90E+03	2.36E+02	1.29E+01	3.91E+00	1.11E+02	1.69E+03	8.91E+02	1.26E-02	1.92E+04	1.88E-01	5.00E+01	Weber, 1993
V79	1.45E-01		Ar-40	9.10E+03	3.64E+02	1.99E+01	8.58E+00	1.96E+02	1.38E+03	7.19E+02	1.93E-02	1.40E+04	2.43E-01	3.20E+01	Wulf, 1985
V79	1.59E-01		Ar-40	9.10E+03	3.64E+02	1.99E+01	8.58E+00	1.96E+02	1.38E+03	7.19E+02	1.93E-02	1.40E+04	2.43E-01	3.50E+01	Wulf, 1985
V79	2.59E-01		Ar-40	1.04E+04	4.16E+02	2.28E+01	1.09E+01	2.37E+02	1.28E+03	6.67E+02	2.20E-02	1.26E+04	2.67E-01	5.30E+01	Wulf, 1985
V79	3.48E-01		Ar-40	1.42E+04	5.68E+02	3.12E+01	1.90E+01	3.73E+02	1.04E+03	5.42E+02	2.98E-02	9.85E+03	3.47E-01	5.80E+01	Wulf, 1985
V79	4.72E-01		Ar-40	1.69E+04	6.76E+02	3.71E+01	2.58E+01	4.85E+02	9.10E+02	4.72E+02	3.54E-02	8.52E+03	4.11E-01	6.87E+01	Wulf, 1985
V79	4.00E-01		Ar-40	2.00E+04	8.00E+02	4.40E+01	3.48E+01	6.31E+02	8.24E+02	4.27E+02	4.16E-02	7.38E+03	4.64E-01	5.27E+01	Wulf, 1985
V79	5.47E-01		Ar-40	3.33E+04	1.33E+03	7.37E+01	8.43E+01	1.45E+03	5.70E+02	2.98E+02	6.78E-02	4.69E+03	7.12E-01	4.99E+01	Hall, 1977
V79	7.98E-01		Ar-40	3.35E+04	1.34E+03	7.42E+01	8.54E+01	1.46E+03	1.11E+02	5.52E+01	6.79E-02	4.61E+03	5.00E+00	1.42E+01	Hall, 1977
V79	6.13E-01		Ar-40	3.50E+04	1.40E+03	7.76E+01	9.22E+01	1.57E+03	5.38E+02	2.79E+02	7.12E-02	4.48E+03	7.68E-01	5.27E+01	Wulf, 1985
V79	5.47E-01		Ar-40	4.93E+04	1.97E+03	1.10E+02	1.66E+02	2.83E+03	4.09E+02	2.14E+02	9.80E-02	3.29E+03	1.05E+00	3.58E+01	Hall, 1977
V79	7.53E-01		Ar-40	6.20E+04	2.48E+03	1.40E+02	2.47E+02	4.17E+03	3.49E+02	1.78E+02	1.21E-01	2.67E+03	1.29E+00	4.21E+01	Hall, 1977
V79	5.48E-01		Ar-40	6.63E+04	2.65E+03	1.49E+02	2.76E+02	4.70E+03	3.40E+02	1.74E+02	1.29E-01	2.52E+03	1.33E+00	2.98E+01	Hall, 1977
V79	7.52E-01		Ar-40	7.45E+04	2.98E+03	1.69E+02	3.38E+02	5.76E+03	3.05E+02	1.59E+02	1.43E-01	2.27E+03	1.48E+00	3.67E+01	Hall, 1977
V79	7.53E-01		Ar-40	8.38E+04	3.35E+03	1.91E+02	4.13E+02	7.09E+03	2.75E+02	1.45E+02	1.58E-01	2.04E+03	1.64E+00	3.32E+01	Hall, 1977
V79	8.42E-01		Ar-40	1.65E+05	6.60E+03	3.91E+02	1.25E+03	2.33E+04	1.69E+02	8.80E+01	2.79E-01	1.16E+03	2.91E+00	2.28E+01	Wulf, 1985
V79	1.73E+00		Ar-40	4.26E+05	1.70E+04	1.14E+03	5.12E+03	1.33E+05	9.79E+01	4.91E+01	8.47E-01	5.64E+02	5.17E+00	2.71E+01	Wulf, 1985
V79	1.29E-01		Ti-48	4.40E+03	2.11E+02	9.60E+00	2.28E+00	7.30E+01	2.61E+03	1.38E+03	9.39E-03	3.15E+04	1.12E-01	5.40E+01	Kranert, 1990

Cells (Types/Lines)	$\alpha(Gy^{-1})$	$\beta(Gy^{-2})$	Ions	E/m (keV/amu)	E(MeV)	$E_{m,\alpha}$(keV)	$R_{m,\alpha}$(μm)	R_i(μm)	L_T(keV/μm)	$L_{100,T}$(keV/μm)	β^2	z^{*2}/β^2	λ(nm)	$\sigma(\mu m^2)$	Reference
V79	2.17E-01		Ti-48	1.48E+04	7.10E+02	3.25E+01	2.04E+01	3.47E+02	1.44E+03	7.48E+02	3.11E-02	1.36E+04	2.53E-01	5.00E+01	Kranert, 1990
V79	2.69E-02		Fe-56	1.00E+02	5.60E+00	2.18E-01	9.69E-03	4.44E+00	1.86E+03	1.77E+03	2.15E-04	1.05E+05	7.42E-02	8.00E+00	Wulf, 1985
V79	1.96E-01		Fe-56	1.30E+04	7.28E+02	2.85E+01	1.62E+01	2.63E+02	2.08E+03	1.08E+03	2.74E-02	1.99E+04	1.72E-01	6.50E+01	Wulf, 1985
V79	2.52E-01		Fe-56	1.70E+04	9.52E+02	3.74E+01	2.61E+01	3.83E+02	1.74E+03	9.00E+02	3.56E-02	1.63E+04	2.16E-01	7.00E+01	Wulf, 1985
V79	4.70E-01		Fe-56	6.00E+04	3.36E+03	1.35E+02	2.33E+02	2.78E+03	7.28E+02	3.71E+02	1.18E-02	5.67E+03	6.20E-01	5.48E+01	Wulf, 1985
V79	5.93E-01		Fe-56	8.01E+04	4.49E+03	1.82E+02	3.83E+02	4.54E+03	5.89E+02	3.05E+02	1.52E-01	4.41E+03	7.78E-01	5.59E+01	Wulf, 1985
V79	5.41E-01		Fe-56	9.50E+04	5.32E+03	2.17E+02	5.12E+02	6.08E+03	5.27E+02	2.74E+02	1.77E-01	3.81E+03	8.80E-01	4.56E+01	Wulf, 1985
V79	9.48E-01		Fe-56	4.00E+05	2.24E+04	1.06E+03	4.66E+03	6.79E+04	2.12E+02	1.07E+02	5.11E-01	1.32E+03	2.62E+00	3.22E+01	Wulf, 1985
V79	1.84E-02		Ni-59	7.00E+02	4.13E+01	1.53E+00	1.22E-01	1.53E+01	4.08E+03	3.02E+03	1.50E-03	8.57E+04	4.83E-02	1.20E+01	Wulf, 1985
V79	3.73E-02		Ni-59	1.80E+03	1.06E+02	3.92E+00	5.13E-01	3.02E+01	4.36E+03	2.37E+03	3.86E-03	6.52E+04	5.43E-02	2.60E+01	Wulf, 1985
V79	5.79E-02		Ni-59	2.50E+03	1.48E+02	5.45E+00	8.75E-01	3.99E+01	4.21E+03	2.27E+03	5.35E-03	5.74E+04	6.31E-02	3.90E+01	Wulf, 1985
V79	1.02E-01		Ni-59	4.50E+03	2.66E+02	9.82E+00	2.37E+00	7.03E+01	3.62E+03	1.92E+03	9.60E-03	4.34E+04	8.12E-02	5.90E+01	Wulf, 1985
V79	1.08E-01		Ni-59	6.10E+03	3.60E+02	1.33E+01	4.16E+00	9.78E+01	3.30E+03	1.74E+03	1.30E-02	3.67E+04	9.40E-02	5.70E+01	Wulf, 1985
V79	1.44E-01		Ni-58	9.00E+03	5.22E+02	1.97E+01	8.41E+00	1.53E+02	2.82E+03	1.48E+03	1.91E-02	2.89E+04	1.18E-01	6.50E+01	Kranert, 1990
V79	2.53E-01		Ni-58	1.46E+04	8.47E+02	3.20E+01	2.00E+01	2.87E+02	2.15E+03	1.12E+03	3.07E-02	2.07E+04	1.70E-01	8.70E+01	Kranert, 1990
V79	4.80E-02		Kr-84	2.85E+03	2.39E+02	6.22E+00	1.09E+00	5.08E+01	5.47E+03	2.93E+03	6.10E-03	7.28E+04	4.84E-02	4.20E+01	Wulf, 1985
V79	8.80E-02		Kr-84	1.10E+04	9.24E+02	2.41E+01	1.21E+01	2.06E+02	3.77E+03	1.96E+03	2.32E-02	3.72E+04	9.19E-02	5.30E+01	Wulf, 1985
V79	9.31E-02		Kr-84	1.11E+04	9.32E+02	2.43E+01	1.22E+01	2.08E+02	3.76E+03	1.96E+03	2.34E-02	3.70E+04	9.22E-02	5.60E+01	Wulf, 1985
V79	1.40E-01		Kr-84	1.79E+04	1.50E+03	3.94E+01	2.86E+01	3.85E+02	2.90E+03	1.50E+03	3.74E-02	2.70E+04	1.30E-01	6.50E+01	Wulf, 1985
V79	1.49E-01		Kr-84	1.80E+04	1.51E+03	3.96E+01	2.89E+01	3.88E+02	2.89E+03	1.50E+03	3.76E-02	2.69E+04	1.31E-01	6.90E+01	Wulf, 1985
V79	3.23E-02		Xe-132	3.75E+03	4.95E+02	8.18E+00	1.73E+00	7.09E+01	8.32E+03	4.43E+03	8.01E-03	1.03E+04	3.38E-02	4.30E+01	Wulf, 1985
V79	3.53E-02		Xe-132	5.30E+03	7.00E+02	1.16E+01	3.22E+00	9.61E+01	7.97E+03	4.20E+03	1.13E-02	9.21E+04	3.80E-02	4.50E+01	Wulf, 1985
V79	3.22E-02		Xe-132	5.30E+03	7.00E+02	1.16E+01	3.22E+00	9.61E+01	7.97E+03	4.20E+03	1.13E-02	9.21E+04	3.80E-02	4.10E+01	Wulf, 1985
V79	3.51E-02		Xe-132	5.90E+03	7.79E+02	1.29E+01	3.91E+00	1.06E+02	7.81E+03	4.11E+03	1.26E-02	8.83E+04	3.96E-02	4.38E+01	Kraft, 1982
V79	4.02E-02		Xe-132	6.20E+03	8.18E+02	1.35E+01	4.29E+00	1.11E+02	7.77E+03	4.09E+03	1.32E-02	8.66E+04	4.00E-02	5.00E+01	Wulf, 1985
V79	5.64E-02		Xe-132	6.51E+03	8.59E+02	1.42E+01	4.68E+00	1.17E+02	7.64E+03	4.02E+03	1.38E-02	8.49E+04	4.14E-02	6.90E+01	Wulf, 1985
V79	5.71E-02		Xe-132	1.01E+04	1.33E+03	2.21E+01	1.04E+01	1.83E+02	6.78E+03	3.54E+03	2.14E-02	6.95E+04	5.07E-02	6.20E+01	Wulf, 1985
V79	5.44E-02		Xe-132	1.01E+04	1.33E+03	2.21E+01	1.04E+01	1.83E+02	6.78E+03	3.54E+03	2.14E-02	6.95E+04	5.07E-02	5.90E+01	Wulf, 1985
V79	6.50E-02		Xe-132	1.06E+04	1.40E+03	2.32E+01	1.13E+01	1.92E+02	6.73E+03	3.51E+03	2.24E-02	6.79E+04	5.13E-02	7.00E+01	Kranert, 1990
V79	6.38E-02		Xe-132	1.13E+04	1.49E+03	2.48E+01	1.27E+01	2.06E+02	6.66E+03	3.47E+03	2.38E-02	6.57E+04	5.21E-02	6.80E+01	Wulf, 1985
V79	1.01E-01		Xe-132	1.14E+04	1.50E+03	2.50E+01	1.29E+01	2.09E+02	6.52E+03	3.40E+03	2.41E-02	6.54E+04	5.38E-02	1.05E+02	Weber, 1993
V79	1.01E-01		Xe-132	1.14E+04	1.50E+03	2.50E+01	1.29E+01	2.09E+02	6.52E+03	3.40E+03	2.41E-02	6.54E+04	5.38E-02	1.05E+02	Weber, 1993
V79	5.63E-02		Xe-132	1.33E+04	1.76E+03	2.92E+01	1.69E+01	2.48E+02	6.21E+03	3.23E+03	2.80E-02	6.03E+04	5.78E-02	5.60E+01	Wulf, 1985

Cells (Types/Lines)	$\alpha(Gy^{-1})$	$\beta(Gy^{-2})$	Ions	E/m (keV/amu)	E(MeV)	$E_{m,s}$(keV)	$R_{m,s}$(μm)	R_i(μm)	L_T(keV/μm)	$L_{100,T}$(keV/μm)	β^2	z^{*2}/β^2	λ(nm)	$\sigma(\mu m^2)$	Reference
V79	5.93E-02		Xe-132	1.33E+04	1.76E+03	2.92E+01	1.69E+01	2.48E+02	6.21E+03	3.23E+03	2.80E-02	6.03E+04	5.78E-02	5.90E+01	Wulf, 1985
V79	7.34E-02		Xe-132	1.58E+04	2.09E+03	3.47E+01	2.29E+01	3.04E+02	5.88E+03	3.05E+03	3.31E-02	5.47E+04	6.25E-02	6.90E+01	Wulf, 1985
V79	6.81E-02		Xe-132	1.77E+04	2.34E+03	3.89E+01	2.80E+01	3.48E+02	5.60E+03	2.91E+03	3.69E-02	5.12E+04	6.68E-02	6.10E+01	Wulf, 1985
V79	6.92E-02		Xe-132	1.77E+04	2.34E+03	3.89E+01	2.80E+01	3.48E+02	5.60E+03	2.91E+03	3.69E-02	5.12E+04	6.68E-02	6.20E+01	Wulf, 1985
V79	7.03E-02		Au-197	9.80E+03	1.93E+03	2.14E+01	9.80E+00	1.79E+02	1.11E+04	5.80E+03	2.07E-02	1.14E+05	3.07E-02	1.25E+02	Weber, 1993
V79	7.03E-02		Au-197	9.80E+03	1.93E+03	2.15E+01	9.80E+00	1.79E+02	1.11E+04	5.80E+03	2.07E-02	1.14E+05	3.07E-02	1.25E+02	Weber, 1993
V79	5.27E-02		Pb-208	1.56E+04	3.24E+03	3.43E+01	2.24E+01	2.93E+02	1.04E+04	5.43E+03	3.27E-02	7.84E+04	3.52E-02	8.80E+01	Kranert, 1990
V79	2.30E-02		U-238	1.10E+03	2.62E+02	2.40E+00	2.38E-01	3.63E+01	1.12E+04	9.03E+03	2.36E-03	2.03E+05	2.04E-02	4.10E+01	Wulf, 1985
V79	2.25E-02		U-238	1.70E+03	4.05E+02	3.71E+00	4.68E-01	4.80E+01	1.28E+04	9.42E+03	3.64E-03	1.98E+05	1.92E-02	4.60E+01	Wulf, 1985
V79	2.15E-02		U-238	1.70E+03	4.05E+02	3.71E+00	4.68E-01	4.80E+01	1.28E+04	9.42E+03	3.64E-03	1.98E+05	1.92E-02	4.40E+01	Wulf, 1985
V79	1.99E-02		U-238	2.00E+03	4.76E+02	4.36E+00	6.08E-01	5.34E+01	1.34E+04	9.27E+03	4.28E-03	1.95E+05	1.90E-02	4.26E+01	Kraft, 1982
V79	1.80E-02		U-238	2.50E+03	5.95E+02	5.45E+00	8.75E-01	6.21E+01	1.39E+04	8.69E+03	5.35E-03	1.90E+05	1.91E-02	4.00E+01	Wulf, 1985
V79	2.19E-02		U-238	2.75E+03	6.55E+02	6.00E+00	1.02E+00	6.64E+01	1.40E+04	8.51E+03	5.88E-03	1.87E+05	1.92E-02	4.90E+01	Wulf, 1985
V79	2.44E-02		U-238	3.20E+03	7.62E+02	6.98E+00	1.32E+00	7.40E+01	1.41E+04	7.54E+03	6.83E-03	1.83E+05	1.93E-02	5.50E+01	Wulf, 1985
V79	2.11E-02		U-238	3.85E+03	9.16E+02	8.40E+00	1.81E+00	8.49E+01	1.42E+04	7.57E+03	8.21E-03	1.77E+05	1.98E-02	4.80E+01	Wulf, 1985
V79	2.51E-02		U-238	3.85E+03	9.16E+02	8.40E+00	1.81E+00	8.49E+01	1.42E+04	7.57E+03	8.21E-03	1.77E+05	1.98E-02	5.70E+01	Wulf, 1985
V79	2.51E-02		U-238	4.10E+03	9.76E+02	8.95E+00	2.02E+00	8.81E+01	1.42E+04	7.56E+03	8.74E-03	1.74E+05	2.02E-02	5.70E+01	Wulf, 1985
V79	2.29E-02		U-238	4.10E+03	9.76E+02	8.95E+00	2.02E+00	8.81E+01	1.42E+04	7.56E+03	8.74E-03	1.74E+05	2.02E-02	5.20E+01	Wulf, 1985
V79	2.51E-02		U-238	4.10E+03	9.76E+02	8.95E+00	2.02E+00	8.81E+01	1.42E+04	7.56E+03	8.74E-03	1.74E+05	2.02E-02	5.70E+01	Wulf, 1985
V79	2.07E-02		U-238	4.70E+03	1.12E+03	1.03E+01	2.58E+00	9.91E+01	1.42E+04	7.54E+03	1.00E-02	1.69E+05	2.07E-02	4.70E+01	Wulf, 1985
V79	3.47E-02		U-238	4.70E+03	1.12E+03	1.03E+01	2.58E+00	9.91E+01	1.42E+04	7.54E+03	1.00E-02	1.69E+05	2.07E-02	7.90E+01	Kranert, 1988
V79	3.13E-02		U-238	5.10E+03	1.21E+03	1.11E+01	3.00E+00	1.06E+02	1.42E+04	7.50E+03	1.09E-02	1.66E+05	2.12E-02	7.10E+01	Kranert, 1990
V79	2.43E-02		U-238	5.40E+03	1.29E+03	1.18E+01	3.33E+00	1.11E+02	1.42E+04	7.49E+03	1.15E-02	1.64E+05	2.14E-02	5.51E+01	Kraft, 1982
V79	3.18E-02		U-238	6.90E+03	1.64E+03	1.51E+01	5.20E+00	1.36E+02	1.40E+04	7.34E+03	1.47E-02	1.53E+05	2.27E-02	7.10E+01	Wulf, 1985
V79	2.95E-02		U-238	6.90E+03	1.64E+03	1.51E+01	5.20E+00	1.36E+02	1.40E+04	7.34E+03	1.47E-02	1.53E+05	2.27E-02	6.60E+01	Wulf, 1985
V79	3.97E-02		U-238	7.60E+03	1.81E+03	1.66E+01	6.20E+00	1.48E+02	1.38E+04	7.25E+03	1.61E-02	1.49E+05	2.34E-02	8.78E+01	Kraft, 1982
V79	2.87E-02		U-238	8.20E+03	1.95E+03	1.79E+01	7.11E+00	1.59E+02	1.40E+04	7.16E+03	1.74E-02	1.45E+05	2.41E-02	6.40E+01	Wulf, 1985
V79	4.99E-02		U-238	1.06E+04	2.52E+03	2.32E+01	1.13E+01	2.02E+02	1.32E+04	6.87E+03	2.24E-02	1.33E+05	2.62E-02	1.05E+02	Kranert, 1990
V79	4.58E-02		U-238	1.23E+04	2.93E+03	2.70E+01	1.47E+01	2.33E+02	1.28E+04	6.68E+03	2.59E-02	1.25E+05	2.75E-02	9.40E+01	Wulf, 1985
V79	4.78E-02		U-238	1.33E+04	3.17E+03	2.92E+01	1.69E+01	2.52E+02	1.26E+04	6.53E+03	2.80E-02	1.22E+05	2.83E-02	9.60E+01	Wulf, 1985
V79	4.75E-02		U-238	1.37E+04	3.26E+03	3.01E+01	1.78E+01	2.60E+02	1.25E+04	6.51E+03	2.88E-02	1.21E+05	2.87E-02	9.50E+01	Wulf, 1985
V79	4.58E-02		U-238	1.41E+04	3.36E+03	3.09E+01	1.88E+01	2.67E+02	1.23E+04	6.39E+03	2.96E-02	1.19E+05	2.96E-02	9.00E+01	Kranert, 1990

AII-2 Charged Particles on Mouse Cells

Cells (Types/Lines)	$\alpha(Gy^{-1})$	$\beta(Gy^{-2})$	Ions	E/m (keV/amu)	E(MeV)	$E_{m,s}$(keV)	$R_{m,s}$(μm)	R_i(μm)	L_T(keV/μm)	$L_{100,T}$(keV/μm)	β^2	z^{*2}/β^2	λ(nm)	σ(μm^2)	Reference
C3H10T1/2	4.30E-01	1.30E-02	p	1.16E+03	1.16E+00	2.53E+00	2.58E-01	3.11E+01	2.36E+01	1.32E+01	2.47E-03	4.05E+01	8.70E+00	1.63E+00	Goodhead, 1992
C3H10T1/2	4.30E-01	1.30E-02	p	1.38E+03	1.38E+00	3.01E+00	3.37E-01	4.10E+01	2.14E+01	1.18E+01	2.93E-03	3.41E+01	1.01E+01	1.47E+00	Goodhead, 1992
C3H10T1/2	7.53E-01		p	2.25E+03	2.25E+00	4.91E+00	7.36E-01	9.16E+01	1.51E+01	8.24E+00	4.78E-03	2.09E+02	1.62E+01	1.82E+00	Miller, 1995
EATC	8.23E-01		p	3.40E+03	3.40E+00	7.42E+00	1.46E+00	1.85E+02	1.09E+01	5.85E+00	7.20E-03	1.39E+02	2.50E+01	1.44E+00	Bertsche, 1987
C3H10T1/2	3.10E-01	3.00E-02	p	4.00E+03	4.00E+00	8.73E+00	1.93E+00	2.40E+02	1.00E+01	5.20E+00	8.46E-03	1.18E+02	2.87E+01	4.96E-01	Hei, 1988
EATC	5.93E-01		p	6.20E+03	6.20E+00	1.35E+01	4.29E+00	5.24E+02	6.90E+00	3.65E+00	1.31E-02	7.65E+01	4.48E+01	6.55E-01	Bertsche, 1987
EATC	4.27E-01		p	1.13E+04	1.13E+01	2.48E+01	1.27E+01	1.52E+03	4.31E+00	2.26E+00	2.37E-02	4.23E+01	8.00E+01	2.95E-01	Bertsche, 1987
EATC	2.99E-01		p	2.07E+04	2.07E+01	4.56E+01	3.69E+01	4.50E+03	2.66E+00	1.39E+00	4.27E-02	2.34E+01	1.43E+02	1.27E-01	Bertsche, 1987
EATC	2.93E-01		p	2.07E+04	2.07E+01	4.56E+01	3.69E+01	4.50E+03	2.66E+00	1.39E+00	4.27E-02	2.34E+01	1.43E+02	1.25E-01	Bertsche, 1980
C3H10T1/2	5.00E-02	4.10E-02	p	3.10E+04	3.10E+01	6.86E+01	7.47E+01	9.36E+03	1.87E+00	9.75E-01	6.29E-02	1.59E+01	2.16E+02	1.49E-02	Bettega, 1990
C3H10T1/2	5.00E-02	4.10E-02	p	3.10E+04	3.10E+01	6.86E+01	7.47E+01	9.36E+03	1.87E+00	9.75E-01	6.29E-02	1.59E+01	2.16E+02	1.49E-02	Bettega, 1990
C3H10T1/2	1.72E+00		D	2.75E+02	5.50E-01	5.99E-01	3.35E-02	8.37E+00	5.81E+01	3.44E+01	5.86E-04	1.68E+03	2.15E+00	1.60E+01	Miller, 1995
C3H10T1/2	7.41E-01		D	5.50E+02	1.10E+00	1.20E+00	8.60E-02	2.00E+01	4.00E+01	2.27E+01	1.17E-03	8.53E+02	4.10E+00	4.74E+00	Miller, 1990
C3H10T1/2	4.10E-01	1.60E-01	D	5.50E+02	1.10E+00	1.20E+00	8.60E-02	2.03E+01	4.00E+01	4.00E+01	1.17E-03	8.53E+02	4.10E+00	2.62E+00	Hei, 1988
EATC	7.89E-01		D	1.25E+03	2.50E+00	2.72E+00	2.89E-01	7.00E+01	2.30E+01	1.28E+01	2.66E-03	3.76E+02	9.12E+00	2.90E+00	Bertsche, 1980
EATC	4.45E-01		D	5.00E+03	1.00E+01	1.09E+01	2.89E+00	7.18E+02	8.22E+00	4.37E+00	1.06E-02	9.46E+01	3.59E+01	5.85E-01	Bertsche, 1987
C3H10T1/2	2.02E-01		D	1.29E+04	2.58E+01	2.83E+01	1.60E+01	3.85E+02	3.90E+00	2.04E+00	2.70E-02	3.71E+01	9.04E+01	1.26E-01	Miller, 1995
C3H10T1/2	1.30E+00		He-3	3.33E+01	1.00E-01	7.26E-02	3.02E-03	1.34E+00	1.20E+02	1.20E+02	7.12E-05	3.17E+04	6.41E-01	2.50E+01	Hei, 1988a
EATC	7.31E-01		He-3	7.80E+02	2.34E+00	1.70E+00	1.42E-01	1.48E+01	1.23E+02	7.00E+01	1.66E-03	2.40E+03	1.49E+00	1.44E+01	Bertsche, 1987
C3H10T1/2	1.14E+00		He-3	1.47E+03	4.40E+00	3.20E+00	3.71E-01	3.64E+01	8.00E+01	8.00E+01	3.13E-03	1.28E+03	2.69E+00	1.46E+01	Hei, 1988
C3H10T1/2	1.70E+00		He-3	1.67E+03	5.00E+00	3.63E+00	4.54E-01	4.44E+01	7.37E+01	4.12E+01	3.55E-03	1.13E+03	3.03E+00	2.01E+01	Miller, 1995a
EATC	1.22E+00		He-3	5.00E+03	1.50E+01	1.09E+01	2.89E+00	2.76E+02	3.17E+01	1.71E+01	1.06E-02	3.78E+02	9.26E+00	6.18E+00	Bertsche, 1987
EATC	3.87E-01		He-3	8.60E+03	2.58E+01	1.88E+01	7.75E+00	7.12E+02	2.13E+01	1.14E+01	1.81E-02	2.21E+02	1.52E+01	1.32E+00	Bertsche, 1980
EATC	5.54E-01		He-3	8.67E+03	2.60E+01	1.90E+01	7.86E+00	7.22E+02	2.13E+01	1.13E+01	1.83E-02	2.19E+02	1.53E+01	1.88E+00	Bertsche, 1987
C3H10T1/2	1.45E+00		He-4	3.60E+02	1.44E+00	7.84E-01	4.79E-02	7.89E+00	1.97E+02	1.12E+02	7.72E-04	4.87E+03	7.21E-01	4.57E+01	Miller, 1995
C3H10T1/2	1.19E+00		α	4.50E+02	1.80E+00	9.80E-01	6.50E-02	9.86E+00	1.77E+02	1.01E+02	9.65E-04	4.02E+03	8.68E-01	3.38E+01	Napolitano, 1992
C3H10T1/2	1.30E+00		α	4.50E+02	1.80E+00	9.80E-01	6.50E-02	9.86E+00	1.77E+02	1.01E+02	9.65E-04	4.02E+03	8.68E-01	3.69E+01	Napolitano, 1992
C3H10T1/2	2.18E+00		He-4	5.93E+02	2.37E+00	1.29E+00	9.56E-02	1.35E+01	1.48E+02	8.40E+01	1.27E-03	7.12E+03	1.14E+00	5.17E+01	Miller, 1995
C3H10T1/2	1.65E+00		α	6.75E+02	2.70E+00	1.47E+00	1.15E-01	1.58E+01	1.40E+02	7.76E+01	1.45E-03	2.75E+03	1.28E+00	3.70E+01	Hieber, 1987
C3H10T1/2	1.65E+00		α	6.75E+02	2.70E+00	1.47E+00	1.15E-01	1.58E+01	1.37E+02	7.76E+01	1.45E-03	2.75E+03	1.28E+00	3.62E+01	Hieber, 1987
C3H10T1/2	1.65E+00		α	8.00E+02	3.20E+00	1.74E+00	1.48E-01	1.97E+01	1.25E+02	7.05E+01	1.71E-03	2.33E+03	1.47E+00	3.29E+01	Roberts, 1987
C3H10T1/2	1.91E+00		He-4	8.33E+02	3.33E+00	1.81E+00	1.57E-01	2.08E+01	1.18E+02	6.68E+01	1.78E-03	2.24E+03	1.59E+00	3.60E+01	Miller, 1995

Cells (Types/Lines)	$\alpha(Gy^{-1})$	$\beta(Gy^{-2})$	Ions	E/m (keV/amu)	E(MeV)	$E_{m,a}$(keV)	$R_{m,a}$(μm)	R_i(μm)	L_T(keV/μm)	$L_{100,T}$(keV/μm)	β^2	z^{*2}/β^2	λ(nm)	σ(μm^2)	Reference
C3H10T1/2	1.65E+00		α	1.04E+03	4.15E+00	2.26E+00	2.18E-01	2.84E+01	1.01E+02	5.68E+01	2.22E-03	1.80E+03	1.98E+00	2.67E+01	D.Bettega, 1990
EATC	1.55E+00		α	1.08E+03	4.30E+00	2.34E+00	2.30E-01	2.99E+01	9.96E+01	5.61E+01	2.30E-03	1.74E+03	2.02E+00	2.47E+01	U. Bertsche, 1980
C3H10T1/2	1.65E+00		α	1.08E+03	4.30E+00	2.34E+00	2.30E-01	2.99E+01	9.96E+01	5.61E+01	2.30E-03	1.74E+03	2.01E+00	2.63E+01	Bettega, 1990
C3H10T1/2	1.44E+00		He-4	1.28E+03	5.12E+00	2.79E+00	3.00E-01	3.88E+01	9.00E+01	5.05E+01	2.74E-03	1.46E+03	2.32E+00	2.07E+01	R.Miller, 1995a
EATC	2.49E+00		He-4	1.33E+03	5.30E+00	2.89E+00	3.17E-01	4.09E+01	8.47E+01	4.77E+01	2.84E-03	1.41E+03	2.50E+00	3.37E+01	U. Bertsche, 1987
C3H10T1/2	1.43E+00		α	1.35E+03	5.40E+00	2.94E+00	3.26E-01	4.21E+01	8.42E+01	4.74E+01	2.89E-03	1.38E+03	2.52E+00	1.92E+01	Nagasawa, 1990
C3H10T1/2	1.67E+00		α	1.40E+03	5.60E+00	3.05E+00	3.45E-01	4.45E+01	8.31E+01	4.68E+01	3.00E-03	1.34E+03	2.57E+00	2.22E+01	Lloyd, 1979
EATC	1.06E+00		He-4	1.88E+03	7.50E+00	4.09E+00	5.48E-01	7.07E+01	6.64E+01	3.67E+01	4.01E-03	9.97E+02	3.52E+00	1.12E+01	U. Bertsche, 1987
EATC	7.45E-01		He-4	2.88E+03	1.15E+01	6.27E+00	1.10E+00	1.43E+02	5.00E+01	2.72E+01	6.14E-03	6.51E+02	5.17E+00	5.96E+00	U. Bertsche, 1987
EATC	7.89E-01		He-4	4.40E+03	1.76E+01	9.60E+00	2.28E+00	2.94E+02	3.57E+01	1.92E+01	9.38E-03	4.27E+02	8.02E+00	4.50E+00	U. Bertsche, 1980
EATC	8.40E-01		He-4	4.40E+03	1.76E+01	9.60E+00	2.28E+00	2.94E+02	3.57E+01	1.92E+01	9.38E-03	4.27E+02	8.02E+00	4.79E+00	U. Bertsche, 1983
EATC	3.35E-01		He-4	4.40E+03	1.76E+01	9.60E+00	2.28E+00	2.94E+02	3.57E+01	1.92E+01	9.38E-03	4.27E+02	8.02E+00	1.91E+00	U. Bertsche, 1987
C3H10T1/2	4.80E-01	1.40E-02	α	7.60E+03	3.04E+01	1.66E+01	6.20E+00	7.62E+01	2.29E+01	1.22E+01	1.61E-02	2.48E+02	1.40E+01	1.76E+00	D. Goodhead, 1992
C3H10T1/2	4.80E-01	1.40E-02	α	8.80E+03	3.52E+01	1.93E+01	8.08E+00	9.89E+01	2.06E+01	1.10E+01	1.86E-02	2.15E+02	1.59E+01	1.58E+00	D. Goodhead, 1992
C3H10T1/2	1.79E+00		C-12	5.36E+03	6.43E+01	1.17E+01	3.28E+00	1.58E+02	2.71E+02	1.43E+02	1.14E-02	3.04E+02	1.11E+00	7.76E+01	R.Miller, 1995a
C3H10T1/2	2.71E-01		C-12	4.74E+05	5.69E+03	1.29E+03	5.96E+03	3.88E+05	1.00E+01	5.00E+00	5.77E-01	6.33E+01	9.03E+01	4.33E-01	Yang, 1985
C3H10T1/2	1.01E+00		O-16	6.04E+03	9.66E+01	1.32E+01	4.08E+00	1.55E+02	4.18E+02	2.20E+02	1.28E-02	4.68E+03	7.43E-01	6.74E+01	Miller, 1995
C3H10T1/2	1.50E+00		F-19	4.82E+03	9.16E+01	1.05E+01	2.71E+00	1.10E+02	6.09E+02	3.22E+02	1.03E-02	7.01E+03	4.84E-01	1.46E+02	Miller, 1995
C3H10T1/2	4.28E-01		Ne-20	4.25E+05	8.50E+03	1.14E+03	5.10E+03	1.65E+05	3.20E+01	1.60E+01	5.11E-01	2.02E+02	2.62E+01	2.19E+00	Yang, 1985
C3H10T1/2	6.59E-01		Si-28	3.20E+05	8.96E+03	8.16E+02	3.38E+03	5.10E+05	8.20E+01	4.10E+01	3.70E-01	5.40E+02	1.05E+01	8.64E+00	Yang, 1985
C3H10T1/2	4.06E-01		Si-28	6.70E+05	1.88E+04	1.98E+03	9.65E+03	2.75E+05	5.00E+01	2.50E+01	6.74E-01	2.95E+02	1.96E+01	3.24E+00	Yang, 1985
EATC	1.09E-01		Ar-40	1.80E+04	7.20E+02	3.96E+01	2.89E+01	5.35E+02	8.91E+02	4.62E+02	3.76E-02	8.08E+03	4.22E-01	1.55E+01	Bertsche, 1987
C3H10T1/2	8.49E-01		Ar-40	3.30E+05	1.32E+04	8.45E+02	3.54E+03	5.30E+04	1.40E+02	7.00E+01	3.40E-01	9.50E+02	6.10E+00	1.90E+01	Yang, 1985
EATC	2.36E-01		Ti-48	7.50E+03	3.60E+02	1.64E+01	6.05E+00	1.38E+02	2.11E+03	1.10E+03	1.59E-02	2.24E+04	1.53E-01	7.95E+01	Bertsche, 1983
C3H10T1/2	6.12E-01		Fe-56	3.00E+05	1.68E+04	7.58E+02	3.08E+03	6.80E+03	5.00E+02	2.65E+02	1.80E-01	3.90E+03	1.47E+00	4.90E+01	Yang, 1985
C3H10T1/2	6.92E-01		Fe-56	4.00E+05	2.24E+04	1.06E+03	4.68E+03	2.50E+04	3.00E+02	1.50E+02	3.50E-01	2.10E+03	2.80E+00	3.32E+01	Yang, 1985
C3H10T1/2	9.02E-01		Fe-56	6.00E+05	3.36E+04	1.72E+03	8.29E+03	1.10E+05	1.90E+02	9.50E+01	5.90E-01	1.10E+03	5.10E+00	2.74E+01	Yang, 1985
EATC	6.11E-02		Kr-84	2.89E+03	2.43E+02	6.31E+00	1.12E+00	5.16E+01	5.47E+03	2.93E+03	6.20E-03	7.24E+04	4.86E-02	5.35E+01	Bertsche, 1983
EATC	1.69E-02		U-238	6.50E+03	1.55E+03	1.42E+01	4.67E+00	1.30E+02	1.40E+04	7.36E+03	1.38E-02	1.56E+05	2.25E-02	3.77E+01	Bertsche, 1983
C3H10T1/2	2.44E-01		U-238	9.60E+05	2.28E+05	3.16E+03	1.56E+04	9.00E+04	1.90E+03	9.60E+02	7.67E-01	1.11E+04	5.40E-01	7.42E+01	Yang, 1985

AII-3 Charged Particles on Human Cells

Cells (Types/Lines)	$\alpha(Gy^{-1})$	$\beta(Gy^{-2})$	Ion Type	E/m (keV/amu)	E(MeV)	E_{max}(keV)	R_{max}(μm)	R_i(μm)	L_T(keV/μm)	$L_{100,T}$(keV/μm)	β^2	z^{*2}/β^2	λ(nm)	σ(μm^2)	Reference
HeLa	1.54E-02		π^-	1.50E+04	1.50E+01	3.29E+01	2.09E+01	1.00E+04	7.50E-01	3.75E-01	1.85E-01	5.42E+00	4.47E+02	1.85E-03	Reading, 1981
HeLa	1.63E-01		π^-	2.00E+04	2.00E+01	4.40E+01	3.48E+01	3.00E+04	6.00E-01	3.00E-01	2.35E-01	4.26E+00	5.92E+02	1.56E-02	Reading, 1981
HeLa	2.80E-02		π^-	3.00E+04	3.00E+01	6.64E+01	7.05E+01	4.00E+04	4.60E-01	2.30E-01	3.23E-01	3.10E+00	8.21E+02	2.06E-03	Reading, 1981
HeLa	1.38E-01		π^-	3.50E+04	3.50E+01	7.76E+01	9.22E+01	5.00E+04	4.00E-01	2.00E-01	3.61E-01	2.77E+00	9.65E+02	8.84E-03	Reading, 1981
HeLa	1.14E-01		π^-	4.50E+04	4.50E+01	1.00E+02	1.42E+02	8.00E+04	3.57E-01	1.78E-01	4.28E-01	2.34E+00	1.13E+03	6.49E-03	Reading, 1981
HeLa	8.39E-02		π^-	6.00E+04	6.00E+01	1.35E+02	2.33E+02	1.20E+05	3.07E-01	1.54E-01	5.11E-01	1.96E+00	1.36E+03	4.12E-03	Reading, 1981
HeLa	1.16E-01		π^-	6.80E+04	6.80E+01	1.53E+02	2.89E+02	1.50E+05	2.80E-01	1.40E-01	5.48E-01	1.83E+00	1.52E+03	5.20E-03	Reading, 1981
HeLa	8.50E-01	3.70E-02	p	1.16E+03	1.16E+00	2.53E+00	2.58E-01	3.11E+01	2.36E+01	1.35E+01	2.47E-03	4.05E+01	8.70E+00	3.21E+00	Goodhead, 1992
HeLa-S3	1.01E+00	-1.00E-03	p	1.16E+03	1.16E+00	2.53E+00	2.58E-01	3.11E+01	2.36E+01	1.32E+01	2.47E-03	4.05E+01	8.70E+00	3.82E+00	Goodhead, 1992
HeLa-S3	6.50E-01	3.70E-02	p	1.38E+03	1.38E+00	3.01E+00	3.37E-01	4.10E+01	2.14E+01	1.18E+01	2.93E-03	3.41E+01	1.01E+01	2.22E+00	Goodhead, 1992
HeLa	5.30E-01	8.40E-02	p	1.38E+03	1.38E+00	3.01E+00	3.37E-01	4.10E+01	2.14E+01	1.18E+01	2.93E-03	3.41E+01	1.01E+01	1.81E+00	Goodhead, 1992
HSF	5.46E-01		p	3.70E+03	3.70E+00	8.07E+00	1.69E+00	2.13E+02	1.00E+01	5.41E+00	7.84E-03	1.28E+02	2.76E+01	8.73E-01	Hei, 1988
Human cells (EUE)	8.40E-01		p	8.00E+03	8.00E+00	1.75E+01	6.80E+00	8.21E+02	5.69E+00	3.00E+00	1.68E-02	5.94E+01	5.69E+01	7.65E-01	Bettega, 1979
Human cells (EUE)	6.17E-01		p	1.20E+04	1.20E+01	2.63E+01	1.41E+01	1.69E+03	4.01E+00	2.01E+00	2.51E-02	3.99E+01	8.72E+01	3.96E-01	Bettega, 1979
Human cells (EUE)	2.93E-01		p	3.10E+04	3.10E+01	6.86E+01	7.47E+01	9.36E+03	1.87E+00	9.75E-01	6.29E-02	1.59E+01	2.16E+02	8.74E-02	Bettega, 1979
HeLa	2.21E-01		p	9.00E+04	9.00E+01	2.05E+02	4.67E+02	6.37E+04	8.05E-01	4.22E-01	1.67E-01	5.98E+00	5.69E+02	2.85E-02	Wainson, 1972
HSF	1.38E+00		D	5.50E+02	1.10E+00	1.20E+00	8.60E-02	2.03E+01	4.00E+01	2.27E+01	1.17E-03	8.53E+02	4.10E+00	8.84E+00	Hei, 1988
HSF	9.00E-01		D	1.50E+03	3.00E+00	3.27E+00	3.84E-01	9.39E+01	2.00E+01	1.09E+01	3.19E-03	3.13E+02	1.12E+01	2.88E+00	Hei, 1988
Human Kid. T1	6.06E-01		D	1.50E+03	3.00E+00	3.27E+00	3.84E-01	9.39E+01	1.99E+01	1.10E+01	3.19E-03	3.13E+02	1.12E+01	1.93E+00	Barendsen, 1966
Human Kid. T1	4.14E-01		D	1.75E+03	3.50E+00	3.81E+00	4.90E-01	1.21E+02	1.81E+01	9.90E+00	3.72E-03	2.69E+02	1.28E+01	1.20E+00	Barendsen, 1963
Human Kid. T1	3.20E-01		D	3.15E+03	6.30E+00	6.87E+00	1.29E+00	3.24E+02	1.17E+01	6.31E+00	6.68E-03	1.50E+02	2.28E+01	6.00E-01	Barendsen, 1963
Human Kid. T1	2.79E-01		D	6.60E+03	1.32E+01	1.44E+01	4.80E+00	1.17E+03	6.43E+00	3.40E+00	1.39E-02	7.18E+01	4.89E+01	2.87E-01	Todd, 1965
Human Kid. T1	2.40E-01		D	7.44E+03	1.49E+01	1.63E+01	5.96E+00	1.44E+03	5.86E+00	3.09E+00	1.57E-02	6.38E+01	5.49E+01	2.24E-01	Barendsen, 1963
Human Kid. T1	2.50E-01		D	7.45E+03	1.49E+01	1.63E+01	5.98E+00	1.45E+03	5.85E+00	3.09E+00	1.57E-02	6.37E+01	5.50E+01	2.34E-01	Barendsen, 1966
HSF	2.24E+00		He-3	6.00E+02	1.80E+00	1.31E+00	9.73E-02	1.08E+01	1.50E+02	8.55E+01	1.28E-03	3.09E+03	1.11E+00	5.37E+01	Hei, 1988
HSF	2.08E+00		He-3	8.33E+02	2.50E+00	1.82E+00	1.57E-01	1.62E+01	1.20E+02	6.84E+01	1.78E-03	2.25E+03	1.54E+00	3.99E+01	Hei, 1988
HSF	1.91E+00		He-3	1.47E+03	4.40E+00	3.20E+00	3.71E-01	3.64E+01	8.00E+01	4.50E+01	3.13E-03	1.28E+03	2.68E+00	2.44E+01	Hei, 1988
Human Kid. T1	1.03E+00		α	4.50E+02	1.80E+00	9.80E-01	6.50E-02	9.86E+00	1.77E+02	1.01E+02	9.65E-04	4.02E+03	8.68E-01	2.93E+01	Barendsen, 1964
Human Kid. T1	1.27E+00		α	6.25E+02	2.50E+00	1.36E+00	1.03E-01	1.43E+01	1.46E+02	8.26E+01	1.34E-03	2.96E+03	1.17E+00	2.95E+01	Barendsen, 1966
Human Kid. T1	1.27E+00		α	6.25E+02	2.50E+00	1.36E+00	1.03E-01	1.43E+01	1.46E+02	8.26E+01	1.34E-03	2.96E+03	1.17E+00	2.95E+01	Barendsen, 1964
Human Kid. T1	1.61E+00		α	7.75E+02	3.10E+00	1.69E+00	1.41E-01	1.89E+01	1.26E+02	7.13E+01	1.66E-03	2.40E+03	1.45E+00	3.25E+01	Barendsen, 1964
Human Kid. T1	1.56E+00		α	8.50E+02	3.40E+00	1.85E+00	1.62E-01	2.14E+01	1.17E+02	6.63E+01	1.82E-03	2.19E+03	1.60E+00	2.93E+01	Barendsen, 1966
Human Kid. T1	1.56E+00		α	9.00E+02	3.60E+00	1.96E+00	1.76E-01	2.32E+01	1.15E+02	6.50E+01	1.93E-03	2.07E+03	1.65E+00	2.87E+01	Barendsen, 1964

Cells (Types/Lines)	$\alpha(Gy^{-1})$	$\beta(Gy^{-2})$	Ion Type	E/m (keV/amu)	E(MeV)	$E_{m,s}$(keV)	$R_{m,s}$(μm)	R_i(μm)	L_T(keV/μm)	$L_{100,T}$(keV/μm)	β^2	z^{*2}/β^2	λ(nm)	$\sigma(\mu m^2)$	Reference
Human Kid. T1	1.75E+00		α	1.00E+03	4.00E+00	2.18E+00	2.06E-01	2.69E+01	1.06E+02	6.01E+01	2.14E-03	1.92E+03	1.84E+00	2.99E+01	Barendsen, 1964
Human Kid. T1	1.75E+00		α	1.00E+03	4.00E+00	2.18E+00	2.06E-01	2.69E+01	1.06E+02	6.01E+01	2.14E-03	1.87E+03	1.84E+00	2.99E+01	Barendsen, 1966
HFL4916	3.03E+00		α	1.03E+03	4.10E+00	2.23E+00	2.14E-01	2.79E+01	1.06E+02	5.95E+01	2.20E-03	1.82E+03	1.86E+00	5.00E+01	Min, 1986 / Simmons, 1996
HFL4916	2.38E+00		α	1.04E+03	4.15E+00	2.26E+00	2.18E-01	2.84E+01	1.01E+02	5.66E+01	2.22E-03	1.80E+03	1.98E+00	3.85E+01	Min, 1986 / Simmons, 1996
HFL4916	2.78E+00		α	1.14E+03	4.55E+00	2.48E+00	2.51E-01	3.25E+01	9.76E+01	5.50E+01	2.44E-03	1.64E+03	2.07E+00	4.35E+01	Min, 1986 / Simmons, 1996
Human Kid. T1	1.43E+00		α	1.28E+03	5.10E+00	2.78E+00	2.98E-01	3.86E+01	9.01E+01	5.05E+01	2.73E-03	1.47E+03	2.32E+00	2.06E+01	Barendsen, 1966
Human Kid. T1	1.56E+00		α	1.30E+03	5.20E+00	2.83E+00	3.07E-01	3.97E+01	8.95E+01	5.02E+01	2.78E-03	1.44E+03	2.34E+00	2.24E+01	Barendsen, 1963
T1 Human Kid.	4.99E-01		α	1.33E+03	5.30E+00	2.96E+00	3.09E-01	2.76E+01	8.47E+01	4.77E+01	2.84E-03	1.41E+03	2.50E+00	6.76E+00	Barendsen, 1962
HeLa-S3	4.00E+00		α	1.38E+03	5.50E+00	3.00E+00	3.35E-01	2.76E+01	8.37E+01	4.71E+01	2.93E-03	1.36E+03	2.54E+00	5.36E+01	H.Sasaki, 1983
HF19 strain	3.16E+00		He-4	1.48E+03	5.90E+00	3.21E+00	3.74E-01	4.83E+01	7.84E+01	4.39E+01	3.16E-03	1.27E+03	2.79E+00	3.97E+01	Cox, 1979
HF19 strain	2.57E+00		He-4	1.85E+03	7.40E+00	4.03E+00	5.36E-01	6.92E+01	6.67E+01	3.69E+01	3.96E-03	1.01E+03	3.50E+00	2.74E+01	Cox, 1979
Human Kid. T1	1.19E+00		α	2.08E+03	8.30E+00	4.52E+00	6.45E-01	8.33E+01	6.14E+01	3.38E+01	4.44E-03	9.01E+02	3.92E+00	1.17E+01	Barendsen, 1966
Human Kid. T1	9.35E-01		α	2.08E+03	8.30E+00	4.52E+00	6.45E-01	8.33E+01	6.14E+01	3.38E+01	4.44E-03	9.01E+02	3.92E+00	9.18E+00	Barendsen, 1963
HF19 strain	1.98E+00		He-4	2.93E+03	1.17E+01	6.38E+00	1.14E+00	1.47E+02	4.76E+01	2.59E+01	6.25E-03	6.40E+02	5.52E+00	1.51E+01	Cox, 1979
HF19 strain	1.25E+00		He-4	6.10E+03	2.44E+01	1.33E+01	4.16E+00	5.18E+02	2.74E+01	1.46E+01	1.30E-02	3.09E+02	1.12E+01	5.49E+00	Cox, 1979
Human Kid. T1	6.06E-01		α	6.25E+03	2.50E+01	1.37E+01	4.35E+00	5.41E+02	2.71E+01	1.45E+01	1.32E-02	3.01E+02	1.13E+01	2.63E+00	Barendsen, 1966
Human Kid. T1	4.69E-01		He-4	6.58E+03	2.63E+01	1.44E+01	4.77E+00	5.91E+02	2.54E+01	1.35E+01	1.40E-02	2.87E+02	1.23E+01	1.91E+00	Todd, 1965
Human Kid. T1	5.08E-01		α	6.70E+03	2.68E+01	1.46E+01	4.93E+00	6.11E+02	2.52E+01	1.34E+01	1.42E-02	2.81E+02	1.24E+01	2.05E+00	Barendsen, 1963
HeLa	6.50E-01	5.90E-02	α	7.60E+03	3.04E+01	1.66E+01	6.20E+00	7.62E+01	2.29E+01	1.22E+01	1.61E-02	2.48E+02	1.40E+01	2.38E+00	Goodhead, 1992
HeLa-S3	7.90E-01	6.00E-03	α	7.60E+03	3.04E+01	1.66E+01	6.20E+00	7.62E+01	2.29E+01	1.22E+01	1.61E-02	2.48E+02	1.40E+01	2.90E+00	Goodhead, 1992
HF19 strain	1.09E+00		He-4	8.73E+03	3.49E+01	1.91E+01	7.95E+00	9.73E+02	2.07E+01	1.10E+01	1.85E-02	2.17E+02	1.58E+01	3.61E+00	Cox, 1979
HeLa-S3	7.10E-01	1.30E-02	α	8.80E+03	3.52E+01	1.93E+01	8.08E+00	9.89E+01	2.06E+01	1.10E+01	1.86E-02	2.15E+02	1.59E+01	2.34E+00	Goodhead, 1992
HeLa	4.20E-01	8.00E-02	α	8.80E+03	3.52E+01	1.93E+01	8.08E+00	9.89E+02	2.06E+01	1.10E+01	1.86E-02	2.15E+02	1.59E+01	1.39E+00	Goodhead, 1992
HeLa-S3	3.18E-01		α	1.00E+04	4.00E+01	2.19E+01	1.02E+01	1.24E+03	1.87E+01	9.91E+00	2.11E-02	1.39E+02	1.79E+01	9.52E-01	Deering, 1962
Chang H.Liver	1.15E+00		Li-7	6.58E+03	4.61E+01	1.44E+01	4.77E+00	4.59E+02	6.02E+01	3.17E+01	1.40E-02	6.45E+02	5.20E+00	1.11E+01	Todd, 1975
Human Kid. T1	6.99E-01		Li-7	6.59E+03	4.61E+01	1.44E+01	4.78E+00	4.59E+02	6.02E+01	3.17E+01	1.40E-02	6.45E+02	5.20E+00	6.74E+00	Todd, 1965
HeLa-S3	4.57E-01		Li-7	9.86E+03	6.90E+01	2.16E+01	9.91E+00	9.32E+02	4.27E+01	2.23E+01	2.08E-02	4.33E+02	7.97E+00	3.12E+00	Deering, 1962
HF19 strain	2.00E+00		B-10	4.98E+03	4.98E+01	1.09E+01	2.87E+00	1.62E+02	2.00E+02	1.06E+02	1.06E-02	2.30E+03	1.49E+00	6.39E+01	Cox, 1979
HF19 strain	2.79E+00		B-10	6.56E+03	6.56E+01	1.43E+01	4.75E+00	2.52E+02	1.66E+02	8.72E+01	1.39E-02	1.77E+03	1.89E+00	7.40E+01	Cox, 1979
Human Kid. T1	1.20E+00		B-11	6.58E+03	7.24E+01	1.44E+01	4.78E+00	2.79E+02	1.64E+02	8.64E+01	1.40E-02	1.77E+03	1.91E+00	3.17E+01	Todd, 1965
HF19 strain	2.96E+00		B-10	1.07E+04	1.07E+02	2.34E+01	1.15E+01	5.74E+02	1.10E+02	5.71E+01	2.26E-02	1.10E+03	3.16E+00	5.19E+01	Cox,1979
Chang H.Liver	5.29E-01		C-12	6.58E+03	7.90E+01	1.44E+01	4.77E+00	2.19E+02	2.31E+02	1.22E+02	1.40E-02	2.52E+03	1.36E+00	1.96E+01	Todd, 1975
Human Kid. T1	1.52E+00		C-12	6.60E+03	7.92E+01	1.44E+01	4.80E+00	2.20E+02	2.31E+02	1.22E+02	1.40E-02	2.51E+03	1.36E+00	5.60E+01	Todd, 1968

Cells (Types/Lines)	$\alpha(Gy^{-1})$	$\beta(Gy^{-2})$	Ion Type	E/m (keV/amu)	E(MeV)	$E_{m,s}$(keV)	$R_{m,s}$(μm)	R_i(μm)	L_T(keV/μm)	$L_{100,T}$(keV/μm)	β^2	z^{*2}/β^2	λ(nm)	$\sigma(\mu m^2)$	Reference
HeLa-S3	1.82E+00		C-12	8.75E+03	1.05E+02	1.91E+01	8.00E+00	3.48E+02	1.82E+02	9.53E+01	1.85E-02	1.92E+03	1.83E+00	5.31E+01	Deering, 1962
Human Kid. T1	7.40E-01	1.10E-01	C-12	1.23E+04	1.48E+02	2.70E+01	1.48E+01	6.20E+02	1.46E+02	7.58E+01	2.60E-02	1.38E+03	2.42E+00	1.72E+01	Blakely, 1979
Human Kid. T1	8.10E-01	6.90E-02	C-12	1.55E+04	1.87E+02	3.41E+01	2.23E+01	9.21E+02	1.18E+02	6.14E+01	3.26E-02	1.10E+03	3.11E+00	1.53E+01	Blakely, 1979
Human Kid. T1	3.90E-01	8.80E-02	C-12	4.85E+04	5.82E+02	1.08E+02	1.62E+02	7.06E+03	4.73E+01	2.47E+01	9.66E-02	3.73E+02	9.03E+00	2.95E+00	Blakely, 1979
Human Kid. T1	3.30E-01	5.30E-02	C-12	6.90E+04	8.28E+02	1.56E+02	2.96E+02	1.32E+04	3.64E+01	1.87E+01	1.33E-01	2.70E+02	1.24E+01	1.92E+00	Blakely, 1979
Human Kid. T1	3.80E-01	4.00E-02	C-12	9.76E+04	1.17E+03	2.24E+02	5.36E+02	2.47E+04	2.75E+01	1.43E+01	1.81E-01	1.99E+02	1.69E+01	1.67E+00	Blakely, 1979
Human Kid. T1	2.20E-01	4.00E-02	C-12	1.75E+05	2.10E+03	4.17E+02	1.36E+03	6.93E+04	1.82E+01	9.43E+00	2.91E-01	1.24E+02	2.73E+01	6.40E-01	Blakely, 1979
Human Kid. T1	2.50E-01	4.40E-02	C-12	2.08E+05	2.50E+03	5.04E+02	1.78E+03	9.34E+04	1.60E+01	8.25E+00	3.32E-01	1.08E+02	3.19E+01	6.40E-01	Blakely, 1979
Human Kid. T1	2.80E-01	2.60E-02	C-12	3.33E+05	4.00E+03	8.55E+02	3.59E+03	2.04E+05	1.24E+01	6.26E+00	4.58E-01	7.87E+01	4.39E+01	5.54E-01	Blakely, 1979
HF19 strain	1.38E+00		N-14	3.70E+03	5.18E+01	8.07E+00	1.69E+00	8.26E+01	4.59E+02	2.45E+02	7.90E-03	5.59E+03	6.05E-01	1.01E+02	Cox,1979
Human Kid. T1	1.18E+00		N-14	6.50E+03	9.10E+01	1.42E+01	4.67E+00	1.91E+02	3.16E+02	1.66E+02	1.36E-02	3.42E+03	9.92E-01	5.95E+01	Todd, 1968
IMR-90	1.49E+00		N-14	2.80E+04	3.92E+02	6.19E+01	6.26E+01	2.26E+03	9.92E+01	5.15E+01	5.75E-02	8.52E+02	4.04E+00	2.37E+01	Ohno, 1984
Human Kid. T1	1.08E+00		O-16	6.56E+03	1.05E+02	1.43E+01	4.75E+00	1.76E+02	3.91E+02	2.05E+02	1.40E-02	4.35E+03	8.11E-01	6.73E+01	Todd, 1968
HeLa-S3	9.52E-01		O-16	8.13E+03	1.30E+02	1.78E+01	7.00E+00	2.45E+02	3.48E+02	1.82E+02	1.72E-02	3.59E+03	9.39E-01	5.31E+01	Deering, 1962
Human Kid. T1	5.00E-01		Ne-20	1.70E+03	3.40E+01	3.71E+00	4.68E-01	2.73E+01	1.18E+03	6.43E+02	3.64E-03	1.79E+04	1.97E-01	9.43E+01	Todd, 1968
Human Kid. T1	9.71E-01		Ne-20	6.60E+03	1.32E+02	1.44E+01	4.80E+00	1.54E+02	6.08E+02	3.19E+02	1.40E-02	6.51E+03	5.17E-01	9.44E+01	Todd, 1968
Human Kid. T1	1.00E+00	0.00E+00	Ne-20	8.08E+03	1.62E+02	1.77E+01	6.92E+00	2.07E+02	5.27E+02	2.76E+02	1.71E-02	5.47E+03	6.21E-01	8.44E+01	Blakely, 1979
Human Kid. T1	1.02E+00	8.00E-03	Ne-20	1.86E+04	3.72E+02	4.08E+01	3.05E+01	7.96E+02	2.88E+02	1.49E+02	3.87E-02	2.56E+03	1.31E+00	4.69E+01	Blakely, 1979
Human Kid. T1	1.04E+00	2.70E-03	Ne-20	3.64E+04	7.27E+02	8.07E+01	9.84E+01	2.56E+03	1.66E+02	8.62E+01	7.37E-02	1.35E+03	2.49E+00	2.76E+01	Blakely, 1979
Human Kid. T1	9.50E-01	6.00E-02	Ne-20	5.60E+04	1.12E+03	1.26E+02	2.07E+02	5.50E+03	1.19E+02	6.02E+01	1.10E-01	9.07E+02	3.78E+00	1.81E+01	Blakely, 1979
Human Kid. T1	5.70E-01	6.30E-02	Ne-20	9.03E+04	1.81E+03	2.06E+02	4.69E+02	1.29E+04	8.02E+01	4.17E+01	1.69E-01	5.92E+02	5.76E+00	7.31E+00	Blakely, 1979
Human Kid. T1	3.40E-01	8.00E-02	Ne-20	1.32E+05	2.64E+03	3.07E+02	8.75E+02	2.53E+04	6.11E+01	3.19E+01	2.33E-01	4.30E+02	7.84E+00	3.32E+00	Blakely, 1979
Human Kid. T1	3.30E-01	6.70E-02	Ne-20	2.41E+05	4.81E+03	5.91E+02	2.22E+03	7.15E+04	4.04E+01	2.07E+01	3.68E-01	2.71E+02	1.29E+01	2.13E+00	Blakely, 1979
Human Kid. T1	2.40E-01	8.20E-02	Ne-20	3.75E+05	7.50E+03	9.80E+02	4.26E+03	1.48E+05	3.28E+01	1.66E+01	4.92E-01	2.03E+02	1.67E+01	1.26E+00	Blakely, 1979
Chang H.Liver	2.57E-01		Ar-40	5.50E+03	2.20E+02	1.20E+01	3.44E+00	1.01E+02	1.77E+03	9.34E+02	1.17E-02	2.02E+04	1.72E-01	7.29E+01	Todd, 1975
Human Kid. T1	4.81E-01		Ar-40	5.70E+03	2.28E+02	1.25E+01	3.68E+00	1.06E+02	1.76E+03	9.25E+02	1.21E-02	1.97E+04	1.74E-01	1.35E+02	Todd, 1968
Human Kid. T1	5.80E-01	1.00E-03	Ar-40	1.48E+04	5.93E+02	3.25E+01	2.05E+01	3.97E+02	1.03E+03	5.34E+02	3.11E-02	9.51E+03	3.53E-01	9.54E+01	Blakely, 1979
Human Kid. T1	7.50E-01	2.00E-03	Ar-40	3.71E+04	1.48E+03	8.24E+01	1.02E+02	1.74E+03	5.26E+02	2.73E+02	7.52E-02	4.25E+03	7.88E-01	6.31E+01	Blakely, 1979
Human Kid. T1	7.90E-01	2.10E-02	Ar-40	5.85E+04	2.34E+03	1.31E+02	2.23E+02	3.79E+03	3.77E+02	1.91E+02	1.15E-01	2.81E+03	1.20E+00	4.76E+01	Blakely, 1979
Human Kid. T1	7.40E-01	8.70E-02	Ar-40	8.38E+04	3.35E+03	1.91E+02	4.13E+02	7.09E+04	2.80E+02	1.45E+02	1.58E-01	2.04E+03	1.64E+00	3.32E+01	Blakely, 1979
Human Kid. T1	8.30E-01	8.00E-02	Ar-40	1.19E+05	4.75E+03	2.75E+02	7.50E+02	1.31E+04	2.05E+02	1.07E+02	2.14E-01	1.52E+03	2.32E+00	2.73E+01	Blakely, 1979
HSF	1.61E+00		Ar-40	1.50E+05	6.00E+03	3.53E+02	1.07E+03	1.98E+04	1.75E+02	9.09E+01	2.58E-01	1.25E+03	2.80E+00	4.50E+01	Chen, 1994
Human Kid. T1	7.90E-01	9.90E-02	Ar-40	1.68E+05	6.73E+03	3.99E+02	1.28E+03	2.41E+04	1.62E+02	8.40E+01	2.83E-01	1.15E+03	3.07E+00	2.05E+01	Blakely, 1979

Cells (Types/Lines)	$\alpha(Gy^{-1})$	$\beta(Gy^{-2})$	Ion Type	E/m (keV/amu)	E(MeV)	$E_{m,s}$(keV)	$R_{m,s}$(μm)	R_f(μm)	L_T(keV/μm)	$L_{100,T}$(keV/μm)	β^2	z^{*2}/β^2	λ(nm)	$\sigma(\mu m^2)$	Reference
Human Kid. T1	7.30E-01	8.90E-02	Ar-40	3.36E+05	1.35E+04	8.63E+02	3.64E+03	7.66E+04	1.09E+02	5.51E+01	4.60E-01	7.04E+02	5.00E+00	1.28E+01	Blakely, 1979
Human Kid. T1	5.20E-01	9.80E-02	Ar-40	4.00E+05	1.60E+04	1.06E+03	4.68E+03	1.01E+05	1.02E+02	5.12E+01	5.11E-01	6.34E+02	5.45E+00	8.48E+00	Blakely, 1979
HSF	1.15E+00		Ar-40	4.80E+05	1.92E+04	1.31E+03	6.07E+03	3.61E+02	9.50E+01	4.66E+01	2.53E-02	1.28E+04	6.12E+00	1.75E+01	Chen, 1994
HSF	1.24E+00		Fe-56	9.40E+04	5.26E+03	2.15E+02	5.03E+02	5.97E+03	5.29E+02	2.75E+02	1.75E-01	3.84E+03	8.76E-01	1.05E+02	Chen, 1994
HSF	1.42E+00		Fe-56	2.01E+05	1.13E+04	4.85E+02	1.69E+03	2.21E+04	3.07E+02	1.58E+02	3.24E-01	2.09E+03	1.65E+00	6.98E+01	Chen, 1994
HSF	5.30E-01		La-139	4.07E+05	5.66E+04	1.08E+03	4.80E+03	3.80E+04	9.75E+02	4.60E+02	5.10E-01	5.80E+03	9.50E-01	8.27E+01	Chen, 1994
HSF	1.50E+00		Fe-56	4.22E+05	2.36E+04	1.13E+03	5.05E+03	7.39E+04	2.00E+02	1.05E+02	2.22E-02	3.05E+04	2.66E+00	4.80E+01	Chen, 1994

AII-4 Neutrons on Hamster Cells

Cells (Types/Lines)	$\alpha(Gy^{-1})$	$\beta(Gy^{-2})$	Type	E(keV)	$E_{m,\delta}$(keV)	$R_{m,\delta}$(μm)	R_i(μm)	L_T(keV/μm)	$L_{100,T}$(keV/μm)	L_D(keV/μm)	$L_{100,D}$(keV/μm)	β^2	z^{*2}/β^2	λ(nm)	σ(μm²)	Reference
V79	1.49E+00		n	5.55E+02	4.52E-01	2.63E-02	1.03E+01	5.95E+01	3.92E+01	6.38E+01	4.39E+01	4.42E-04	3.79E+03	1.67E+00	1.42E+01	Sinclair, 1985
V79	7.28E-01		n	8.00E+02	7.04E-01	4.69E-02	1.75E+01	5.31E+01	3.37E+01	5.81E+01	3.90E+01	6.88E-04	2.76E+03	2.08E+00	6.18E+00	Sinclair, 1985
V79	1.24E+00		n	1.10E+02	6.21E-02	2.70E-03	1.74E+00	5.39E+01	4.86E+01	6.39E+01	5.60E+01	6.07E-05	9.13E+03	1.22E+00	1.07E+01	Hall, 1975
V79	1.41E+00		n	2.20E+02	1.41E-01	6.52E-03	3.21E+00	6.29E+01	4.80E+01	6.99E+01	5.32E+01	1.38E-04	6.93E+03	1.24E+00	1.42E+01	Hall, 1975
V79	1.64E+00		n	3.40E+02	2.45E-01	1.24E-02	5.33E+00	6.39E+01	4.50E+01	6.89E+01	4.95E+01	2.40E-04	5.41E+03	1.36E+00	1.67E+01	Hall, 1975
V79	1.47E+00		n	4.30E+02	3.29E-01	1.77E-02	7.22E+00	6.25E+01	4.25E+01	6.69E+01	4.69E+01	3.22E-04	4.61E+03	1.48E+00	1.47E+01	Hall, 1975
V79	1.21E+00		n	6.80E+02	5.81E-01	3.64E-02	1.37E+01	5.61E+01	3.62E+01	6.07E+01	4.12E+01	5.68E-04	3.19E+03	1.87E+00	1.09E+01	Hall, 1975
V79	1.01E+00		n	1.00E+03	9.13E-01	6.67E-02	2.46E+01	4.85E+01	3.02E+01	5.42E+01	3.60E+01	8.92E-04	2.23E+03	2.43E+00	7.86E+00	Hall, 1975
V79	9.21E-01		n	2.00E+03	1.98E+00	2.03E-01	7.55E+01	3.37E+01	1.99E+01	4.14E+01	2.67E+01	1.93E-03	1.09E+03	4.33E+00	4.96E+00	Hall, 1975
V79	3.36E-01		n	6.00E+03	6.13E+00	1.31E+00	4.98E+02	1.61E+01	8.94E+00	2.39E+01	1.49E+01	6.13E-03	3.27E+02	1.25E+01	8.63E-01	Hall, 1975
V79	2.99E-01		n	1.50E+04	1.61E+01	6.84E+00	2.54E+03	8.03E+00	4.33E+00	1.40E+01	8.45E+00	1.54E-02	1.20E+02	3.17E+01	3.84E-01	Hall, 1975
V79	3.76E-01		n	1.49E+04	1.60E+01	6.76E+00	2.51E+03	8.07E+00	4.36E+00	1.40E+01	8.49E+00	1.53E-02	1.21E+02	3.15E+01	4.85E-01	Hall, 1975
V79	2.86E-01		n	2.10E+04	2.27E+01	1.25E+01	4.65E+03	6.16E+00	3.29E+00	1.13E+01	6.77E+00	2.16E-02	8.38E+01	4.47E+01	2.82E-01	Hall, 1975
V79-379A	9.46E-01		n	2.30E+03	2.31E+00	2.56E-01	9.54E+01	3.09E+01	1.81E+01	3.99E+01	2.49E+01	2.25E-03	9.39E+02	4.92E+00	4.67E+00	Fox, 1988
V79	6.01E-01		n	6.10E+03	6.40E+00	1.34E+00	5.13E+02	1.59E+01	8.85E+00	2.37E+01	1.47E+01	6.22E-03	3.22E+02	1.27E+01	1.53E+00	Hall, 1982
V79	8.12E-01		n	7.10E+03	7.50E+00	1.77E+00	6.70E+02	1.42E+01	7.86E+00	2.18E+01	1.35E+01	7.27E-03	2.72E+02	1.48E+01	1.84E+00	Hall, 1982
V79	6.83E-01		n	7.80E+03	8.27E+00	2.10E+00	7.92E+02	1.32E+01	7.29E+00	2.06E+01	1.27E+01	8.01E-03	2.45E+02	1.63E+01	1.44E+00	Hall, 1982
V79	6.36E-01		n	8.10E+03	8.56E+00	2.23E+00	8.46E+02	1.29E+01	7.10E+00	2.02E+01	1.24E+01	8.29E-03	2.36E+02	1.69E+01	1.31E+00	Hall, 1982
V79	6.73E-01		n	1.40E+04	1.50E+01	6.05E+00	2.24E+03	8.47E+00	4.58E+00	1.46E+01	8.83E+00	1.44E-02	1.30E+02	2.96E+01	9.12E-01	Hall, 1982
V79	5.58E-01		n	1.43E+04	1.54E+01	6.33E+00	2.33E+03	8.32E+00	4.49E+00	1.44E+01	8.70E+00	1.48E-02	1.26E+02	3.03E+01	7.43E-01	Hall, 1982
V79	5.45E-01		n	1.93E+04	2.08E+01	1.08E+01	4.00E+03	6.59E+00	3.53E+00	1.19E+01	7.16E+00	1.99E-02	9.18E+01	4.10E+01	5.74E-01	Hall, 1982
V79	8.60E-01		n	2.53E+04	2.74E+01	1.75E+01	6.51E+03	5.31E+00	2.83E+00	1.00E+01	5.97E+00	2.60E-02	6.88E+01	5.41E+01	7.30E-01	Hall, 1982
V79	4.76E-01		n	3.24E+04	3.53E+01	2.71E+01	1.02E+04	4.35E+00	2.31E+00	8.50E+00	5.04E+00	3.31E-02	5.30E+01	6.95E+01	3.31E-01	Hall, 1982
V79	2.52E-01		n	5.00E+04	5.49E+01	5.81E+01	2.23E+04	3.06E+00	1.61E+00	6.35E+00	3.72E+00	5.04E-02	3.38E+01	1.08E+02	1.23E-01	Hall, 1982
V79-379A	6.33E-01	6.61E-02	n	2.30E+03	2.31E+00	2.56E-01	9.54E+01	3.09E+01	1.81E+01	3.89E+01	2.49E+01	2.25E-03	9.39E+02	4.92E+00	3.13E+00	Prise, 1987
CHO	8.26E-01		n	1.47E+04	1.58E+01	6.60E+00	2.45E+03	8.16E+00	4.40E+00	1.41E+01	8.56E+00	1.51E-02	1.23E+02	3.11E+01	1.08E+00	Raillton, 1973
CHO	9.80E-01		n	1.47E+04	1.58E+01	6.60E+00	2.45E+03	8.16E+00	4.40E+00	1.41E+01	8.56E+00	1.51E-02	1.23E+02	3.11E+01	1.28E+00	Raillton, 1974
CHO	1.33E+00		n	3.50E+03	3.54E+00	5.16E-01	1.94E+02	3.18E+01	1.35E+01	3.54E+01	2.01E+01	3.50E-03	5.94E+02	7.33E+00	6.79E+00	Key, 1971
CHO	1.61E+00		n	5.83E+02	4.71E-01	2.74E-02	1.11E+01	5.87E+01	3.85E+01	6.31E+01	4.32E+01	4.71E-04	3.63E+03	1.71E+00	1.51E+01	Key, 1971
CHO	2.22E+00		n	4.33E+02	3.28E-01	1.81E-02	7.35E+00	6.24E+01	4.25E+01	6.68E+01	4.69E+01	3.25E-04	4.59E+03	1.48E+00	2.22E+01	Key, 1971
CHO	3.57E+00		n	1.76E+02	1.08E-01	5.04E-03	2.66E+00	6.07E+01	4.87E+01	6.89E+01	5.45E+01	1.05E-04	7.68E+03	1.22E+00	3.47E+01	Key, 1971
V79	3.40E-01	7.51E-02	n	1.70E+04	1.84E+01	8.65E+00	3.18E+03	7.26E+00	3.90E+00	1.29E+01	7.78E+00	1.76E-02	1.05E+02	3.61E+01	3.95E-01	Cox, 1977.

AII-5 Neutrons on Mouse Cells

Cells (Types/Lines)	$\alpha(Gy^{-1})$	$\beta(Gy^{-2})$	Type	E(keV)	$E_{m,a}$(keV)	$R_{m,a}$(μm)	R_i(μm)	L_T(keV/μm)	$L_{100,T}$(keV/μm)	L_D(keV/μm)	$L_{100,D}$(keV/μm)	β^2	z^{*2}/β^2	λ(nm)	$\sigma(\mu m^2)$	Reference
C3H10T1/2	1.60E+00	7.00E-02	n	2.30E+02	1.48E-01	7.07E-03	3.34E+00	6.32E+01	4.78E+01	7.00E+01	5.29E+01	1.46E-04	6.78E+03	1.25E+00	1.62E+01	Miller, 1989
C3H10T1/2	2.00E+00	7.00E-02	n	3.50E+02	2.52E-01	1.30E-02	5.58E+00	6.38E+01	4.47E+01	6.87E+01	4.98E+01	2.49E-04	5.31E+03	1.37E+00	2.04E+01	Miller, 1989
C3H10T1/2	1.40E+00	7.00E-02	n	4.50E+02	3.43E-01	1.90E-02	7.61E+00	6.20E+01	4.20E+01	6.64E+01	4.64E+01	3.42E-04	4.45E+03	1.51E+00	1.39E+01	Miller, 1989
C3H10T1/2	3.26E+00		n	5.00E+02	3.87E-01	2.18E-02	8.93E+00	6.09E+01	4.06E+01	6.60E+01	4.52E+01	3.89E-04	4.11E+03	1.58E+00	3.17E+01	Barrendsen, 1985
C3H10T1/2	5.00E-02	6.80E-01	n	7.00E+02	6.01E-01	3.80E-02	1.43E+01	5.56E+01	3.57E+01	6.03E+01	4.08E+01	5.87E-04	3.11E+03	1.91E+00	4.45E-01	Blacer-Kubiczek, 1991
C3H10T1/2	1.20E+00	7.00E-02	n	7.00E+02	6.01E-01	3.80E-02	1.43E+01	5.56E+01	3.58E+01	6.03E+01	4.08E+01	5.87E-04	3.11E+03	1.91E+00	1.07E+01	Miller, 1989
C3H10T1/2	1.30E+00	7.00E-02	n	9.60E+02	8.67E-01	6.31E-02	2.32E+01	4.93E+01	1.13E+01	5.49E+01	3.08E+01	8.52E-04	2.32E+03	2.36E+00	1.03E+01	Miller, 1989
C3H10T1/2	1.20E+00	7.00E-02	n	1.96E+03	1.92E+00	1.96E-01	7.39E+01	3.40E+01	2.01E+01	4.18E+01	2.69E+01	1.89E-03	1.12E+03	4.25E+00	6.53E+00	Miller, 1989
C3H10T1/2	1.55E+00		n	4.20E+03	4.23E+00	7.07E-01	2.66E+02	2.07E+01	1.17E+01	2.90E+01	1.82E+01	4.24E-03	4.86E+02	8.77E+00	5.14E+00	Barendsen, 1985
C3H10T1/2	1.40E+00	7.00E-02	n	5.90E+03	6.06E+00	1.33E+00	5.00E+02	1.63E+01	9.08E+00	2.42E+01	1.50E+01	6.01E-03	3.34E+02	1.23E+01	3.64E+00	Miller, 1989
C3H10T1/2	5.00E-02	6.80E-01	n	9.70E+03	1.06E+01	3.17E+00	1.19E+03	5.56E+01	3.57E+01	6.03E+01	4.08E+01	5.87E-04	3.11E+03	1.91E+00	4.45E-01	Blacer-Kubiczek, 1991
C3H10T1/2	1.20E+00	7.00E-02	n	1.37E+04	1.38E+01	6.38E+00	2.13E+03	8.26E+00	4.66E+00	1.48E+01	8.96E+00	1.41E-02	1.32E+02	2.89E+01	1.59E+00	Miller, 1989
P388F	7.69E-01		n	1.40E+04	1.50E+01	6.05E+00	2.24E+03	8.47E+00	4.58E+00	1.46E+01	8.83E+00	1.44E-02	1.30E+02	2.96E+01	1.04E+00	Nias, 1967
C3H10T1/2	8.20E-01		n	1.50E+04	1.61E+01	6.84E+00	2.54E+03	8.03E+00	4.33E+00	1.40E+01	8.45E+00	1.54E-02	1.20E+02	3.17E+01	1.05E+00	Barrendsen, 1985

AII-6 Neutrons on Human Cells

Cells (Types/Lines)	$\alpha(Gy^{-1})$	$\beta(Gy^{-2})$	Ions	E(keV)	$E_{m,a}$(keV)	$R_{m,a}$(μm)	R_i(μm)	L_T(keV/μm)	$L_{100,T}$(keV/μm)	L_D(keV/μm)	$L_{100,D}$(keV/μm)	β^2	z^{*2}/β^2	λ(nm)	$\sigma(\mu m^2)$	Ref.
HeLa	7.10E-01		n	2.40E+01	1.32E-02	6.98E-04	1.86E-01	3.08E+01	3.08E+01	3.68E+01	3.68E+01	1.29E-05	1.28E+04	1.44E+00	3.50E+00	Morgan, 1986
Human Kidney T1	1.26E+00		n	9.00E+02	8.10E-01	5.67E-02	2.09E+01	5.07E+01	3.18E+01	5.60E+01	3.74E+01	7.92E-04	2.47E+03	2.25E+00	1.02E+01	Broerse, 1968
Human Kidney T1	1.08E+00		n	3.00E+03	3.06E+00	3.98E-01	1.50E+02	2.60E+01	1.50E+01	3.43E+01	2.18E+01	2.98E-03	7.03E+02	6.33E+00	4.50E+00	Broerse, 1968
Human Kid. T1	9.52E-01		n	4.40E+03	4.56E+00	7.54E-01	2.90E+02	2.01E+01	1.14E+01	2.83E+01	1.78E+01	4.43E-03	4.62E+02	9.16E+00	3.06E+00	Barendsen, 1966
Human Kidney T1	7.43E-01		n	6.50E+03	6.85E+00	1.51E+00	5.74E+02	1.52E+01	8.42E+00	2.29E+01	1.42E+01	6.64E-03	3.00E+02	1.36E+01	1.80E+00	Broerse, 1968
Human Kidney T1	8.63E-01		n	8.00E+03	8.46E+00	2.18E+00	8.28E+02	1.30E+01	7.16E+00	2.03E+01	1.25E+01	8.19E-03	2.39E+02	1.67E+01	1.79E+00	Broerse, 1968
HeLa	7.30E-01		n	1.40E+04	2.29E+02	5.59E+02	2.24E+03	8.47E+00	4.58E+00	1.46E+01	8.83E+00	1.44E-02	1.30E+02	2.96E+01	9.89E-01	Nias, 1967
Human Kidney T1	6.54E-01		n	1.50E+04	1.61E+01	6.84E+00	2.54E+03	8.03E+00	4.33E+00	1.40E+01	8.45E+00	1.54E-02	1.20E+02	3.17E+01	8.40E-01	Broerse, 1968
HeLa	5.40E-01		n	2.50E+04	2.71E+01	1.71E+01	6.37E+03	5.36E+00	2.85E+00	1.01E+01	6.02E+00	2.57E-02	6.96E+01	5.34E+01	4.63E-01	Britten, 1992
HF19	1.31E+00		n	1.00E+05	1.84E+01	8.65E+00	3.18E+03	7.26E+00	3.90E+00	1.29E+01	7.78E+00	1.76E-02	1.05E+02	3.61E+01	1.52E+00	Cox, 1977

AII-7 Sparsely Ionising Radiation on Hamster Cells

Cells (Types/Lines)	Dose rate	$\alpha(Gy^{-1})$	$\beta(Gy^{-2})$	Ions	Source	E_p(keV)	R_{max}(μm)	R_i(μm)	L_T(keV/μm)	$L_{100,T}$(keV/μm)	L_D(keV/μm)	$L_{100,D}$(keV/μm)	λ(nm)	$\sigma(\mu m^2)$	Reference
V79-171	9.0 Gy/min	1.70E-01	3.90E-02	e		1.10E+04	2.60E+04	5.42E+04	1.98E-01	1.28E-01			5.86E+02	5.39E-03	Spadinger, 1992
CHO	9.0 Gy/min	1.40E-01	6.60E-02	e		1.10E+04	2.60E+04	5.42E+04	1.98E-01	1.28E-01			5.86E+02	4.44E-03	Spadinger, 1992
V79	2.5 Gy/min	4.80E-01	2.70E-01	C_k x-rays	0.277 KeV	1.29E-01			2.21E+01	2.21E+01	2.30E+01	2.29E+01	2.04E+00	1.70E+00	Goodhead, 1979
V79		5.23E-01		Al_k x-rays	1.486 KeV	5.34E-01			1.67E+01	1.51E+01	1.77E+01	1.67E+01	2.88E+00	1.40E+00	Goodhead, 1980
V79	5.0 Gy/min	4.38E-01	6.56E-02	Al_k x-rays	1.486 KeV	5.34E-01			1.67E+01	1.51E+01	1.77E+01	1.67E+01	2.88E+00	1.17E+00	Cox, 1977
V79-379A	2.5	5.70E-01	6.20E-02	Al_k x-rays	1.486 KeV	5.34E-01			1.67E+01	1.51E+01	1.77E+01	1.67E+01	2.88E+00	1.53E+00	Prise, 1989
V79		4.53E-01		Ti_k x-rays	4.510 KeV	2.49E+00			7.70E+00	5.70E+00	9.51E+00	8.21E+00	7.80E+00	5.58E-01	Goodhead, 1980
V79-171	1.1Gy/min	2.90E-01	4.10E-02	x-rays	55 KVp	8.29E+00			8.34E+00	7.12E+00	9.66E+00	8.80E+00	6.39E+00	3.87E-01	Spadinger, 1992
CHO	1.1Gy/min	3.00E-01	7.70E-02	x-rays	55 KVp	8.29E+00			8.34E+00	7.12E+00	9.66E+00	8.80E+00	6.39E+00	4.00E-01	Spadinger, 1992
CHO-SC1 & -tsH1	1 Gy/min	1.90E-01	6.00E-02	x-rays	150 KVp	8.50E+00			7.03E+00	5.74E+00	8.48E+00	7.55E+00	8.11E+00	2.14E-01	Chang, 1992
V79/4		1.37E-01		x-rays	180 KVp	1.00E+01			6.10E+00	4.89E+00	7.54E+00	6.64E+00	9.56E+00	1.34E-01	Tolkendorf, 1983
V79-753B	1 Gy/min	1.28E-01	4.60E-02	x-rays	200 KVp	1.12E+01			5.40E+00	4.26E+00	6.83E+00	5.96E+00	1.07E+01	1.11E-01	Belli, 1989
V79		1.36E-01	2.70E-03	x-rays	210 KVp	1.21E+01			5.19E+00	4.05E+00	6.59E+00	5.74E+00	1.13E+01	1.13E-01	Hall, 1972
V79	2.7 Gy /min	1.77E-01		x-rays	225 KVp	1.35E+01			4.86E+00	3.79E+00	6.23E+00	5.40E+00	1.22E+01	1.37E-01	Ngo, 1981
V79-379A		1.30E-01	4.80E-02	x-rays	240 KVp	1.50E+01			4.57E+00	3.38E+00	5.82E+00	5.00E+00	1.33E+01	9.52E-02	Folkard, 1996
CHO	1.8 Gy/min	2.00E-01	7.30E-02	x-rays	250 KVp	1.58E+01			4.31E+00	3.33E+00	5.63E+00	4.85E+00	1.37E+01	1.38E-01	Spadinger, 1992
V79-4		9.40E-02	3.32E-02	x-rays	250 KVp	1.58E+01			4.31E+00	3.33E+00	5.63E+00	4.85E+00	1.37E+01	6.48E-02	Thacker, 1982
V79-379A	1.8	1.10E-01	2.70E-02	x-rays	250 KVp	1.58E+01			4.31E+00	3.33E+00	5.63E+00	4.85E+00	1.37E+01	7.58E-02	Prise, 1990
V79	0.5-2.Gy/min	1.43E-01	2.59E-02	x-rays	250 KVp	1.58E+01			4.31E+00	3.33E+00	5.63E+00	4.85E+00	1.37E+01	9.86E-02	Thacker, 1979
V79	0.1 Gy/min	2.38E-01		x-rays	250 KVp	1.58E+01			4.31E+00	3.33E+00	5.63E+00	4.85E+00	1.37E+01	1.64E-01	Schlag, 1981
V79-171	1.8 Gy/min	2.30E-01	5.10E-02	x-rays	250 KVp	1.58E+01			4.31E+00	3.33E+00	5.63E+00	4.85E+00	1.37E+01	1.59E-01	Spadinger, 1992
V79	6.5 Gy/min	1.40E-01	5.50E-03	γ-rays	Co-60	3.55E+02			4.44E-01	2.84E-01	6.88E-01	5.15E-01	1.71E+02	9.95E-03	Perris, 1986
CHO	3.4 Gy/min	1.40E-01	6.60E-02	γ-rays	Co-60	3.55E+02			4.44E-01	2.84E-01	6.88E-01	5.15E-01	1.71E+02	9.95E-03	Spadinger, 1992
CHO-10B		2.30E-01	3.00E-02	γ-rays	Co-60	3.55E+02			4.44E-01	2.84E-01	6.88E-01	5.15E-01	1.71E+02	1.63E-02	Raju, 1991
V79-171	3.4 Gy/min	1.70E-01	3.90E-02	γ-rays	Co-60	3.55E+02			4.44E-01	2.84E-01	6.88E-01	5.15E-01	1.71E+02	1.21E-02	Spadinger, 1992
V79	2.0-3.50	1.80E-01	1.96E-02	γ-rays	Co-60	3.55E+02			4.44E-01	2.84E-01	6.88E-01	5.15E-01	1.71E+02	1.28E-02	Millar, 1978
V79	3 Gy/min	2.38E-01		γ-rays	Co-60	3.55E+02			4.44E-01	2.84E-01	6.88E-01	5.15E-01	1.71E+02	1.69E-02	Schlag, 1981
CHO	0.7 Gy/min	2.19E-01		γ-rays	Co-60	3.55E+02			4.44E-01	2.84E-01	6.88E-01	5.15E-01	1.71E+02	1.56E-02	Raillton, 1973
CHO	0.15 Gy/min	2.88E-01		γ-rays	Co-60	3.55E+02			4.44E-01	2.84E-01	6.88E-01	5.15E-01	1.71E+02	2.05E-02	Raillton, 1974
V79/4(AH1)	16.0 Gy/min	2.24E-01	1.28E-02	γ-rays	Co-60	3.55E+02			4.44E-01	2.84E-01	6.88E-01	5.15E-01	1.71E+02	1.59E-02	Morgan, 1986
V79		1.40E-01	1.50E-02	γ-rays	Co-60	3.55E+02			4.44E-01	2.84E-01	6.88E-01	5.15E-01	1.71E+02	9.95E-03	Raju, 1991
V79	1.20 Gy/min	1.43E-01	2.59E-02	γ-rays	Co-60	3.55E+02			4.44E-01	2.84E-01	6.88E-01	5.15E-01	1.71E+02	1.02E-02	Thacker, 1979
V79		2.67E-01		γ-rays	Co-60	3.55E+02			4.44E-01	2.84E-01	6.88E-01	5.15E-01	1.71E+02	1.89E-02	Goodhead, 1980

AII-8 Sparsely Ionising Radiation on Mouse Cells

Cells (Types/Lines)	Dose rate	$\alpha(Gy^{-1})$	$\beta(Gy^{-2})$	Ions	Source	E_p(keV)	$R_{m,i}$(μm)	R_i(μm)	L_T(keV/μm)	$L_{100,T}$(keV/μm)	L_D(keV/μm)	$L_{100,D}$(keV/μm)	λ(nm)	$\sigma(\mu m^2)$	Reference
C3H10T1/2	0.43 Gy/min	3.36E-01		Cr x-rays	5.4 KeV	3.09E+00			6.70E+00	4.90E+00	8.55E+00	7.31E+00	9.18E+00	3.61E-01	Hieber, 1990
C3H10T1/2		2.70E-01	3.00E-02	x-rays	80 KVp	7.44E+00			8.36E+00	7.02E+00	9.77E+00	8.84E+00	6.45E+00	3.61E-01	Napolitano, 1992
C3H10T1/2		2.34E-01		x-rays	250 kVp	1.58E+01			4.31E+00	3.33E+00	5.63E+00	4.85E+00	1.37E+01	1.61E-01	Miller, 1995
C3H10T1/2		5.65E-02	7.00E-02	x-rays	250 kVp	1.58E+01			4.31E+00	3.33E+00	5.63E+00	4.85E+00	1.37E+01	3.90E-02	Miller, 1989
C3H10T1/2	1.8 Gy/min	1.93E-01		x-rays	250 kVp	1.58E+01			4.31E+00	3.33E+00	5.63E+00	4.85E+00	1.37E+01	1.33E-01	Goodhead, 1992
C3H10T1/2	1.25 Gy/min	1.80E-01	4.40E-02	x-rays	250 kVp	1.58E+01			4.31E+00	3.33E+00	5.63E+00	4.85E+00	1.37E+01	1.24E-01	Hei, 1988a
P388F	0.1 Gy/min	3.22E-01		x-rays	300 KV	1.91E+01			3.97E+00	3.04E+00	5.23E+00	4.49E+00	1.50E+01	2.04E-01	Nias, 1967
C3H10T1/2		2.50E-01	3.60E-02	x-rays	300 KV	1.91E+01			3.97E+00	3.04E+00	5.23E+00	4.49E+00	1.50E+01	1.59E-01	Barrendsen, 1985
C3H10T1/2		1.85E-01	2.15E-02	γ	C0-60	3.55E+02			4.44E-01	2.84E-01	6.88E-01	5.15E-01	1.71E+02	1.31E-02	Roberts, 1987
C3H10T1/2		1.42E-01		γ	Co-60	3.55E+02			4.44E-01	2.84E-01	6.88E-01	5.15E-01	1.71E+02	1.01E-02	Hieber, 1987
C3H10T1/2	0.5 Gy/min	2.49E-01		γ	Co-60	3.55E+02			4.44E-01	2.84E-01	6.88E-01	5.15E-01	1.71E+02	1.77E-02	Hieber, 1990

AII-9 Sparsely Ionising Radiation on Human Cells

Cells (Types/Lines)	Dose rate	$\alpha(Gy^{-1})$	$\beta(Gy^{-2})$	Rad. Type	Source	E_p(keV)	R_{max}(μm)	R_i(μm)	L_T(keV/μm)	$L_{100,T}$(keV/μm)	L_D(keV/μm)	$L_{100,D}$(keV/μm)	λ(nm)	$\sigma(\mu m^2)$	Ref.
T1 Human Kid.		7.80E-02		β	Y-90	9.35E+02	1.76E+03	4.37E+03	2.04E-01	1.16E-01			4.46E+02	2.55E-03	Barendsen, 1962
HF19	2.5 Gy/min	3.00E+00		C-k x-rays	0.277 KeV	1.29E-01			2.21E+01	2.21E+01	2.30E+01	2.29E+01	2.04E+00	1.06E+01	Goodhead,1979
HF19		2.93E+00		Ck x-rays	0.277 KeV	1.29E-01			2.21E+01	2.21E+01	2.30E+01	2.29E+01	2.04E+00	1.04E+01	Goodhead, 1980
HF19	5.0 Gy/min	1.60E+00		Al-k x-ray	1.486 KeV	5.34E-01			1.67E+01	1.51E+01	1.77E+01	1.67E+01	2.88E+00	4.82E+00	Cox, 1977.
HF19		1.60E+00		Alk x-rays	1.486 KeV	5.34E-01			1.67E+01	1.51E+01	1.77E+01	1.67E+01	2.88E+00	4.82E+00	Goodhead, 1980
HF19		1.46E+00		Tik x-rays	4.510 KeV	2.49E+00			7.70E+00	5.70E+00	9.51E+00	8.21E+00	7.80E+00	1.80E+00	Goodhead, 1980
T1 Human Kid.		1.29E-01		x-rays	20 KVp	8.78E+00			5.35E+00	4.51E+00	6.78E+00	6.04E+00	9.95E+00	1.10E-01	Barendsen, 1962
Human Kid. T1	4.06 Gy/min	2.58E-01		x-rays	50 KVp	8.48E+00			8.28E+00	7.09E+00	9.58E+00	8.74E+00	6.43E+00	3.41E-01	Todd, 1965
T1 Human Kid.		1.03E-01		x-rays	200 KVp	1.12E+01			5.40E+00	4.26E+00	6.83E+00	5.96E+00	1.07E+01	8.88E-02	Barendsen, 1962
HeLa-S3	0.3 Gy/min	3.54E-01		x-rays	200 KVp	1.12E+01			5.40E+00	4.26E+00	6.83E+00	5.96E+00	1.07E+01	3.06E-01	Sasaki, 1983
Human Kid. T1	2.7 Gy/min	5.10E-01	1.40E-01	x-rays	220 KVp	1.30E+01			4.97E+00	3.88E+00	5.52E+00	5.63E+00	1.19E+01	4.05E-01	Blakely, 1979
Human Kid. T1	0.75 Gy/min	2.22E-01		x-rays	250 KVp	1.58E+01			4.31E+00	3.33E+00	5.63E+00	4.85E+00	1.37E+01	1.53E-01	Barendsen, 1966
HF19 strain		7.97E-01		x-rays	250 KVp	1.58E+01			4.31E+00	3.33E+00	5.63E+00	4.85E+00	1.37E+01	5.49E-01	Cox,1 979
HeLa-S3	1.8 Gy/min	5.59E-01		x-rays	250 KVp	1.58E+01			4.31E+00	3.33E+00	5.63E+00	4.85E+00	1.37E+01	3.85E-01	Goodhead, 1992
HeLa	0.5 Gy/min	3.80E-03	5.90E-04	x-rays	250 KVp	1.58E+01			4.31E+00	3.33E+00	5.63E+00	4.85E+00	1.37E+01	2.62E-03	Morgan, 1986
HeLa	1.8 Gy/min	5.92E-01		x-rays	250 KVp	1.58E+01			4.31E+00	3.33E+00	5.63E+00	4.85E+00	1.37E+01	4.08E-01	Goodhead, 1992
HeLa-S3	3.5 Gy/min	1.97E-01		x-rays	250 KVp	1.58E+01			4.31E+00	3.33E+00	5.63E+00	4.85E+00	1.37E+01	1.36E-01	Deering, 1962
HeLa	0.30 Gy/min	1.28E-01		x-rays	300 KVp	1.91E+01			3.97E+00	3.04E+00	5.23E+00	4.49E+00	1.50E+01	8.12E-02	Nias, 1967
HeLa	1Gy/min	2.22E-01		x-rays	300 KVp	1.91E+01			3.97E+00	3.04E+00	5.23E+00	4.49E+00	1.50E+01	1.41E-01	Nias, 1969
Human cells(EUE)		5.52E-01		γ	Co-60	3.55E+02			4.44E-01	2.84E-01	6.88E-01	5.15E-01	1.71E+02	3.92E-02	Bettega, 1979
IMR-90	1 Gy/min	3.11E-01		γ	Co-60	3.55E+02			4.44E-01	2.84E-01	6.88E-01	5.15E-01	1.71E+02	2.21E-02	Ohno, 1984
HF19		1.19E+00		γ	Co-60	3.55E+02			4.44E-01	2.84E-01	6.88E-01	5.15E-01	1.71E+02	8.44E-02	Goodhead, 1980
HSF		2.47E-01		γ	Cs-137	1.59E+02			7.53E-01	5.05E-01	1.19E+00	9.27E-01	9.42E+01	2.98E-02	Hei, 1988

AIII Chromosome Dicentrics Database

AIII-1 Charged Particles on Human Cells

Cells (Types/Lines)	α(dic's/Gy-cell)	β(dic's/Gy^2-cell)	Ions	E(keV/amu)	E(MeV)	L_T(keV/μm)	$L_{100,T}$(keV/μm)	β^2	z^{*2}/β^2	λ(nm)	σ(μm^2)	Reference
Human Lymphocyte	1.09E-01	3.18E-02	pi-meson	1.10E+04	1.10E+01	8.70E-01	4.35E-01	1.41E-01	7.10E+00	3.69E+02	1.52E-02	Lloyd, 1975
Human Lymphocyte	5.69E-02	2.80E-02	pi-meson	6.00E+04	6.00E+01	3.07E-01	1.54E-01	5.11E-01	1.96E+00	1.36E+03	2.80E-03	Lloyd, 1975
Human Lymphocyte	2.76E-01	1.36E-01	p	4.90E+03	4.90E+00	8.28E+00	4.41E+00	1.04E-02	9.65E+01	3.56E+01	3.66E-01	Takatsuji, 1983
Human Lymphocyte	5.10E-02	5.30E-03	p	7.40E+03	7.40E+00	5.87E+00	3.10E+00	1.56E-02	6.42E+01	5.48E+01	4.79E-02	Bocian, 1973
Human Lymphocyte	2.30E-01	3.00E-02	p	8.00E+03	8.00E+00	5.69E+00	3.00E+00	1.68E-02	5.94E+01	5.69E+01	2.09E-01	Bettega, 1981
Human Lymphocyte	4.36E-02	5.81E-02	p	8.70E+03	8.70E+00	5.25E+00	2.77E+00	1.83E-02	5.47E+01	6.28E+01	3.66E-02	Edwards, 1986
Human Lymphocyte	1.00E-01	4.00E-02	p	1.20E+04	1.20E+01	4.01E+00	2.10E+00	2.51E-02	3.99E+01	8.70E+01	6.42E-02	Bettega, 1981
Human Lymphocyte	1.78E-01	3.08E-02	p	1.40E+04	1.40E+01	3.60E+00	1.88E+00	2.92E-02	3.43E+01	9.95E+01	1.02E-01	Matsubara, 1990
Human Lymphocyte	4.40E-02	1.90E-02	p	1.65E+04	1.65E+01	3.21E+00	1.68E+00	3.43E-02	2.92E+01	1.14E+02	2.26E-02	Rimpl, 1990
Human Lymphocyte	1.43E-01	2.65E-02	p	2.20E+04	2.20E+01	2.48E+00	1.29E+00	4.53E-02	2.21E+01	1.55E+02	5.67E-02	Matsubara, 1990
Human Lymphocyte	5.00E-02	3.00E-02	p	3.10E+04	3.10E+01	1.87E+00	9.75E-01	6.29E-02	1.59E+01	2.16E+02	1.49E-02	Bettega, 1981
Human Lymphocyte	8.72E-02	4.03E-02	p	3.90E+04	3.90E+01	1.53E+00	8.00E-01	8.01E-02	1.25E+01	2.72E+02	2.13E-02	Matsubara, 1990
Human Lymphocyte	5.40E-02	1.19E-02	p	5.00E+04	5.00E+01	1.27E+00	6.66E-01	9.86E-02	1.01E+01	3.36E+02	1.09E-02	Todorov, 1975
Human Lymphocyte	4.05E-01	-7.80E-01	He-3	7.83E+03	2.35E+01	2.78E+01	1.49E+01	1.25E-02	3.20E+02	1.10E+01	1.80E+00	Edwards, 1986
Human Lymphocyte	5.20E-01	5.30E+01	α	6.97E+02	2.79E+00	1.36E+02	7.68E+01	1.49E-03	2.67E+03	1.30E+00	1.13E+01	Vulpis, 1973
HFL6052	5.70E-01		α	1.03E+03	4.10E+00	1.06E+02	5.95E+01	2.20E-03	1.82E+03	1.86E+00	9.62E+00	Simmon, 1996
HFL5496	6.60E-01		α	1.04E+03	4.15E+00	1.01E+02	5.66E+01	2.22E-03	1.80E+03	1.98E+00	1.07E+01	Simmon, 1996
HFL4916	6.40E-01		α	1.14E+03	4.55E+00	9.76E+01	5.50E+01	2.44E-03	1.64E+03	2.07E+00	1.00E+01	Simmon, 1996
Human Lymphocyte	2.86E-01		α	1.23E+03	4.90E+00	1.35E+02	8.23E+01	2.62E-03	1.53E+03	1.13E+00	6.19E+00	Edwards, 1980
Human Lymphocyte	3.72E-01		α	1.29E+03	5.15E+00	8.98E+01	5.04E+01	2.76E-03	1.45E+03	2.33E+00	5.35E+00	Purrott, 1980
Human Lymphocyte	4.90E+00		α	1.41E+03	5.65E+00	8.29E+01	4.66E+01	3.02E-03	1.32E+03	2.58E+00	6.50E+01	Dufrain, 1979
Human Lymphocyte	7.55E-01	2.10E-02	α	5.75E+03	2.30E+01	2.94E+01	1.57E+01	1.22E-02	3.27E+02	1.03E+01	3.55E+00	Takatsuji,1984
Human Lymphocyte	8.00E-01		C-12	3.54E+04	4.25E+02	5.93E+01	3.08E+01	7.18E-02	5.02E+02	6.99E+00	7.59E+00	Edwards, 1994
Human Lymphocyte	3.80E-01		O-16	6.23E+04	9.96E+02	6.94E+01	3.54E+01	1.21E-01	5.27E+02	6.51E+00	4.22E+00	Edwards, 1994
Human Lymphocyte	5.10E-01	1.72E-01	O-16	9.25E+04	1.48E+03	5.10E+01	2.66E+01	1.72E-01	3.71E+02	9.06E+00	4.16E+00	Edwards, 1994
Human Lymphocyte	4.10E-03		Ne-20	9.45E+03	1.89E+02	4.61E+02	2.41E+02	2.00E-02	4.77E+03	7.36E-01	3.02E-01	Edwards, 1994

AIII-2 Charged Particles on Mouse and Hamster Cells

Cells (Types/Lines)	α(dic's/Gy-cell)	β(dic's/Gy^2-cell)	Ions	E(keV/amu)	E(MeV)	L_T(keV/μm)	$L_{100,T}$(keV/μm)	β^2	z^{*2}/β^2	λ(nm)	σ(μm^2)	Reference
CH2B2	8.75E-02		He-4	1.00E+04	4.00E+01	1.87E+01	9.91E+00	2.11E-02	1.39E+02	1.79E+01	2.62E-01	Skarsgard, 1967
CH2B2	3.11E-01		Li-6	5.00E+03	3.00E+01	8.16E+01	4.33E+01	9.12E-03	9.87E+02	3.54E+00	4.06E+00	Skarsgard, 1967
CH2B2	1.75E-01		Li-6	9.67E+03	5.80E+01	5.02E+01	2.63E+01	1.75E-02	5.14E+02	6.53E+00	1.40E+00	Skarsgard, 1967
CH2B2	4.40E-01		B-11	9.27E+03	1.02E+02	1.26E+02	6.58E+01	1.96E-02	1.27E+03	2.66E+00	8.87E+00	Skarsgard, 1967
CH2B2	5.29E-01		C-12	8.83E+03	1.06E+02	1.82E+02	9.50E+01	1.87E-02	1.90E+03	1.84E+00	1.54E+01	Skarsgard, 1967
CH2B2	2.01E-01		O-16	8.19E+03	1.31E+02	3.47E+02	1.82E+02	1.73E-02	3.56E+03	9.43E-01	1.12E+01	Skarsgard, 1967
V79	1.49E-01		p	4.00E+03	4.00E+00	1.00E+01	5.24E+00	8.47E-03	1.18E+02	2.87E+01	2.39E-01	Geard, 1985
V79	5.75E-01		D	5.50E+02	1.10E+00	4.00E+01	2.27E+01	1.17E-03	8.53E+02	4.10E+00	3.68E+00	Geard, 1985
V79	2.48E-01		D	1.50E+03	3.00E+00	2.00E+01	1.10E+01	3.19E-03	3.13E+02	1.12E+01	7.93E-01	Geard, 1985
V79	5.31E-01		He-3	1.47E+03	4.40E+00	8.00E+01	4.52E+01	3.13E-03	1.28E+03	2.69E+00	6.80E+00	Geard, 1985
V79-4	2.58E-01		He-4	4.50E+02	1.80E+00	1.58E+02	8.93E+01	1.17E-03	3.37E+03	1.04E+00	6.50E+00	Tolkendorf, 1983
V79	3.00E-01		α	1.04E+03	4.14E+00	1.02E+02	5.72E+01	2.22E-03	1.80E+03	1.95E+00	4.89E+00	Simmon, 1996
V79-4	1.16E-01		He-4	1.05E+03	4.20E+00	9.87E+01	5.56E+01	2.36E-03	1.69E+03	2.04E+00	1.82E+00	Tolkendorf, 1983
V79-4	9.37E-02		He-4	2.93E+03	1.17E+01	4.98E+01	2.71E+01	6.20E-03	6.45E+02	5.19E+00	7.46E-01	Tolkendorf, 1983

AIII-3 Neutrons on Human Cells

Cells (Types/Lines)	Dose rate	α(dic's/Gy-cell)	β(dic's/Gy^2-cell)	Rad. Type	E(keV)	L_T(keV/μm)	$L_{100,T}$(keV/μm)	L_D(keV/μm)	$L_{100,D}$(keV/μm)	β^2	z^{*2}/β^2	λ(nm)	σ(μm^2)	Reference
Human Lymphocyte		8.21E-01		n	2.40E+01	3.08E+01	3.08E+01	3.68E+01	3.68E+01	1.29E-05	1.28E+04	1.44E+00	4.05E+00	Edwards, 1990
Human Lymphocyte		3.42E-01		n	4.00E+01	3.75E+01	3.75E+01	4.54E+01	4.54E+01	2.12E-05	1.17E+04	1.31E+00	2.06E+00	Sevankaev, 1979
Human Lymphocyte		4.06E-01		n	9.00E+01	5.05E+01	4.78E+01	6.03E+01	5.58E+01	4.87E-05	9.71E+03	1.23E+00	3.28E+00	Sevankaev, 1979
Human Lymphocyte		1.37E+00		n	3.50E+02	6.38E+01	4.47E+01	6.87E+01	4.92E+01	2.49E-04	5.31E+03	1.37E+00	1.39E+01	Sevankaev, 1979
Human Lymphocyte		8.96E-01		n	4.00E+02	6.31E+01	4.34E+01	6.76E+01	4.78E+01	2.49E-04	4.85E+03	1.44E+00	9.04E+00	Vulpis, 1978
Human Lymphocyte	0.5	8.35E-01		n	7.00E+02	5.56E+01	3.58E+01	6.07E+01	4.08E+01	5.87E-04	3.11E+03	1.91E+00	7.43E+00	Lloyd, 1976
Human Lymphocyte		8.75E-01		n	8.50E+02	5.19E+01	3.28E+01	5.71E+01	3.82E+01	7.38E-04	2.61E+03	2.16E+00	7.26E+00	Sevankaev, 1979
Human Lymphocyte	0.12	6.48E-01		n	9.00E+02	5.07E+01	3.18E+01	5.60E+01	3.74E+01	7.92E-04	2.47E+03	2.25E+00	5.25E+00	Biola, 1974
Human Lymphocyte	0.0333	7.28E-01		n	9.00E+02	5.07E+01	3.18E+01	5.60E+01	3.74E+01	7.92E-04	2.47E+03	2.25E+00	5.90E+00	Lloyd, 1976
Human Lymphocyte	0.03- 0.07	8.74E-01		n	1.90E+03	3.47E+01	2.06E+01	4.24E+01	2.74E+01	1.83E-03	1.16E+03	4.13E+00	4.85E+00	Biola, 1974
Human Lymphocyte		7.45E-01		n	2.03E+03	3.34E+01	1.97E+01	4.12E+01	2.65E+01	1.96E-03	1.08E+03	4.38E+00	3.98E+00	Sasaki, 1971
Human Lymphocyte		5.54E-01		n	2.13E+03	3.24E+01	1.91E+01	4.03E+01	2.59E+01	2.07E-03	1.02E+03	4.59E+00	2.87E+00	Zhang, 1982
Human Lymphocyte		6.00E-01		n	2.13E+03	3.24E+01	1.91E+01	4.03E+01	2.59E+01	2.07E-03	1.02E+03	4.59E+00	3.11E+00	Lloyd, 1978
Human Lymphocyte		9.01E-01		n	2.40E+03	3.01E+01	1.76E+01	3.82E+01	2.44E+01	2.35E-03	8.99E+02	5.11E+00	4.34E+00	Biola, 1974
Human Lymphocyte		3.34E-01		n	4.40E+03	2.01E+01	1.14E+01	2.83E+01	1.78E+01	1.43E-03	4.62E+01	9.16E+00	1.07E+00	Zhang, 1982
Human Lymphocyte	0.0473	3.38E-01		n	4.40E+03	2.01E+01	1.14E+01	2.83E+01	1.78E+01	4.43E-03	4.62E+02	9.16E+00	1.09E+00	Biola, 1974
H.L. Go	0.03	3.89E-01	8.10E-02	n	6.50E+03	1.52E+01	8.42E+00	2.29E+01	1.42E+01	6.64E-03	3.00E+02	1.36E+01	9.43E-01	Fabry, 1985
Human Lymphocyte		4.78E-01	6.40E-02	n	7.60E+03	1.35E+01	7.46E+00	2.10E+01	1.29E+01	7.78E-03	2.53E+02	1.59E+01	1.03E+00	Lloyd, 1976
Human Lymphocyte	0.30	4.75E-01	6.40E-02	n	7.60E+03	1.35E+01	7.46E+00	2.10E+01	1.29E+01	7.78E-03	2.53E+02	1.59E+01	1.03E+00	Lloyd, 1976
H.L. Go	0.21	1.81E-01	1.00E-01	n	1.40E+04	8.47E+00	4.58E+00	1.46E+01	8.83E+00	1.44E-02	1.30E+02	2.96E+01	2.45E-01	Fabry, 1985
Human Lymphocyte		2.50E-01		n	1.41E+04	8.42E+00	4.55E+00	1.45E+01	8.79E+00	1.45E-02	1.29E+02	2.98E+01	3.37E-01	Sasaki, 1971
Human Lymphocyte		2.62E-01	8.80E-02	n	1.47E+04	8.16E+00	4.40E+00	1.41E+01	8.56E+00	1.51E-02	1.23E+02	3.11E+01	3.42E-01	Lloyd, 1976
Human Lymphocyte		1.85E-01	9.44E-02	n	1.47E+04	8.16E+00	4.40E+00	1.41E+01	8.56E+00	1.51E-02	1.22E+02	3.11E+01	2.41E-01	Sevankaev, 1979
Human Lymphocyte	0.30	2.62E-01	8.80E-02	n	1.47E+04	8.16E+00	4.40E+00	1.41E+01	8.56E+00	1.51E-02	1.23E+02	3.11E+01	3.41E-01	Lloyd, 1976
Human Lymphocyte	1.0	1.95E-01	1.19E-01	n	1.49E+04	8.07E+00	4.36E+00	1.40E+01	8.49E+00	1.53E-02	1.21E+02	3.15E+01	2.52E-01	Lloyd, 1984
Human Lymphocyte	0.30	2.89E-01	4.04E-02	n	1.50E+04	8.03E+00	4.33E+00	1.40E+01	8.45E+00	1.54E-02	1.20E+02	3.17E+01	3.71E-01	Muramatsu, 1977
Human Lymphocyte	0.12	1.41E-01	3.77E-02	n	1.50E+04	8.03E+00	4.33E+00	1.40E+01	8.45E+00	1.54E-02	1.20E+02	3.17E+01	1.81E-01	Bauchinger, 1975
Human Lymphocyte		4.58E-02		n	1.60E+04	7.63E+00	4.11E+00	1.34E+01	8.10E+00	1.65E-02	1.12E+02	3.39E+01	5.60E-02	Barjaktarovic, 1980
H.L. Go	0.78	1.12E-01	8.81E-02	n	2.10E+04	6.16E+00	3.29E+00	1.13E+01	6.77E+00	2.16E-02	8.38E+01	4.47E+01	1.10E-01	Fabry, 1985

Cells (Types/Lines)	Dose rate	α(dic's/Gy-cell)	β(dic's/Gy^2-cell)	Rad. Type	E(keV)	L_T(keV/μm)	$L_{100,T}$(keV/μm)	L_D(keV/μm)	$L_{100,D}$(keV/μm)	β^2	z^{*2}/β^2	λ(nm)	σ(μm^2)	Reference
AG1522		5.68E-01		n	2.20E+02	6.29E+01	4.80E+01	6.99E+01	5.32E+01	1.38E-04	6.93E+03	1.24E+00	5.72E+00	Pandita, 1996
AG1522		5.77E-01		n	3.40E+02	6.39E+01	4.50E+01	6.89E+01	4.95E+01	2.40E-04	5.41E+03	1.36E+00	5.90E+00	Pandita, 1996
AG1522		7.11E-01		n	4.30E+02	6.25E+01	4.25E+01	6.69E+01	4.69E+01	3.22E-04	4.61E+03	1.48E+00	7.11E+00	Pandita, 1996
AG1522		5.09E-01		n	1.00E+03	4.85E+01	3.02E+01	5.42E+01	3.60E+01	8.92E-04	2.23E+03	2.43E+00	3.95E+00	Pandita, 1996
AG1522		3.33E-01		n	5.90E+03	1.63E+01	9.08E+00	2.42E+01	1.50E+01	6.01E-03	3.34E+02	1.23E+01	8.67E-01	Pandita, 1996
AG1522		2.59E-01		n	1.37E+04	8.26E+00	4.66E+00	1.48E+01	8.96E+00	1.41E-02	1.32E+02	2.89E+01	3.42E-01	Pandita, 1996

AIII-4 Neutrons on Hamster Cells

Cells (Types/Lines)	Dose rate	α(dic's/Gy-cell)	β(dic's/Gy^2-cell)	Rad. Type	E(keV)	L_T(keV/μm)	$L_{100,T}$(keV/μm)	L_D(keV/μm)	$L_{100,D}$(keV/μm)	β^2	z^{*2}/β^2	λ(nm)	σ(μm^2)	Reference
Syrian Hamster	1.00E-01	5.60E-01	1.00E-03	n	2.10E+03	3.27E+01	1.92E+01	4.05E+01	2.61E+01	2.04E-03	1.04E+03	4.53E+00	2.93E+00	Roberts, 1985
Syrian Hamster	5.83E-02	2.40E-01	6.00E-02	n	1.48E+04	8.12E+00	4.38E+00	1.41E+01	8.52E+00	1.52E-02	1.22E+02	3.13E+01	3.12E-01	Roberts, 1985
V79/4(AH1)	1.80E-01	3.20E-01		n	2.40E+00	3.08E+01	3.08E+01	3.68E+01	3.68E+01	1.29E-05	1.28E+04	1.44E+00	1.58E+00	Roberts, 1987

AIII-5 Sparsely Ionising Radiation on Human Cells

Cells (Types/Lines)	Dose rate	Dose range	α(dic's/Gy-cell)	β(dic's/Gy²-cell)	Rad. Type	Source	E_P(keV)	L_T(keV/μm)	$L_{100,T}$(keV/μm)	L_D(keV/μm)	$L_{100,D}$(keV/μm)	λ(nm)	σ(μm²)	Reference
Human Lymphocyte	1.7 - 4.2 Gy/hr	1 -4 Gy	1.07E-01	-3.00E-03	β	H-3	5.70E+00	6.75E+00	5.47E+00	1.25E+01	1.28E+01	8.92E+00	1.16E-01	Brandenberg, 1982
Human Lymphocyte		0.25 - 9 Gy	1.28E-01	5.78E-02	β	H-3	5.70E+00	6.75E+00	5.47E+00	1.25E+01	1.28E+01	8.92E+00	1.38E-01	Vulpis, 1984
Human Lymphocyte		1 -4 Gy	8.00E-02	5.50E-02	β	P-32	6.90E+02	4.06E-01	2.84E-01	6.55E+00	8.48E+00	1.78E+02	5.20E-03	Brandenberg, 1982
Human Lymphocyte	5.00E-01	1.28 - 4.32	2.60E-02	3.47E-02	e		3.00E+03	1.85E-01	1.10E-01			5.76E+02	7.70E-04	Schmid, 1974
Human Lymphocyte			4.10E-02	3.02E-02	e		1.30E+04	2.00E-01	1.31E-01			5.86E+02	1.31E-03	Virsik, 1981
Human Lymphocyte			4.47E-02	6.07E-02	e		1.40E+04	2.01E-01	1.33E-01			5.87E+02	1.44E-03	Matsubara, 1986
Human Lymphocyte	1.00E-01	0.44 - 7.42	5.50E-03	5.66E-02	e		1.50E+04	2.02E-01	1.34E-01			5.87E+02	1.78E-04	Purrott, 1977
Human Lymphocyte		0.53 - 7.64	9.00E-03	6.08E-02	e (pulse)		1.50E+04	2.02E-01	1.34E-01			5.87E+02	2.91E-04	Purrott, 1977
Human Lymphocyte	1.4 - 3.0	0.46 - 3.69	2.72E-01	3.62E-02	C_k x-rays	1.5 KVp	1.29E-01	2.21E+01	2.21E+01	2.30E+01	2.29E+01	2.04E+00	9.61E-01	Virsik, 1980
Human Lymphocyte	1.40E+00	0.34 - 6.17	2.35E-01	-3.70E-03	Al_k x-rays	3 KVp	5.34E-01	1.67E+01	1.51E+01	1.77E+01	1.67E+01	2.88E+00	6.29E-01	Virsik, 1980
Human Lymphocyte			2.10E-01		Ag_k x-rays	6 KVp	9.78E+00	6.99E+00	6.08E+00	8.23E+00	7.52E+00	7.60E+00	2.35E-01	Virsik, 1980
Human Lymphocyte			1.35E-01	2.50E-02	Cr x-rays	10 KVp	3.09E+00	6.70E+00	4.90E+00	8.55E+00	7.31E+00	9.18E+00	1.45E-01	Virsik, 1981
Human Lymphocyte	6.20E-01	0.17 - 3.22	1.54E-01	7.84E-02	Mo x-rays	30 KVp	9.03E+00	5.52E+00	4.66E+00	6.89E+00	6.16E+00	1.00E+01	1.36E-01	Virsik, 1981
Human Lymphocyte	6.20E-01	0.17 - 3.22	1.11E-01	8.67E-02	x-rays	30 KVp	8.78E+00	6.27E+00	5.30E+00	7.63E+00	6.86E+00	8.74E+00	1.11E-01	Virsik, 1977
Human Lymphocyte			1.77E-01	6.30E-02	x-rays	35.0 KVp	8.77E+00	6.71E+00	5.70E+00	8.05E+00	7.27E+00	8.14E+00	1.90E-01	Matsubara, 1986
Human Lymphocyte			1.10E-01	4.90E-02	x-rays	80.0 KVp	7.44E+00	8.36E+00	7.02E+00	9.77E+00	8.84E+00	5.45E+00	1.47E-01	Matsubara, 1986
Human Lymphocyte	6.80E-01	0.65 - 4.63	-2.00E-03	7.33E-02	x-rays	150 KVp	8.50E+00	7.03E+00	5.74E+00	8.48E+00	7.55E+00	8.11E+00	-2.25E-03	Virsik, 1977
Human Lymphocyte	6.80E-01	0.65 - 4.63	1.27E-01	5.42E-02	x-rays	150 KVp	6.27E+00	7.88E+00	6.42E+00	9.42E+00	8.41E+00	7.02E+00	1.60E-01	Virsik, 1981
Human Lymphocyte		0.49 - 4.49	4.54E-02	2.54E-02	x-rays	180 KVp	1.25E+01	6.06E+00	4.81E+00	7.61E+00	6.66E+00	9.97E+00	4.40E-02	Liniecki, 1973
Human Lymphocyte	1.21E-01	0.115 - 0.575	5.95E-02	-2.02E-02	x-rays	180 KVp	1.25E+01	6.06E+00	4.81E+00	7.61E+00	6.66E+00	9.97E+00	5.77E-02	Ziemba-Zoltowska, 1980
Human Lymphocyte	6.78E-01	0.25 - 5.0	5.40E-02	2.02E-02	x-rays	180 KVp	1.25E+01	6.06E+00	4.81E+00	7.61E+00	6.66E+00	9.97E+00	5.24E-02	Todorov, 1975
Human Lymphocyte		0.5 - 3.0	8.41E-02	8.54E-02	x-rays	200 KVp	1.12E+01	5.40E+00	4.26E+00	6.83E+00	5.96E+00	1.07E+01	7.27E-02	Stenstrand, 1979
Human Lymphocyte	1.10E+00	0.48 - 3.84	3.66E-02	8.01E-02	x-rays	200 KVp	1.12E+01	5.40E+00	4.26E+00	6.83E+00	5.96E+00	1.07E+01	3.16E-02	Murmatsu, 1977
Human Lymphocyte		0.20 - 4.0	7.51E-02	7.11E-02	x-rays	200 KVp	1.12E+01	5.40E+00	4.26E+00	6.83E+00	5.96E+00	1.07E+01	6.49E-02	Sasaki, 1971
Human Lymphocyte	5.00E-01	0.25 - 4.0	7.80E-02	4.15E-02	x-rays	220 KVp	1.67E+01	5.01E+00	3.87E+00	6.54E+00	5.63E+00	1.18E+01	6.25E-02	Schmid, 1972
Human Lymphocyte	5.00E-01	0.25 - 4.0	7.90E-02	5.36E-02	x-rays	220 KVp	1.67E+01	5.01E+00	3.87E+00	6.54E+00	5.63E+00	1.18E+01	6.33E-02	Schmid, 1976
Human Lymphocyte	5.00E-01	0.25 - 4.5	8.31E-02	4.70E-02	x-rays	220 KVp	1.67E+04	5.01E+00	3.87E+00	6.54E+00	5.63E+00	1.18E+01	6.66E-02	Banchinger, 1973
Human Lymphocyte		0.05 - 0.5	3.70E-02		x-rays	250 KVp	1.58E+01	4.31E+00	3.33E+00	5.63E+00	4.85E+00	1.37E+01	2.55E-02	Kucerova, 1972
Human Lymphocyte	3.54E-01	0.05 - 4.0	1.78E-02	7.49E-02	x-rays	250 KVp	1.58E+01	4.31E+00	3.33E+00	5.63E+00	4.85E+00	1.37E+01	1.23E-02	Vulpis, 1976
Human Lymphocyte	1.00E+00	0.05 - 6.0	3.64E-02	6.67E-02	x-rays	250 KVp	1.58E+01	4.31E+00	3.33E+00	5.63E+00	4.85E+00	1.37E+01	2.51E-02	Lloyd, 1986
Human Lymphocyte	1.00E+00	0.05 - 8.0	4.76E-02	6.19E-02	x-rays	250 KVp	1.58E+01	4.31E+00	3.33E+00	5.63E+00	4.85E+00	1.37E+01	3.28E-02	Lloyd, 1975
H.L. Go	1.00E-01	0.05 - 1.0	4.16E-02	5.48E-02	x-rays	250 KVp	1.58E+01	4.31E+00	3.33E+00	5.63E+00	4.85E+00	1.37E+01	2.87E-02	Fabry, 1985

Cells (Types/Lines)	Dose rate	Dose range	α(dic's/Gy-cell)	β(dic's/Gy^2-cell)	Rad. Type	Source	E_P(keV)	L_T(keV/μm)	$L_{100,T}$(keV/μm)	L_D(keV/μm)	$L_{100,D}$(keV/μm)	λ(nm)	σ(μm^2)	Reference
Human Lymphocyte			8.10E-02	4.10E-02	x-rays	250 KVp	1.58E+01	4.31E+00	3.33E+00	5.63E+00	4.85E+00	1.37E+01	5.58E-02	Matsubara, 1994
Human Lymphocyte	7.50E-01	1.0 - 5.0	3.75E-02	7.24E-02	x-rays	250 KVp	1.58E+01	4.31E+00	3.33E+00	5.63E+00	4.85E+00	1.37E+01	2.59E-02	Barjaktarovic, 1980
Human Lymphocyte	5.00E-01	0.5 - 3.0	4.64E-02	6.19E-02	x-rays	250 KVp	1.58E+01	4.31E+00	3.33E+00	5.63E+00	4.85E+00	1.37E+01	3.20E-02	Bender, 1969
Human Lymphocyte	1.00E+00	0.5 - 4.0	5.21E-02	7.20E-02	x-rays	250 KVp	1.58E+01	4.31E+00	3.33E+00	5.63E+00	4.85E+00	1.37E+01	3.59E-02	Leonard, 1977
Human Lymphocyte	4.96E-01	0.05 - 4.0	4.33E-02	4.31E-02	γ	Cs-137	1.59E+02	7.53E-01	5.05E-01	1.19E+00	9.27E-01	9.42E+01	5.22E-03	Takahashi, 1982
Human Lymphocyte		0.05 - 3.0	4.53E-02	4.45E-02	γ	Co-60	3.55E+02	4.44E-01	2.84E-01	6.88E-01	5.15E-01	1.71E+02	3.22E-03	Stenstrand, 1979
H.L. Go		0.05 - 2.0	2.54E-02	6.11E-02	γ	Co-60	3.55E+02	4.44E-01	2.84E-01	6.88E-01	5.15E-01	1.71E+02	1.80E-03	Fabry, 1985
Human Lymphocyte	9.00E-01	0.5 - 4.0	3.93E-02	8.16E-02	γ	Co-60	3.55E+02	4.44E-01	2.84E-01	6.88E-01	5.15E-01	1.71E+02	2.79E-03	Brewen, 1972
Human Lymphocyte	1.2 - 1.5	0.5 - 6.0	3.31E-03	3.36E-02	γ	Co-60	3.55E+02	4.44E-01	2.84E-01	6.88E-01	5.15E-01	1.71E+02	2.35E-04	Liniecki, 1977
Human Lymphocyte		0.05 - 5.0	6.94E-02	4.90E-02	γ	Co-60	3.55E+02	4.44E-01	2.84E-01	6.88E-01	5.15E-01	1.71E+02	4.93E-03	Sevankaev, 1979
Human Lymphocyte	5.00E-01	0.25 - 4.0	2.70E-02	4.75E-02	γ	Co-60	3.55E+02	4.44E-01	2.84E-01	6.88E-01	5.15E-01	1.71E+02	1.92E-03	Bauchinger, 1979
Human Lymphocyte	2.80E-01	0.25 - 4.0	4.90E-02	5.31E-02	γ	Co-60	3.55E+02	4.44E-01	2.84E-01	6.88E-01	5.15E-01	1.71E+02	3.48E-03	Lunchnik, 1975
Human Lymphocyte		0.20 - 4.0	9.10E-03	6.82E-02	γ	Co-60	3.55E+02	4.44E-01	2.84E-01	6.88E-01	5.15E-01	1.71E+02	6.46E-04	Sasaki, 1971
Human Lymphocyte	0.5 (1975)	0.25 - 5.0	1.64E-02	4.93E-02	γ	Co-60	3.55E+02		2.84E-01	6.88E-01	5.15E-01	1.71E+02	1.17E-03	Lloyd, 1984
Human Lymphocyte	5.00E-01	0.25 - 8.0	1.57E-02	5.00E-02	γ	Co-60	3.55E+02	4.44E-01	2.84E-01	6.88E-01	5.15E-01	1.71E+02	1.12E-03	Lloyd, 1975
Human Lymphocyte	3.00E-01	0.25 - 8.0	1.76E-02	2.91E-02	γ	Co-60	3.55E+02	4.44E-01	2.84E-01	6.88E-01	5.15E-01	1.71E+02	1.25E-03	Lloyd, 1975
Human Lymphocyte	(1 h)	0.103 - 5.37	1.13E-02	4.96E-02	γ	Co-60	3.55E+02	4.44E-01	2.84E-01	6.88E-01	5.15E-01	1.71E+02	8.03E-04	Lloyd, 1984
Human Lymphocyte	5.00E-01	0.05 - 5.05	1.42E-02	7.59E-02	γ	Co-60	3.55E+02	4.44E-01	2.84E-01	6.88E-01	5.15E-01	1.71E+02	1.01E-03	Lloyd, 1986
Human Lymphocyte	(3 h)	0.105 - 5.04	1.74E-02	3.75E-02	γ	Co-60	3.55E+02	4.44E-01	2.84E-01	6.88E-01	5.15E-01	1.71E+02	1.24E-03	Lloyd, 1984
Human Lymphocyte	(6 h)	0.103 - 5.06	1.83E-02	3.41E-02	γ	Co-60	3.55E+02	4.44E-01	2.84E-01	6.88E-01	5.15E-01	1.71E+02	1.30E-03	Lloyd, 1984
Human Lymphocyte	(12 h)	0.28 - 4.94	2.94E-02	1.60E-02	γ	Co-60	3.55E+02	4.44E-01	2.84E-01	6.88E-01	5.15E-01	1.71E+02	2.09E-03	Lloyd, 1984
Human Lymphocyte	(1975)		1.57E-02	5.00E-02	γ	Co-60	3.55E+02	4.44E-01	2.84E-01	6.88E-01	5.15E-01	1.71E+02	1.12E-03	Lloyd, 1976
Human Lymphocyte			1.14E-02	6.83E-02	γ	Co-60	3.55E+02	4.44E-01	2.84E-01	6.88E-01	5.15E-01	1.71E+02	8.10E-04	Matsubara, 1986

AIII-6 Sparsely Ionising Radiation on Hamster Cells

Cells (Types/Lines)	Dose rate	Dose range	α(dic's/Gy-cell)	β(dic's/Gy^2-cell)	Rad. Type	Source	E_P(keV)	L_T(keV/μm)	$L_{100,T}$(keV/μm)	L_D(keV/μm)	$L_{100,D}$(keV/μm)	λ(nm)	σ(μm^2)	Reference
CH2B2			7.26E-02		x-rays	250 KVP	1.58E+01	4.31E+00	3.33E+00	5.63E+00	4.85E+00	1.37E+01	5.01E-02	Skarsgard, 1967
Syrian Hamster	3.00E-01	1.0 - 10.02	4.60E-02	4.90E-02	x-arys	250 KVp	1.58E+01	4.31E+00	3.33E+00	5.63E+00	4.85E+00	1.37E+01	3.17E-02	Roberts, 1985
Syrian Hamster	2.50E-01	0.62 - 6.59	4.60E-02	4.90E-02	γ	Co-60	3.55E+02	4.44E-01	2.84E-01	6.88E-01	5.15E-01	1.71E+02	3.27E-03	Roberts, 1985
V79-4			2.80E-02		x-rays	180 KVp	1.25E+01	6.06E+00	4.81E+00	7.61E+00	6.66E+00	9.97E+00	2.71E-02	Tolkendorf, 1983
V79/4(AH1)	3.00E-02		4.90E-02	1.30E-02	γ	Co-60	3.55E+02	4.44E-01	2.84E-01	6.88E-01	5.15E-01	1.71E+02	3.48E-03	Roberts, 1987

AIV HPRT Mutations Database

AIV-1 Charged Particles on Hamster Cells

Cells (Types/Lines)	α(mut's/Gy-cell)	β(mut's/Gy^2-cell)	Ions	E/m (keV/amu)	E(MeV)	L_T(keV/μm)	$L_{100,T}$(keV/μm)	β^2	z^{*2}/β^2	λ(nm)	σ(μm^2)	Reference
V79-753B	5.80E-05		p	7.60E+02	7.60E-01	3.19E+01	1.81E+01	1.62E-03	6.18E+02	5.68E+00	2.96E-04	Belli, 1993
V79-753 B	4.60E-05		p	1.16E+03	1.16E+00	2.36E+01	1.32E+01	2.47E-03	4.05E+02	8.78E+00	1.74E-04	Belli, 1991
V79-4	1.99E-05		p	1.23E+03	1.23E+00	2.32E+01	1.29E+01	2.62E-03	3.82E+02	9.04E+00	7.37E-05	Belli,1992
V79-753B	2.57E-05		p	1.41E+03	1.41E+00	2.12E+01	1.17E+01	3.00E-03	3.34E+02	1.02E+01	8.71E-05	Belli, 1993
V79-4	1.87E-05		p	1.44E+03	1.44E+00	2.10E+01	1.16E+01	3.06E-03	3.27E+02	1.03E+01	6.30E-05	Belli,1992
V79-753 B	3.26E-05		p	1.70E+03	1.70E+00	1.83E+01	1.00E+01	3.61E-03	2.77E+02	1.26E+01	9.52E-05	Belli, 1991
V79-753B	2.08E-05		p	3.20E+03	3.20E+00	1.17E+01	6.27E+00	6.78E-03	1.47E+02	2.29E+01	3.88E-05	Belli, 1993
V79-753 B	3.00E-05		p	3.36E+03	3.36E+00	1.10E+01	5.88E+00	7.12E-03	1.41E+02	2.49E+01	5.26E-05	Belli, 1991
V79-753B	5.54E-05		D	2.75E+02	5.50E-01	5.70E+01	3.40E+01	5.86E-04	1.68E+03	2.15E+00	5.05E-04	Belli, 1994
V79-753B	2.75E-05		D	5.50E+02	1.10E+00	3.95E+01	2.27E+01	1.17E-03	8.53E+02	4.10E+00	1.74E-04	Belli, 1994
V79-753B	2.53E-05		D	8.00E+02	1.60E+00	3.08E+01	1.78E+01	1.70E-03	5.87E+02	5.83E+00	1.25E-04	Belli, 1994
V79-753B	1.58E-05		D	1.65E+03	3.30E+00	1.84E+01	1.01E+01	3.51E-03	2.85E+02	1.24E+01	4.65E-05	Belli, 1994
V79	4.56E-05		α	5.13E+02	2.05E+00	1.63E+02	9.25E+01	1.10E-03	3.57E+03	9.91E-01	1.19E-03	Kranert, 1992
V79-4	8.62E-05		α	6.25E+02	2.50E+00	1.46E+02	8.26E+01	1.34E-03	2.96E+03	1.17E+00	2.01E-03	Thacker, 1982
V79	6.19E-05		α	7.50E+02	3.00E+00	1.27E+02	7.21E+01	1.60E-03	2.48E+03	1.43E+00	1.26E-03	Kranert, 1988
CHO	4.79E-05		α	9.25E+02	3.70E+00	1.12E+02	6.34E+01	1.96E-03	2.04E+03	1.71E+00	8.59E-04	Barnhart, 1979
V79	1.44E-04		He-4	1.50E+03	6.00E+00	7.80E+01	4.36E+01	3.21E-03	1.25E+03	2.81E+00	1.80E-03	Kranert, 1990
V79	4.78E-05		He-4	1.85E+03	7.40E+00	6.67E+01	3.69E+01	3.96E-03	1.01E+03	3.50E+00	5.10E-04	Munson, 1979
V79	1.04E-04		He-4	1.90E+03	7.60E+00	6.61E+01	3.66E+01	4.06E-03	9.84E+02	3.54E+00	1.10E-03	Kranert, 1990
V79	6.76E-05		He-4	2.90E+03	1.16E+01	4.90E+01	2.71E+01	6.19E-03	6.46E+02	5.19E+00	5.30E-04	Kranert, 1990
V79	4.90E-05	8.04E-06	He-4	2.93E+03	1.17E+01	4.76E+01	2.59E+01	6.25E-03	6.40E+02	5.52E+00	3.73E-04	Munson, 1979
V79-4	1.01E-05		α	5.08E+03	2.03E+01	3.23E+01	1.73E+01	1.08E-02	3.70E+02	9.11E+00	5.21E-05	Belli, 1992
V79	2.08E-05		He-4	6.10E+03	2.44E+01	2.74E+01	1.46E+01	1.30E-02	3.09E+02	1.12E+01	9.12E-05	Munson, 1979
V79-4	9.60E-06		α	7.63E+03	3.05E+01	2.29E+01	1.22E+01	1.62E-02	2.48E+02	1.40E+01	3.51E-05	Belli, 1992
V79	1.02E-05	3.58E-06	He-4	8.73E+03	3.49E+01	2.07E+01	1.10E+01	1.85E-02	2.17E+02	1.58E+01	3.38E-05	Munson, 1979
V79	6.21E-05	3.30E-05	B-10	4.98E+03	4.98E+01	2.00E+02	1.06E+02	1.06E-02	2.30E+03	1.49E+00	1.99E-03	Munson, 1979
V79	1.62E-04		B-11	5.00E+03	5.50E+01	1.98E+02	1.05E+02	1.06E-02	2.29E+03	1.51E+00	5.12E-03	Kranert, 1990
V79	6.18E-05	3.00E-05	B-10	1.07E+04	1.07E+02	1.10E+02	5.71E+01	2.26E-02	1.10E+03	3.16E+00	1.08E-03	Munson, 1979
V79	1.55E-04		B-11	1.07E+04	1.18E+02	1.14E+02	5.93E+01	2.26E-02	1.10E+03	3.02E+00	2.82E-03	Kranert, 1990
V79	4.77E-05		N-14	3.70E+03	5.18E+01	4.59E+02	2.45E+02	7.90E-03	5.59E+03	6.05E-01	3.50E-03	Munson, 1979
V79	4.87E-05		N-14	3.70E+03	5.18E+01	4.59E+02	2.45E+02	7.90E-03	5.59E+03	6.05E-01	3.58E-03	Kranert, 1990
V79	8.90E-06		O-16	1.90E+03	3.04E+01	8.00E+02	4.34E+02	4.07E-03	1.18E+04	2.98E-01	1.14E-03	Stoll, 1995

Cells (Types/Lines)	α(mut's/Gy-cell)	β(mut's/Gy^2-cell)	Ions	E/m (keV/amu)	E(MeV)	L_T(keV/μm)	$L_{100,T}$(keV/μm)	β^2	z^{*2}/β^2	λ(nm)	σ(μm^2)	Reference
V79	3.60E-05		O-16	8.20E+03	1.31E+02	3.47E+02	1.82E+02	1.74E-02	3.56E+03	9.43E-01	2.00E-03	Kranert, 1990
V79	3.85E-05		O-16	8.80E+03	1.41E+02	3.25E+02	1.70E+02	1.86E-02	3.34E+03	1.03E+00	2.00E-03	Stoll, 1995
V79	2.15E-05		O-16	1.07E+04	1.71E+02	2.77E+02	1.44E+02	2.26E-02	2.78E+03	1.25E+00	9.50E-04	Stoll, 1995
V79	1.44E-05		O-16	8.80E+04	1.41E+03	5.20E+01	2.71E+01	1.65E-01	3.87E+02	8.87E+00	1.20E-04	Stoll, 1995
V79	5.25E-06		O-16	3.96E+05	6.34E+03	2.02E+01	1.02E+01	5.08E-01	1.26E+02	2.75E+01	1.70E-05	Stoll, 1995
V79	2.52E-05		Ne-20	8.00E+03	1.60E+02	5.29E+02	2.77E+02	1.70E-02	5.52E+03	6.18E-01	2.13E-03	Stoll, 1995
V79	5.86E-06		Ne-20	8.90E+03	1.78E+02	4.90E+02	2.56E+02	1.89E-02	5.03E+03	6.81E-01	4.60E-04	Kranert, 1990
V79	3.30E-05		Ne-20	9.80E+03	1.96E+02	4.55E+02	2.38E+02	2.07E-02	4.62E+03	7.48E-01	2.40E-03	Kranert, 1992
V79	2.32E-05		Ne-20	1.07E+04	2.14E+02	4.23E+02	2.20E+02	2.26E-02	4.26E+03	8.19E-01	1.57E-03	Stoll, 1995
V79	2.41E-05		Ne-20	1.20E+04	2.40E+02	3.89E+02	2.02E+02	2.53E-02	3.84E+03	9.09E-01	1.50E-03	Kranert, 1990
V79	2.41E-05		Ne-20	1.20E+04	2.40E+02	3.89E+02	2.02E+02	2.53E-02	3.84E+03	9.09E-01	1.50E-03	Stoll, 1995
V79	1.38E-05		Ne-20	1.43E+04	2.86E+02	3.48E+02	1.81E+02	3.00E-02	3.27E+03	1.04E+00	7.70E-04	Stoll, 1995
V79	3.44E-05		Ne-20	1.48E+04	2.96E+02	3.44E+02	1.79E+02	3.11E-02	3.16E+03	1.06E+00	1.89E-03	Kranert, 1992
V79	1.59E-05		Ne-20	6.50E+04	1.30E+03	1.06E+02	5.42E+01	1.26E-01	7.92E+02	4.26E+00	2.70E-04	Stoll, 1995
V79	1.48E-05		Ne-20	1.91E+05	3.82E+03	4.63E+01	2.39E+01	3.11E-01	3.21E+02	1.09E+01	1.10E-04	Stoll, 1995
V79	1.98E-05		Ne-20	3.95E+05	7.90E+03	3.16E+01	1.59E+01	5.07E-01	1.97E+02	1.76E+01	1.00E-04	Stoll, 1995
V79	3.48E-06		Ca-40	1.41E+04	5.64E+02	1.26E+03	6.54E+02	2.96E-02	1.19E+04	2.88E-01	7.00E-04	Kranert, 1990
V79	3.35E-06		Ti-48	4.40E+03	2.11E+02	2.61E+03	1.38E+03	9.39E-03	3.15E+04	1.12E-01	1.40E-03	Kranert, 1990
V79	3.73E-06		Ti-48	1.48E+04	7.10E+02	1.44E+03	7.48E+02	3.11E-02	1.36E+04	2.53E-01	8.60E-04	Kranert, 1990
V79	1.72E-06		Ni-58	6.00E+03	3.48E+02	3.30E+03	1.74E+03	1.28E-02	3.70E+04	9.40E-02	9.10E-04	Stoll, 1996
V79	1.72E-06		Ni-58	6.00E+03	3.48E+02	3.30E+03	1.74E+03	1.28E-02	3.70E+04	9.40E-02	9.10E-04	Stoll, 1996
V79	1.84E-06		Ni-58	9.00E+03	5.22E+02	2.82E+03	1.48E+03	1.91E-02	2.89E+04	1.18E-01	8.30E-04	Kranert, 1990
V79	1.66E-06		Ni-58	1.46E+04	8.47E+02	2.15E+03	1.12E+03	3.07E-02	2.07E+04	1.70E-01	5.70E-04	Kranert, 1990
V79	7.64E-06		Ni-58	1.36E+05	7.89E+03	4.58E+02	2.39E+02	2.39E-01	3.28E+03	1.05E+00	5.60E-04	Stoll, 1996
V79	7.64E-06		Ni-58	1.36E+05	7.89E+03	4.58E+02	2.39E+02	2.39E-01	3.28E+03	1.05E+00	5.60E-04	Stoll, 1996
V79	1.38E-05		Ni-58	3.87E+05	2.24E+04	2.50E+02	1.26E+02	5.01E-01	1.56E+03	2.22E+00	5.50E-04	Stoll, 1996
V79	1.38E-05		Ni-58	3.87E+05	2.24E+04	2.50E+02	1.26E+02	5.01E-01	1.56E+03	2.22E+00	5.50E-04	Stoll, 1996
V79	1.86E-05		Ni-58	6.30E+05	3.65E+04	2.08E+02	1.04E+02	6.30E-01	1.27E+03	4.56E+00	6.20E-04	Stoll, 1996
V79	1.86E-05		Ni-58	6.30E+05	3.65E+04	2.08E+02	1.04E+02	6.30E-01	1.27E+03	4.56E+00	6.20E-04	Stoll, 1996
V79	1.11E-06		Xe-132	1.06E+04	1.40E+03	6.73E+03	3.51E+03	2.24E-02	6.79E+04	5.13E-02	1.20E-03	Kranert, 1990
V79	2.14E-07		Au-197	2.20E+03	4.33E+02	1.20E+04	7.60E+03	4.71E-03	1.70E+05	2.15E-02	4.10E-04	Stoll, 1996
V79	2.14E-07		Au-197	2.20E+03	4.33E+02	1.20E+04	7.60E+03	4.71E-03	1.70E+05	2.15E-02	4.10E-04	Stoll, 1996
V79	4.56E-07		Au-197	8.70E+03	1.71E+03	1.14E+04	5.95E+03	1.84E-02	1.20E+05	2.94E-02	8.30E-04	Stoll, 1996

Cells (Types/Lines)	α(mut's/Gy-cell)	β(mut's/Gy^2-cell)	Ions	E/m (keV/amu)	E(MeV)	L_T(keV/μm)	$L_{100,T}$(keV/μm)	β^2	z^{*2}/β^2	λ(nm)	σ(μm^2)	Reference
V79	4.56E-07		Au-197	8.70E+03	1.71E+03	1.14E+04	5.95E+03	1.84E-02	1.20E+05	2.94E-02	8.30E-04	Stoll, 1996
V79	5.03E-07		Pb-207	1.16E+04	2.40E+03	1.08E+04	5.77E+03	2.63E-02	1.11E+05	4.85E-02	8.70E-04	Stoll, 1996
V79	5.03E-07		Pb-207	1.16E+04	2.40E+03	1.08E+04	5.77E+03	2.63E-02	1.11E+05	4.85E-02	8.70E-04	Stoll, 1996
V79	5.51E-07		Pb-207	1.57E+04	3.24E+03	1.04E+04	5.43E+03	3.27E-02	7.84E+04	3.52E-02	9.20E-04	Kranert, 1990
V79	2.61E-06		Pb-207	1.50E+05	3.11E+04	3.47E+03	1.82E+03	2.58E-01	2.53E+04	2.27E-01	1.45E-03	Stoll, 1996
V79	2.61E-06		Pb-207	1.50E+05	3.11E+04	3.47E+03	1.82E+03	2.58E-01	2.53E+04	2.27E-01	1.45E-03	Stoll, 1996
V79	2.94E-06		Pb-207	5.00E+05	1.04E+05	1.889e3	9.48E+02	5.77E-01	1.17E+04	4.95E-01	8.90E-04	Stoll, 1996
V79	2.94E-06		Pb-207	5.00E+05	1.04E+05	1.89E+03	9.48E+02	5.77E-01	1.17E+04	4.95E-01	8.90E-04	Stoll, 1996
V79	3.41E-06		Pb-207	9.80E+05	2.03E+05	1.52E+03	7.65E+02	7.67E-01	8.78E+03	6.77E-01	8.30E-04	Stoll, 1996
V79	3.41E-06		Pb-207	9.80E+05	2.03E+05	1.52E+03	7.65E+02	7.67E-01	8.78E+03	6.77E-01	8.30E-04	Stoll, 1996
V79	3.03E-07		U-238	4.70E+03	1.12E+03	1.42E+04	7.54E+03	1.00E-02	1.69E+05	2.07E-02	6.90E-04	Kranert, 1988
V79	6.61E-07		U-238	5.10E+03	1.21E+03	1.42E+04	7.50E+03	1.09E-02	1.66E+05	2.12E-02	1.50E-03	Kranert, 1990
V79	4.04E-07		U-238	1.06E+04	2.52E+03	1.32E+04	6.87E+03	2.24E-02	1.33E+05	2.62E-02	8.50E-04	Kranert, 1990
V79	2.29E-07		U-238	1.41E+04	3.36E+03	1.23E+04	6.39E+03	2.96E-02	1.19E+05	2.96E-02	4.50E-04	Kranert, 1990

AIV-2 Charged Particles on Human Cells

Cells (Types/Lines)	α(mut's/Gy-cell)	β(mut's/Gy^2-cell)	Ions	E/m (keV/amu)	E(MeV)	L_T(keV/μm)	$L_{100,T}$(keV/μm)	β^2	z^{*2}/β^2	λ(nm)	σ(μm^2)	Reference
HSF	2.13E-04		D	3.50E+02	7.00E-01	5.00E+01	3.03E+01	7.46E-04	1.33E+03	2.66E+00	1.70E-03	Hei, 1988
HSF	1.54E-05		D	1.50E+03	3.00E+00	2.00E+01	1.09E+01	3.19E-03	3.13E+02	1.12E+01	4.93E-05	Hei, 1988
HSF	6.20E-04		He-3	6.00E+02	1.80E+00	1.50E+02	8.55E+01	1.28E-03	3.09E+03	1.11E+00	1.49E-02	Hei, 1988
HSF	4.15E-04		He-3	8.33E+02	2.50E+00	1.20E+02	6.84E+01	1.78E-03	2.25E+03	1.54E+00	7.97E-03	Hei, 1988
HSF	2.84E-04		He-3	1.47E+03	4.40E+00	8.00E+01	4.50E+01	3.13E-03	1.28E+03	2.68E+00	3.64E-03	Hei, 1988
HF19 strain	2.20E-04		He-4	1.48E+03	5.90E+00	7.84E+01	4.39E+01	3.16E-03	1.27E+03	2.79E+00	2.76E-03	Cox, 1979
HF19 strain	1.35E-04		He-4	1.85E+03	7.40E+00	6.67E+01	3.69E+01	3.96E-03	1.01E+03	3.50E+00	1.44E-03	Cox, 1979
HF19 strain	8.99E-05		He-4	2.93E+03	1.17E+01	4.76E+01	2.59E+01	6.25E-03	6.40E+02	5.52E+00	6.84E-04	Cox, 1979
HF19 strain	4.85E-05		He-4	6.10E+03	2.44E+01	2.74E+01	1.46E+01	1.30E-02	3.09E+02	1.12E+01	2.13E-04	Cox, 1979
HF19 strain	3.94E-05		He-4	8.73E+03	3.49E+01	2.07E+01	1.10E+01	1.85E-02	2.17E+02	1.58E+01	1.30E-04	Cox, 1979
HF19 strain	2.07E-04		B-10	4.98E+03	4.98E+01	2.00E+02	1.06E+02	1.06E-02	2.30E+03	1.49E+00	6.62E-03	Cox, 1979
HF19 strain	1.78E-04		B-10	6.56E+03	6.56E+01	1.66E+02	8.72E+01	1.39E-02	1.77E+03	1.89E+00	4.72E-03	Cox, 1979
HF19 strain	2.01E-04		B-10	1.07E+04	1.07E+02	1.10E+02	5.71E+01	2.26E-02	1.10E+03	3.16E+00	3.52E-03	Cox, 1979
HF19 strain	8.50E-05		N-14	3.70E+03	5.18E+01	4.59E+02	2.45E+02	7.90E-03	5.59E+03	6.05E-01	6.24E-03	Cox, 1979
HSF	2.30E-05		Ne-20	5.03E+05	1.21E+04	2.50E+01	1.33E+01	6.30E-01	1.61E+02	3.58E+01	9.20E-05	Chen, 1994
HSF	1.32E-04		Ar-40	1.50E+05	6.00E+03	1.75E+02	9.09E+01	2.58E-01	1.25E+03	2.80E+00	3.69E-03	Chen, 1994
HSF	8.30E-05		Ar-40	4.80E+05	1.92E+04	9.50E+01	4.66E+01	2.53E-02	1.28E+04	6.12E+00	1.26E-03	Chen, 1994
HSF	4.10E-05		Fe-56	9.40E+04	5.26E+03	5.29E+02	2.75E+02	1.75E-01	3.84E+03	8.76E-01	3.47E-03	Chen, 1994
HSF	7.20E-05		Fe-56	2.01E+05	1.13E+04	3.07E+02	1.58E+02	3.24E-01	2.09E+03	1.65E+00	3.54E-03	Chen, 1994
HSF	9.80E-05		Fe-56	4.22E+05	2.36E+04	2.00E+02	1.05E+02	2.22E-02	3.05E+04	2.66E+00	3.14E-03	Chen, 1994
HSF	1.10E-05		La-139	4.07E+05	5.66E+04	9.75E+02	4.60E+02	5.10E-01	5.80E+03	9.50E-01	1.72E-03	Chen, 1994

AIV-3 Neutrons on Mammalian Cells

Cells (Types/Lines)	Dose rate	α(mut's/Gy-cell)	β(mut's/Gy^2-cell)	Rad. Type	E(keV)	L_T(keV/μm)	$L_{100,T}$(keV/μm)	L_D(keV/μm)	$L_{100,D}$(keV/μm)	β^2	z^{*2}/β^2	λ(nm)	σ(μm^2)	Reference
C3H10T1/2		1.80E-04		n	7.00E+02	5.56E+01	3.57E+01	6.03E+01	4.08E+01	5.87E-04	3.11E+03	1.91E+00	0.0016	Blacer-Kubiczek, 1991
V79	0.65 Gy/min	1.97E-05	6.25E-06	n	1.70E+04	7.26E+00	3.90E+00	1.29E+01	7.78E+00	1.76E-02	1.05E+02	3.61E+01	2.3E-05	Cox, 1977
HF19	0.65 Gy/min	4.87E-05		n	1.70E+04	7.26E+00	3.90E+00	1.29E+01	7.78E+00	1.76E-02	1.05E+02	3.61E+01	5.7E-05	Cox, 1977

AIV-4 Sparsely Ionising Radiation on Hamster Cells

Cells (Types/Lines)	Dose rate	α(mut's/Gy-cell)	β(mut's/Gy^2-cell)	Rad. Type	Source	E_P(keV)	L_T(keV/μm)	$L_{100,T}$(keV/μm)	L_D(keV/μm)	$L_{100,D}$(keV/μm)	λ(nm)	σ(μm^2)	Reference
V79	2.5 Gy/min	1.10E-05	7.30E-06	Ck x-rays	1.5 KVp	1.29E-01	2.21E+01	2.21E+01	2.30E+01	2.29E+01	2.04E+00	3.89E-05	Goodhead, 1979
V79	5.0 Gy/min	7.40E-06	4.50E-06	Alk x-rays	3 KVp	5.34E-01	1.67E+01	1.51E+01	1.77E+01	1.67E+01	2.88E+00	1.98E-05	Cox, 1977
V79-753 B	1 Gy/min	6.00E-06	1.20E-06	x-rays	250 KVp	1.58E+01	4.31E+00	3.33E+00	5.63E+00	4.85E+00	1.37E+01	4.14E-06	Belli, 1991
V79-4		6.60E-06	7.10E-07	x-rays	250 KVp	1.58E+01	4.31E+00	3.33E+00	5.63E+00	4.85E+00	1.37E+01	4.55E-06	Thacker, 1982
V79	1.20 Gy/min	3.50E-06	8.60E-07	γ	Co-60	3.55E+02	4.44E-01	2.84E-01	6.88E-01	5.15E-01	1.71E+02	2.49E-07	Thacker, 1979
V79		1.58E-06		γ	Co-60	3.55E+02	4.44E-01	2.84E-01	6.88E-01	5.15E-01	1.71E+02	1.12E-07	Kent, 1993
V79		8.14E-06		γ	Co-60	3.55E+02	4.44E-01	2.84E-01	6.88E-01	5.15E-01	1.71E+02	5.78E-07	Kent, 1993
V79		3.61E-06		γ	Co-60	3.55E+02	4.44E-01	2.84E-01	6.88E-01	5.15E-01	1.71E+02	2.56E-07	Kent, 1993

AIV-5 Sparsely Ionising Radiation on Human Cells

Cells (Types/Lines)	Dose rate	α(mut's/Gy-cell)	β(mut's/Gy^2-cell)	Rad. Type	Source	E_P(keV)	L_T(keV/μm)	$L_{100,T}$(keV/μm)	L_D(keV/μm)	$L_{100,D}$(keV/μm)	λ(nm)	σ(μm^2)	Reference
HF19	2.5 Gy/min	6.70E-05		Ck x-rays	1.5 KVp	1.29E-01	2.21E+01	2.21E+01	2.30E+01	2.29E+01	2.04E+00	2.37E-04	Goodhead, 1979
HF19	5.0 Gy/min	7.59E-05		Alk x-rays	3 KVp	5.34E-01	1.67E+01	1.51E+01	1.77E+01	1.67E+01	2.88E+00	2.03E-04	Cox, 1977
HF19		3.10E-05		x-rays	250 KVp	1.58E+01	4.31E+00	3.33E+00	5.63E+00	4.85E+00	1.37E+01	2.14E-05	Cox, 1979
HSF		6.70E-05		γ	Cs-137	1.59E+02	7.53E-01	5.05E-01	1.19E+00	9.27E-01	9.42E+01	8.07E-06	Hei, 1988

AV Oncogenic Transformations Database

AV-1 Charged Particles on Mouse Cells

Cells (Types/Lines)	α(tran's/Gy-cell)	β(tran's/Gy^2-cell)	Ion Type	E(keV/amu)	E(MeV)	L_T(keV/μm)	$L_{100,T}$(keV/μm)	β^2	z^{*2}/β^2	λ(nm)	σ(μm^2)	Reference
C3H10T1/2	7.83E-04		p	2.25E+03	2.25E+00	1.51E+01	8.24E+00	4.78E-03	2.09E+02	1.62E+01	1.90E-03	Miller, 1995
C3H10T1/2	2.20E-05	5.20E-06	p	4.00E+03	4.00E+00	1.00E+01	5.20E+00	8.46E-03	1.18E+02	2.87E+01	3.52E-05	Hei, 1988
C3H10T1/2	1.30E-05	3.90E-05	p	3.10E+04	3.10E+01	1.87E+00	9.75E-01	6.29E-02	1.59E+01	2.16E+02	3.88E-06	Bettega, 1990
C3H10T1/2	2.45E-04		p	2.40E+05	2.40E+02	4.05E-01	2.08E-01	3.66E-01	2.73E+00	1.28E+03	1.59E-05	Yang, 1996
C3H10T1/2	9.85E-04		D	2.75E+02	5.50E-01	5.81E+01	3.44E+01	5.86E-04	1.68E+03	2.15E+00	9.15E-03	Miller, 1995
C3H10T1/2	3.60E-05	1.00E-06	D	5.50E+02	1.10E+00	4.00E+01	2.44E+01	1.17E-03	8.53E+02	4.10E+00	2.30E-04	Hei, 1988
C3H10T1/2	1.09E-03		D	5.50E+02	1.10E+00	4.00E+01	2.27E+01	1.17E-03	8.53E+02	4.10E+00	7.01E-03	Miller, 1990
C3H10T1/2	2.92E-04		D	1.29E+04	2.58E+01	3.90E+00	2.04E+00	2.70E-02	3.71E+01	9.04E+01	1.82E-04	Miller, 1995
C3H10T1/2	5.10E-04		He-3	8.33E+02	2.50E+00	1.20E+02	7.00E+01	1.78E-03	2.34E+03	1.56E+00	9.79E-03	Hei, 1988
C3H10T1/2	3.00E-04	5.80E-05	He-3	1.47E+03	4.40E+00	8.00E+01	4.50E+01	3.13E-03	1.28E+03	2.69E+00	3.84E-03	Hei, 1988
C3H10T1/2	2.35E-03		He-3	1.67E+03	5.00E+00	7.37E+01	4.12E+01	3.55E-03	1.13E+03	3.03E+00	2.77E-02	Miller, 1995
C3H10T1/2	1.67E-03		He-4	3.60E+02	1.44E+00	1.97E+02	1.12E+02	7.72E-04	4.87E+03	7.21E-01	5.28E-02	Miller, 1995
C3H10T1/2	1.94E-03		He-4	5.93E+02	2.37E+00	1.48E+02	8.40E+01	1.27E-03	7.12E+03	1.14E+00	4.61E-02	Miller, 1995
C3H10T1/2	2.90E-04		α	6.75E+02	2.70E+00	1.40E+02	7.76E+01	1.45E-03	2.75E+03	1.28E+00	6.50E-03	Hieber, 1987
C3H10T1/2	2.50E-03		He-4	8.33E+02	3.33E+00	1.18E+02	6.68E+01	1.78E-03	2.24E+03	1.59E+00	4.72E-02	Miller, 1995
C3H10T1/2	6.20E-04	2.90E-04	α	1.04E+03	4.15E+00	1.01E+02	5.68E+01	2.22E-03	1.80E+03	1.98E+00	1.00E-02	Bettega, 1990
C3H10T1/2	5.00E-03		α	1.08E+03	4.30E+00	9.96E+01	5.61E+01	2.30E-03	1.74E+03	2.01E+00	7.97E-02	Bettega, 1992
C3H10T1/2	2.56E-03		He-4	1.28E+03	5.12E+00	9.00E+01	5.05E+01	2.74E-03	1.46E+03	2.32E+00	3.69E-02	Miller, 1995
C3H10T1/2	7.98E-04		C-12	5.36E+03	6.43E+01	2.71E+02	1.43E+02	1.14E-02	3.04E+02	1.11E+00	3.45E-02	Miller, 1995
C3H10T1/2	7.45E-05		C-12	4.74E+05	5.69E+03	1.00E+01	5.00E+00	5.77E-01	6.33E+01	9.03E+01	1.19E-04	Yang, 1985
C3H10T1/2	5.05E-04		O-16	6.04E+03	9.66E+01	4.18E+02	2.20E+02	1.28E-02	4.68E+03	7.43E-01	3.38E-02	Miller, 1995
C3H10T1/2	6.18E-04		F-19	4.82E+03	9.16E+01	6.09E+02	3.22E+02	1.03E-02	7.01E+03	4.84E-01	6.01E-02	Miller, 1995
C3H10T1/2	3.62E-04		Ne-20	4.25E+05	8.50E+03	3.20E+01	1.60E+01	5.11E-01	2.02E+02	2.82E+01	1.85E-03	Yang, 1996
C3H10T1/2	7.40E-05		Ne-20	4.25E+05	8.50E+03	3.20E+01	1.60E+01	5.11E-01	2.02E+02	2.82E+01	3.79E-04	Yang, 1985
C3H10T1/2	4.48E-04		Si-28	3.20E+05	8.96E+03	8.20E+01	4.10E+01	3.70E-01	5.40E+02	1.05E+01	5.88E-03	Yang, 1985
C3H10T1/2	5.63E-05		Si-28	6.70E+05	1.88E+04	5.00E+01	2.50E+01	8.74E-01	2.95E+02	1.96E+01	4.50E-04	Yang, 1985
C3H10T1/2	2.34E-04		Ar-40	2.38E+05	9.50E+03	1.40E+02	7.00E+01	3.80E-01	8.80E+03	4.30E+00	5.25E-03	Palcic, 1985
C3H10T1/2	1.78E-04		Ar-40	3.30E+05	1.32E+04	1.13E+02	5.72E+01	4.55E-01	7.12E+02	4.79E+00	3.22E-03	Yang, 1996
C3H10T1/2	5.66E-04		Ar-40	4.00E+05	1.60E+04	1.02E+02	5.12E+01	5.11E-01	6.34E+02	5.45E+00	9.23E-03	Yang, 1996
C3H10T1/2	1.36E-04		Ar-40	3.30E+05	1.32E+04	1.40E+02	7.00E+01	3.40E-01	9.50E+02	6.10E+00	3.06E-03	Yang, 1985
C3H10T1/2	8.15E-05		Fe-56	3.00E+05	1.68E+04	5.00E+02	2.65E+02	1.80E-01	3.90E+03	1.47E+00	6.52E-03	Yang, 1985
C3H10T1/2	1.53E-04		Fe-56	4.00E+05	2.24E+04	3.00E+02	1.50E+02	3.50E-01	2.10E+03	2.80E+00	7.34E-03	Yang, 1985
C3H10T1/2	6.26E-04		Fe-56	6.00E+05	3.36E+04	1.90E+02	9.50E+01	5.90E-01	1.10E+03	5.10E+00	1.90E-02	Yang, 1985
C3H10T1/2	9.52E-05		U-238	9.60E+05	2.28E+05	1.90E+03	9.60E+02	7.67E-01	1.11E+04	5.40E-01	2.89E-02	Yang, 1985

AV-2 Neutrons on Mouse Cells

Cells (Types/Lines)	α(tran's/Gy-cell)	β(tran's/Gy^2-cell)	Type	E(keV)	L_T(keV/μm)	$L_{100,T}$(keV/μm)	L_D(keV/μm)	$L_{100,D}$(keV/μm)	β^2	z^{*2}/β^2	λ(nm)	σ(μm^2)	Reference
C3H10T1/2	6.80E-04	2.90E-05	n	2.30E+02	6.32E+01	4.78E+01	7.00E+01	5.29E+01	1.46E-04	6.78E+03	1.25E+00	6.88E-03	Miller, 1989
C3H10T1/2	1.61E-03	2.90E-05	n	3.50E+02	6.38E+01	4.47E+01	6.87E+01	4.98E+01	2.49E-04	5.31E+03	1.37E+00	1.64E-02	Miller, 1989
C3H10T1/2	8.20E-04	2.90E-05	n	4.50E+02	6.20E+01	4.20E+01	6.64E+01	4.64E+01	3.42E-04	4.45E+03	1.51E+00	8.14E-03	Miller, 1989
C3H10T1/2	2.40E-03		n	5.00E+02	6.09E+01	4.06E+01	6.60E+01	4.52E+01	3.89E-04	4.11E+03	1.58E+00	2.34E-02	Barendsen, 1985
C3H10T1/2	8.34E-04	1.50E-06	n	9.70E+03	5.56E+01	3.57E+01	6.03E+01	4.08E+01	5.87E-04	3.11E+03	1.91E+00	7.42E-03	Blacer-Kubiczek, 1991
C3H10T1/2	1.00E-03	2.90E-05	n	7.00E+02	5.56E+01	3.58E+01	6.03E+01	4.08E+01	5.87E-04	3.11E+03	1.91E+00	8.90E-03	Miller, 1989
C3H10T1/2	6.00E-04	2.90E-05	n	9.60E+02	4.93E+01	1.13E+01	5.49E+01	3.08E+01	8.52E-04	2.32E+03	2.36E+00	4.73E-03	Miller, 1989
C3H10T1/2	9.60E-04	2.90E-05	n	1.96E+03	3.40E+01	2.01E+01	4.18E+01	2.69E+01	1.89E-03	1.12E+03	4.25E+00	5.23E-03	Miller, 1989
C3H10T1/2	1.30E-03		n	4.20E+03	2.07E+01	1.17E+01	2.90E+01	1.92E+01	4.24E-03	4.86E+02	8.77E+00	4.31E-03	Barendsen, 1985
C3H10T1/2	4.72E-04		n	5.90E+03	1.63E+01	9.08E+00	2.42E+01	1.50E+01	6.01E-03	3.34E+02	1.23E+01	1.23E-03	Miller, 1990
C3H10T1/2	7.60E-04	2.90E-05	n	5.90E+03	1.63E+01	9.08E+00	2.42E+01	1.50E+01	6.01E-03	3.34E+02	1.23E+01	1.98E-03	Miller, 1989
C3H10T1/2	8.60E-04	2.90E-05	n	1.37E+04	8.26E+00	4.66E+00	1.48E+01	8.96E+00	1.41E-02	1.32E+02	2.89E+01	1.14E-03	Miller, 1989
C3H10T1/2	9.00E-04	3.00E-04	n	1.50E+04	8.03E+00	4.33E+00	1.40E+01	8.45E+00	1.54E-02	1.20E+02	3.17E+01	1.16E-03	Barendsen, 1985

AV-3 Sparsely Ionising Radiation on Mouse Cells

Cells (Types/Lines)	Dose rate	α(tran's/Gy-cell)	β(tran's/Gy^2-cell)	Rad. Type	Source	E(keV)	L_T(keV/µm)	$L_{100,T}$(keV/µm)	L_D(keV/µm)	$L_{100,D}$(keV/µm)	λ(nm)	σ(µm^2)	Reference
C3H10T1/2	2 - 3 Gy/min	1.43E-05	1.22E-05	Ck X-rays	1.5 KVp	1.29E-01	2.21E+01	2.21E+01	2.30E+01	2.29E+01	2.04E+00	5.05E-05	Frankenberg, 1995
C3H10T1/2		1.44E-05		x-rays	225 KVp	1.35E+01	4.86E+00	3.79E+00	6.23E+00	5.40E+00	1.22E+01	1.12E-05	Palcic, 1985
C3H10T1/2	1.25 Gy/min	3.20E-05	4.60E-06	x-rays	250 KVp	1.58E+01	4.31E+00	3.33E+00	5.63E+00	4.85E+00	1.37E+01	2.21E-05	Hei, 1988a
C3H10T1/2		1.46E-04		x-rays	250 kVp	1.58E+01	4.31E+00	3.33E+00	5.63E+00	4.85E+00	1.37E+01	1.01E-04	Miller, 1995
C3H10T1/2		4.60E-05	2.90E-05	x-rays	250 KVp	1.58E+01	4.31E+00	3.33E+00	5.63E+00	4.85E+00	1.37E+01	3.17E-05	Miller, 1989
C3H10T1/2		2.00E-04	5.00E-05	x-rays	300 KVp	1.91E+01	3.97E+00	3.04E+00	5.23E+00	4.49E+00	1.50E+01	1.27E-04	Barrendsen, 1985
C3H10T1/2	0.7 Gy/min	3.60E-06	3.90E-06	γ	Co-60	3.55E+02	4.44E-01	2.84E-01	6.88E-01	5.15E-01	1.71E+02	2.56E-07	Frankenberg, 1995

AVI Single Strand Breaks of DNA Database

AVI-1 Densely Ionising Radiation on Cells

Cells (Types/Lines)	α(ssb's-Gy^{-1})	β(ssb's-Gy^{-2})	Ion Type	E(keV/amu)	E(MeV)	L_T(keV/μm)	$L_{100,T}$(keV/μm)	L_D(keV/μm)	$L_{100,D}$(keV/μm)	β^2	(z/b)2	λ(nm)	σ(μm^2)	Reference
V79-4	3.88E-01		n	6.00E+03	6.00E+00	1.61E+01	8.98E+00	2.39E+01	1.49E+01	6.13E-03	3.27E+02	1.25E+01	9.96E-01	Kampf, 1988
V79-379A	4.79E-01		p	7.60E+02	7.60E-01	3.19E+01	1.81E+01			1.62E-03	6.18E+02	5.68E+00	2.44E+00	Prise, 1990
V79-S171	2.84E-02		p	1.15E+03	1.15E+00	2.47E+01	1.38E+01			2.45E-03	4.09E+02	8.26E+00	1.12E-01	Ritter, 1977
V79-379A	2.76E-01		p	1.15E+03	1.15E+00	2.47E+01	1.38E+01			2.45E-03	4.09E+02	8.26E+00	1.09E+00	Prise, 1990
V79-379A	7.53E-01		p	1.90E+03	1.90E+00	1.68E+01	9.19E+00			4.04E-03	2.48E+02	1.41E+01	2.02E+00	Prise, 1990
V79-S171	5.26E-02		p	4.00E+03	4.00E+00	9.80E+00	5.24E+00			8.47E-03	1.18E+02	2.87E+01	8.25E-02	Ritter, 1977
V79-4	4.80E-01		H-2	6.28E+03	1.26E+01	6.86E+00	3.63E+00			1.33E-02	7.54E+01	4.51E+01	5.27E-01	Kampf, 1988
V79-379A	2.85E-01		α	9.50E+02	3.80E+00	1.08E+02	6.12E+01			2.04E-03	1.96E+03	1.79E+00	4.94E+00	Prise, 1990
V79-4	4.12E-01		He-4	4.90E+03	1.96E+01	3.27E+01	1.75E+01			1.04E-02	3.83E+02	8.96E+00	2.15E+00	Kampf, 1988
V79-4	3.68E-01		He-4	1.95E+03	7.81E+00	6.54E+01	3.62E+01			4.18E-03	9.58E+02	3.59E+00	3.85E+00	Kampf, 1988
V79-S171	1.82E-02		Be-9	4.00E+03	3.60E+01	1.53E+02	8.16E+01			8.52E-03	1.84E+03	1.84E+00	4.47E-01	Ritter, 1977
V79-4	2.30E-01		C-12	3.47E+03	4.17E+01	3.51E+02	1.87E+02			7.15E-03	4.47E+03	7.90E-01	1.29E+01	Kampf, 1988
V79-S171	1.30E-02		C-12	3.80E+03	4.56E+01	3.41E+02	1.81E+02			8.11E-03	4.13E+03	8.21E-01	7.09E-01	Ritter, 1977
V79-S171	9.20E-03		Ne-20	3.80E+03	7.60E+01	8.19E+02	4.35E+02			8.11E-03	1.02E+04	3.45E-01	1.20E+00	Ritter, 1977
V79-4	2.06E-01		Ne-22	3.19E+03	7.01E+01	9.05E+02	4.84E+02			6.81E-03	1.16E+04	2.98E-01	2.98E+01	Kampf, 1988
V79-S171	9.40E-03		A-40	3.90E+03	1.56E+02	2.06E+03	1.09E+03			8.33E-03	2.53E+04	1.38E-01	3.10E+00	Ritter, 1977
V79-S171	9.60E-03		A-40	1.50E+03	6.00E+01	2.69E+03	1.47E+03			3.22E-03	4.23E+04	8.36E-02	4.13E+00	Ritter, 1977
Bacteriophage T7	6.47E-03		H	3.18E+03	3.18E+00	1.17E+01	6.29E+00			6.74E-03	1.48E+02	2.28E+01	1.21E-02	Neary, 1970
Bacteriophage T7	5.83E-03		H	1.39E+03	1.39E+00	2.13E+01	1.18E+01			2.96E-03	3.38E+02	1.02E+01	1.99E-02	Neary, 1972
Bacteriophage T7	6.67E-03		H	1.39E+03	1.39E+00	2.13E+01	1.18E+01			2.96E-03	3.38E+02	1.02E+01	2.27E-02	Neary, 1970
Bacteriophage T7	5.45E-03		He-4	3.00E+03	1.20E+01	4.76E+01	2.59E+01			6.25E-03	6.40E+02	5.52E+00	4.15E-02	Neary, 1972
Bacteriophage T7	6.79E-03		He-4	1.33E+03	5.33E+00	8.45E+01	4.76E+01			2.85E-03	1.40E+03	2.51E+00	9.18E-02	Neary, 1972
Bacteriophage T7	6.79E-03		He-4	1.33E+03	5.33E+00	8.45E+01	4.76E+01			2.85E-03	1.40E+03	2.51E+00	9.18E-02	Neary, 1970
Bacteriophage T7	9.70E-03		B-10	6.00E+03	6.00E+01	1.71E+02	9.03E+01			1.27E-02	1.93E+03	1.81E+00	2.66E-01	Neary, 1972
Bacteriophage T7	1.41E-02		C-12	5.69E+03	6.83E+01	2.54E+02	1.34E+02			1.21E-02	2.88E+03	1.21E+00	5.74E-01	Neary, 1972
Bacteriophage T7	1.41E-02		C-12	5.69E+03	6.83E+01	2.54E+02	1.34E+02			1.21E-03	2.88E+03	1.21E+00	5.74E-01	Neary, 1970
ϕx-174	8.50E-05		D	7.50E+03	1.50E+01	5.84E+00	3.08E+00			1.58E-02	6.33E+01	5.52E+01	7.94E-05	Christensen, 1972
ϕx-174	8.16E-05		He-4	4.63E+03	1.85E+01	3.50E+01	1.88E+01			9.85E-03	4.06E+02	8.13E+00	4.57E-04	Christensen, 1972
ϕx-174	7.82E-05		Li-7	4.71E+03	3.30E+01	7.87E+01	4.17E+01			1.00E-02	8.98E+02	3.71E+00	9.84E-04	Christensen, 1972
ϕx-174	6.80E-05		B-11	4.18E+03	4.60E+01	2.29E+02	1.22E+02			8.91E-03	2.70E+03	1.25E+00	2.49E-03	Christensen, 1972
ϕx-174	5.44E-05		C-12	3.88E+03	4.65E+01	3.33E+02	1.77E+02			8.27E-03	4.06E+03	8.50E-01	2.90E-03	Christensen, 1972
ϕx-174	3.74E-05		O-16	4.00E+03	6.40E+01	5.51E+02	2.93E+02			8.54E-03	6.64E+03	5.14E-01	3.30E-03	Christensen, 1972
ϕx-174	4.42E-05		Ar-40	2.40E+03	9.60E+01	2.42E+03	1.30E+03			5.14E-03	3.35E+04	1.05E-01	1.71E-02	Christensen, 1972

AVI-2 Sparsely Ionising Radiation on Cells

Cells (Types/Lines)	Dose rate	α(ssb's-Gy^{-1})	β(ssb's-Gy^{-2})	Rad. Type	Source	E(keV)	L_T(keV/μm)	$L_{100,T}$(keV/μm)	L_D(keV/μm)	$L_{100,D}$(keV/μm)	λ(nm)	σ(μm^2)	Reference
V79-379A	2.50E+00	1.50E-01		Alk x-rays	3 KVp	5.34E-01	1.67E+01	1.51E+01	1.77E+01	1.67E+01	2.88E+00	4.02E-01	Prise, 1989
GM38		1.25E+03		X-rays	225 KVp	1.35E+01	4.86E+00	3.79E+00	6.23E+00	5.40E+00	1.22E+01	9.71E+02	Rydberg, 1996
V79-379A	1.80E+00	3.10E-01		x-rays	250 KVp	1.58E+01	4.31E+00	3.33E+00	5.63E+00	4.85E+00	1.37E+01	2.14E-01	Prise, 1989
V79-379A		3.62E-01		x-rays	250 KVp	1.58E+01	4.31E+00	3.33E+00	5.63E+00	4.85E+00	1.37E+01	2.50E-01	Prise, 1990
V79-S171		5.34E-02		x-rays	300 KVp	1.91E+01	3.97E+00	3.04E+00	5.23E+00	4.49E+00	1.50E+01	3.39E-02	Ritter, 1977
V79-4		5.30E-01		γ	Co-60	3.55E+02	4.44E-01	2.84E-01	6.88E-01	5.15E-01	1.71E+02	3.77E-02	Kampf, 1988
Bacteriophage T7		4.64E-03		γ	Co-60	3.55E+02	4.44E-01	2.84E-01	6.88E-01	5.15E-01	1.71E+02	3.30E-04	Neary, 1972
Bacteriophage T7		4.08E-03		γ	Co-60	3.55E+02	4.44E-01	2.84E-01	6.88E-01	5.15E-01	1.71E+02	2.90E-04	Neary, 1972
ϕx-174		1.26E-04		γ	Co-60	3.55E+02	4.44E-01	2.84E-01	6.88E-01	5.15E-01	1.71E+02	8.94E-06	Christensen, 1972

AVII Double Strand Breaks of DNA Database

AVII-1 Charged Particles on Cells

Cells (Types/Lines)	α(dsb's/Gy-cell)	β(dsb's/Gy^2-cell)	Ion Type	E(keV/amu)	E(MeV)	L_∞(keV/μm)	$L_{100,\infty}$(keV/μm)	β^2	z^{*2}/β^2	λ(nm)	σ(μm^2)	Reference
V79-379A	1.92E-02		p	7.60E+02	7.60E-01	3.19E+01	1.81E+01	1.62E-03	6.18E+02	5.68E+00	9.78E-02	Prise, 1990
V79	9.16E+00		p	8.20E+02	8.20E-01	3.00E+01	1.69E+01	1.75E-03	5.73E+02	6.24E+00	4.40E+01	Jenner, 1992
V79	1.07E+01		p	8.80E+02	8.80E-01	2.92E+01	1.65E+01	1.87E-03	5.34E+02	6.46E+00	4.98E+01	Belli, 1994/ 1996
V79-379A	1.15E-02	2.70E-04	p	1.15E+03	1.15E+00	2.47E+01	1.38E+01	2.45E-03	4.09E+02	8.26E+00	4.54E-02	Prise, 1990
V79-S171	1.30E-03		p	1.15E+03	1.15E+00	2.47E+01	1.38E+01	2.45E-03	4.09E+02	8.26E+00	5.12E-03	Ritter, 1977
V79	7.88E+00		p	1.50E+03	1.50E+00	2.00E+01	1.10E+01	3.19E-03	3.14E+02	1.12E+01	2.52E+01	Jenner, 1992
V79	1.04E+01		p	1.50E+03	1.50E+00	1.99E+01	1.10E+01	3.19E-03	3.14E+02	1.12E+01	3.32E+01	Belli, 1994/ 1996
V79-379A	6.50E-03	8.70E-04	p	1.90E+03	1.90E+00	1.69E+01	9.19E+00	4.04E-03	2.48E+02	1.41E+01	1.75E-02	Prise, 1990
V79	1.30E+01		p	3.24E+03	3.24E+00	1.17E+01	6.27E+00	6.78E-03	1.47E+02	2.29E+01	2.42E+01	Belli, 1994/ 1996
V79-S171	8.12E-04		p	4.00E+03	4.00E+00	9.80E+00	5.24E+00	8.47E-03	1.18E+02	2.87E+01	1.27E-03	Ritter, 1977
V79-4	1.10E-02		H-2	3.41E+03	6.81E+00	1.09E+01	5.85E+00	7.22E-03	1.39E+02	2.50E+01	1.92E-02	Kampf, 1988
V79-379A	2.30E-02		α	7.50E+02	3.00E+00	1.27E+02	7.21E+01	1.61E-03	2.48E+03	1.43E+00	4.68E-01	Prise, 1987
V79-4	9.90E-02		α	8.28E+02	3.31E+00	1.18E+02	6.69E+01	1.77E-03	2.25E+03	1.58E+00	1.87E+00	Jenner, 1993
V79-379A	1.45E-02		α	9.50E+02	3.80E+00	1.08E+02	6.12E+01	2.04E-03	1.96E+03	1.79E+00	2.51E-01	Prise, 1990
V79-4	1.72E-02		He-4	1.95E+03	7.81E+00	6.54E+01	3.62E+01	4.18E-03	9.58E+02	3.59E+00	1.80E-01	Kampf, 1988
V79-4	1.35E-02		He-4	4.90E+03	1.96E+01	3.27E+01	1.75E+01	1.04E-02	3.83E+02	8.96E+00	7.06E-02	Kampf, 1988
V79	1.07E+01		α	5.50E+03	2.20E+01	3.00E+01	1.60E+01	1.17E-02	3.43E+02	1.00E+01	5.11E+01	Jenner, 1992
V79	1.09E+01		α	8.88E+03	3.55E+01	2.00E+01	1.10E+01	1.85E-02	2.17E+02	1.58E+01	3.48E+01	Jenner, 1992
V79-S171	3.65E-03		Be-9	4.00E+03	3.60E+01	1.53E+02	8.16E+01	8.52E-03	1.84E+03	1.84E+00	8.95E-02	Ritter, 1977
V79-4	1.63E-02		C-12	3.47E+03	4.17E+01	3.51E+02	1.87E+02	7.15E-03	4.47E+03	7.90E-01	9.16E-01	Kampf, 1988
V79-S171	2.58E-03		C-12	3.80E+03	4.56E+01	3.41E+02	1.81E+02	8.11E-03	4.13E+03	8.21E-01	1.41E-01	Ritter, 1977
V79	4.08E-03		O-16	1.08E+04	1.73E+02	2.76E+02	1.44E+02	2.28E-02	2.76E+02	1.26E+00	1.80E-01	Weber, 1993
V79-S171	1.84E-03		Ne-20	3.80E+03	7.60E+01	8.19E+02	4.35E+02	8.11E-03	1.02E+04	3.45E-01	2.41E-01	Ritter, 1977
V79	2.14E-03		Ne-20	1.40E+04	2.80E+02	3.51E+02	1.83E+02	2.94E-02	3.33E+03	1.03E+00	1.20E-01	Weber, 1993
V79-S171	1.70E-03		Ar-40	3.90E+03	1.56E+02	2.06E+03	1.09E+03	8.33E-03	2.53E+04	1.38E-01	5.60E-01	Ritter, 1977
V79	1.92E-03		Ar-40	5.90E+03	2.36E+02	1.69E+03	8.91E+02	1.26E-02	1.92E+04	1.88E-01	5.20E-01	Weber, 1993
V79	1.77E+00		Kr-84	5.70E+03	4.79E+02	4.72E+03	2.49E+03	1.21E-02	5.38E+04	6.53E-02	1.33E+03	Rydberg, 1985
V79	3.95E+00		Kr-84	1.79E+04	1.50E+03	2.90E+03	1.50E+03	3.74E-02	2.70E+04	1.30E-01	1.83E+03	Rydberg, 1985
V79	2.09E-03		Xe-132	1.14E+04	1.50E+03	6.52E+03	3.40E+03	2.41E-02	6.54E+04	5.38E-02	2.18E+00	Weber, 1993
V79	6.45E-02		Au-197	1.10E+02	2.17E+01	2.42E+03	2.42E+03	2.79E-05	2.88E+03	1.07E-01	2.50E+01	Rydberg, 1985

Cells (Types/Lines)	α(dsb's/Gy-cell)	β(dsb's/Gy^2-cell)	Ion Type	E(keV/amu)	E(MeV)	L_T(keV/μm)	$L_{100,T}$(keV/μm)	β^2	z^{*2}/β^2	λ(nm)	σ(μm^2)	Reference
V79	3.35E-02		Pb-208	1.30E+02	2.70E+01	4.39E+03	4.22E+03	2.79E-04	1.43E+05	3.94E-02	2.35E+01	Rydberg, 1985
V79	1.04E-03		Au-197	9.80E+03	1.93E+03	1.11E+04	5.80E+03	2.07E-02	1.14E+05	3.07E-02	1.85E+00	Weber, 1993
CHO-K1	9.80E-03		D	2.90E+03	5.80E+00	1.20E+01	6.50E+00	6.20E-03	1.60E+02	2.18E+01	1.88E-02	Taucher-Scholz, 1995
CHO-K1	3.16E-02		D	6.10E+03	1.22E+01	6.60E+00	3.60E+00	1.30E-02	7.90E+01	5.52E+01	3.34E-02	Taucher-Scholz, 1995
CHO-K1	2.64E-02		D	7.10E+03	1.42E+01	6.00E+00	3.10E+00	1.50E-02	6.30E+01	5.52E+00	2.53E-02	Taucher-Scholz, 1995
CHO-K1	1.19E+01		C12	2.80E+03	3.36E+01	4.00E+02	2.14E+02	5.85E-03	5.30E+03	9.00E-01	7.62E+02	Heilmann, 1995
CHO-K1	1.41E+01		C12	5.40E+03	6.48E+01	2.28E+02	1.39E+02	1.18E-02	3.01E+03	2.00E+00	5.14E+02	Heilmann, 1995
CHO-K1	2.56E+01		C12	1.09E+04	1.31E+02	1.54E+02	8.09E+01	2.28E-02	1.53E+03	3.00E+00	6.31E+02	Heilmann, 1995
CHO-K1	3.66E+01		C12	1.81E+04	2.17E+02	1.03E+02	5.63E+01	3.76E-02	9.92E+02	5.60E+00	6.03E+02	Heilmann, 1995
CHO-K1	3.87E+01		C12	1.86E+05	2.23E+03	1.70E+01	8.80E+00	3.01E-01	1.10E+02	5.00E+01	1.05E+02	Heilmann, 1995
CHO-K1	3.46E+01		C12	2.61E+05	3.13E+03	1.40E+01	6.80E+00	3.98E-01	8.03E+01	6.50E+01	7.75E+01	Heilmann, 1995
CHO-K1	3.26E-03		O-16	1.08E+04	1.73E+02	2.76E+02	1.44E+02	2.28E-02	2.76E+03	1.26E+00	1.44E-01	Taucher-Scholz, 1996
CHO-K1	7.46E-03		O-16	1.14E+04	1.82E+02	2.50E+02	1.30E+02	2.63E-02	2.40E+03	2.10E+00	2.99E-01	Taucher-Scholz, 1995
CHO-K1	9.08E-03		O-16	5.50E+04	8.80E+02	7.71E+01	3.89E+01	1.08E-01	5.90E+02	5.84E+00	1.12E-01	Taucher-Shcolz, 1996
CHO-K1	1.05E-02		O-16	2.02E+05	3.23E+03	2.92E+01	1.51E+01	3.25E-01	1.97E+02	1.74E+01	4.90E-02	Taucher-Shcolz, 1996
CHO-K1	8.78E-03		O-16	3.07E+05	4.91E+03	2.28E+01	1.16E+01	4.34E-01	1.47E+02	2.36E+01	3.20E-02	Taucher-Shcolz, 1996
CHO-K1	4.30E-02		O-16	3.86E+05	6.18E+03	2.03E+01	1.02E+01	5.00E-01	1.28E+02	2.73E+01	1.40E-01	Taucher-Shcolz, 1996
CHO-K1	5.13E-02		O-16	3.97E+05	6.35E+03	2.00E+01	9.98E+00	5.11E-01	1.25E+02	4.54E+01	1.64E-01	Taucher-Scholz, 1995
CHO-K1	9.43E-03		Ar-40	5.30E+03	2.12E+02	1.73E+03	9.50E+02	1.10E-02	2.00E+04	2.50E-01	2.62E+00	Taucher-Scholz, 1995
CHO-K1	1.37E-02		Ar-40	1.33E+04	5.32E+02	1.05E+03	5.10E+02	3.10E-02	9.60E+03	5.40E-01	2.29E+00	Taucher-Scholz, 1995
CHO-K1	1.16E-03		Ca-40	6.90E+03	2.76E+02	1.87E+03	9.82E+02	1.47E-02	2.04E+04	1.70E-01	3.47E-01	Taucher-Shcolz, 1996
CHO-K1	6.85E-03		Ni-58	4.00E+05	2.32E+04	2.10E+02	2.05E+02	6.10E-01	1.30E+03	4.50E+00	2.30E-01	Taucher-Shcolz, 1996
CHO-K1	3.90E-03		Ni-58	6.50E+05	3.77E+04	2.02E+02	1.01E+02	6.52E-01	1.21E+03	4.78E+00	1.26E-01	Taucher-Shcolz, 1996
CHO-K1	1.54E-03		Xe-132	9.10E+03	1.20E+03	7.99E+03	5.20E+03	3.20E-03		4.10E-01	1.97E+00	Taucher-Scholz, 1995
CHO-K1	4.35E-03		Xe-132	1.18E+04	1.56E+03	7.29E+03	3.82E+03	1.70E-02	7.85E+04	6.67E-02	5.07E+00	Taucher-Scholz, 1995
CHO-K1	1.08E-02		Pb-207	4.82E+05	9.98E+04	1.66E+03	8.30E+02	6.74E-01	9.96E+03	5.85E-01	2.86E+00	Taucher-Scholz, 1995
EATC	6.69E+01		α	8.50E+02	3.40E+00	1.17E+02	6.63E+01	1.82E-03	2.19E+03	1.60E+00	1.25E+03	Blocher, 1988
mammalian cells	6.97E-03		Ne-20	4.20E+03	8.40E+01	7.72E+02	4.09E+02	8.96E-03	9.39E+03	3.75E-01	8.60E-01	Heilmann, 1993
mammalian cells	8.56E-03		Ne-20	1.04E+04	2.08E+02	4.46E+02	2.32E+02	2.20E-02	4.38E+03	7.68E-01	6.10E-01	Heilmann, 1993
mammalian cells	1.29E-02		Ne-20	1.12E+04	2.24E+02	4.16E+02	2.17E+02	2.36E-02	4.09E+03	8.36E-01	8.60E-01	Heilmann, 1993
mammalian cells	1.09E-02		Ne-20	1.42E+04	2.84E+02	3.49E+02	1.82E+02	2.98E-02	3.29E+03	1.04E+00	6.10E-01	Heilmann, 1993
mammalian cells	3.95E+00		Ar-40	2.70E+03	1.08E+02	2.34E+03	1.25E+03	5.78E-03	3.14E+04	1.12E-01	1.48E+03	Heilmann, 1993
mammalian cells	2.57E-03		Ar-40	6.10E+03	2.44E+02	1.68E+03	8.83E+02	1.30E-02	1.88E+04	1.86E-01	6.90E-01	Heilmann, 1993

Cells (Types/Lines)	α(dsb's/Gy-cell)	β(dsb's/Gy^2-cell)	Ion Type	E(keV/amu)	E(MeV)	L_T(keV/μm)	$L_{100,T}$(keV/μm)	β^2	z^{*2}/β^2	λ(nm)	σ(μm^2)	Reference
mammalian cells	3.08E-03		Ar-40	9.40E+03	3.76E+02	1.32E+03	6.88E+02	1.99E-02	1.37E+04	2.57E-01	6.50E-01	Heilmann, 1993
mammalian cells	3.95E+00		Ar-40	1.05E+04	4.20E+02	1.23E+03	6.42E+02	2.22E-02	1.26E+04	2.81E-01	7.80E+02	Heilmann, 1993
mammalian cells	3.54E-03		Ar-40	1.31E+04	5.24E+02	1.11E+03	5.77E+02	2.76E-02	1.05E+04	3.21E-01	6.30E-01	Heilmann, 1993
mammalian cells	2.97E-03		Ti-48	4.00E+03	1.92E+02	2.80E+03	1.49E+03	7.86E-03	3.49E+04	9.97E-02	1.33E+00	Heilmann, 1993
mammalian cells	3.95E+00		Ti-48	4.67E+03	2.24E+02	2.58E+03	1.37E+03	9.96E-03	3.04E+04	1.14E-01	1.63E+03	Heilmann, 1993
mammalian cells	3.95E+00		Ti-48	1.19E+04	5.72E+02	1.65E+03	8.57E+02	2.51E-02	1.60E+04	2.13E-01	1.04E+03	Heilmann, 1993
mammalian cells	3.95E+00		Ni-56	5.00E+03	2.80E+02	3.53E+03	1.86E+03	1.07E-02	4.11E+04	8.46E-02	2.23E+03	Heilmann, 1993
mammalian cells	3.95E+00		Ni-56	1.54E+04	8.62E+02	2.10E+03	1.09E+03	3.23E-02	1.99E+04	1.76E-01	1.33E+03	Heilmann, 1993
mammalian cells	3.41E-03		Ge-74	1.01E+04	7.47E+02	3.21E+03	1.67E+03	2.14E-02	3.29E+04	1.07E-01	1.75E+00	Heilmann, 1993
mammalian cells	2.43E-04		Kr-84	5.00E+03	4.20E+02	4.89E+03	2.58E+03	1.07E-02	5.74E+04	6.15E-02	1.90E-01	Heilmann, 1993
mammalian cells	6.41E-04		Kr-84	1.19E+04	1.00E+03	3.61E+03	1.88E+03	2.51E-02	3.54E+04	9.76E-02	3.70E-01	Heilmann, 1993
mammalian cells	3.95E+00		La-139	1.01E+04	1.40E+03	7.34E+03	3.83E+03	2.14E-02	7.47E+04	4.66E-02	4.65E+03	Heilmann, 1993
HSF	4.89E+01		p	5.00E+03	5.00E+00	8.00E+00	4.00E+00	1.06E-02	9.46E+01	3.59E+01	6.26E+01	Frankenberg, 1997
HSF	4.59E+01		α	7.50E+02	3.00E+00	1.26E+02	7.20E+01	1.61E-03	2.48E+03	1.43E+00	9.25E+02	Frankenberg, 1997
Caski	4.30E-03		O-16	1.08E+04	1.73E+02	2.76E+02	1.44E+02	2.28E-02	2.76E+02	1.26E+00	1.90E-01	Weber, 1993
Caski	3.75E-03		Ne-20	1.00E+04	2.00E+02	4.50E+02	2.36E+02	2.11E-02	4.53E+03	7.54E-01	2.70E-01	Weber, 1993
Caski	3.56E-03		Ne-20	1.40E+04	2.80E+02	3.51E+02	1.83E+02	2.94E-02	3.33E+03	1.03E+00	2.00E-01	Weber, 1993
Caski	2.36E-03		Ar-40	5.90E+03	2.36E+02	1.69E+03	8.91E+02	1.26E-02	1.92E+04	1.88E-01	6.40E-01	Weber, 1993
Caski	2.23E-03		Xe-132	1.14E+04	1.50E+03	6.52E+03	3.40E+03	2.41E-02	6.54E+04	5.38E-02	2.33E+00	Weber, 1993
GM38	1.85E+01		N-14	2.93E+04	4.10E+02	9.70E+01	5.06E+01	5.90E-02	8.35E+02	4.09E+00	2.87E+02	Rydberg, 1996
GM38A	2.64E+01		Ne-20	4.25E+05	8.50E+03	3.20E+01	1.60E+01	5.11E-01	2.02E+02	2.82E+01	1.35E+02	Lobrich, 1994
GM38	1.15E+01		Fe-56	1.25E+05	7.00E+03	4.40E+02	2.30E+02	2.22E-01	3.23E+03	1.82E+00	8.10E+02	Rydberg, 1996
GM38	1.35E+01		Fe-56	1.61E+05	9.00E+03	3.50E+02	1.78E+02	2.60E-01	2.60E+03	2.20E+00	7.56E+02	Rydberg, 1996
GM38A	1.68E+01		Fe-56	2.50E+05	1.40E+04	3.50E+02	1.90E+02	2.67E-01	2.60E+04	2.24E+00	9.41E+02	Lobrich, 1994
GM38A	1.68E+01		Fe-56	4.00E+05	2.24E+04	2.40E+02	1.24E+02	4.28E-01	1.60E+03	3.56E+00	6.45E+02	Lobrich, 1994
GM38	1.60E+01		Fe-56	5.00E+05	2.80E+04	1.90E+02	9.60E+01	5.78E-01	1.20E+03	4.78E+00	4.86E+02	Rydberg, 1996
GM38A	1.68E+01		Fe-56	6.00E+05	3.36E+04	1.90E+02	9.70E+01	5.77E-01	1.20E+03	4.70E+00	5.11E+02	Lobrich, 1994
Bovine lens epithelial cells	1.54E-03		O-16	3.50E+03	5.60E+01	5.24E+02	5.80E+02	7.30E-03	7.50E+03	4.50E-01	1.30E-01	Aufderheide, 1987
Bovine lens epithelial cells	4.26E-03		O-16	8.70E+03	1.39E+02	2.85E+02	3.10E+02	1.80E-02	3.40E+03	1.10E+00	1.95E-01	Aufderheide, 1987
Bovine lens epithelial cells	7.94E-03		Ar-40	1.93E+04	7.72E+02	7.90E+02	8.20E+02	7.10E+03	4.10E-02	4.50E-01	1.00E+00	Aufderheide, 1987
Bovine lens epithelial cells	4.59E-03		Kr-84	1.80E+04	1.51E+03	3.04E+03	2.70E+03	4.60E-02	2.54E+04	2.10E-01	2.23E+00	Aufderheide, 1987
Bovine lens epithelial cells	9.24E-04		Xe-132	5.40E+03	7.13E+02	8.80E+03	7.80E+03	1.20E-02	9.10E+04	5.60E-02	1.30E+00	Aufderheide, 1987
Bovine lens epithelial cells	2.02E-03		Xe-132	1.01E+04	1.33E+03	7.20E+03	6.71E+03	2.12E-02	7.06E+04	7.47E-02	2.33E+00	Aufderheide, 1987

Cells (Types/Lines)	α(dsb's/Gy-cell)	β(dsb's/Gy^2-cell)	Ion Type	E(keV/amu)	E(MeV)	L_T(keV/μm)	$L_{100,T}$(keV/μm)	β^2	z^{*2}/β^2	λ(nm)	σ(μm^2)	Reference
Bovine lens epithelial cells	4.00E-03		Xe-132	1.65E+04	2.18E+03	6.20E+03	5.70E+03	3.90E-02	4.20E+04	9.80E-02	3.97E+00	Aufderheide, 1987
Bovine lens epithelial cells	3.08E-04		U-238	1.50E+03	3.57E+02	1.42E+04	1.24E+04	3.21E-03		2.74E-02	7.00E-01	Aufderheide, 1987
Bovine lens epithelial cells	6.58E-04		U-238	4.10E+03	9.76E+02	1.52E+04	1.41E+04	8.53E-03	1.76E+05	2.97E-02	1.70E+00	Aufderheide, 1987
Yeast, 211-rad22	1.44E-01		α	8.75E+02	3.50E+00	1.16E+02	6.56E+01	1.88E-03	2.13E+03	1.63E+00	2.67E+00	Frankenberg, 1990/81
Yeast, diploid 211*B	1.58E-02		α	8.75E+02	3.50E+00	1.16E+02	6.56E+01	1.88E-03	2.13E+03	1.63E+00	2.93E-01	Lobrich, 1993
Yeast, diploid 211*B	1.40E-02		α	8.80E+02	3.52E+00	1.16E+02	6.55E+01	1.89E-03	2.12E+03	1.63E+00	2.60E-01	Ikpeme, 1995
Yeast, diploid 211*B	6.66E-03		C-12	3.40E+03	4.08E+01	3.66E+02	1.95E+02	7.26E-03	4.55E+03	7.46E-01	3.90E-01	Ikpeme, 1995
Yeast, diploid 211*B	1.86E-02		C-12	1.80E+04	2.16E+02	1.04E+02	5.39E+01	3.76E-02	9.57E+02	3.63E+00	3.10E-01	Ikpeme, 1995
Yeast, diploid 211*B	6.96E-03		O-16	2.90E+03	4.64E+01	6.64E+02	3.56E+02	6.20E-03	8.58E+03	3.95E-01	7.40E-01	Ikpeme, 1995
Yeast, diploid 211*B	7.67E-03		O-16	8.00E+03	1.28E+02	3.50E+02	1.83E+02	1.70E-02	3.64E+03	9.33E-01	4.30E-01	Ikpeme, 1995
Yeast, diploid 211*B	1.04E-02		O-16	1.07E+04	1.71E+02	2.77E+02	1.44E+02	2.26E-02	2.78E+03	1.25E+00	4.60E-01	Ikpeme, 1995
Yeast, diploid 211*B	4.24E-03		Ar-40	1.40E+04	5.60E+02	1.05E+03	5.44E+02	2.94E-02	9.97E+03	3.45E-01	7.10E-01	Akpa, 1992
Yeast, diploid 211*B	5.60E-03		Ne-20	4.90E+03	9.80E+01	7.14E+02	3.77E+02	1.04E-02	8.32E+03	4.16E-01	6.40E-01	Akpa, 1992
Yeast, diploid 211*B	7.97E-03		Ne-20	9.80E+03	1.96E+02	4.55E+02	2.38E+02	2.07E-02	4.62E+03	7.48E-01	5.80E-01	Akpa, 1992
Yeast, diploid 211*B	7.38E-03		Ne-20	1.44E+04	2.88E+02	3.47E+02	1.81E+02	3.02E-02	3.25E+03	1.04E+00	4.10E-01	Akpa, 1992
Yeast, diploid 211*B	1.08E-02		Ne-20	1.44E+04	2.88E+02	3.47E+02	1.81E+02	3.02E-02	3.25E+03	1.04E+00	6.00E-01	Ikpeme, 1995
Yeast, diploid 211*B	1.32E-02		Ne-20	1.50E+04	3.00E+02	3.27E+02	1.70E+02	3.15E-02	3.12E+03	1.12E+00	6.90E-01	Ikpeme, 1995
Yeast, diploid 211*B	3.23E-03		Ar-40	5.00E+03	2.00E+02	1.86E+03	9.82E+02	1.07E-02	2.15E+04	1.60E-01	9.60E-01	Akpa, 1992
Yeast, diploid 211*B	4.27E-03		Ar-40	5.70E+03	2.28E+02	1.76E+03	9.25E+02	1.21E-02	1.97E+04	1.74E-01	1.20E+00	Ikpeme, 1995
Yeast, diploid 211*B	3.92E-03		Ar-40	1.29E+04	5.16E+02	1.12E+03	5.80E+02	2.72E-02	1.07E+04	3.19E-01	7.00E-01	Akpa, 1992
Yeast, diploid 211*B	3.35E-03		Ar-40	1.34E+04	5.36E+02	1.06E+03	5.52E+02	2.82E-02	1.03E+04	3.39E-01	5.70E-01	Akpa, 1992
Yeast, diploid 211*B	2.46E-03		Ni-58	1.21E+04	7.02E+02	2.41E+03	1.25E+03	2.55E-02	2.36E+04	1.47E-01	9.50E-01	Ikpeme, 1995
Yeast, diploid 211*B	1.87E-03		Kr-84	1.12E+04	9.41E+02	3.75E+03	1.95E+03	2.36E-02	3.68E+04	9.24E-02	1.12E+00	Ikpeme, 1995
Yeast, diploid 211*B	2.48E-03		Xe-132	1.18E+04	1.56E+03	6.48E+03	3.38E+03	2.49E-02	6.42E+04	5.43E-02	2.57E+00	Akpa, 1992
Yeast, diploid 211*B	4.59E-03		Xe-132	1.40E+04	1.85E+03	6.15E+03	3.20E+03	2.94E-02	5.86E+04	5.86E-02	4.52E+00	Ikpeme, 1995
Yeast, diploid 211*B	2.96E-03		Au-197	9.10E+03	1.79E+03	1.13E+04	5.92E+03	1.93E-02	1.18E+05	2.96E-02	5.37E+00	Akpa, 1992
Yeast, diploid 211*B	2.56E-03		Au-197	9.30E+03	1.83E+03	1.13E+04	5.91E+03	1.97E-02	1.17E+05	2.97E-02	4.63E+00	Ikpeme, 1995
Yeast, diploid 211*B	3.95E+00		Au-197	1.17E+04	2.30E+03	1.08E+04	5.61E+03	2.47E-02	1.06E+05	3.25E-02	6.81E+03	Ikpeme, 1995
Yeast, diploid 211*B	1.62E-03		Pb-207	1.27E+04	2.63E+03	1.10E+04	5.80E+03	2.50E-02	1.10E+05	4.80E-02	2.85E+00	Akpa, 1992
Bacillus spores	1.76E-03		Ne-20	1.39E+03	2.88E+02	3.47E+02	1.81E+02	3.02E-02	3.25E+03	1.04E+00	9.80E-02	Micke, 1994
Bacillus spores	1.08E-03		Ar-40	8.90E+03	3.56E+02	1.39E+03	7.24E+02	1.89E-02	1.43E+04	2.41E-01	2.40E-01	Micke, 1994
Bacillus spores	8.11E-04		Ar-40	1.05E+04	4.20E+02	1.23E+03	6.42E+02	2.22E-02	1.26E+04	2.81E-01	1.60E-01	Micke, 1994
Bacillus spores	4.17E-04		Ar-40	1.39E+04	5.56E+02	1.05E+03	5.45E+02	2.92E-02	1.00E+04	3.44E-01	7.00E-02	Micke, 1994

Cells (Types/Lines)	α(dsb's/Gy-cell)	β(dsb's/Gy^2-cell)	Ion Type	E(keV/amu)	E(MeV)	L_T(keV/μm)	$L_{100,T}$(keV/μm)	β^2	z^{*2}/β^2	λ(nm)	σ(μm^2)	Reference
Bacillus spores	2.31E-04		Pb-207	4.30E+03	8.90E+02	1.27E+04	6.75E+03	9.17E-03	1.54E+05	2.27E-02	4.70E-01	Micke, 1994
Bacillus spores	3.22E-04		Pb-207	1.27E+04	2.63E+03	1.11E+04	5.76E+03	2.67E-02	1.08E+05	3.20E-02	5.70E-01	Micke, 1994
Bacteriophage T7	2.67E-04		H	1.39E+03	1.39E+00	2.13E+01	1.18E+01	2.96E-03	3.38E+02	1.02E+01	9.10E-04	Neary, 1972
Bacteriophage T7	2.57E-04		H	1.39E+03	1.39E+00	2.13E+01	1.18E+01	2.96E-03	3.38E+02	1.02E+01	8.76E-04	Neary, 1970
Bacteriophage T7	2.06E-04		H	3.18E+03	3.18E+00	1.17E+01	6.29E+00	6.74E-03	1.48E+02	2.28E+01	3.85E-04	Neary, 1970
Bacteriophage T7	2.63E-04		He-4	1.33E+03	5.33E+00	8.45E+01	4.76E+01	2.85E-03	1.40E+03	2.51E+00	3.56E-03	Neary, 1972
Bacteriophage T7	2.91E-04		He-4	1.33E+03	5.33E+00	8.45E+01	4.76E+01	2.85E-03	1.40E+03	2.51E+00	3.94E-03	Neary, 1970
Bacteriophage T7	2.86E-04		He-4	3.00E+03	1.20E+01	4.76E+01	2.59E+01	6.25E-03	6.40E+02	5.52E+00	2.18E-03	Neary, 1972
Bacteriophage T7	3.80E-04		B-10	6.00E+03	6.00E+01	1.71E+02	9.03E+01	1.27E-02	1.93E+03	1.81E+00	1.04E-02	Neary, 1972
Bacteriophage T7	5.72E-04		C-12	5.69E+03	6.83E+01	2.54E+02	1.34E+02	1.21E-02	2.88E+03	1.21E+00	2.33E-02	Neary, 1972
Bacteriophage T7	4.88E-04		C-12	5.69E+03	6.83E+01	2.54E+02	1.34E+02	1.21E-03	2.88E+03	1.21E+00	1.99E-02	Neary, 1970
SV40	8.35E-05		U-238	4.71E+03	1.12E+03	1.42E+04	7.54E+03	1.00E+02	1.69E+05	2.07E-02	1.90E-01	Stanton, 1990
SV40	1.12E-04		Xe-131	3.82E+03	5.00E+02	8.40E+03	4.40E+03	8.01E-03	1.04E+05	3.38E-02	1.50E-01	Stanton, 1990
SV40	3.27E-04		Ne-20	1.10E+04	2.20E+02	4.20E+02	2.18E+02	2.32E-02	4.16E+03	8.29E-01	2.20E-02	Stanton, 1990
SV40	2.98E-04		Ne-20	1.09E+04	2.18E+02	4.20E+02	2.19E+02	2.30E-02	4.19E+03	8.26E-01	2.00E-02	Stanton, 1990
SV40	1.86E-04		Ar-40	1.13E+04	4.50E+02	1.21E+03	6.29E+02	2.36E-02	1.19E+04	2.88E-01	3.60E-02	Stanton, 1990
SV40	1.33E-04		Ar-40	8.26E+03	3.31E+02	1.46E+03	7.64E+02	1.75E-02	1.51E+04	2.25E-01	3.10E-02	Stanton, 1990
SV40	1.09E-04		Ar-40	4.17E+03	1.67E+02	2.00E+03	1.05E+03	8.90E-03	2.42E+04	1.46E-01	3.50E-02	Stanton, 1990
SV40	2.17E-04		Kr-84	8.93E+03	7.50E+02	4.03E+03	2.11E+03	1.89E-02	4.22E+04	9.34E-02	1.40E-01	Stanton, 1990
SV40	1.47E-04		Xe-132	5.56E+03	7.34E+02	8.50E+03	4.57E+03	5.03E-03	1.18E+05	2.98E-02	2.00E-01	Stanton, 1990
SV40	8.35E-05		U-238	4.03E+03	9.60E+02	1.42E+04	7.56E+03	8.60E-03	1.75E+05	2.01E-02	1.90E-01	Stanton, 1990
ϕx-174	3.06E-06		D	7.50E+03	1.50E+01	5.84E+00	3.08E+00	1.58E-02	6.33E+01	5.52E+01	2.86E-06	Christensen, 1972
ϕx-174	7.24E-06		He-4	4.63E+03	1.85E+01	3.50E+01	1.88E+01	9.65E-03	4.06E+02	8.13E+00	4.05E-05	Christensen, 1972
ϕx-174	8.50E-06		Li-7	4.71E+03	3.30E+01	7.87E+01	4.17E+01	1.00E-02	8.98E+02	3.71E+00	1.07E-04	Christensen, 1972
ϕx-174	1.53E-05		B-11	4.18E+03	4.60E+01	2.29E+02	1.22E+02	8.91E-03	2.70E+03	1.25E+00	5.60E-04	Christensen, 1972
ϕx-174	1.90E-05		C-12	3.88E+03	4.65E+01	3.33E+02	1.77E+02	8.27E-03	4.06E+03	8.50E-01	1.01E-03	Christensen, 1972
ϕx-174	2.07E-05		O-16	4.00E+03	6.40E+01	5.51E+02	2.93E+02	8.54E-03	6.64E+03	5.14E-01	1.83E-03	Christensen, 1972
ϕx-174	1.62E-05		Ar-40	2.40E+03	9.60E+01	2.42E+03	1.30E+03	5.14E-03	3.35E+04	1.05E-01	6.25E-03	Christensen, 1972

mammalian cells: either bovine lense epithelial cells or HF

AVII-2 Neutrons on Cells

Cells (Types/Lines	Dose rate	α(dsb's/Gy-cell)	β(dsb's/Gy^2-cell)	Type	E(keV)	L_T(keV/µm)	$L_{100,T}$(keV/µm)	L_D(keV/µm)	$L_{100,D}$(keV/µm)	β^2	z^{*2}/β^2	λ(nm)	σ(µm^2)	Reference
V79-379A		1.60E-02	3.26E-04	n	2.30E+03	3.09E+01	1.81E+01	3.89E+01	2.49E+01	2.25E-03	9.39E+02	4.92E+00	7.90E-02	Prise, 1987
V79-4		2.34E-02		n	6.00E+03	1.61E+01	8.98E+00	2.39E+01	1.49E+01	6.13E-03	3.27E+02	1.25E+01	6.01E-02	Kampf, 1988
Caski		7.63E-02		n	9.05E+03	1.20E+01	6.55E+00	1.90E+01	1.17E+01	9.29E-03	2.11E+02	1.90E+01	1.47E-01	Weber, 1993

AVII-3 Sparsely Ionising Radiation on Cells

Cells (Types/Lines)	Dose rate	α(dsb's/Gy-cell)	β(dsb's/Gy^2-cell)	Rad. Type	Source	E_p(keV)	L_T(keV/µm)	$L_{100,T}$(keV/µm)	L_D(keV/µm)	$L_{100,D}$(keV/µm)	λ(nm)	σ(µm^2)	Reference
V79-379A	2.50E+00	2.20E-02	7.00E-04	Alk x-rays	3 KVp	5.34E-01	1.67E+01	1.51E+01	1.77E+01	1.67E+01	2.88E+00	5.89E-02	Prise, 1989
V79		3.63E+01		x-rays	50 kVp	8.48E+00	8.28E+00	7.09E+00	9.58E+00	8.74E+00	6.43E+00	4.81E+01	Weber, 1993
V79-379A		9.90E-03	7.40E-04	x-rays	250 KVp	1.58E+01	4.31E+00	3.33E+00	5.63E+00	4.85E+00	1.37E+01	6.83E-03	Prise, 1990
V79-379A	1.80E+00	1.30E-02	4.78E-04	x-rays	250 KVp	1.58E+01	4.31E+00	3.33E+00	5.63E+00	4.85E+00	1.37E+01	8.96E-03	Prise, 1987
V79-379A	1.80E+00	8.30E-03	7.00E-04	x-rays	250 KVp	1.58E+01	4.31E+00	3.33E+00	5.63E+00	4.85E+00	1.37E+01	5.72E-03	Prise, 1989
V79-S171		9.10E-04		x-rays	300 KVp	1.91E+01	3.97E+00	3.04E+00	5.23E+00	4.49E+00	1.50E+01	5.14E-04	Ritter, 1977
V79-4		9.00E-03		γ	Co-60	3.55E+02	4.44E-01	2.84E-01	6.88E-01	5.15E-01	1.71E+02	6.39E-04	Kamf, 1988
V79-4		1.17E-01		γ	Co-60	3.55E+02	4.44E-01	2.84E-01	6.88E-01	5.15E-01	1.71E+02	8.31E-03	Jenner, 1993
V79		4.54E+01		γ	Co-60	3.55E+02	4.44E-01	2.84E-01	6.88E-01	5.15E-01	1.71E+02	3.22E+00	Weber, 1993
CHO		7.79E+01		x-rays	200 KVp	1.12E+01	5.40E+00	4.26E+00	6.83E+00	5.96E+00	1.07E+01	6.74E+01	Baumstark-Khan, 1993
CHO-K1	6 Gy/min	6.25E-03		x-rays	250 KVp	1.58E+01	4.31E+00	3.33E+00	5.63E+00	4.85E+00	1.37E+01	4.31E-03	Taucher-Scholz, 1996
CHO-K1	7 Gy/min	1.96E-02		x-rays	250 KVp	1.58E+01	4.31E+00	3.33E+00	5.63E+00	4.85E+00	1.37E+01	1.35E-02	Taucher-Scholz, 1995
CHO-K1	7 Gy/min	3.60E+01		x-rays	250 KVp	1.58E+01	4.31E+00	3.33E+00	5.63E+00	4.85E+00	1.37E+01	2.48E+01	Heilmann, 1995
EATC	40.20 Gy/min	4.10E+01		x-rays	140KVp	7.70E+00	7.49E+00	6.16E+00	8.95E+00	8.00E+00	7.35E+00	4.91E+01	Blocher, 1988
HSF		3.50E+01		e		1.80E+04	2.50E-01	1.50E-01			5.87E+02	1.40E+00	Frankenberg, 1997
NHF		1.72E+02		x-rays	300 KVp	1.91E+01	3.97E+00	3.04E+00	5.23E+00	4.49E+00	1.50E+01	1.09E+02	Baumstark-Khan, 1993
Caski		9.65E-02		x-rays	50 kVp	8.48E+00	8.28E+00	7.09E+00	9.58E+00	8.74E+00	6.43E+00	1.28E-01	Weber, 1993
Caski		1.11E-01		γ	Co-60	3.55E+02	4.44E-01	2.84E-01	6.88E-01	5.15E-01	1.71E+02	7.91E-03	Weber, 1993
GM38		2.90E+01		X-rays	225 KVp		2.00E-01					9.28E-01	Rydberg, 1996
Yeast, 211-rad22	23.4 Gy/min	5.57E-02		e		3.00E+04	2.09E-01	1.45E-01			5.87E+02	1.86E-03	Frankenberg, 1990/81
Yeast, diploid 211*B		8.75E-03		x-rays	80 KeV	7.44E+00	8.36E+00	7.02E+00	9.77E+00	8.84E+00	6.45E+00	1.17E-02	Lobrich, 1993
Bacteriophage T7		2.61E-04		γ	Co-60	3.55E+02	4.44E-01	2.84E-01	6.88E-01	5.15E-01	1.71E+02	1.85E-05	Neary, 1972
Bacteriophage T7		1.48E-04		γ	Co-60	3.55E+02	4.44E-01	2.84E-01	6.88E-01	5.15E-01	1.71E+02	1.05E-05	Neary, 1972
Bacteriophage T7		2.21E-04		Alk x-rays	3 KVp	5.34E-01	1.67E+01	1.51E+01	1.77E+01	1.67E+01	2.88E+00	5.92E-04	Neary, 1970
ϕx-174		6.12E-06		γ	Co-60	3.55E+02	4.44E-01	2.84E-01	6.88E-01	5.15E-01	1.71E+02	4.35E-07	Christensen, 1972

AVIII Database References

DATABASE REFERENCES

Akpa, T. C., K. J. Weber, et al. (1992). "Heavy Ion-Induced DNA Double Strand Breaks in Yeast." Int.J.Radiat.Biol. **62:** 279-287.

Aufderheide, E., H. Rink, et al. (1987). "Heavy Ions Effects on Cellular DNA: Strand Break Induction and Repair in Cultured Diploid Lens Epithelial Cells." Int.J.Radiat.Biol. **51**: 779-790.

Barendsen, G. W. (1962). "Dose-Survival Curves of Human Cells in Tissue Culture Irradiated with Alpha-, Beta-, 20 kV. X- and 200-kV. X-Radiation." Nature **193**: 1153-1155.

Barendsen, G. W. (1964). "Impairment of the Proliferative Capacity of Human Cells in Culture by a-Particles with Differing Linear-Energy Transfer." Int. J. Radiat. Biol. **8**: 453-466.

Barendsen, G. W. and J. F. Gaiser (1985). "Cell Transformation *in vitro* by Fast Neutrons of Different Energies: Implications for Mechanisms." Radiat.Prot.Dosim. **13**: 145-148.

Barendsen, G. W., C. J. Koot, et al. (1966). "The Effect of Oxygen on Impairment of the Proliferative Capacity of Human Cells in Culture by Ionizing Radiations of Different LET." Int. J. Radiat. Biol. **10**: 317-327.

Barendsen, G. W. and H. M. D. Walter (1963). "Effects of Different Ionizing Radiations on Human Cells in Tissue Culture." Radiat. Res. **18**: 106-119.

Bauchinger, M. and E. Schmid (1973). "Chromosome Aberrations in Lymphocytes after X-irradiation *in vitro*. II. Analysis of the Primary Processes in the Formation of Dicentric Chromosomes." Muatation Res. **20**: 107-113.

Bauchinger, M., E. Schmid, et al. (1979). "Calculation of the Dose-Rate Dependence of The Dicentric Yield after ^{60}Co γ-Irradiation of Human Lymphocytes." Int. J. Radiat. Biol. **.35**: 229-233.

Bauchinger, M., E. Schmid, et al. (1975). "Chromosome Aberrations in Human Lymphocytes after Irradiation with 15.0 MeV Neutrons *in vitro*. I. Dose-Response Relation and RBE." Mutation Res. **27**: 103-1-9.

Bayonove, J. F., A. Mir, et al. (1994). "Effects of Long-Duration Space-Flight on Rice Seed (or Embryo) Radiation Sensitivity and Element Microlocalizations." Adv. Space Res. **14**(10): 109-113.

Belli, M. (1994). "Molecular and Cellular Effectiveness of Charged Particles (Light and Heavy Ions) and neutrons." In: Progress Report, Contract FI3P-CT920053.

Belli, M., F. Cera, et al. (1994). "Inactivation Induced by Deuterons of Various LET in V79 Cells." Radiat. Prot.Dosim. **52**: 305-310.

Belli, M., F. Cera, et al. (1991). "Mutation induction and RBE-LET Relationship of Low-energy Protons in V79 cells." Int.J.Radiat. Biol. **59**: 459-465.

Belli, M., F. Cera, et al. (1992). "RBE-LET Relationship for Survival and Mutation Induction of V79 Cells Irradiated with Low-Energy Protons: Re-Evaluation of the LET Values at the LNL Facility." Int.J.Radiat.Biol. **61**: 145-146.

Belli, M., F. Cera, et al. (1993). "Inactivation and Mutation Induction in V79 Cells by Low Energy Protons: Re-Evaluation of the Results at the LNL Facility." Int.J.Radiat.Biol. **63**: 331-337.

Belli, M., F. Cera, et al. (1994). "DNA Double-Strand Breaks Induced by Low Energy Protons in V79 Cells." Int.J.Radiat.Biol. **65**: 529-536.

Belli, M., R. Cherubini, et al. (1989). "RBE-LET Relationship for The Survival of V79 Cells Irradiated with Low Energy Protons." Int.J. Radiat. Biol. **55**: 93-104.

Belli, M., D. T. Goodhead, et al. (1992). "Direct Comparison of Biological Effectiveness of Proton and Alpha-Particles of the Same LET. II. Mutation Induction at the HPRT Locus in V79 Cells." Int.J.Radiat.Biol. **61**: 625-629.

Belli, M., F. Ianzini, et al. (1995). "DNA Double-Strand Break Production and Rejoining in V79 Cells Irradiated with Light-Ions." Adv. Space Res. **18**(1/2): 73-82.

Bender, M. A. and J. G. Brewen (1969). "Factors Influencing Chromosome Aberration Yield in the Human Peripheral Leukocyte System." Mutation Res. **8**: 383-399.

Bertsche, U. and G. Iliakis (1987). "Modification in Repair and Expression Of Potentially Lethal Damage (α-PLD) as Measured by Delayed Plating or Treatment with β-araA in Plateau-Phase Ehrlich Ascites Tumor after Exposure to Charged Particles of Various Specific Energies." Radiat. Res. **111**: 26-46.

Bertsche, U., G. Iliakis, et al. (1983). "Inactivation of Ehrlich Ascites Tumor cells by Heavy Ions." Radiat. Res. **95**: 57-67.

Bertsche, U. and G. Illiakis (1980). "Compartive Analysis of Survival Curves Obtained with Various Radiation Qualities for Ehrlich Ascites Tumor Cells." **In: Proceedings of the Seventh Symposium on Microdosimetry,** Oxford, UK; edited by J. Booz, H.D. Hartfield and H.G. Ebert . Harwood Academic Publisher; CEC EUR 7147 DE-EN-FR: pp 1251-1262.

Bettega, D., C. Birattari, et al. (1979). "Relative Biological Effectiveness for Proton of Energies up to 31 MeV." Radiat. Res. **77**: 85-97.

Bettega, D., P. Calzolari, et al. (1992). "Transforamtion of C3H10T1/2 Cells with 4.3 MeV α-Particles at Low Doses: Effects of Single and Fractionated Doses." Radiat. Res. **131**: 66-71.

Bettega, D., P. Calzolari, et al. (1990). "Oncogenic Transformation Induced by High and Low LET Radiations." Radiat.Prot.Dosim. **31**(1-4): 279-283.

Bettega, D., S. Dubini, et al. (1981). "Chromosome Aberrations Induced by Protons up to 31 MeV in Cultured Human Cells." Radiat. Environ. Biophys. **19**: 91-100.

Biola, M.-T., R. Le Go, et al. (1974). "Efficacite Reative de divers Rayonnements Mixtes gamman neutrons pour l'induction *in vitro* d'anomalies Chromosomiques dans les lymphocytes Humans." In: Proceedings Series on The effects of Neutrons Irradiation Upon Cell Function. Biological Eeffects of Neutron Irradiation, Vienna, 1974: 221-236.

Bird, R. and H. J. Burki (1975). "Survival of Sychronized Chinese Hamster Cells Exposed to Radiation of Different Linear-Energy Transfer." Int.J.Radiat.Biol. **27**: 105-120.

Blakely, E. A., F. Q. Ngo, et al. (1984). "Heavy-Ion Radiobiology: Cellular Studies." **In: Advances in Radiation Biology;** edited by J. T. Lett, U. K. Ehmann and A. B. Cox. Orlando, Florida, Academic Press, Inc. pp 295-389

Blakely, E. A., C. A. Tobias, et al. (1979). "Inactivation of Human Kidney Cells by High-energy Monoenergetic Heavy-ion Beams." Radiat. Res. **80**: 122-160.

Blocher, D. (1988). "DNA Double-Strand Break Repair Determines the RBE of α-particles." Int. J. Radiat. Biol. **54**: 761-771.

Bocian, E., S. Pszona, et al. (1973). "Dose-Response Curve for Chromosome Aberrations in Human Lymphocytes Irradiated with 7.4 MeV Protons *in vitro*." studia biophysica **39**: 167-176.

Brandenberg, K., U. Seydel, et al. (1982). "The Induction of Chromosome aberrations in Human Lymphocyte Cultures by Internal β-Emitters as Compared to X- and γ-Irradiation." **In: Proceedings of the Eighth Symposium in Microdosimetry;** GmbH Jülich, Germany; edited by J. Booz and H.G. Ebert. Harwood Academic Publishers; ECE EUR 8395 EN: pp 797-807.

Brewen, J. G., R. J. Preston, et al. (1972). "Radiation-induced Human chromosome aberration Yields Following an Accidental Whole-Body Exposure to ^{60}Co γ-rays." Radiat. Res. **49**: 647-656.

Britten, R. A. (1992). "The Inherent Cellular Sensitivity to 62.5 MeV (p -->Be+) Neutrons of Human Cells Differing in Photon Sensitivity." Int. J. Radiat. Biol. **61**: 805-812.

Broerse, J. J. (1968). "Survival of Cultured Human Cells after Irradiation with fast Neutrons of Different Energies in Hypoxic and Oxygenated Conditions." Int. J. Radiat. Biol. **13**: 559-572.

Chen, D. J., K. Tsuboi, et al. (1994). "Charged-particle Mutagensis II. Mutagenic Effect of High Energy Charged Particles in Normal human fibroblasts." Adv. Space Res. **14 (10)**: (10)347-(10)354.

Cherubini, R. (1994). "Molecular and Cellular Effectiveness of Charged Particles (Light and Heavy Ions) and Neutrons Project 1." In: Progress Report (FI3P-CT920053); sector: B13.

Christensen, R. C. and C. A. Tobias (1972). "Heavy-Ion-Induced Single- and Double-Strand Breaks in ϕX-174 Replicative for DNA." Int. J. Radiat. Biol. **22**: 457-477.

Cox, R. and W. K. Masson (1979). "Mutation and Inactivation of Cultured Mammalian Cells Exposed to Beams of Accelerated Ions. III. Human Fibroblasts." Int.J.Radiat.Biol. **36**: 149-160.

Cox, R., J. Thacker, et al. (1977). "Inactivation and Mutation of Cultured Mammalian Cells by Aluminum Characteristic Ultrasoft X-rays. II.Dose-Responses of Chinese Hamster and Human Diploid Cells to Aluminum X-rays and Radiations of Different LET." Int.Radiat.J.Biol. **31**: 561-576.

Cox, R., J. Thacker, et al. (1977). "Mutation and Inactivation of Mammalian Cells by Various Ionising Radiation." Nature **267**: 425-427.

Deering, R. A. and R. Rice (1962). "Heavy Ion Irradiation of HeLa Cells." Radiat. Res. **17**: 774-786.

Duffrain, R. J., L. G. Littlefield, et al. (1979). "Human Cytogenetic Dosimetry: A Dose-response Relationship for Alpha Radiation from ^{241}Am." Health Phys. **37**: 279-.

Edwards, A. A. (1994). " The Induction of Chromosomal Changes in Human and Rodent Cells by Accelerated Changed Particles: Early and Late Effects." In: Progress Report. F13P-CT920064i.

Edwards, A.A., P. Finnon, et al. (1994). "The Effectiveness of High Energy Neon Ions in Producing Chromosomal Aberrations in Human Lymphocytes." Radiat. Prot. Dosim. **52**: 299-303.

Edwards, A.A., D.C. Lloyd, et al. (1990). "The Induction of Chromosome-Aberrations in Human-Lymphocytes By 24- keV Neutrons." Radiat.Prot.Dosim. **31**: 265-268.

Edwards, A.A., D.C. Lloyd, et al. (1986). "Chromosome Aberrations Induced in Human Lymphocytes by 8.7 MeV Protons and 23.5 Mev Helium-3 Ions." Int. J. Radiat. Biol. **50**: 137-145.

Edwards, A. A., R. J. Purrott, et al. (1980). "The Induction of Chromosome Aberrations in Human Lymphocytes by Alpha-Radiation." Int. J. Radiat. Biol. **38**: 83-91.

Fabry, L., A. Leonard, et al. (1985). "Induction of Chromosome Aberrations in G_0 Human Lymphocytes by Low Doses of Ionizing Radiations of Different Quality." Radiat. Res. **103**: 122-134.

Folkard, M., K. M. Prise, et al. (1989). "The Irradiation of V79 Mammalian Cells by Protons with Energies Below 2 MeV. Part I: Experimental Arrangement and Measurements of Cell Survival." Int. J. Radiat. Biol. **56**: 321-237.

Folkard, M., K. M. Prise, et al. (1996). "Inactivation of V79 by Low-energy Protons, Deutrons and Helium-3 Ions." Int.J.Radiat.Biol. **69**: 729-738.

Fox, J. C. and N. J. McNally (1988). "Cell Survival and DNA Double-Strand Break Repair Following X-ray or Neutron Irradiation of V79." Int. J. Raadiat. Biol. **54**: 1021-1030.

Frankenberg, D., -. S. Frankenberg, M., et al. (1981). "Evidence for DNA double strand breaks as critical lesions in Yeast cells Irradiated with Sparsely or Densely Ionizing Radiation under Oxic or Anoxic Conditions." Radiat. Res. **88**: 524-532.

Frankenberg, D., M. Frankenberg-schwager, et al. (1990). "The Contribution of OH* in Densely Ionizing Electron Track Ends or Particle Tracks to the Induction of DNA Double Strand Breaks." Radiat.Prot.Dosim. **31**: 249-252.

Frankenberg, D., H. Kuhn, et al. (1995). "0.3 keV carbon K Ultrasoft X-rays are four times more Effective than γ-rays when inducing Oncogenic Cell Transformation at Low Doses." Int.J.Radiat.Biol. **68**: 593-601.

Frankenberg, D., C. Steinmetz, et al. (1997). "Yields of DNA Double -Strand Breaks in Human Skin Fibroblasts After Exposure to 18 MeV Electrons, 5 MeV Protons and 3 MeV α-particles using Calibrated PFGE." **In: Proceedings of twelfth Symposium on Microdosimetry**: Oxford (In Press).

Geard, C. (1985). "Charged Particle Cytogenetics: Effects of LET, Fluence, and Particle Separation on Chromosome Aberrations." Radiat. Res. **104**: S112-S121.

Geard, C. R. (1985). "Chromosomal Aberration Production by Track Segment Charged-Particles as a Function of Linear Energy-Transfer." Radiat.Prot.Dosim. **13**: 199-204.

Goodhead, D. T., M. Belli, et al. (1992). "Direct Comparison Between Protons and Alpha-Particles of the Same LET: I. Irradiation Methods and Inactivation of Asychronous V79, HeLa and C3H10T1/2 cells." Int. J. Radiat. Biol. **61**: 611-624.

Goodhead, D. T., R. J. Munson, et al. (1980). "Mutation and Inactivation of Cultured Mammalian Cells Exposed to Beam of Accelerated Heavy Ions. IV. Biophysical Interpretation." Int.J.Radiat.Biol. **37**: 135-167.

Goodhead, D. T., J. Thacker, et al. (1979). "Effectiveness of 0.3 keV Carbon Ultrasoft X-rays for the Inactivation and Mutation of Cultured Ammalian Cells." Int.J.Radiat.Biol. **36**: 101-114.

Hall, E. J., R. P. Bird, et al. (1977). "Biophysical Studies with High-Energy Argon Ions. 2.Determination Of The Relative Biologial Effectiveness, the Oxygen Enhancement Ratio, and Cell Cycle Response." Radiat. Res. **70**: 469-479.

Hall, E. J., W. Gross, et al. (1972). "Survival Curves and Age Response Functions for Chinese Hamster Cells Exposed to X-rays or High Alpha-particles." Radiat. Res. **52**: 88-98.

Hall, E. J., A. M. Kellerer, et al. (1982). "Dependence on Neutron Energy of the OER and RBE." Int.J.Radiat.Oncol.Biol.Phys. **8**: 1567-1572.

Hall, E. J., A. M. Kellerer, et al. (1978). "The Relative Biological Effectiveness of 160 MeV Protons. II. Biological Data and their Interpretation in terms of Microdosimetry." Int. J. Radiat. Oncol. Biol. Phys. **4**: 1009-1013.

Hall, E. J., J. K. Novak, et al. (1975). "RBE as a Function of Neutron Energy. I.Experimental Observations." Radiat.Res. **64**: 245-255.

Hei, T. K., D. J. Chen, et al. (1988). "Mutation Induction by Charged Particles of Defined Linear Energy Transfer." Carcinogenesis **9**: 1233-1236.

Hei, T. K., K. Komatsu, et al. (1988). "Oncogenic Transformation by Charged Particles of Defined LET." Carcinogenesis **9**: 747-750.

Heilmann, J., H. Rink, et al. (1993). "DNA Strand Break Induction, Rejoining and Cellular Recovery in Mammalian Cells after Heavy Ion Irradiation." Radiat. Res. **135**: 46-55.

Heilmann, J., G. Taucher-Scholz, et al. (1995). "Induction of DNA double-strand breaks in CHO-K1 cells by carbon ions." Int J. Radiat.Biol. **68**: 153-162.

Hieber, L., G. Ponsel, et al. (1987). "Absent of a Dose-Rate Effect in the Transformation of C3H101/2 Cells by α-particles." Int J. Radiat. Biol. **52**: 859-869.

Hieber, L., K. Trutschler, et al. (1990). "Radiation-Induced Cell Transformation: Transformation Efficiencies of Different Types of Ionizing Radiation and Molecular Changes in Radiation Transformation and Tumor Cell Lines." Environ. Health Presp. **88**: 169-174.

Ikpeme, S., M. Lobrich, et al. (1995). "Heavy-Ion-Induced DNA Double-Strand Breaks with Yeast as a Model System." Radiat. Environ. Biophys. **34**: 95-99.

Jenner, T. J., M. Belli, et al. (1992). "Direct Comparison of Biological Effectiveness of Protons And Alpha-Particles of the Same LET. III. Initial Yield of DNA Double-Strand Breaks in V79." Int. J. Radiat. Biol. **61**: 631-637.

Jenner, T. J., C. M. deLara, et al. (1993). "Induction and Rejoining of DNA-Strand Breaks in V79-4 Mammalian Cells Following γ- and α-irradiation." Int. J. Radiat. Biol. **64**: 265-273.

Kampf, G. and K. Eichhorn (1983). "DNA Strand Breaks by Different Radiation Qualities and relations to Cell Killing: Further Results after the Influence of α-Particles And Carbon Ions." studia biophysica. **93**: 17-26.

Kent, C. R. H., S. M. Edwards, et al. (1993). "Mutation Induction by Ionizing Radiation in Three Human Bladder Tumor Cell Lines." Int.J.Radiat.Biol. **63**: 1-5.

Key, M. (1971). "Comparative effects of neutrons and x-rays on Chinese Hamster cells." In: Proceedings Series "Biophysical Aspects of Radiation Quality". IAEA. Vienna: 431-444.

Kraft, G., W. Kraft-Weyrather, et al. (1982). "The Influence of Radiation Quality on the Biological Effectiveness of Heavy Charged Particles." **In: Proceedings of the Eighth Symposium on Microdosimetry,** GmbH Jülich, Germany; edited by J. Booz and H.G. Ebert. Harwood Academic Publishers; ECE EUR 8395 EN: pp 743-753.

Kranert, T., E. Schneider, et al. (1990). "Mutation induction in V79 Chinese Hamster Cells by Very Heavy Ions." Int.J.Radiat.Biol. **58**: 975-987.

Kranert, T., U. Stoll, et al. (1992). "Mutation Induction in Mammalian Cells by Very Heavy Ions." Adv.Space Res. **12 (2-3)**: (2)111-(2)118.

Kronenberg, A. (1991). "Perspective on Fast-Neutron Mutagenesis of Human Lymphoblastoid Cells." Radiat.Res. **128**: S87-S93.

Kronenberg, A. (1994). "Mutation-Induction In Human Lymphoid-Cells By Energetic Heavy-Ions." Adv. Space Res. **14(10)**: 339-346.

Kucerova, M., A. J. B. Anderson, et al. (1972). "X-ray-Induced Chromosome Aberrations in Human Peripheral Blood Leococytes: The Response to Low Level of Exposure *in vitro*." Int. J. Radiat. Biol. **21**: 389-396.

Leonard, A., G. Decat, et al. (1977). "The Chromosomal Radiosensitivity of Lymphocytes from the Chimpanzee (Pan Troglodyytes)." Mutation Res. **45**: 69-76.

Liniecki, J., A. Bajerska, et al. (1973). "The Influence of Blood Oxygenation During *in vitro* Irradiation Upon the Yield of Dicentric Chromosomal Aberrations in Lymphocytes." Bull. Acad. Pol. Sco. Cl .VI **Vol.XXI,No.1**: 69-76

Liniecki, J., A. Bajerska, et al. (1977). "Gamma-Radiation-Induced Chromosomal Aberrations in Human Lymphocytes: Dose-Rate Effects is Stimulated and Non-Stimulated Cells." Mutation Res. **43**: 291-304.

Lloyd, D. C., A. A. Edward, et al. (1992). "Chromosomal Aberrations in Human Lymphocytes Induced *in vitro* by Very Low Doses of X-rays." Int. J. Radiat. Biol. **61**: 335-343.

Lloyd, D. C., A. A. Edward, et al. (1984). "Chromosome Aberrations Induced in Human Lymphocytes by d-T Neutrons." Radiat.Res. **98**: 561-573.

Lloyd, D. C., A. A. Edwards, et al. (1986). "Chromosome Aberrations Induced in Human Lymphocytes by *in vitro* acute X- and γ– Radiation." Radiat. Prot. Dosim. **15**: 83-88.

Lloyd, D. C., R. J. Purrott, et al. (1976). "Chromosome Aberrations Induced in Human by Neutron Irradiation." Int.J.Radiat.Biol. **29**: 169-182.

Lloyd, D. C., R. J. Purrott, et al. (1975). "An Investigation of The Characteristics of A Negative Pion Beam by Means of Induced Chromosome Aberrations in Human Peripheral Blood Lymphocytes." Int. J. Radiat. Biol. **27**: 223-236.

Lloyd, D. C., R. J. Purrott, et al. (1978). "Chromosome Aberrations Induced in Human Lymphocytes from ^{252}Cf." Int.J.Radiat.Biol. **34**: 177-186.

Lloyd, D. C., P. R.J., et al. (1975). "The Relationship Between Chromosome Aberrations and LET Radiation Dose to Human Lymphocytes." Int. J. Radiat. Biol. **28**: 75-90.

Lloyd, E. L., M. A. Gemmell, et al. (1979). "Cell Survival Following Multiple-Track Alpha Particle." Int. J. Radiat. Biol. **35**: 23-31.

Lobrich, M., S. Ikpeme, et al. (1993). "DNA Double-Strand Break Induction in Yeast by X-rays and α-particles Measured by Pulsed-Field Gel Electrophoresis." Int. J. Radiat. Biol. **64**: 539-546.

Lobrich, M., B. Rydeberg, et al. (1994). "DNA Double-Strand Breaks Induced by High-Energy Neon and Iron in Human Fibroblasts. II. Probing Individual Noti Fragment by Hypridization." Radiat. Res. **139**: 142-151.

Luchnik, N. V. (1975). "Do One-Hit Chromosome Exchanges Exist?" Radiat. Environ. Biophys. **12**: 197-204.

Lucke-Huhle, C., E. A. Blakely, et al. (1979). "Drastic G_2 Arrest in Mammalian Cells after Irradiation With Heavy-Ion Beams." Radiat. Res. **79**: 97-112.

Matsubara, S., T. Katoh, et al. (1994). "The Effects of X-ray Energy and an Iodine-Based Contrast Agent on Chromosome Aberrations." Radiat. Res. **137**: 231-237.

Matsubara, S., Y. Kuwabara, et al. (1986). "A Comparative Study of Dose Distribution of a High-Energy Electron Beam and Chromosome Aberration Frequencies." The British J. Radiology **59**: 1001-1005.

Matsubara, S., H. Ohara, et al. (1990). "Chromosome Aberration Frequencies Produced by a 70-MeV Proton Beam." Radiat. Res. **123**: 182-191.

Micke, U., G. Horneck, et al. (1994). "Double Strand Breaks in the DNA of Bacillus Subtilis Cells Irradiated by Heavy Ions." Adv. Space Res. **14**: (10)207-(10)211.

Miller, B. L., E. Fielden, et al. (1978). "Interpretation of Survival-Curve Data for Chinese Hamster Cells, Line V79 Using the Multi-Target with Initial Slope, and α, β equation." Int. J. Radiat. Biol. **33**: 599-603.

Miller, R. C., D. J. Brenner, et al. (1990). "The Effects of The Temporal Distribution of Dose on Oncogenic Transformation by Neutrons and Charged Particles of Intermediate LET." Radiat. Res. **124:** S62-S68.

Miller, R. C., C. R. Geard, et al. (1989). "Neutron-Energy-Dependent Oncogenic Transformation of C3H10T1/2 Mouse Cells." Radiat. Res. **117**: 114-127.

Miller, R. C., C. R. Geard, et al. (1995). "Neutron-Induced Cell-Dependent Oncogenic Transformation of C3H10T1/2 Cells." Radiat.Res. **142**: 270-275.

Miller, R. C., S. A. Marino, et al. (1995). "The Biological Effectiveness of Radon-Progeny Alpha Particles. II. Oncogenic Transformation as a Function of Linear Energy Transfer." Radiat. Res. **142**: 54-60.

Min, T., P. Cohn, et al. (1985). "The Sensitivity of Three Diploid Human Cell Lines to Alpha- Irradiation." In: Proceedings of 2nd Workshop on Lung Dosimetry. Cambridge.

Morgan, G. R., C. J. Roberts, et al. (1986). "Inactivation of Chinese Hamster V79/4(AH1) and HeLa Cells by 24 keV Neutrons." Int. J. Radiat. Biol. **50**: 35-40.

Mortimer, R., T. Brustad, et al. (1965). "Influence of Linear Energy Transfer and Oxygen Tension on The Effectiveness of Ionizing Radiations for Induction of Mutation and Lethality in Saccharomyces Cerevisae." Radiat.Res. **26**: 465-482.

Munson, R. J., D. A. Bance, et al. (1979). "Mutation and Inactivation of Cultured Mammalian Cells Exposed to Beams of Accelerated Ions. I. Irradiation Facilities and Methods." Int.J.Radiat.Biol. **36**: 127-136.

Muramatsu, S. and T. Maruyama (1977). "Chromosome Aberrations in Human Lymphocytes after Irradiation with NIRS-Cyclotron Fast Neutrons *in vitro*. A Preliminary Report." Nippon Act. Radiol. **37**: 995-997.

Nagasawa, H., J. Robertson, et al. (1990). "Induction of Chromosomal Aberrations and Sister Chromatid Exchanges by Alpha Particles in Density-Inhibited Cultures of Mouse 10T1/2 and 3T3 Cells." Int. J. Radait. Biol. **57**: 35-44.

Napolitano, M., M. Durante, et al. (1992). "Inactivation of C3H10T1/2 Cells by Monoenergetic High LET Alpha-Particles." Int J. Radiat. Biol. **61**: 813-820.

Neary, G.J. (1970). "The Influence of Radiation Quility and Oxygen on Strand Breaks in Dry DNA." Int.J.Radiat.Biol. **18**: 25-40.

Neary, G. J., V. J. Horgan, et al. (1972). "Further Data on DNA Strand Breakage by various Radiation Qualities." Int.J.Radiat.Biol. **22**: 525-537.

Ngo, F.Q.H., E.A. Blakely, et al. (1981). "Sequential Exposures of Mammalian Cells to low- and high-LET Radiations." Radiat. Res. **87**: 59-78.

Nias, A. H. and M. Ebert (1969). "Effects of Single and Continuous Irradiation of HeLa Cells at -169 ^{o}C." Int.J.Radiat.Biol. **16**: 31-41.

Nias, A. H. W., D. Green, et al. (1967). "Effect of 14 MeV Monoenergetic Neutrons on HeLa and P388F Cells *in vitro*." Int J. Radiat. Biol. **13**: 449-456.

Norman, A. and M. S. Sasaki (1966). "Chromosome-Exchange Aberrations in Human Lymphocytes." Int. J. Radiat. Biol. **11**: 421-328.

Ohno, T., T. Nishimura, et al. (1984). "Differential Recovery from Potentially Lethal Damage in Normal Human Lung Fibroblasts After Irradiation with ^{60}Co γ-rays and Accelarated N- Ion Beams." Int. J. Radiat. Biol. **45**: 21-26.

Palcic, B., J. W. Brosing, et al. (1985). "The Requirement for Survival Measurements at Low Doses." In: Proceedings of the Berkeley Conference in Honor of Jersy Neyman and Jack Kiefer. Vol.I; edited by: L.M.Le Cam, and R.A. Olshen.Wadsworth, Inc.: pp 331-352.

Pandita, T. K. and C. R. Geard (1996). "Chromosome Aberrations in Human Fibroblasts Induced by Monoenergetic Neutrons. I.Relative Biological Effectiveness." Radiat.Res. **145**: 730-739.

Perris, A., P. Pialoglou, et al. (1986). "Biological Effectiveness of Low Energy Protons. I. Survival of Chinese Hamster Cells." Int.J. Radiat. Biol. **50**: 1093-1101.

Prise, K. M., S. Davies, et al. (1987). "The Relationship Between Radiation-Induced DNA Double-Strand Breaks and Cell Kill in Hamster V79 Fibroblasts Irradiated with 250 kVp X-rays. 2.3 MeV Neutrons or ^{238}Pu α-particles." Int. J. Radiat. Biol. **52**: 893-902.

Prise, K. M., M. Folkard, et al. (1990). "The Irradiation of V79 Mammalian Cells by Protons with Energies Below 2 MeV. Part II. Measurement of Oxygen Enhancement Ratios and DNA Damage." Int. J. Radiat. Biol. **58**: 261-277.

Prise, K. M., M. Folkard, et al. (1989). "Measurement of DNA Damage and Cell Killing in Chinese Hamster V79 Cells Irradiated with Aluminum Characteristic Ultrasoft X-rays." Radiat. Res. **117**: 489-499.

Purrott, R. J. (1977). "Chromosome Aberration Yields Induced in Human Lymphocytes by 15 MeV Electrons Given at a Conventional Dose-Rate and in microsecond Pulse." Int. J. Radiat. Biol. **31**: 251-256.

Purrott, R. J., A. A. Edwards, et al. (1980). "The Induction of Chromosome Aberrations in Human Lymphocytes by *in vitro* Irradiation with α-particles from Plutonium-239." Int. J. Radiat. Biol. **38**: 277-284.

Railton, R., R. c. Lawson, et al. (1973). "Neutron Spectrum Dependence of RBE. and OER. values." Int.J.Radiat.Biol. **23**: 509-518.

Railton, R., D. Porter, et al. (1974). "The Oxygen Enhancement Ratio and Relative Biological Effectiveness for Combined Irradiations of Chinese Hamster Cells by Neutrons and γ-rays." Int. J. Radiat. Biol. **25**: 121-127.

Raju, M. R., Y. Eisen, et al. (1991). "Radiobiology of α particles. III.Cell Inactivation by α-particle Traversals of the Cell Nucleus." Radiat. Res. **128**: 204-209.

Reading, D. H., M. A. Hynes, et al. (1981). "Negative Pion Depth-Dose Profile Examined by Means of HeLa Cell-Survival Curves." British Journal Radiology **54**: 606-614.

Rimpl, G. R., E. Schmid, et al. (1990). "Chromosome Aberrations Induced in Human Lymphocytes by 16.5 MeV Protons." Int.J.Radiat. Biol. **58**: 999-1007.

Ritter, M. A., J. E. Cleaver, et al. (1977). "High-LET Radiations Induce a Large Proportion of non-rejoining DNA Breaks." Nature **266**: 653-655.

Roberts, C. J. (1987). "The Production of Chromosome Aberration in Chinese Hamster Fibroblasts Exposed to 24 keV Neutrons." Int. J. Radiat. Biol. **51**: 341-351.

Roberts, C. J. and D. Holt (1985). "Induction of Chromosome Aberration and Cell Killing in Syrian Hamster Fibroblasts By γ-rays and Fast Neutrons." Int. J. Radiat. Biol. **48**: 927-939.

Rydberg, B. (1985). "DNA Strand Breaks Induced by Low-Energy Heavy Ions." Int. J. Radiat. Biol. **47**: 57-61.

Rydberg, B. (1996). "Clusters of DNA Damage Induced by Ionizing Radiation: Formation of Short Fragments. II. Experimental Detection." Radiat.Res. **145**: 200-209.

Sasaki, H. (1983). "Time-lapse Photographic Studies on Proliferation Kinetics of HeLa Cells Irradiated with Alpha-Particles As Compared to X-rays." In: Proceedings of the Seventh International Congress of Radiation Research. Biology.: B5-34.

Sasaki, M. (1971). "Radiation-induced Chromosome Aberrations in Lymphocytes: Possible Biological Dosimeter in Man." In: Proceeding of the International Symposium of Biological Aspects of Radiation Protection, Kyoto, Oct. 1969.: pp 81-90.

Schlag, H. and C. Luck-Huhle (1981). "The Influence of Ionization Density on the DNA Synthetic Phase and Survival of Irradiated Mammalian Cells." Int. J. Radiat. Biol. **40**: 75-85.

Schmid, E., M. Bauchinger, et al. (1972). "Chromosome Aberrations of Human Lymphocytes after X-irradiation *in vitro*. I. Qualitative and Quantitative Aspects of Dose-Response Curves." Mutation Res. **16**: 307-317.

Schmid, E., M. Bauchinger, et al. (1976). "Analysis of the Time Relationship of X-ray-Induced Primary Breaks in the Formation of Dicentric Chromosomes." Int.J.Radiat.Biol. **30**: 339-346.

Schmid, E., G. Rimpl, et al. (1974). "Dose-response Relation Of Chromosome Aberrations in Human Lymphocytes after *in vitro* Irradiation with 3-MeV Electrons." Radiat. Res. **57**: 228-238.

Sevankaev, A. V., E. A. Zherbin, et al. (1979). "Cytogenetic Effects Produced by Neutrons in Lymphocytes of Human Peripheral Blood *in vitro*." Genetica **15**: 1046-1060.

Simmons, J. A., P. Cohn, et al. (1996). "Survival and Yields of Chromosomes Aberrations in Hamster and Human Lung Cells Irradiated by Alpha Particles." Radiat. Res. **145**: 174-180.

Sinclair, W. K. (1985). "Experimental RBE values of high LET Radiations at Low-Doses and the Implications for Quality Factor Assignment." Radiat.Prot.Dosim. **13**: 319-326.

Skarsgard, L. D., B. A. Kihlman, et al. (1967). "Survival, Chromosome Abnormalities, and Recovery in Heavy Ion- and X-irradiated Mammalian Cells." Radiat. Res. Suppl. **7**: 208-221.

Spadinger, I. and B. Palcic (1992). "The relative biological effectiveness of ^{60}Co γ-rays, 55 kVp X-rays, 250 KVp X-rays, and 11 MeV Electrons at Low Doses." Int. J. Radiat. Biol. **61**: 345-353.

Stanton, J., G. Taucher-Scholz, et al. (1993). "Protection of DNA from high LET radiation by Two OH Radical Scavengers, tris (hydroxymethyl) amino-methane and 2-mercaptoethanol." Radiat. Environ. Biophys. **32**: 21-32.

Stanton, J., G. Taucherscholz, et al. (1990). "Comparison Between Indirect and Direct Effects For High and Low Let Radiations in SV40 DNA Strand Break Induction." Radiat.Prot.Dosim. **31**: 253-256.

Stenerlow, B., E. Blomquist, et al. (1996). "Rejoining of DNA Double-Strand Breaks Induced by Accelarated Nitrogen ions." Int.J.Radiat.Biol. **70**: 413-420.

Stenstrand, K., H. Toivonen, et al. (1979). "Radiation-Induced Chromosome Aberrations in Human Lymphocytes. STL-A29. Institute of Radiation Protection, Helsinki." .

Stoll, U., B. Barth, et al. (1996). "HPRT Mutations in V79 Chinese Hamster Cells Induced by Accelarated Ni, Au and Pb ions." Int.J.Radiat.Biol. **70**: 15-22.

Stoll, U., A. Schmidt, et al. (1995). "Killing and Mutation of Chinese Hamster V79 Cells Exposed to Accelerated Oxygen and Neon Ions." Radiat. Res. **142**: 288-294.

Stoll, U., E. Schneider, et al. (1995). "Induction of HPRT(-) Mutants in Chinese-Hamster V79 Cells after Heavy-Ion Exposure." Radiat. Environ. Biophys. **34**: 91-94.

Takahashi, E., M. Hirai, et al. (1982). "Radiation-Induced Chromosome Aberrations In Lymphocytes from Man and Crab-Eating Monkey. The Dose-Response Relationship at Low Doses." Mutation Res. **94**: 115-123.

Takatsuji, T. (1984). "Dose-Effect Relationship of Chromosome Aberrations Induced by 23 MeV Alpha Particles in Human Lymphocytes." Int. J. Radiat. Biol. **45**: 237-243.

Takatsuji, T. and H. Takekoshi (1983). "Induction of Chromosome Aberrations by 4.9 MeV Protons in Human Lymphocytes." Int. J. Radiat. Biol. **44**: 553-562.

Taucher-Scholz, G., J. Heilmann, et al. (1996). "Induction and Rejoining of DNA Double-Strand Breaks in CHO Cells after Heavy-Ion Irradiation." Adv. Space Res. **18**(1/2): 83-92.

Taucher-Scholz, G., J. Heilmann, et al. (1996). "Induction of DNA Strand Breaks by Heavy Ions." Nucl.Instrum.Meth.Phys.,Res.B **107**: 318-322.

Taucher-Scholz, G., J. Heilmann, et al. (1995). "Detection Of Heavy-Ion-Induced DNA Double-Strand Breaks Using Static- Field Gel-Electrophoresis." Radiat. Environ. Biophys. **34**: 101-106.

Thacker, J., A. Stretch, et al. (1982). "The Mutagenicity of α particles from Plutonium-238." Radiat.Res. **92**: 343-352.

Thacker, J., A. Stretch, et al. (1979). "Mutation and Inactivation of Cultured Mammalian Cells Exposed to Beams of Accelerated ions. II. Chinese Hamster V79 Cells." Int.J.Radiat.Biol. **36**: 137-148.

Thacker, J., R. E. Wilkinson, et al. (1986). "The Induction Of Chromosome Exchange Aberrations by Carbon Ultrasoft X-rays in V79 Hamster Cells." Int. J. Radiat. Biol. **49**: 645-656.

Todd, P. (1965). "Reversible and Irreversible Effects of Densely Ionizing Radiations Upon The Reproductive Capacity of Cultured Human Cells." Medical College of Virginia Quarterly. **1**: 2-14.

Todd, P. W. (1975). "Heavy-ion Irradiation of Human and Chinese Cells *in vitro*." Radiat. Res. **61**: 288-297.

Todd, P. W., J. T. Lyman, et al. (1968). "Dosimetry and Apparatus for Heavy Ion Irradiation of Mammalian Cells *in vitro*." Radiat.Res. **34**: 1-23.

Todorov, S., S. Bulanova, et al. (1973). "Aberrations Induced by Fission Neutrons in Human Peripheral Lymphocytes." Mutation Res. **17**: 377-382

Todorov, S. L. (1975). "Radiation-induced Chromosome Aberrations in Human Peripheral Lymphocytes. Exposure to X-rays or Protons." Strahlentherapie **149**: 197-204.

Tolkendorf, E. and K. Eichohorn (1983). "Effect of Ionizing Radiation of Different Linear Energy Transfer of The Induction of Cellular Death and of Chromosome Aberrations in Cells of the Chinese Hamster." studia biophysica **95**: 43-56.

Virsik, R. P. and D. Harder (1981). "Analysis of Radiation-induced Acentric Fragments in Human G_0 Lymphocytes." Radiat. Environ. Biophys. **19**: 29-40.

Virsik, R. P., D. Harder, et al. (1977). "The RBE of 30 kV X-rays for the Induction of Dicentric Chromosomes in Human Lymphocytes." Radiat. Environ. Biophys. **14**: 109-121.

Virsik, R. P., C. H. Schafer, et al. (1980). "Chromosome Aberrations Induced in Human Lymphocytes by Al_k and C_k X-rays." Int.J. Radiat. Biol. **38**: 545-557.

Vulpis, N. (1973). "Chromosome Aberrations Induced in Human Peripheral Blood Lymphocytes Using Heavy Particles from B-10(n-α)Li-7 Reaction." Mutation Res. **18**: 103-111.

Vulpis, N. (1984). "The Induction of Chromosome Aberrations in Human Lymphocytes by *in vitro* Irradiation with β Particles from Tritiated Water." Radiat. Res. **97**: 511-518.

Vulpis, N., G. Panetta, et al. (1976). "Radiation-induced Chromosome Aberrations in Radiological Protection Dose-Response Curves at Low Dose-Levels." Int. J. Radiat. Biol. **29**: 595-600.

Vulpis, N. and L. Tognacci (1978). "Chromosome Aberration as a Dosimetric Technique for Fission Neutrons Over the Dose-Range 0.2-50 rad." Int. J. Radiat. Biol. **33**: 301-306.

Wainson, A. A., M. F. Lomamov, et al. (1972). "The RBE of Accelerated Protons in Different Parts of the Bragg Curve." British J. Radiol. **45**: 525-529.

Weber, K. J. and M. Flentje (1993). "Lethality of Heavy Ion-Induced DNA Double-Strand Breaks in Mammalian Cells." Int.J.Radiat. Biol. **64**: 169-178.

Wouters, B. G., G. K. Y. Lam, et al. (1996). "Measurements of Relative Biological Effectiveness of the 70 MeV proton beam at TRIUMF Using Chinese Hamster V79 Cells and the High-Precision Cell Sorter Assay." Radiat.Res. **146**: 159-170.

Wulf, H., W. Kraft-Weyrather, et al. (1985). "Heavy-ion Effects on Mammalian Cells: Inactivation Measurements with Different Cell Lines." Radiat. Res. **134**: S122-S134.

Yang, T. C.-H., L. Craise, et al. (1985). "Neoplastic Cell Transformation by Heavy Charged Particles." Radiat.Res. **104**: S177-S187.

Ziemba-Zoltowska, B., E. Bocian, et al. (1980). "Chromosome Aberrations Induced by Low Doses of X-rays in Human Lymphocytes *in vitro*." Int. J. Radiat. Biol. **37**: 231-236.

Appendix BI

```
c       Program 'nanospectra.for'.  For unified dosimetry in the condensed phase.
c       Calculates  the integer yield of photons output from a scintillation
c       material containing a known concentration of active centres each
c       having cross-sectional area 'siga'.  The calculation determines the
c       concentration of ionizations produced and hence the fluence of excitons
c       assuming a migration length for excitons.  Distributions are
c       calculated from Poisson statistics although Vavilov would be better.

c       Note that this is a pilot study with simplifying approximations.  A
c       more rigorous calculation should include the mean chord distributions;
c       the instantaneous ionisation and the Caswell type analysis of crossers,
c       insiders, stoppers and starters, etc.  Fuller details of the activator
c       concentration are also required.

        implicit none
        real*8 frel(280),fel(200),
       1 tel(200),zel(200),fwr(200),rel(200),rna(280),rnkv(280),fwkv(280),
       2 rxna(280),fxwr(280),flex(280),pact(280),stp(200),ran(200),ciz(280),
       3 cxiz(280),rrsc(280),fxex(280),pxact(280),felkv(280),frkv(280),
       4 arg(280),r2pr(280),po2(280),tech(280),ps2nm(280),lamda(280),
       5 egam,rmep,rmfp,exra,ftrl,ftkv,tpr,
       6 xa,pizl,adis,chrd,siga,vsc,tciz,txciz,rangel,dfex,recstp,stel,px,
       7 totfr,rmass,rho,area,ftot,tnph,tphx,tpem,avca,thk,fact
        integer ina(280),kc,ndp,na,jump,ifact
        common/int/ rho
        external pizl,adis,rangel,recstp,stel,px,ifact,fact
        open(unit=36,access='sequential',status='old',file=
       1 'am241dam.dat')
        open(unit=40,access='sequential',status='unknown',file=
       1 'nanam241.dat')
        open(unit=43,access='sequential',status='unknown',file=
       1 'pham241.dat')
c       Density is for NE102A in g/cm2.(rho), vol. of scint = vsc cm3.
c       mass = rmass in g.
c       avca is the average concentration of active centres in the
c       scintillant,cm-3.
c       xa is the mean distance between activator centres.
        jump=1
        avca=1.d+20
        thk=2.0d-3
        rho=1.032
        rmass=5.0d-4
        vsc=rmass/rho
        area=vsc/thk
c       Note xa is given in nanometres!
        xa=adis(avca)
        exra=xa*1.d-7/2.0
        dfex=5.d-7
```

```
      if (dfex.lt.exra) exra=dfex
      siga=3.1414*exra*exra
      write(40,602) rho,rmass,vsc,area,thk,xa,dfex,siga
602   format(1h ,'Density of scint., (rho),g/cm3, = ',1pe9.3,/,1h ,
     1 'Mass of scintillator,g=',1pe9.3,/,1h ,'Vol. of scint.,cm3 = ',
     2 1pe9.3,/,1h ,'Area of scint., g.cm2 = ',1pe9.3,/,1h ,
     3 'Thickness of scint,cm = ',1pe9.3,/,1h ,
     4 'Distance (mean) between active centres, nm =',1pe9.3,/,1h ,
     4 'Migration length for excitons,cm = ',1pe9.3,/,1h ,
     5 'Cross-section for light emission from active centre,cm2 = ',1pe9.3,/)

c     Reads equilibrium spectrum data calculated from pelsld.for.
      read(36,18)
18    format(a)
      read(36,*) egam,rmep,rmfp
      read(36,*) ndp
      do 500 kc=1,ndp
      read(36,*) tel(kc),felkv(kc),tech(kc)
      if (tel(kc).lt.5.d-2) ndp=kc
      if (tel(kc).lt.5.d-2) goto 3500
      fel(kc)=felkv(kc)*tech(kc)
500   continue
3500  continue

c     The above product converts fluence per keV (fel(kc)) to fluence
c     per channel (felkv(kc)).
      ftot=0.0
      ftkv=0.0
      do 598 kc=1,ndp
      ftot=ftot+fel(kc)
      ftkv=ftkv+felkv(kc)
598   continue
      do 597 kc=1,ndp
      frel(kc)=fel(kc)/ftot
      frkv(kc)=felkv(kc)/ftkv
597   continue
      write(40,596) ftot,ftkv
596   format(1h ,'ftot=',1pe9.3,3x,'ftkv = ',1pe9.3/)
      write(40,599) egam,rmep,rmfp
599   format(1h ,'Initial energy (X-ray), keV=',1pe9.3,/,1h ,
     1 'Inverse mean free path for incoh. scatter, cm2/g =',1pe9.3,/,1h ,
     2 'Inverse mean free path for energy transfer, cm2/g =',1pe9.3,/)

c     fel(kc) is the fl. of equilbm. electrons per unit source concn.
      write(40,302)
302   format(/,1h ,2x,'kc',5x,'Eltn.Engy.',5x,'Fl.elns/sce.con.',2x,
     1 'Chan.width',/,1h ,12x,'keV',14x,'cm',12x,'keV',/)
      do 501 kc=1,ndp
      write(40,600) kc,tel(kc),fel(kc),tech(kc)
600   format(1h ,i3,4x,1pe9.3,10x,1pe9.3,6x,1pe9.3)
501   continue

c     Calculation of concentration of excitons (ciz(kc)) and fluence of
c     excitons (flex(kc)) produced.
      write(40,301)
```

```
301     format(//,1h ,'El.Engy',13x,'Prim.Inzn.',6x,
        1 'Concn.Excitns.',10x,'Conc. Excitns',/,1h ,3x,'keV',12x,'cm-1',
        2 14x,'per srce. concn.(dimls)',2x,'per unit X-ray fluence, cm-1',/)
        do 502 kc=1,ndp
        zel(kc)=pizl(tel(kc))*1.d+4
        ciz(kc)=fel(kc)*zel(kc)
        cxiz(kc)=ciz(kc)*rmfp
        write(40,700) tel(kc),zel(kc),ciz(kc),cxiz(kc)
700     format(1h ,2x,1pe9.3,10x,1pe9.3,10x,1pe9.3,10x,1pe9.3)
502     continue

c       ciz(kc) is the conc. of electrons per unit source
c       concn, (dimensionless).  Mult. by rmfp to get Conc. for unit
c       incident X-ray fluence, (cm-1).  Mult. by X-ray fluence for total conc.

c       Total conc. of excitons per unit X-ray flnce (txciz) or per
c       unit source concn.(tciz).
        tciz=0.0
        txciz=0.0
        do 503 kc=1,ndp
        tciz=tciz+ciz(kc)
        txciz=txciz+cxiz(kc)
503     continue

        write(40,701) dfex,tciz,txciz
701     format(/,1h ,'Diffn. length of excitons, nm = ',1pe9.3,2x,/,1h ,
        1 'Total conc. of excitons per unit source concn. =',1pe9.3,
        2 /,1h ,'Total concn. of excitons for unit X-ray fluence, cm-1 = ',
        3  1pe9.3,/)

c       Calculate the probability that an exciton will activate the activator
c       centre per unit source concentration of electrons, also the total
c       number of reactions.  Uses the diffusion length, not velocity.
c       Calculate the mean number of scintillation centres,na, activated per
c       track.
        write(40,300)
300     format(//,1h ,'Conc.excns.',4x,'Fl.excns.,cm.',2x,'Fl.excns.(dim),',2x,
        1 'Prby.actn.(cm3)',2x,'Prby.actn. (cm2)',2x,'Scint.emiss.',
        2 /,1h ,'/Srce.Conc.',2x,'/Srce. conc.',2x,'/X-ray fl',2x,
        3 '/Srce.Concn',2x,'/X-ray fl.',3x,'/Srce.Conc.(cm3)',/)
        do 702 kc=1,ndp
c       if (ciz(kc).eq.0.0) goto 111
        flex(kc)=ciz(kc)*dfex
        fxex(kc)=flex(kc)*rmfp
        pact(kc)=flex(kc)*siga*avca
        if (pact(kc).gt.1.0) pact(kc)=1.0
c       pact(kc)=flex(kc)*siga
        pxact(kc)=fxex(kc)*siga*avca
        if (pxact(kc).gt.1.0) pxact(kc)=1.0
c       pxact(kc)=fxex(kc)*siga
        rrsc(kc)=pact(kc)*vsc
        write(40,601) ciz(kc),flex(kc),fxex(kc),pact(kc),pxact(kc),rrsc(kc)
601     format(1h ,1pe9.3,9x,1pe9.3,9x,1pe9.3,6x,1pe9.3,6x,1pe9.3,6x,1pe9.3)
702     continue
111     continue
```

```
      if (jump.eq.1) goto 7400
      do 999 kc=1,ndp
      stp(kc)=stel(tel(kc))
      ran(kc)=rangel(tel(kc))
      write(40,888) tel(kc),stp(kc),ran(kc)
888   format(1h ,'tel=',1pe9.3,3x,'stp=',1pe9.3,2x,'range=',1pe9.3)
999   continue
7400  continue

c     Calculation of the average number of active centres at risk
c     per track- weighted for equilbm. spectrum.
      totfr=0.0
      tnph=0.0
      tphx=0.0
      tpem=0.0
      chrd=thk
      write(40,705)
705   format(/,1h ,'El.Engy,keV',4x,'Int. numb.',4x.'No. of Scints,norm',4x,
     1 'No. of Sc./keV',4x,'No. of scints/X-ray fl.',/,1h ,14x,
     2 'of Scints.norm',8x,'rna(kc)',14x,'rnkv(kc)',10x,'rxna(kc)',/)
      do 1000 kc=1,ndp
      rel(kc)=rangel(tel(kc))
      if (rel(kc).gt.chrd) rel(kc)=chrd
      fwr(kc)=frel(kc)*rel(kc)
      fxwr(kc)=fel(kc)*rel(kc)*rmfp
      fwkv(kc)=frkv(kc)*rel(kc)
      rna(kc)=fwr(kc)*1.d7/xa
      rnkv(kc)=fwkv(kc)*1.d7/xa
      ina(kc)=abs(rna(kc)+0.5)
      rxna(kc)=fxwr(kc)*1.d7/xa
      totfr=totfr+fwr(kc)*1.d7
      tnph=tnph+rna(kc)
      tphx=tphx+rxna(kc)

c     tpem is the total number of photons emitted by the electron track.
      tpem=tpem+rna(kc)*pact(kc)
      write(40,704) tel(kc),ina(kc),rna(kc),rnkv(kc),rxna(kc)
704   format(1h ,1pe9.3,9x,i5,9x,1pe9.3,9x,1pe9.3,9x,1pe9.3)
1000  continue
1010  continue
c     Convert total track length to nanometres.
c     Mean number of active centres at risk for whole equilbm specrum
c     (normalised to unity) = na.
      na=abs(totfr/xa)
c     Total mean number of photons emitted per unit incident
c     fluence of X-rays is tphx.
      write(40,800) na,xa,totfr,tnph,tphx,tpem
800   format(/,1h ,'Number(integral) of active centres at risk = ',
     1 i6,/,1h ,'Mean distance between active centres, nm =',1pe9.3,
     2 /,1h ,'Total track length, nanometre, = ',1pe9.3,/,
     3 1h ,'Total photons for eln. spectrm norml. = ',1pe9.3,
     4 /,1h ,'Total photons emitted per unit X-ray fluence = ',1pe9.3,
     5 /,1h ,'Total photons emitted per electron track = ',1pe9.3,//)

c     Calculate,for each kc energy band,the frequency of  events that are
```

```
c       spaced at 2nm.

        write(43,3399)
3399    format(1h ,3x,'kc',3x,'tel(kc)',3x,'Prob.x=2nm',3x,'Prob.Inzn.2nm',3x,
     1 'No.hv./keV',3x,'No.*Prob.=dsb',3x,'Prim.Inzn,nm-1',2x,'Inzmfp, nm',/)
        ftrl=fact(2)
        do 348 kc=1,ndp
        po2(kc)=px(2,xa,ftrl)
        arg(kc)=zel(kc)*1.d-4/5.55d+2
        ps2nm(kc)=1.0-dexp(-arg(kc))*(1.0+arg(kc))
        r2pr(kc)=rnkv(kc)*po2(kc)*ps2nm(kc)
        lamda(kc)=1.d7/zel(kc)
        write(43,3400) kc,tel(kc),po2(kc),ps2nm(kc),rnkv(kc),r2pr(kc),
     1 zel(kc)*1.d-7,lamda(kc)
3400    format(1h ,i5,2x,1pe9.3,4x,1pe9.3,4x,1pe9.3,6x,1pe9.3,5x,1pe9.3,
     1 3x,1pe9.3,5x,1pe9.3)
348     continue

c       Calculate the total number of equivalent dsb's.
        tpr=0.0
        do 611 kc=1,ndp
        tpr=tpr+r2pr(kc)*tech(kc)
611     continue
        write(43,3550) egam,rmfp,tpem,tpr
3550    format(//,1h ,'Egam,keV=',1pe9.3,2x,'Engy transf. coefft, cm=',1pe9.3,/,
     1 1h ,'Total photons=',1pe9.3,2x,'Total dsbs=',1pe9.3,//)
        write(40,7000) tpem,tpr
7000    format(1h ,'Total number of scintln. photons/track = ',
     1 1pe9.3,/,1h ,'Total number of scint. pairs paced at 2nm, dsbs = '
     2 1pe9.3,//)
        stop
        end

c       Calculate linear primary ionisation for electrons,
c       (average over whole track).  Energy, ex, in keV.  pizl in no./um.

        real*8 function pizl(ex)
        implicit none
        real*8 ex,rex,ogx,a,b
        if (ex.lt.0.05) goto 1000
        rex=ex/0.27
        ogx=dlog(rex)
        if (ex.ge.0.05.and.ex.le.0.27) goto 1100
        if (ex.le.3.0) goto 1200
        if (ex.le.2000.0) goto 1300
1100    continue
        pizl=488.4*(1.0+0.02*ogx-0.19*ogx*ogx+0.115*(ogx**3)+0.032*ogx**4)
        goto 1400
1200    continue
        pizl=488.4*((rex**-0.76)*(1.0+0.76*ogx)-0.025*ogx**2.8+0.002*ogx**5)
        goto 1400
1300    continue
        a=-0.75351
        b=0.786129
        pizl=488.4*dexp(-(a+b*ogx))
```

```
      goto 1400

1000  continue
      pizl=0.0
1400  continue
      return
      end

c     Calculation of mean distance,xa,between active centres. Also
c     probability that exactly s nanometres will be the space between 2
c     centres.  Let 'ca' be conc of active sites (no./unit mass).
c     rho = density of material.  Vol. of acive site with diffuse
c     boundary = 4/3. pi. xbar^3.= 1/(ca.rho).  Rad of
c     site = (3/(4pi.ca.rho)^(1/3).  Mean dist = twice.
c     Distance x = r.exp(-r/lamda), lamda= diffusion length.

      real*8 function adis(ca)
      implicit none
      real*8 xu,ca,va,ra,rho,fact
      integer ixa
      common/int/ rho
      external fact

c     Volume of active site .
c     Constant= 3/4pi = 0.23873.
      va=1.0/(ca*rho)
      ra=0.6204*(va**(1.0/3.0))

c     Convert to nanometres.
      ra=ra*1.d+7
      xu=2.0*ra
      ixa=abs(xu+0.5)
      write(40,604) ixa,ra,xu
604   format(1h ,'integer dist. between act. centres, nm =',i6,/,
     1 1h ,'mean radius,nm =',1pe9.3,
     2 2x,'real mean distance between active centres, nm =',1pe9.3,/)
      adis=xu
      return
      end

      real*8 function fact(n)
      implicit none
      real*8 a(280)
      integer j,n,ntop
      data ntop,a(1)/0,1./
      if (n.le.0) write(40,506)
506   format(1h ,'negative function obtained for factorial',/)
      if (n.le.0) goto 7000
      if (n.le.ntop) fact=a(n+1)
      if (n.le.ntop) goto 7000
      if (n.le.279) goto 7001
7001  continue
      do 5000 j=ntop+1,n
      a(j+1)=j*a(j)
5000  continue
```

```
      ntop=n
      fact=a(n+1)
7000  continue
      return
      end

c     Calculation of factorial n, n!.
      integer function ifact(n)
      implicit none
      integer ia(80),j,n,ntop
      data ntop,ia(1)/0,1/
      if (n.lt.0) write(40,605)
605   format(1h ,'negative function obtained for factorial',/)
      if (n.le.0) goto 700
      if (n.le.ntop) ifact=ia(n+1)
      if (n.le.ntop) goto 700
      if (n.le.79) goto 701
701   continue
      do 400 j=ntop+1,n
      ia(j+1)=j*ia(j)
400   continue
      ntop=n
      ifact=ia(n+1)
700   continue
      return
      end

c     Calculation of csda stopping powers for electrons.
c     Units are keV.cm2.g-1.
      real*8 function stel(ey)
      implicit none
      real*8 ey,zze,eth,rmza,rlx,oln,oxtm,a0,a1,a2,a3,a4
      rmza=0.5556
      eth=0.01
      if (ey.lt.eth) ey=eth
      if (ey.le.0.07) goto 3178
      if (ey.lt.10.0) goto 3179
      if (ey.gt.10.0.and.ey.le.300.0) goto 3180
      if (ey.gt.300.0.and.ey.lt.2000.0) goto 3181
      if (ey.gt.2000.0.and.ey.le.31000.0) goto 3183
3178  continue
      stel=2.5*1.d5*dsqrt(ey/0.07)

c     Units are keV.cm2.g-1.
      goto 3184
3179  continue

c     Convert low energy values to eV.
      zze=ey*1.d3
      oln=dlog(zze)
      oxtm=dexp(-4.5467+0.31104*oln+0.07773*oln*oln)
      oxtm=oxtm/rmza
      stel=zze/(oxtm*(0.15546*oln+0.31104))
      stel=stel*1.0d3
      goto 3184
```

```
3180    continue
        oln=dlog(ey)
        oxtm=(2.0*oln-8.00637)/3.4012
        rlx=1.8205-1.1598*oxtm+0.16429*oxtm*oxtm
        stel=dexp(rlx)
        stel=stel*1.d3
        goto 3184
3181    continue
        oln=dlog(ey)
        oxtm=(2.0*oln-13.304685)/1.89712
        rlx=0.63749-0.12199*oxtm+0.09112*oxtm*oxtm
        stel=dexp(rlx)
        stel=stel*1.0d3
        goto 3184
3183    continue
        oln=dlog(ey)
        a0=1.333117d1
        a1=-5.41576
        a2=8.475313d-1
        a3=-5.798398d-2
        a4=1.477839d-3
        stel=a0+a1*oln+a2*oln*oln+a3*(oln**3)+a4*(oln**4)
        stel=dexp(stel)*1.0d3

c       stel is converted from MeV to keV.cm2.g-1.
3184    continue
c       write(6,6666) ey,stel
6666    format(1h ,'ey, keV=',1pe9.3,3x,'stpwr, keV.cm2.g-1=',1pe9.3)
        return
        end

c       Calculation of reciprocal stopping power for ranges.
c       Calculation of the csda range for electrons using reciprocal
c       stopping power.
        real*8 function recstp(ey)
        implicit none
        real*8 ey,stel
        external stel
        recstp=1.0/stel(ey)
        return
        end

c       Calculation of electron csda ranges in keV.g-1.cm2, by integration of
c       reciprocal stopping powers.
        real*8 function rangel(ey)
        implicit none
        real*8 ey,ans,a,b,epsr,relerr,eth,rth,recstp
        integer ifail,n,nlimit
        real*8 d01ahf
        external recstp
        eth=0.01
        rth=5.0d-6*eth
        a=eth
        nlimit=0
        epsr=1.d-5
```

```
      ifail=1
      b=ey
      ans=d01ahf(a,b,epsr,n,relerr,recstp,nlimit,ifail)
      rangel=abs(ans)+rth
      continue
      return
      end
      real*8 function px(nx,rnu,frl)
      implicit none
      real*8 rnu,frl,az,ax,ay
      integer nx

c     mnu is the mean number along track.
c     nx is the specific number required.
c     Calculate probability that active centres will be a specified
c     distance (nx) apart.
c     rnu=float(mnu)
      ax=dexp(-rnu)
      ay=rnu**nx
      az=ax*ay/frl
      px=az
c     write(40,2002) nx,rnu,frl,rnu,ax,ay,az,px
2002  format(1h ,'nx=',i5,2x,'rnu=',1pe9.3,2x,'frl=',1pe9.2,3x,'rnu=',
     1 1pe9.3,2x,'ax=',1pe9.3,2x,'ay=',1pe9.3,2x,'az=',1pe9.3,
     2 2x,'px=',1pe9.3)
      return
      end
```